

The Behavior of Uranium in the Environment: Bacterial Reduction of an Aqueous Uranium Species

by

Matthew R. Lewis

B.S. Engineering Physics
United States Military Academy, 1991

SUBMITTED TO THE DEPARTMENT OF NUCLEAR ENGINEERING
IN PARTIAL FULFILLMENT OF THE REQUIREMENTS FOR THE DEGREE OF

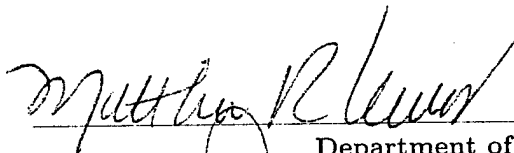
MASTER OF SCIENCE IN NUCLEAR ENGINEERING AT THE
MASSACHUSETTS INSTITUTE OF TECHNOLOGY

JUNE 2000

© 2000 Matthew R. Lewis. All rights reserved.

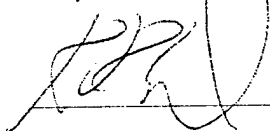
The author hereby grants to MIT permission to reproduce
and to distribute publicly paper and electronic
copies of this thesis document in whole or in part.

Signature of Author



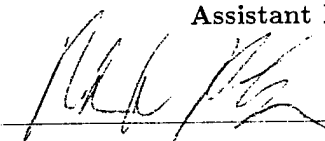
Department of Nuclear Engineering
May 5, 2000

Certified by



Kenneth R. Czerwinski
Assistant Professor of Nuclear Engineering
Thesis Supervisor

Certified by



Martin Polz
Assistant Professor of Civil and Environmental Engineering
Thesis Reader

Accepted by

Sow-Hsin Chen
Chairman, Committee on Graduate Students
Department of Nuclear Engineering

DTIC QUALITY INSPECTED 2

DISTRIBUTION STATEMENT A
Approved for Public Release
Distribution Unlimited

20000522 053

The Behavior of Uranium in the Environment: Bacterial Reduction of an Aqueous Uranium Species

by

Matthew R. Lewis

Submitted to the Department of Nuclear Engineering
on May 5, 2000 in Partial Fulfillment of the
Requirements for the Degree of Master of Science in
Nuclear Engineering

ABSTRACT

Experimental and analytical studies were performed to investigate the behavior of uranium with bacteria in an anaerobic environment. Laboratory studies used *Shewanella putrefaciens* because of its ability to grow rapidly in aerobic conditions and reduce metals in anaerobic conditions. Under anaerobic conditions, *Shewanella putrefaciens* use aqueous uranium as the electron acceptor in lieu of oxygen. The reduction of U(VI) to U(IV) removes uranium from solution and forms an insoluble compound known as uraninite. Ultraviolet/Visible Spectroscopy was used to analyze uranium ion complexation with several oxazine dyes that included Brilliant Cresyl Blue, Celestine Blue, and Gallomine Triethiodide. Complexation and resultant color changes with U(VI) and U(IV) with the dye solutions were tested at a variety of pH levels. The dye behavior was evaluated for future use as a visible reduction indicator for microbial reduction when performing direct plating experiments. These studies showed the best visual indicator to be Celestine Blue. Significant absorbance changes in the 400 to 800 nm wavelength range for Brilliant Cresyl Blue and Gallomine Triethiodide solutions were not detected.

X Ray Diffraction and Electron Microprobe Spectroscopy characterized the solid precipitates by the bacteria. The dark black precipitate exhibited visible characteristics of both $\text{UO}_2(\text{s})$ and $\text{U}_3\text{O}_8(\text{s})$. Electron microprobe showed a very small crystal formed by the bacteria, but was inconclusive with respect to the elemental composition of the mineral. The XRD spectra determined that precipitate was uranium dioxide $\text{UO}_2(\text{s})$.

The investigation included a time phased uranium isotope analysis in the precipitate and supernatant samples. Thermal Ionization Mass Spectrometry (TIMS) measured the uranium isotopic ratio of $^{238}\text{U}/^{235}\text{U}$ to determine if microbial reduction of U(VI) to U(IV) affected these ratios. The isotopic ratios of both the supernatant and precipitate were measured at times ranging from zero to 95 hours. An enriched uranium solution was created by dissolving an enriched sample of $\text{U}_3\text{O}_8(\text{s})$ in nitric acid. The $\text{U}_3\text{O}_8(\text{s})$ was standard reference material (SRM) from the New Brunswick National Laboratory, and was enriched to roughly 50 percent ^{235}U . The results of the TIMS experiment showed that there was not a detectable level of fractionation.

Thesis Supervisor: Kenneth R. Czerwinski
Assistant Professor of Nuclear Engineering

Thesis Reader: Martin Polz
Assistant Professor of Civil and Environmental Engineering

Acknowledgments

This thesis is the result of nearly a year's worth of experimental research. It is the product of the support and guidance received from a very long list of individuals. I would like to thank the United States Army, the United States Military Academy, and the Lord for the opportunity to attend graduate school. I would especially like to thank Colonel Raymond Winkel, Department Head of Physics at West Point, whose efforts made this path in my Army career possible. I wish to thank Professor Kenneth Czerwinski in the Nuclear Engineering Department at the Massachusetts Institute of Technology for the guidance and support throughout the research. Professor Czerwinski's encouragement and thorough knowledge of actinide chemistry provided invaluable guidance throughout this research. I would also like to thank Professor Martin Polz at the MIT Department of Civil and Environmental Engineering who offered important insight on the microbial selection process, and whose notable work on the reduction of metals provided the motivation for the research on the uranium isotopes. Lingping Kuai and Vanja Klepac, post doctorate and graduate student in the microbiology lab at the Ralph Parson's Laboratory, supplied invaluable assistance preparing the cultures used to stimulate the microbial reduction experiments. I also wish to thank Professor Sam Bowring, Mark Schmitz, and Kalsoum Kabbasi from the Department of Earth, Atmosphere, and Planetary Sciences at MIT for devoting their time and resources for the TIMS measurements. A special thanks goes to Mark Schmitz for the long interview on the physics and operation TIMS machine, and assisting with the long chemical preparation of the samples for TIMS analysis.

The most important thanks goes to my wife Anne, and our children Matthew Jr. and Daniel. My family's love, patience, and support throughout the past two years provided me with the encouragement and stamina required to complete this thesis and my degree.

Table of Contents

	Page
Title Page	1
Abstract	2
Acknowledgments	3
Table of Contents	4
List of Figures	7
List of Tables	9
 Chapter 1: Introduction	 11
1.1 Background and Motivation	11
1.2 The Chemistry of Uranium	12
1.3 Oxidation States of Aqueous Uranium	15
1.3.1 Tetravalent Uranium Ions U(IV)	16
1.3.2 Hexavalent Uranium Ions	16
1.4 Environmental Behavior of Uranium	18
1.5 Research Goals	19
 Chapter 2: Application of Photometric Dyes to Determine Local Bacterial Reduction	 23
2.1 Principles of UV/Visible Spectroscopy	24
2.2 Determining Uranium Concentration Using Arsenazo(III) by UV/Visible Spectroscopy	26
2.2.1 Arsenazo(III) Complexation with Uranium in pH2 Buffer	29
2.2.2 Arsenazo(III) Complexation with Uranium in Strong Acid and pH2 Buffer	32
2.2.3 Results and Conclusions using Arsenazo(III) to Determine Uranium Concentration	37
2.3 Photometric Determination of the Reduction Process with Oxazine Dyes	38
2.3.1 Oxazine Dye Complexation Behavior with Uranium (VI)	39
2.3.2 UV/ Visible Spectroscopy Results with U(VI)	42
2.3.3 Oxazine Dye Complexation Behavior with Uranium (IV)	45
2.3.4 UV/ Visible Spectroscopy Results with U(IV)	53
2.3.5 Comparison of the Absorbance Spectra for the Oxazine Dyes with U(VI) and U(IV)	53
2.4 Conclusions	56
 Chapter 3: The Reduction of Uranium by Bacteria	 60
3.1 Inductively Coupled Plasma- Atomic Emission Spectroscopy (ICP-AES)	60
3.1.1 Principles of ICP-AES	61

3.1.2 ICP-AES Hardware Specifications	64
3.1.3 Determination of Uranium by ICP-AES	66
3.2 Producing Enriched Uranium Acetate	67
3.2.1 Benchmarking the Chemical Procedure for $U_3O_8(s)$	69
3.2.2 Production of Enriched Uranium Acetate	74
3.3 Microbiology Experimental Procedures	84
3.4 Physical Structures of the Crystals	89
3.4.1 X-Ray Diffraction	89
3.4.2 Scanning Electron Microprobe	94
3.5 Conclusions	96
Chapter 4: Analysis of Uranium Isotopic Ratio of Precipitates from Bacteria	100
4.1 Background	100
4.2 TIMS Fundamentals	102
4.3 Preparation for TIMS Analysis	104
4.3.1 Chemical Preparation	105
4.3.2 TIMS Filament Loading	118
4.4 TIMS Operation	123
4.5 Observations	129
4.6 Results and Conclusions	146
Chapter 5: Conclusions and Recommendations for Future Work	150
5.1 Organic Indicator Dye Results	150
5.2 Microbiological Work and Uranium Acetate Preparation	153
5.3 Outcome of the Isotopic Fraction Investigation	155
5.4 Final Thoughts	157
Appendix 1 Chemical Equilibrium and Stability Constants	159
Appendix 2 Annex A	161
-1 Bacterial Growth Media	
-2 UV/Visible Spectrometer Instructions	
Annex B Arsenazo(III) Spectra Results	168
-1 Arsenazo(III) Experiment One (pH2 Buffer)	
-2 Arsenazo(III) Experiment Two (4 N HNO_3)	
-3 Arsenazo(III) Experiment Two (pH2 Buffer)	
Annex C Color Photos Comparing the Visual Change of the Oxazine Dyes with U(VI)	178
-1 Gallomine Triethiodide	
-2 Celestine Blue	
-3 Brilliant Cresyl Blue	
Annex D Brilliant Cresyl Blue Spectra Results with U(VI)	182
Annex E Celestine Blue Spectra Results with U(VI)	194
Annex F Gallomine Triethiodide Spectra Results with U(VI)	206
Annex G ICP-AES Concentration of U(IV) Source	218
Annex H Brilliant Cresyl Blue Spectra Results with U(IV)	221
Annex I Celestine Blue Spectra Results with U(IV)	229
Annex J Gallomine Triethiodide Spectra Results with U(IV)	237

Annex K	Brilliant Cresyl Blue Spectra Comparison of U(VI) and U(IV)	245
Annex L	Celestine Blue Spectra Comparison of U(VI) and U(IV)	252
Annex M	Gallomine Triethiodide Spectra Comparison of U(VI) and U(IV)	259
Appendix 3	Annex A New Brunswick Certified Reference Material Certificate of Analysis	266
	Annex B ICP-AES Operating Instructions	267
	Annex C Detailed Media Contents for Cultivating Shewanella	270
	Annex D X-Ray Diffraction Graphs	272
Appendix 4	Annex A Anion Exchange Resin Behavior for AG1-X8 Cl ⁻ Form	280
	Annex B Order in the Carousel	281
	Annex C Column Chemistry Log	282
	Annex D TIMS Turret Loading	284
	Annex E TIMS Results of Sample AO	288
	-1 Raw Database	
	-2 Chart of Isotopic Ratios versus Time	
	-3 Chart of Isotopic Ratios versus Temperature	
	Annex F TIMS Results of Turret One	292
	-1 Raw Database	
	-2 Isotope Ratio Charts	
	Annex G TIMS Results of Turret Two	313
	-1 Raw Database	
	-2 Isotope Ratio Charts	
	Annex H TIMS Results of Turrets Three through Five	324
	-1 Raw Database	
	-2 Isotope Ratio Charts	
	Annex I TIMS Results of Turret Six	363
	-1 Raw Database	
	-2 Isotope Ratio Charts	
	Annex J Estimated Concentration of the Precipitate Solutions	377
	Bibliography	379

List of Figures

	Page
2.1 Uranium Calibration (Arsenazo(III))	31
2.2 Spectra Obtained for U-Arsenazo(III) Calibration Curve	32
2.3 4.0 N HCl Spectra Obtained for U-Arsenazo(III) Calibration Curve	34
2.4 4.0 N HCl Uranium Calibration	35
2.5 pH 2 Spectra Obtained for U-Arsenazo(III) Calibration Curve	36
2.6 pH 2 Buffer Uranium Calibration	37
2.7 Uraninite Production Photo	45
2.8 ICP-AES of C45 (U(IV) Source)	49
2.9 Celestine Blue with U(VI) and U(IV)	54
2.10 Celestine Blue Complexation with U(IV) and U(VI) at 1 N HNO ₃	55
3.1 Coaxial Design of the ICP Torch	61
3.2 Schematic of the Major Components of a Typical ICP-AES	62
3.3 Components of the Spectroflame ICP D ICP-AES	63
3.4 Calibration Curve and Concentration Determination for the Non-Enriched Uranium Acetate Solutions	73
3.5 Calibration Curve and Concentration Determination for the Enriched Uranium Acetate Solutions	77
3.6 Calibration Curve and Concentration Determination for the Re-prepared Enriched Uranium Acetate Solutions	83
3.7 Rigaku RU300 X-Ray Generator	91
3.8 Zero Background Sample Holder	92
3.9 Background and Ka2 X-Rays subtracted from the Original X-Ray Spectra.	93
3.10 The Raw Spectra of the Silicon Sample Holder and Collodian with and without Sample	94
3.11 SEM picture of the Uranium Precipitate by Bacterial Reduction	96
4.1 Principles of a Mass Spectrometer	103
4.2 Calibration Curve and Concentration Determination for the Enriched Uranium Acetate Supernatant Solutions	108
4.3 Conversion of Uranyl Acetate into Uraninite	109
4.4 50 µL Columns in Draining Stand	113
4.5 Molecular Structure of Styrene-Divinylbenzene Crosslinked Co-Polymers with Attached Groups for AG1	114
4.6 Column Carousel Picture	116
4.7 TIMS Filament Picture	120
4.8 Drying Down Filament Picture	122
4.9 Vector 54 Thermal Ionization Mass Spectrometer Picture	123
4.10 Comparison of Fraction Behavior with the Temperature and Load Sample Size in Turret One	131
4.11 Control Samples C0, C4, C8, and C95	133

4.12	Sandwich Loading Technique with U500	135
4.13	Sandwich Loading Technique with U500 as a Function of Temperature	136
4.14	Test Sample Supernatant Isotope Ratios	139
4.15	S95 Supernatant and Precipitate Ratio Comparison	140
4.16	Calibration Curve and Concentration Determination for the Enriched Uranium Acetate Precipitate Solutions	142
4.17	Comparison of 95 Hour Sample Isotopic Ratios	145

List of Tables

		Page
1.1	The Natural Occurrence of Uranium	13
1.2	Uranium Isotopes	13
1.3	Radii of Uranium Ions	14
1.4	pH Values of 0.02M Solutions of Uranium Ions	15
2.1	Arsenazo(III) and Uranium Complexation Data	27
2.2	Observations of Samples A1-B3	27
2.3	Uranium Concentration in pH 2 Buffer	29
2.4	pH2 Buffer Integrated Absorbance and Corrected Integrated Absorbance	30
2.5	Uranium Concentration in pH2 Buffer and 4 N HCl	33
2.6	4 N HCl Integrated Absorbance and Corrected Integrated Absorbance	34
2.7	pH2 Buffer Integrated Absorbance and Corrected Integrated Absorbance	36
2.8	Dye Stock Solutions	39
2.9	U(VI) Samples	40
2.10	Qualitative Observations of U(VI) Dye Samples	41
2.11	U(IV) Solution Preparation	50
2.12	Qualitative Observations of U(IV) Dye Samples	50
2.13	Visible Wavelengths	53
2.14	Oxazine Dye Results	57
3.1	ICP-AES Hardware	65
3.2	ICP-AES Setting for URANIUM Method	66
3.3	ICP-AES Data for Non-Enriched U_3O_8 Conversion to Uranium Acetate	72
3.4	Estimated Concentration of the Non-Enriched Uranium Acetate Solution	74
3.5	ICP-AES Data for Enriched U_3O_8 Conversion to Uranium Acetate	76
3.6	pH Measurements of the Rinse Solutions	81
3.7	ICP-AES Data for Re-prepared Enriched U_3O_8 Conversion to Uranium Acetate	82
3.8	Summary of the Steps Involved in Preparing the Anaerobic Media and the Bacteria for the Uranium Reduction Experiments	85
3.9	Components of the Uranium Media	87
3.10	PDF 41-1422 XRD Spectroscopic Data for Uraninite	90
3.11	The Scan Parameters for the Two XRD Analyses Performed on the Bacterial Precipitate	92
3.12	Peak Intensities of Measured Spectra from the Bacterial Precipitate and the Reference Values for Uraninite	93

4.1	ICP-AES Data for the Enriched Uranium Acetate Supernatant	107
4.2	Column Chemistry for Concentrating the Uranium with an Anion Exchange Resin	115
4.3	Acid Properties used in Columns	117
4.4	Uranium Spike Weights	118
4.5	New Brunswick Certified Reference Material Certificate of Analysis for CRM U500, Uranium Isotope Standard	130
4.6	Isotope Dilution Calculations of Blank Uranium Concentrations	134
4.7	ICP-AES Data for the Precipitate Solutions in the 1.5 mL Microcentrifuge Tubes	143
4.8	Filament Load Amounts for the Controls and Test Samples	144

Chapter 1

Introduction

The purpose of this chapter is to introduce the goals of the investigation. Chapters 2 through 4 provide a detailed description of the laboratory method and equipment used to gather specific results. Section 1.1 discusses the background and motivation of the experimental research. Section 1.2 and 1.3 present some pertinent information on the chemical behavior and physical properties of uranium. Section 1.4 briefly discusses the environmental aspects of bacteria and uranium contaminated ground waters. Section 1.5 completes the discussion by clearly describing the two primary investigation goals. The ultimate aim of this chapter is to explain the motivation for this research and outline the scientific basis for the experiments.

1.1 Background and Motivation

There are many uses of uranium in modern society. Uranium is used to fuel many civilian power utilities and in many different military roles. In the early 1960s, the United States Army began developing armor piercing ammunition consisting of depleted uranium (DU) alloyed with other metals. Density, tensile strength, and pyrophoric properties made DU munitions an effective armor piercer. It was also considered for penetrators because it was relatively inexpensive as a byproduct from the enrichment process¹.

One of the largest firms to produce depleted uranium products was Nuclear Metals Incorporated (NMI). The company, now re-named the Starmet Corporation, is located in Concord, Massachusetts and specialized in these materials from 1958 through 1985. For many years, the company stored uranium wastes, directly related from producing these weapons, in an unlined holding basin. There was a total of 400,000 pounds of uranium disposed in the holding basin. In 1985, the basin was capped because of concerns raised about contamination of the ground water. Remediation did not begin until 1997 and the company is currently applying for EPA Superfund site designation to help finance the clean up².

Technical data on fate and transport of the uranium plume has primarily been researched by the private environmental firm Goldberg-Zoino Associates Geoenvironmental, Inc (GZA). The site has also been the subject of many public and private university studies. Of particular concern is the effect that natural anaerobic processes may have in controlling the movement of this plume. One of these processes occurs with subsurface bacteria that are able to reduce the oxidation states of dissolved elements, such as sulfur or uranium, as part of their metabolic process.³

1.2 The Chemistry of Uranium

Uranium was first discovered as an element in the eighteenth century as an unusual mineral known as pitchblende. Although it is considered a rare element, there is more uranium present in the earth's crust than such common elements as silver, mercury, cadmium, and bismuth⁴. The average

uranium content in the earth's crust is 4×10^{-6} grams per gram of soil for a total of about 10^{14} tons. There also is a significant amount in the ocean, which holds nearly 10^{10} tons of uranium. Table 1.1 shows the abundance of uranium in nature⁵. Minerals found in the environment tend to be U(IV)

Table 1.1 The Natural Occurrence of Uranium⁵

<i>Substance</i>	<i>Concentration (Mass U/g)</i>
Igneous Rocks	4 µg
Basalt	0.2 µg
Granites	25 µg
Sedimentary Rocks	2 µg
Phosphate Rocks	100 µg
Bituminous shale	65 µg
Lignite	50 µg
Ocean Water	1 ng

Table 1.2 Uranium Isotopes: This chart displays the synthetic and natural isotopes. The percentage of occurrence in nature is in parenthesis.⁶

<i>Isotope</i>	<i>Primary Decay</i>	<i>Half Life</i>	<i>Source</i>
228	EC, α	9.3 min	Synthetic
229	EC, α	58 min	Synthetic
230	α	20.8 days	Synthetic
231	EC	4.2 days	Synthetic
232	α	73.6 days	Synthetic
233	α	1.62×10^5 years	Synthetic
234	α	2.48×10^5 years	Natural (0.0055)
235	α	7.13×10^8 years	Natural (0.720)
236	α	2.39×10^7 years	Synthetic
237	β	6.75 min	Synthetic
238	α	4.50×10^9 years	Natural (99.2745)
239	β	23.5 min	Synthetic
240	β	14.1 hours	Synthetic
241	β	16.8 min	Synthetic
EC-Electron Capture			
α -Alpha Decay			
β -Beta Decay			

compounds which oxidize to U(VI) during environmental weathering processes.

Uranium consists of a variety of isotopes that are listed in Table 1.2⁶. All the isotopes of uranium are radioactive to some extent with some isotope half lives as long as 4 billion years. Natural uranium consists of uranium isotopes 234, 235, and 238. Synthetic isotopes are also shown in Table 1.2.

Uranium in its metallic form is soft and silvery white⁷. Uranium falls into the actinide series of elements in which the 5f shell is in the course of being filled. The ground state electronic configuration of uranium involves the six valence electrons 5f³, 6d¹, and 7s² ⁷. The energy levels of the 5f, 6d, and 7s shells are very close together and the order they are filled in can be erratic. While uranium is most commonly found in the oxidation state of +6, involving the loss of all these electrons, uranium may also exist in lower oxidation states. The four well-defined oxidation states of uranium are

<i>Table 1.3 Radii of Uranium Ions⁸</i>	
<i>ION</i>	<i>IONIC RADIUS</i>
U ³⁺	1.03 Å
U ⁴⁺	0.93 Å
U ⁵⁺	0.89 Å
U ⁶⁺	0.83 Å

+3(5f³), +4(5f²), +5(5f¹), and +6(5f⁰). The atomic radii of uranium ions are in Table 1.3⁸.

The chemical properties of uranium are determined largely by the closeness of the energy levels of the 5f and 6d electrons. The 5f radius is large compared to the 4f radius corresponding to the lanthanide series. It

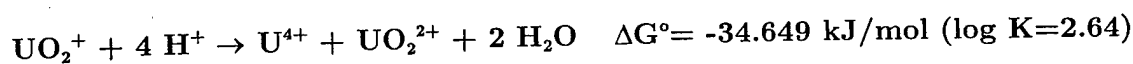
produces an overlap with the electron clouds of close neighbors and a mixing of their ligand wave functions in aqueous or organic solutions.⁹

1.3 Oxidation States of Uranium in Aqueous Solutions

In aqueous solutions, uranium may occur as trivalent U^{3+} , tetravalent U^{4+} (uranous ion), pentavalent UO_2^+ , or the hexavalent UO_2^{2+} (uranyl ion). However, oxidation states of three and five are very rare. U^{3+} is unstable, spontaneously oxidizing to U^{4+} by the following reaction in water¹⁴:



(Note: The thermodynamic data above and all subsequent reactions are found in [10] derived from a standard reference temperature of 298.15 K, standard pressure of 0.1 MPa, and $I=0$). UO_2^+ is also unstable by disproportionating into U^{4+} and UO_2^{2+} by the following half reactions:



Thus, only the uranous and uranyl ions are of practical importance¹¹.

Hydrolysis complexes form with all ionic uranium species. The order of increasing hydrolysis depends on charge size of the ion. U^{4+} is more easily

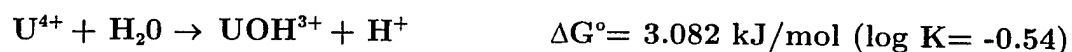
<i>Table 1.4 pH Values of 0.02M Solutions of Uranium Ions</i>	
Ion	pH
U^{3+}	2.4
U^{4+}	1.3
UO_2^{2+}	2.9

hydrolyzed compared to the uranyl ion UO_2^{2+} ¹². As a result of hydrolysis, solutions with uranium salts tend to be acidic. pH values for 0.02 M

uranium solutions are in Table 1.4. Equilibrium constants for other uranium ion complexes can be found in Appendix 1.

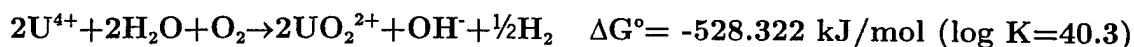
1.3.1 Tetravalent Uranium Ions U(IV)

Uranium (IV) in acid solutions is present simply as U^{4+} . Solutions of U(IV) salts are acidic as a result of hydrolysis. In ¹³, the hydrolysis constants for U^{4+} are highly dependent on temperature. Hydrolysis of U^{4+} proceeds by the following reaction at standard conditions¹⁴:



U(IV) complexes usually form with a coordination number of eight. Ligands coordinate around the central atom in a cubic manner. Although U(IV) has a coordination number of eight, in practice ligands often occupy not one, but two coordinate positions. This is true for both U(IV) and U(VI)¹⁵.

The oxidation of aqueous uranous ions by dissolved gaseous oxygen occurs spontaneously, but slowly according to the following reaction:



1.3.2 Hexavalent Uranium Ions U(VI)

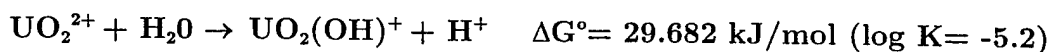
Almost all the compounds of U(VI) contain not the U^{6+} ion, but the uranyl group UO_2^{2+} . This group is characterized by the fact that the distances between the uranium and the two oxygen atoms (1.7- 2.0 Å) are shorter than the distances between uranium and any other elements entering into the composition of various compounds. The uranyl group, having a linear structure, also differs from other groups in its exceptional chemical

stability; as a rule, it enters into the composition of the new compound unchanged. The strength of the group is related to the fact that the uranium atoms have at their disposal a large number of 6d and 5f orbitals, some of which remain free after the usual covalent bonds between uranium and the oxygen atom $O=U=O$, have been formed¹⁶.

The exception to the integrity of this bonding occurs in oxidation reactions of uranium to U(VI) and the subsequent reactions with halides in the absence of moisture. However, the tendency to form the uranyl bonding is so great that UF_6 transforms very rapidly when water is present back to the uranyl group. It is extremely important that the complex compounds of uranium U(VI) almost always preserve this grouping. Thus the complex ion UO_2^{2+} and not U^{6+} is considered by convention as the central ion¹⁶.

The structure of complex formation with ligands is usually a dodecahedron, with the central uranium in the center, the two oxygen atoms perpendicular one above the plane and the other below the plane, with six ligand sites in the plane. The oxygen atoms are closer to the uranium than any other ligand bond (2.2-3.0 Å) and relatively inert in chemical reactions. Six is considered the maximum coordination number for the uranyl ion, but it is not the only possible coordination number. The coordination number depends on the size of the ligands, density of the charges, and other factors. Ligands normally occupy two coordination sites. Uranyl ions can form both cationic and anionic complexes¹⁵.

Uranyl ions (UO_2^{2+}) also hydrolyze, but not nearly as much as U^{4+} . Hydrolysis of U^{6+} proceeds by the following reaction¹⁴:



The stability constants with organic compounds can be referenced to the constants with humic and fulvic acids. The stability constants for pH values 4.0 to 6.0 range from $10^{5.11}$ to $10^{7.8}$ for humic acids and $10^{6.41}$ and $10^{7.4317}$. This indicates the possibility of strong sorption occurring with the bacteria cells in the relevant biological pH range of 4.0 to 8.0.

1.4 Environmental Behavior of Uranium

Surface waters or ground waters may have an undesirable amount of dissolved uranium as the result of natural processes or from contamination from uranium mining and processing activities. Although U(VI) tends to be very soluble in water, U(IV) substances are normally insoluble. Thus, microbial reduction of U(VI) has the potential to convert uranium from a soluble form to an insoluble form.

There are many studies on the ability of microorganisms to use certain metals and non-metals as part of their anaerobic respiration process. The metals serve as the electron acceptor in lieu of oxygen in aerobic processes. Microorganisms that use these elements in their metabolic process can greatly affect the fate and transport of these metals and non-metals in the environment. The element in its reduced form may be more or less soluble than in its original oxidation state. For uranium, microbial reduction offers a unique method of removing the more soluble species to an insoluble form. Uranyl ions and its complexes dominate most oxidizing aquatic environments. When it is reduced to U(IV), it forms UO_2 (s), an insoluble

mineral commonly known as uraninite. This inherently natural process denotes a unique way of stabilizing aquatic bodies that are contaminated with uranium¹⁸.

Traditional approaches in environmental microbiology have attempted to model these processes. However, classic isolation techniques tended to be heavily biased and typically only yielded organisms that grew quickly in the culture media generated in the laboratory. While there are isolated microbial cultures capable of metal reduction, it is difficult to characterize the exact role the specific bacteria play in the actual field environment. Laboratory studies clearly show metal reducing bacteria such as *Shewanella putrefaction* and *Geobacter metralireducens* (GS-15) have the ability to remove uranium as part of the metabolic reduction process. The yellowish uranyl solution is reduced to a clear solution with dark black solids forming adjacent to cultured bacteria in a test tube. It is much more difficult to see this process in the soil because the dark precipitate is quickly lost among the other dark solids in the soil matrix.

1.5 Research Goals

The purpose of this investigation is to better understand the bacterial processes with uranium in the subsurface. The enrichment cultures used previously were adopted because they grew well in the high nutrient concentrations of the laboratory medium. A better modeling for environmental behavior of the bacteria would be direct plating soil samples and identifying areas where the reduction of uranium occurs. Identification

of uraninite production in the soil matrix by direct plating is somewhat difficult.

The first part of this study seeks to identify a chemical dye that complexes with the uranium metal ions in solution and visibly changes color during the reduction process. This research evaluates a series of reduction indicating dyes and selects the dye that presents the best visible color change signifying the microbial reduction process in the soil matrix. This study investigates the behavior of the dyes at various pH levels in aerobic and anaerobic conditions. Ultra violet (UV)/ Visible spectroscopy will be used to quantify the color change of the dye during the redox reactions. The dye should also be able to locally target the redox reaction thereby identifying the location of the anaerobic bacteria in the soil matrix.

The second part of this study investigates the isotopic ratio of uranium atoms during the reduction process. Changing the isotopic ratio of an element is referred to as isotopic fractionation. It is normally a result of a kinetic difference in certain processes for each isotope based on its mass. The influent uranium solution has a particular isotopic ratio that may or may not be the same as the ratio in the reduced uranium solid. There is recent evidence of iron isotope fractionation during a similar process by other researchers¹⁹. Their experiments of dissimilarity reductive dissolution of iron oxide (Ferrihydrite) by bacteria (*Shewanella*) showed that biological organisms could fractionate Fe isotopes by up to 1.3 per mil for the $^{56}\text{Fe}/^{54}\text{Fe}$ ratio. The ability for bacteria to preferentially precipitate out the lighter isotopes as opposed to heavier isotopes has not been investigated with

uranium. Although the mass difference is not as great as the iron isotope mass difference, there may be some degree of fractionation. The isotope ^{235}U is roughly 1.28% lighter than the naturally abundant ^{238}U where as iron isotope ^{52}Fe is 3.84% lighter than ^{54}Fe . At a macroscopic level atomic behavior and therefore chemical behavior of uranium should be the same regardless of its isotopic state. If fractionation occurs during microbial reduction, it could demonstrate an ability to naturally enrich a uranium sample, although predictably at a slower rate than the results with iron. The measurement of the isotopic ratio will be accomplished using a Thermal Ionization Mass Spectrometer (TIMS).

¹Tanya P. Oxenberg, "The Use of Catchboxes to Minimize the Impact to the Environment from Testing Depleted Uranium Penetrators," Masters thesis, Georgia Institute of Technology, 1997, 1.

²Scott Allen, "Concord Firm Halts Clean Up," The Boston Globe, 17 May 1999, B1, B5.

³C. Sherman, "Using Vegetation and Surface Water Samples to Trace Depleted Uranium Contamination from Starmet Corporation in Concord, MA," Bachelor of Science Thesis, Massachusetts Institute of Technology, 1998, 5-6.

⁴P. N. Palei, Analytical Chemistry of Uranium (Ann Arbor, Michigan: Ann Arbor-Humphrey Science Publishers, 1970), 2.

⁵Glenn T. Seaborg and Joseph J. Katz, The Actinide Elements (New York, New York: McGraw-Hill Book Company, 1954), 131.

⁶Ibid., 132.

⁷E. H. Cordfunke, The Chemistry of Uranium. (New York, NY: Elsevier Publishing Company, 1969), 21.

⁸Ibid., 98.

⁹Ibid., 99.

¹⁰I. Grenthe, J. Fuger, R.J.M. Konings, R. J. Lemire, A. B. Muller, C. Nguyen-Trung, and H. Wanner, Chemical Thermodynamics of Uranium, Volume 1, (New York, NY: Elsevier Science Publishing Company, 1992).

¹¹Mason Benedict, Thomas H. Pigford, and Hans Wolfgang Levi, Nuclear Chemical Engineering, (Boston, MA: McGraw-Hill Company, 1981), 229.

¹² Cordfunke, 105

¹³ Palei, 21

¹⁴ Grenthe, 51

¹⁵I.I. Chernyaev, Complex Compounds of Uranium. (Jerusalem, Israel: Academy of Sciences of the U.S.S.R, 1966), 4-6.

¹⁶ Chernyaev, 1-2

¹⁷K.R. Czerwinski, G. Buckau, F. Scherbaum, and J.I. Kim, "Complexation of the Uranyl Ion with Aquatic Humic Acid," Radiochimica Acta 65, (March 1994): 118.

¹⁸Yuri A. Gorby and Derek Lovley, "Enzymatic Uranium Precipitation," Environmental Science and Technology 26, (1992): 205-207.

¹⁹ACS March 1999, 1 Abstracts GEOC#068, Iron Isotope Fractionation by the Bacteria *Shewanella* during Dissimilatory Reductive Dissolution of Ferrihydrite.

Chapter 2

Application of Photometric Dyes to Determine Local Bacterial Reduction

The purpose of this chapter is to develop a method to detect the microbial reduction process of uranium in an environmental sample. Visibly detecting the uraninite mineral produced in the reduction of U(VI) to U(IV) is difficult in a soil sample when isolation procedures or direct plating experiments are used. However, aqueous uranium complexes formed with organic ligands can provide a visible indication of reduction by evaluating the absorbance differences of U(VI) and U(IV). Uranyl or uranous ions and the complexes that these ions form with most inorganic ligands do not offer significant absorbance differences that complexes with certain organic ligands present. Therefore, the primary focus in these experiments is to identify a reduction indicator that provides a significant visible color difference between the complexes formed with U(VI) and U(IV). Section 2.1 provides a brief overview on the theory behind Ultra-Violet (UV)/Visible Spectrometry. Section 2.2 provides the experimental results using an organic complexing agent known as Arsenazo(III) to determine the uranium concentration in aqueous solutions. Section 2.3 examines the color differences of three oxazine dyes with solutions of U(VI) and U(IV) at various acid and buffer solutions. Section 2.4 concludes the study with some

recommendations on using the dyes in a media containing bacteria to identify localized areas where microbial reduction of uranium is occurring.

2.1 Principles for UV/Visible Spectroscopy

UV/Visible Spectroscopy is a method used to determine the concentration of uranium in a solution by observing the absorbance intensity of light by uranium complexes. The energy difference between states during molecular or atomic transitions from one state to another are discrete quantities. Typically these types of transitions occur over a wide range of frequencies on the electromagnetic spectrum, but processes involving transitions of the valence electrons in the atomic or molecular systems are especially prevalent towards the longer wavelength area where visible light lies. When this transition energy difference is exactly equal to a specific frequency, ν , that lies in the UV/ Visible region, it is either absorbed or emitted (equation 2.1)¹. The reflected wavelengths in the visible range will define the color of the solution as viewed by a person.

$$h\nu = |\Delta E| \quad (2.1)$$

h = Planck's constant (6.626E-34 J s)

ΔE = Energy difference between the initial and final states,

ν = frequency of the light absorbed/emitted [1/s].

In UV/Visible Spectroscopy, the intensity of the source at the frequency of a given chromophore (the energy difference in the state transitions of a given aqueous complex) that is adsorbed passing through a sample solution is measured to determine the concentration of that chromophore in the solution. The Beer-Lambert law, shown in equation 2.2,

governs the relationship between the observed intensity and the concentration.²

$$I = I_0 10^{\epsilon C x} \quad (2.2)$$

I = intensity of light at a given wavelength that passes through the sample

I_0 = the intensity of the light incident on the sample,

ϵ = the molar absorption coefficient (or extinction coefficient) of the chromophore [$M^{-1} \text{ cm}^{-1}$]

C = the molar concentration of the chromophore

x = the path length of the light as it passes through the sample

By defining the transmittance, T , as the ratio of the intensity of light that passes through the sample over the incident intensity (equation 2.3) and the absorbance, A , as the \log_{10} of the inverse of the transmittance (equation 2.4), the absorbance can be related to the concentration of the chromophore by equation 2.5.

$$T \equiv \frac{I}{I_0} \quad (2.3)$$

$$A \equiv -\log_{10} T \quad (2.4)$$

$$T = 10^{-A} \quad (2.5)$$

$$A = \epsilon C x \quad (2.6)$$

Because the system obeys Beer's Law, equation 2.5 shows that with all other parameters fixed by the experiment, the concentration of the chromophore is directly proportional to the observed absorbance intensity at the wavelength typical of the chromophore of interest.

The UV/ Visible Spectrometer used in this experiment was Ocean Optics Fiber Optic Spectrometer Model PC1000. The UV/Visible Spectrometer system consisted of a deuterium/halogen light source, a

spectrometer (SD2000 Fiber Optic Spectrometer), and a PC-based computer data collection system. LabView 4.1 for Windows was used as the software interface with the hardware. The light source is directed into the solution through a standard cuvette sample holder. The samples are placed in polystyrene cuvettes (Elkay Ultra-Vu Model 127-1010-007, minimum volume = 3 mL, light path = 10 mm), which are then placed one at a time in the cuvette holder (Ocean Optics, CUV -ALL-FLR sample holder). The light source leaves the source, passes through the solution, and returns to the spectrometer by optic cables. All fiber optic cables and other optics equipment used in the UV/Visible Spectrometer system were also from Ocean Optics, Inc.

A detailed description of the exact steps in using the UV/Visible Spectrometer system is in Appendix 2, Annex A-2. Some critical software parameters applied in the raw data gathering of the spectrum were³:

- 1) *Integration/frequency*: 6 (Integration frequency refers to the number of "shots" that are used to measure a single spectrum. In this case it adds counts per 6 milliseconds)
- 2) *Box car smoothing*: 5 (boxcar smoothing refers to the number of pixels that are averaged together into 1 bin and basically specifies number of channels per frequency range)
- 3) *Average*: 5 (average refers to the number of spectra that are taken and averaged together to make each displayed/recorded spectrum. This adjusts for slight variation in each spectrum. Higher numbers increase measurement time.)
- 4) *Absorbance*: ON
- 5) *Frequency range*: 400-800nm

2.2 Determining Uranium Concentration using Arsenazo(III) Complexation by UV/Visible Spectroscopy

The first organic dye was not used as a reduction indicator. Rather its purpose was to determine the uranium concentration in aqueous

solutions. UV/Visible Spectrometry was used to measure the absorbance of the complexes formed with Arsenazo(III) and uranyl ions present in a bacterial medium. The reason for this measurement was to determine if uranium remained in a medium that when added to bacteria failed to precipitate the black uraninite solid.

As stated earlier, neither uranyl ions nor its normal inorganic

Table 2.1 Arsenazo(III) and Uranium Complexation Data: This data from ⁴ discusses the complexation behavior UV/ Visible absorbance parameters of these complexes.

For simultaneous measurement of U(IV) and U(VI). The molar absorption coefficients for the uranium-Arsenazo(III) complexes are:

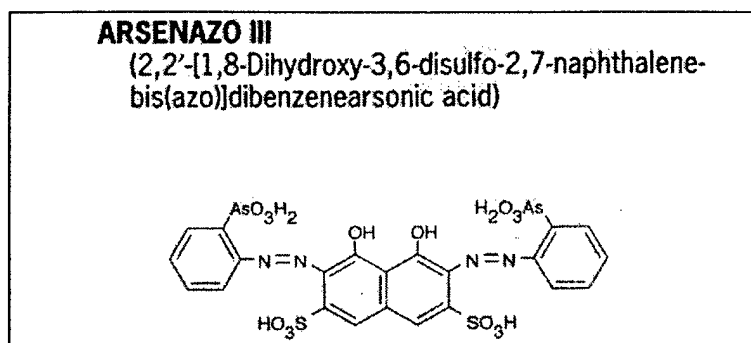
<i>Element</i>	<i>Conditions of sensitivity</i>	<i>Molar Absorption Coefficient</i>
	<i>Max sensitivity</i>	ϵ ($L M^{-1} cm^{-1}$)
U ⁴⁺	4M HCL; l=670 nm	100000
UO ₂ ²⁺	pH=2; l=655 nm	53000

complexes have significant absorbance in the UV/Visible frequency range for

Table 2.2 Observations of A1-B3: This table contains the information on the first experiment using the bacteria *Shewanella putrefaciens*. There was no visible uraninite in any of the samples except possibly the tiny specs of black in sample B2.

<i>Sample</i>	<i>Electron Donor</i>	<i>Electron Acceptor</i>	<i>Visual Observation</i>
A1	NaCH ₃ COO	NaNO ₃	Clear
A2	NaCH ₃ COO	NaNO ₃	Clear supernatant with a yellow precipitate at the bottom
B1	NaCH ₃ COO	UO ₂ (CH ₃ COO) ₂	Clear supernatant with a yellow precipitate at the bottom
B2	NaCH ₃ COO	UO ₂ (CH ₃ COO) ₂	Yellowish tinge to the supernatant, smaller amount of precipitate. Mostly white solid with dark specs on the bottom
B3	NaCH ₃ COO	Fe-citrate UO ₂ (CH ₃ COO) ₂	Yellowish tinge to the supernatant, smaller amount of precipitate

direct spectroscopy. Arsenazo(III) is an organic compound that acts as a visual complexing agent to measure the free uranium in solution. Some physical observations using Arsenazo(III) complexation with both U(VI) and U(IV) are found in [4], and significant constants for Arsenazo(III) are shown in Table 2.1⁴. Arsenazo(III) has the following chemical structure shown below⁵. From earlier work in [6], the concentration of Arsenazo(III) must be chosen higher than the uranium concentration to ensure all free uranium available may bind with the Arsenazo(III) ligand. This technique of ensuring



an overabundance of Arsenazo(III) molecules to complex the uranium in solution is further discussed in [6] and [4].

The samples were originally capped in 25 mL glass culture tubes that maintained a sealed N₂-CO₂ atmosphere. Qualitative observations of each culture tube and information on the primary source of electron donors and acceptors are in Table 2.2. The exact composition and concentrations of these solutions can be found in Appendix 2, Annex A-1. The pH of the entire medium was adjusted to 6.5-7.0 with a 1 N HCl solution. Two samples aimed to test the chemical behavior of the medium without the bacteria. Another two samples had the bacteria and uranium in the solution. The only difference between these two samples was the primary

electron acceptor: in one it was nitrate and in the other it was uranyl acetate. The last sample was inoculated with the strain, but added approximately 10-20 mM of iron citrate to about 1 mM of uranyl acetate to act as the electron acceptors.

After manually shaking each glass test tube to suspend all solid phases present, the samples were all uncapped with a pair of standard pliers and poured into 15 mL disposable polypropylene centrifuge tubes (Corning model 430052). The aliquots were centrifuged for 30 minutes on a Sigma laboratory centrifuge model 204.

2.2.1 Arsenazo(III) Complexation with Uranium in pH 2 Buffer

Nine total samples in this experiment were analyzed and are listed in

Table 2.3 Uranium Concentration in pH 2 Buffer: This table contains a list of samples and description of the method used to prepare them with pH 2 buffer for UV/Visible spectroscopy.

<i>Sample</i>	<i>Aliquot Source</i>
1	Deionized water
2	Uranium Standard 1.0 mM
3	Uranium Standard 0.5 mM
4	Uranium Standard 0.1 mM
5	A1 Supernatant
6	A2 Supernatant
7	B1 Supernatant
8	B2 Supernatant
9	B3 Supernatant
<p>Analysis Solution: 4.0 mL of pH2 Buffer (VWR Lot No: 9812123) 0.5 mL of source above 0.5 mL of 1.9 mM Arsenazo(III) solution</p>	

Table 2.3. A 1.16 mM uranium acetate stock solution was used as the free-metal uranium source for this experiment. This solution was diluted with

Table 2.4 Integrated Absorbance and Corrected Integrated Absorbance: This table contains the absorbance, integrated from 625 to 670 nm, for the spectra taken as part of the calibration curve experiment. The corrected integrated absorbance is determined by subtracting the blank value from the integrated

<i>Cuvette</i>	<i>ΣAbsorbance 625-670 nm</i>	<i>Corrected Absorbance</i>	<i>U Conc</i>
BLANK	2.622	0	0 mM (Trace)
STD 1	224.381	221.758	1.0 mM
STD 2	214.605	211.983	0.5 mM
STD 3	124.396	121.774	0.1 mM
A1	22.397	0	
A2	39.452	17.055	
B1	26.234	3.836	
B2	74.004	51.607	
B3	228.252	205.855	

deionized water to make 10 mL of 1.0 mM, 0.5 mM, and 0.1 mM standard uranium solutions. A 1.9 mM Arsenazo(III) dye solution (Aldrich Chemical Company Lot No: 1668-00-4) was used as the indicator dye in this experiment with the pH2 buffer.

The solution used for the analysis consisted of 4 mL of pH 2 buffer, 0.5 mL of sample, and 0.5 mL of Arsenazo(III) solution, and were mixed in a 5 mL polypropylene vial. This mixture was then transferred into a 3 mL cuvette using a disposable transfer pipette. The standard and sample absorbance spectrum is graphed in Figure 2.2. Larger versions of these graphs that separate sample and standard spectra are also found in Appendix 2, Annex B.

The broad peak centered in the spectrum between 500 and 600 nm represents the absorbance of the free or non-complexed Arsenazo(III). A second peak that develops in the 625 and 670 nm range represents the

absorbance of the Arsenazo(III) complexed to the uranyl ion (UO_2^{2+}). To

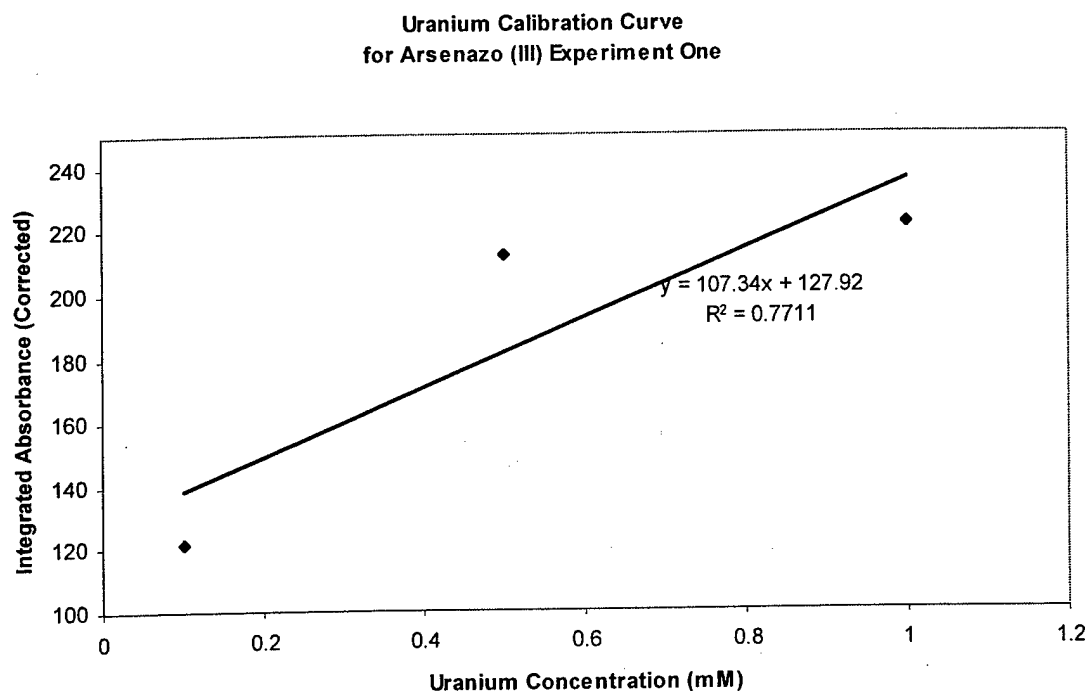


Figure 2.1 Uranium Calibration: This figure contains the calibration curve obtained for the determination of Uranium by UV/Vis spectroscopy, generated from the background corrected, integrated absorbance values given in Table 2.4.

generate a calibration curve, each spectrum is integrated over the second peak by summing all of the absorbances for wavelengths between 625 and 670 nm. The integrated value for the blank sample is then subtracted to give the corrected integrated absorbance for each standard. The blank buffer solution was used to remove the background in the standards and A1 was used to remove the background from the samples. These corrected absorbances are given in Table 2.4, and the resulting calibration curve is shown in Figure 2.1.

Arsenazo(III) Experiment
Standards and Samples in pH2 Buffer (Normalized)

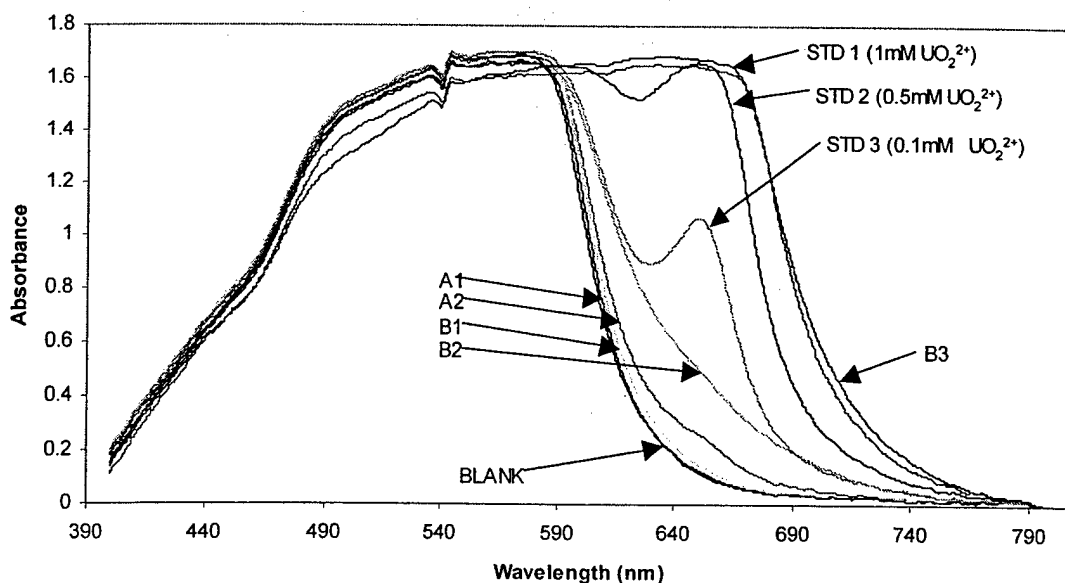


Figure 2.2 Spectra obtained for U-Arsenazo(III) Calibration Curve: This figure shows the standard and sample spectra obtained during the determination of a calibration curve for the determination of Uranium by UV/Vis spectroscopy using Arsenazo(III) as an indicator dye.

2.2.2 Arsenazo(III) Complexation with Uranium in Strong Acid and pH 2 Buffer

This experiment repeated the previous procedure with two important changes. The uranium concentration for the standards was an order of magnitude lower and a strong acid series was added, in addition to the pH 2 buffer series. The samples are listed in Table 2.5. A 4 N solution of hydrochloric acid (HCl) was made from concentrated HCL (J.T. Baker, Lot No: N31067), and 50 mL of 1.24 mM Arsenazo(III) was prepared. The uranium standards were made from a uranium acetate solid (Fisher Scientific Company, Lot number or catalog number unavailable). A 0.3395 mM solution of uranium acetate was made first. Uranium acetate or

$\text{UO}_2(\text{CH}_3\text{COO})_2$ breaks down into free uranyl ions (UO_2^{2+}), acetate ions (CH_3COO^-), and various other uranyl and acetate complexes as a function of

Table 2.5 Uranium Concentration in pH 2 Buffer and 4.0 N HCl This table contains a list of samples and description of the method used to prepare them with pH2 buffer for UV/Visible spectroscopy. Two separate series were used to prepare these samples for analysis. Note the changes in analysis solutions prepared in this experiment compared to those in Table 2.3.

<i>Sample</i>	<i>Aliquot Source</i>
1	Deionized water
2	Uranium Standard 1.0 mM
3	Uranium Standard 0.5 mM
4	Uranium Standard 0.1 mM
5	A1 Supernatant
6	A2 Supernatant
7	B1 Supernatant
8	B2 Supernatant
9	B3 Supernatant
<p>Analysis Solution: 2.0 mL of pH2 Buffer or 4.0 N HCl 1.0 mL of source above 1.0 mL of 0.1 mM Arsenazo(III) solution</p>	

pH. The stock solution was then diluted using deionized water to make 0.05 mM, 0.01 mM, and a 0.005 mM solutions.

With the 4.0 N HCl and 1.24 mM Arsenazo(III) stock solutions, the steps described in Section 2.2.1 were repeated with some modifications to the mixture procedure. Data from the previous experiment indicated a very low concentration of uranium in any of the samples. To improve the measurement of the unknown uranium concentration in the samples, only 2.0 instead of 4.0 mL of 4 N HCl or pH2 buffer were added. Changes were also made to the Arsenazo(III) solutions. In this experiment 1.0 mL of 0.1 mM Arsenazo(III) was used as opposed to 0.5 mL of 1.0 mM. Lastly, the source volume was increased from 0.5 to 1.0 mL from the samples and standards.

The reactants were mixed in the 5 mL vials as before, and then

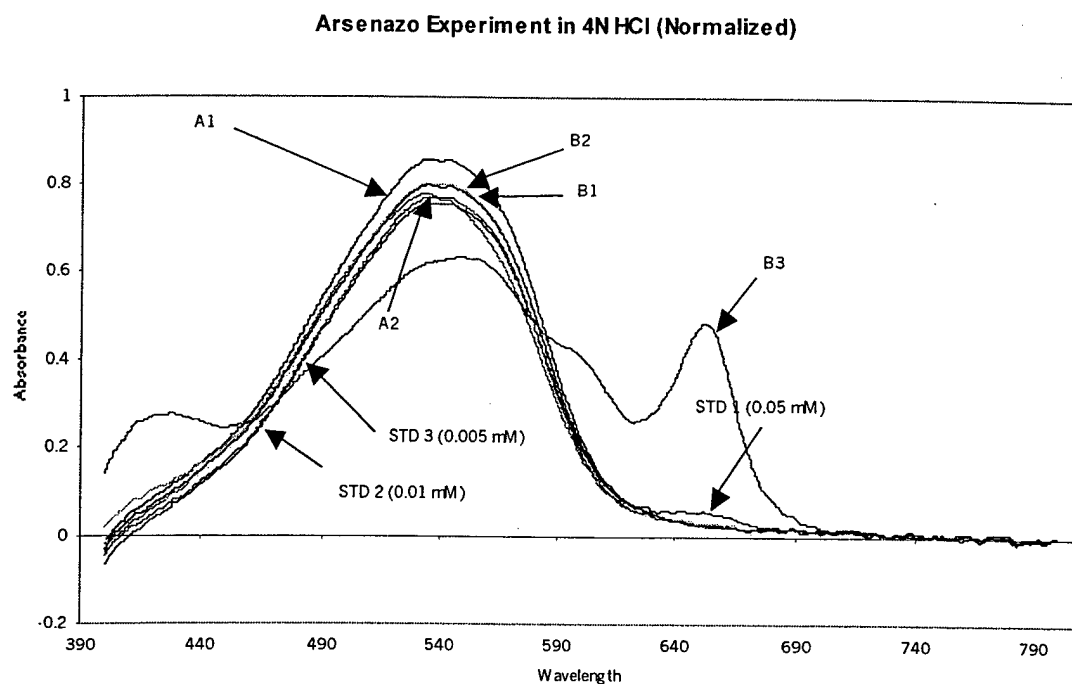


Figure 2.3 4.0 N HCl Spectra obtained for U-Arsenazo(III) Calibration Curve: This figure shows the standard and sample spectra obtained during the determination of a calibration curve for the determination of Uranium by UV/Visible spectroscopy using Arsenazo(III) as an indicator dye in 4.0 N HCl.

Table 2.6 4.0 N HCl Integrated Absorbances and Corrected Integrated Absorbances: This table contains the absorbance, integrated from 625 to 670 nm, for the spectra taken as part of the calibration curve experiment for 4.0 N HCl. The corrected integrated absorbance is determined by subtracting the blank value from the integrated absorbance.

<i>Cuvette</i>	<i>ΣAbsorbance 625-670 nm</i>	<i>Corrected Absorbance</i>	<i>U Conc</i>
BLANK	2.227	0	0 mM (Trace)
STD 1	7.590	5.363	0.05 mM
STD 2	4.724	2.497	0.01 mM
STD 3	4.890	2.663	0.005 mM
A1	4.639	0	
A2	4.429	-0.595	
B1	4.044	-0.595	
B2	4.044	-0.595	
B3	4.044	-0.595	

transferred into cuvettes with a disposable transfer pipette. The UV/Visible

Uranium Calibration Curve with 4.0 N HCl

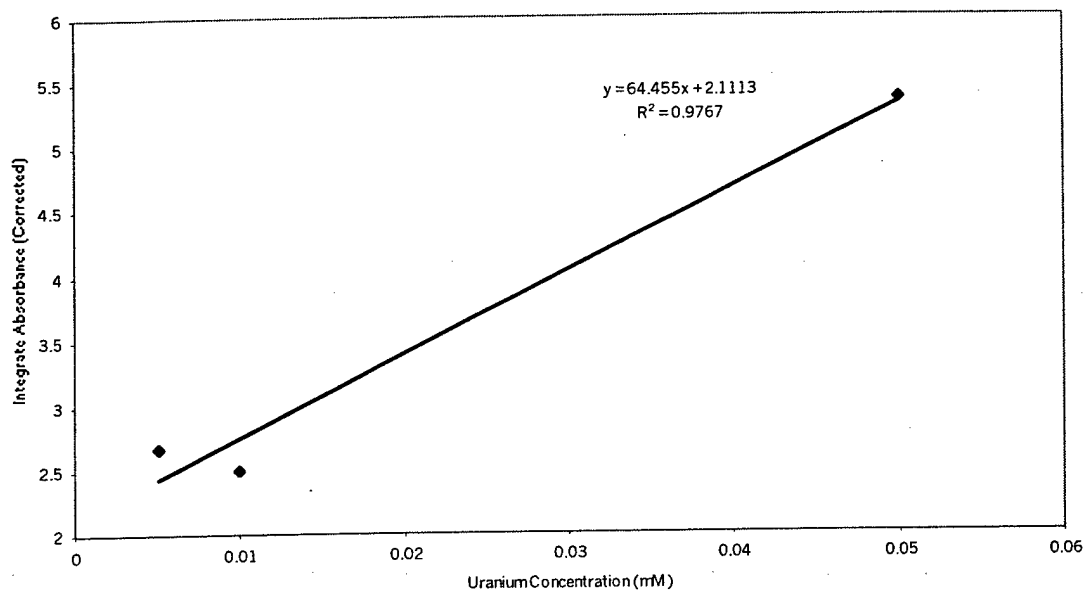


Figure 2.4 4.0 N HCl Uranium Calibration: This figure contains the calibration curve obtained for the determination of Uranium by UV/Vis spectroscopy, generated from the background corrected, integrated absorbance values given in Table 2.6.

Spectrometer analyzed the samples using the same parameters as described in Section 2.1. The cuvettes used for the 4.0 N acid experiment were a slightly different model than those used in the pH 2 buffer experiment. Any differences in the absorbance spectrum are unique to the pH 2 or the HCl experiment respectively. Figure 2.3 shows the complete spectrum of samples and standards with the 4.0 N HCl acid and Figure 2.5 the same information for the pH 2 buffer. The integrate absorbance values are in Table 2.6 for the acid and Table 2.7 for the buffer. The Calibration curve for the 4.0 N acid and pH2 buffer are then plotted in Figure 2.3 and Figure 2.5 respectively.

The final calculated uranium concentrations for samples A1-B3 are also in Tables 2.6 and 2.7.

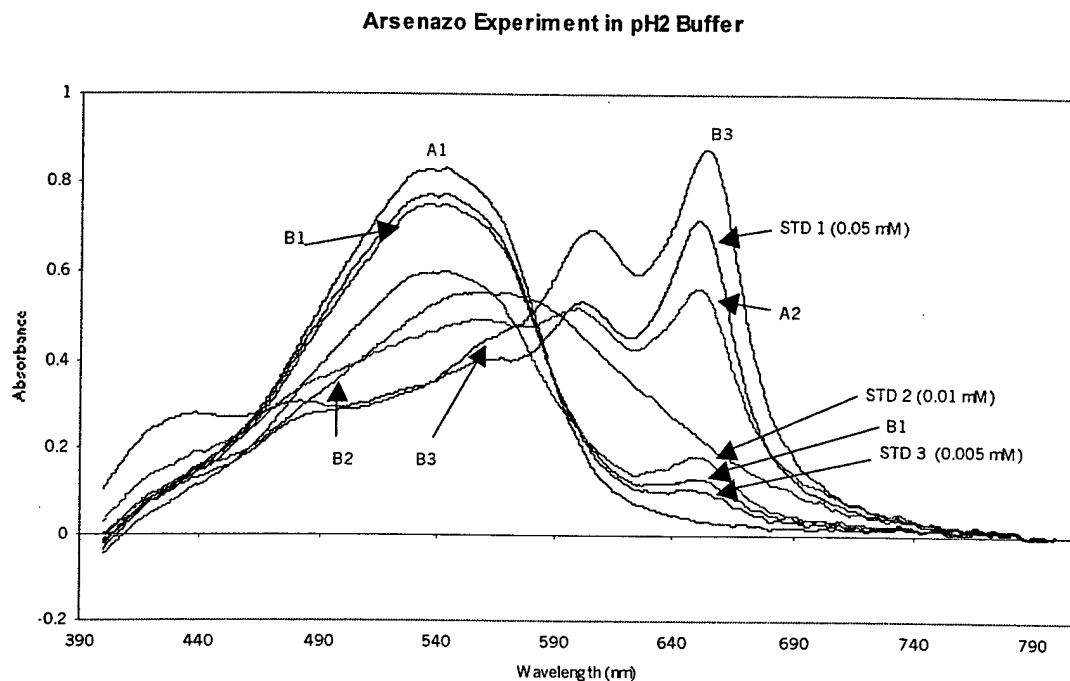


Figure 2.5 pH2 Spectra obtained for U-Arsenazo(III) Calibration Curve: This figure shows the standard and sample spectra obtained during the determination of a calibration curve for the determination of Uranium by UV/Vis spectroscopy using Arsenazo(III) as an indicator dye in pH 2 Buffer.

Table 2.7 pH 2 Buffer Integrated Absorbance and Corrected Integrated Absorbance: This table contains the absorbance, integrated from 625 to 670 nm, for the spectra taken as part of the calibration curve experiment for pH 2 Buffer. The corrected integrated absorbance is determined by subtracting the blank value from the integrated absorbance.

<i>Cuvette</i>	<i>ΣAbsorbance 625-670 nm</i>	<i>Corrected Absorbance</i>	<i>U Conc</i>
BLANK	2.521	0	0 mM (Trace)
STD 1	78.193	75.671	0.05 mM
STD 2	21.283	18.762	0.01 mM
STD 3	13.215	10.693	0.005 mM
A1	5.775	0	
A2	64.865	59.090	
B1	16.080	10.306	
B2	33.572	27.797	
B3	98.747	92.972	

Uranium calibration Curve for pH2 Buffer in Experiment Two

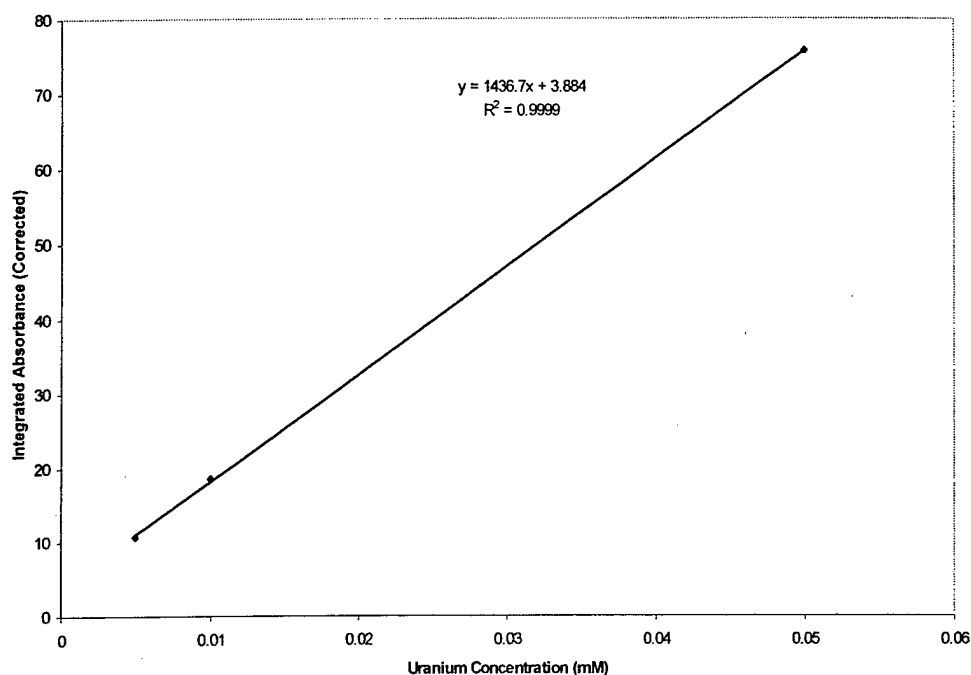


Figure 2.6 pH 2 Buffer Uranium Calibration: This figure contains the calibration curve obtained for the determination of Uranium by UV/Vis spectroscopy, generated from the background corrected, integrated absorbance values given in Table 2.7.

2.2.3 Results and Conclusions using Arsenazo(III) to Determine Uranium Concentration

The absence of any dark black precipitate in the samples with the uranium media and the bacteria, and low uranium concentrations of the medium was initially troubling. Further review of the medium composition indicated that most of the uranium was precipitating out as a phosphate solid, preventing the bacteria from reducing the uranium ions. The sample containing nitrate also superceded uranium reduction by the more favorable reduction of nitrate ions over the uranyl ions. In the sample without nitrate,

the localized black specks in the bacteria indicated areas in which the forward and reverse rate of the dissolution of the uranium phosphate solid at equilibrium was enough to cause small, localized reduction of uranium.

Later reduction experiments were repeated in medium without phosphate. These experiments resulted in the appearance of a dark colored precipitate formed in the bottom of the culture tubes with the bacteria. The uraninite produced from these reactions was used as the source for U(IV) in Section 2.3.3, was evaluated for the mineral structure in Chapter 3, and was analyzed for the isotopic composition discussed further in Chapter 4.

2.3 Photometric Determination of the Reduction Process with Oxazine Dyes

Three oxazine dyes were initially chosen to evaluate their ability to visibly indicate the uranium reduction process. These three oxazine dyes [Gallomine Triethiodide ($C_{30}H_{60}I_3N_3O_3$), Celestine Blue ($C_{17}H_{18}ClN_3O_4$), and Brilliant Cresyl Blue ($C_{17}H_{20}ClN_3O$)] were selected based on a literature search and a description of their color change during oxidation and reduction with a variety of metals including uranium⁷. The complexation behavior of each indicator dye with uranium aqueous ions was measured with UV/Visible Spectrometry to determine wavelength shifts over a variety of pH levels for both U(VI) and U(IV). The behavior of the complexes was evaluated at various pH values using a series of nitric acid and pH buffer solutions. Table 2.9 and 2.12 list the sample and mixture compositions for U(VI) and U(IV) respectively. U(VI) data was collected in an open air environment while U(IV) measurements were gathered in an argon

environment maintained inside a glove box. The source of U(VI) was the same uranyl acetate used to make the media added to the bacteria and standards for the Arsenazo experiments. Uraninite from one of the reduction reactions was dissolved and used as the source for U(IV).

The oxazine dye mixtures were made in solutions of deionized water. Gallomine Triethiodide (GT) and Celestine Blue (CB) were purchased from Aldrich Chemical Company (Lot No: 04410TS and 65-29-2 respectively). Brilliant Cresyl Blue (BCB) was purchased from Sigma

Table 2.8 Dye Stock Solutions: This table lists the mass and volume used to make the stock solutions for the indicator dyes. These will be diluted down to 1mM.

Conc	Molar Mass (g)	Mass used in Solution (g)	Purity of Indicator (%)	Volume of DI Water (mL)	Final Solution (mM)
BCB	317.8	0.2305	62	50.0	8.99
CB	363.8	0.2186	80	50.0	9.61
GT	891.54	0.4228	98	50.0	9.30

Chemical company (Lot No: 027H440). Information on each of the dyes is in Table 2.8.

2.3.1 Oxazine Dye Complexation Behavior with Uranium (VI)

The oxazine dye solutions were prepared first. A stock solution of each dye was prepared in sterile, self-standing 50 mL disposable polypropylene centrifuge tubes (Corning model 430921). The mass and final concentration of the stock solutions are in Table 2.8 above. The stock

solutions were then diluted to a 1.0 mM concentration in separate 50 mL centrifuge tubes.

The next step was to create the defined acidic solutions. The pH 1, 2, 3, 5, and 7 buffer solutions were purchased directly from VWR. 50 mL of each buffer solution were transferred into a 50 mL centrifuge tube. Then 30 mL of the strong acid solutions of 1, 2, 4, and 6 N were made from concentrated nitric acid (J.T. Baker, Lot L07056). The last chemical preparation step was to make the uranium stock solution and further dilute to the 1.0 mM concentration used in the experiment.

The first experiment with the oxazine dyes analyzed the complexation

Table 2.9 U(VI) Samples: This table shows the labeling procedure used to identify the 63 five mL poly sample bottles. The first label showed what acid series was used and the second label specified the exact solution composition.

<i>First Label</i>		<i>Second Label</i>	
A	pH 1 Buffer	1	4 mL acid only
B	pH 2 Buffer	2	3.5 mL acid + BCB(500µl)
C	pH 3 Buffer	3	3 mL acid +BCB(500µl)+ Uranyl
D	pH 5 Buffer		Solution(500µl)
E	pH 7 Buffer	4	3 mL acid +CB(500µl)
F	1 N HNO ₃	5	3 mL acid +CB(500µl)+ Uranyl
G	2 N HNO ₃		Solution(500µl)
H	4 N HNO ₃	6	3 mL acid +GT(500µl)
I	6 N HNO ₃	7	3 mL acid +GT(500µl)+ Uranyl
			Solution(500µl)

BCB- Brilliant Cresyl Blue
 CB- Celestine Blue
 GT- Gallomine Triethiodide

For example: The solution in A3 was 3 mL of pH1 buffer, 0.5 mL of 1mM BCB indicator dye, and 0.5 mL of a uranium acetate solution.

with uranium in the hexavalent oxidation state. To maintain consistency with the uranium medium introduced to the bacteria, a uranium acetate salt

was used. Dissolution of the yellow uranium acetate salt crystals to form a 6.13 mM stock solution in a glass volumetric flask was assisted with a sonic bath mixer (Cole Parmer Model 8850). This solution was diluted with deionized water to make 20.0 mL of a 1.0 mM uranium acetate solution.

Each of the 63 samples to be analyzed by UV/Visible Spectroscopy was mixed in a 5 mL polyethylene vial (VWR Products). The labeling of these sample bottles and the exact composition is in Table 2.11. Qualitative results were recorded immediately after all 63 solutions were made. These observations are in Table 2.10 and digital color photos are in Appendix 2,

Table 2.10 Qualitative Observations of Dye Samples with U(VI): This table gives the qualitative visual color comparison associated with each sample series with uranium (VI) and the indicator dyes. Refer to Table 2.11 for the sample labeling method.

<i>Row</i>	<i>Composition</i>	<i>Observation</i>
1	Blanks	All clear
2	BCB (no Uranium)	I2 is the only one that really differs. All the other samples (A2-H2) appear a dark rich blue color, while I2 loses its color and appears black or brownish
3	BCB (with Uranium)	Same as above except there appears to be more blue in I3 compared to I2
4	CB (no Uranium)	Lots of change as a function of pH in the behavior of this dye A4 and B4 appear purple. C4 transitions to a purple/blue color. D4 is most a rich blue, while E4 becomes a light blue. F4 is mostly purple again, while the solutions with the strong Nitric acid (2,4 and 6N) appear clear with a slight yellow tinge.
5	CB (with Uranium)	Same as above except D5 and E5 have a purple tinge to the blue.
6	GT (no Uranium)	Clear except G6-I6. Slight orange tinge to the solutions.
7	GT (with Uranium)	Clear except H7 and I7 that still have an orange tinge.

Annex C.

The samples were then analyzed using the UV/ Visible Spectrometer using the procedure described in the previous section. The graphs of the absorbance behavior with the different acid solutions are in Appendix 2, Annex D (BCB), E (CB), and F (GT). The first graph of each series shows the behavior of the indicator dye as a function of changing acid solutions without uranium present and the second chart shows the same information with uranium. The rest of the graphs in each annex compare the spectra with and without the uranium present at a specific acid concentration.

2.3.2 UV/Visible Spectroscopy Results with U(VI)

The absorbance behavior of Celestine Blue (CB) is located in Appendix 2, Annex E. Annex E-1 shows the behavior of the dye without any uranium present. The absorbance spectrum changes as the solution conditions become more basic. At highly acidic conditions, the absorbance peak of CB was centered near 540 nm. As the pH increased, the peak shifted and increased to a peak centered near 640 nm. This is especially prevalent at pH 5 and pH 7 in Annex E-1. The absorbance spectrum with uranyl ions present is in Annex E-2. In Annex E-2 the peak shift occurs, but it is not nearly as intense and there is also a slight peak near 490 nm builds as the solution becomes more acidic. In Annexes E-9 through E-11, which show the complexation behavior with the highest concentrations of nitric acid, there is no apparent absorbance with or without U(VI). At 1 N HNO₃, the peak shapes are nearly identical for the samples with and without uranium. There is a slight increase in absorbance when U(VI) is added

shown in Annex E-8. The same type of behavior is observed in Annex E-7 with the pH 1 buffer but the increase is not quite as apparent. The absorbance spectrum for pH 2 buffer solutions in Annex E-6 resemble the absorbance peaks of the pH 1 buffer sample, but in this case, the absorbance was stronger without the hexavalent uranium present. In Annex E-5 for the pH 3 sample, the difference in the magnitude of the absorbance spectrum is much greater without the uranium present and suggests that a CB-U(VI) complex is forming outside the observed UV/Visible range of 400-800 nm.

The absorbance spectrum for the pH 3 and pH 5 solutions changes significantly. It shifts the dye absorbance peak from 540 nm at pH3 to 640 nm at pH 5 when hexavalent uranium is not present. The spectrum observed in Annex E-4 for the pH 5 sample with U(VI) shows two much smaller peaks, one centered at 490 nm and one near 640 nm. The absorbance peaks increase in pH 7 shown in Annex E-3, but are located in the same place as pH 5.

The absorbance behavior for Brilliant Cresyl Blue (BCB) is located in Appendix 2, Annex D. BCB did not have nearly the same amount of changes as observed with CB. The complexation behavior based on the absorbance spectra with and without U(VI) are nearly identically shown in Annexes D-3 through D-8 corresponding to pH 7 through 1 N HNO₃ respectively. The absorbance peaks are centered between 540 and 650 nm. At 2 N HNO₃, the peak is located in the same spot that the pH7 through 1 N HNO₃ charts indicate, however the addition of the uranium lowers the peak considerably without observance of another peak anywhere within the

400-800 nm range. Annex D-9 for the 2 N HNO_3 samples suggests that another complex, this time between U(VI) and BCB, falls into an absorbance range outside 400-800nm, thus reducing the uncomplexed BCB peak absorbance in 540 through 650 nm range. At 4 N HNO_3 , the absorbance spectrum shown in Annex D-10 gently shifts toward higher wavelengths, but still generally maintains the same behavior with and without U(IV). It almost appears at 4.0 N HNO_3 that a second peak develops near the 700nm wavelength. The absorbance peak at 700 nm is slightly higher for the BCB with U(VI) spectra than the BCB without U(VI). At 6 N HNO_3 , the absorbance behavior in Annex D-11 shifts back to the left where the original pH 7-1 N spectrum lied at a drastically reduced intensity.

Gallomine Triethiodide (GT) does not change much at all and its spectra lie very close to the blank sample. The absorbance behavior for GT is located in Appendix 2, Annex F. There is an interesting effect in the high acid concentrations. The absorbance spectrum in Annexes F-10 and F-11 for the 4 and 6 N HNO_3 samples both have the GT with U(VI) absorbance spectra greater than without U(VI), although the shapes are nearly identical. At 2 N HNO_3 , the absorbance spectrum switches places, this time the GT with U(VI) has less absorbance than without U(VI). The difference is only slight and within the error of solution concentrations. The remaining figures in Annex F have almost identical spectra and zero absorbance in the 400-800 nm range.

2.3.3 Oxazine Dyes Complexation Behavior with Uranium (IV)

Although there were no visible signs of uraninite precipitation in the Arsenazo experiments, three identical time-phased experiments succeeded in producing uraninite by bacterial reduction. The timed series were labeled A, B or C and the time that formaldehyde was added stopping the reaction by killing the bacteria. There was no difference in experimental procedure used for A, B, or C. The absence of any phosphate in the uranium medium during these experiments kept the uranium in solution and enabled the bacteria the opportunity to produce the black precipitate. The uraninite

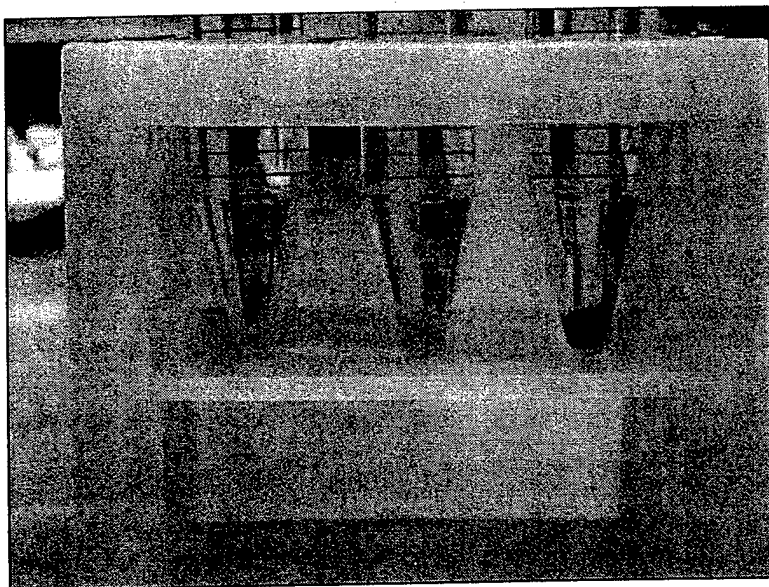


Figure 2.7 Uraninite Production: This is a picture of three of the samples clearly showing the black precipitate produced by bacterial reduction.

produced by the anaerobic respiration of the *Shewanella putrefaciens* bacteria originated from the same uranium acetate salt that was used in the

previous set of indicator dye experiments. The uraninite from these experiments would then be used for three purposes:

- An isotopic analysis with a Thermal Ionization Mass Spectrometer (TIMS). The results of this work is in Chapter 4.
- The primary source of U(IV) for the indicator dye experiments.
- X-Ray diffraction analysis to fully determine the mineral structure of the precipitate. Both U_3O_8 and UO_2 have similar color, but different X Ray diffraction patterns. The results of this work and electron microprobe pictures of the crystals are in chapter 3.

Two samples that had interacted for 45 hours with the bacteria were used as the source of uranium for the next set of experiments. The uraninite produced by bacterial reduction became the source of U(IV) for evaluating the indicator dye behavior. These samples were originally capped in glass culture tubes that maintained a nitrogen and carbon dioxide environment. Previous work in [4] found U(IV) unstable in aerobic aqueous solutions, but stable in de-oxygenized solutions long enough to perform speciation analysis. U(IV) in solution was found to slowly oxidize in air to form UO_2^{2+} (aq). In [4], the oxidation took only ten hours. For this reason special care was made to operate in a non-reactive argon environment. The transfer chamber in a Mbraun Glove Box operating at 2.9 mbar was depressurized to -1.0 mbar three times and flushed with argon gas before placing any material into the main chamber. The glass test tubes were uncapped inside the glove box to prevent any oxidation. The bulk of the supernatant was removed using disposable pipettors and the remaining 9 mL solution , along with the dead

cells and precipitate, was transferred into 15 mL centrifuge tubes. The 15 mL centrifuge tubes were tightly sealed and then removed from the glove box. The samples were centrifuged on a Sigma Model 204 Centrifuge for 30 seconds. The samples were returned into the glove box where, after removing as much supernatant as possible with the disposable pipettor, they were washed with 10 mL of deionized water. The tubes were shaken manually, removed from the glove box, and re-centrifuged for 30 seconds. This washing procedure was then repeated a second time.

After the second rinse, the two centrifuge tubes were returned into the glove box. The supernatant was again removed until only a wet solid remained. A large glass desiccator was placed inside the glove box. The two samples were placed uncapped inside the desiccator, and then the desiccator was sealed by rotating the neck valve. The samples were then removed from the glove box inside the desiccator and began freeze-drying. They remained in the freeze dryer for approximately 14 hours. Both appeared now as a black powder at the bottom of their respective centrifuge tubes. The large desiccator was sealed and returned into the glove box. The desiccator was then opened and the tubes re-capped. One sample remained in the glove box until further analysis in Chapter 3 with X ray diffraction and electron microprobe.

The black uraninite powder from the other sample was dissolved in acid and would be used as the U(IV) source for the indicator dyes. Approximately 2-3 mL of 6 N HNO_3 acid were added to the sample with a clean disposable pipettor. The black powder dissolved almost immediately in

the strong acid. There was still a small amount of undissolved organic matter on the bottom of the centrifuge tube. The supernatant was drawn off placed into another 15 mL centrifuge tube. The total volume of the supernatant was about 2.5 mL. A 1 mL aliquot was removed to determine the total dissolved uranium concentration.

Inductively Coupled Plasma-Atomic Emission Spectroscopy (ICP-AES) was used to determine the total uranium concentration. Chapter 3 describes the method of using ICP-AES to determine concentration in greater detail. A certified standard uranium atomic absorption solution of 990 μg per mL in 1 weight percent HNO_3 (Aldrich Chemical Company, Lot No: 01611HQ) was used to make standard solutions for quantitative determination of the uranium concentration in a solution. The certified standard solution was diluted with 5% by weight HNO_3 to make a 300, 100, 10, and 1 μg per mL solution.

The next step was to prepare the samples. A rough estimate of the total amount of uranium dissolved in the 2.5 mL of 6N nitric acid is in equation 2.9 where 5 mL is the volume of 2 mM uranium acetate media introduced to the bacteria and assumes that 80% of the uranium in solution

$$5 \text{ mL} \times \frac{2 \times 10^{-3} \text{ mol (UO}_2\text{Ac)}}{1000 \text{ mL}} \times \frac{1 \text{ mol U}}{1 \text{ mol (UO}_2\text{Ac)}} \times \frac{238 \times 10^3 \text{ mg}}{1 \text{ mol U}} \times 0.80 \approx 1.9 \text{ mg of U} \quad (2.9)$$

is converted into uraninite by bacterial reduction. This translates into an estimated concentration of 3.2 mM of uranium in the 2.5 mL solution. A 1.0 mL aliquot was removed from this sample for further dilution and preparation.

The 1.0 mL aliquot was first diluted with 10 mL of DI water. This helped increase the volume for analysis with the ICP-AES and diluted the acid strength from 6.0 N to approximately 0.5 N HNO₃, discounting any speciation effects. This dilution adjusted the estimated uranium concentration to 0.29 mM or 69.1 ppm. This was then further diluted with DI water for three separate 5 mL samples. The solutions were then analyzed with the ICP-AES for absolute uranium concentration analysis using the procedure outline in Chapter 3. The resulting data and graphed results are in Appendix 2, Annex G. The linear calibration of the standards is in Figure

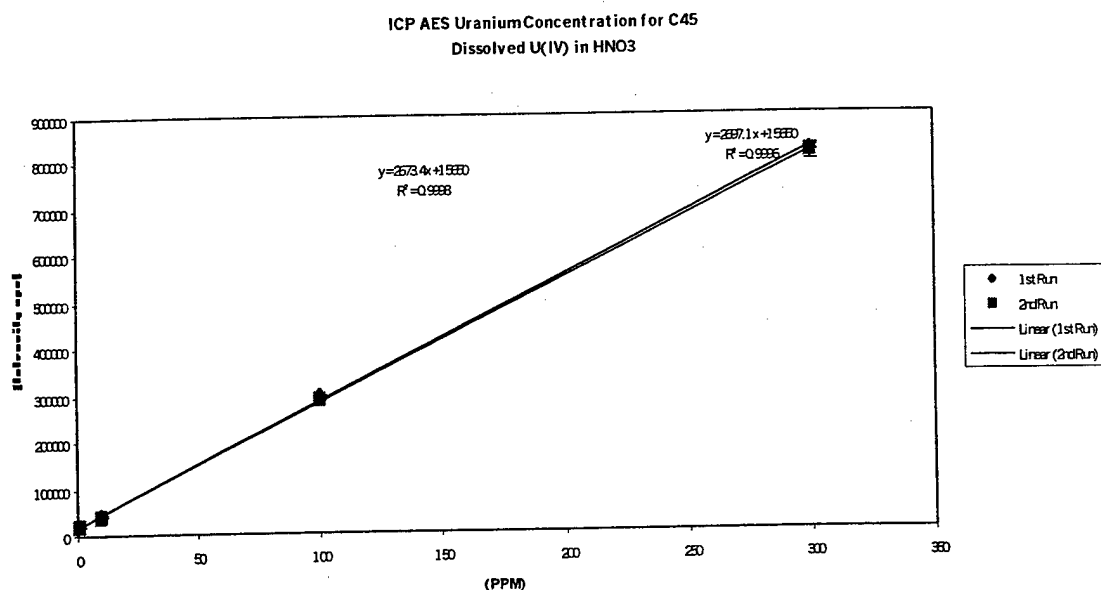


Figure 2.8 ICP AES Concentration of C45: This figure shows the linear regression of the uranium standards used to calculate an unknown sample uranium concentration for C45. The data is located in Appendix 2, Annex G.

2.8. Using the linear equation of line in Figure 2.8, the uranium concentration of each sample is determined. Working backward through the

dilution steps, the concentration of the 1 mL aliquot was 5.73 ± 0.20 mM. This is also the concentration of the remaining 1.5 mL that remained in the 15 mL centrifuge tube and would be used as the source of U(IV).

Table 2.11 U(IV) Solution Preparation: This table shows the labeling procedure used to identify the 63 five mL poly sample bottles. The first label showed what acid series was used and the second label specified the exact solution composition.

<i>First Label</i>		<i>Second Label</i>	
A	pH1 Buffer 1	4 ml acid only	
C	pH3 Buffer 2	3.5 ml acid + BCB(500 μ l)	
E	pH7 Buffer 3	3 ml acid +BCB(500 μ l)+ Uranyl	
F	1.0 N HNO ₃	Solution(500 μ l)	
H	4.0 N HNO ₃ 4	3 ml acid +CB(500 μ l)	
	5	3 ml acid +CB(500 μ l)+ Uranyl Solution(500 μ l)	
	6	3 ml acid +GT(500 μ l)	
	7	3 ml acid +GT(500 μ l)+ Uranyl Solution(500 μ l)	

For example: The solution in A3 was 3 ml of pH1 buffer, 0.5 ml of 1mM BCB indicator dye, and 0.5 ml of a uranium acetate solution.

The remaining 1.5 mL of uranium solution was then used to test the

Table 2.12 Qualitative Observations of Dye Samples with U(IV): This table gives the qualitative visual color comparison associated with each sample series for the uranium IV with the indicator dyes.

<i>Series</i>	<i>Composition</i>	<i>Observation</i>
A	pH1	All appear blue or purple except the GT samples A6 and A7 which both appear faint orange
C	pH3	Same as above
E	pH7	E6-E7 have much less color than A6-A7 and C6-C7.
F	1.0 N HNO ₃	F4 had color while F5 was nearly clear. F6-F7 resemble A6-A7 and C6-C7.
H	4.0 N HNO ₃	H4-H5 are now both clear. F6-F7 resemble A6-A7 and C6-C7.

behavior of the indicator dyes with U(IV). 1.4 mL of the uranium solution was diluted with 0.1 N NaOH down to a 1.0 mM solution for a total volume of 7.89 mL. The dilution with the base helped reduce the effects of the 1.4 mL uranium solution in the strong 6 N acid. Assuming no complexation and discounting specific ion activity correction the dissociation constant for water, this approximately increased the pH from -0.78 (-log 6.0) to +0.01 (-log 0.9825). The limited volume of 1 mM U(IV) prevented the analysis over all the acid ranges that were performed on U(VI). The following pH and acid ranges were chosen: pH 1, pH 3, pH 7, 1 N HNO₃, and 4 N HNO₃. Table 2.11 outlines the preparation of the samples for UV/Visible absorbance analysis.

The protocol for spectrographic analysis remained identical to that used with the U(VI) in terms of concentration and amounts of acids, dyes, and metal solution. This time the spectrometer, along with all the samples, was arranged in the glove box containing the argon environment to prevent oxidation of the metal. The qualitative observations of the solutions are in Table 2.12. The spectra for the indicator dyes is located in Appendix 2, Annex H (BCB), Annex I (CB), and Annex J (GT). The first graph of each annex represents the dye complexation and absorbance behavior without any uranium metal across the entire pH buffer/ HNO₃ acid range. The second graph is similar except the 1.0 mM U(IV) solution is introduced. The remainder of the graphs compare and contrast the shape of the spectra with and without uranium at each pH buffer or nitric acid concentration.

2.3.4 UV/Visible Spectroscopy Results with U(IV)

The CB complexation with U(IV) provided some interesting results. The 4 N HNO₃ samples in Annex I-7 show the strong acid suppressing the absorbance behavior of CB completely with and without U(IV). The spectrum resembles that of the blank sample. In Annex I-6, the samples in 1 N HNO₃ provided probably the most significant result. The spectra without U(IV) shows a strong absorbance peak centered at 540 nm, but when U(IV) is introduced, the 1 N HNO₃ spectrum drastically reduces to that of the blank again. This suggests a strong CB-U(IV) complex forms with an absorbance frequency that is outside the UV/Visible range. The absorbance spectrum shown in Annex I-5 for the samples in the pH 1 buffer is nearly identical between the samples with and without U(IV). In Annex I-4, the pH 3 samples show a small shift in the CB absorbance into the 640 nm area that is suppressed when U(IV) solution is added. This may be the effect of the nitric acid strength in the 500 µl U(IV) solution. Annex I-3 with the pH 7 samples, illustrate another split in the absorbance spectra between CB with and without U(IV). The CB absorbance without tetravalent uranium peak solely in the 630-640 nm wavelength range while the U(IV) solution peak back at the original uncomplexed CB peak centered at 540 nm.

There were less characteristic changes between the other two indicator dyes using U(IV) as opposed to U(VI). The complexation with BCB and U(IV) is nearly indistinguishable between solutions with and without tetravalent uranium. The only separation in the spectra between the two occurs at the 4 N HNO₃ revealed in Annex H-7. At 4 N HNO₃, there is

slightly less absorbance when the U(IV) is introduced. This effect is attributed to the low pH of the U(IV) solution. The GT absorbance spectra are almost indistinguishable between solutions with and without tervalent uranium. The only separation occurs in Annex J-6 with the 1 N HNO₃ samples. There is a U(IV)-GT complex that slightly increases the absorbance spectrum with a peak centered at the lower end of the frequency range near 480 nm.

2.3.5 Comparison of the Absorbance Spectra for the Oxazine Dyes with U(IV) and U(VI)

The absorbance charts for each pH buffer and acid value that were similar to both experiments with U(VI) and U(IV) are located in Appendix 2, Annex K (BCB, Annex L (CB), and M (GT). The first graph in each Annex plots the entire spectrum for all acid and buffer values with uranium at both its oxidation states. The remaining graphs in the Annexes elucidate the first comparison by showing each pH value or acid concentration separately. As each dye is evaluated towards achieving the ultimate goal of

Table 2.13 Visible Wavelengths: This table shows the frequency range for electromagnetic radiation available to the human eye and the color associated to that frequency range.

Visible Wavelengths

400-440nm	Violet
440-480nm	Blue
480-560nm	Green
560-590nm	Yellow
590-630nm	Orange
630-700nm	Red

a reduction indicator capable of a significant visual color change between the

different oxidation states of uranium, the visible color and frequency range is listed in Table 2.13. This reference helps visualize the color changes associated with the location of the absorbance peaks.

Among the three dyes, CB appears to distinguish the best between the complexes formed with U(IV) and those with U(VI). The complete

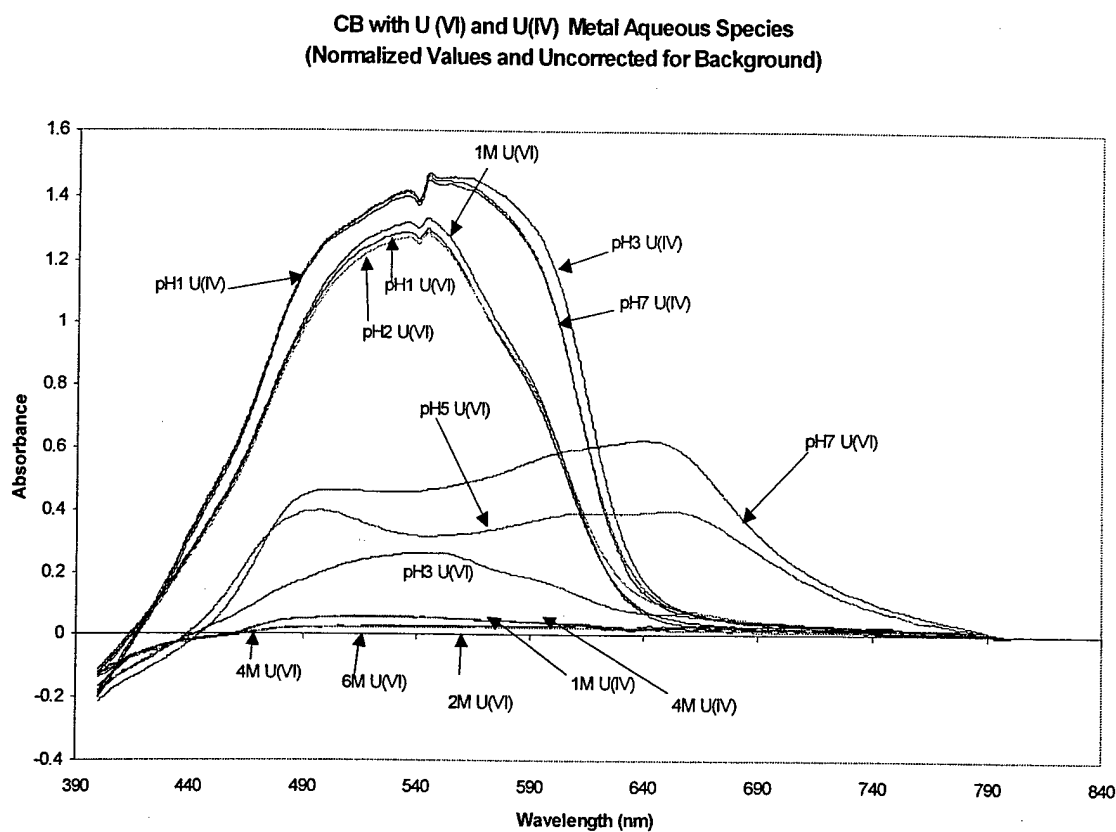


Figure 2.9 Celestine Blue with U(VI) and U(IV): This figure shows the complete absorbance spectrum for Celestine Blue with U(VI) and U(IV) solutions. The spectra for each acid concentration and pH buffer solution is chosen that coincide for both uranium oxidation state solutions. The separate charts at each pH value or acid concentration are in Appendix 2, Annex L.

spectrum is located in Figure 2.9. The spectrum in the buffer solutions of pH7 and pH 3 not only have a different shape to their spectra, but even in

the areas where their peaks are collocated there is a significant absorbance intensity difference. In pH 7, U(IV) clearly dominates the peak at 540 nm range, where as the spectra for U(VI) has two much smaller peaks, one at 500 and the other near 640 nm. At pH 3, the peaks are collocated, but the U(IV) absorbance peak is much higher than U(VI). At pH 1, the behavior is just like pH 7, but the gap is narrowed.

The absorbance spectrum for most pH buffer solutions has been

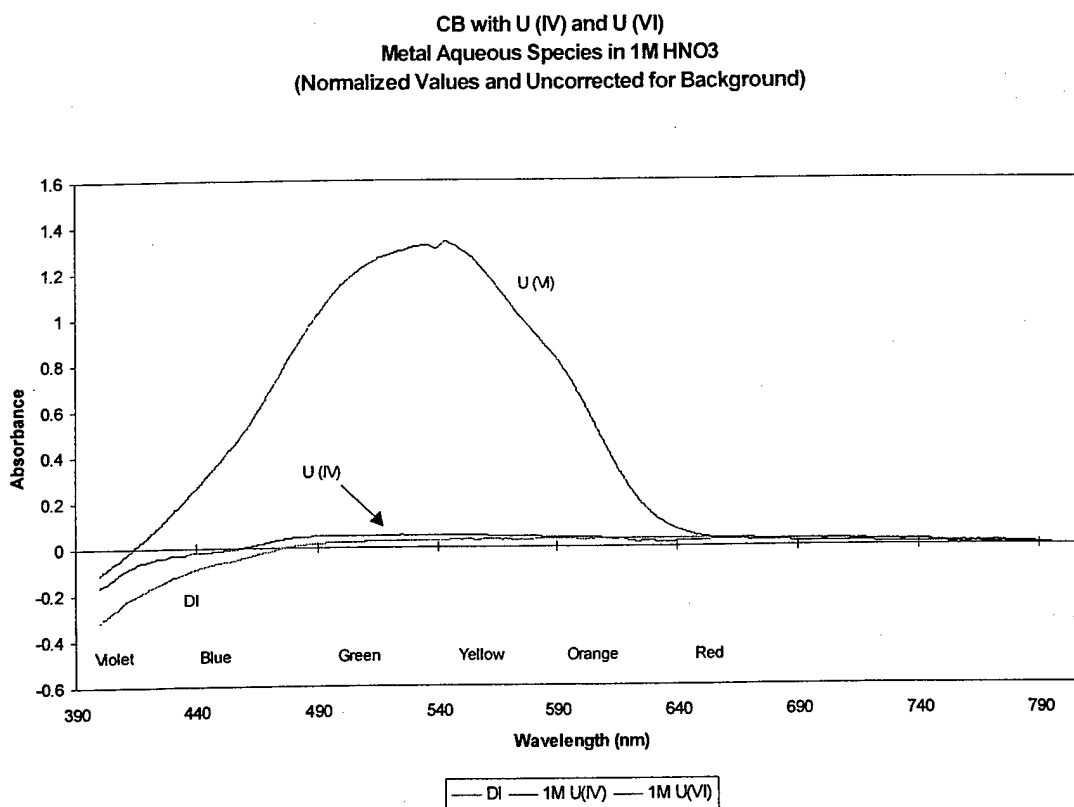


Figure 2.10 Celestine Blue Complexation with U(VI) and U(IV) at 1 N HNO₃: This chart shows the absorbance of CB complexes with U(VI) and U(IV) between 400-800nm. The dramatic reduction in the absorbance spectra for U(IV) as opposed to U(VI) strongly suggests its suitability as a visual reduction indicator.

dominated by the U(IV) absorbance spectra. At 1 N HNO₃, this trend

dramatically reverses. There is a strong absorbance spectrum for the U(VI) complex centered on a peak at about 540 nm. This is sharply contrasted against a nearly non-existent U(IV) absorbance spectrum. This chart is located in Figure 2.10 and represents the best conditions to distinguish the areas of localized reduction of U(VI) to U(IV). The areas where this reduction occurs will change from a purple color to near colorless.

The other two indicator dyes did not show favorable results when it came to producing a significant color change in the absorbance spectra. BCB spectra for U(VI) and U(IV) is nearly identical in terms of peak location and shape, with a slight gap between them that is inconsistent and within the experimental error of the concentration of the reagents. The only slight indication is at 4 N HNO₃ when the U(VI) complex with BCB has a higher absorbance in the last portion of the UV/Visible frequency range. The charts for GT are nearly identical as well and are very nearly equivalent to the blank. The only area where there is a slight deviation is at the upper nitric acid concentration end. The 1 N and 4 N HNO₃ show a slightly higher absorbance spectrum for U(IV) than U(VI), but it is so small that a visual inspection of this would be difficult.

2.4 Conclusions

The purpose of this work was to use the complexation of organic dyes with uranium metal in solution to determine the concentration and the oxidation state of the uranium aqueous species. Arsenazo(III) complexes were used for the concentration measurements and a series of oxazine dyes

were evaluated to determine qualitatively which one gives the most visible color difference between complexes formed with U(VI) and U(IV).

Although U(VI) tends to be much more soluble than U(IV), the first experiment showed the complications that occur when phosphate ions are present. Uranium phosphate is a very insoluble compound that forms when solutions of uranyl cations is mixed with phosphate anions. Therefore it is important to avoid the use of any phosphate in medium designed to study the bacterial reduction processes with uranium.

The oxazine dye experiments analyzed the absorbance intensity in UV/ Visible range of the electromagnetic spectrum between 400-800 nm in a variety of pH buffer and nitric acid solutions. A baseline spectrum without the uranium present was measured first. Then solutions containing U(VI) and U(IV) were added and the changes to the absorbance spectrum were compared to the baseline spectrum of the dyes. Then the two uranium complexation spectrums for U(VI) and U(IV) were compared against one another to determine a difference in absorbance between the complexes

Table 2.14 Oxazine Dye Results: This table shows the areas where differences exist between the complexation behavior of U(VI) and U(IV).

	Gallomine Triethiodide	Brilliant Cresyl Blue	Celestine Blue
pH 7	No	No	Possible
pH 3	No	No	Possible
pH 1	No	No	No
1 N HNO ₃	No	No	Yes
4 N HNO ₃	No	No	No

formed with the uranium metal species. Table 2.14 summarizes the results of the comparisons between the complexation behavior of the two oxidation states.

Celestine Blue seemed to offer the biggest difference in color behavior compared to Gallomine Triethiodide and Brilliant Cresyl Blue. In 1 N nitric acid, there is a large difference in the spectrum that was shown in Figure 2.10. The U(VI) complex has a large absorbance peak where the U(IV) is nearly colorless. Future experiments should test Celestine Blue with different solutions of U(VI) and U(IV) in circular plates with agar and bacterial growth media. The plates should then be photographed and compared to determine if the color difference is sufficient to locally detect the reduction process by bacteria.

There are many areas for future study. The behavior of the U(IV) complexes may be affected by the concentration of the acid used to dissolve the uraninite. Monitoring the pH levels of the U(IV) and U(VI) may help prevent this from disguising the true differences in the complexation behavior between U(VI) and U(IV). [7] also referred to another indicator dye, Galloxyanine, which may provide a good color change, going from pink to colorless at the end point for the reduction of U (VI) to U (IV).

Another possible technique would be a reduction titration in sequence with the UV/Visible Spectrometer. Starting with a solution U(VI) and a particular indicator, slowly titrate Fe(II), which oxidize to Fe(III) and reduce the uranium to U(IV).

	Potential, volts ⁸
$\text{Fe}^{3+} + \text{e}^- \rightarrow \text{Fe}^{2+}$	0.770
$\text{UO}_2^{+2} + 4\text{H}^+ + 2\text{e}^- \rightarrow \text{U}^{+4} + 2\text{H}_2\text{O}$	0.334

The titrator can also then monitor the pH changes and using a mobile dip probe, the spectrometer can simultaneously take periodic measurements of the absorbance intensity. This would probably be the best technique to simulate the color change that would occur with the bacterial reduction process.

¹ Walter J. Moore, Basic Physical Chemistry (London, England: Prentice Hall International, 1983), 53-59.

²Ibid., 604.

³ Spectro Analytical Instruments GMBH. Spectroflame Modula; Spectroflame EOP Operation Manual. Kleve, Germany. (Not Dated)

⁴ De Beer, H. & Coetzee (1992). Ion Chromatographic Separation and Spectrophotometric Determination of U(IV) and U(VI). Radiochimica Acta, 57, 113-117.

⁵Aldrich Catalog Handbook of Fine Chemicals (1998-1999), 127.

⁶Paul E. Owen, "Waste Characteristics of Spent Fuel from a Pebble Bed Reactor," Master's Thesis, Massachusetts Institute of Technology 1999, 83-97.

⁷ K. Vijaya Raju and G. Madhu Gautam, "Iron (II) Titration of some Metal Ions with Oxazine Dye Indicators," Talanta, 35, no. 6, (1988): 490-492.

⁸ Robert C. Weast and George L. Tuve, eds., CRC Handbook of Chemistry and Physics (Cleveland, Ohio: Chemical Rubber Company, 1958), D111-113.

Chapter 3

The Reduction of Uranium by Bacteria

The purpose of this chapter is to study in detail the reduction of dissolved uranium into a solid precipitate using bacteria. Section 3.1 discusses the principles and use of Inductively Coupled Plasma - Atomic Emission Spectroscopy (ICP-AES) for determining the concentration of total uranium in a solution. Section 3.2 presents in depth the chemical preparation of uranium acetate $\text{UO}_2(\text{CH}_3\text{COO})_2$ from solid triuranium octaoxide U_3O_8 . Section 3.3 explains the microbiology work at the Ralph M. Parsons laboratory and the reductive process that converts the uranium in solution into a solid uraninite UO_2 precipitate. Section 3.4 looks at the precipitate in great detail using X-Ray Diffraction (XRD) and the Electron Microprobe (EMP). Section 3.5 concludes with some lessons learned during the procedure. The overall objective of this chapter is to present an overview of the microbiological and chemical processes that were used throughout this investigation.

3.1. Inductively Coupled Plasma - Atomic Emission Spectroscopy (ICP-AES)

Many of the experiments conducted in this work used Inductively Coupled Plasma - Atomic Emission Spectroscopy (ICP-AES) to determine total uranium concentrations in solution. This section provides an overview of the

physical principles behind ICP-AES(3.1.1), describes the machine parameters of the Spectroflame ICP D used in this study(3.1.2), and explains the method used to determine uranium with the ICP-AES (3.1.3).

3.1.1 Principles of ICP-AES

The ICP-AES operates on the general principle of a hot plasma generated by ionizing argon atoms with an igniting device. These ions move back and

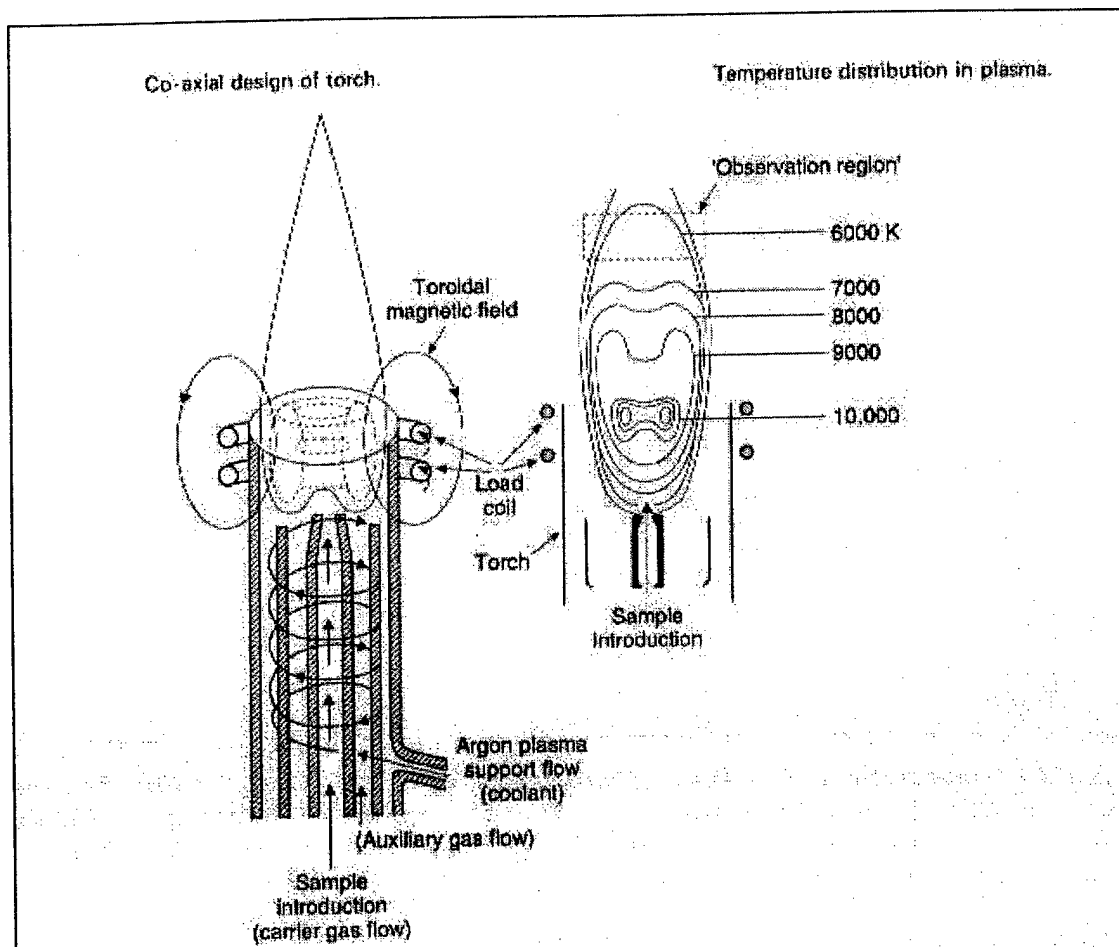
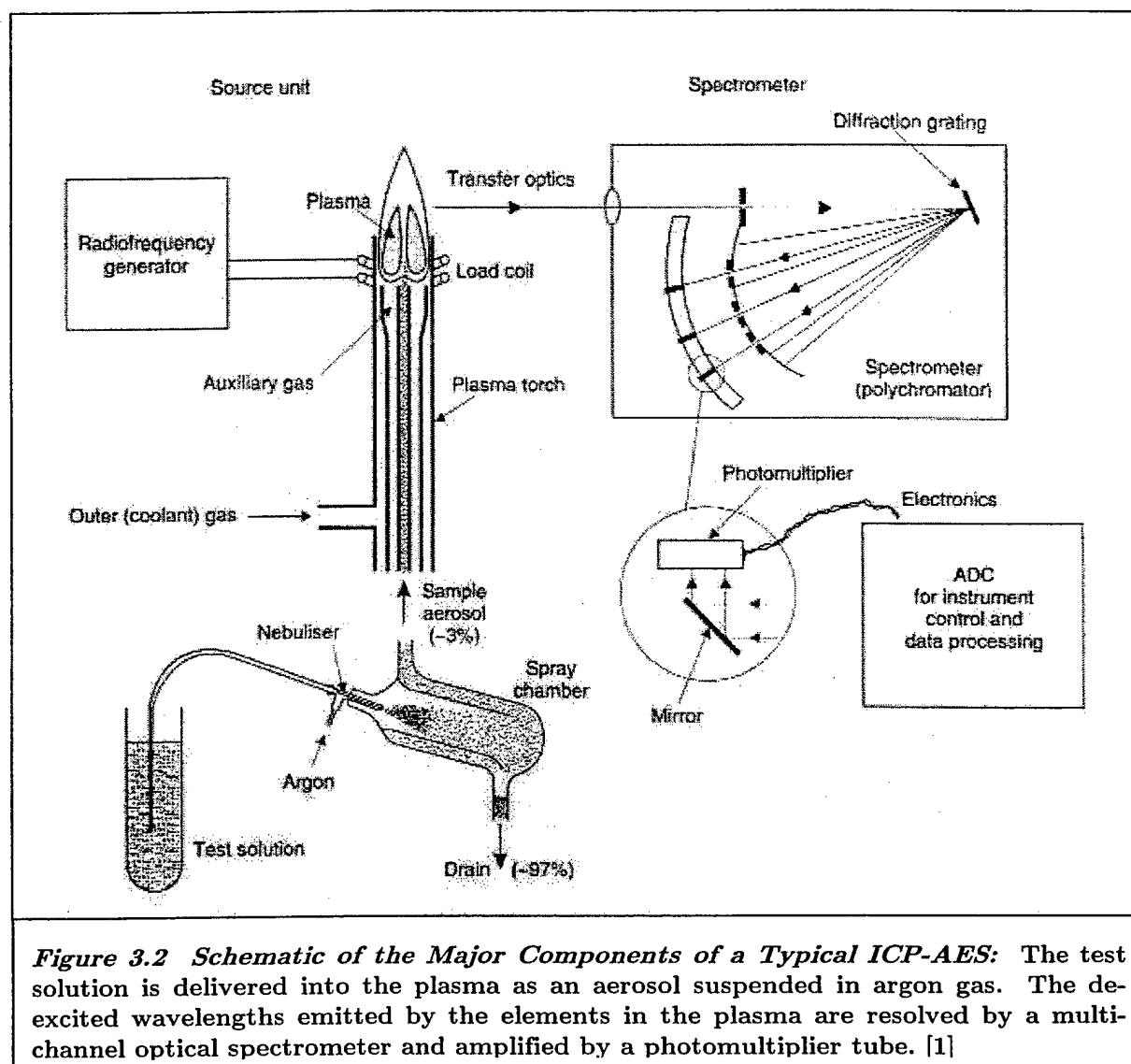


Figure 3.1 Coaxial Design of the ICP Torch: This a diagram of the quartz torch and the oscillation field of the coil. It is important to ensure that the coil does not touch the torch in the pre operating checks (see Appendix 3, Annex B). [1]

forth rapidly in an oscillating electromagnetic field established by a high frequency coil wrapped around a quartz torch. This oscillation causes collisions and a transfer of energy to other argon atoms, which in turn become ionized, generating secondary argon ions and electrons¹.



The number of ions steadily increases until the plasma reaches a steady state. The filtered liquid sample is then introduced using a peristaltic pump into the nebulizer, which injects a fine aerosol mist from the sample solution into the

nebulizer chamber and is then carried upward by argon gas into the plasma. The nebulizer chamber also acts as a filter and removes droplets that are too large to be excited by the plasma. Because of this process only 1% to 3% of the nebulized material is transported to the plasma. An argon humidifier is used during operation to humidify the nebulizing argon and prevent any sample material from crystallizing on the nebulizer or becoming encrusted within the nebulizing chamber. The argon humidifier is filled one third full with deionized water for optimum operating conditions. When sample atoms are introduced into the plasma, they collide with the rapidly moving plasma ions and become excited. The excited sample atoms and ions pass through the plasma, and relax to lower energy states, emitting characteristic photons. A spectrometer measures the intensity of the selected characteristic photon directly related to a

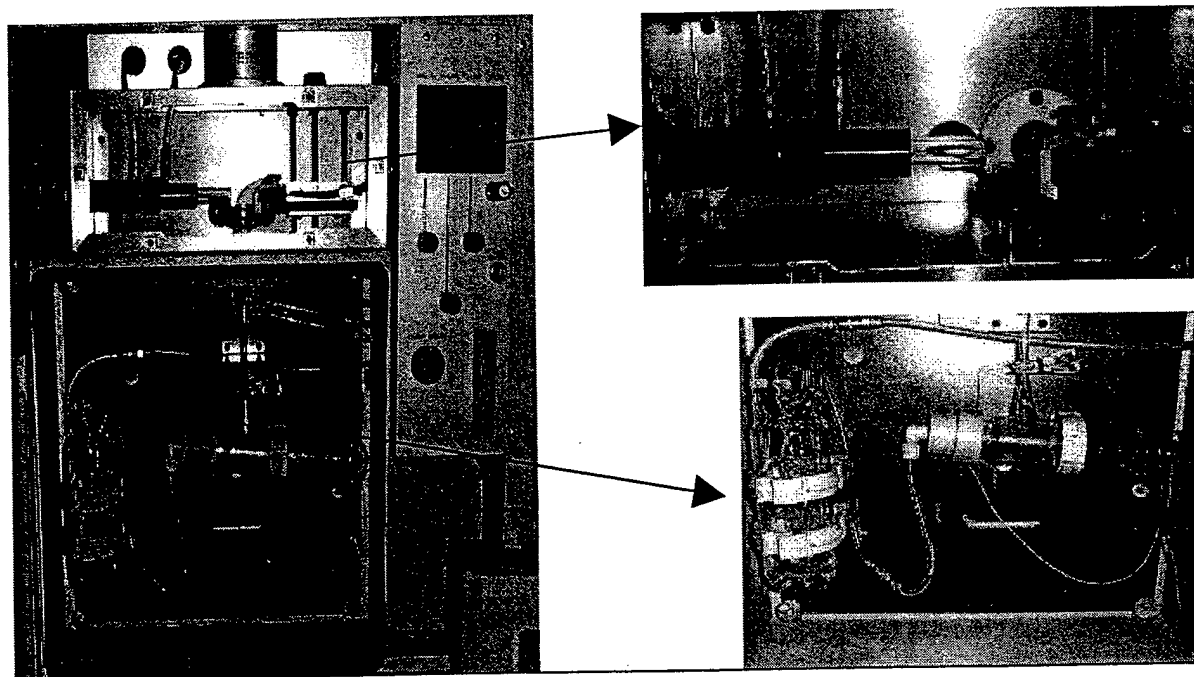


Figure 3.3 *Components of the Spectroflame ICP D ICP-AES:* These are the actual components of the schematic diagram shown in Figure 3.2.

particular element¹. By calibrating the system using known standards, the concentration of a given element can be determined from the intensity observed at the characteristic wavelength(s) for that element. Figure 3.2 shows a schematic of this process.

3.1.2 ICP-AES Hardware Specifications

The ICP-AES system used for this work is the Spectroflame ICP-D model ICP-AES system. Figure 3.3 is a detailed photograph of the ICP-D model components that are sketched in Figure 3.1 and Figure 3.2. The specific machine details of the Spectroflame ICP-D ICP-AES system are presented in Table 3.1. The start up procedures and general software operating procedure are in Appendix 3, Annex B.

Table 3.1 ICP-AES Hardware: This table contains the specifications for the hardware in the Spectroflame ICP-D model ICP-AES system. The specifications were obtained from the equipment documentation, and have not been effected by the upgrade to the operating system.

Spectrometer

- Direct Wavelength drive - No peak search
- Fixed grating
- Pashen-Runge mount
- Focal length 750 mm
- Holographic grating on Zerodur blank
- Temperature stabilized construction
- Four entrance slits

Monochromator #1

- Grating 2400 l/mm
- Dispersion 0.55 nm/mm
- Wavelength coverage: 190 - 460 nm
- w/ nitrogen purge: 165 - 460 nm
- Flushed direct optical path for low wavelength

Monochromator #2

- Grating 1200 l/mm
- Dispersion 1.1 nm/mm
- Wavelength coverage: 240 - 790 nm

Sample Introduction

- Integral peristaltic pump
- Pneumatic nebulizer w/ conical spray chamber
- Fixed torch
- Argon humidifier
- Temperature controlled sample presentation compartment

RF Generator

- 2.5 kW max. output power
- 27.12 MHz operating frequency
- Power and frequency stabilized
- Microprocessor controlled
- Auto-start
- Integrated water cooling system

3.1.3 Determination of Uranium by ICP-AES

Uranium concentration was measured by ICP-AES using the method URANIUM, written for these experiments (Table 3.2). Uranium concentration is determined by measuring the intensity of the 385.958 nm wavelength photons². The output from the ICP-AES gave the raw intensity, average, and standard deviation of three consecutive measurements.

Table 3.2 ICP Settings for URANIUM Method: This table contains the equipment settings contained in the method URANIUM, which was created for the determination of Uranium by ICP-AES using the 385.958 nm line.

Coolant Temperature:	15°C
Argon Pressure:	100 psig
Coolant Flow Setting:	40
Nebulizer Pressure:	3.3 bar
Pre-Flush Time:	30 s
High Flush Time:	10 s
Pump Speed Setting:	2 (high flush) 1(preflush/measurement)
Measurement Time:	100 % (100% = 2 seconds)
Number of Measurements:	3 per

The standard and sample mixtures were all diluted to their desired concentration using a 0.1 N HNO₃ solution, except where noted. The acid matrix was chosen in order to minimize the potential for sorption of the uranium to the containers and piping network of the ICP. Nitric acid was the acid chosen to remain consistent with the other acid chemistry in the experiments. The dilutions were performed using variable volume pipettors (Gilson Pipetman series) and volumetric flasks (Kimax and/or Pyrex brands; VWR Scientific).

After the system optics were reprofiled for the 385.958 nm wavelength, blank samples of deionized water and the 0.1 N HNO₃ solution, which were used for the dilutions, were measured to get the background intensity. The spectral intensities reported by the ICP-AES are given in units of counts per second (cps). The uranium standards were then analyzed in order of increasing concentration to minimize any potential hold-up effects in the system. The standards, with a known concentration of uranium, yielded a corresponding photon peak intensity. The average spectral intensity values for each known uranium concentration were graphed and a linear regression analysis was performed calibrating those values into a linear equation as a function of their concentration. The results of this calibration for each experiment are shown in the next section.

3.2 Producing Enriched Uranium Acetate

There are many techniques to make a solution of uranium acetate. In Chapter 2, the uranium acetate came directly from an older source by Fisher Chemical Company. The uranium acetate for the dye experiments and the first two bacterial experiments was made simply by dissolving the salt in deionized water to the concentration necessary to establish a media concentration of 2mM.

The isotopic ratio from the supernatant of sample AO (see Chapter 2, Section 2.3 for label definitions) was later analyzed with a Thermal Ionization Mass Spectrometer (See Chapter 4, Section 4.5). The results from sample AO determined that the uranium acetate had originally been a depleted uranium

source with a $^{238}\text{U}/^{235}\text{U}$ isotopic ratio of 307. Uranium occurs in nature with a ratio of approximately 142^3 . The instrumental error associated with the measured ratio of 307 was much too high for the precision needed to investigate any biological isotopic fractionation that is performed in Chapter 4. The swamping effect of the depleted uranium acetate source prompted the use of an enriched uranium source that would give a clearer isotopic signature.

The enriched uranium sample came from the New Brunswick Laboratory in Argonne, Illinois operated by the United States Department of Energy. The certified reference uranium standard U500 was selected giving a nearly one to one ratio of ^{235}U to ^{238}U . Two grams of U500 were purchased in the form of U_3O_8 (cr). The U_3O_8 came as a black granular powder and the specific isotope atomic and weight percents are in Appendix 3, Annex A. This black powder was then converted chemically into a uranium acetate salt suitable for the bacteria.

A non-enriched U_3O_8 sample was first used to benchmark the chemical procedure. In general terms, the solid was dissolved and oxidized in strong nitric acid to form the uranyl ion UO_2^{2+} (aq) and associated metal-ligand complexes with the nitrate (See Sections 1.2 and 1.3 in Chapter 1). Then a strong base was added to cause $\text{UO}_2(\text{OH})_2$ (s) to precipitate. The supernatant was removed and the solid rinsed with deionized water or more base to remove any remaining nitrate from the solution. After the last rinse, the uranium hydroxide was dissolved in pure acetic acid. This solution was then dried down on a hot plate in the hood to form the uranium acetate salt. The salt was then

re-dissolved in deionized water to an appropriate concentration and measured by ICP-AES.

3.2.1 Benchmarking the Chemical Procedure for U_3O_8

The first step in the experiment was to make the reagents. A 6.0 N potassium hydroxide (KOH) solution was made by dissolving 95.842g of KOH(s) (Mallinckrodt, Lot No: 6984KJXJ, 87.8% pure) in 250 mL of deionized water. The solution was mixed in a glass volumetric flask aided with the sonic bath mixer.

The next step involved the dissolution of the non-enriched U_3O_8 solid. An empty sterile 50 mL Corning polypropylene self-standing centrifuge tube was weighed on a Sartorius Model ISO9001 scale. A small amount of U_3O_8 was added using a clean Teflon spatula into the centrifuge tube. The centrifuge tube was re-weighed and subtracting the blank centrifuge tube mass, the total mass of U_3O_8 was 0.2297 grams giving 0.2728 millimoles of U_3O_8 and 0.8184 millimoles of uranium (three moles of uranium per mole of U_3O_8). Then 10 ml of a 6.0 N HNO_3 acid solution made from a concentrated nitric acid solution (JT Baker, Lot No: L07056) was added into the centrifuge tube.

According to the [F CRC], U_3O_8 is soluble in nitric and sulfuric acids. Initially there seemed to be no reaction of the black powder with the acid solution. A similar experiment on the dissolution rates of U_3O_8 in [4] showed the kinetic rate constants in 6.0 N HNO_3 at 60°C to be $3.88 \times 10^{-7} \text{ mol} \cdot \text{cm}^{-2} \cdot \text{min}^{-1}$ with decreasing rates at lower temperatures. In [5] another experiment on the

dissolution rates was performed investigating the effect of temperature, acid concentration, and agitation. In dissolving 0.8 grams of U_3O_8 with 400 ml of 6.0 N nitric acid at 30°C with a constant agitation of 500 rpm, the dissolution rate started slowly for the first 60 minutes and then steeply increased from 60 until 85 minutes and then continued to increase at a slower rate until the solid was fully dissolved at 180 minutes. Because there was no agitation in the centrifuge tube and the temperature was near 20°C, the dissolution for the U_3O_8 for this experiment took considerably longer. By the next day though, the entire black U_3O_8 had dissolved in the 6.0 N nitric acid and the solution changed from colorless to yellow.

The next step was to add the strong base. A 10 mL solution of 6.0 N KOH was added slowly into the centrifuge tube that was nestled in a cool water bath. After all the KOH had been added, an orangish cloudy precipitate formed. The centrifuge tube was placed in a Sigma 204 centrifuge for five minutes. The pH of the solution was assessed with ColorpHast Indicator Strips 7.5-14 by EM-Reagents (Lot No: 80311068) and was in excess of 14. The supernatant was poured off into a 150 mL nalgene waste container. The volume of the amorphous uranium hydroxide solid at the bottom of the centrifuge tube was about 5 mL. Deionized water was added to the 25 mL line to wash the solid. The solution was centrifuged for five minutes and the rinse solution placed into the waste container. This rinse procedure was repeated two more times. The total rinse solution in the nalgene was now 66 mL. A final rinse was performed with 35 mL and centrifuged for nearly two hours. This final rinse was added into the 66 mL making a total rinse volume of 101 mL.

The next step was to dissolve the remaining solid in the centrifuge tube with acetic acid. Concentrated Glacial Acetic Acid (Mallinckrodt, 17.34M, Lot No: 3121.0N25A12) was used in this experiment. Forty mL of acetic acid were added into the centrifuge tube and placed in the ultra sonic bath to increase the dissolution rate. The total dissolution took approximately 10 minutes. The yellow colored solution was poured from the centrifuge tube into a 150 mL Pyrex glass beaker and placed on a VWR Model 370 hot plate at a low setting of two. The beaker remained under a hood and dried down overnight.

In the morning, a visual inspection of the glass beaker showed small, clear yellow clear crystals. Approximately 112 mL of deionized water were added into the glass beaker to dissolve the crystals. The crystals were tightly sorbed onto the glass and were difficult to dissolve. Once most of the crystals were brought into solution by scraping the bottom of the glass beaker with a Teflon spatula, the uranium waste and acetate solutions were ready for concentration analysis by ICP-AES. The method for using the ICP-AES is discussed in Section 3.1 of this chapter.

The samples and standards for the ICP- AES were run next. The uranium acetate solution appeared to be over saturated because a yellow precipitate had formed on the bottom of the beaker. A wide range of standards was chosen to determine the detection limit of the ICP-AES for uranium with the URANIUM method and provide a linear equation for concentration determination of the unknown samples. The linear diagram is in Figure 3.4.

The U in Table 3.3 represents the label used for the uranium acetate solution and the W represents the rinse or waste solution.

Table 3.3 ICP-AES Data for Non-Enriched U_3O_8 conversion to Uranium Acetate: This table shows the raw data from the ICP-AES used to determine the detection limit and concentration of an unknown sample.

Sample	Concentration (M)	Spectral Intensity (Mean Value of 3 Measurements)	Standard Deviation	
water	unk (~0)	16491	22.65	
water	unk (~0)	16376	132	
so (0.1M HNO3)	unk (~0)	15916	304	
s7	1.00E-07	16183	112	
s6	1.00E-06	17041	125.5	
s5	1.00E-05	25149	147	
s4	1.00E-04	97020	540	
s3	1.00E-03	815448	6929	
U3	3.00313E-05	40867	333.5	
U2	3.22131E-04	274547	1004	
W3	1.69625E-06	18199	187.6	
W2	1.83563E-05	31527	369.4	
		0.1 M HNO3 (μ l)	Original Solution (μ l)	Calculated Original Concentration
U3	1:100	9909	90.9	3.30E-03
U2	1:10	9090.9	909	3.54E-03
W3	1:100	9909	90.9	1.87E-04
W2	1:10	9090.9	909	2.02E-04

The rough calculations of the expected concentrations and the comparison to the actual values determined by ICP-AES are in Table 3.4. The strong sorption to the glass and over saturation of the solution noted above in the observation of the fine yellow dust of the bottom of the beaker accounted for the uranium that is not in either the rinse or the uranium acetate solution. The pH of the uranium acetate, measured with ColorpHast indicator strips pH 0-6 (Lot

ICP AES Non Enriched Uranium Acetate Samples
8 November 1999

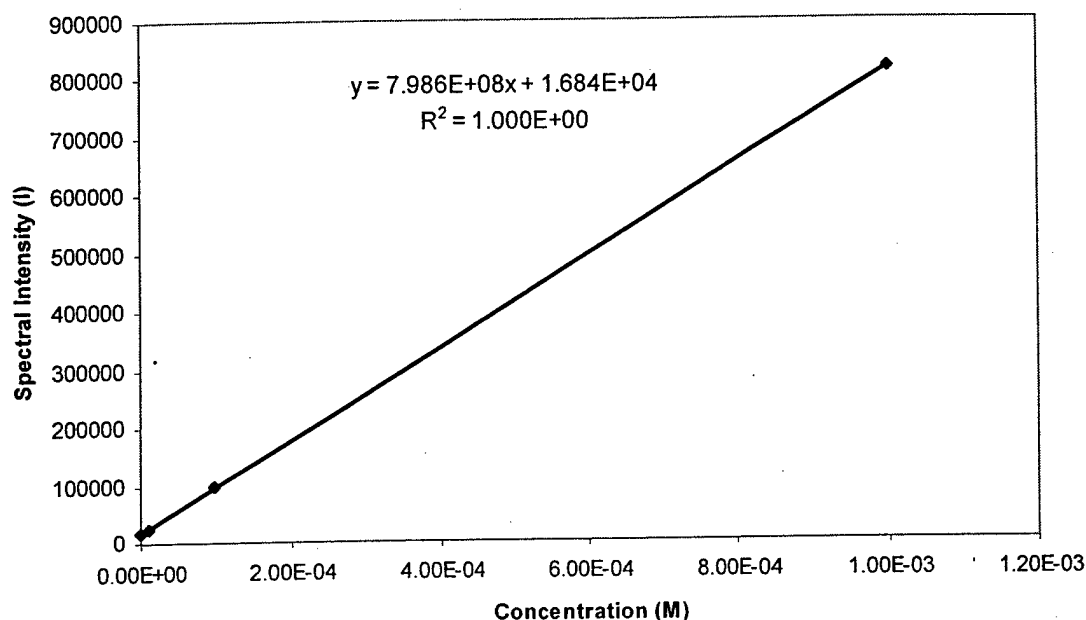
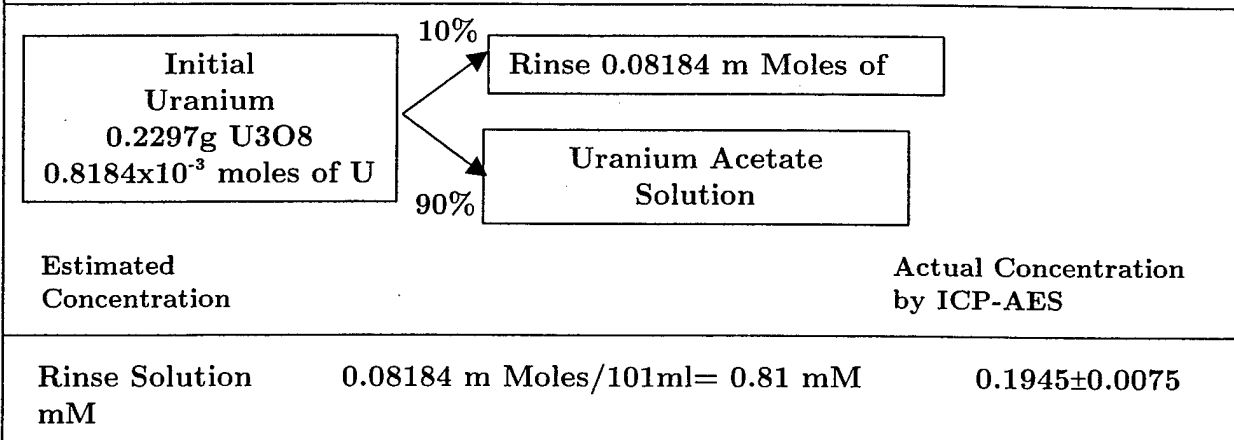


Figure 3.4 Calibration curve and Concentration Determination for Non-Enriched Uranium Acetate Solution: The photon intensities of 385.958nm for the standard non-enriched uranium solutions with a known concentration are graphed and linearly regressed. This regression gives an equation for intensities as a function of concentration to determine the total uranium concentration in an unknown sample

No: 80332224), was pH5. The loss associated with this initial run would attempt to be avoided in the next experiment using the enriched uranium sample.

Table 3.4 Estimated Concentration of the Non-Enriched Uranium Acetate Solution:
This diagram expresses the expected and actual uranium concentrations in the uranium acetate and waste solutions.



3.2.2 Production of Enriched Uranium Acetate

The U500 enriched uranium sample was taken over to the clean lab located on the. A mass of 0.5457 grams was measured into a 60 mL Teflon beaker. Static electricity spread some of the black powder around the beaker. Then 20 mL of 7.0 N ultra clean HNO_3 acid, measured with a glass graduated cylinder, were added to the beaker and rolled gently to get all the U_3O_8 off the sides. The temperature in the clean room was slightly lower than the outside temperature and held constant at 17°C. Using the atomic percentages in Appendix 3, Annex A (U500 molar mass of U_3O_8 is 837.64 grams/mol), this amounts to 6.52×10^{-3} moles of U_3O_8 and 1.955×10^{-3} moles of uranium. In the 20 mL of nitric acid, this amounted to a concentration of 9.78×10^{-2} M. A small aliquot of 1.1687 grams of the solution was removed that would be used later as the internal standard for the empirical behavior of U500 in the TIMS machine. Using a rough assumption that 1.2 grams of solution is equal to 1 mL ([6] for the

density of 7.0 N HNO_3), this amounts to 9.52×10^{-5} moles removed, leaving a total of 1.86×10^{-3} moles of uranium left in the teflon beaker.

The uranium solution was divided into two 50 mL sterile polypropylene centrifuge tubes (approximately ten mL in each tube). Prior to adding the strong base, the tubes were placed in a cool water bath to absorb the heat. Then 10 mL of 6.0 N KOH were slowly added to each centrifuge tube. The orangish precipitate formed almost immediately. The exothermic reaction was allowed to cool in the bath for twenty minutes until cool to the touch. The tubes were then placed into an International Clinical Company (No: W7926) centrifuge and spun for twenty minutes at approximately 1600 revolutions per minute (rpm).

The supernatant was removed by pouring the solution into a 250 mL nalgene container. Then 25 mL of deionized water was added to each tube to wash the solid. The tubes were shaken manually to suspend the solids and wash away any remaining ions. The tubes were again centrifuged and the supernatant poured off into the nalgene. The next rinse used 36.5 mL of deionized water into each culture tube. The procedure was repeated once more. The total rinse solution in the nalgene container was now 196 mL.

The remaining solid was dissolved by adding 40 mL of the glacial acetic acid into each centrifuge tube. The solutions were placed into the sonic mixer to increase the mixing rate. The yellow solutions were then placed into a 150 mL Pyrex glass beaker and placed on the hot plate to dry down in the hood overnight. The sides were rinsed with acetic acid to see if any yellow residue

appeared to help reduce the loss. When the solution had dried completely, 60 mL of deionized water were added into beaker to dissolve the salts this time with a 5 mm magnetic stirrer bar. After mixing for 45 minutes on a VWR Scientific Products Hot Plate/ Magnetic Stirrer model 370 at a speed setting such that a small vortex formed, all the uranium acetate crystals had dissolved.

Table 3.5 ICP-AES Data for Enriched U_3O_8 conversion to Uranium Acetate: This table shows the raw data from the ICP-AES used to determine the detection limit and concentration of an unknown sample.

Sample	Concentration (M)	Spectral Intensity (Mean Value of 3 Measurements)	Standard Deviation	
water	unk (~0)	14202	66.30	
water	unk (~0)	13893	65.50	
water	unk (~0)	13921	26.09	
so (.1M HNO3)	unk (~0)	13749	43.33	
so (.1M HNO3)	unk (~0)	13823	126.80	
s7	1.00E-07	13920	55.70	
s6	1.00E-06	14373	116.20	
s5	1.00E-05	19473	196.50	
s4	1.00E-04	60265	623.00	
s4	1.00E-04	60124	933.00	
s3	1.00E-03	476152	2192.00	
rinse no dilution	2.691E-05	26631	298.80	
water	unk (~0)	14361	238.00	
rinse 1:1 dilution	1.698E-05	22044	154.00	
rinse 1:4 dilution	7.358E-06	17600	78.9	
uranium 1:40	3.458E-04	173933	2424.00	
uranium 1:80	1.763E-04	95628	678	
		0.1 N HNO3 (ml)	Original Solution (ml)	Calculated Original Concentration
rinse no dilution	0	0	10	2.69E-05
rinse 1:1 dilution	1:1	5	5	3.40E-05
rinse 1:4 dilution	1:4	8	2	3.68E-05
Uranium 1:40	1:40	9.75	0.25	1.38E-02
Uranium 1:80	1:80	9.875	0.125	1.41E-02

This solution was then poured into a 100 mL volumetric flask. The sides of the beaker were rinsed with deionized water and also poured into the flask. Then a

final volume was added to the flask to bring it to the 100 mL line. The 100 mL solution was then poured into a clean Savillex Mpls Teflon 180 mL beaker. The solution and the rinse solution were analyzed by the ICP- AES for total uranium concentration. The raw data for the spectral intensities is in Table 3.5. The calibration curve and the linear equation are in Figure 3.5.

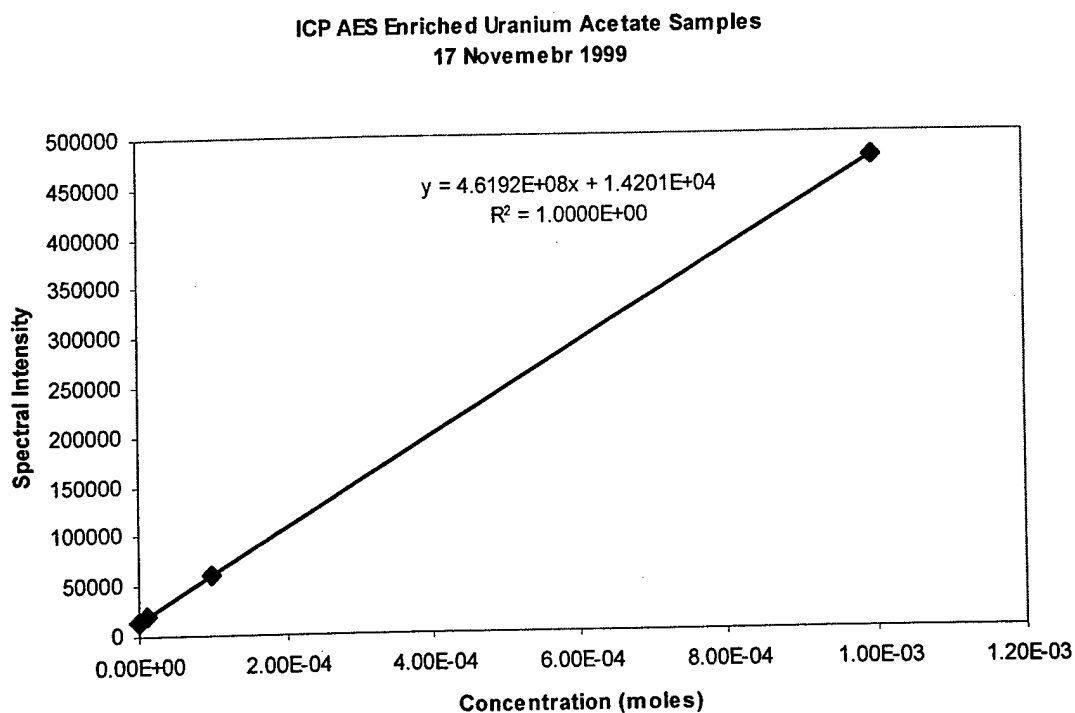


Figure 3.5 Calibration curve and Concentration Determination for the Enriched Uranium Acetate Solution: The photon intensities of 385.958nm for the standard enriched uranium solutions with a known concentration are graphed and linearly regressed. This regression gives an equation for intensities as a function of concentration to determine the total uranium concentration in an unknown sample.

The average concentration of the rinse solution was $3.26 \pm 0.51 \times 10^{-6}$ M and the uranium acetate solution was $1.40 \pm 0.02 \times 10^{-2}$ M. The undiluted rinse sample

was a bright orange and the basic properties of the original rinse solution may or may not have affected this intensity. Normally the solutions are filtered and diluted in acid prior to the analysis by the ICP-AES, but in the case of the rinse, the concentration was very close to the detection limit so an attempt was made to evaluate the spectral intensity untreated. Because the calculated concentration of the rinse with no dilution was two standard deviations from the mean of the other two, this measurement was not included into the average for the rinse concentration. This also meant that of the original 1.860×10^{-3} moles of uranium, 4.565×10^{-4} moles was lost again to sorption to the glassware during the mixing steps or that the solution had started to come out of solution as a result of the pH. This time the pH was measured around 4.75 using the pH indicator strips. This equaled a net recovery of 75.11% of the original uranium that was dissolved in the nitric acid. This solution was used for the next bacterial reduction experiment. A small amount of yellow precipitate had settled on the bottom of the teflon beaker once again indicating the probable over saturation of the solution.

The enriched uranium solution was poured into a glass bottle and the fine yellow solids on the bottom were treated with a small amount of 1.0 N hydrochloric acid (HCl) to dissolve the precipitate. This was then consolidated into a clean glass bottle. The small volume of acid did not change the concentration of the solution a significant amount. A small amount of this solution was used to make the uranium media for the bacteria in a process that will be described in greater detail in the next section. Two series of culture tubes were made, one a control series and the other an interaction series. Each

series added formaldehyde to stop any reaction at time 0, 4, and 8 hours. Additionally two culture tubes were allowed to interact indefinitely without any formaldehyde added. None of the bacteria samples reduced the uranium as they had before. There was no sign of any black precipitate in any of the culture tubes after over two weeks.

The continued presence of nitrate ions would have prevented the reduction of the uranium ions in solution. The bacteria would continue reducing the nitrate as opposed to the uranium ions for its anaerobic respiration. A rough estimate of the nitrate concentration was made with the assumption that 2 mL of 6.0 N HNO_3 remained in the centrifuge tubes after the supernatants were removed. After the first rinse with 73 mL of deionized water, the concentration should have been about 0.162 M of nitrate. After the second rinse again with 73 mL, the concentration would have been 4.38 mM in the 2 mL of solid and solution mixture at the bottom of the centrifuge tube. This was later diluted with the acetic acid, dried down, and then later brought back into the 112 mL of deionized water. So there appeared that there was a possibility that enough nitrate existed requiring the more thorough washing of the hydroxide solid. The uranium hydroxide would be re-precipitated from the uranium acetate solution that had been used to make the uranium media, however this time the solids would be washed for five to six times to ensure all the nitrate ions were removed.

The glass bottle and ten glass culture tubes containing the controls and samples with the enriched uranium acetate solution were returned to the

laboratory. The pH of the uranium acetate solution was assessed with the pH indicator strips to be pH 4, slightly lower than its original reading because of the 1.0 N HCl acid added that was described earlier. The uranium acetate solution in the glass bottle was dried down to a volume of 80 mL and then poured into three 50 mL centrifuge tubes. The first had approximately 25 mL, the second 25 mL, and the third 30 mL. Using a disposable pipettor, 6.0 N KOH was added into each tube until no more precipitate formed. The orangish precipitate formed almost immediately as the drips of base hit the solution. All three tubes became completely clouded after two additions of 2-3 mL of the base from the pipettor such that additional precipitate formation could not be detected. The samples were placed in the International Clinical Company centrifuge at 1600 rpm for five minutes bringing the solid to the bottom and allowing visual inspection of the solution again. Three more drops of base were added into each of these two centrifuge tubes without anymore visible precipitate formation. The samples were then shaken manually to ensure a good equilibrium and centrifuged one last time for five minutes.

The next step was the separation of the uranium hydroxide and the wash of the solids. Approximately 41-42 mL of deionized water were added to the solids, manually shaken, and then placed into the centrifuge for five minutes. The pH of the solutions was more closely monitored, testing each rinse with the pH indicator strips (Table 3.6). The rinse solutions were poured off into three 250 mL nalgene containers. By the fourth rinse, the decreasing pH and decreasing hydroxide concentration began to dissolve some of the precipitate.

Using a disposable pipettor, 4-5 drops of the 6.0 N KOH were added to stabilize the solid. This final rinse was then poured off into the nalgene containers.

Table 3.6 pH Measurements of the Rinse Solutions:
Re-preparation of the enriched uranium acetate to remove any nitrate ions remaining in solution.

Rinse	Bottle	pH
0	1	>14
	2	>14
	3	>14
	DI H ₂ O	7
1	1	13
	2	12.5
	3	14
2	1	11.5
	2	11.0
	3	12.0
3	1	10.0
	2	8.5
	3	9.5
4	1	8.5
	2	8.0
	3	8.0

The next step was dissolving the hydrated uranium hydroxide solid with the acetic acid. Fifteen mL of deionized water were added to each centrifuge tube. The acetic acid was added using a disposable pipettor until the solid dissolved. After two additions of approximately 2-3 mL of acetic acid, the solids disappeared. The solutions in the three centrifuge tubes were poured into a 100 mL volumetric flask. The tubes were each rinsed with acetic acid which was also poured into the 100 mL flask. The flask was then topped off to the 100 mL line with deionized water.

Table 3.7 ICP-AES Data for Re-prepared Enriched Uranium Acetate: This table shows the raw data from the ICP-AES used to determine the detection limit and concentration of an unknown sample.

Sample	Concentration (M)	Spectral Intensity (Mean Value of 3 Measurements)	Standard Deviation	
DI	unk (~0)	22418	167.9	
DI	unk (~0)	21969	90.7	
0.1 HNO ₃	unk (~0)	21958	177.6	
10-7 STD	unk (~0)	21825	31.45	
10-6 STD	0.000001	22585	66	
10-5 STD	0.00001	30306	55.4	
10-4 STD	0.0001	94757	350.6	
10-3 STD	0.001	728203	5671	
1mM Old Sample	1.02E-03	741833	7009	
Sample 1	3.06E-03	2183900	33153	
Sample 2	5.57E-04	415969	3740	
Sample 3	5.53E-05	62079	248.2	
DI	unk (~0)	21545	222.2	
Sample 3	5.57E-05	62350	320.9	
		0.1 N HNO ₃ (ml)	Original Solution	Calculated Original Concentration (M)
Sample 1	5:5	5	5	6.13E-03
Sample 2	1:10	10	1	6.13E-03
Sample 3	0.1:10	10	0.1	5.62E-03
Sample 3	0.1:10	10	0.1	5.58E-03

Next the solutions were dried down on a hot plate to obtain the uranium acetate salts. The 100 mL solution was poured into a 250 mL volumetric flask. In addition, there appeared to be some yellow precipitate in the bottom of the second of three rinse solution bottles. At this point, an effort was made to recover as much of the enriched uranium as possible. The 250 mL in the nalgene rinse container was divided into six 50 mL centrifuge tubes (about 40-45 mL in each). Concentrated acetic acid was added to nalgene container to dissolve the yellow precipitate that remained on the bottom, and was poured

into the 250 mL volumetric flask. Three drops of 6.0 N KOH were added to stabilize any hydroxide solids in the centrifuge tubes. These were spun in the centrifuge, the supernatant poured off, and any remaining yellow solid was dissolved with 2.5 mL of acetic acid. All this was added into the 250 mL

U500 Uranium Acetate Solution ICP AES

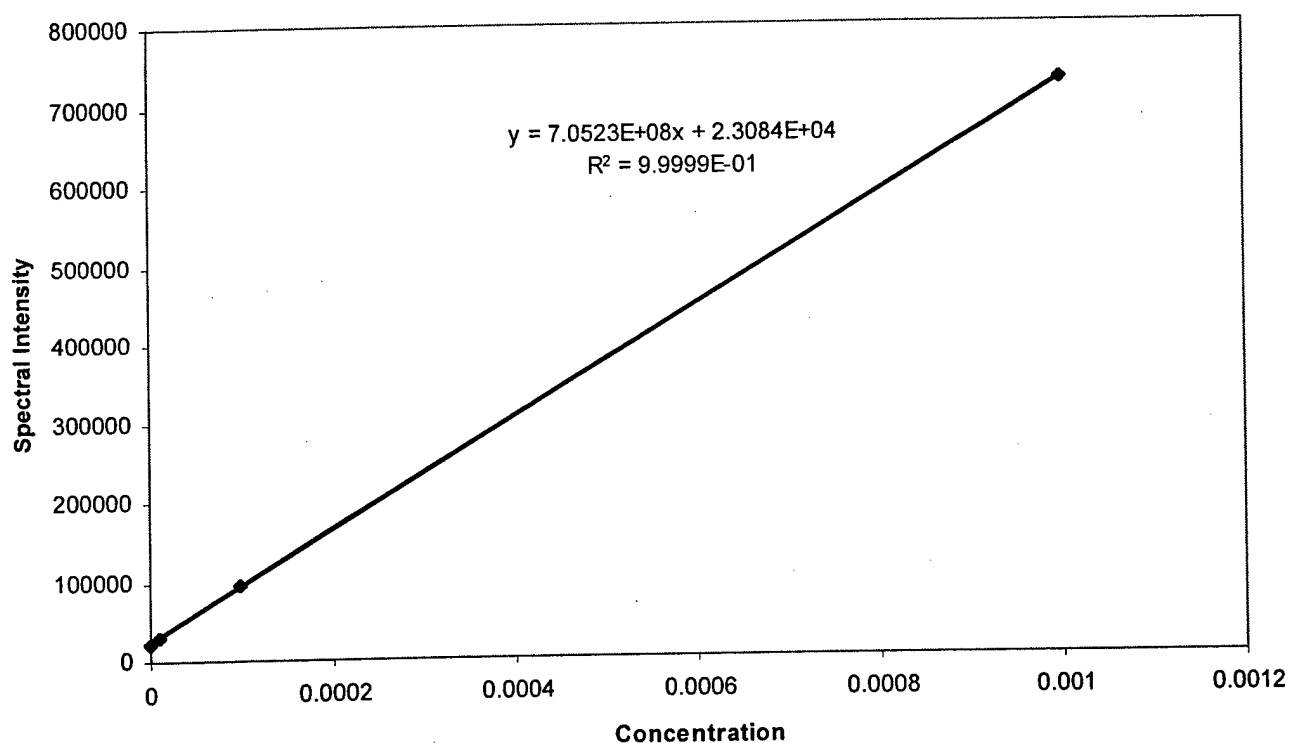


Figure 3.6: Calibration curve and Concentration Determination for the Re-prepared Enriched Uranium Acetate Solution: The photon intensities of 385.958nm for the standard enriched uranium solutions with a known concentration are graphed and linearly regressed. This regression gives an equation for intensities as a function of concentration to determine the total uranium concentration in an unknown sample.

volumetric flask. The flask was then placed on the hot plate and brought to a

gentle boil. The boil was monitored to ensure no loss of uranium to the boil outside the flask. After over 15 hours, the uranium acetate salts had dried completely. The flask was removed from the hot plate and allowed to cool.

The final step was adding 250 mL of deionized water and then analyzing the final uranium concentration. This time a larger volume was chosen to ensure that the solution was less concentrated and not over saturated, and yet still high enough that the solution could be diluted to the 2mM concentration needed for the bacterial medium. The results from the ICP-AES are in Table 3.7 and calibration graph is in Figure 3.6.

The average uranium concentration was $5.87 \times 10^{-3} \pm 3.03 \times 10^{-4} \text{M}$. The pH was tested with the pH indicator strips to be 4.5. This solution would be used to make the enriched uranium media described in the next section.

3.3 Microbiology Experimental Procedures

Many bacteria use oxygen in their metabolic process. Some bacteria are capable of using metals and a few non-metals as the electron acceptor in anaerobic respiration. There were three environmental bacteria strains known to reduce aqueous uranium: *Geobacter metallireducens* (GS15), *Shewanella putrefactions*, and many strains of *Sulfur Reducing Bacterium* (SRB). GS15 and SRB are inherently anaerobic and, thus grow slowly. Because *Shewanella* can grow aerobically and anaerobically, it was much easier and faster to produce large amounts of material. *Shewanella* also reduced uranyl ions quicker than the other two bacteria and can not use sulphate as the reductant.

Up to this point, three experiments using cultured specimens of *Shewanella Putrefaciens* had been carried out. These experiments were performed twice for the indicator dye study and once with the enriched uranium

Table 3.8 Summary of the Steps Involved in Preparing the Anaerobic Media and the Bacteria for the Uranium Reduction Experiment.

- | | |
|-----------------|---|
| Inoculum | <ol style="list-style-type: none"> 1. Grow <i>Shewanella Putrefaciens</i> (SP) in LB medium (usually 2-3 days) 2. Collect the cells by centrifugation at 10,000 rpm for ten minutes 3. Wash the cells with NaHCO_3 (2.5g/L), three times 4. Ready for inoculation |
|-----------------|---|

- | | |
|--|--|
| U^{6+}
medium | <ol style="list-style-type: none"> 1. Add 5 ml of media per tube 2. Flush with CO_2+N_2 gas for 2 minutes 3. Autoclave 4. Cool down to room temperature 5. Inoculate with SP (10^7-10^8 cells/ml) 6. Keep in warm environment until sampling time is complete |
|--|--|



- | | |
|---|--|
| { | <ul style="list-style-type: none"> • $\text{UO}_2(\text{CH}_3\text{COO})_2$, 2mM • Lactate-Na, 5mM • NaHCO_3, 2.5g/L • Basal Salts, 100x, 10ml/L (free of phosphate, PO_4^{3-}) • Trace Elements 1000x, 1ml/L • Vitamins 1000x, 1ml/L • CaCl_2 1000x, 1 ml/L |
|---|--|

Time Course Experiments

- | | |
|---------------|---|
| Sampling Time | <div style="display: inline-block; vertical-align: middle;"> $\left\{ \begin{array}{l} \text{T=0 hour} \\ \text{T=4 hour} \\ \text{T=8 hour} \\ \text{T=24 hour} \\ \text{T=96 hour} \end{array} \right.$ </div> |
|---------------|---|

acetate attempting to precipitate enriched uraninite by microbial reduction. Only one of the three succeeded in the reduction of uranium. The first experiment failed because of phosphate in the medium that precipitated out the uranium. The first experiment with the enriched uranium acetate failed because

of suspect contamination of the media with nitrate. The basic procedure for preparing the biological samples is in Table 3.8.

The same procedure outlined in Table 3.8 was used to make the culture tubes for the second trial with the enriched uranium samples. *Shewanella* are first grown aerobically in a luria-bertani (LB) medium. A small amount of *Shewanella* are grown in a warm environment near room temperature for two to three days in the LB medium. The bacteria are then spun in a Beckman model J2-21 centrifuge and washed with a bicarbonate buffer. Simultaneously 25mL anaerobic culture tubes containing a solution of salts, vitamins, bicarbonate buffer, and the uranium media are prepared. These solutions are flushed with a nitrogen/ carbon dioxide mix to de-oxygenize the mixture and are then capped. The culture tubes are then autoclaved in a Castle Thermatic Model 60 at 15 psi and near 120°C to sterilize the media. After an appropriate cool down time, the tubes are then inoculated by adding the strain with a sterile Becton -Dickinson needle and BD 23G 1 mL syringe.

An LB solution was made by dissolving 12.50 grams of dry LB powder from DIFCO Laboratories into 500 mL of deionized water in a 1 liter glass bottle. The bottle is then autoclaved and allowed to cool. A concentrated stock amount of the *Shewanella Putrefaciens* strain, labeled MR-1 in 2.5g/L NaHCO₃, was kept in a 20 mL glass culture tube in the freezer. After the cells thawed to room temperature, two mL of *Shewanella* stock were added directly into the 500 mL LB broth. The glass bottle cap was run directly over an open flame to prevent contamination and then applied loosely back on the bottle. The bottle

was then placed at 30°C with a magnetic stirrer bar added to help prevent clumping during growth. The bacteria were then allowed to grow in this media for approximately three days.

While the bacteria grew in the LB broth, two sequential events occurred: 1) preparation of the re-conditioned enriched uranium acetate described above in Section 3.2.2 and 2) preparation of the uranium media and the culture tubes. The concentration of the enriched uranium acetate solution rinsed clean of nitrate ions was evaluated by ICP-AES to be 5.87 mM. The uranium solution was mixed according to the procedure in Table 3.9, to make 100 mL of the uranium media (the specific components of the ingredients in Table 3.9 are in Appendix 3, Annex C). The uranium concentration was made slightly higher than 2mM (actual 2.10 mM) to account for the standard deviation in the ICP-AES value of the concentration determination. The media was mixed in a 100 mL volumetric flask. The contents in Table 3.9 were added first and then deionized water up to the 100 mL line on the flask. The pH was tested with an indicator strip to be pH 7 which was within the pH 6.5 to 7.0 required for the

Table 3.9 Components of the Uranium Media: A 100 ml of this uranium was prepared, with 5 ml of the media in each culture tube.

1.	NaHCO ₃ (100x100g/L)	2.5g/L	02.5 ml
2.	Basal Salts	10 ml/L	1 ml
3.	Trace Elements	1 ml/L	0.1 ml
4.	Vitamins	1 ml/L	0.1 ml
5.	CaCl ₂ (1000x)	1 ml/L	0.1 ml
6.	Lactate (100x)	5mM	1ml
7.	UO ₂ (CH ₃ COO) ₂	2mM	35.71 ml

bacteria.

Five mL of this media was then added to each glass culture tube shown in the photo with Table 3.8. Nitrogen and carbon dioxide gas are bubbled into the solution for two minutes and then sealed prior to insertion into the autoclave. After all the culture tubes are sealed, they are placed into the autoclave which brought the temperature up to 120°C for 25 minutes. The culture tubes are then cooled for 30 minutes.

The *Shewanella* bacteria were removed from the oven after four days of growth. The LB broth and the bacteria were poured into two 250 mL centrifuge cups. They were placed into a Beckman Model JL-21 centrifuge at a speed of 10,000 rpm and temperature of 30°C for 10 minutes. After the centrifuge, the bacteria laid in a small, pinkish clump at the bottom. The LB broth was poured off and a 2.5g/L bicarbonate solution was poured into the cup just enough to cover the cells. A spatula was used to improve the rinsing of the cells. This was then returned into the centrifuge where this was repeated two more times. After the third rinse, the bicarbonate was drained off exposing only the cells. Then another solution of 2.5g/ L bicarbonate was poured into the cup just enough to cover the cells and the cells re-suspended with the spatula. A metal syringe inserted 0.2 mL of this solution through the rubber stopper that sealed the culture tubes to inoculate the five sample bottles. These five, now labeled with blue tape as the controls, were placed immediately into the autoclave to kill the cells. The five culture tubes were autoclaved for 25 minutes and allowed to cool for 35 minutes.

The remaining five culture tubes were inoculated with 0.2mL of the bacteria and bicarbonate solution. These five culture tubes were labeled with pink tape. After inoculation, all ten culture tubes were returned into the oven that maintained a 30°C environment and were allowed to interact. After the specific interaction time, 0.5 mL of formaldehyde was added to both the blue and pink respective culture tubes to kill the cells and stop the reduction reaction. There were clear signs of uraninite formation in all culture tubes. This uraninite was then analyzed in Chapter 4 for any biological fractionation in the uranium isotopic ratio.

3.4 Physical Structure of the Crystals

This section is out of sequence in terms of the experimental order, but not in terms of significance. The source of the uraninite precipitate came from the freeze-dried sample discussed in Chapter 2, Section 2.3.3. Dried solid samples were analyzed with both a scanning electron microprobe (SEM) and X-Ray Diffraction (XRD) to determine qualitative structure of the crystals and verify indeed that the solid forming was uraninite, UO_2 (s), and not triuranium octaoxide, U_3O_8 (s), which has a similar physical appearance.

3.4.1 X-Ray Diffraction

X-rays interact with a crystal lattice in the same way that light interacts with a conventional diffraction grating. They are dispersed in different directions according to wavelength. The diffraction of X-rays by crystals is described by Bragg's Law of $n\lambda=2d\sin\theta$. Incoming waves are scattered by

successive planes of atoms. Scattered rays for which Bragg's equation is satisfied experience constructive interference and will form a diffracted beam at an angle θ equal to the angle of incidence of the incoming rays. The crystal planes act as a selective mirror. X-rays that do not satisfy Bragg's Law undergo a form of destructive interference and do not form a reflective pattern. The diffraction pattern is indicative of the specific lattice spacing associated with each crystal. In this way, the uranium solid precipitated by the bacteria will be tested for its lattice spacing and then compared against the library and matched with a specific crystal in the Primary Data File (PDF). An example of PDF 41-1422, the reference used for uraninite is shown in Table 3.10.

Table 3.10 PDF 41-1422 XRD Spectroscopic Data for Uraninite UO_2 (s)

Uraninite-1JTC\RG U O2										Specimen from Alm Bos, Italy. Chemical and microprobe analysis (U860+ and U (total) polarographically; calculation by standard addition method) (wt.%): \Al2 O3\ 0.010, CaO 0.466, \U O2\ 98.197, \Ce2 O3\ 0.125, \Ti O2\ 0.009, \Th O2\ 0.249, PbO 0.544, \Si O2\ 0.150, FeO 0.015; \U O2.06\, To replace 5-550, 9-206, 13-225 and 20-1344. Black															
Radiation : CuK α 1			Lambda: 1.54056			Filter: Quartz																			
Calibration: Internal(SCD)			d-Cutoff:			1/c(RIR):																			
Ref: Fritzsche, R., Sussieck-Fornefeld, C., Min.-Petr. Inst., Univ. Heidelberg, G ICDD Grant-in-Aid (1988)																									
System: Cubic(Powder Diffraction)			S.G.: Fm3m (225)			Z= 4																			
Cell Parameters= 5.467			mp=																						
Ref: Willis, B.																									
Nature (London), 197 755 (1963)																									
Dx= 10.975 Dm= 10.950 Hwt= 270.03			Vol(RC)= 40.85			F(9)=78.1(-0.0128,9)																			
ee=			nm8=			ey=			Sign:											2V=					
Ref:																									
9 Reflections. Radiation: Cu_1.540598. Strong Lines: 3.15/X 2.73/5 1.93/5 1.65/5 1.25/2 1.22/2 1.12/2 1.37/1 1.58/1																									
#	d(A)	I(fix)	I(var)	h	k	l	2-Theta	Theta	1/(2d)	#	d(A)	I(fix)	I(var)	h	k	l	2-Theta	Theta	1/(2d)						
1>	3.1530	100	100	1	1	1	28.282	14.141	0.15858	6>	1.3670	10	23	4	0	0	68.596	34.298	0.36576						
2>	2.7330	50	57	2	0	0	32.741	16.371	0.18295	7>	1.2543	20	30	3	3	1	75.777	37.888	0.39863						
3>	1.9330	50	81	2	2	0	46.969	23.484	0.25867	8>	1.2224	15	38	4	2	0	78.123	39.061	0.40903						
4>	1.6474	45	86	3	1	1	55.755	27.878	0.30351	9>	1.1158	15	42	4	2	2	87.317	43.658	0.44811						
5>	1.5782	8	16	2	2	2	58.430	29.215	0.31682																

A Rigaku RU300 X-Ray Generator with 250mm and 185mm Diffractometers were used for the analysis.

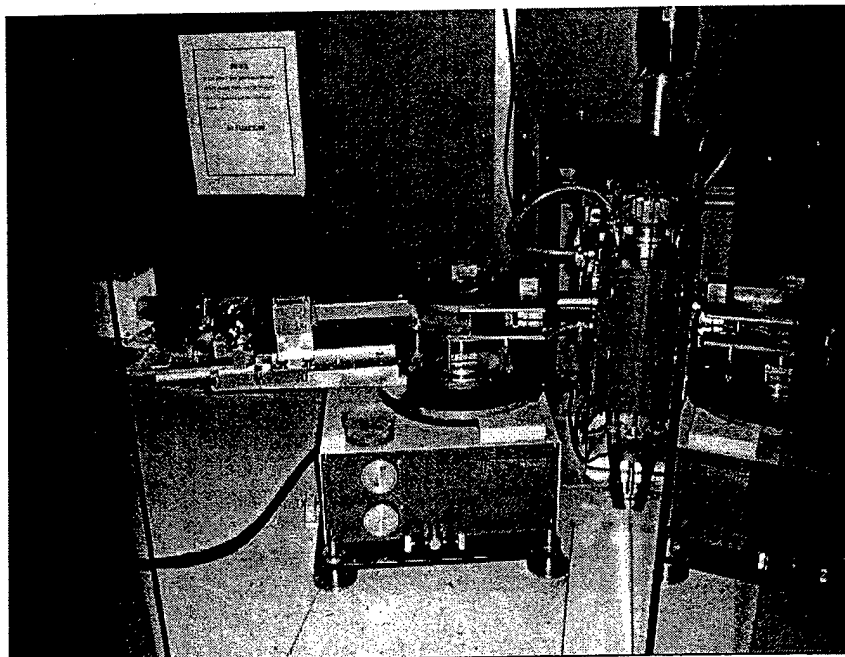


Figure 3.7 Rigaku RU300 X-Ray Generator

A zero background polished silicon sample holder was provided to mount the uranium crystals using a pre-mixed bottle of nitro-cellulose (also known as collodian) as the binder for the uranium powder to the sample holder. The sample holder was returned to the glove box where uraninite sample was stored after it had completed drying down in the freezer dryer. Using a disposable pipettor in the glove box, a small dusting of dried uranium precipitate was placed on the sample holder. Five drops of collodian were placed on top of crystal and allowed to dry for four hours.

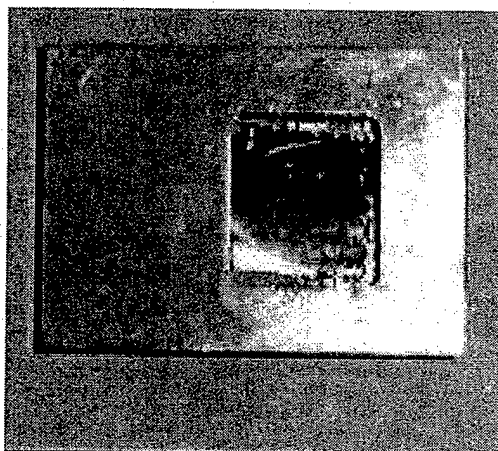


Figure 3.8 Zero Background Sample Holder

After four hours, the sample holder was placed in the lid of 50 mL centrifuge tube and sealed with plexifilm to avoid and contamination or oxidation. The sample was delivered to X-Ray Diffraction machine location.

Table 3.11 The Scan Parameters for the two XRD Analyses Performed on the Bacterial Precipitate.

Analysis 1 Preliminary Scan

File: Z14534.raw
 Scan Range: 25°-90°
 Scan Speed: 20°/min
 Sampling Interval: 0.02°

Analysis 2 Increased Intensity Scan

File Z14535.raw
 Scan Range: 20°-90°
 Scan Speed: 2°/min
 Sampling Interval: 0.02°

Two broad band X-Ray scans were performed on the target. The parameters for each is in Table 3.11. The preliminary scan did not observe much of a signature. The scan was slowed down by a factor of 10 to increase the intensity, but

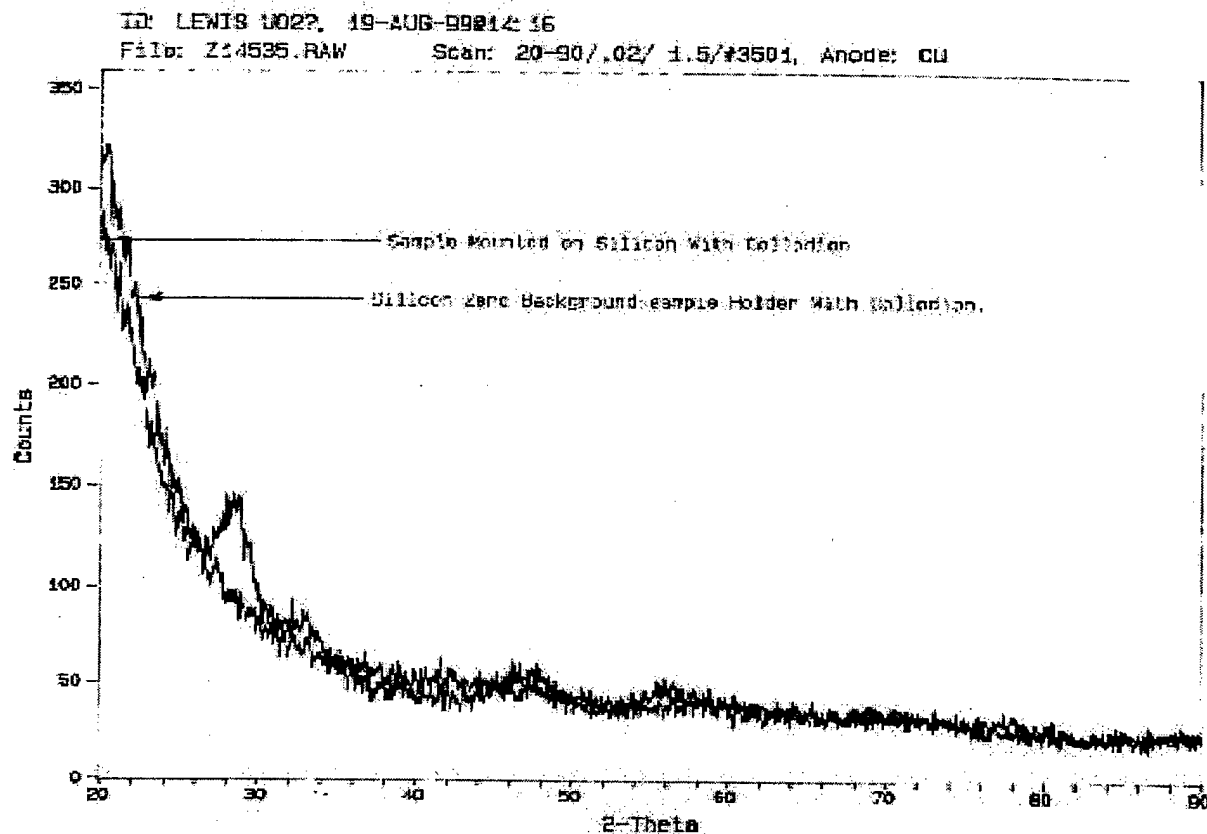


Figure 3.10 The X-Ray Spectra of the Silicon Sample Holder and Collodion with and without the sample (i.e. background spectra).

3.4.2 Scanning Electron Microprobe

The Electron Microprobe is a useful tool to observe mineral structure and determine relative concentrations for elements forming the mineral. It focuses a high-energy electron beam to create images and uses characteristic X-rays from the exposed specimen to determine its chemical composition. It provides a non-destructive approach of analyzing chemical variation at a micrometer scale. The JEOL JXA-733 "Superprobe" was used to study the uranium precipitate. The

JEOL Superprobe is known as a wavelength dispersive (WD) X-Ray spectrometer. The X Ray source, the crystal, and the detector lie on the circumference of a hypothetical circle with constant radius called the Rowland circle. It then applies Bragg's law to determine which is most suitable to view a particular diffracted X-Ray scattered off a crystal. The electron beam penetrates approximately 2 μm for elemental composition. For EDS (energy dispersive spectral) analysis a Si-Li drifted crystal detector was used. WDS (wavelength dispersive spectrometry) was performed using TAP, PET and LIF crystals.

There are some limitations for the SEM which impeded the use of the SEM as a secondary source to the XRD for crystal characterization. The XRD used lattice spacing to distinguish between U_3O_8 and UO_2 . SEM would need to quantitatively measure the chemical composition of the grains, however quantitative measurements of oxygen based compounds with the SEM are very difficult. Analyzing light elements like oxygen that have atomic numbers below 10 are very difficult for the following reasons:

- 1) Low energy or soft x-rays are strongly absorbed in the specimen or the detector, so count rates are low.

- 2) Spectral interference from L and M lines of the heavier elements and rising continuum intensity at long wavelengths leads to low peak to background ratios.

For these reasons, the actual count of uranium to oxygen atoms in the uranium crystals in the SEM was inconclusive in determining whether the

crystal was U_3O_8 or UO_2 . It did provide some qualitative results demonstrating the crystal size to be very small, normally less than one micron. A picture of the dried uranium mounted on sticky carbon paper is shown in Figure 3.11



Figure 3.11 SEM Picture of the Uranium Precipitate by Bacterial Reduction.

3.5 Conclusions

The objective of this chapter was to provide a broad overview of the general methods used in laboratory for the bacterial reduction of uranium using *Shewanella putrefaciens*. The last portion of this chapter explained the structure of the precipitate that was identified as the mineral uraninite UO_2 . There were some important lessons that were learned through each step.

The first was the kinetics involved in the dissolution of U_3O_8 with nitric acid. The literature states the improved dissolution kinetics with heat and agitation. This would have increased the dissolution times in our research. The interesting effect here that is also addressed in Chapter 2, is the uranium speciation in the acid. The mixed oxidation state of U_3O_8 is dissolved entirely into the uranyl ion UO_2^{2+} (aq) by oxidizing the uranium (IV) to U(VI). In the dye experiment in Chapter 2, the uranium was also dissolved in nitric acid, although in the glove box, but into a different species (known by the observed complex behavior with a few of the dyes).

The next lesson was the solubility and over saturation of the uranium acetate solution. In both the non-enriched case and the first enriched case, the over saturation of the solution was observed by the fine yellow solid particles at the bottom of the solutions. This accounted for a significant part of the loss during the chemical preparation. The target concentration of the solution was initially 10mM. Raising the pH up to level safe for the bacteria made this uranium concentration too high. This was mitigated in the second solution with the enriched uranium by only raising the concentration up to a concentration of just over 5mM.

The most lesson observed was oversight of the nitrate ion concentration and the impact that a small amount of nitrate had on the reduction of the uranium. The further rinses completed with the uranium hydroxide in the second run with the enriched uranium acetate forced the bacteria to use the uranium metal as the electron acceptor. This is important when evaluating this

process in the environment. For the bacterial reduction to occur, all other oxidants must have been used up before the bacteria will use uranium. This includes not only nitrate, but any other dissolved environmental metals or ligands capable of being reduced and are thermodynamically more favorable.

The rinse procedure also showed the requirement to maintain very basic conditions in the rinse. The solid volume of the precipitate seemed to decrease around pH8 which was stopped by adding a small amount of a basic solution to bring the pH up to level that would stabilize the hydroxide solid. The use of deionized water may be replaced by rinsing with a basic solution for the first few rinses, as long as the metal cation does not present a problem in the reaction. The basic solution should not be too concentrated though, to prevent higher order uranium hydroxide complexes from forming.

Lastly in terms of the crystal identification, the X-Ray diffraction approach is much more suitable for identification than an elemental analysis of the crystal with the electron microprobe. Future study would have included a solid X-Ray pattern of UO_2 and U_3O_8 to compare each against the other. The data in the report clearly show a similarity with the library reference peaks of uraninite, but a comparison with a small amount of U_3O_8 solid crystal may have formed a better comparison. The issue now to be addressed in Chapter 4 will be the isotopic ratios with the precipitates as a function of time. There is significant evidence with other elements, but no data yet established whether biological fractionation occurs with uranium.

¹ Robin, Gill, (1997). Modern Analytical Geochemistry. (Singapore, Indonesia: Longman Singapore Publishers Limited, 1997), 41-59.

² SPECTRO ANALYTICAL INSTRUMENTS. *SpectroFlame ICP Limits of Detection in Aqueous Solutions (2 s) in ppb*. Spectro Analytical Instruments. Fitchburg, MA. (Not Dated)

³ Josef R. Parrington, Harold D. Knox, Susan L. Breneman, Adward M. Baum, and Frank Feiner, Nuclides and Isotopes, Fifteenth Edition, (San Jose, Ca.: General Electric Company, 1996), 48-49.

⁴ Yoshiyuki Yasuike, Yasuhisa Ikeda, and Yoichi Takashima, "Kinetic study on dissolution of U_3O_8 powders in nitric acid," Journal of Nuclear Science and Technology, 32, no. 6, (1995)596-598.

⁵ Akihiko Inoue and Takeshi Tsujino, "Dissolution rates of U_3O_8 in nitric acid," Industrial Chemical Process Development, 23, (1984), 122-125.

⁶ Robert C. Weast and George L. Tuve, eds., CRC Handbook of Chemistry and Physics (Cleveland, Ohio: Chemical Rubber Company, 1958), D199.

Chapter 4

Analysis of Uranium Isotopic Ratios of Precipitates formed by Bacteria

The purpose of this chapter is to determine whether the bacterial reduction of aqueous U(VI) species to solid U(IV) affects the isotopic ratio of uranium atoms. Natural uranium primarily consists of a mixture of three isotopes: ^{234}U , ^{235}U , and ^{238}U . The natural atomic abundances of these isotopes are ^{234}U (0.0056%), ^{235}U (0.718%), and ^{238}U (99.276%)¹ Changing the isotopic ratio of an element is referred to as isotopic fractionation. The objective of this chapter is to determine if there is any change in the isotopic ratio of the uranium atoms during the bacterial reduction of uranium by *Shewanella putrefaciens*.

4.1 Background

It is well documented that the mass of isotopes affects the kinetics of chemical reactions. Thermodynamically favorable processes often result in an isotopic fractionation where the lighter isotopic elements of a molecule react quicker than their heavier counterparts. This change is more prevalent in the lighter isotopes where the mass difference among the isotopes is more pronounced, but a recent investigation of iron isotopic fractionation in terrestrial and lunar materials seemed to indicate a significant biological fractionation of iron in sedimentary rocks². The authors in 2 concluded that

the iron fractionation was a result of biological processes, and were in the processes of conducting experiments using iron reducing and iron oxidizing bacteria to produce iron biomaterials to quantify the extent of this biological fractionation. In a similar study of iron isotope fractionation by the bacterium *Shewanella putrefaciens* (the same bacteria used in this thesis), it showed biological organisms could fractionate iron isotopes by up to 1.3 per thousand for the ratio of $^{56}\text{Fe}/^{54}\text{Fe}$ during the reductive dissolution of iron oxide (ferrihydrite)³. The mass difference of the iron isotopes ^{56}Fe and ^{54}Fe as a percent difference (3.70% compared to ^{54}Fe and 3.57% compared to ^{56}Fe) is comparable to the mass difference of the uranium isotopes ^{235}U and ^{238}U (1.27% compared to ^{235}U and 1.26% compared to ^{238}U)⁴.

This phase of the research on the bacterial reduction of uranium investigated whether or not the mass difference of the uranium isotopes was sufficient to yield a fractionation between the precipitate and the supernatant. Theoretically, if a fractionation occurred, the precipitate formed by the reduction of the uranyl species from UO_2^{2+} to the solid uraninite mineral UO_2 would be enriched with ^{235}U . A measurable amount of isotopic fractionation depends on many factors affecting the precipitation and an analytical technique capable of detecting this level of fractionation. Thermal Ionization Mass Spectrometry (TIMS) is the most accurate technique that is widely available to determine these isotopic ratios. TIMS is a high precision mass analyzer employed by many geologists to measure the isotopic ratios that are then used to date minerals and rocks. For these reasons, TIMS was selected as the method to examine the ability and rate of

bacteria to fractionate uranium isotopes during the reductive process of uraninite formation.

4.2 TIMS Fundamentals

The basic objective of any mass spectrometer is to quantitatively separate a sample into its constituent parts based on their mass. Mass spectrometry probes the elemental or isotopic composition of a species in a sample, whether graphically or numerically as ratios of different isotopes.

The basic components of any mass spectrometer are:

- Ion source
- Mass analyzer
- Ion collector

Figure 4.1 illustrates a generic layout of the components of a mass analyzer. The design of these devices is unique to each machine according to the sample types and objectives of the measurement⁵. TIMS is a method that measures the isotopic composition of samples introduced in the solid form that are capable of being thermally ionized. TIMS is used widely by geologists for the following purposes:

- Measurement of the isotopic compositions of elements where natural variations occur (principally as a result of radioactive decay). These are then used to provide absolute age determination rocks and minerals, and to determine the origins of geologic materials by reference to their isotopic composition⁶.
- Precise measurement of element concentrations by isotope dilution⁷.
Isotope dilution was used in this study to measure the amount of

uranium in the reagents used in the chemical preparation of the samples. A more detailed description of this technique and the results are described in Section 4.5 of this chapter.

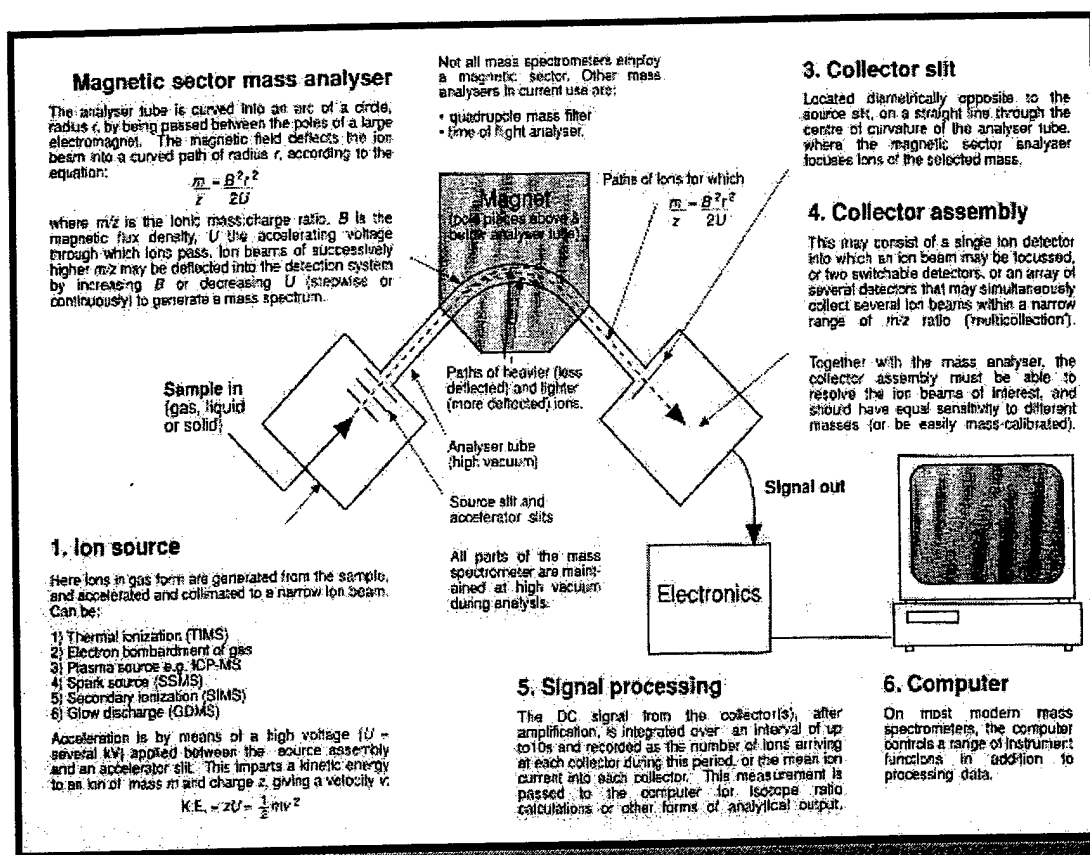


Figure 4.1 Principles of a Mass Spectrometer: This is a simplified diagram showing the primary components of a mass spectrometer. Figure 4.2 shows a photo of the thermal ionization mass spectrometer used to determine the uranium isotopic ratio⁵.

Both of these objectives are determined by the evaluation of isotopic ratios or the relative amount of each isotope in a sample.

TIMS has been most effective in analyzing the isotopic variations of heavy elements produced by radioactive decay, compared with which biologic and mass fractionation effects are negligible or may be easily corrected.

TIMS is generally unsuited to the determination of small, natural, mass dependent isotopic variations in the lighter elements unless they can be ionized as a high mass polyatomic ion (e.g. Cs_2BO_2^+) because instrumental fractionation effects generally mask any natural fractionation effects. This is also the case for high precision isotope analysis with transition metals and certain actinides⁸.

Instrumental or mass fractionation is the tendency during the thermal ionization process of the lighter isotopes to leave a heated filament before the heavier isotopes. This affects the ion flux intensities that are measured by the TIMS for each isotope. Mass fractionation is affected mostly by filament analysis time, filament temperature or amperage, sample loading technique, and the amount of analyte loaded on the filament. The two major challenges in constructing a precise uranium isotope analysis necessary to distinguish the effects of any biologic fractionation are the necessity to correct for the significant mass fractionation effects and the low ionization efficiency of uranium. Mass fractionation is usually corrected empirically with a certified standard or rigorously with a double spike method⁹.

4.3 Preparation for TIMS analysis

For nearly all TIMS applications it is essential to separate the element of interest from a sample prior to isotope analysis. This is to minimize or eliminate isobaric interference from other elements and to reduce the proportion of other constituents of the sample to a level that they do not inhibit the ionization of the element of interest. Reagents and laboratory

procedures must be carefully applied to minimize the contamination of the true isotopic signature of the element of interest.

All of the chemical preparation was performed in a clean room where gloves, hair caps, boot covers, and full body gowns were standard operating procedures. Extra steps were taken to purify all analytical grade reagents. Analytical grade acids were further purified in the laboratory with evaporation by infra red lamps and distillation in Teflon bottles as opposed to any Pyrex glassware. Reverse osmosis by Millipore water purification systems known as Milli Q was used in place of deionized water. Ion exchange was used to purify and concentrate the element of interest in the sample, and to prevent isobaric interferences from any other elements.

4.3.1 Chemical Preparation

Samples used in this test came from the reduction experiment with the enriched uranium acetate described in the microbiological process in Section 3.2 and 3.3 in Chapter 3. Each glass culture tube used in the experiment was labeled in a pattern that provided information on the time and type of interaction. The glass culture tubes that were used as the controls for the experiment were labeled with blue tape, the letter C, and the time that formaldehyde was introduced into the culture tubes. For example, the five control samples were labeled C0, C4, C8, C24, and C95. The control samples were autoclaved immediately after inoculation for 25 minutes, thereby killing the bacteria and preventing any biological interaction with the uranium solution. The formaldehyde was added to mirror the procedure of their respective test sample. The overall purpose of

the control samples was to determine whether chemical fractionation was a factor in the experiment.

The samples that interacted with the bacteria carried an S and the time in hours that the formaldehyde was introduced thus killing the bacteria and stopping the reduction reaction discussed in Section 3.3. After the inoculations and timed microbial reduction reactions in the Parsons Laboratory, the ten glass culture tubes were placed in the freezer and remained in the freezer for thirteen days. The ten culture tubes inoculated with the *S. putrefaciens* bacteria and the enriched uranium media were removed from the freezer and transferred to the TIMS laboratory.

Once the samples arrived in the laboratory, they were thawed at room temperature. The size of the glass culture tubes prevented their direct insertion into an International Clinical Company (No: W7926) centrifuge, so the samples were transferred into ten sterile 15 mL Corning polypropylene centrifuge tubes. Similar labeling discussed above was used to mark the ten centrifuge tubes. Each glass culture tube was shaken manually to suspend the solids on the bottom of the tube. The culture tubes were then uncapped with pliers and poured into its respective 15 mL centrifuge tube. Each centrifuge tube was spun at the high speed setting for five minutes. After the centrifuge, the solutions were clear with a beige solid biomatter and a varying degree of a blackish precipitate on the bottom of the tube.

Aliquots of the supernatant were first removed and transferred into 1.5 mL Sarstedt polypropylene microcentrifuge tubes. First, twenty 1.5 mL microcentrifuge tubes were labeled using the same technique described above

Table 4.1 ICP-AES Data for Enriched Uranium Acetate Supernatant: This table shows the raw data from the ICP-AES used to determine the detection limit and concentration of the uranium in the supernatants of S0, S4, S8, S24, and S95.

Sample	Concentration (M)	Spectral Intensity (Mean Value of 3 Measurements)	Standard Deviation		
water		20170	106.80		
0.1 HNO3		19938	134.10		
0.1 HNO3		20108	3.06		
water		20024	120.60		
0.1 HNO3		19813	124.50		
10-7 STD	1.00E-07	19727	143.80		
10-6 STD	1.00E-06	20635	68.70		
10-5 STD	1.00E-05	28684	72.00		
10-4 STD	1.00E-04	97007	285.90		
10-3 STD	1.00E-03	760525	5157.00		
5x10-4M	5.00E-04	751806	6583.00		
2.5x10-4M	2.50E-04	383638	876.00		
1.0x10-4	1.00E-04	165175	259.50		
7.5x10-5	7.50E-05	128392	621.00		
5.0x10-5	5.00E-05	86522	128.10		
2.5x10-5	2.50E-05	55280	259.00		
1.0x10-5	1.00E-05	31225	119.70		
	Calculated Concentration			Concentration (M)	Concentration (mM)
SOS 1:10	1.53E-04	134049	529.00	1.68E-03	1.68E+00
SOS 1:100	1.37E-05	31079	140.70	1.39E-03	1.39E+00
S4S 1:10	1.25E-04	113420	743.00	1.38E-03	1.38E+00
S4S 1:100	1.08E-05	28866	101.90	1.09E-03	1.09E+00
S8S 1:10	1.06E-04	99581	410.80	1.17E-03	1.17E+00
S8S 1:100	8.32E-06	27069	76.90	8.41E-04	8.41E-01
water	-2.98E-06	18708	151.10	-2.98E-06	-2.98E-03
S24S 1:5	8.15E-05	81239	279.60	4.89E-04	4.89E-01
S24S 1:10	4.35E-05	53082	99.20	4.78E-04	4.78E-01
S95S 1:5	2.27E-06	22594	76.70	1.36E-05	1.36E-02
S95S 1:10	-9.20E-08	20843	101.00	-1.01E-06	-1.01E-03
S95S 1:1	1.30E-05	30506	110.30	2.59E-05	2.59E-02
Time (Hours)	Total Uranium Concentration (mM)	Standard Deviation	Concentration of Uranium in the media (discounting sorption, 5 ml + 0.2 ml + 0.5 ml formaldehyde)		
0	1.535	0.208	1.842		
4	1.231	0.205			
8	1.005	0.233			
24	0.484	0.059			
95	0.020	0.009			

except this time adding a P or S to the end of the label. The P referred to

the precipitate samples and the S to the supernatant. Using S8S as an example, S referred to the test samples that interacted with the bacteria, 8 indicates that at the eighth hour formaldehyde was added to stop the reaction, and S for supernatant analysis. A small aliquot of 100 μL was drawn off each supernatant and placed into its respective microcentrifuge tube. Then, 900 μL of 7.0 N HNO_3 were added to each one of these tubes to stabilize the dissolved metals.

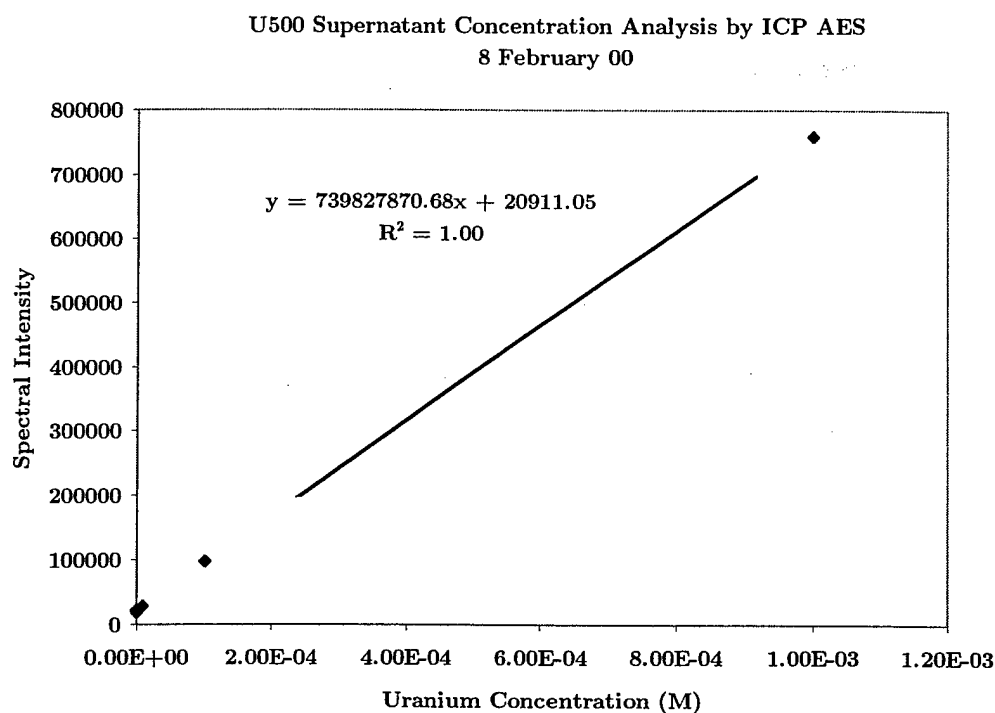


Figure 4.2 Calibration Curve and Concentration Determination for Enriched Uranium Acetate Supernatant Solutions: The photon intensities of 385.958nm for the standard uranium solutions with a known concentration are graphed and linearly regressed. This regression gives an equation for intensities as a function of concentration to determine the total uranium concentration in the supernatants for S0, S4, S8, S24, and S95.

The next step was to obtain the solid samples for analysis. Extra care was taken to separate the solid from any amount of uranium in the

supernatant to obtain the true isotopic signature of the uraninite precipitate. The majority of the supernatant was first poured off into a new set of 15 mL centrifuge tubes using a disposable pipettor for each culture tube. The concentration of this supernatant was analyzed later with ICP-AES in the method described earlier in Chapter 3. The raw photon intensity data is in Table 4.1 and the calibration curve is in Figure 4.2.

The data from the ICP-AES showed significant sorption occurring with the bacteria. The 5 mL uranium media in each culture tube was 2.1 mM before inoculation. After dilution with 0.5 mL of formaldehyde and 0.2 mL of the cells in the bicarbonate solution, the total uranium concentration

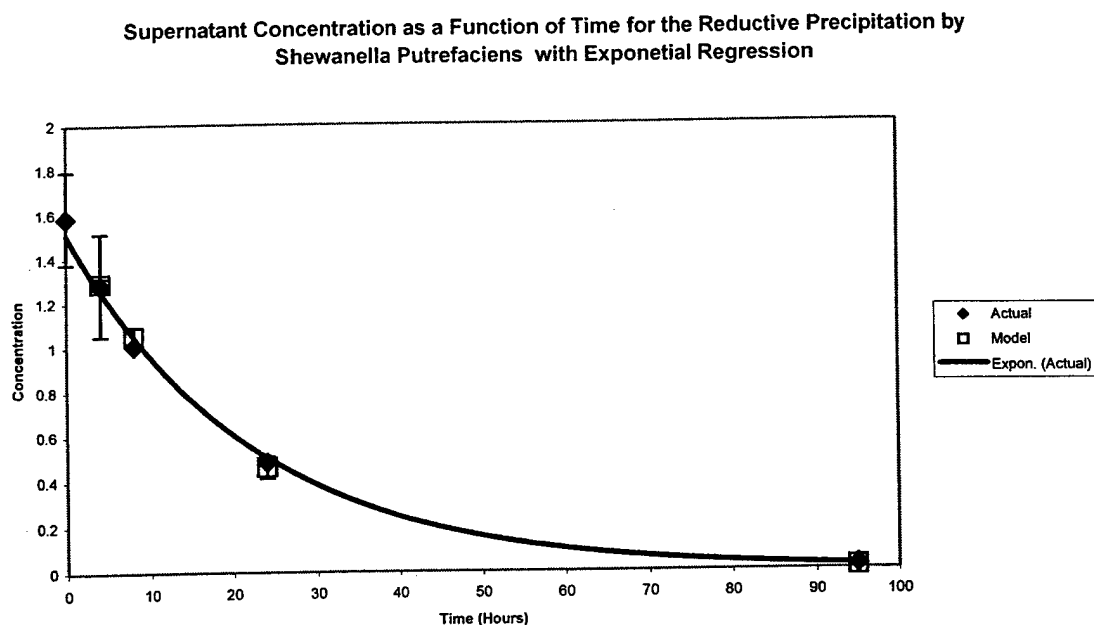


Figure 4.3 Conversion of Uranyl Acetate into Uraninite: This chart shows the decay rate of uranium remaining in solution as uraninite is produced by bacterial reduction.

was 1.842 mM. The measured concentration of S0 was 1.535 ± 0.208 mM indicating a loss to sorption onto the cells. This strong sorption was somewhat expected based on the high stability constants of uranium with humic and fulvic acids shown in Chapter 1. The conversion of the uranium solution into uraninite is graphed in Figure 4.3. The data points are fitted almost perfectly to an exponential decay with an R^2 value of 1.00. This gives the rate of conversion of the soluble uranium into the solid phase. The kinetics fit a first order rate equation. The model data points are plotted on

$$\ln[A_0] - \ln[A] = kt$$

A concentration at time t

A_0 initial concentration

k constant ($5.14 \times 10^{-2} \pm 4.72 \times 10^{-3}$)

Figure 4.8 as well. The error bars for the standard deviation values for both the ICP-AES calculated concentration values and the model predicted values are plotted in Figure 4.8 as well.

The solid substrates in each of 15 mL centrifuge tubes were rinsed by adding ten mL of Milli Q water (MQ H₂O) to the solid remaining and shaken vigorously using a Fisher Scientific Touch Mixer Model 231 for about five to ten seconds at the vortex setting. These were then centrifuged for five minutes and the supernatant rinse removed into a nalgene bottle as uranium waste. This washing procedure was repeated five times for each culture tube to remove any uranium in solution or any uranium ions adsorbed on the biomatter. The high number of rinses was to ensure that the true isotopic ratio of the solid uraninite would not be affected by any lingering uranyl ion

species in solution or adsorbed onto the bacteria. The last rinse solution was removed very carefully using a disposable pipettor that had a disposable pipette tip and spaghetti tubing to get as much of the liquid off the solid as possible.

On the bottom of the 15 mL centrifuge tube remained approximately 80 μL of a slurry containing bacteria and black uraninite solid. To slightly increase the volume, two drops ($\sim 30 \mu\text{L}$) of MQ H_2O were added to get the volume to at least 100 μL . Using a 100 μL Kimax pipettor, 100 μL of this slurry was removed and placed it into its respective 1.5 mL microcentrifuge tube. To each of these microcentrifuge tubes, 900 μL of 7.0 N HNO_3 were added just like supernatants samples. When adding the nitric acid, the black uraninite solids dissolved immediately, leaving only the beige, dead bacteria cells visible.

The microcentrifuge tubes were then spun in a unispeed microcentrifuge (Qualitron catalog number DW41) for five minutes. The solid matter settled on the bottom and sides of the microcentrifuge tube. The centrifuge process was repeated in an attempt to get all the biomatter on the bottom and off the sides of the tubes by increasing the time to fifteen minutes, however the results were the same. While the centrifuge process continued, twenty 3 mL polyfluoroyl (PFA) Teflon Savillex beakers were prepared. PFA is the cleanest form of Teflon in terms of trace metals as compared to PTE, another common form of Teflon. The beakers had been cleaned and were stored in 6.0 N hydrochloric acid (HCl). The small drop of 6.0 N HCl was rolled on its side to remove any condensation and was then

removed. Any remaining liquid in the threads of the cap was tapped out until it was completely dry. The Savillex beakers were then labeled with the same markings found on the microcentrifuge tube (S0S, S0P, C0S, etc.).

When the beakers were ready and the last sample centrifuged, 250 μL of the supernatant in each one of the microcentrifuge tubes were placed into its respective Savillex beaker. Next, 250 μL of concentrated nitric acid and 250 μL of hydrogen peroxide (Ultrarex 30% H_2O_2) were added to each Savillex beaker to dissolve any organics. The beakers with the 750 μL solutions were then capped tightly and placed on a teflon hot plate operating at approximately 250°C. The samples remained on the plate and fluxed for nearly 24 hours.

While the samples fluxed in the acid and hydrogen peroxide solution, anion exchange columns were prepared. Because of the number of samples and the limited supply of column material, there were two series of columns. The first series was used to prepare the supernatant samples and blanks, while the other set was used for the precipitate samples. The fifteen 50 μL columns were mounted on a stiff, flat FTP Teflon sheet. They were removed from a storage bath of 30% HNO_3 . The columns can be seen in Figure 4.4.

The columns were first surface rinsed with MQ H_2O and then thoroughly rinsed using a squirt bottle containing MQ H_2O . Fixing the spout of the bottle to the bottom of the stem, water was gently forced through a 35 micron frit up the stem until the stem was full. Then the column was turned over and the reservoir completely filled. The column was then

turned upside down and flicked to get all the water out of the reservoir and

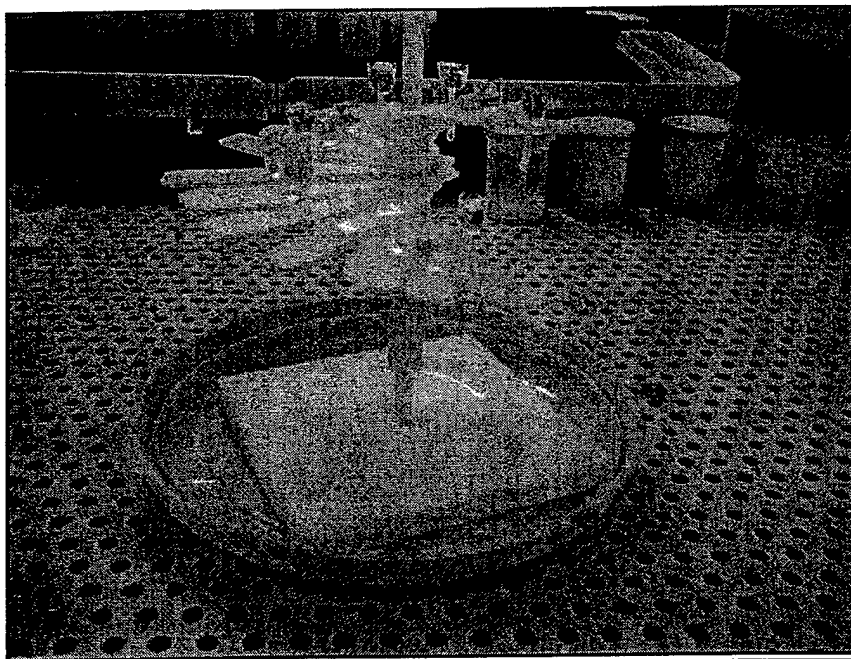


Figure 4.4 50 μ L Columns in Draining Stand: After the third and final rinse with MQ H₂O, the columns were placed in this draining stand. The hot plate is in the background.

stem. This rinse procedure was performed three times for each column.

A styrene divinylbenzene anion exchange resin called AG1-X8 Cl-form 200-400 dry mesh (Bio Rad Lot No: 25195A8) was used to concentrate the uranium in the samples. AG1 indicates that the resin is analytical grade and type 1, meaning a strongly basic anion exchanger containing quaternary ammonium groups. X8 refers to the extent of crosslinking within the resin bead and the physical characteristics such as pore size, permeability, swelling and shrinking effects, and sensitivity. In this case there is an 8% divinylbenzene crosslinkage of the styrene divinylbenzene polymer. A diagram of the molecular structure of AG1 resin is shown in Figure 4.5. 200-400 mesh is used for high-resolution analytical

work because it reduces the flow rate through the column, but increases the efficiency of the resin for a given volume. The exchange capacity for AG1-X8 resin is 3.2 milliequivalents per gram of dry resin or 1.4 milliequivalents per milliliter of hydrated resin¹⁰. A copy of the anion exchange resin behavior for different metals as a function of the concentration of HCl is found in

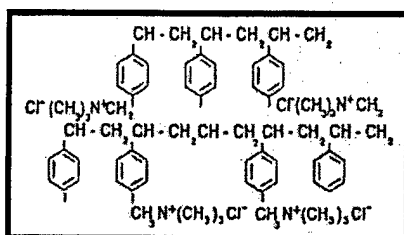


Figure 4.5 Molecular Structure of Styrene-Divinylbenzene Crosslinked Copolymers with Attached Groups for AG1: Bio Rex Resin AG1 showing a molecular diagram of the strongly basic anion exchange resin.

Appendix 4, Annex A.

After the third and final column rinse, the same technique was used to fill the stem with MQ H₂O, but the reservoir was only filled a third of the way up with water. A key part of the column preparation was to ensure that no air bubbles remained in the stem. This can cause problems, mainly a very slow to nil flow rate through the column. After shaking a saturated mixture of resin in a small squirt bottle until the resin was fully suspended, the remainder of the reservoir was filled with the mixture. The column was then placed in a settling stand that is shown in Figure 4.4. After the resin settled in the stem, the excess resin material remaining in the reservoir was removed with a 100 μ L pipettor moved in a slow circular motion around the

sides of the reservoir. More water or more resin mixture was added until a small concave bead remained at the top of the resin in the stem.

The column chemistry was divided into five basic steps: cleaning, equilibrating, loading, washing, and eluting. The column chemistry is

**COLUMN CHEMISTRY FOR URANIUM USING AG1X8 CL- FORM
ANION EXCHANGE RESIN**

Pre-Clean reservoir	500 μ L	6.0 N HCl	1x
Clean	500 μ L	0.1 N HCl	9x
Equilibrate	200 μ L	3.0 N HCl	1x
Load Sample	150 μ L	3.0 N HCl	1x
Wash One Drop~30 μ l	30 μ L	3.0 N HCl	3x
Wash	200 μ L	3.0 N HCl	3x
Wash	200 μ L	6.0 N HCl	1x
Elute U	250 μ L	0.1 N HCl	1x

Table 4.2 Column Chemistry for Concentrating the Uranium with an Anion Exchange Resin: This table show the volume and steps taken to elute the uranium from the aliquot taken from the microcentrifuge tube. Note the concentration of the hydrochloric acid through the steps.

expressly written out in Table 4.2.

After properly preparing each column and ensuring a good flow rate, they were removed from the settling stand and placed into a carousel shown in Figure 4.6. The order that each sample was loaded in the carousel is in Appendix 4, Annex B.

After the beakers fluxed in the hot acid and hydrogen peroxide bath, they were uncapped and were allowed to dry down under the fume hood. After two hours, some of the samples had completely dried down (S8S and C8S) and five drops or 150 μ L of 3.0 N HCl were added to these samples. The drying down process continued for the rest of the samples, closely

monitored to ensure that none of the salts escaped from the beaker. After just over three hours, all the samples in the beakers were dry and 150 μL of 3.0 N HCl were added to each one. The beakers were capped and then set aside to cool. After the columns were cleaned and equilibrated, the supernatant solutions and blanks were loaded onto the first series of columns. The precipitate solutions were saved for the second series of columns.

The solutions that seep through the columns up until the elution step

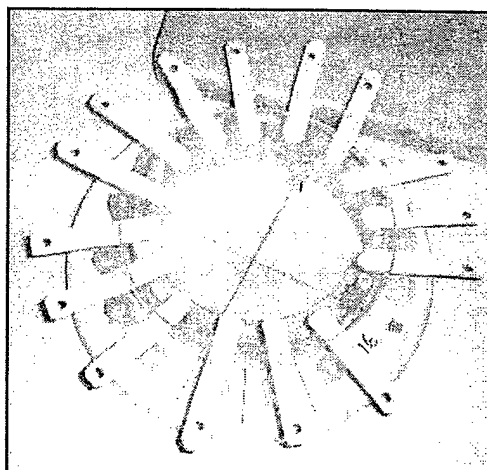
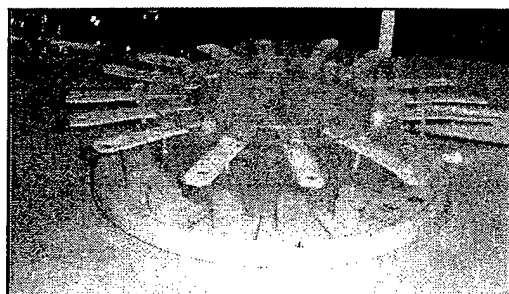


Figure 4.6 Column Carousel: The anion exchange columns were set in this carousel as the column chemistry steps were executed. Number labels fall on each spot where a column is set up.

are caught into a small basin underneath the column. This rinse was later discarded. For the elution, a new set of Savillex beakers was used. They were placed under the column just prior to the elution. After the elution step for series one columns, the beakers were capped. These were later opened in the lead laboratory where a small drop of 0.1 M H_3PO_4 was added

to the beaker solutions. The drop of phosphoric acid comes out of a modified dropper bottle with thin spaghetti tubing such that each drop is approximately 3-5 μl . H_3PO_4 is used because of its high boiling point. Properties of concentrated hydrochloric and phosphoric acids are listed in Table 4.3 to show the large difference in boiling points. The time that each step of Table 4.1 was performed is recorded in Appendix 4, Annex C.

<i>Table 4.3 Acid Properties used in the Columns:</i> This table shows the large difference in boiling temperatures between HCl and H_3PO_4 .				
<i>ACID</i>	<i>Density (g/mL)</i>	<i>N</i>	<i>Boiling Point ($^{\circ}\text{C}$)</i>	<i>Boiling Point ($^{\circ}\text{F}$)</i>
H_3PO_4	1.84	18.32	339.0	642.2
HCl	1.10	6.15	109.7	229.5

During the final drying, the 250°C temperature drives away all the chloride ions and leaves behind the uranium in the small amount of phosphoric acid. The uranium is now in the final form that will be used in the loading procedure for the filaments. In addition to the phosphoric acid, the blank samples labeled blank 11 through blank 15 are spiked with a mixed lead/ uranium spike to determine the uranium present in the reagents. The spike is a standard solution with specific isotopic ratios of ^{205}Pb , ^{233}U , and ^{235}U . The weight of the spike bottle after each application is measured with a Mettler 160 scale. The spike weights are listed above in Table 4.4. The spiked samples were then placed onto the hot plate to complete the process described above.

Table 4.4 Uranium Spike Weights: The weights of the spike bottle are used in determining the uranium concentration of the blank samples.

Weight in Spike Bottle (g)		
30.0069		
29.9960	Δ in Blank 11	0.0109
29.9846	Δ in Blank 12	0.0114
29.9769	Δ in Blank 13	0.0077
29.9685	Δ in Blank 14	0.0084
29.9583	Δ in Blank 15	0.0102

The second series of columns for the precipitate samples was then initiated. The same cleaning and preparation procedure described above for the columns and resin setup was performed. The column reservoirs were first filled completely with 6.0 N HCl and later with the first of six 0.1 N HCl flushes. After the last flush, the column procedures in Table 4.2 were started for the second set of columns. The time that each column step was accomplished is also in Appendix 4, Annex C. After the column steps were complete, the Savillex beakers from the second series were placed for the final dry down with the phosphoric. After the drying down process, the samples from this series were capped tightly and awaited final TIMS filament loading with the samples from the first series of columns.

4.3.2 TIMS Filament Loading

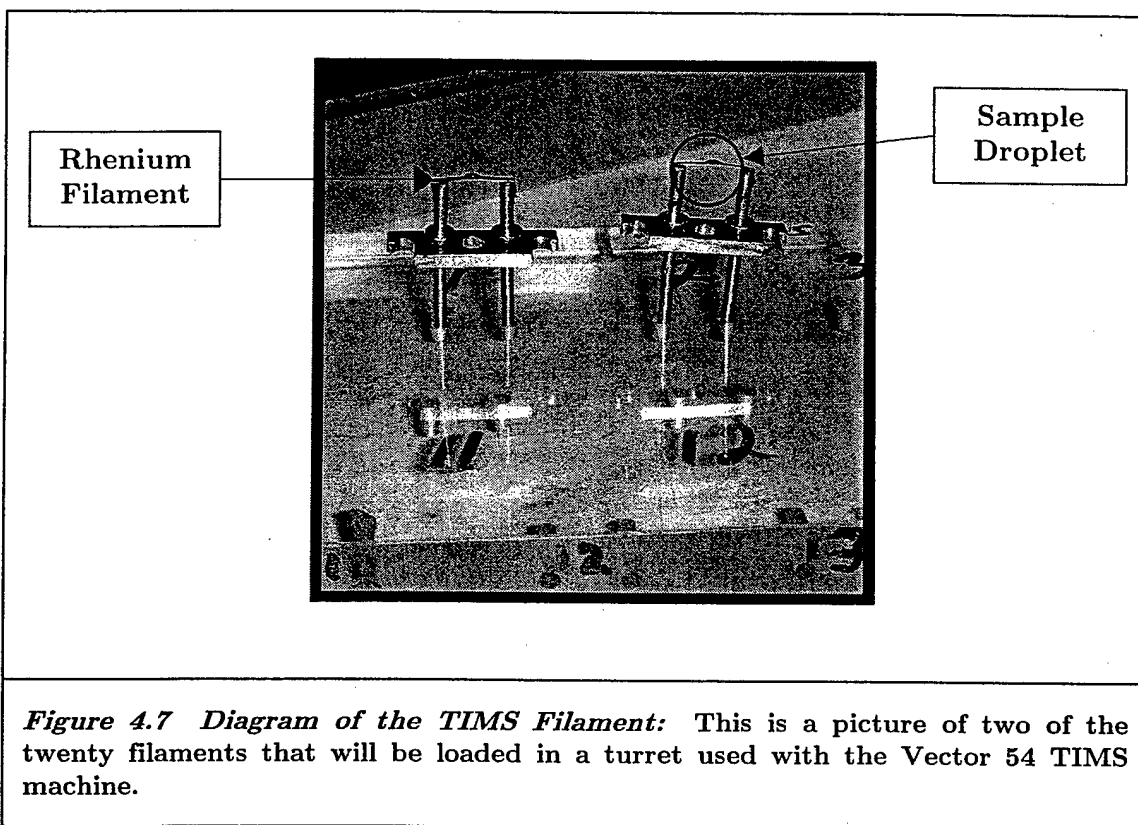
In most TIMS machines, including the machine used in this study, the solid analyte is emitted from a heated rhenium filament that has a high work function and low volatility. The filament is welded onto steel posts set in a ceramic insulator. Prior to loading any samples onto the filaments, the

filaments are heated at high temperatures corresponding to two amps applied across the filament for ten minutes and four amps for twenty minutes under a vacuum of approximately 10^{-8} millibars (mb). Once the samples are loaded on the filaments, the mass of the desired element becomes a major concern for many reasons including: 1) enough analyte for a long steady ion current 2) mass fractionation corrections and 3) reproducibility of the results. The TIMS sensitivity primarily depends on the mass of the element of interest on the filament. The limit is normally measured in terms of nanograms (ng or 10^{-9} grams). The minimum amount of uranium needed for a good signal in the VG Sector 54 TIMS that was used for in this research was 100 ng¹¹.

The preparation of the U500 standard samples used as the empirical standard began by re-examining the concentration of the solution produced earlier by dissolving the enriched U_3O_8 in nitric acid. The concentration of the U500 solution produced earlier is converted from moles per liter into parts per million (ppm). The original mass of enriched U500 measured was 0.5457 grams (discussed in Chapter 3). The corrected molar mass of U500 due to the enrichment is 837.64 grams/mol comprised of three uranium atoms and eight oxygen atoms. 0.5457 grams of U500 corresponded to 0.4624 grams of uranium atoms. This was dissolved in 20 mL of 7.0 N nitric acid with a density of approximately 1.2 gram per mL¹² and total solution weight of 24.5457 grams. This equates to 18838 ppm U500 where ppm is defined as μg of uranium per gram of solution or 23120 ng per μl . A aliquot

of this solution was then diluted with MQ H₂O to make a 1 ppm concentrated solution that would be applied to the filaments.

The next step was the actual preparation of the samples and standard solutions on the filament. MQ H₂O, five μ L, was added to each Savillex beaker described at the end of the chemical preparation above. An aliquot (usually around 1-3 μ L) was loaded onto a rhenium filament using a finger pipette and spaghetti tubing. Ultra pure colloidal graphite (Aquadag



Colloidal Graphite produced by Ted Pella Inc, Lot No:040297), one to three μ L depending on the filament, was added to the drop on the filament. Colloidal graphite is essentially a binder that affects the ionization efficiency of the filament. The width of the filament was about 0.03 inches and the

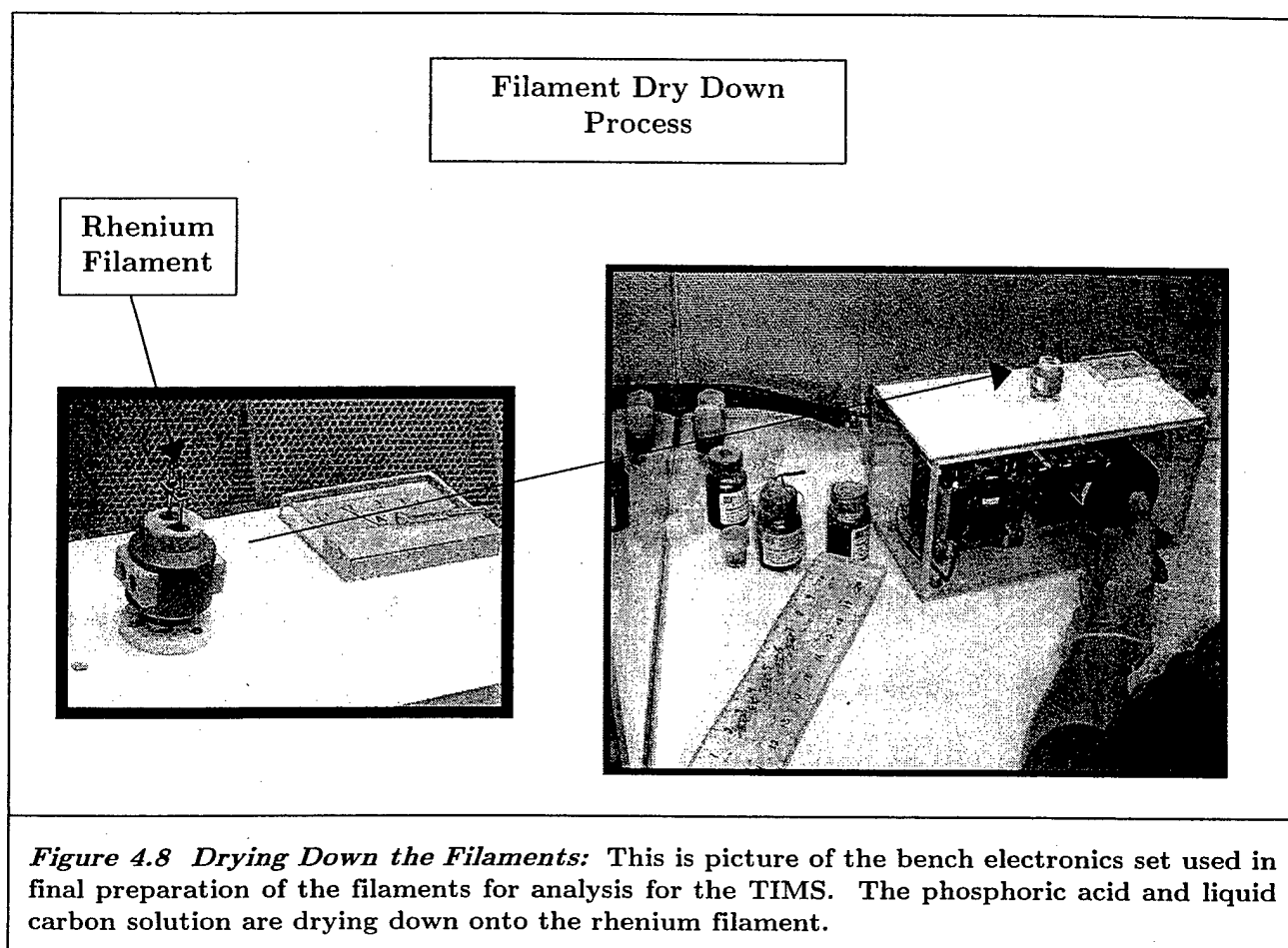
droplets were about the same. A picture of the filament with the droplet is shown in Figure 4.7.

The filament preparation varied for each turret load by the amount of graphite, amount of sample, and order of preparation. This is noted in Appendix 4, Annex D. Except were noted in Annex D, the sample volume was placed first on the filament. Then the colloidal graphite was dropped on the top and dried down in a process using electric current. This loading process is referred to as regular loading. Certain filaments in the second, third, fourth, and fifth turret were prepared using a preparation technique known as the sandwich loading technique. The sandwich method is described in the sequence below:

1. One drop ($\sim 1 \mu\text{L}$) of graphite on filament
2. Air dry down
3. Add H_3PO_4 ($1 \mu\text{L}$ of either 1 M or 0.1M H_3PO_4) and U500 or samples volume
4. Air dry down
5. One drop ($\sim 1 \mu\text{L}$) of graphite on filament
6. Air dry down
7. Amperage applied

The sandwich process was applied without a top layer of graphite for filaments three and four in the second turret. The only other variation in the sample preparation was the thickness of the colloidal graphite solution. After turret one, the colloidal graphite applied to the filaments was mixed slightly thicker from 1:5 to 1:2.

The filaments were allowed to air dry under a fume hood. Once the



filament had finished air drying, it was placed into a sample holder. Current was manually applied on the filament, starting from 0 and slowly increased to 2.6 amps. At this point, the phosphoric acid fumes off and, as soon as a slight glow on the filament was seen, the current was turned off. This process took about a minute for each filament. A picture of the bench where this process took place and of the sample holder used in this process is shown in Figure 4.8. The samples are placed in the twenty filament turret holder and inserted into the TIMS machine.

4.4 TIMS Operation

The principles and operation of most TIMS machines are very similar. The machine used to study the uranium isotope ratios in this research was a VG Sector 54 TIMS. The description in this section is generic for most TIMS machines, but certain parameters are specific to the VG Sector 54. The VG Sector 54 is shown in Figure 4.9.

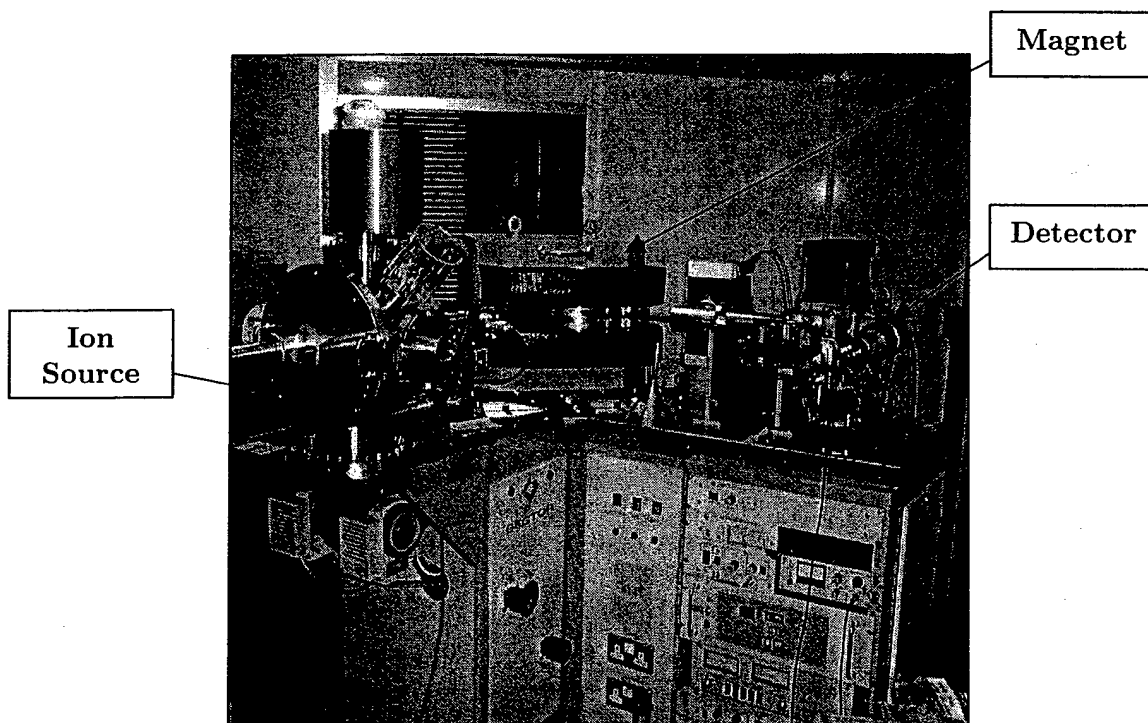


Figure 4.9 Vector 54 Thermal Ionization Mass Spectrometer. This is a digital photo of the Thermal Ionization Mass Spectrometer used to measure the uranium isotope ratio.

Prior to every analysis, the entire chamber in the TIMS machine is pumped down for 45 minutes. Liquid nitrogen is placed in a cold trap decreasing the vacuum to near 5×10^{-8} mb. Within a few hours, this reduces the pressure to near 1×10^{-9} mb and stabilizes. The twenty rhenium filaments loaded on a rotating turret inside the chamber are slowly warmed up in

about ten minutes by increasing the amperage to 4.1 amps. Increasing amperage, and thus increasing temperatures, proceeds manually beyond this point.

The solid analyte is then heated off the rhenium filament in the evacuated chamber using an ion and turbomolecular pump. The temperature of the filament T cause an evaporation of n neutral uranium atoms from the filament, which are accompanied by n^+ positive ions according to equation 4.1¹³.

$$\frac{n^+}{n} = e^{(W-E)/kT} \quad (4.1)$$

W is the work function of the rhenium filament. The work function is a measure of the minimum energy required to extract an electron from the surface of a solid. It is defined more precisely as the energy difference between the state in which an electron has been removed to a distance from the surface of a single crystal face that is large enough that the image force is negligible but small compared to the distance of any other face (typically about 10^{-4} cm), and that the electron is still in the state of the bulk solid. The work function depends on the cleanliness of the crystal surface and for reasonably clean surfaces the work function for rhenium is 4.72 eV for thermionic emission¹⁴. E is the first ionization energy of the evaporated material, which for uranium is 6.194 eV. k is the Boltzmann constant of 8.62×10^{-5} eV/ K and T is the filament temperature in degrees Kelvin¹⁵.

The ratio in equation 4.1 is known as the ionization efficiency and it is another limiting factor on the sensitivity of the TIMS. Equation 4.1 is a good first approximation, however there are many other factors that affect

this ratio. The actual ionization efficiency is a result of the physical characteristics of the sample matrix and the geometry of the bead on the filament. As a first approximation, at 2000°C, a typical temperature during the analysis, the ionization efficiency for uranium using equation 4.1 was 5.52×10^{-4} .

The resultant ions from this process are accelerated towards a mass analyzer by a high voltage applied between the source assembly and an accelerator slit. An applied magnetic field deflects the ion beam along a radius of curvature of 27 cm creating separate ionic beams based on its mass/charge ratio. It is collimated into a tight ion beam by applying smaller potentials to a series of slits. The relative abundances of isotopic masses of a given element in this ion beam are not in general identical to the abundance from the original sample owing to mass fractionation. Mass fractionation refers to the tendency of the sample's lighter isotopes to ionize at a quicker rate at earlier times in the sample analysis. This effect and correction for this will be discussed in greater detail in the observations in Section 4.5¹⁶.

The ability of a mass spectrometer to resolve adjacent ion beams accelerated by the magnetic field depends on the width of the ion beam that is controlled mainly by the width of the source slit and the curvature radius of the analyzer tube. The VG Sector 54 uses a Compaq 386 running DOS based Fisons software version 3.12 to automate many of the functions of the machine. These functions included: 1) selecting the individual filaments for analysis from the twenty filament sample barrel, 2) applying a steady current across the filament, 3) peak searching and source focusing, 4) setting

and maintaining the magnetic field, and 5) data collecting and reducing. The VG Sector 54 normally has seven different Faraday Detectors noted as L1, L2, Axial, H1, H2, H3, and H4 (Note: It also has one Daly detector system available for use on the axial position, but we did not use this detector for the isotopic ratio measurement). The Faraday cup detects ions as positive electric charges, and hence has essentially an equal response to different ionic masses. It consists of a carbon coated metal box with an inclined metal electrode that collects the incoming ions¹⁷.

Positive ions striking the electrode cause an accumulation of positive electric charge, which is neutralized by an electric current flowing from the earth through a large 10^{11} ohm resistor. The potential difference across the resistor, measured by a high impedance voltmeter, is proportional to the ion current (the sensitivity is typically around 10^{-11} Amps per volt). This detector has an equal response to all ions and has low electrical noise. However, the ion signal takes time to build up or decay after switching an ion beam in or out of the cup. Electronic noise in the resistor restricts the Faraday cup to measurement of ion beams greater than 10^{-15} Amps¹⁸.

The slit size is set for each detector. Most of the detectors in the VG Sector have a fixed slit size of 1 mm, except for the axial detector. The axial faraday cup is the only detector that is able to reduce the slit size, thereby increasing its mass resolution, but reducing its sensitivity. However, to keep as many variables as possible constant, a 1 mm slit setting was used on the axial detector to have a comparable signature with the other detectors used in the isotope ratio measurement.

The static multi collector measurement mode was used to collect the isotopic ratio of the samples. The TIMS machine measured the isotopic ratio for uranium by comparing the intensity simultaneously in the two ion beams falling in the faraday cup detectors located at L1 and AX primarily. The L1 and AX Faraday detectors were used to measure the ^{238}U and ^{235}U mass beams respectively (AX: ^{238}U , L1: ^{235}U). The detector spacing for examining uranium metal is in reference to the axial detector using arbitrary motorized steps for the VG Sector 54. For uranium metal, the axial detector is fixed and set for ^{238}U ion flux. L1 is set at the 959 step referenced off the axial detector and set for the ^{235}U ion flux. L2 is at 1495 step and used for the ^{233}U ion flux¹¹.

As the filaments come out of the warm up mode at 4.1 amps, the ^{238}U beam is focused into the AX detector. The spread of the beam peaks is the same, but by adjusting the high voltage potential on the lenses, the beam is focused and centered into the cup until a flat top peak is achieved. The slit focus sequence by the software is in the following order:

- D-Focus
- Z-Focus
- D-Bias
- Z-Bias
- Slit
- Extract
- Source

Adjusting the high voltage of the lenses shifts the whole array of the spectrum. The high voltage tuning is a more stable adjustment than attempting to move the beam by changing the magnetic field, which is kept constant throughout this process¹¹.

Focusing the ion beams is an iterative process. Adjustments are not made by jumping to a particular temperature or amperage (amp) setting and focusing the beam. Rather it is a slower, more methodical adjustment. As it comes out of warm up at 4.1 amps, the first major focusing takes place. The amperage is increased manually in steps of 0.01 amps up to the measurement amperage, usually around 4.3 amps for our analysis. At this point the machine enters into a second focusing adjustment. Subsequent focusing also occurs for every block measurement¹¹.

The software automates much of the ion flux intensity measurements for the isotopes. It divides the measurements in cycles and blocks. Each cycle consists of five individual measurements. There are ten cycles per block, where each block takes about two minutes. In general, ten blocks per bead were recorded at a fixed amperage setting. The actual flux intensity measurements are in Appendix 4, Annexes F through I. The software parameters were set up to disregard up to one cycle measurement if the measured ratio was more than two standard deviations from the mean of the block measurement. The last temperature in the cycle was recorded as the block temperature. When the temperature reached 2030°C, the software interface continued to record only 2030°C. A pyrometer outside of the

machine was then used to get accurate temperatures for blocks operating at temperatures above 2030°C.

The beam intensity is displayed on an LCD display directly on the TIMS in millivolts (mv) or on the computer display in amperages (10 mv on the LCD display equals 1×10^{-13} amps on the print out from the computer generated information). Beam strengths are generally maintained at or above 100 mv or 1×10^{-12} amps. Low beam strengths or values less than above meant that there was very little uranium mass on the filament or that the filament temperature was not hot enough.

4.5 Observations

TIMS was used twice during this research. The first TIMS analysis was performed to investigate the isotopic ratio of the uraninite solid from the second bacterial reduction experiment. The uranium media delivered to the bacteria at that time came from an older uranium acetate salt by Fisher Scientific Company. Lot number and much of the manufacture information were difficult to obtain because the identifying label was nearly gone. The initial results from these experiments can be found in Appendix 4, Annex E. The net result observed from sample AO was that the uranium acetate salt was produced from a depleted uranium source. This pushed the mean $^{238}\text{U}/^{235}\text{U}$ ratio well above 307 with individual block values in a twenty block measurement as high as 308.152 and as low as 305.516. This saturation of ^{238}U and depletion of ^{235}U created problems when trying to compare the ion beam intensities and correct for instrumental or mass fractionation. The ion beam intensity for the ^{235}U was simply too low and unreliable that the TIMS

was unable to resolve the isotopic ratio within a precision necessary to detect any biologic fractionation.

To mediate this dilemma, an enriched uranium sample that had equal amounts of both isotopes was found. The New Brunswick Laboratory operated by the United States Department of Energy supplies enriched certified reference material (CRM) for precise isotopic work. CRM U500 was selected because the ratio between the two isotopes was nearly one to one. The technical data from the certificate of analysis is in Table 4.5.

<i>Table 4.5 New Brunswick Laboratory Certified Reference Material Certificate of Analysis for CRM U500, Uranium Isotope Standard.</i>				
	²³⁴ U	²³⁵ U	²³⁶ U	²³⁸ U
Atom Percent	0.5181 ±0.0008	49.696 ±0.050	0.0755 ±0.0003	49.711 ±0.050
Weight Percent	0.5126	49.383	0.0754	50.029
The uncertainties for the isotopic composition are 95% confidence interval for a single determination.				
July 5, 1994 Argonne, Illinois (Revision of NBL Certificate Dated October 1, 1987)				
Carleton D. Bingham Director				

Using the information in Table 4.5, the baseline isotopic ratio for ²³⁸U to ²³⁵U is 1.0003±0.0014. The key to our ability to identify biological fractionation was to minimize the instrumental or mass fractionation. The purchase and use of U500 served two purposes. It improved our ability to detect any biological fractionation of the reduction process, and it served as an empirical standard to benchmark mass fractionation behavior. U500

arrived in the solid form of U_3O_8 , a mixed oxidative state of uranium VI and IV. The enriched solid sample was then converted into a uranium acetate solution in a method covered in Chapter 3.

The samples loaded in turret number one are listed in Appendix 4, Annex D. Turret one was our first baseline for the empirical behavior of the U500 standard and the first look at supernatant signature of the control samples. The primary effects investigated were the effect of H_3PO_4 , graphite mixture volume (1 and 3 μL), sample load amount (1 and 3 μL), and

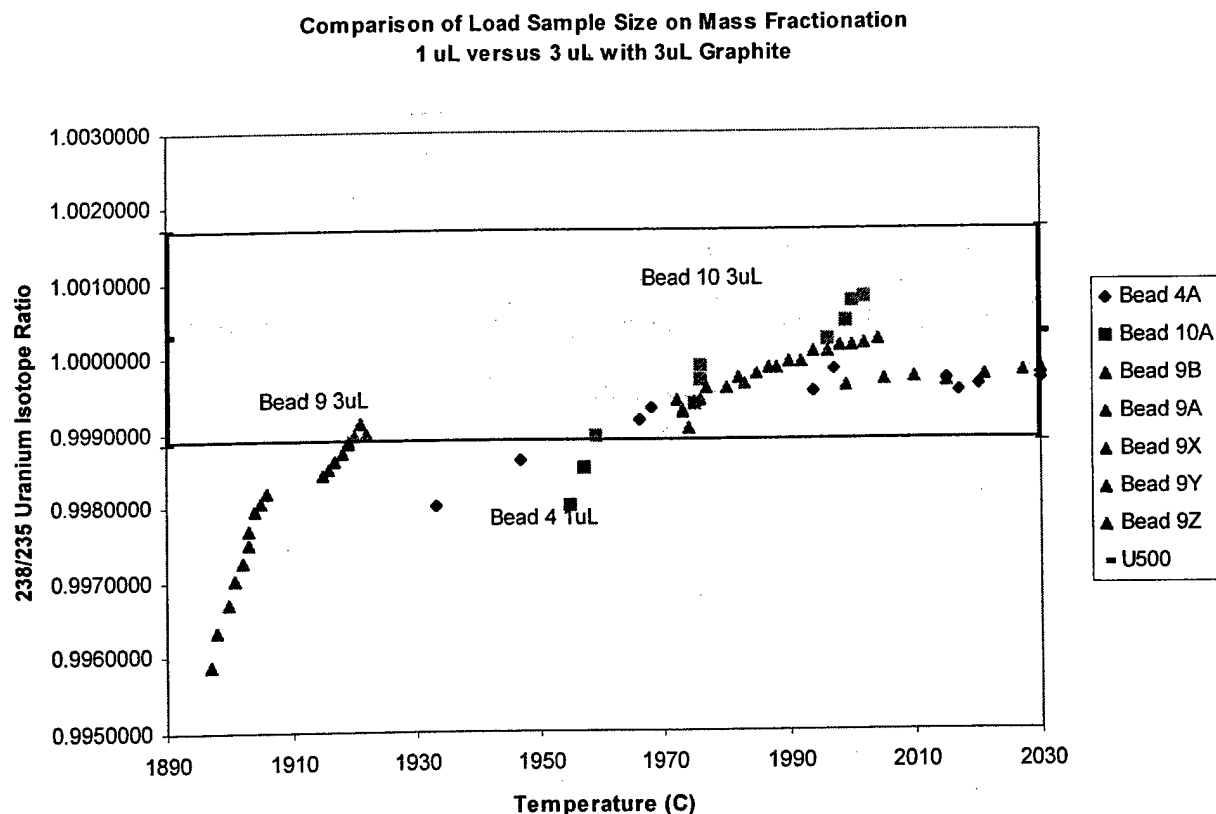


Figure 4.10 Comparison of Fractionation Behavior with Temperature and Load Sample Size in Turret One.

temperature on mass fractionation. All filaments were prepared using the regular technique. Turret one also provided the raw intensities for the

isotope dilution calculations to determine the uranium concentration in the reagents. Generally, most of the filaments provided reliable and stable beam intensities. Beads seven and eight were not run because of the observed behavior of the bead with only 1 μL of graphite in the earlier filaments.

One of the most significant results was then comparison of load size effect on the fractionation behavior. Figure 4.10 looks at samples that were prepared similarly, with the only difference in the load amount. Bead four with 1 μL is compared to beads nine and ten with 3 μL as it fractionates as a function of filament temperature. The pattern is nearly identical in the temperature range of 1970 to 2030 despite a difference of three times the mass of the samples. The shaded region on the isotopic graph represents the isotopic ratio of U500 using the certificate of analysis values and standard deviations of the atomic percentages

The control supernatant samples were prepared with 1 μL of sample and 3 μL of graphite. They were measured in three consecutive blocks of ten at constant amperages 4.30, 4.37, and 4.40. Filament 19, which had control sample C24, showed an extremely low and unreliable beam intensity. The behavior of all other control samples is graphed in Figure 4.10, and it shows similar ratios and mass fractionation behavior for all the control samples. This confirms the assumption earlier that chemical fractionation was not a factor in this experiment. The total isotopic ratio behavior for all filaments in turret one is graphed as a function of consecutive bead measurements. The graphs, along with the raw data are in Appendix 4, Annex F.

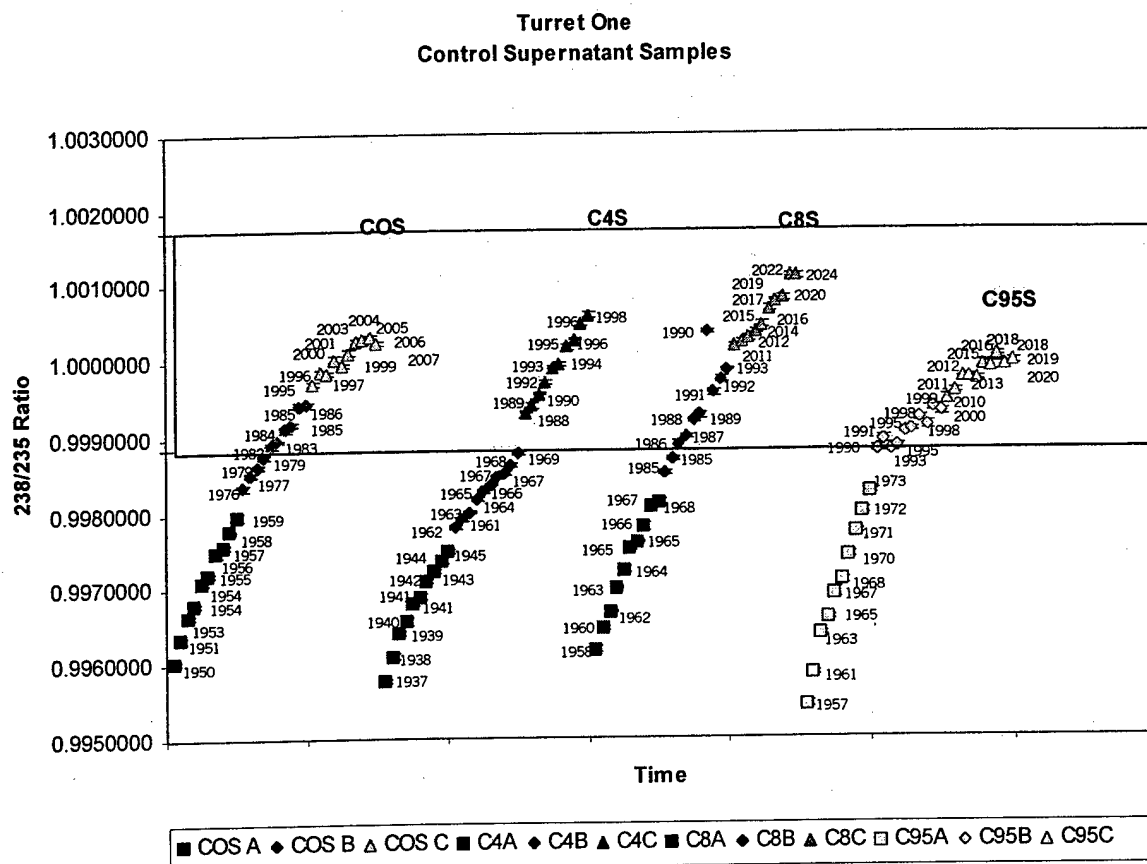


Figure 4.11 Control Samples C0, C4, C8, and C95. This graph shows the similar isotopic ratios of the control samples. It demonstrates similar mass fractionation behavior. A series is at 4.30 amps, B series is at 4.37 amps, and C series is at 4.40 amps with the corresponding filament temperature in degrees Celsius next to the data point.

Table 4.6 shows the uranium concentration of the blank samples using isotope dilution. Isotope dilution is best described in 17. Isotope dilution or ID uses a known mass m_s of spike that is mixed with an unknown sample. The isotopic composition of the element of interest in the mixture is then determined, and expressed by the ratio of two isotopes A and B where $R_{\text{mix}} = A/B$. This is then related to mass by equation 4.2. The natural values for uranium are used for A_E , $X_{A,E}$, and R_{Sample} . The spike's isotopic ratios were 1.01106 for $^{233}\text{U}/^{235}\text{U}$ and 0.007614 for $^{238}\text{U}/^{235}\text{U}$. The results show an

extremely small amount of uranium compared to the amount in the reagents: picograms (10^{-12}) as compared to micrograms (10^{-6}) which is the mass contributed from the test samples.

$$m_E = \frac{m_S A_E C_{B,S} (R_{mix} - R_{spike})}{X_{A,E} (1 - R_{mix} / R_{sample})} \quad (4.2)$$

where:

A_E = relative atomic mass of element E in unspiked sample ($235.196 \text{ g mol}^{-1}$)

$C_{B,S}$ = concentration of isotope B in spike ($1.60967 \times 10^{-9} \text{ mol of } ^{235}\text{U per g}$)

$X_{A,E}$ = atomic fraction of isotope A in element E in unspiked sample (3.79×10^{-3} for ^{238}U)

R_{sample} = isotopic ratio of A/B in unspiked sample ($^{238}\text{U}/^{235}\text{U} = 137.88$ for natural uranium)

R_{spike} = isotopic ratio of A/B in pure spike ($^{238}\text{U}/^{235}\text{U} = 0.007614$)

Table 4.6 Isotope Dilution Calculation of Blank Uranium Concentrations

<i>Sample</i>	<i>m_s (g)</i>	<i>m_E (pg)</i>
Blank 11	0.0109	5.69
Blank 12	0.0114	4.90
Blank 13	0.0077	6.59
Blank 14	0.0084	4.90
Blank 15	0.0102	5.60
Average Mass		5.54±0.62

The data gathered in turret one helped shape our next series in turret two. The addition of phosphoric acid on the U500 filaments helped promote more stable ion beam intensities. This was an important note because all of the test samples were prepared in this acid. In the second turret, samples

with 1 M H_3PO_4 were prepared to investigate its effect on the beam intensity.

It was also generally observed in turret one that at constant amperages as the sample burned off the filament the filament temperature increased and the ion beam intensities decreased with time. To moderate this, a thicker mixture of colloidal graphite was made for turret two that was

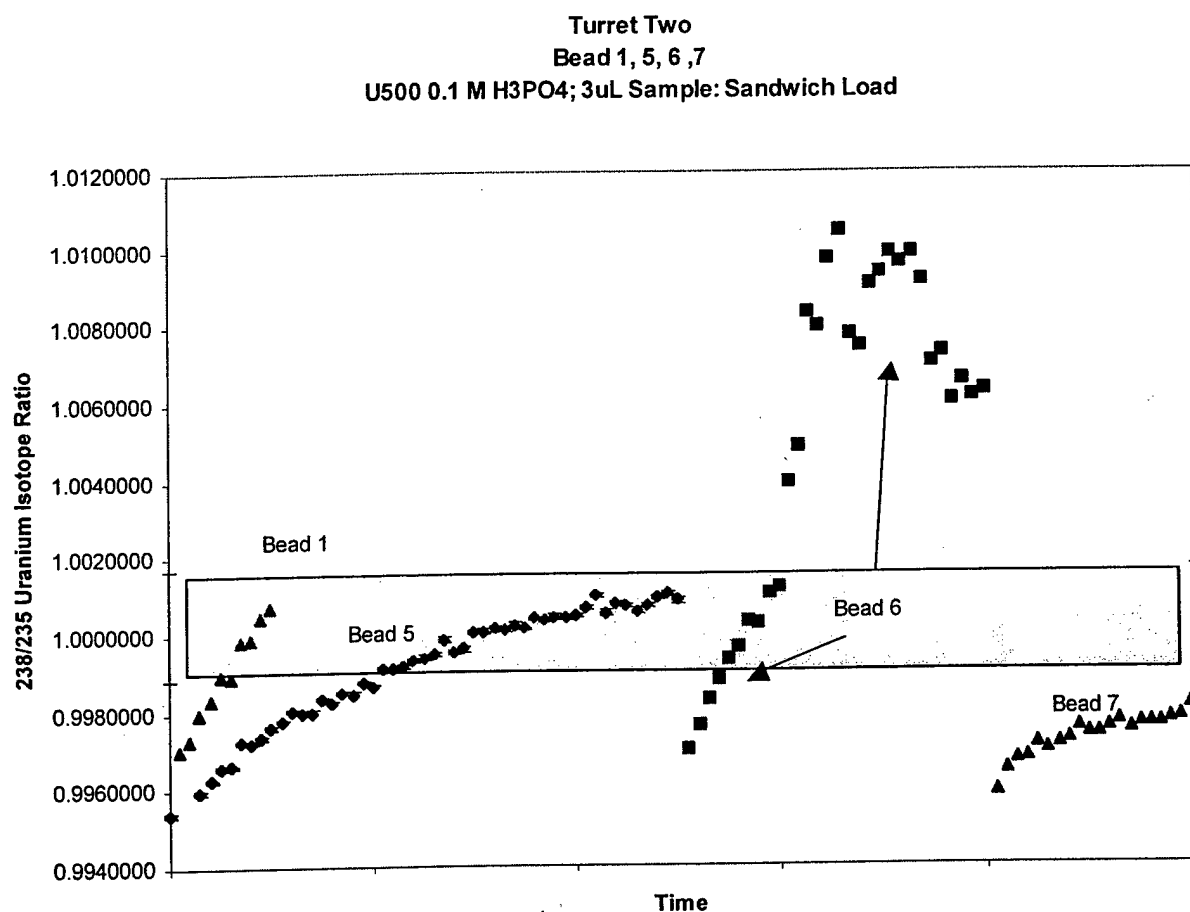


Figure 4.12 Sandwich Loading Technique with U500: This shows the behavior of the U500 standard when prepared using the sandwich method with respect to consecutive block measurements. The results seem to show a more consistent behavior in terms of controlling instrumental fractionation, that is changes in the isotopic measurement between each consecutive measurement. The first sample still showed a steep slope so the other samples with 1M were not run.

also used for the remaining turrets. The graphite mixture was doubled from the original mixture of five parts water, one part graphite to two parts water and one part graphite. In addition, the sandwich technique (described earlier) was used for the filaments in turret two, except for beads three and four, which did not have a top layer of graphite.

The results from turret two provided some interesting results. There were seven filaments prepared for this turret, all using the U500 standard. Only four were actually analyzed. Because of the rapid mass fractionation

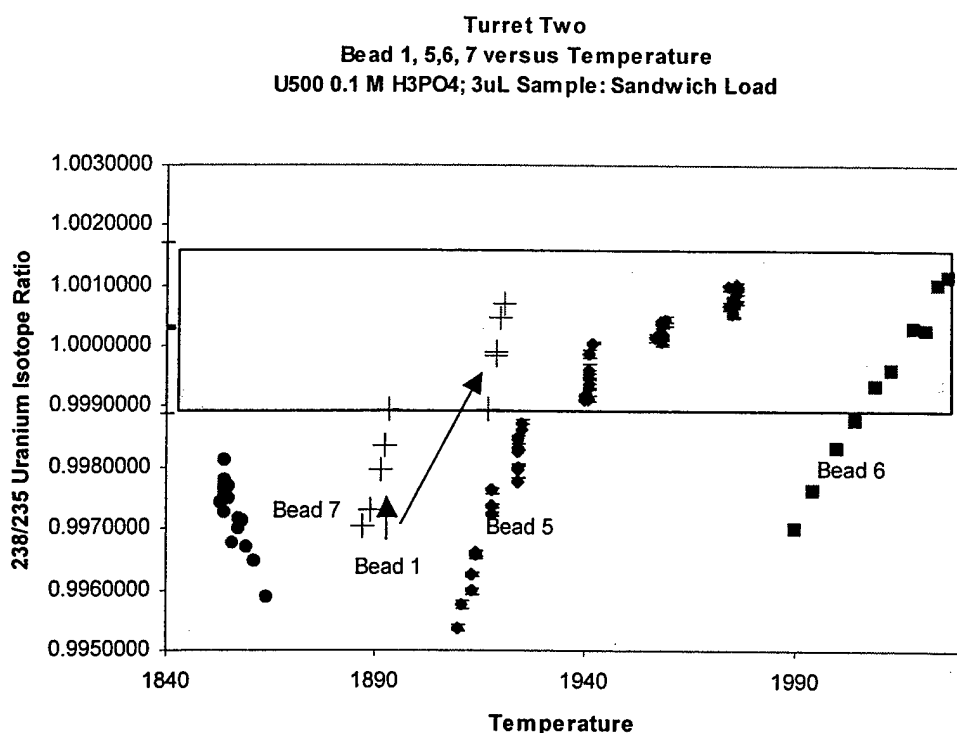


Figure 4.13 Sandwich Loading Technique with U500 as a Function of Temperature: This graph shows the same samples as in Figure 4.11, but referenced off the filament temperature. This chart seems to indicate a more erratic behavior. The amperage is increased in the different block measurement that usually results in increased temperature and isotopic ratio values. Higher temperatures usually reduce the instrumental fractionation but this also causes a more rapid burn off of the element of interest off the filament.

observed in bead one, filaments two through four were not run. This can be seen in the relatively steep slope of bead one in Figure 4.12. Figure 4.12 shows the fractionation behavior with respect to analysis time. Beads five and seven appear to be well behaved. However, when the fraction behavior is compared with respect to temperature in Figure 4.13, it appears to be much more erratic.

The next three turrets, noted as turrets three, four and five, were run that finally offered data of the test sample supernatants and precipitates. The filaments in turret three and four were all prepared with the sandwich technique. Only 1 μL of the sample solution was used to prepare these filaments. Bead seven (C4S) in turret three appeared to flake off yielding no ion flux when it was measured. In addition, very low beam strength values were observed for two beads of turret three (S24S-1, and S95S-1). This was somewhat expected because at these time intervals most of the uranium had been converted into solid uraninite. These were re-loaded with 2 of the remaining 4 μL of sample for filaments in turret four.

The results from turrets three and four indicated that the regular loading technique seemed to offer more consistent results than the sandwich method. The filaments for turret five for test samples S4S, S8S, S24S, and S95S were prepared with two μL and used the regular filament preparation method. The beam currents in this run were all higher except S95. The larger loads in both turret four and five, with 2 μL as compared to 1 μL , show a shallower slope in instrumental fractionation, meaning less

instrumental fractionation with more sample. The final results of all these runs including charted isotopic ratios is in Appendix 4, Annex H.

The charts in Annex H provided some very interesting information and at first glance indicated an apparent biological fractionation. This meant that over a certain period, the $^{238}\text{U}/^{235}\text{U}$ ratio got larger for the supernatants and smaller for the precipitates. Charts H-2-1 through H-2-6 show the total supernatant and precipitate ratios as both functions of filament temperature and consecutive bead measurements, with the regular loaded supernatant samples on a separate chart than the sandwich method. At this point, the precipitate ratios data were all from samples prepared with the sandwich method. However, the sandwich method did not appear to provide the most consistent and well-behaved data. The best results appeared to come from the regularly loaded supernatant samples. An example of these charts is shown in Figure 4.14. In this chart, the trend shows that at the higher temperature values where instrumental fractionation is minimized, the $^{238}\text{U}/^{235}\text{U}$ increased as the allowed bacterial interaction time increased. In other words, $\text{S4S} < \text{S8S} < \text{S24S} < \text{S95S}$ where S95S seemed to clearly stabilize at a much higher value than any of the other ratios.

Turret Three through Five
Test Sample Supernatant Isotopic Ratios as a Function of Temperature
Regular Loading

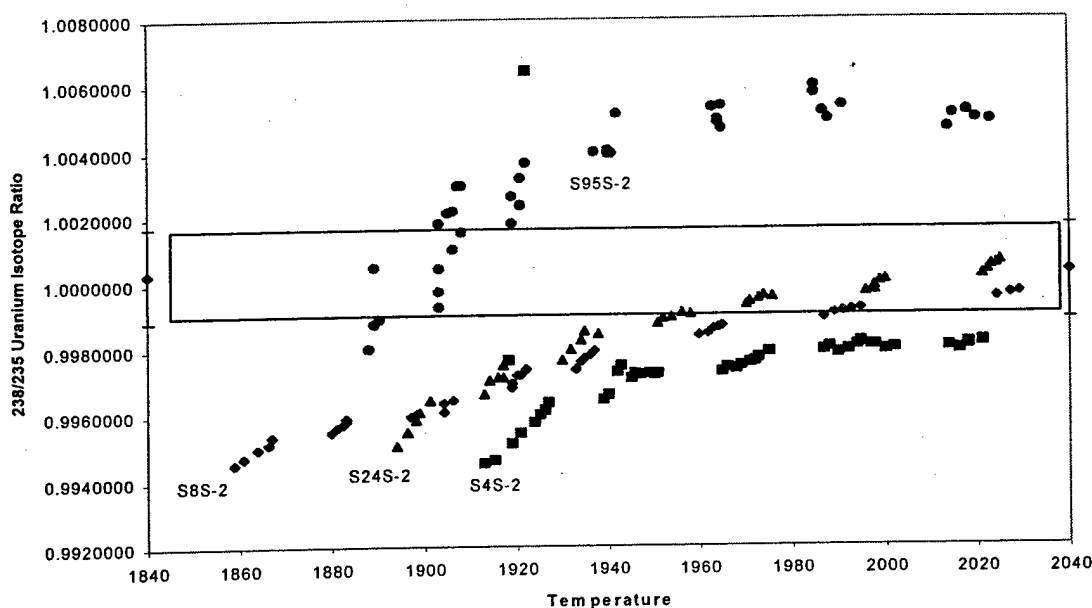


Figure 4.14 Test Sample Supernatant Isotopic Ratios: This chart shows the instrumental fractionation as a function of Temperature using the regular loading method for the filaments. Notice as temperature increases the slope decreases, especially at the 2000°C range. In addition, notice the ratio stabilizes at a higher point with each successive interaction time.

The next series of charts compare the supernatant and precipitate ratios directly for the interaction time periods of 8, 24, and 95 hours. Because the precipitate ratios at this point were all prepared with the sandwich method, only the sandwich method supernatant ratios were used in these charts. The block measurements that are closest in filament temperature are charted together and each chart clearly shows a measurable difference in the isotopic ratios of the precipitate and supernatant with the all supernatants higher than the precipitates. The temperature for each block measurement is shown in parenthesis next to the data point on the chart. The closest temperature comparison that is at a temperature that

minimizes the instrumental fractionation is shown in Figure 4.15 for the 95

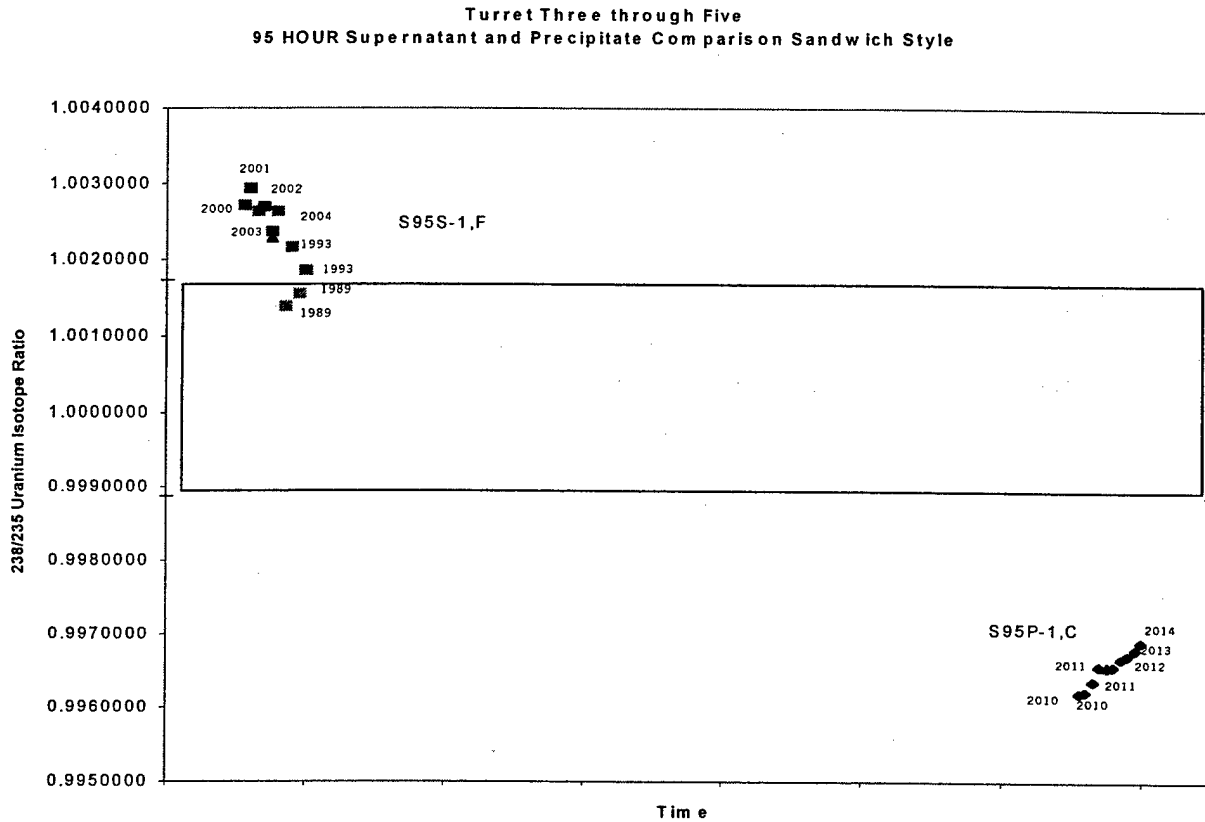


Figure 4.15 S95 Supernatant and Precipitate Ratio Comparison: This graph shows the ratio at similar temperatures of the 95 hour test sample's supernatant and precipitate isotopic ratios using sandwich prepared filaments. Although it seems to indicate biological fractionation, the filament load mass is very different and must be corrected.

hour test sample.

The last series of charts for these runs showed the sandwich and regular loaded samples for both precipitate and supernatants at each specific time interaction. SOS and COS are also charted together to show any isotopic ratio differences. The comparisons were graphed with the ratios as a function of temperature and consecutive block measurements.

Two factors required clarification before making any conclusions. The first was the precipitate and supernatant comparisons were made with the sandwich method, which was not as reliable as the regular loading method was. The second was the issue of filament load size. Although in turret one the data for differences of two or times the mass on the filaments appeared to behave similarly, the issue of three orders of magnitude differences was not adequately studied. It was observed that mass or instrumental fractionation is more severe at the lower temperatures. As the filament is warmed up, it loses more ^{235}U than ^{238}U and then stabilizes at temperatures near 2000°C . This effect has a greater impact on the isotopic ratio than a smaller sample would stabilize at than that of a much larger sample where the reservoir of atoms is much larger. This effect may be the reason that the supernatant ratios are so much different from the precipitate ratios at the 24 and 95 hour samples. Although the 95 hour isotopic ratios seemed to clearly show a fractionation, there was three orders of magnitude difference for uranium present. This can also be seen in the raw data ion beam intensities in Annex H-1.

Before concluding anything beyond this point, a closer evaluation was made of the filament load size that related directly back to the test sample concentrations. Concentration of the supernatant samples could be estimated directly back to the ICP-AES concentration values that were calculated Table 4.1. The precipitate solutions that were still in the microcentrifuge tubes were then analyzed for their concentration. Although the solutions had been sitting idle for almost 30 days, the precipitate samples

were in a strong acid solution of 6.3 N HNO₃ that should have prevented sorption. The microcentrifuge tubes were shaken manually for a few seconds and then spun for ten minutes in the centrifuge. Then 200 µL of the remaining 750 µL was removed with a calibrated Eppendorf 100-1000 µL pipettor and placed into a 15 mL polypropylene centrifuge tube. This was then diluted with five mL of MQ H₂O. The acid concentration was now estimated at 0.242 N HNO₃. Then 9.68 mL of 1.0 N HNO₃ was diluted with MQ H₂O to give 40 mL of 0.242 stock solution that would be used to dilute the ICP-AES uranium standard solutions.

U500 Precipitate Concentration Analysis by ICP AES
6 March 00

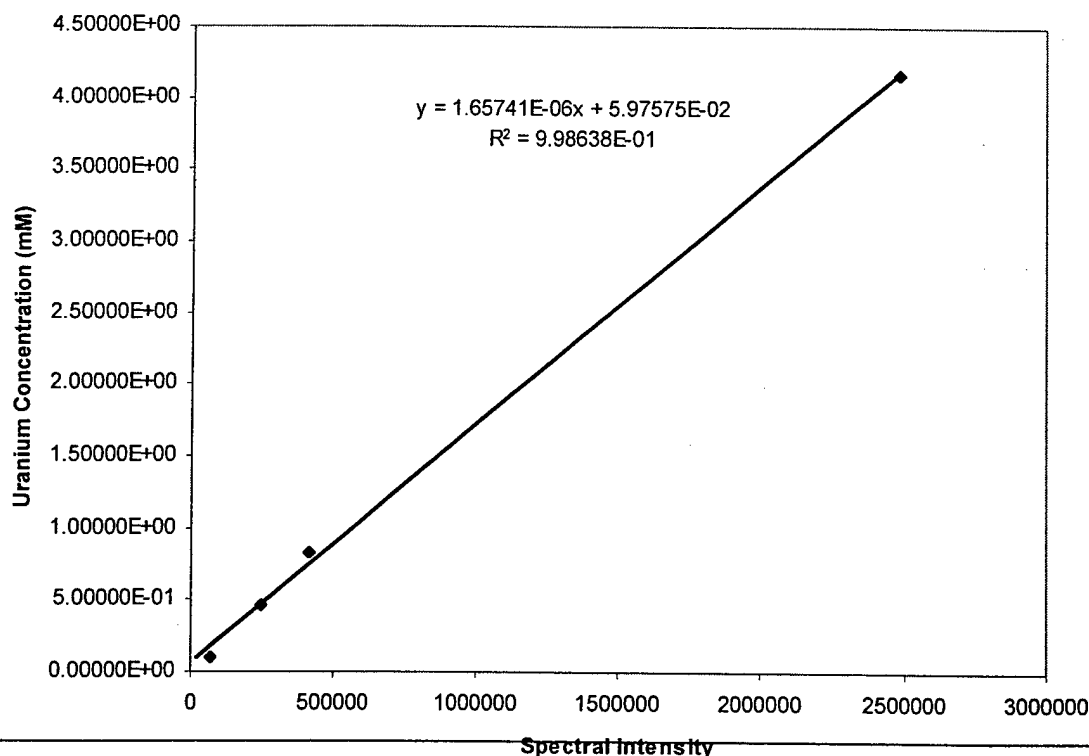


Figure 4.16 Calibration Curve and Concentration Determination for Enriched Uranium Acetate Precipitate Solutions: The photon intensities of 385.958nm for the standard uranium solutions with a known concentration are graphed and linearly regressed. This regression gives an equation for intensities as a function of concentration to determine the total uranium concentration in the precipitate solutions in the microcentrifuge tubes for S4, S8, S24, and S95.

The final ICP-AES data and calibration curve for the uranium standards is Table 4.7. Despite the high estimated concentrations in Table 4.6, the ICP-AES values were much lower. The ICP-AES data provided two

<i>Table 4.7 ICP-AES DATA for the Precipitate Solutions in the 1.5 mL Microcentrifuge Tubes</i>			
Sample	Concentration (mM)	Spectral Intensity (Mean Value of 3 Measurements)	Standard Deviation
Water		22442	127.2
Water		22822	74.4
MQ H2O		22847	196.4
MQ H2O		22510	301.3
STD 1	1.01E-01	70783	610.0
STD 2	8.32E-01	410548	4768.0
Water		22170	6.7
STD 3	4.62E-01	244879	2300.0
STD 4	4.16E+00	2481350	14919.0
S4	5.51E-02	69294	410.2
S8	7.60E-02	81918	758
24	1.30E-01	114190	698
Water		22184	108.8
95	1.40E-01	120490	955
Water		22499	120
	Calculated Concentration in Microcentrifuge Tubes (mM)	Moles of Uranium into dry down of $UO_2(NO_3)_2$	Exchange Capacity of the Resin
S4P	1.43E+00	3.58E-07	7.00E-05
S8P	1.98E+00	4.94E-07	7.00E-05
S24P	3.37E+00	8.42E-07	7.00E-05
S95P	3.64E+00	9.10E-07	7.00E-05

interesting observations. The first is that the concentration in the 1.5 mL tubes was significantly lower than expected. In Appendix 4, Annex J, estimates of the concentration were estimated to be almost three times as

high. This indicates that cellular sorption of uranium increased time as the time allowed interaction with the living cells increased, and that it appears that the rinses worked in removing this uranium from the precipitates. Secondly, the concentration was sufficiently low enough that the uranium did not saturate the resin.

The next step was to dilute the precipitate samples down. There were four μL of the S4P through S95P samples. One of the 5 μL had been used

Table 4.8 Filament Load Amounts for the Control and Test Samples

<i>Samples</i>		<i>Uranium (μg)</i>	<i>Notes</i>
Control		6.23	1/5 added to the CXS Filaments
Supernatants	S4S	5.3	1/5 used first in SXS-1 filaments that were loaded by sandwich method. 2/5 used in -2 samples.
	S8S	2.86	
	S24S	1.71	
	S95S	0.17	
Precipitates	S4P	144.3	1/5 used for SXP-1 filaments 4/5 remained.
	S8P	185.9	
	S24P	293.3	
	S95P	314.5	
Diluted Precipitate	S4P-2	1.11 $\mu\text{g}/\mu\text{L}$	1 μL used to prepare these filaments for turret six.
	S8P-2	1.43 $\mu\text{g}/\mu\text{L}$	
	S24P-2	2.26 $\mu\text{g}/\mu\text{L}$	
	S95P-2	2.42 $\mu\text{g}/\mu\text{L}$	

earlier to prepare the samples for turret three. These remaining 4 μL were diluted with 100 μL of MQ H_2O . Table 4.8 summarizes the calculated uranium amounts in the samples. From the results discussed for turret one earlier as long as filaments are loaded a mass of uranium that is within one

or two times the amount of another, the instrumental fractionation behavior should be similar. Turret six was then loaded according to Annex D using 1 μL of the diluted precipitate solution. The results from turret six including isotopic graphs and raw data are in Appendix 4, Annex I.

The results from the runs of turret six indicated that the separation shown in Figure 4.14 and 4.15 of the isotopic ratios observed in turrets three,

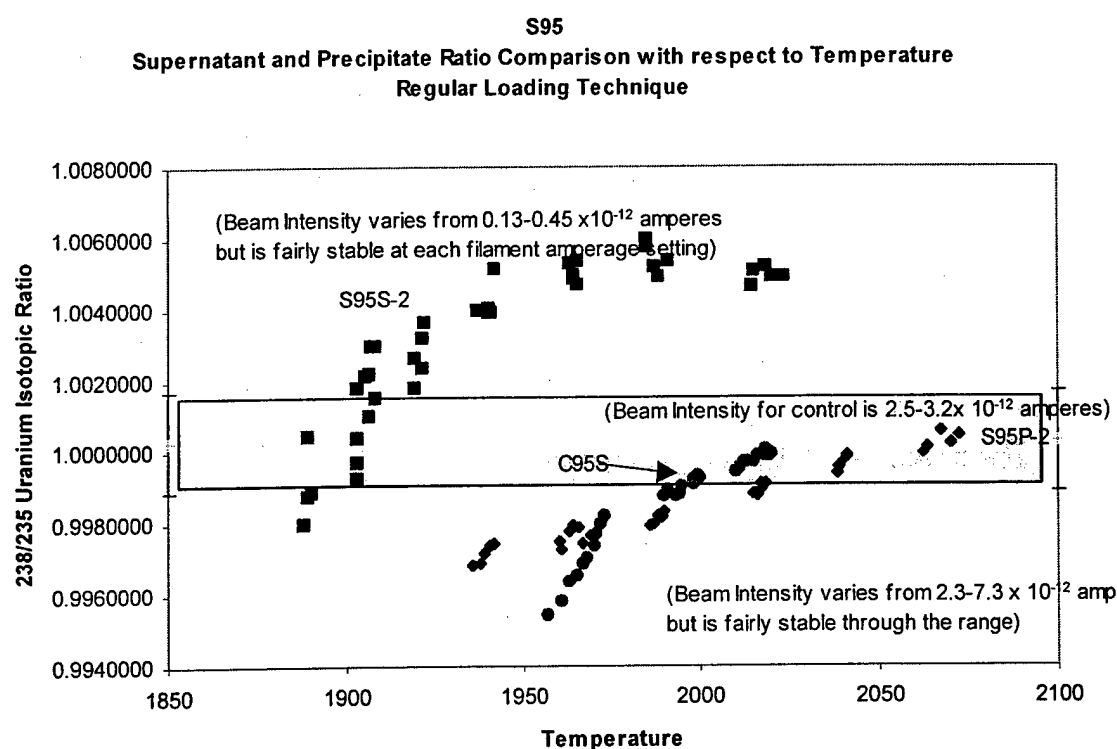


Figure 4.17 Comparison of 95 Hour Sample Isotopic Ratios: This chart shows the instrumental fractionation as a function of temperature using the regular loading method for the filaments. Although there is separation between S95S and S95P, the beam intensities are different indicating that there is a significant mass load difference in these filaments. When compared to C95, whose beam intensities are similar, this almost no difference in the isotopic ratio.

four, and five is a result of instrumental, not biologic fractionation. To help clarify the situation, the control samples were also added to the charts.

What is observed in S4 and S8 is a reverse trend of what was expected showing the precipitates higher than the supernatant ratio. The beam intensities for S4 are very similar indicating that the dilution step of the precipitate samples helped indeed match the filament load sizes. There is some separation between the supernatant and precipitate at the 95 hour sample, but the intensities are different. When the control data is shown, it lies very close to the precipitate behavior. The 95 hour samples are re-graphed this time using the regular loaded supernatant sample, the diluted precipitate sample, and the control sample in Figure 4.17. The remaining graphs in Annex I all indicate that there is not a detectable level of biological fractionation. Any fractionation appears to be more a function of load size and instrumental effects, than a biological kinetics effect.

4.6 Results and Conclusions

TIMS is a high precision device that is widely available to measure the isotopic differences in solid samples. TIMS analyzes these ratios by measuring the ion flux densities emanating off a heated element that forms positive ions as a function principally of the ionization efficiency of the element of interest and the work function of the filament. The ability to detect an accurate ratio requires correction of mass or instrumental fractionation, which is the tendency of the lighter isotopes to leave first. This research attempted to detect if an isotopic difference occurred in the uranium precipitates formed by the bacterial reduction that take places during the anaerobic respiration phase of the organism.

The results of this work are most clearly described in the charts of Appendix 4, Annex I. The isotopic fractionation appears not to be a result of biological fractionation, but instead on the load mass of the element of interest on the filament. Some areas could have been improved for future research of this effect. The first is to perform a more accurate concentration calculation using an ICP-AES or other method after the final chemistry step in the columns. This would give a greater ability to control the load sizes.

The second improvement would be to better remove the supernatant from the precipitate. For this research specifically, a better rinse technique would have been to use a 0.1 N HCl solution as opposed to MQ H₂O. Uraninite does not dissolve in HCl therefore it would have remained solid. However, the HCl would have been a stronger desorbing agent than water for any sorbed uranium species. The large differences between the calculated concentration of precipitate solutions in the microcentrifuge tubes and the estimated values in Appendix 4, Annex J seem to indicate a time dependent enzymatic effect of the organism grasping hold of the aqueous uranium species. In other words, the assumption in this report was that sorption increased with the dissolved uranium interaction time with the living cells.

This report concludes then that there is no concentrated build up of enriched uranium caused by the enzymatic precipitation by anaerobic bacteria living in the soil. The mass difference was not significant enough to cause a distinguishable difference in the reduction rates of either the ²³⁵U or ²³⁸U isotopes.

¹ E.H. Cordfunke, The Chemistry of Uranium, (New York, NY: Elsevier Publishing Company, 1969), 21.

² Brian Beard and Clark M. Johnson, "High precision iron isotope measurements of terrestrial and lunar materials," Geochimica et Cosmochimica, 63, 11/12 (1999): 1653-1660.

³ Iron Isotope Fractionation by the Bacteria *Shewanella* during Dissimilatory Reductive Dissolution of Ferrihydrite. ACS March 1999, 1 Abstracts, GEOC#068.

⁴ Josef R. Parrington, Harold D. Knox, Susan L. Breneman, Adward M. Baum, and Frank Feiner, Nuclides and Isotopes, Fifteenth Edition, (San Jose, Ca: General Electric Company, 1996), 24, 48-49.

⁵ Robin Gill, Modern Analytical Geochemistry. (Singapore, Indonesia: Longman Singapore Publishers Limited, 1997), 137.

⁶ Ibid., 135.

⁷ Ibid., 142.

⁸ Ibid., 141.

⁹ Ibid., 147-149.

¹⁰ Guide to Ion Exchange (Bio Rad Catalog Number 140-9997), 8.

¹¹ Interview with Mark Schmitz, PhD student, Massachusetts Institute of Technology, 31 January 2000.

¹² Robert C. Weast and George L. Tuve, eds., CRC Handbook of Chemistry and Physics 53rd Edition (Cleveland, Ohio: Chemical Rubber Company, 1958), D199.

¹³ Gill, 138.

¹⁴ David Lide and H.P.R Frederikse, eds., CRC Handbook of Chemistry and Physics 78th Edition (New York: Chemical Rubber Company, 1997), 12-214.

¹⁵ Ibid., 10-215.

¹⁶ Gill, 139.

¹⁷ Ibid., 139-146.

¹⁸ Ibid., 140.

Chapter 5

Conclusion and Recommendations for Future Work

The purpose of this chapter is to briefly review the results of the experimental work and provide insight on improvements to the laboratory procedure. Section 5.1 reviews the dye complexation results with uranium and organic dyes. Section 5.2 briefly discusses the microbiological work and uranium acetate preparation. Section 5.3 talks about the isotopic ratio of uranium atoms throughout the bacterial precipitation experiment. Section 5.4 provides some final thoughts on future research in this area.

5.1 Organic Indicator Dye Results

The main purpose of Chapter 2 was to evaluate the complexation of organic dyes with uranium metal in an aqueous solution to determine the concentration and the oxidation state of the uranium species. The primary goal was to identify a dye with significant visible color differences between U(VI) and U(IV) complexes. Arsenazo(III) complexes were used for the concentration measurements. Oxazine dyes Brilliant Cresyl Blue, Gallomine Triethiodide, and Celestine Blue were evaluated in solutions of different pH to determine qualitatively which one provided the most visible color difference between complexes formed with U(VI) and U(IV).

Although U(VI) species are much more soluble than U(IV), the first experiment showed that when phosphate ions were present, U(VI) precipitates out of solution. Therefore when making any medium to be used with bacteria, it is important to avoid the use of any phosphate ions.

The oxazine dye experiments analyzed the absorbance intensity in the UV/Visible range of the electromagnetic spectrum between 400-800 nm wavelengths in a variety of pH buffer and nitric acid solutions. A baseline spectrum without the uranium present was measured first. Then solutions containing U(VI) and U(IV) were added and the changes to the absorbance spectrum were compared to the baseline spectrum of the dyes. The two uranium complexation spectra for U(VI) and U(IV) were also compared against one another to determine a difference in absorbance between the complexes formed with the uranium metal species. Celestine Blue offered the largest color difference over any of the uranium complexes formed with Gallomine Triethiodide and Brilliant Cresyl Blue. The greatest differentiation between the U(VI) and U(IV) complexes with Celestine Blue occurred with 1.0 N nitric acid shown in Figure 2.10. The U(VI) complex had a large absorbance peak where the U(IV) complex was nearly colorless.

The next step to further this research would be to test the behavior of Celestine Blue in the agar media used to culture bacteria on circular plates. First, uranium solutions of U(IV) and U(VI) would be applied and then cultured plates with the metal reducing bacteria in an anaerobic environment would be used. Gradually, the research should move toward

applying subsurface soil from an area where bacteria are found, directly to the plate with a solution of U(VI).

The oxidation of uranium by nitrate ions is of particular concern. The dissolution of uraninite initially forms U(IV) aqueous species, but over time the nitrate ions will be reduced and the uranium will be oxidized. If too much time is allowed to pass from the dissolution of the uraninite, the uranium ions present in solution will be uranyl ions (UO_2^{2+}) and not uranous ions (U^{4+}). This process inhibits the ability to adequately study the complexation behavior of any ligand with U(IV). Another option to study the complexation variations between the two primary oxidation states of uranium is to use a different source. An experiment using uranium chloride salts of UO_2Cl_2 and UCl_4 may be a more reliable source of the characteristic uranium ions.

Another experiment to test the complexation behavior of the dyes with aqueous uranium species is a reduction titration with the UV/Visible Spectrometer. Starting with a solution U(VI) and a particular reduction indicator, slowly titrate Fe(II), which oxidizes to Fe(III) and reduces the uranium to U(IV). The titrator can monitor the pH changes while the UV/Visible spectrometer can simultaneously take periodic measurements of the absorbance intensity of the complexes using a mobile dip probe. This experiment may be the best technique to simulate the color changes that would occur with the bacterial reduction process.

The last recommendation may be to continue the search for a better reduction indicator. Raju and Gautum referred to another indicator dye,

Gallocyanine, which may provide a good color change, going from pink to colorless at the end point for the reduction of U(VI) to U(IV).

5.2 Microbiological Work and Uranium Acetate

Preparation

The purpose of Chapter 3 was to study the reduction of the dissolved uranium into a solid precipitate using bacteria. The overall objective was to present an overview of the microbiological and chemical processes that were used throughout this investigation. It included the general methods used in the laboratory for the uranium acetate preparation and the culture of the bacteria *Shewanella putrefaciens*. The last portion of Chapter 3 explained the structure of the precipitate and identified it as the mineral uraninite UO_2 . A number of lessons were learned in this process.

The first lesson learned involved the dissolution rate of U_3O_8 in nitric acid. The literature indicated the two most effective ways to improve the dissolution rate are heat and agitation. The interesting effect involved in the dissolution is the uranium speciation in the acid. This is also addressed in Chapter 2. The mixed oxidation state of U_3O_8 is dissolved entirely over time into the uranyl ion UO_2^{2+} (aq) by oxidizing the uranium (V) to (VI). In the dye experiment, uraninite was also dissolved in nitric acid, but the kinetics of the oxidation of U(IV) in an argon environment was slow enough to observe a different complexation behavior than U(VI).

The next instance of laboratory improvement concerns the solubility and over saturation of the uranium acetate solution. In both the non-

enriched and the first enriched uranium solutions, fine yellow solid particles settled at the bottom of the mixtures indicating the over saturation. This accounted for a significant part of the loss during the chemical preparation. The targeted concentration of the solution was initially 10 mM. The increase of pH to a level between 6.5 and 7.0 that is suitable for bacterial growth made this uranium concentration too high. This was avoided in the second experiment with the enriched uranium by only raising the concentration to slightly over 5mM.

The third point learned was the impact that a small amount of nitrate had on the bacterial reduction of uranium. With a small amount of nitrate ions present, the bacteria preferentially used these ions as opposed to the uranyl ions as the electron acceptor in the metabolic process. The increased rinses of the uranium hydroxide in the creation of the second mixture of enriched uranium acetate forced the bacteria to reduce the uranium species in its metabolic process. This point is extremely important when evaluating this process in the environment. For the bacterial reduction of uranium to occur, all other oxidants found in the environment must be used up before the bacteria will use uranium. This includes not only nitrate, but any other dissolved environmental metals or ligands capable of being reduced.

The rinse procedure also showed the requirement to maintain very basic conditions in the rinse. The solid volume of the uranium hydroxide precipitate decreased around pH 8. This was stopped by adding a small amount of a basic solution to bring the pH up to a level that stabilized the hydroxide solid. The use of deionized water to wash the hydroxide solid may

be replaced by rinsing with a basic solution for the first few rinses. The basic solution should not be too concentrated though, to prevent higher order uranium hydroxide complexes from forming.

Lastly in terms of the crystal identification, the X-Ray diffraction approach is much more suitable for identification than an elemental analysis of the crystal with the electron microprobe. Future study would have included a solid X-Ray pattern of UO_2 and U_3O_8 to compare each against the other. The data in the report clearly showed a similarity with the library reference peaks of uraninite, but an XRD analysis with a small amount of U_3O_8 and $\text{UO}_2(\text{CH}_3\text{COO})_2$ solid crystals may form a better comparison.

5.3 Outcome of the Isotopic Fractionation Investigation

The intention of Chapter 4 was to determine whether the bacterial reduction of aqueous U(VI) species to solid U(IV) effected the isotopic ratio of uranium atoms. The objective of this chapter was to determine whether there was a measurable change in the isotopic ratio of the supernatant or precipitate ratio during the bacterial reduction of uranium by *Shewanella putrefaciens*.

TIMS analyzed ratios of solid samples by measuring the ion flux densities emanating off of a heated element. The uranium atoms that leave the filament form positive ions as a function principally of the ionization efficiency of the element of interest and the work function of the filament. The ability to detect an accurate ratio requires correction of mass or

instrumental fractionation, which is the tendency of the lighter isotopes to leave first.

The results of this work are most clearly described in the charts of Appendix 4, Annex I. The isotopic fractionation appears not to be a result of biological fractionation, but instead on the load mass of the element of interest on the filament. Kinetics of the reduction of the uranium by the bacteria are also in Chapter 4. The kinetics fit nicely to a first order rate equation with the following form:

$$\ln[A_0] - \ln[A] = kt$$

A concentration at time t

A_0 initial concentration

k constant ($5.14 \pm 0.47 \times 10^{-2}$)

where k was experimentally determined to be 5.14×10^{-2} . A few areas could be improved for future research of this effect.

The first instance is to perform a more accurate concentration calculation using an ICP-AES or other method after the final chemistry step in the columns. This would give a greater ability to control the load sizes. Load size should be kept on the order of 1 μg or 1000 ng and filaments should be loaded using the regular method. In addition, operating at higher temperatures, with a sufficient amount of mass on the filament to retain a stable flux rate, reduced the instrumental fractionation.

The second improvement would be a better method to remove the supernatant from the precipitate. For this research specifically, a better rinse technique would have been to use a 0.1 N HCl solution as opposed to

MQ H₂O. Uraninite does not dissolve in HCl therefore it would have remained solid. However, the HCl would have been a stronger desorbing agent than water for any sorbed uranium species. The large differences between the calculated concentration of precipitate solutions in the microcentrifuge tubes and the estimated values in Appendix 4, Annex J seem to indicate a time dependent enzymatic effect of the organism grasping hold of the aqueous uranium species. In other words, the assumption in this report was that sorption increased with the dissolved uranium interaction time with the living cells.

This report concludes then that there is no concentrated build up of enriched uranium caused by the enzymatic precipitation by anaerobic bacteria living in the soil. The mass difference was not significant enough to cause a distinguishable difference in the reduction rates of either the ²³⁵U or ²³⁸U isotopes.

5.4 Final Thoughts

There are many threats to public health including contamination of ground water resources. The study of the fate and transport of uranium at sites with significant uranium deposits from anthropogenic sources is important to prevent this kind of contamination. Knowledge of the disposition of uranium in surface and subsurface waters, and the processes that control its migration have implications for many that include areas with significant uranium mining, abandoned US Army ranges with exposed DU rounds, and uranium enrichment facilities. One process that may prevent

further movement of uranium or remove it naturally from its aqueous phase is the reduction of uranium by bacteria. There still is no concrete evidence of this process occurring in the soil, especially the selective reduction of uranium as opposed to other elements. In the lab, the presence of a minor amount of nitrate ions prevented the bacteria from reducing the uranium. The presence of other oxidants in the hypolimnion (bottom of large standing water bodies) or ground water presents challenges to engineering this method into a reliable remediation strategy or accurate modeling of the movement process. However, the exact role that bacteria play in the environmental processes controlling the movement of uranium has yet to be determined and requires further investigation.

Appendix 1

Selected Uranium Stability Constants¹(All Except Acetate)

Major Ligands

CO₃²⁻ (Carbonate)
NO₃⁻ (Nitrate)
OH⁻ (Hydroxide)
CH₃COO⁻ (Acetate)
Cl⁻

Major Cations

K⁺
H⁺
UO₂²⁺
U⁴⁺

Reactions

	log K	ΔG°
1) Carbonate		
CO ₃ ²⁻ + UO ₂ ²⁺ ⇌ UO ₂ CO ₃ (aq)	9.68	-55.24
CO ₃ ²⁻ + UO ₂ ²⁺ ⇌ UO ₂ CO ₃ (s)	14.470	-82.595
2CO ₃ ²⁻ + UO ₂ ²⁺ ⇌ UO ₂ (CO ₃) ₂ ²⁻	16.940	-96.694
3CO ₃ ²⁻ + UO ₂ ²⁺ ⇌ UO ₂ (CO ₃) ₃ ⁴⁻	21.600	-123.294
5CO ₃ ²⁻ + U ⁴⁺ ⇌ U(CO ₃) ₅ ⁶⁻	34.000	-194.073
2) Nitrate		
NO ₃ ⁻ + UO ₂ ²⁺ ⇌ UO ₂ NO ₃ ⁺	0.300	-1.712
2NO ₃ ⁻ + U ⁴⁺ ⇌ U(NO ₃) ₂ ²⁺	2.300	-13.128
3) Hydroxide		
H ₂ O(l) + UO ₂ ²⁺ ⇌ UO ₂ OH ⁺ + H ⁺	-5.2	29.682
2H ₂ O(l) + UO ₂ ²⁺ ⇌ UO ₂ (OH) ₂ (aq) + 2H ⁺	<-10.3	>58.793
2H ₂ O(l) + UO ₂ ²⁺ ⇌ UO ₂ (OH) ₂ (s) + 2H ⁺	-4.931	28.148
3H ₂ O(l) + UO ₂ ²⁺ ⇌ UO ₂ (OH) ₃ ⁻ + 3H ⁺	-19.2	109.594
4H ₂ O(l) + UO ₂ ²⁺ ⇌ UO ₂ (OH) ₄ ²⁻ + 4H ⁺	-33.00	188.365
H ₂ O(l) + U ⁴⁺ ⇌ U(OH) ₃ ³⁺ + H ⁺	-0.540	3.082

¹ Grenthe, I., Fuger, J., Konings, R. J. M., Lemire, R. J., Muller, A. B., Nguyen-Trung, C., & Wanner, H. . Chemical Thermodynamics of Uranium, Volume 1, (, Amsterdam Elsevier :, 1992), 51-60.

4) Acetate²

$\text{CH}_3\text{COO}^- + \text{UO}_2^{2+} \rightleftharpoons \text{UO}_2\text{CH}_3\text{COO}^+$	2.631
$2\text{CH}_3\text{COO}^- + \text{UO}_2^{2+} \rightleftharpoons \text{UO}_2(\text{CH}_3\text{COO})_2$	4.658
$3\text{CH}_3\text{COO}^- + \text{UO}_2^{2+} \rightleftharpoons \text{UO}_2(\text{CH}_3\text{COO})_3^-$	6.244

5) Chlorides

$\text{Cl}^- + \text{UO}_2^{2+} \rightleftharpoons \text{UO}_2\text{Cl}^+$	0.170	-0.970
$2\text{Cl}^- + \text{UO}_2^{2+} \rightleftharpoons \text{UO}_2(\text{Cl})_2(\text{s})$	-12.116	69.157
$2\text{Cl}^- + \text{UO}_2^{2+} \rightleftharpoons \text{UO}_2(\text{Cl})_2(\text{aq})$	-1.100	6.279
$\text{Cl}^- + \text{U}^{4+} \rightleftharpoons \text{UCl}_3^+$	1.720	-9.818

² Glenn T. Seaborg and Joseph J. Katz, The Actinide Elements. (New York, New York: McGraw-Hill Book Company, 1954), 168.

Appendix 2, Annex A

- A-1 Bacterial Growth Media Composition**
- A-2 UV/Visible Spectrometer Instructions**

Appendix 2, Annex A-1

Bacterial Growth Media Composition

A-1

Electron donor:

Acetate (NaCH_3COO), 10mM

Electron acceptor:

Nitrate (NaNO_3), 10mM

Other nutrients and buffer:

NaHCO_3 , 2.5g/L

NH_4Cl , 1.5g/L

$\text{NaH}_2\text{PO}_4 \cdot \text{H}_2\text{O}$, 0.6 g/L

KCl, 0.5 g/L

$\text{MgCl}_2 \cdot 6\text{H}_2\text{O}$, 0.4 g/L

$\text{CaCl}_2 \cdot 2\text{H}_2\text{O}$, 0.15 g/L

Trace elements*

Vitamins*

Without inoculation of the strain.

*(The concentrations are shown below)

A-2

Electron donor:

Acetate (NaCH_3COO), 10mM

Electron acceptor:

Nitrate (NaNO_3), 10mM

Other nutrients and buffer:

NaHCO_3 , 2.5g/L

NH_4Cl , 1.5g/L

$\text{NaH}_2\text{PO}_4 \cdot \text{H}_2\text{O}$, 0.6 g/L

KCl, 0.5 g/L

$\text{MgCl}_2 \cdot 6\text{H}_2\text{O}$, 0.4 g/L

$\text{CaCl}_2 \cdot 2\text{H}_2\text{O}$, 0.15 g/L

Trace elements*

Vitamins*

Without inoculation of the strain,

Add extra: uranyl acetate $(\text{CH}_3\text{COO})_2\text{UO}_2$, 1 mM
Acetate $(\text{CH}_3\text{COONa})$, 10mM

B-1

Electron donor:

Acetate $(\text{NaCH}_3\text{COO})$, 10mM

Electron acceptor:

Uranyl Acetate, $(\text{CH}_3\text{COO})_2\text{UO}_2$, 1mM

Other nutrients and buffer:

NaHCO_3 , 2.5g/L

NH_4Cl , 1.5g/L

$\text{NaH}_2\text{PO}_4 \cdot \text{H}_2\text{O}$, 0.6 g/L

KCl , 0.5 g/L

$\text{MgCl}_2 \cdot 6\text{H}_2\text{O}$, 0.4 g/L

$\text{CaCl}_2 \cdot 2\text{H}_2\text{O}$, 0.15 g/L

Trace elements*

Vitamins*

Without inoculation of the strain,

B-2

Electron donor:

Acetate $(\text{NaCH}_3\text{COO})$, 10mM

Electron acceptor:

Nitrate (NaNO_3) , 10mM

Other nutrients and buffer:

NaHCO_3 , 2.5g/L

NH_4Cl , 1.5g/L

$\text{NaH}_2\text{PO}_4 \cdot \text{H}_2\text{O}$, 0.6 g/L

KCl , 0.5 g/L

$\text{MgCl}_2 \cdot 6\text{H}_2\text{O}$, 0.4 g/L

$\text{CaCl}_2 \cdot 2\text{H}_2\text{O}$, 0.15 g/L

Trace elements*

Vitamins*

With inoculation of the strain

B-3

Electron donor:

Acetate $(\text{NaCH}_3\text{COO})$, 10mM

Electron acceptor:

Fe-citrate, about 10-20mM (Supernatant of a 50mM Fe-citrate solution which is not completely dissolved at room temperature)

Uranyl Acetate, $(\text{CH}_3\text{COO})_2\text{UO}_2$, 1mM

Other nutrients and buffer:

NaHCO_3 , 2.5g/L

NH_4Cl , 1.5g/L

$\text{NaH}_2\text{PO}_4 \cdot \text{H}_2\text{O}$, 0.6 g/L

KCl , 0.5 g/L

$\text{MgCl}_2 \cdot 6\text{H}_2\text{O}$, 0.4 g/L

$\text{CaCl}_2 \cdot 2\text{H}_2\text{O}$, 0.15 g/L

Trace elements*

Vitamins*

With inoculation of the strain

*** The amount of trace elements in the medium:**

conc. HCl (37%), .001ml/L

$\text{MnCl}_2 \cdot 4\text{H}_2\text{O}$, 010 mg/L

$\text{CoCl}_2 \cdot 6\text{H}_2\text{O}$, 0.12 mg/L

ZnCl_2 , 0.07 mg/L

H_3BO_3 , 0.06 mg/L

$\text{NiCl}_2 \cdot 6\text{H}_2\text{O}$, 0.025 mg/L

$\text{CuCl}_2 \cdot 2\text{H}_2\text{O}$, 0.015 mg/L

$\text{Na}_2\text{MoO}_4 \cdot 2\text{H}_2\text{O}$, 0.025 mg/L

$\text{FeCl}_2 \cdot \text{H}_2\text{O}$, 1.1 mg/L

*** The amount of vitamins in the medium:**

P-aminobenzonic acid, 0.05 mg/L

Biotin, 0.02 mg/L

Nicotinic acid, 0.05 mg/L

Thiamine HCl , 0.05 mg/L

Pyridoxin HCl (B6), 0.1 mg/L

Cyano cobalamin (B12), 0.001 mg/L

Appendix 2, Annex A-2

Spectrometer Instructions

1. Turn on the computer
2. Turn on the power for the light source on rear of device.
3. Click Windows Start button.
4. Click on Spectrometer. The latest software version loads.
5. Click on run continuously (⚙️) button. A blue line should appear roughly equal to zero
6. Select either the master or slave spectrometer by clicking on the marked toggle switch. The master is good for wavelengths between 200nm and 800nm. The slave is good for wavelengths between 500nm and 1100nm.
7. Place probe in deionized (DI) water or place cuvette with DI in the sample holder to read the reference scans.
8. Click on the scan dark button. Let it wait about five seconds to collect a good dark spectra, then click on the button again.
9. Turn on the halogen lamp (the red button).
10. Adjust the integration frequency until a flat line forms. Then lower the integration frequency until just below the flat line. The intent in this step is to establish the largest spectrum possible with the least amount of integration frequencies. A simultaneous approach is to adjust the optics. This requires you to loosen the screw on the optic return line in an attempt to maximize the spectrum. Then determine the integration frequency value as previously described. A spectrum of 4000 is usually the best attainable value before saturation.
11. Adjusting the boxcar smoothing averages neighboring pixels together to form a smoother curve. The average button average consecutive scans to limit erratic

jumps. A value of 5,5 is usually good; where as a value of one gets lots of noise and huge files.

12. Click the absorbance button on the screen. The screen drastically changes to show what appears to be the top half of a horizontal parabola. You are now reading absorbance. DO NOT CLICK ON THE ABSORBANCE BUTTON AGAIN, OTHERWISE A NEW REFERENCE SCAN (steps 7-12) WILL HAVE TO BE REPEATED.

13. Place the probe into the sample or cuvette with sample into the cell holder.

14. IMPORTANT: Set the beginning and ending wavelength. The graph on the right shows exactly what you will be saving.

15. Type in the name you wish to save.

16. Click on the append button to save the existing file. This places all of the scans in the file name and prevents overwriting the data.

17. Click on the instant save to create a snapshot of the spectrum.

18. For time delay saving, first, make sure the append feature is on. Then click on the instant save to save an initial scan. Next, click on the number box labeled time delay. Type the delay in SECONDS. Do not click or press enter after typing the last number. When you are ready to begin, click on the time delay save button.

The scans will start after the period specified. Then it will scan at every multiple after that. The computer stamps the time with seconds on each saved spectrum.

19. The automatic shutdown is useful for time delay spectroscopy. After pressing the time delay button, look at the number in the scans taken box. Type in this number plus the number of scans taken into the maximum number of scans box.

For example, if the number of scans reads 147 and you wish to take 50 scans, then type 197 in the maximum number of scans box. Then press the button marked auto shutdown.

20. If the spectrometer programming does not seem to work for any reason, stop the spectrometer by clicking on the red octagon button at the top of the screen. Then click on the file, then click on revert. Answer yes to any questions. If that does not seem to work, click on the file open. Next, click on backup.vi. This is a working backup copy of the spectrometer software.

Appendix 2, Annex B

Arsenazo(III) Spectra Results

B-1 Arsenazo(III) Experiment One

- B-1-1 Uranium Standards in pH2 Buffer
- B-1-2 Samples in pH2 Buffer
- B-1-3 Standard and Samples in pH2 Buffer

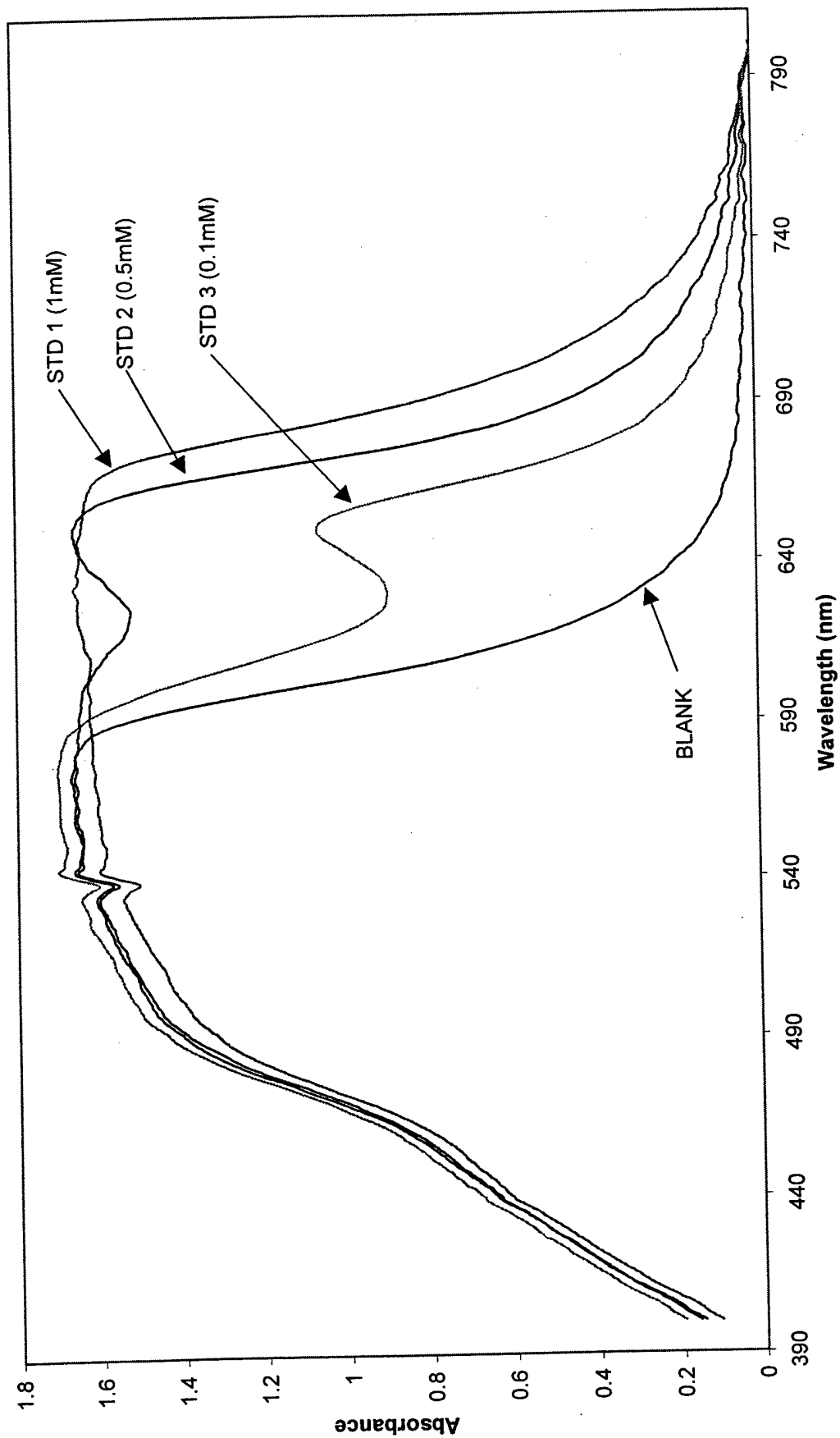
B-2 Arsenazo(III) Experiment Two (4N HNO₃)

- B-2-1 Uranium Standards in 4N HNO₃
- B-2-2 Samples in 4N HNO₃
- B-2-3 Standard and Samples in 4N HNO₃

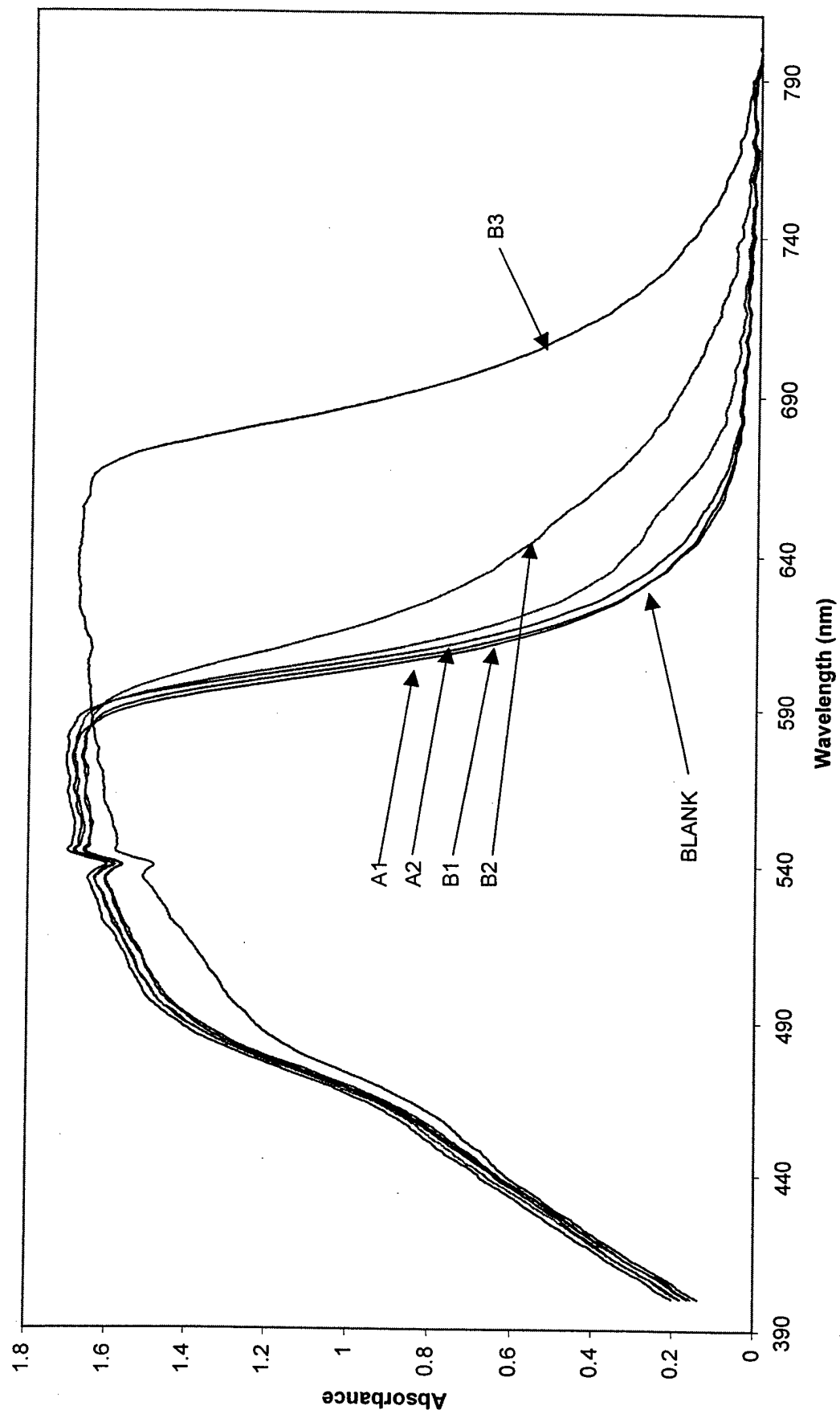
B-3 Arsenazo(III) Experiment Two (pH2 Buffer)

- B-3-1 Uranium Standards in pH2 Buffer
- B-3-2 Samples in pH2 Buffer
- B-3-3 Standard and Samples in pH2 Buffer

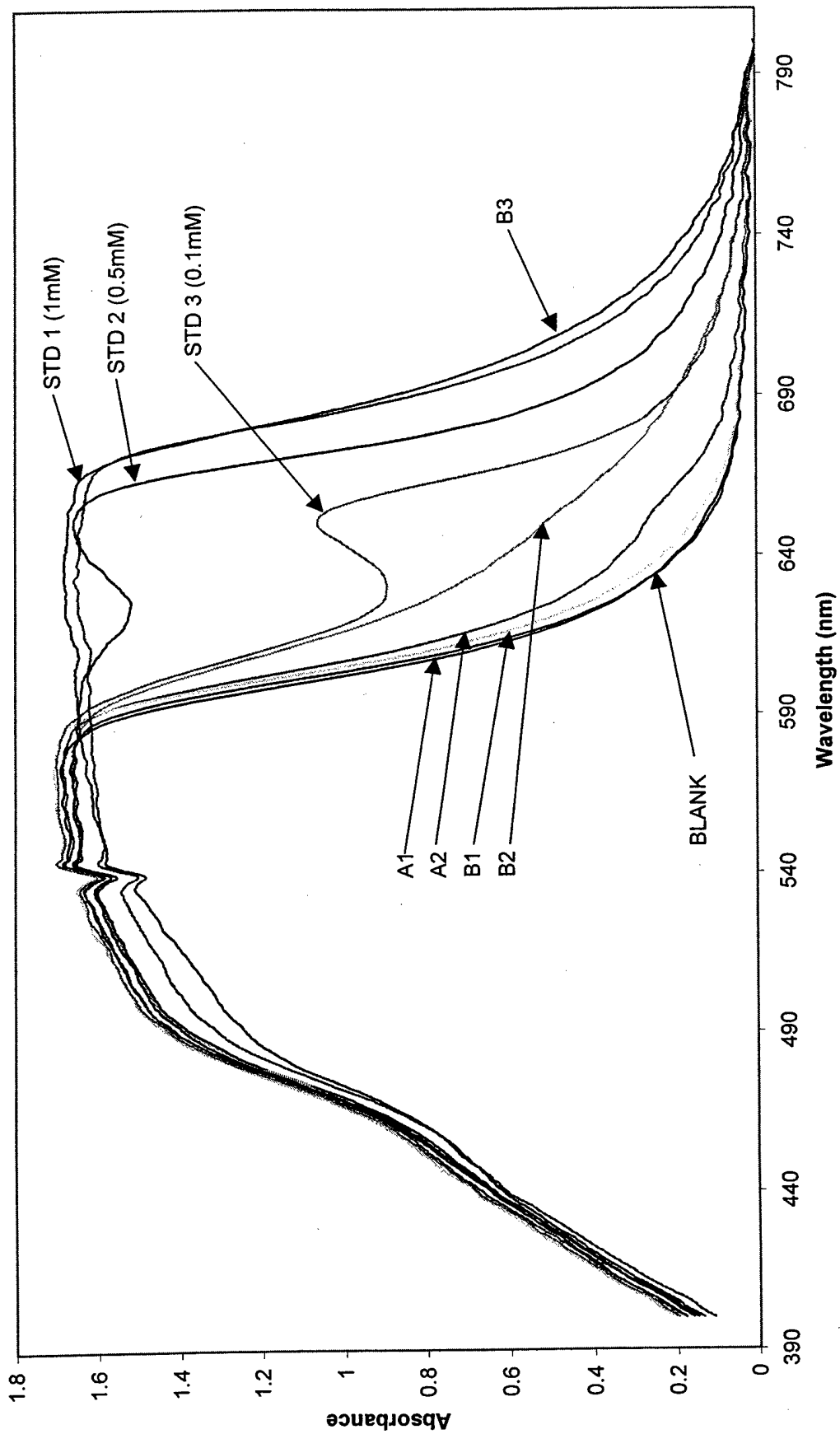
Arsenazo Experiment One Uranium Standards in pH2 Buffer



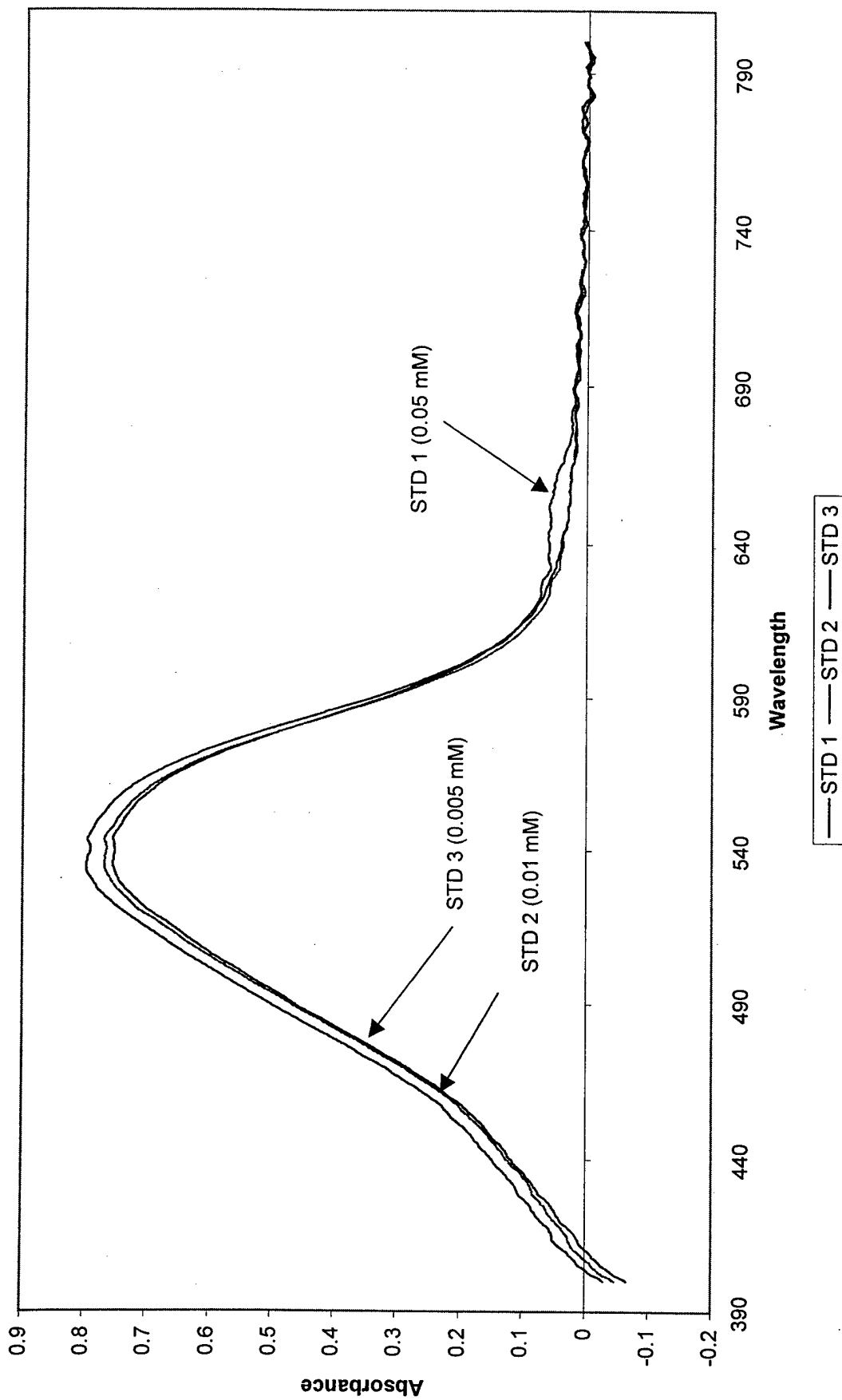
Arsenazo Experiment One
Samples in pH2 Buffer (Normalized)



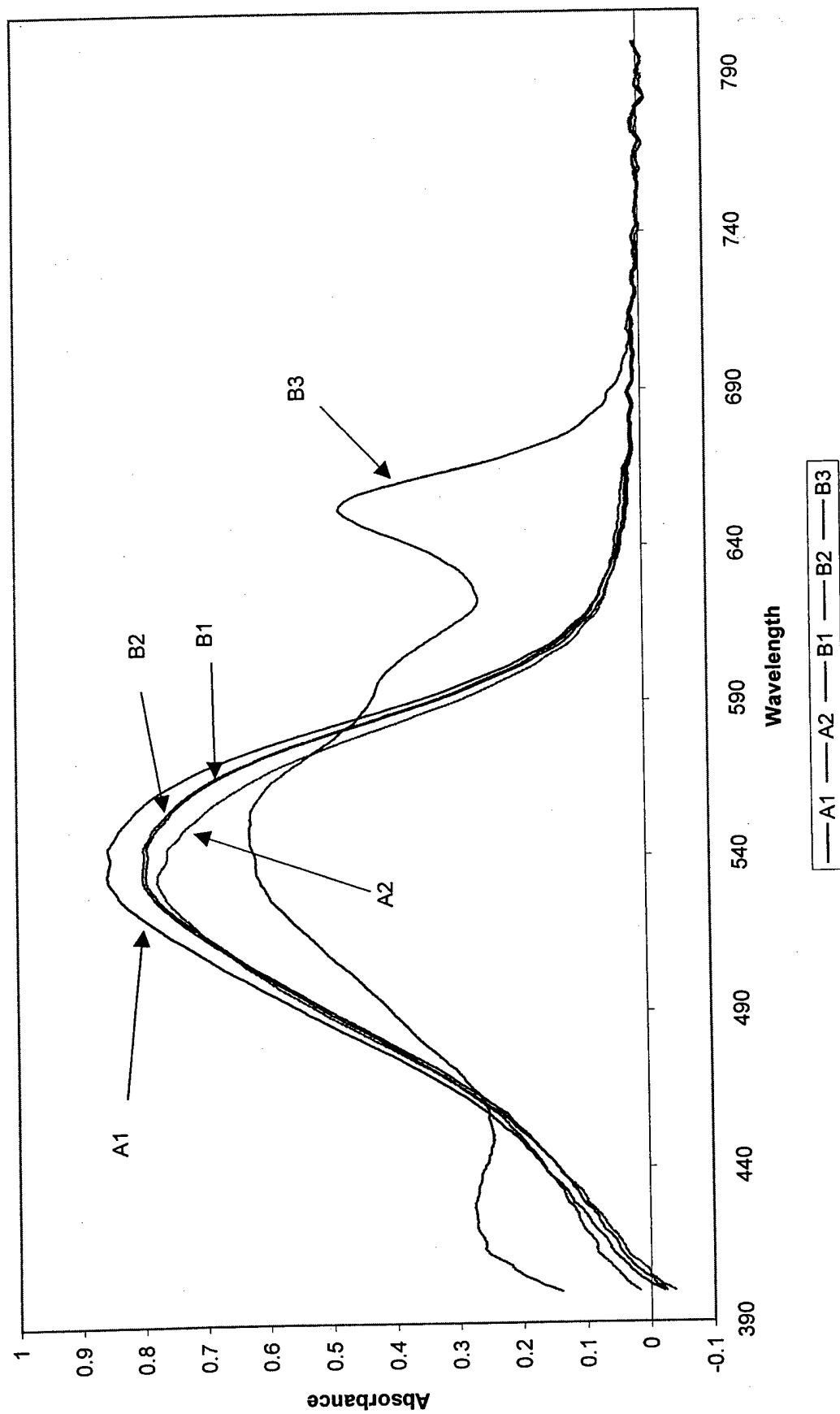
Arsenazo Experiment One
Standards and Samples in pH2 Buffer (Normalized)



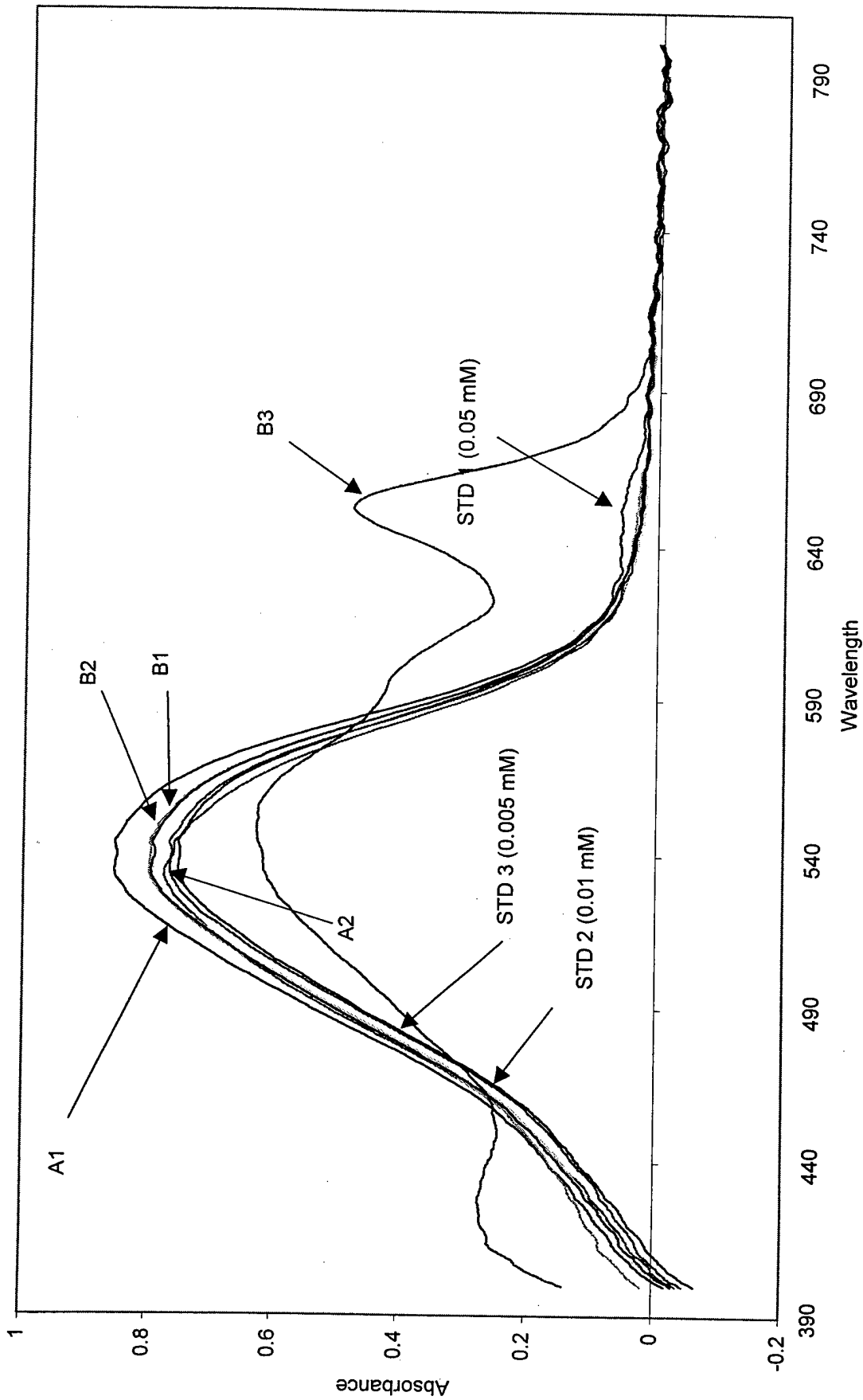
Arsenazo Experiment Two
Uranium Standards in 4M HCl (Normalized)



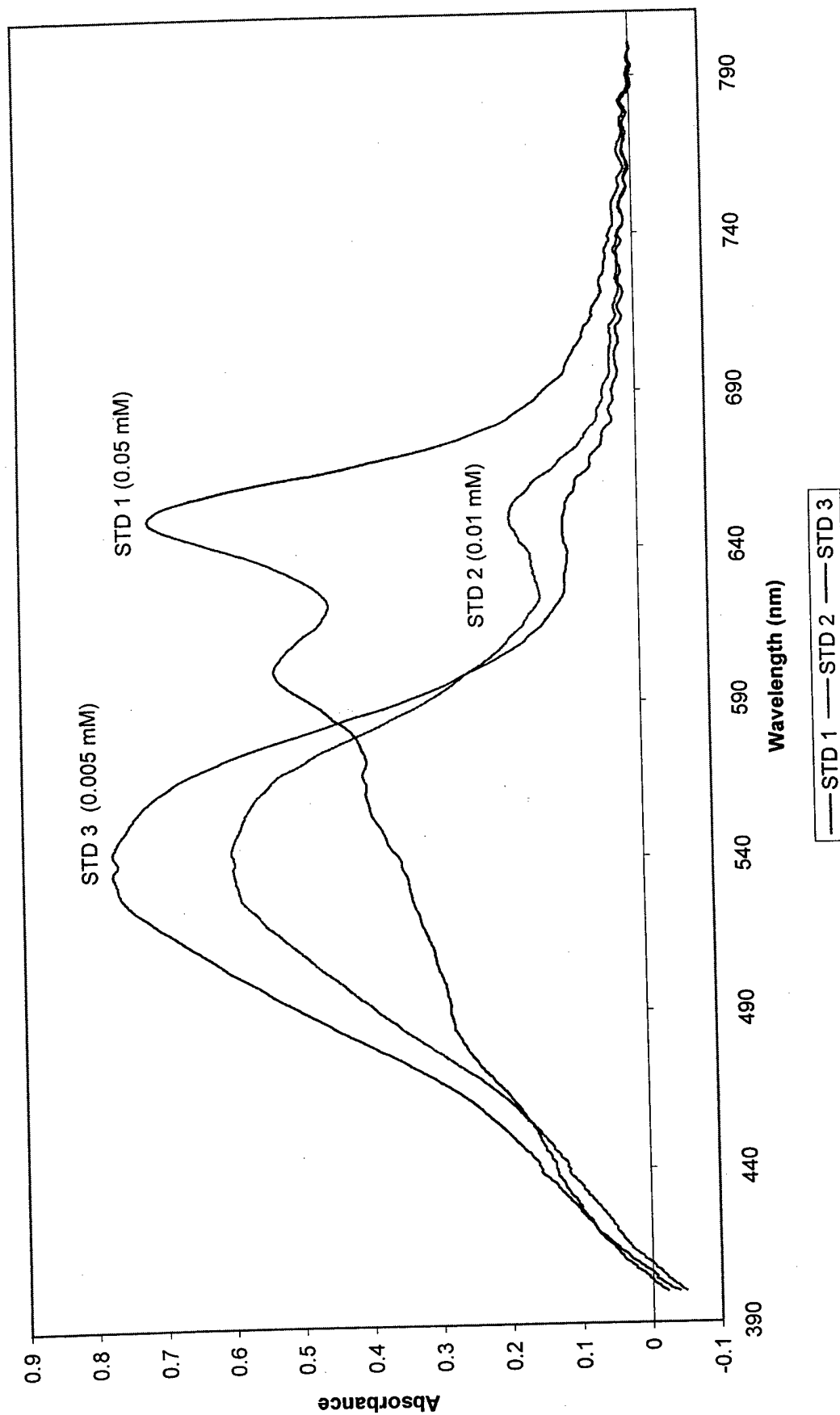
**Arsenazo Experiment Two
Samples in 4M HCl (Normalized)**



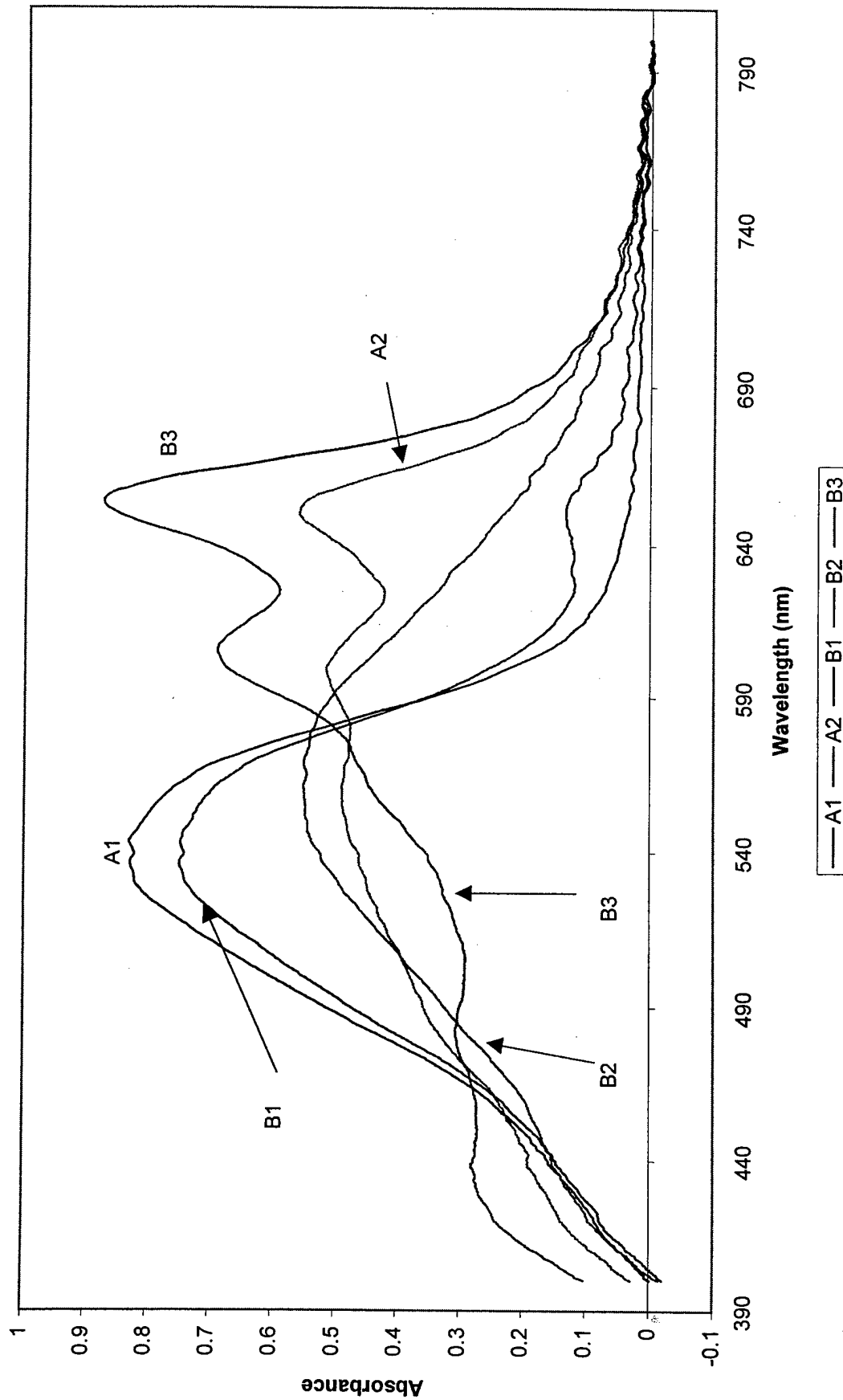
Arsenazo Experiment in 4N HCl (Normalized)



Arsenazo Experiment Two
Uranium Standards in pH2 Buffer



**Arsenazo Experiment Two
Samples in pH2 Buffer**



Appendix 2, Annex C

Color Photos Comparing the Visual Change of the Oxazine Dyes with U(VI)

Annex C-1 Gallomine Triethiodide

Annex C-2 Celestine Blue

Annex C-3 Brilliant Cresyl Blue

Appendix 2, Annex C-1 Gallomine Triethiodide

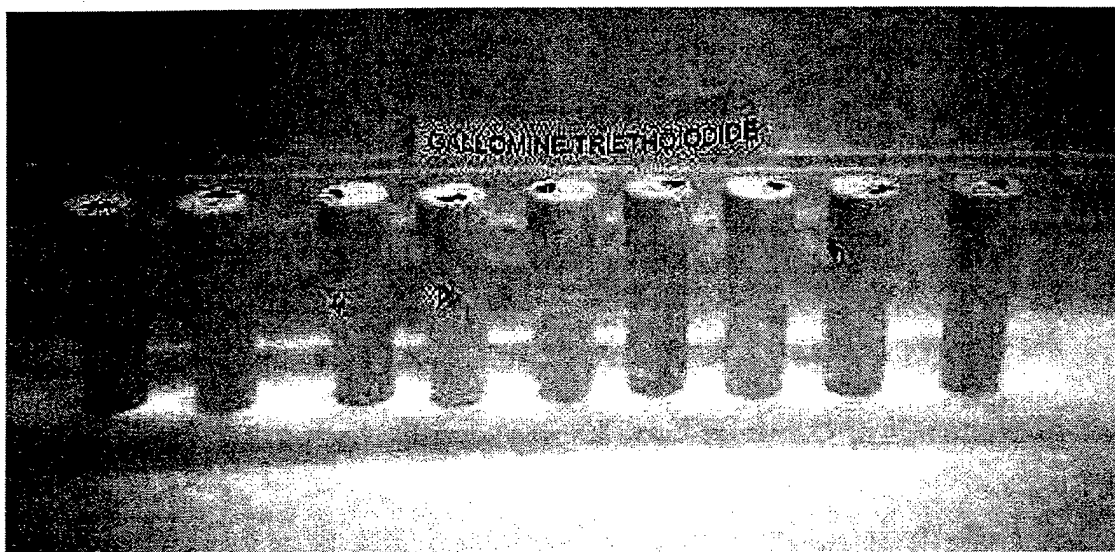


Figure 1 Gallomine Triethiodide with U(VI)

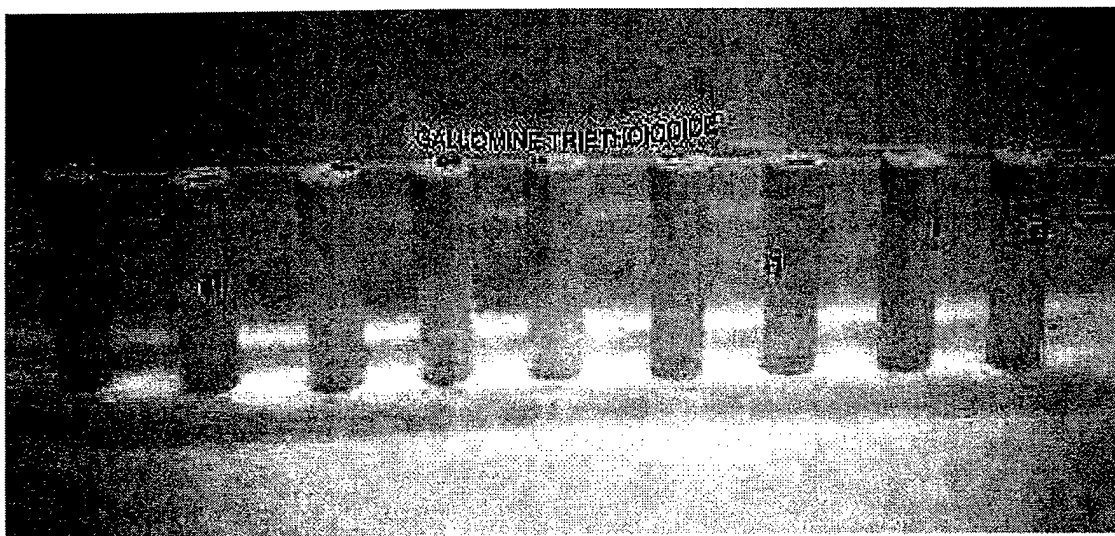


Figure 2 Gallomine Triethiodide without U(VI)

Appendix 2, Annex C-2 Celestine Blue

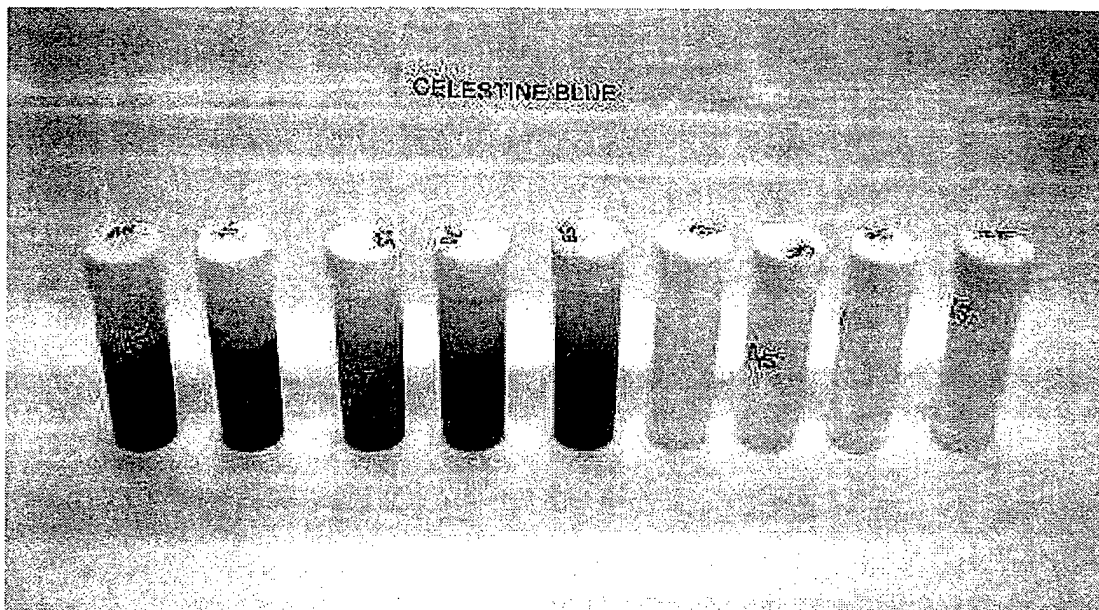


Figure 3 Celestine Blue with U(VI)

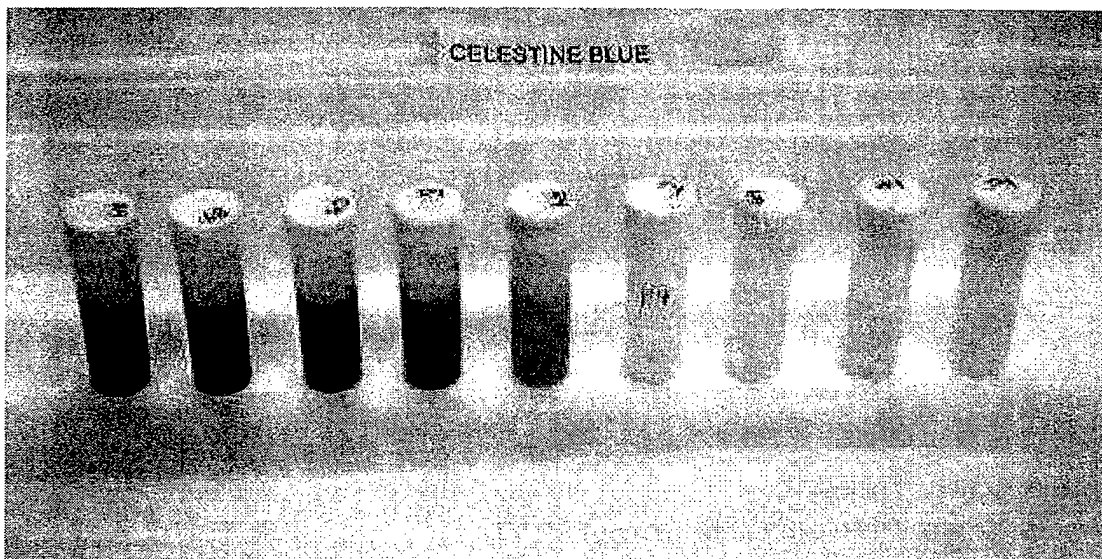


Figure 4 Celestine Blue without U(VI)

Appendix 2, Annex C-3 Brilliant Cresyl Blue

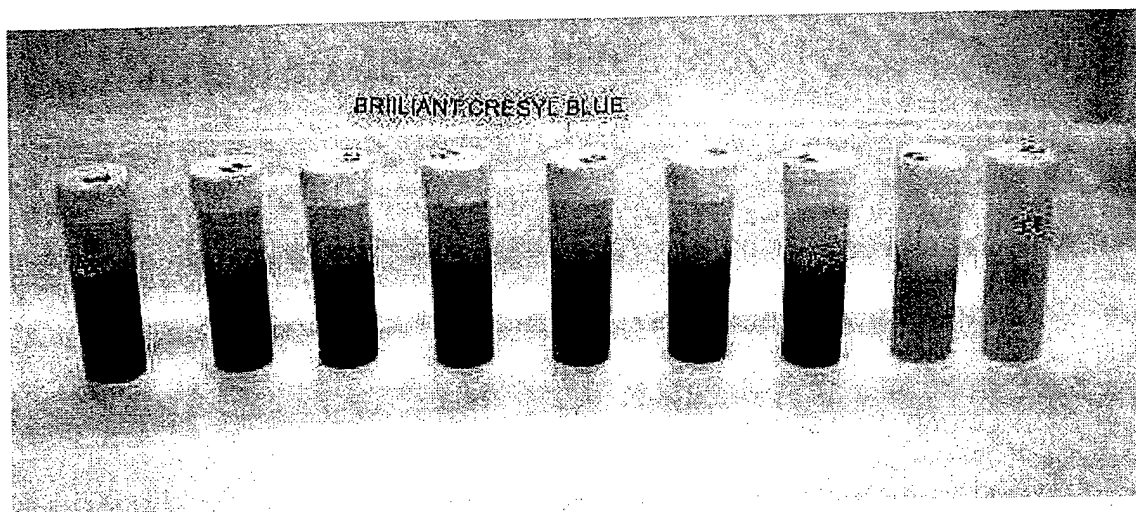


Figure 5 Brilliant Cresyl Blue with U(VI)

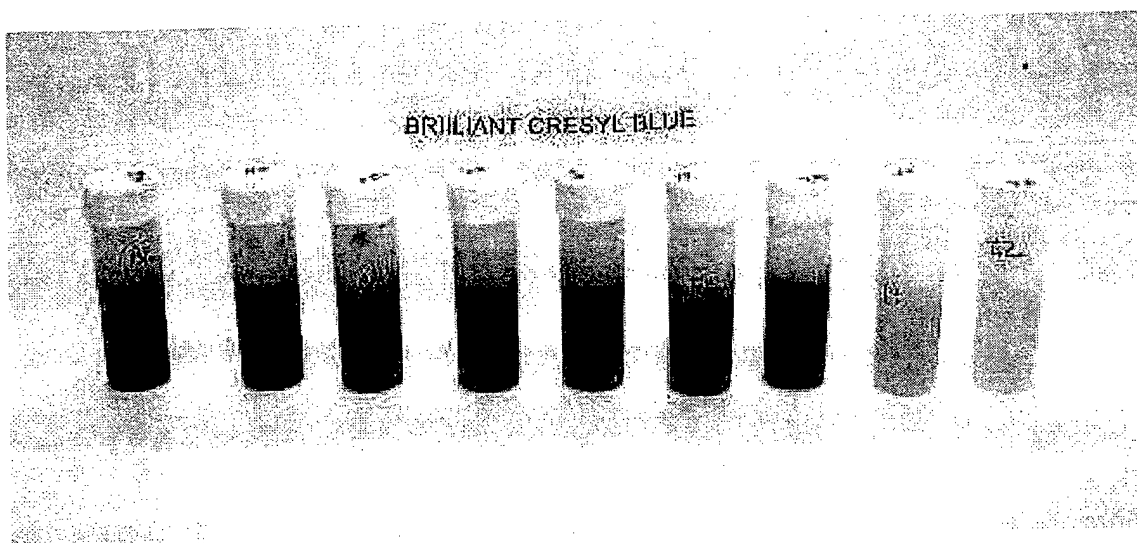


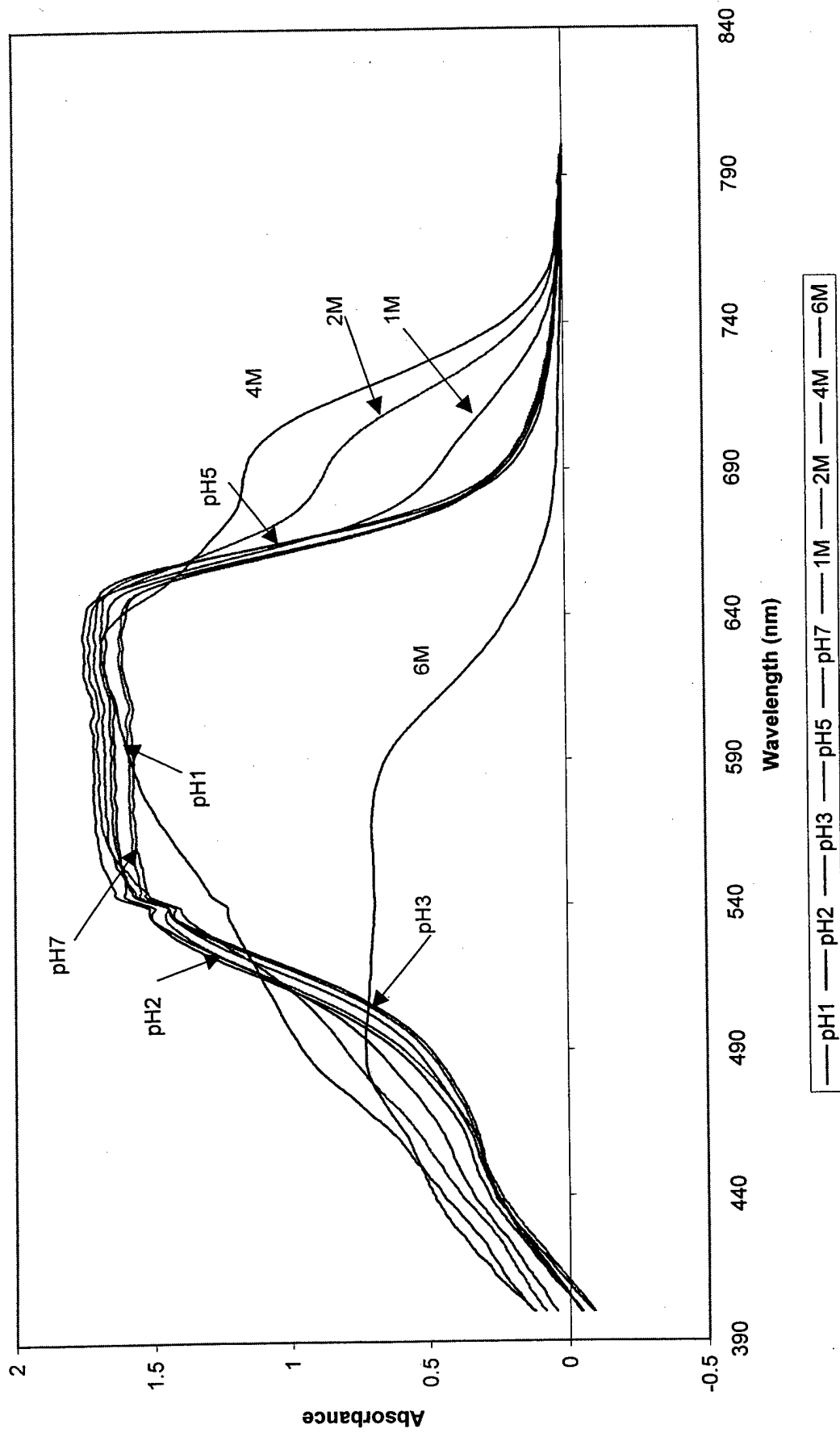
Figure 6 Brilliant Cresyl Blue without U(VI)

Appendix 2, Annex D

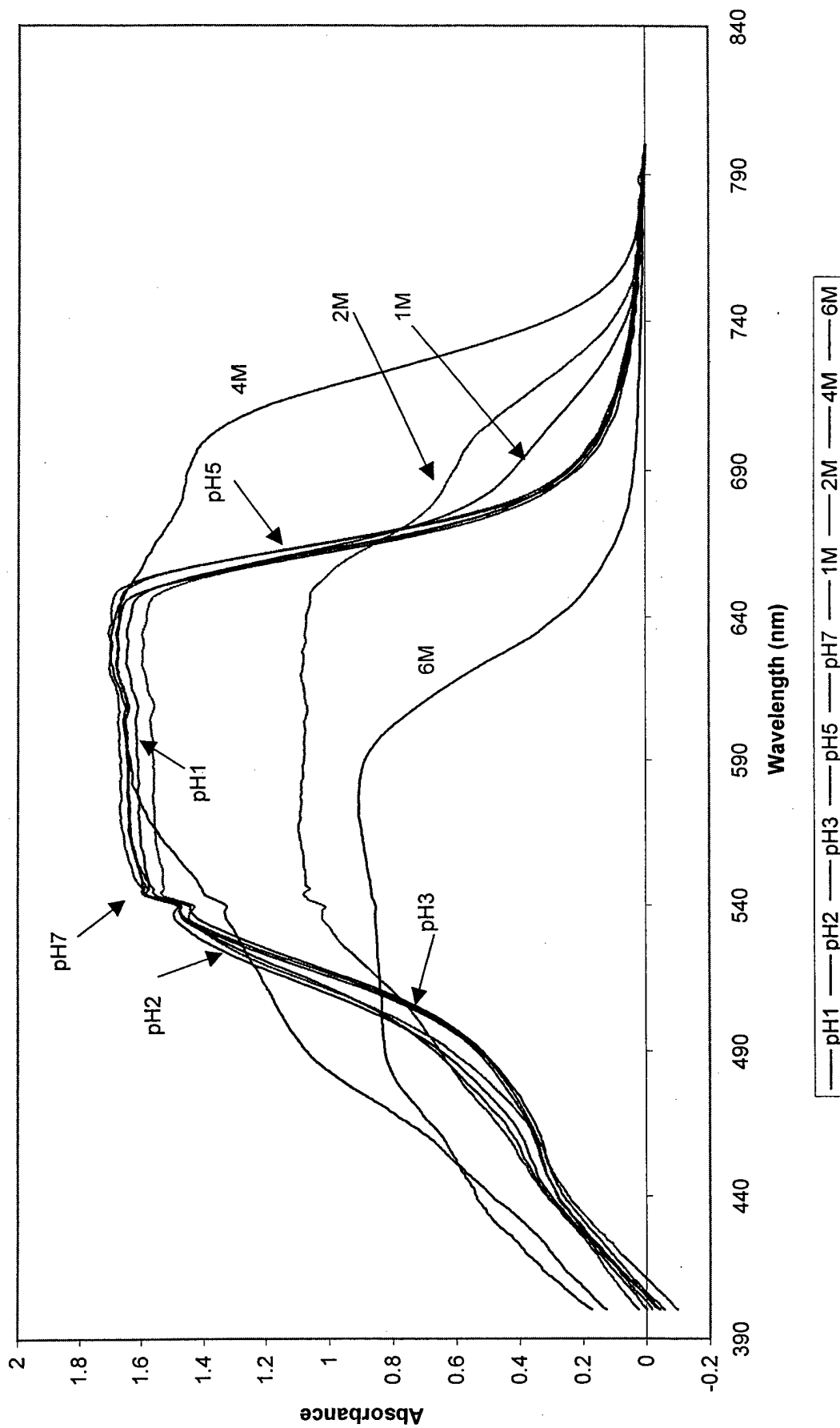
Brilliant Cresyl Blue Spectra Results with U(VI)

- D-1 BCB total without U(VI)
- D-2 BCB total with U(VI)
- D-3 BCB Complexation with U(VI) at pH7
- D-4 BCB Complexation with U(VI) at pH5
- D-5 BCB Complexation with U(VI) at pH3
- D-6 BCB Complexation with U(VI) at pH2
- D-7 BCB Complexation with U(VI) at pH1
- D-8 BCB Complexation with U(VI) at 1N HNO₃
- D-9 BCB Complexation with U(VI) at 2N HNO₃
- D-10 BCB Complexation with U(VI) at 4N HNO₃
- D-11 BCB Complexation with U(VI) at 6N HNO₃

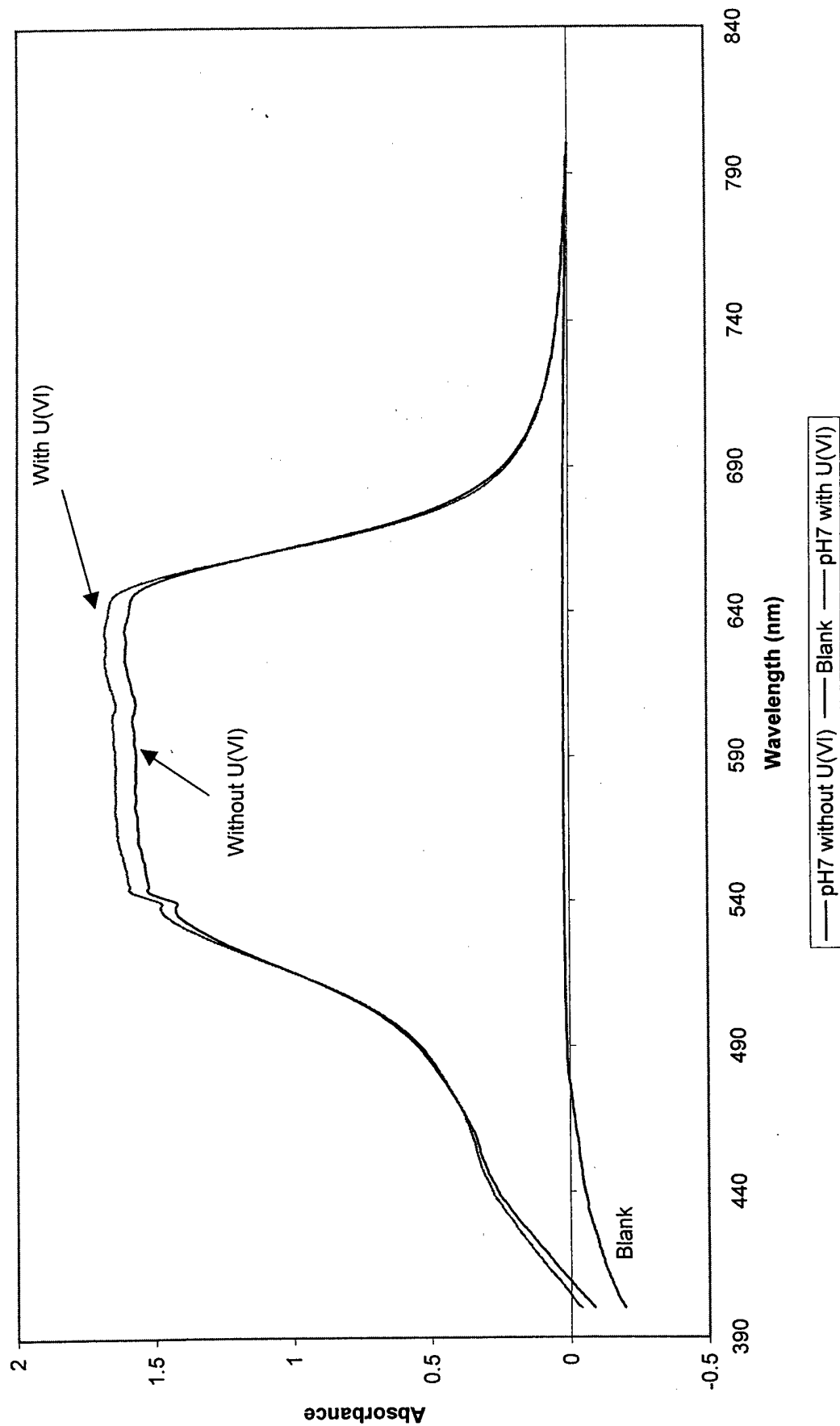
**BCB without U(VI) Metal Aqueous Species
(Normalized Values and Uncorrected for Background)**



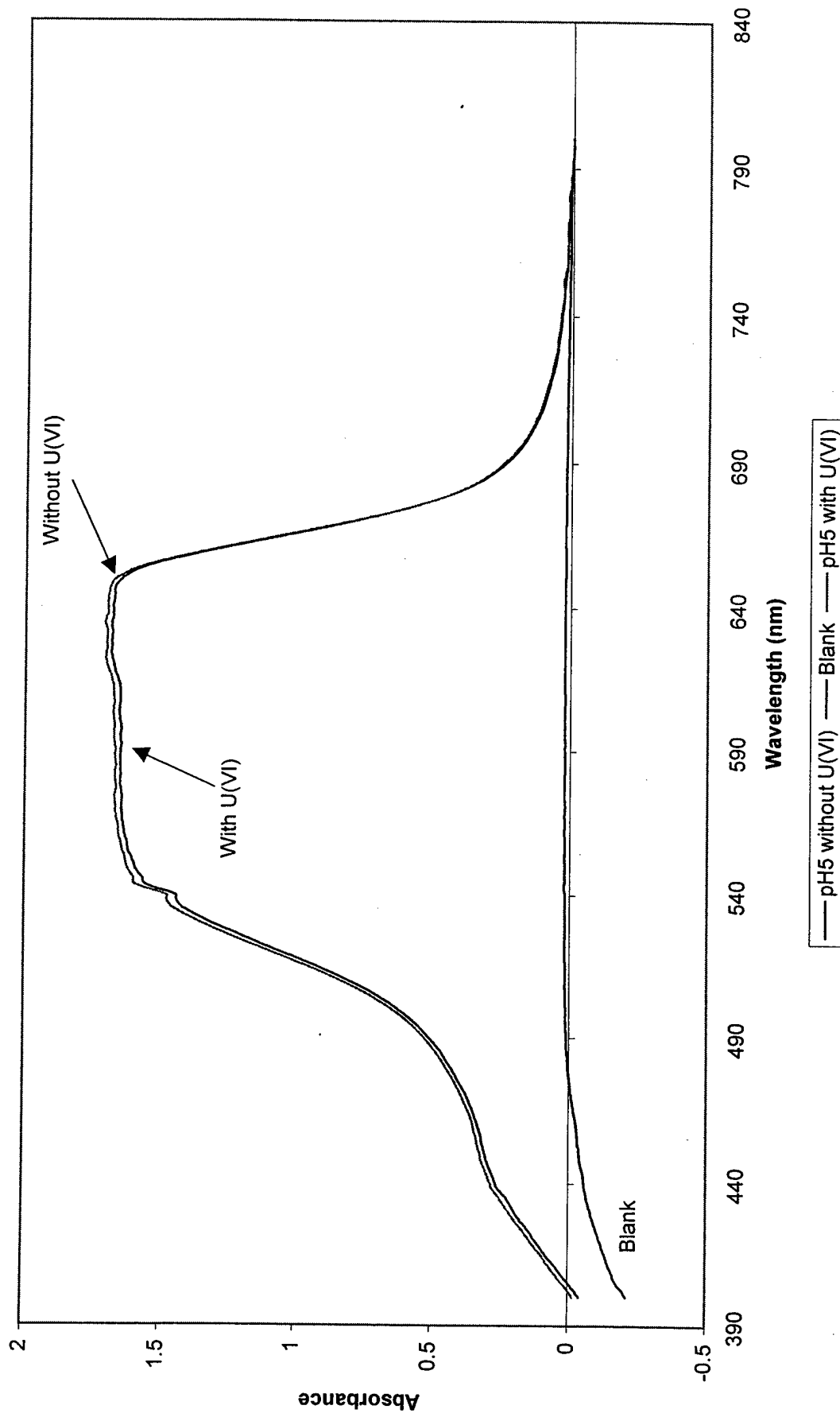
**BCB with U(VI) Metal Aqueous Species
(Normalized Values and Uncorrected for Background)**



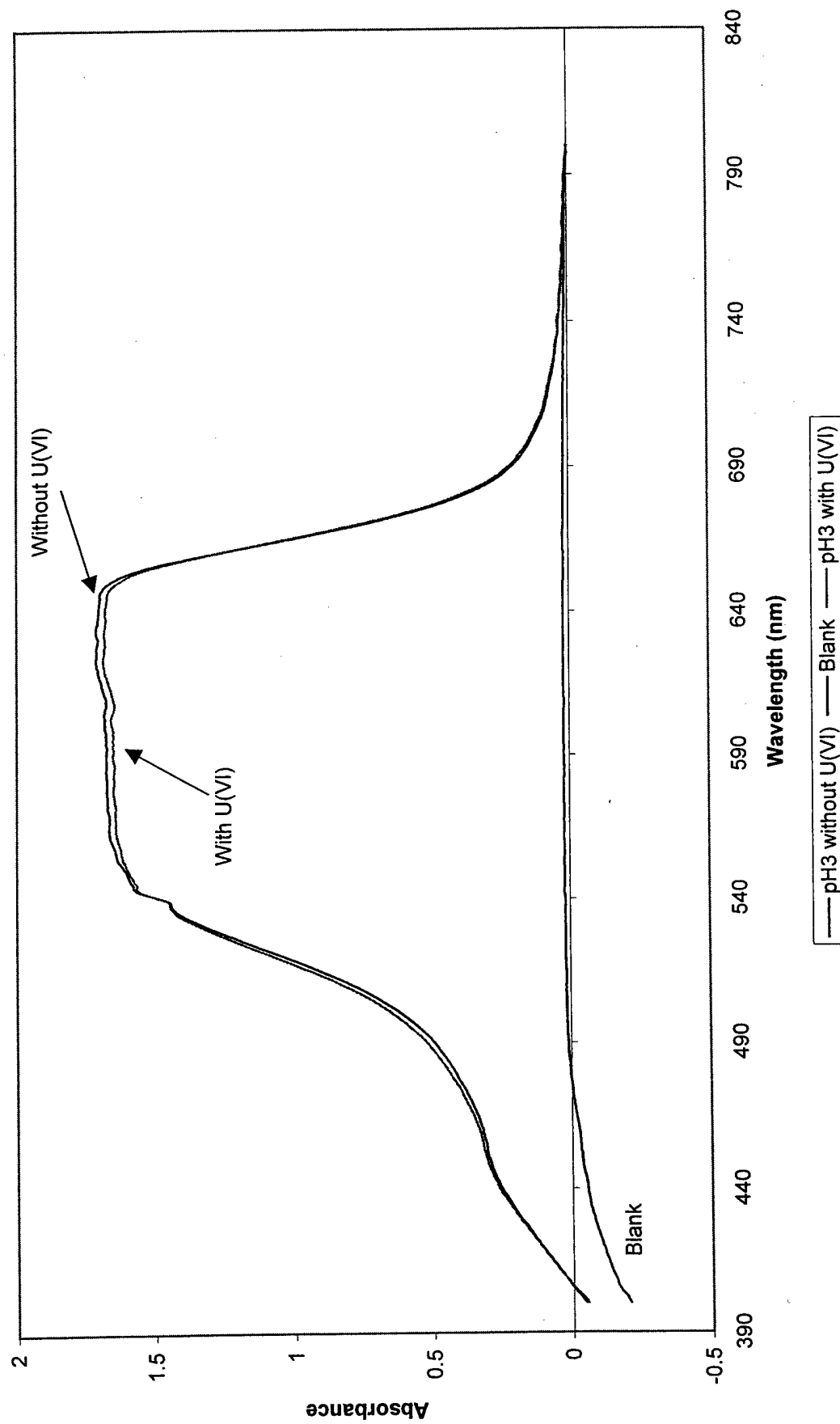
BCB Complexion with U(VI) Metal Aqueous Species in pH7 Buffer (Normalized Values and Uncorrected for Background)



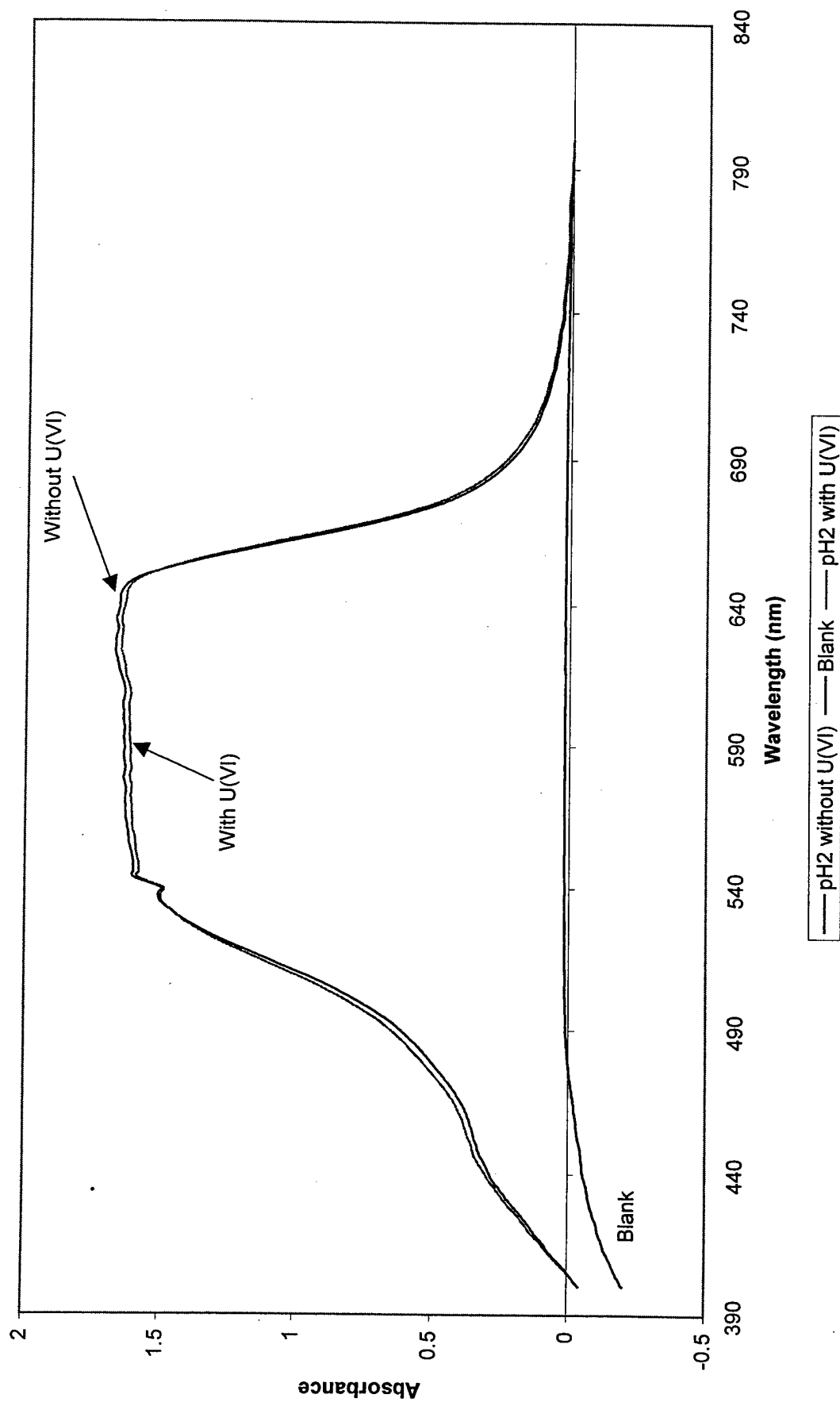
**BCB Complexion with U(VI) Metal Aqueous Species in pH5 Buffer
(Normalized Values and Uncorrected for Background)**



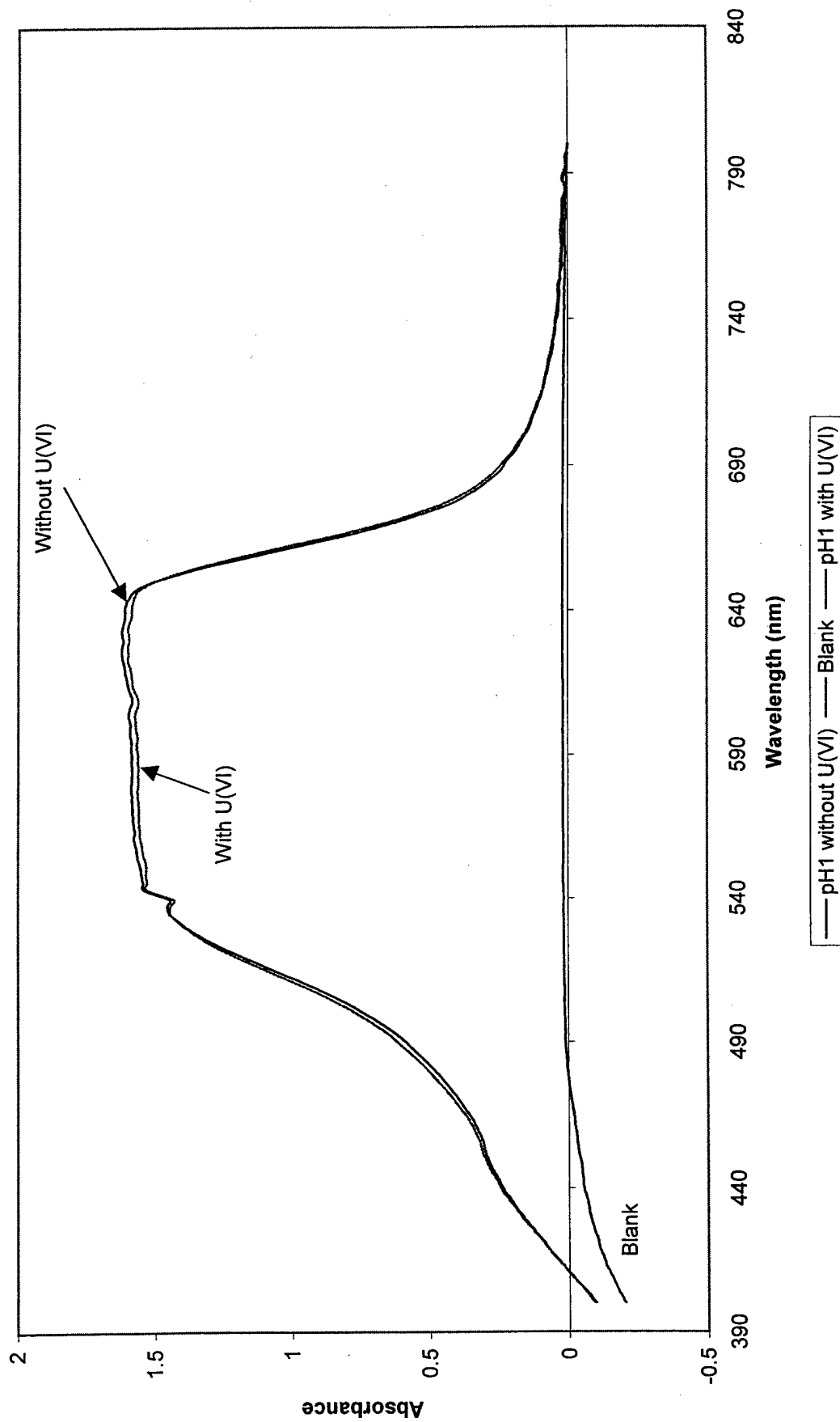
BCB Complexion with U(VI) Metal Aqueous Species in pH3 Buffer (Normalized Values and Uncorrected for Background)



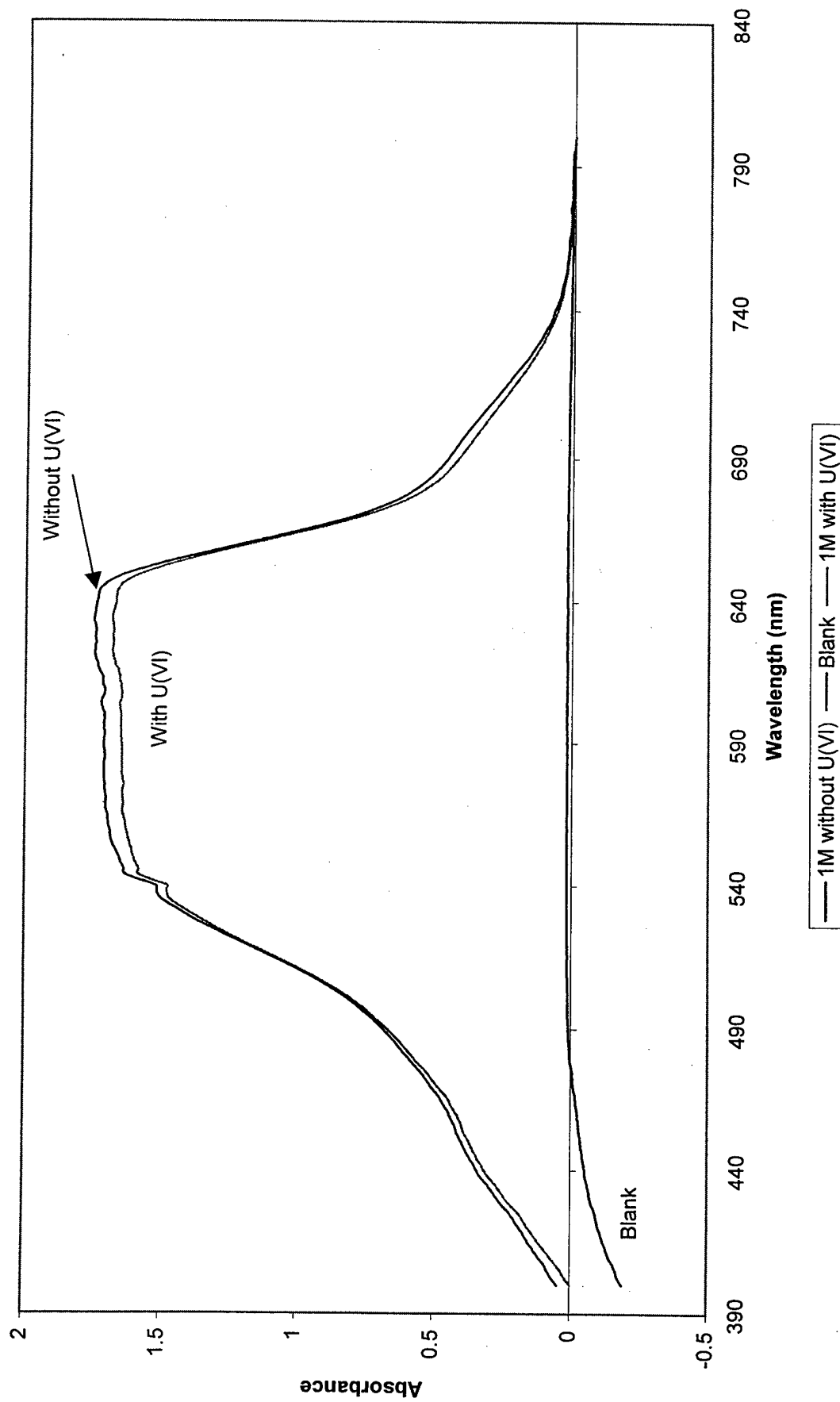
BCB Complexion with U(VI) Metal Aqueous Species in pH2 Buffer (Normalized Values and Uncorrected for Background)



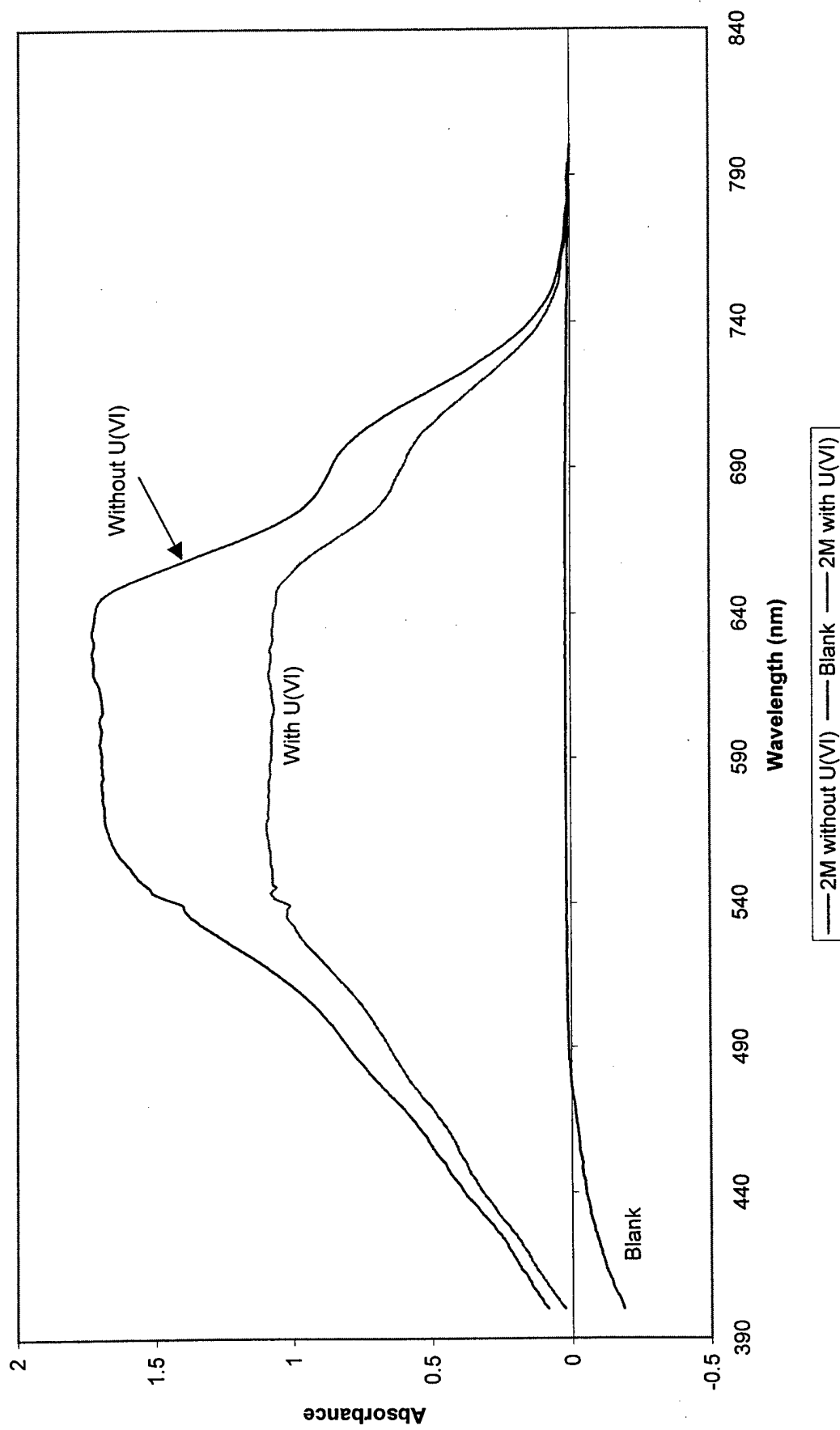
BCB Complexation with U(VI) Metal Aqueous Species in pH1 Buffer (Normalized Values and Uncorrected for Background)



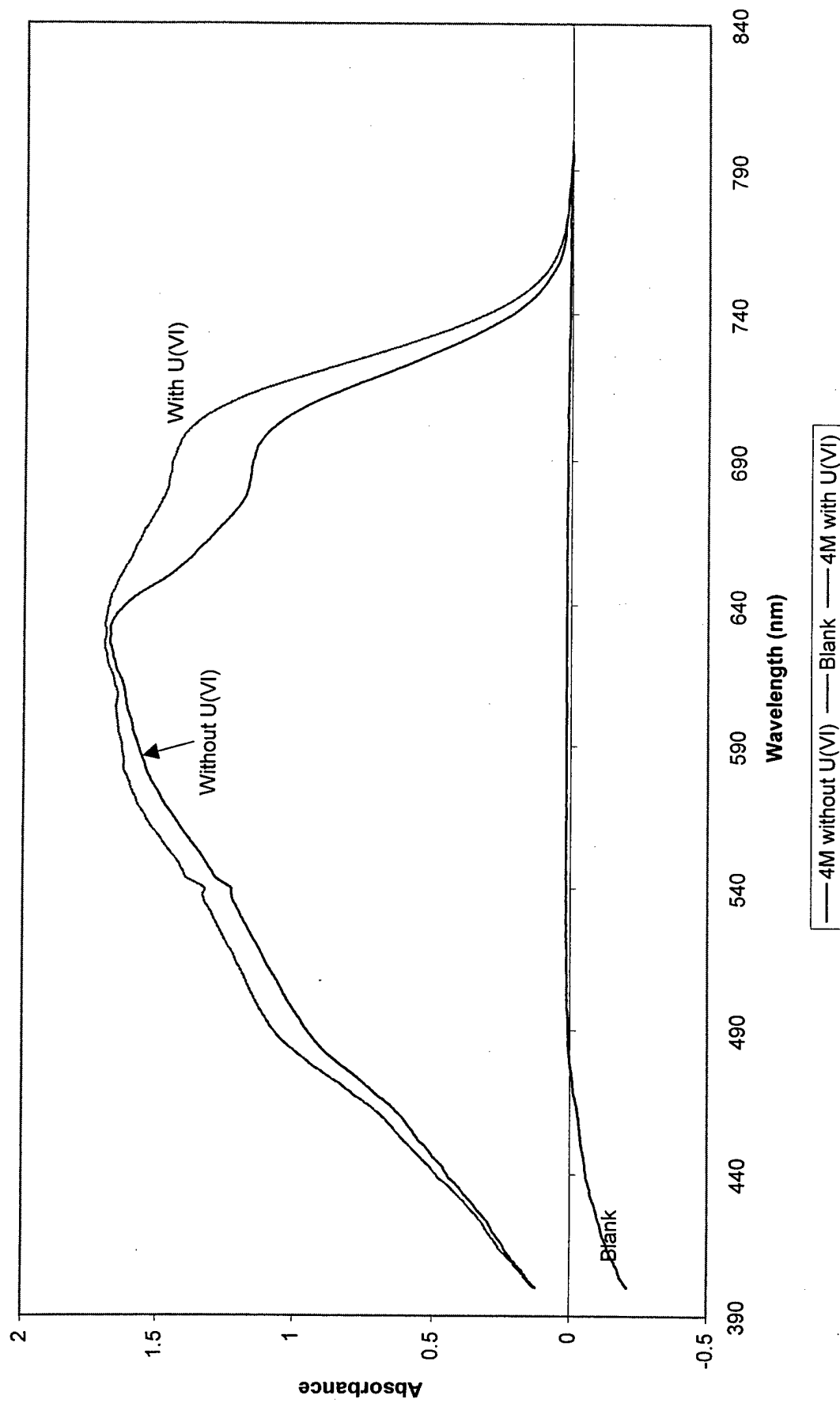
BCB Complexation with U(VI) Metal Aqueous Species in 1M HNO₃
(Normalized Values and Uncorrected for Background)



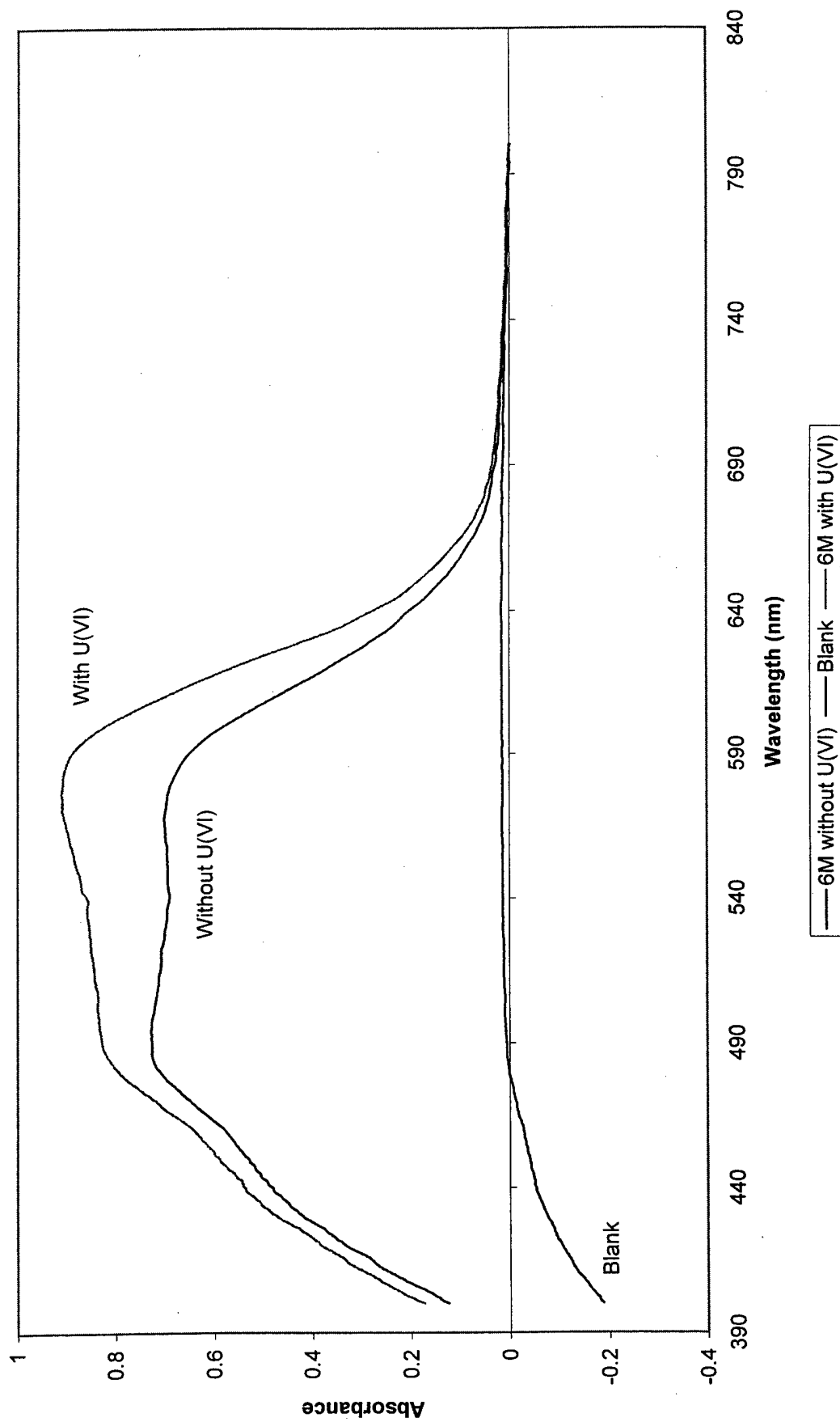
BCB Complexation with U(VI) Metal Aqueous Species in 2M HNO₃
(Normalized Values and Uncorrected for Background)



BCB Complexion with U(VI) Metal Aqueous Species in 4M HNO₃
(Normalized Values and Uncorrected for Background)



BCB Complexation with U(VI) Metal Aqueous Species in 6M HNO₃
(Normalized Values and Uncorrected for Background)

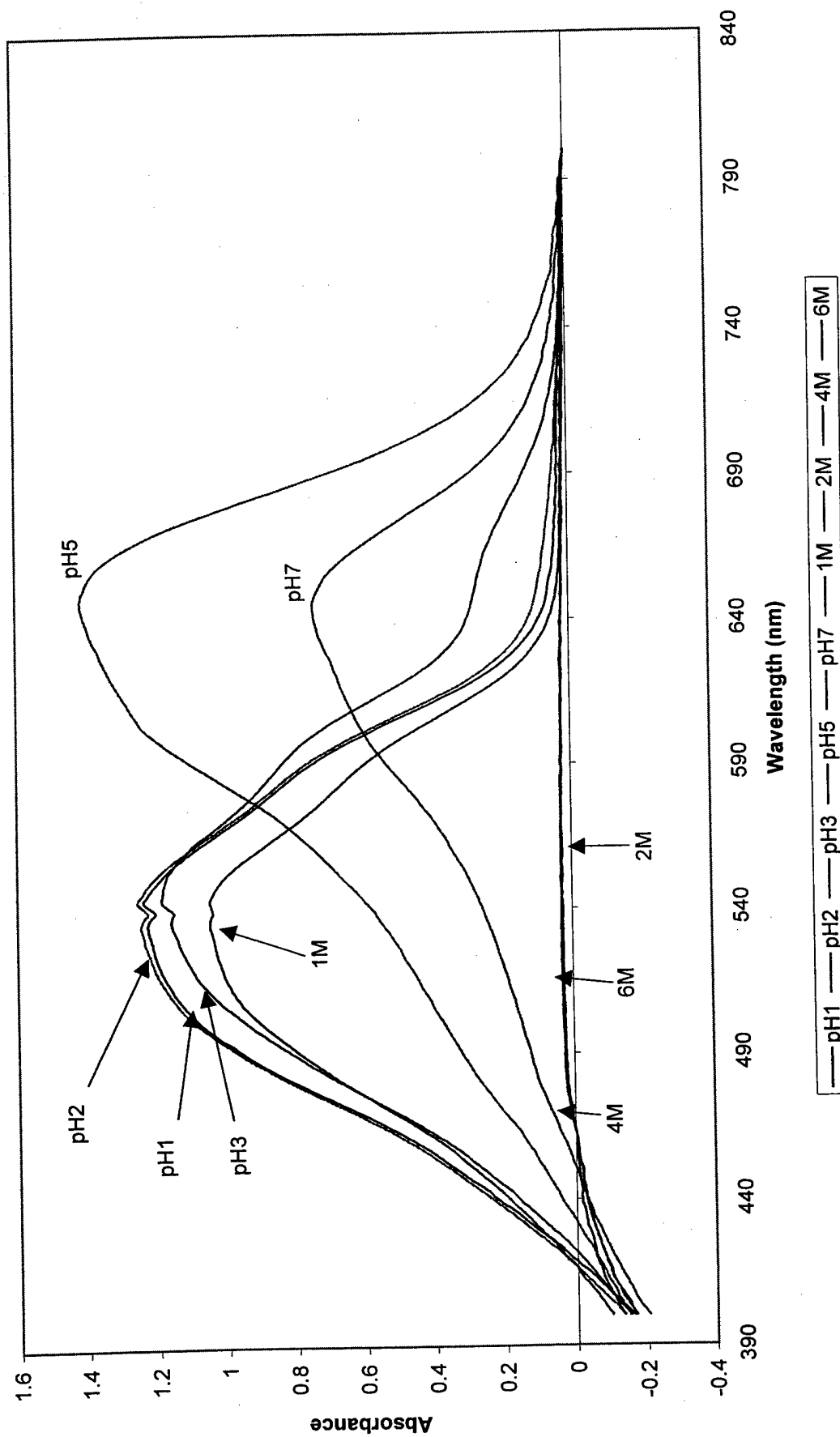


Appendix 2, Annex E

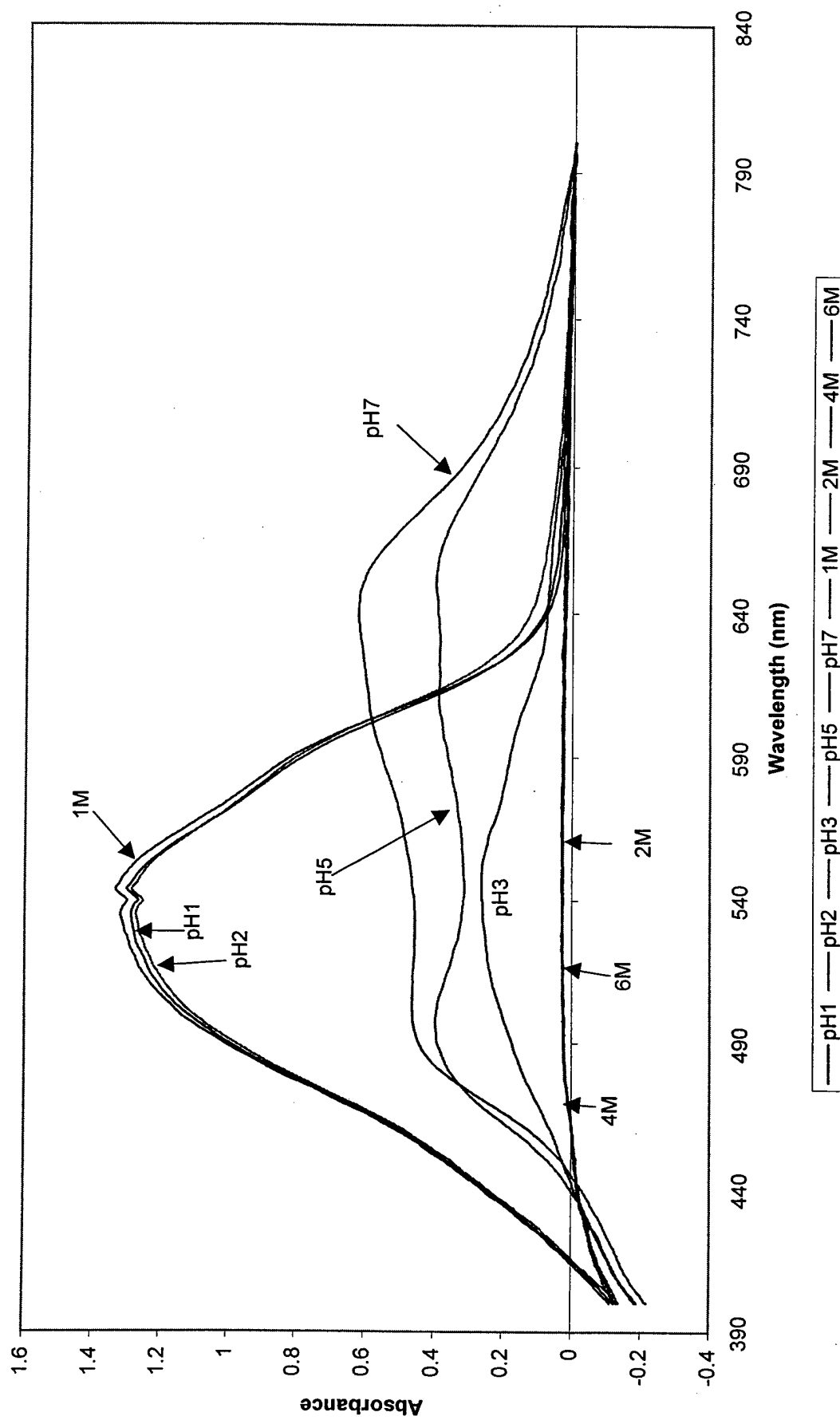
Celestine Blue Spectra Results with U(VI)

- E-1 CB total without U(VI)
- E-2 CB total with U(VI)
- E-3 CB Complexation with U(VI) at pH7
- E-4 CB Complexation with U(VI) at pH5
- E-5 CB Complexation with U(VI) at pH3
- E-6 CB Complexation with U(VI) at pH2
- E-7 CB Complexation with U(VI) at pH1
- E-8 CB Complexation with U(VI) at 1N HNO₃
- E-9 CB Complexation with U(VI) at 2N HNO₃
- E-10 CB Complexation with U(VI) at 4N HNO₃
- E-11 CB Complexation with U(VI) at 6N HNO₃

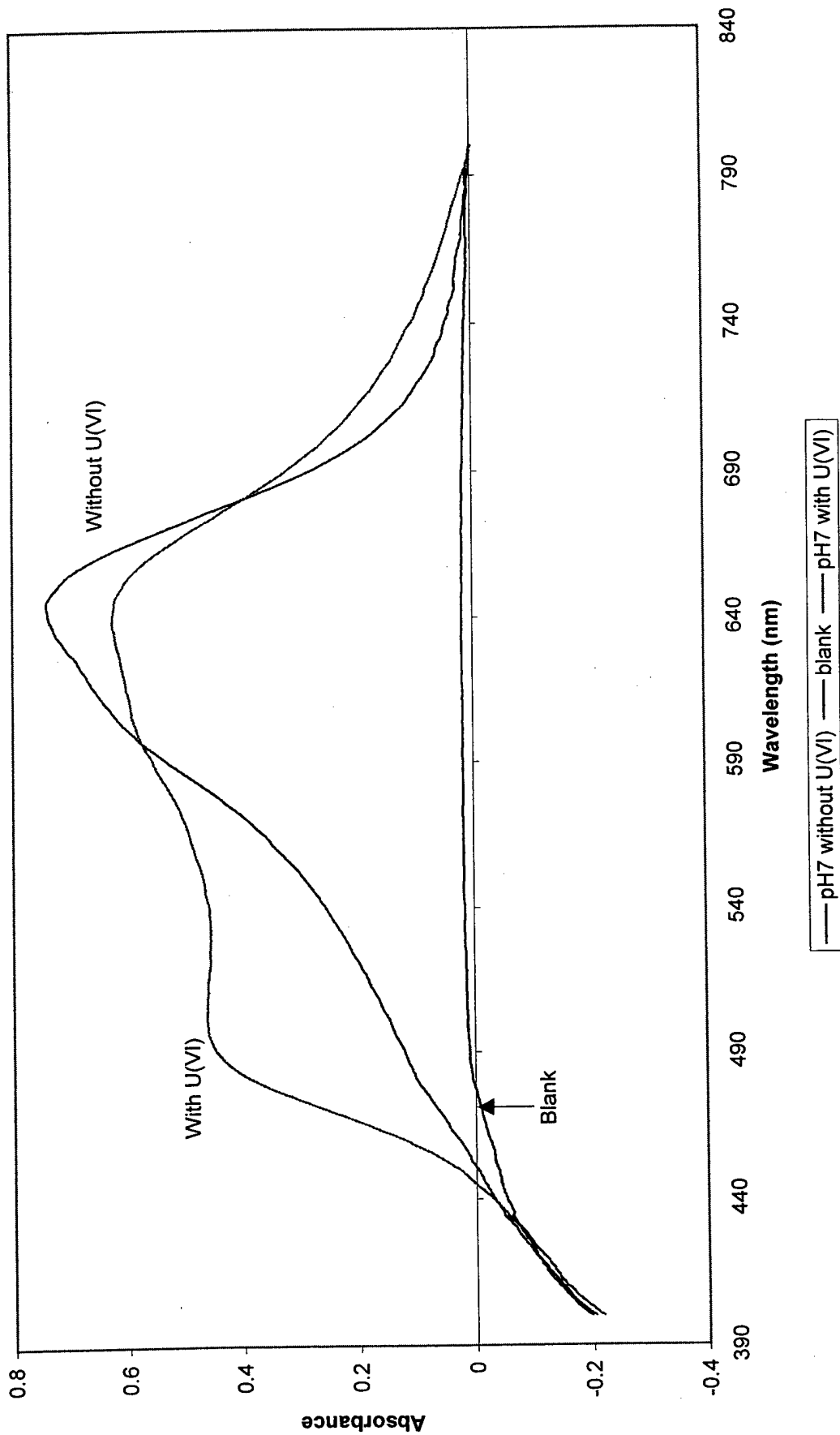
**CB without U (VI) Metal Aqueous Species
(Normalized Values and Uncorrected for Background)**



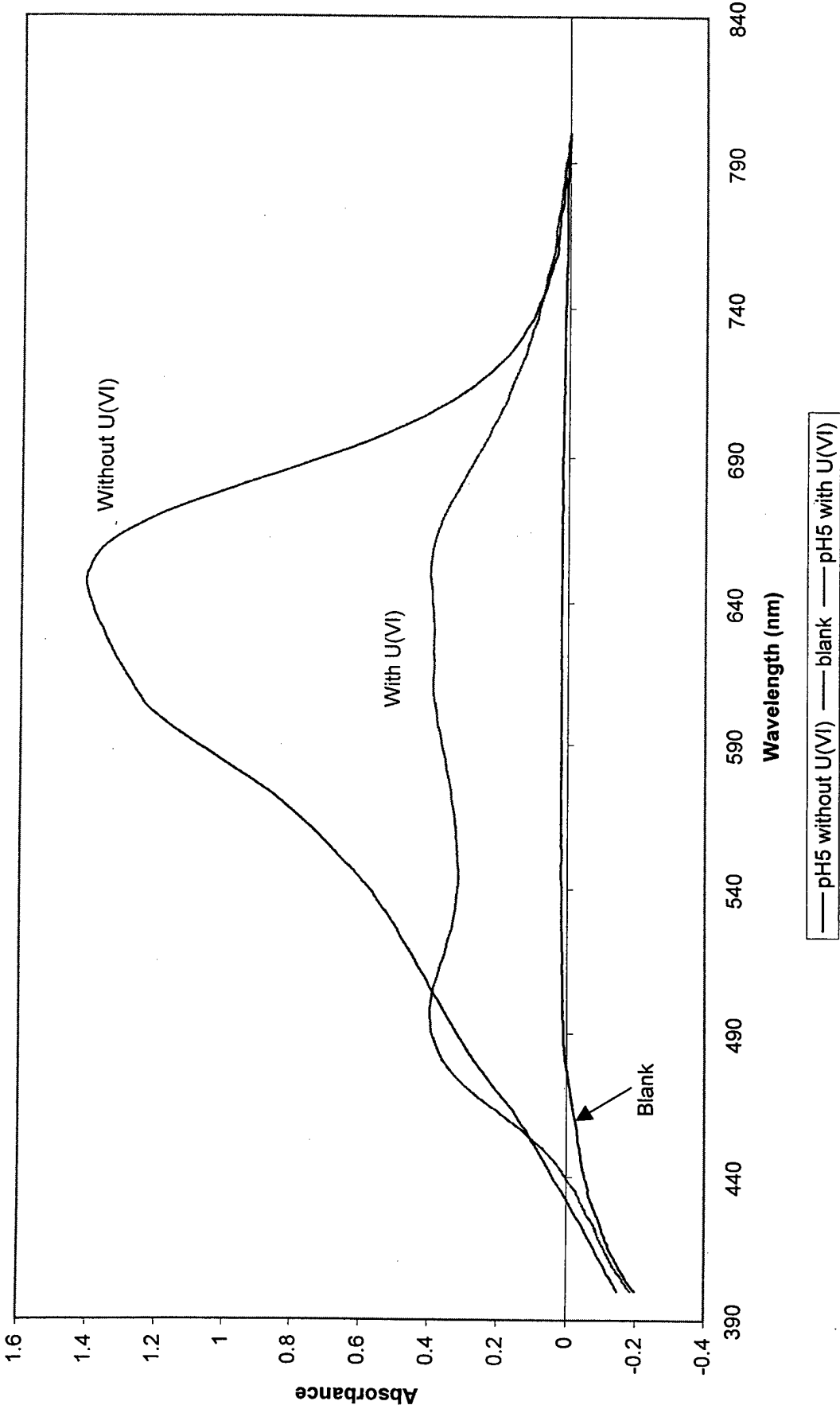
**CB with U (VI) Metal Aqueous Species
(Normalized Values and Uncorrected for Background)**



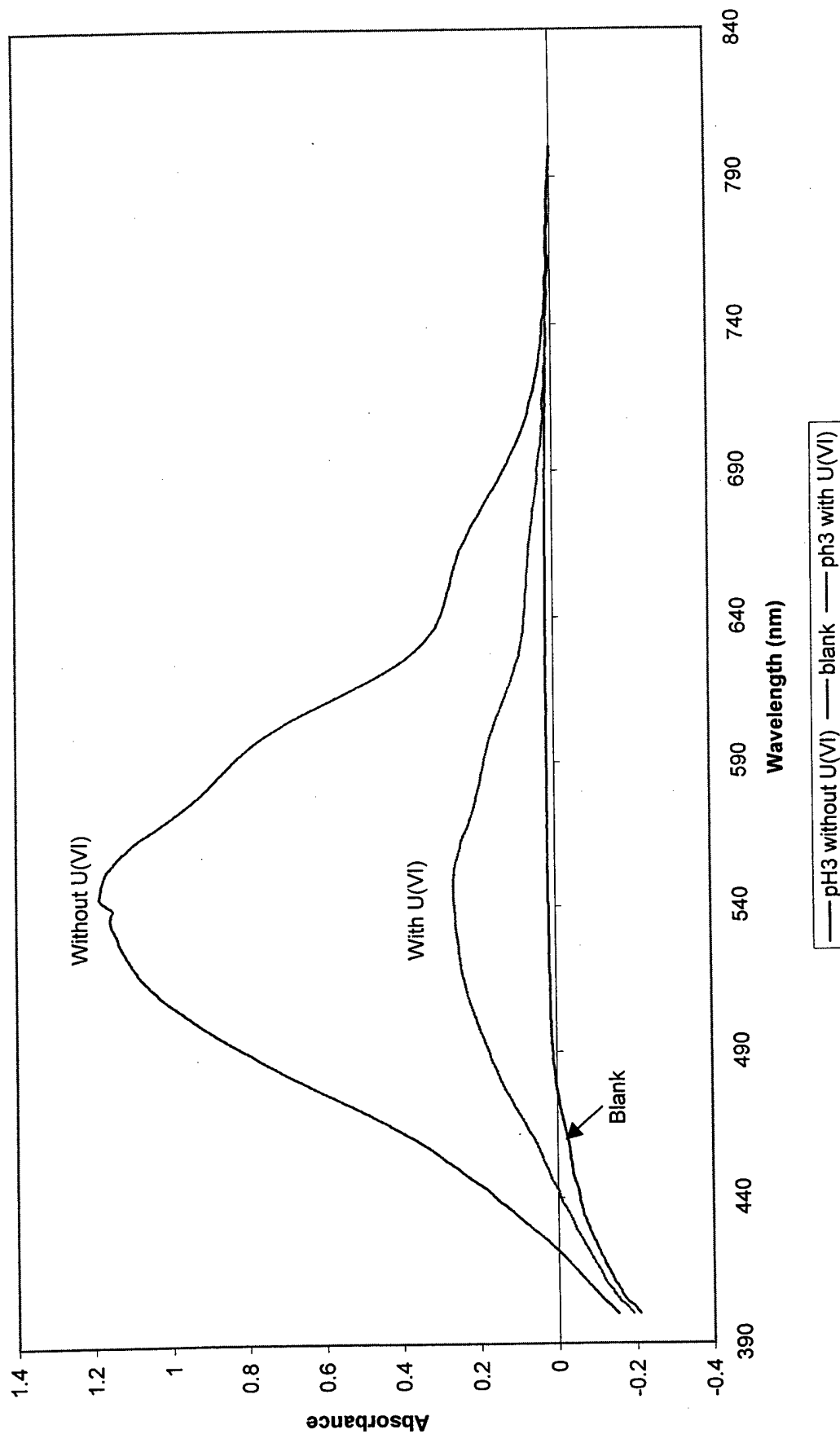
CB Complexion with U (VI) Metal Aqueous Species in pH7 Buffer (Normalized Values and Uncorrected for Background)



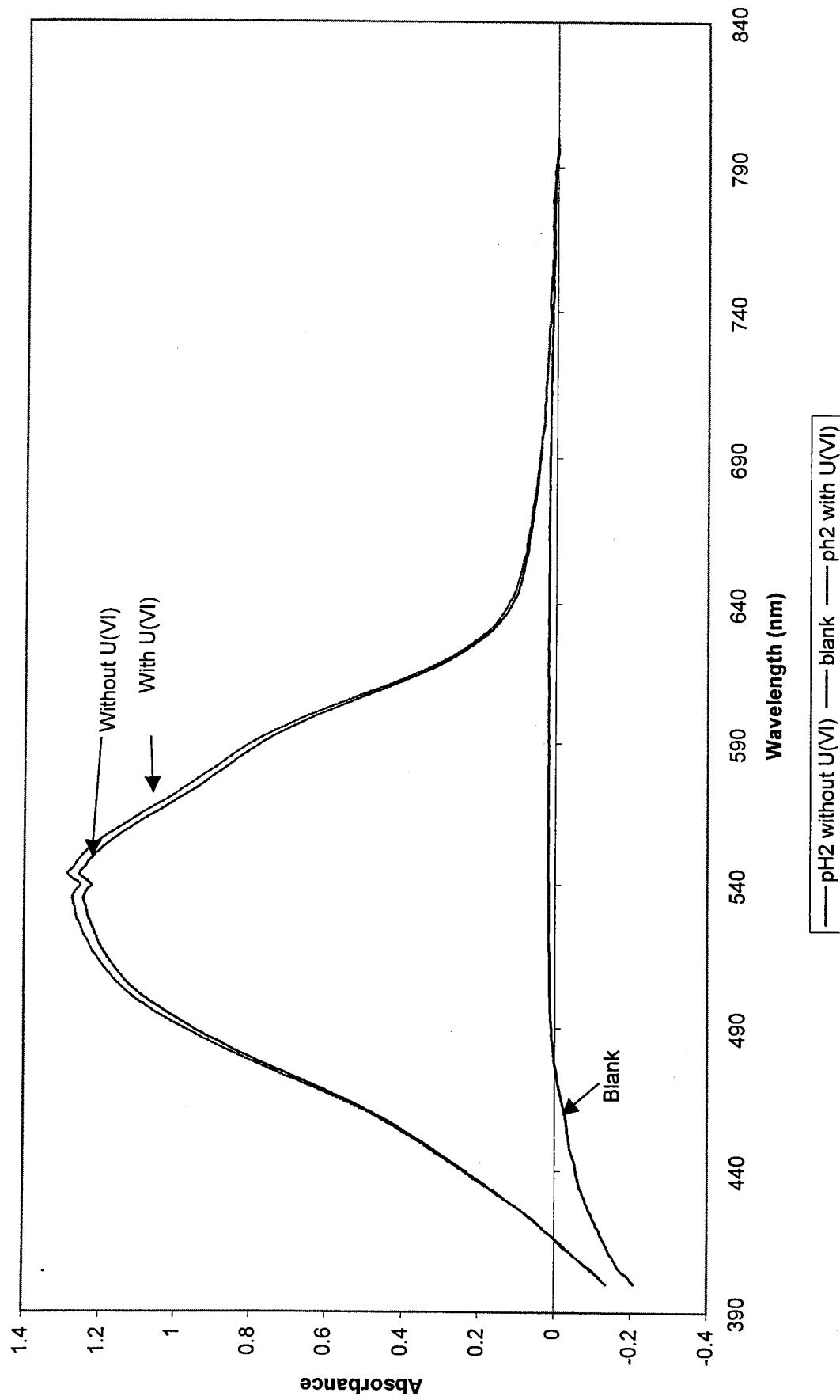
CB Complexion with U (VI) Metal Aqueous Species in pH5 Buffer
(Normalized Values and Uncorrected for Background)



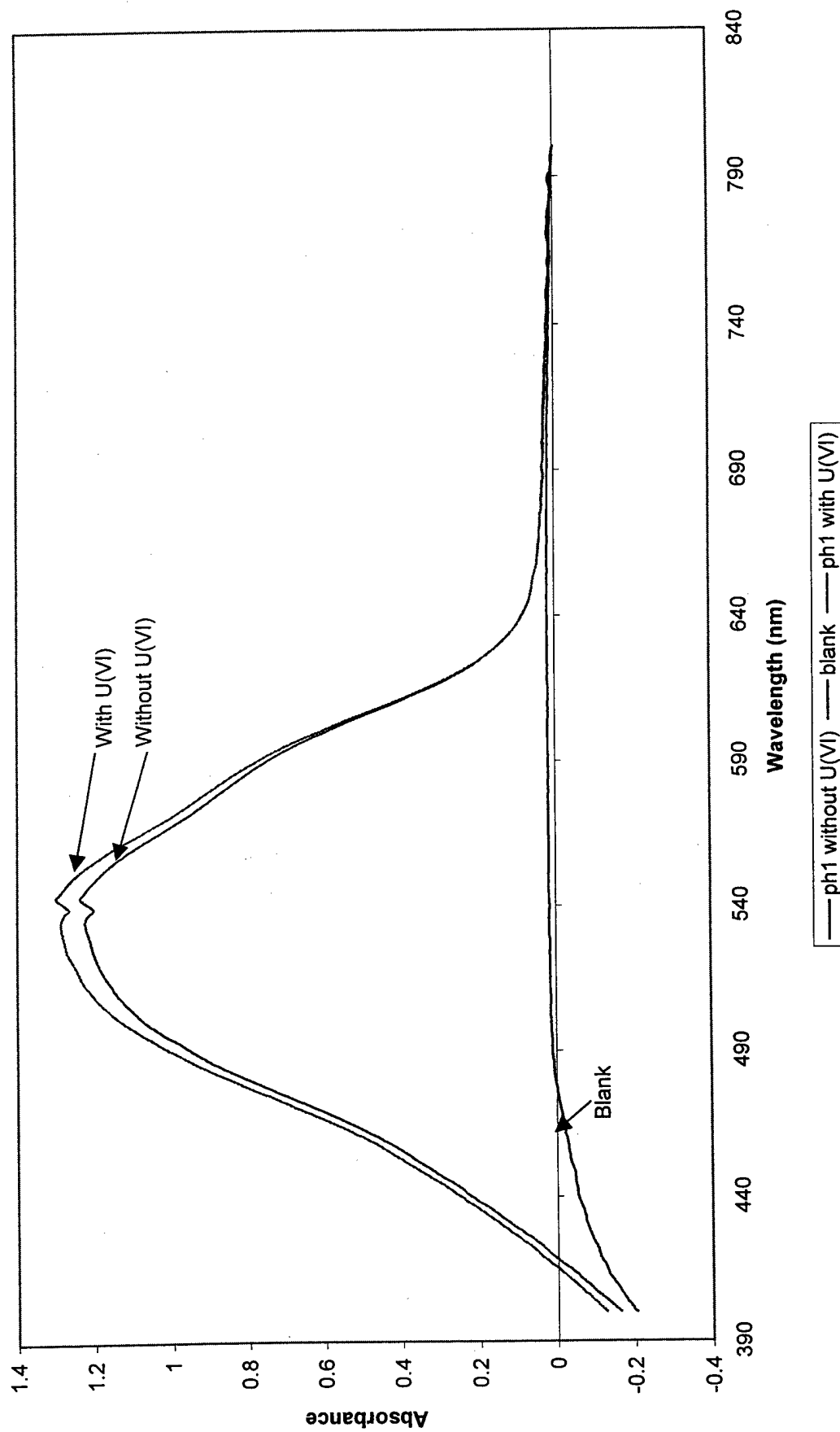
CB Complexation with U (VI) Metal Aqueous Species in pH3 Buffer (Normalized Values and Uncorrected for Background)



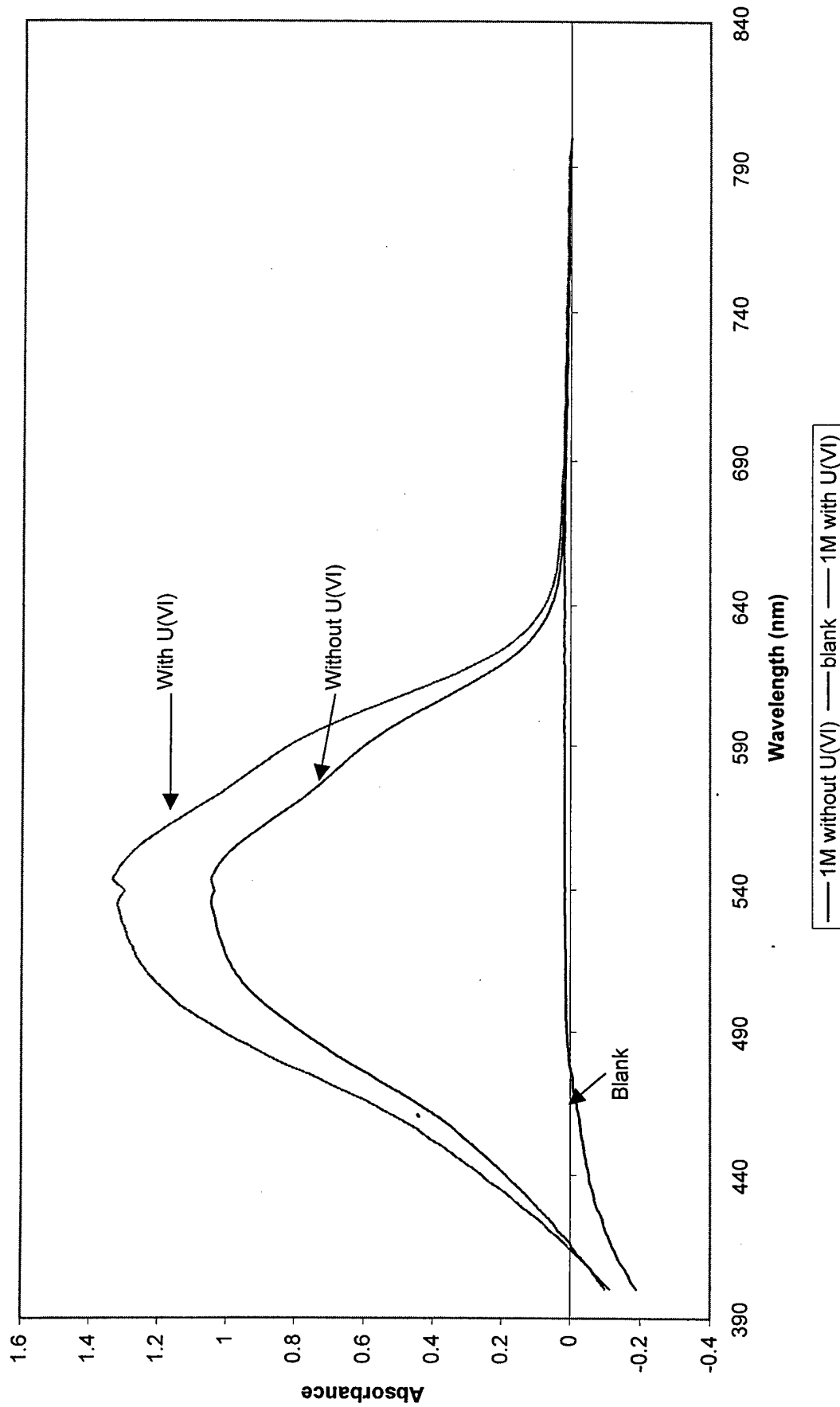
CB Complexation with U (VI) Metal Aqueous Species in pH2 Buffer (Normalized Values and Uncorrected for Background)



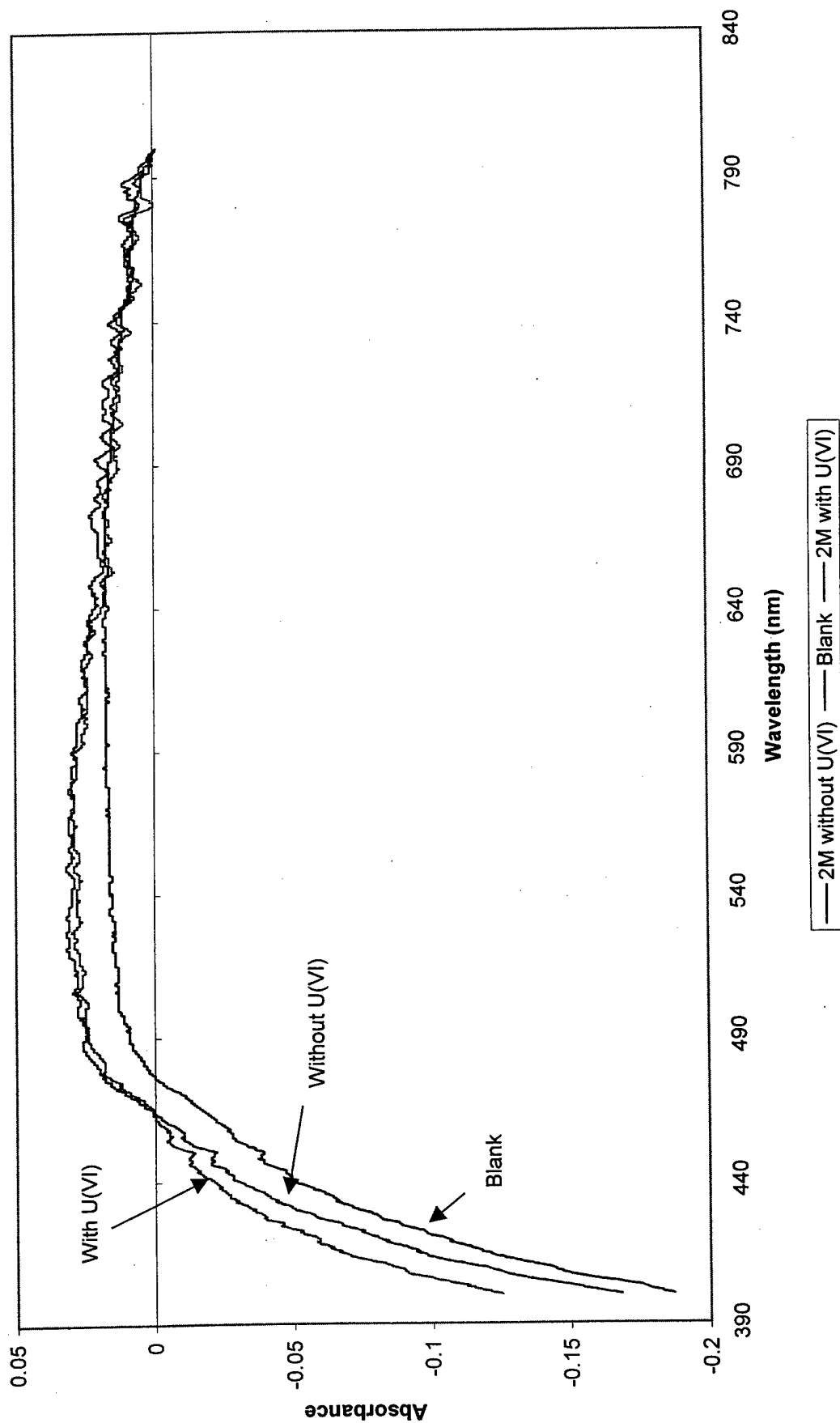
CB Complexion with U (VI) Metal Aqueous Species in pH1 Buffer (Normalized Values and Uncorrected for Background)



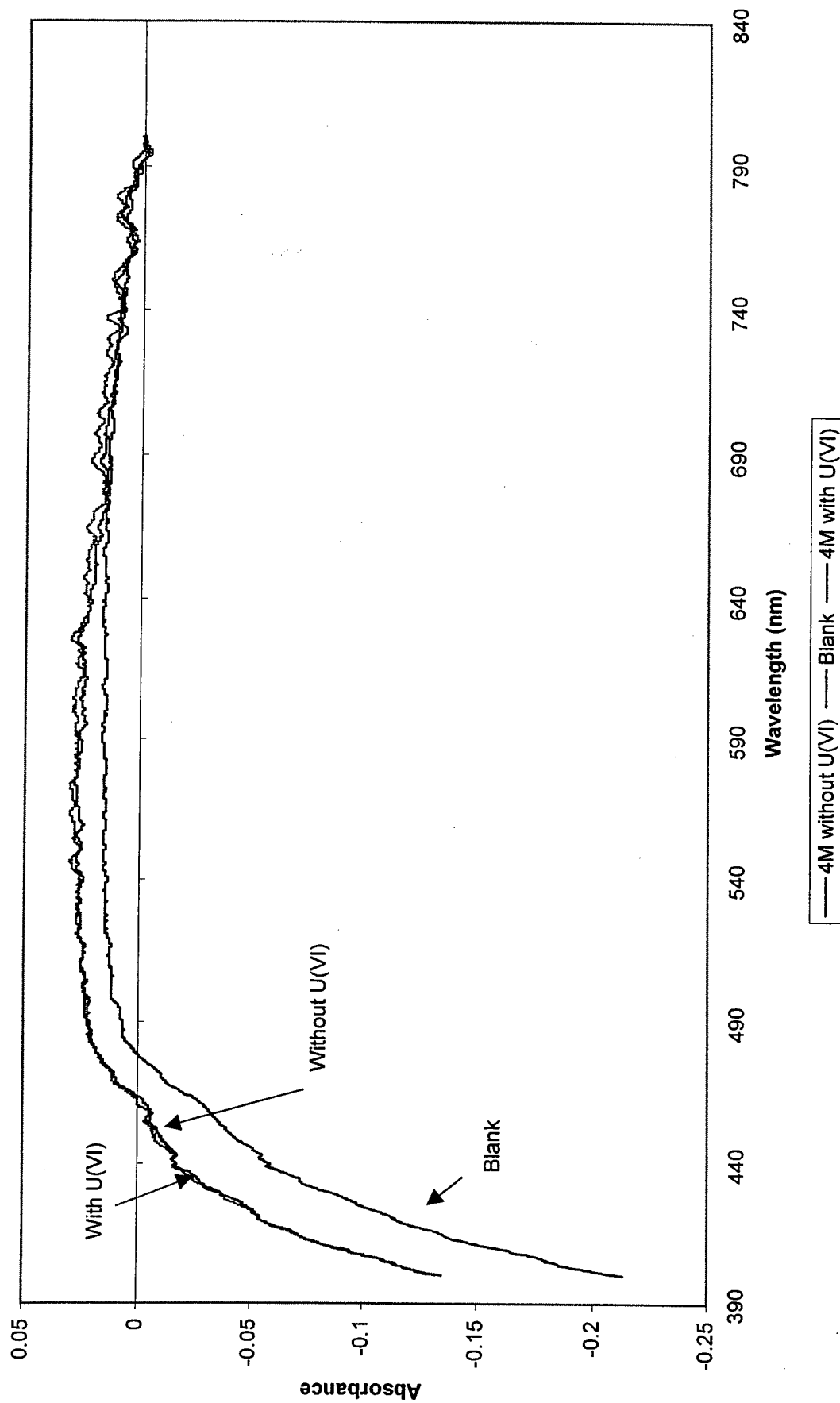
CB Complexion with U (VI) Metal Aqueous Species in 1M HNO₃ **(Normalized Values and Uncorrected for Background)**



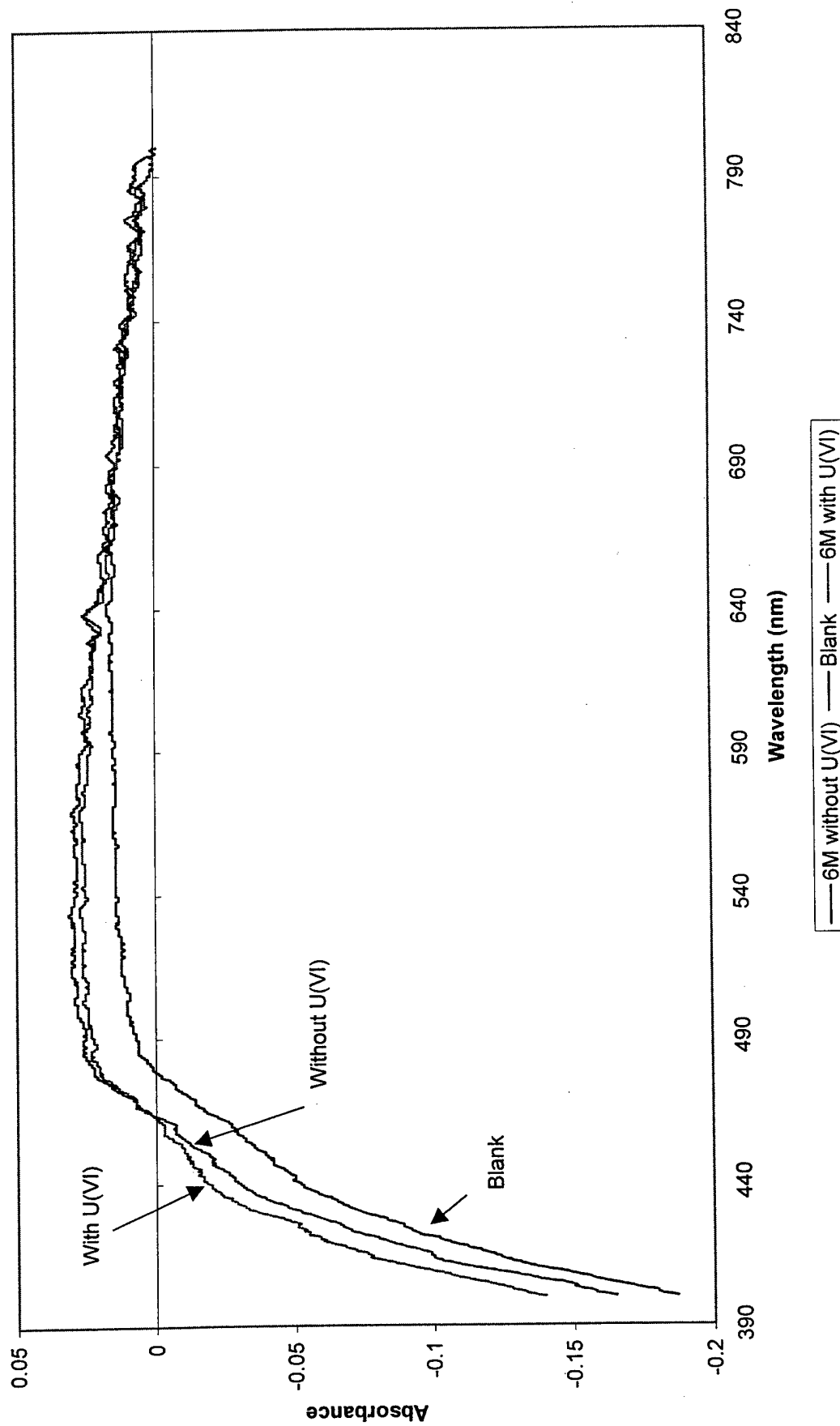
CB Complexion with U (VI) Metal Aqueous Species in 2M HNO₃ (Normalized Values and Uncorrected for Background)



CB Complexion with U (VI) Metal Aqueous Species in 4M HNO₃ **(Normalized Values and Uncorrected for Background)**



CB Complexation with U(VI) Metal Aqueous Species in 6M HNO₃
(Normalized Values and Uncorrected for Background)

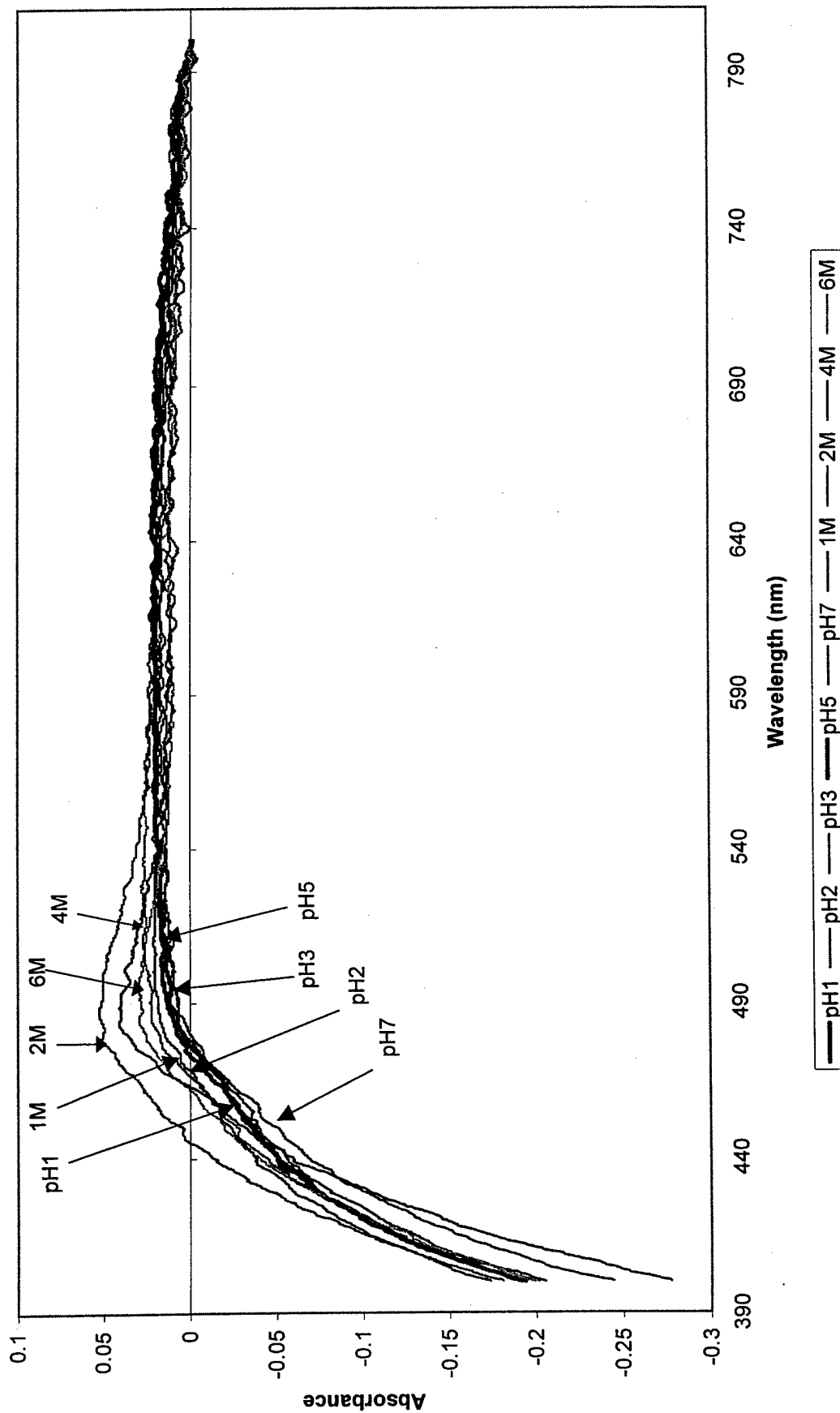


Appendix 2, Annex F

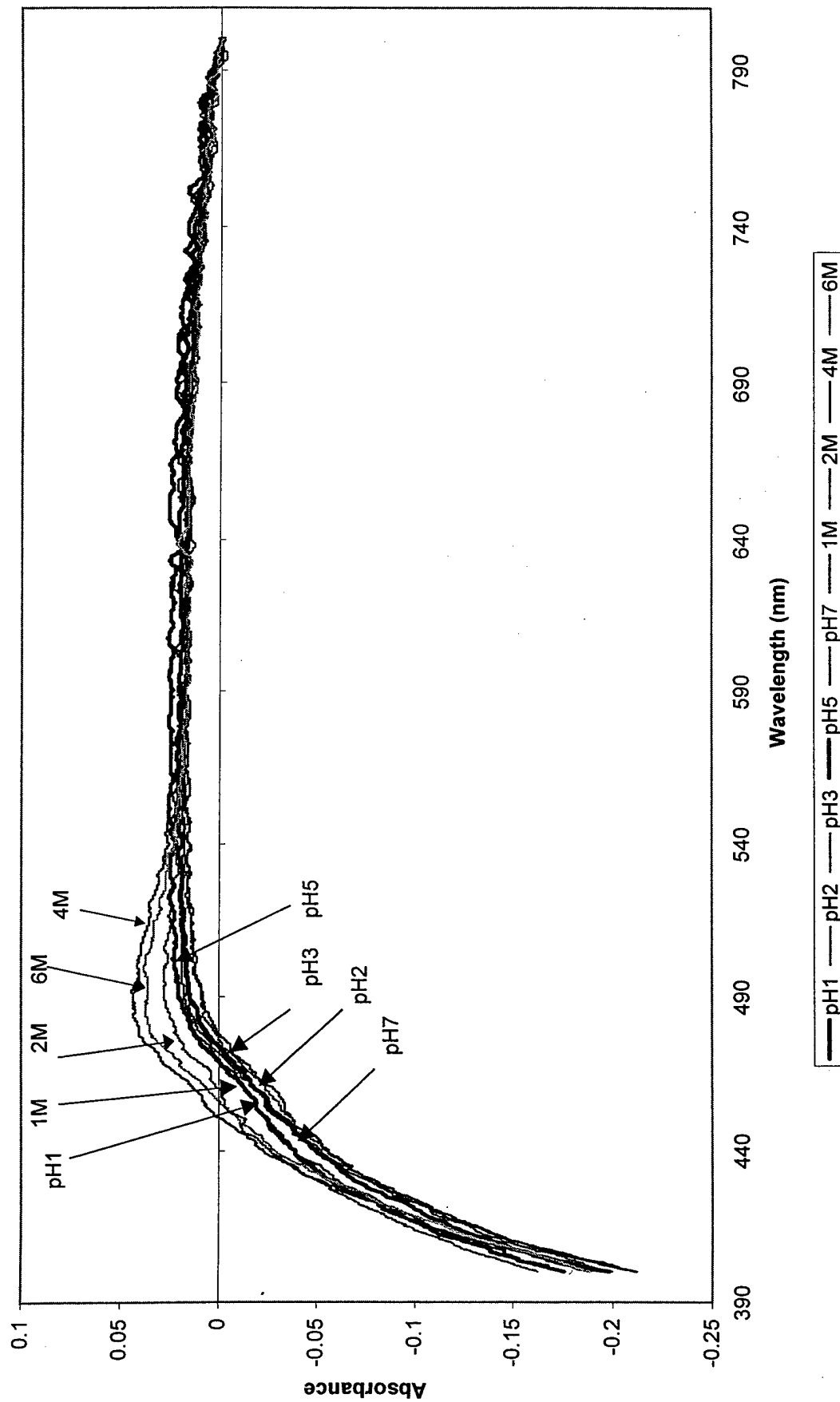
Gallomine Triethiodide Spectra Results with U(VI)

- F-1 GT total without U(VI)
- F-2 GT total with U(VI)
- F-3 GT Complexation with U(VI) at pH7
- F-4 GT Complexation with U(VI) at pH5
- F-5 GT Complexation with U(VI) at pH3
- F-6 GT Complexation with U(VI) at pH2
- F-7 GT Complexation with U(VI) at pH1
- F-8 GT Complexation with U(VI) at 1N HNO₃
- F-9 GT Complexation with U(VI) at 2N HNO₃
- F-10 GT Complexation with U(VI) at 4N HNO₃
- F-11 GT Complexation with U(VI) at 6N HNO₃

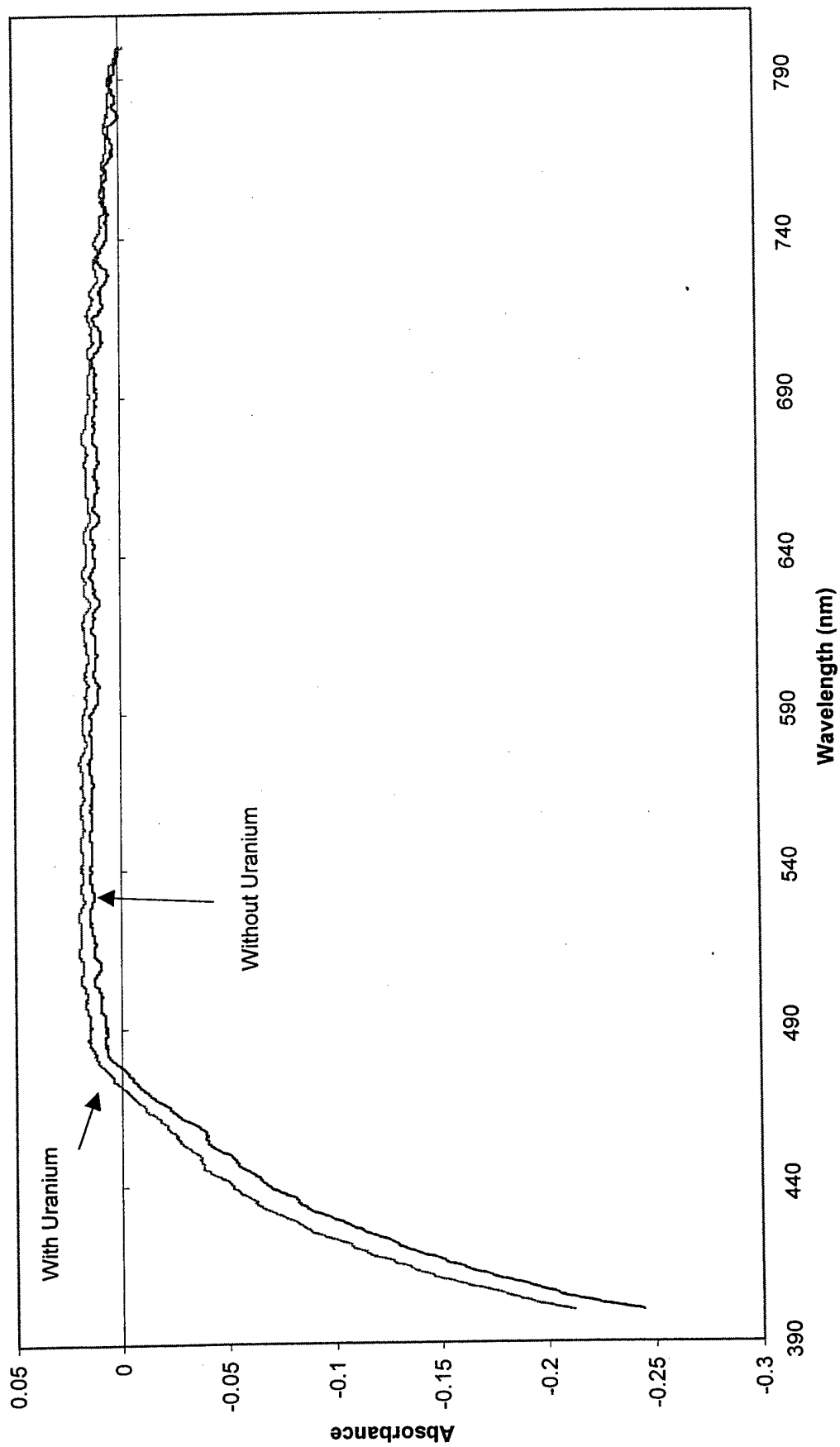
Gallamine Triethiodide without U(VI) Metal Aqueous Species (Normalized and Uncorrected for Background)



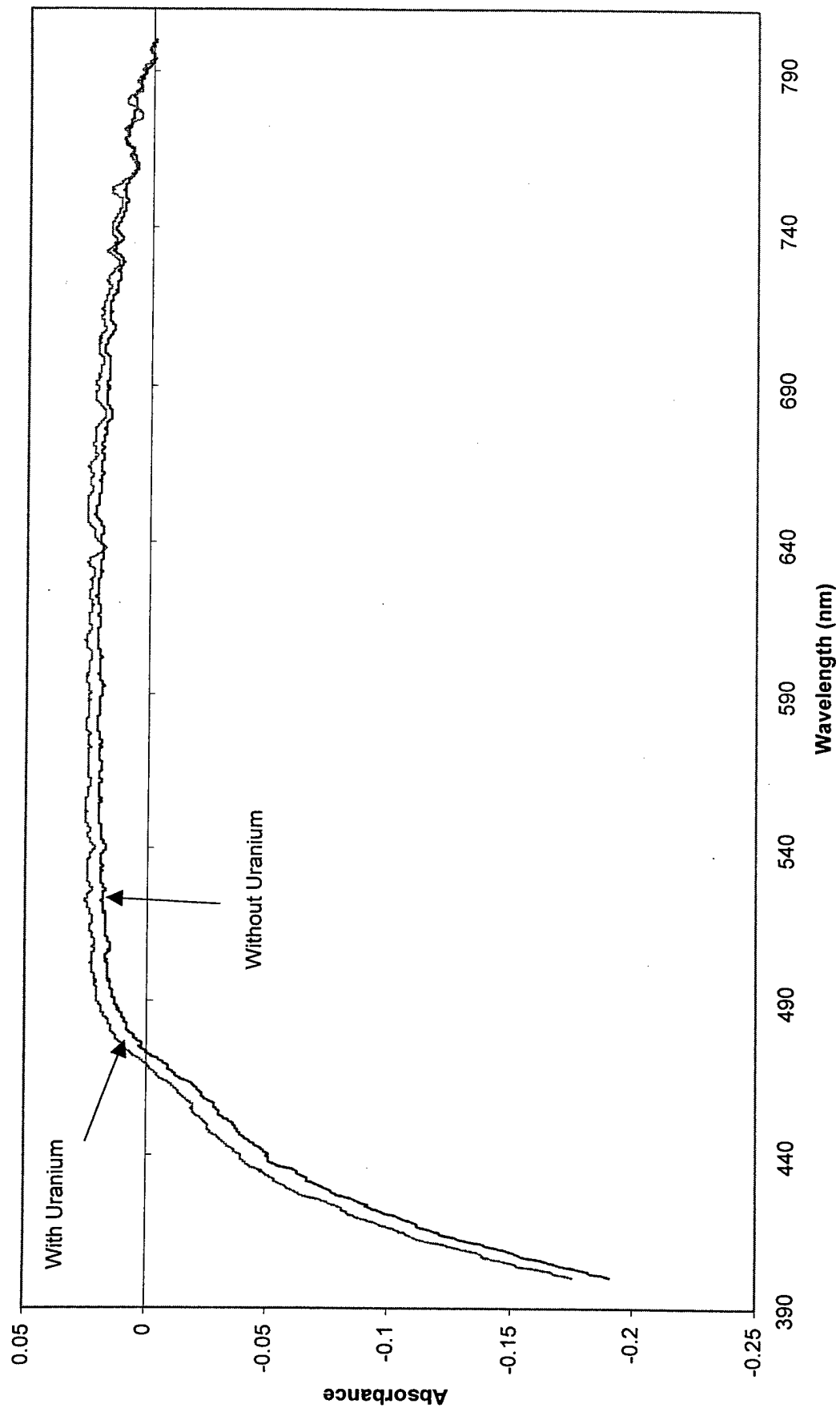
Gallamine Triethiodide with U(VI) Metal Aqueous Species (Normalized and Uncorrected for Background)



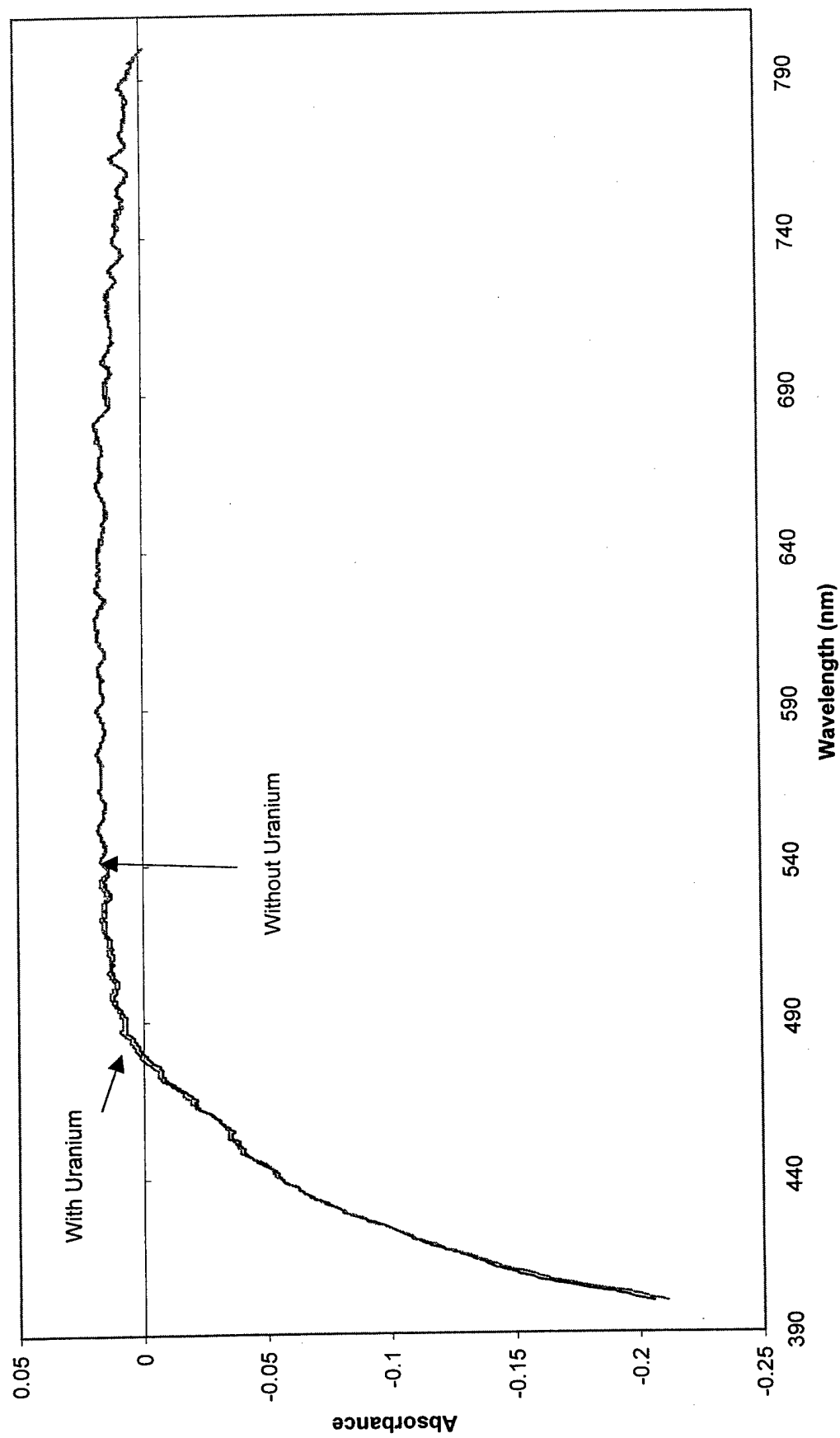
**GT Complexation with U(VI) Metal Aqueous Species in pH7 Buffer
(Normalized and Uncorrected for Background)**



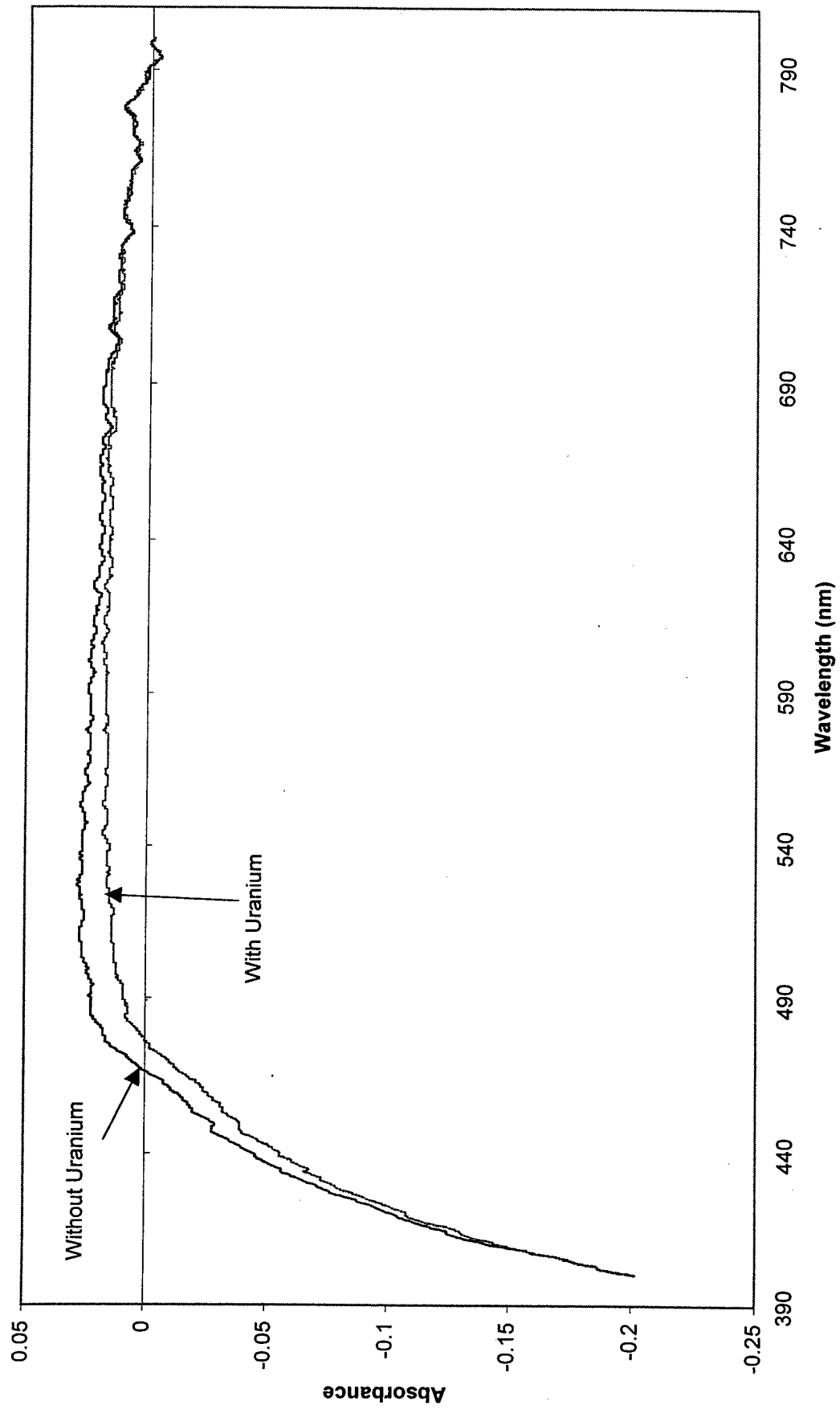
**GT Complexation with U(VI) Metal Aqueous Species in pH5 Buffer
(Normalized and Uncorrected for Background)**



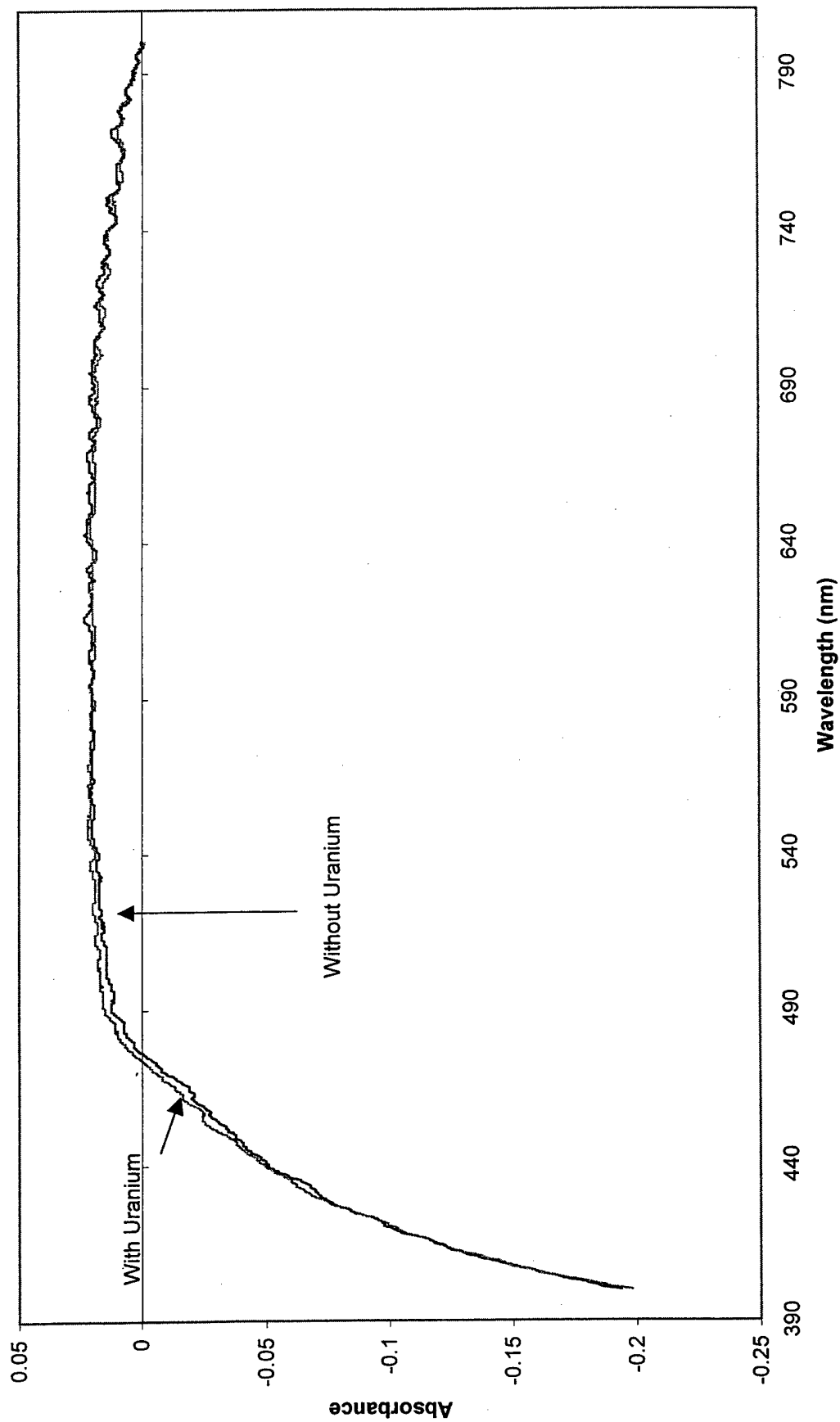
**GT Complexation with U(VI) Metal Aqueous Species in pH3 Buffer
(Normalized and Uncorrected for Background)**



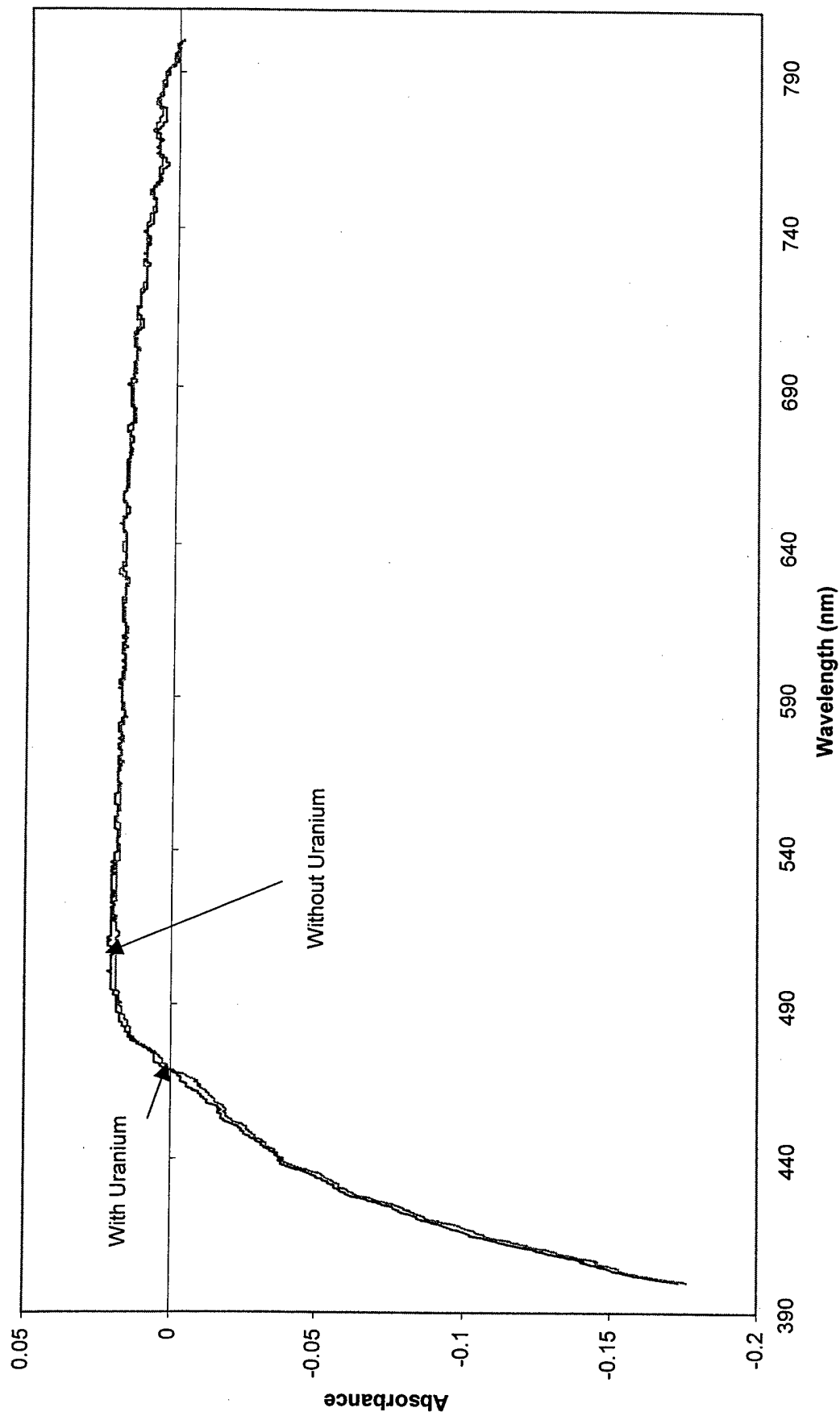
**GT Complexation with U(VI) Metal Aqueous Species in pH2 Buffer
(Normalized and Uncorrected for Background)**



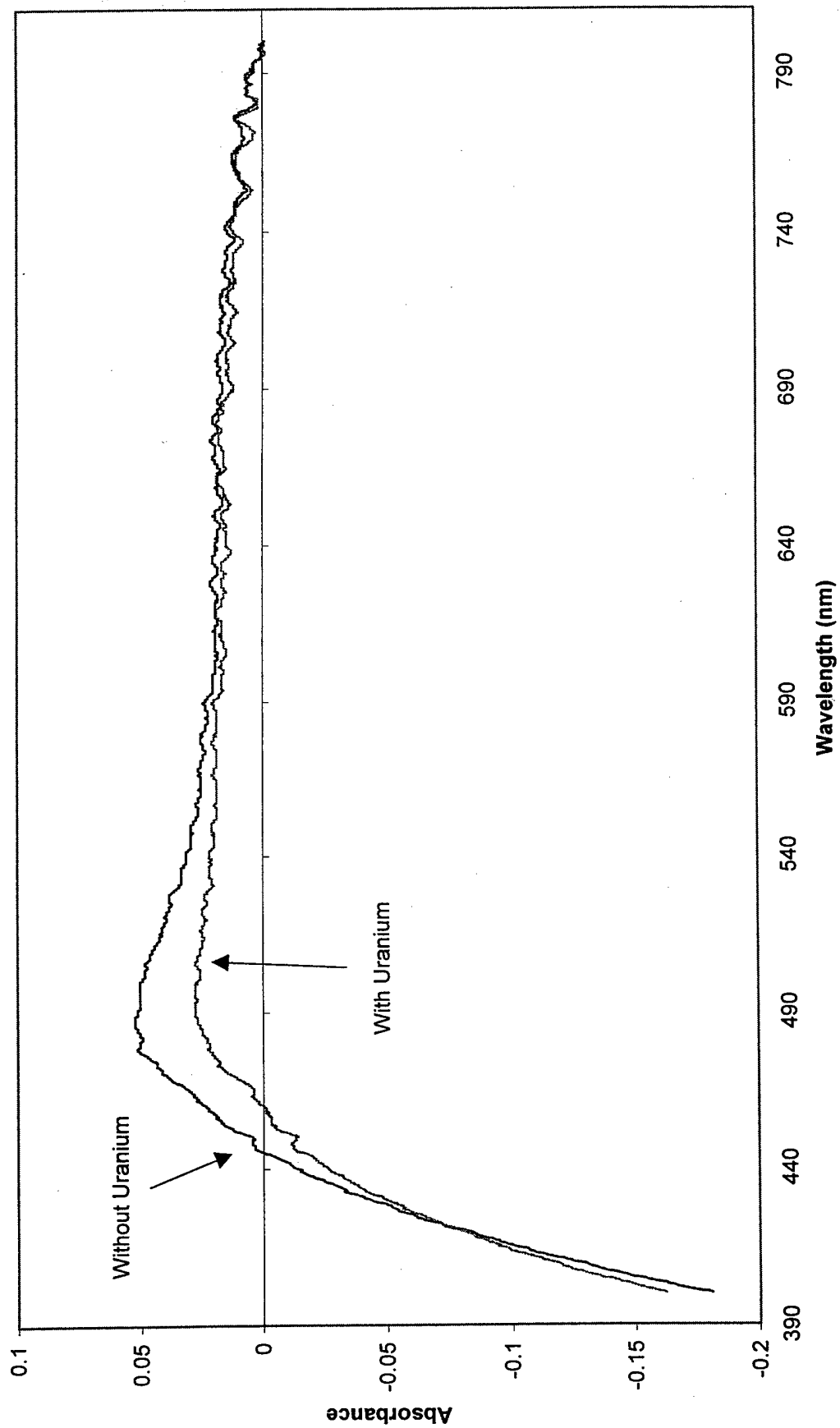
**GT Complexation with U(VI) Metal Aqueous Species in pH1 Buffer
(Normalized and Uncorrected for Background)**



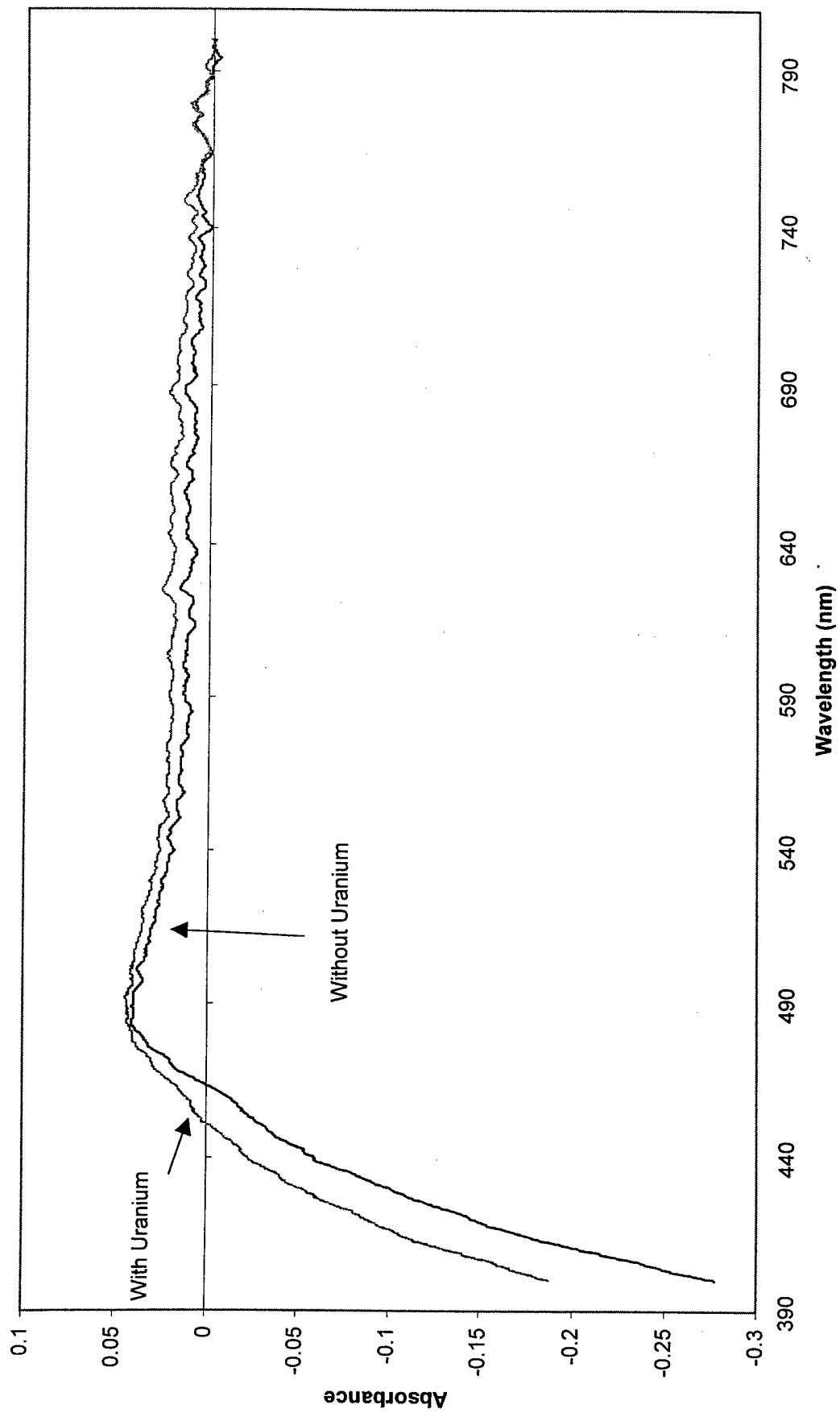
**GT Complexation with U(VI) Metal Aqueous Species in 1M HNO₃
(Normalized and Uncorrected for Background)**



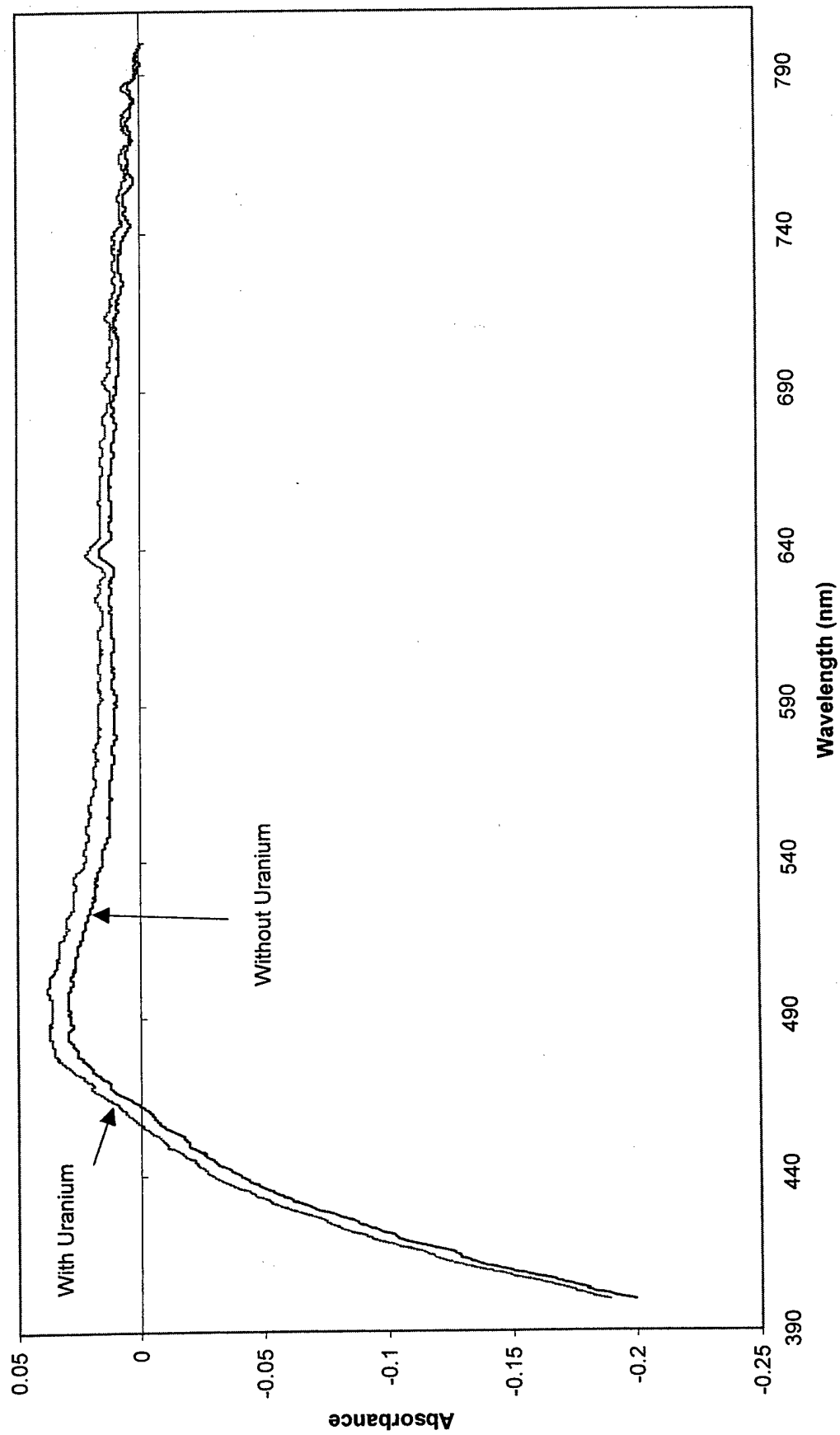
GT Complexation with U(VI) Metal Aqueous Species in 2M HNO₃
(Normalized and Uncorrected for Background)



GT Complexation with U(VI) Metal Aqueous Species in 4M HNO₃
(Normalized and Uncorrected for Background)



GT Complexation with U(VI) Metal Aqueous Species in 6M HNO₃
(Normalized and Uncorrected for Background)



Appendix 2, Annex G

G-1 Database from ICP-AES Data on Concentration of C45

G-2 Calibration for Uranium Standards used to determine the concentration of Uranium in C45

Appendix 2, Annex G-1

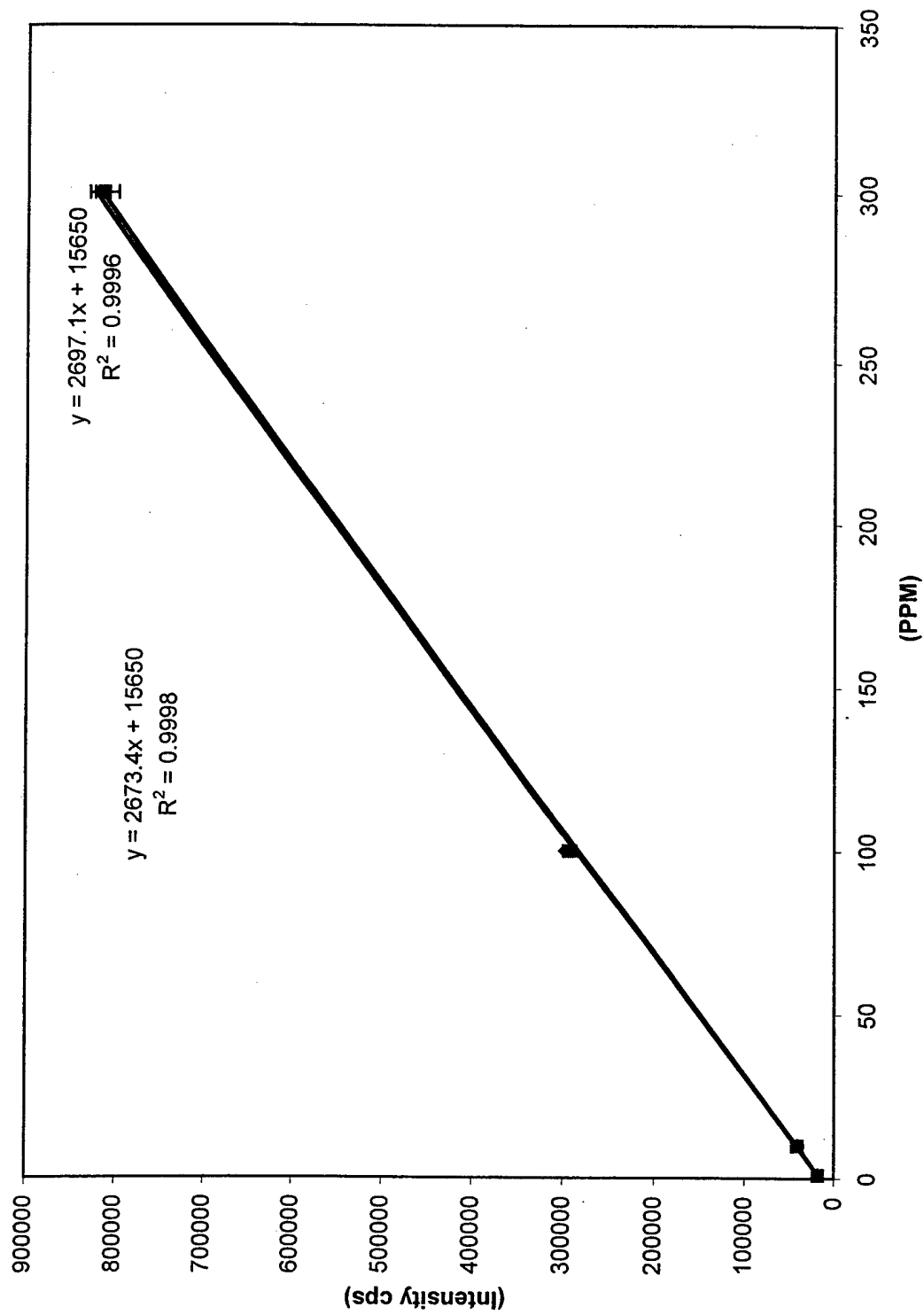
	Concentration (ppm)	Average	Std Dev	Calculated Concentration	
				Run 1 Constants	Run 2 Constants
u blink		15652	59.3	0.000741537	0.000748111
u std 4 1 ppm	1	18277	85.5	0.974009121	0.982643824
u std 3 10 ppm	10	41630	227.5	9.632568314	9.717962146
u std 2 100 ppm	100	296930	982	104.2897927	105.2143338
u std 1 300 ppm	300	820941	16059	298.5766193	301.2235356
u blink 2		15720	61.1	0.025953802	0.026183886
u sample 3		19735	88.1	1.514589745	1.528016758
u blink 3		15578	84.2	-0.026695339	-0.026931997
u sample 2		54242	305.1	14.30870194	14.43555024
u blink 4		15659	101.2	0.003336917	0.0033665
u sample 1		207705	1102	71.20796411	71.83923094
u blink 5		15645	28.96	-0.001853843	-0.001870278
u std 4 1 ppm	1	18196	79	0.943976864	0.952345328
u std 3 10 ppm	10	41466	165.9	9.571762263	9.656617042
u std 2 100 ppm	100	290859	2573	102.0388565	102.9434428
u std 1 300 ppm	300	815084	4524	296.4050276	299.0326925
u blink 6		15727	113.8	0.028549182	0.028802274

	X" Concentration (PPM)	Total (ml)	Stock(ml)	Distilled Water (ml)	X' Conc (ppm)
Sample 1 Avg	71.52359753				
1st Dilution		5	2.947	2.053	121.3498431
2nd Dilution		11	1	10	1334.848274
Sample 2 Avg	14.37212609				
1st Dilution		5	0.5894	4.4106	121.9216668
2nd Dilution		11	1	10	1341.138335
Sample 3 Avg	1.521303251				
1st Dilution		5	0.05894	4.94106	129.055247
2nd Dilution		11	1	10	1419.607717

So Final Resulting Concntration of the original Sample in mM:

U238	238.050785 (DU Source)	
Sample 1	5.607409672	Mean Concentration
Sample 2	5.633832862	Std Dev
Sample 3	5.963465806	5.73490278 0.198381801

ICP AES Uranium Concentration for C45 Dissolved U(IV) in HNO3



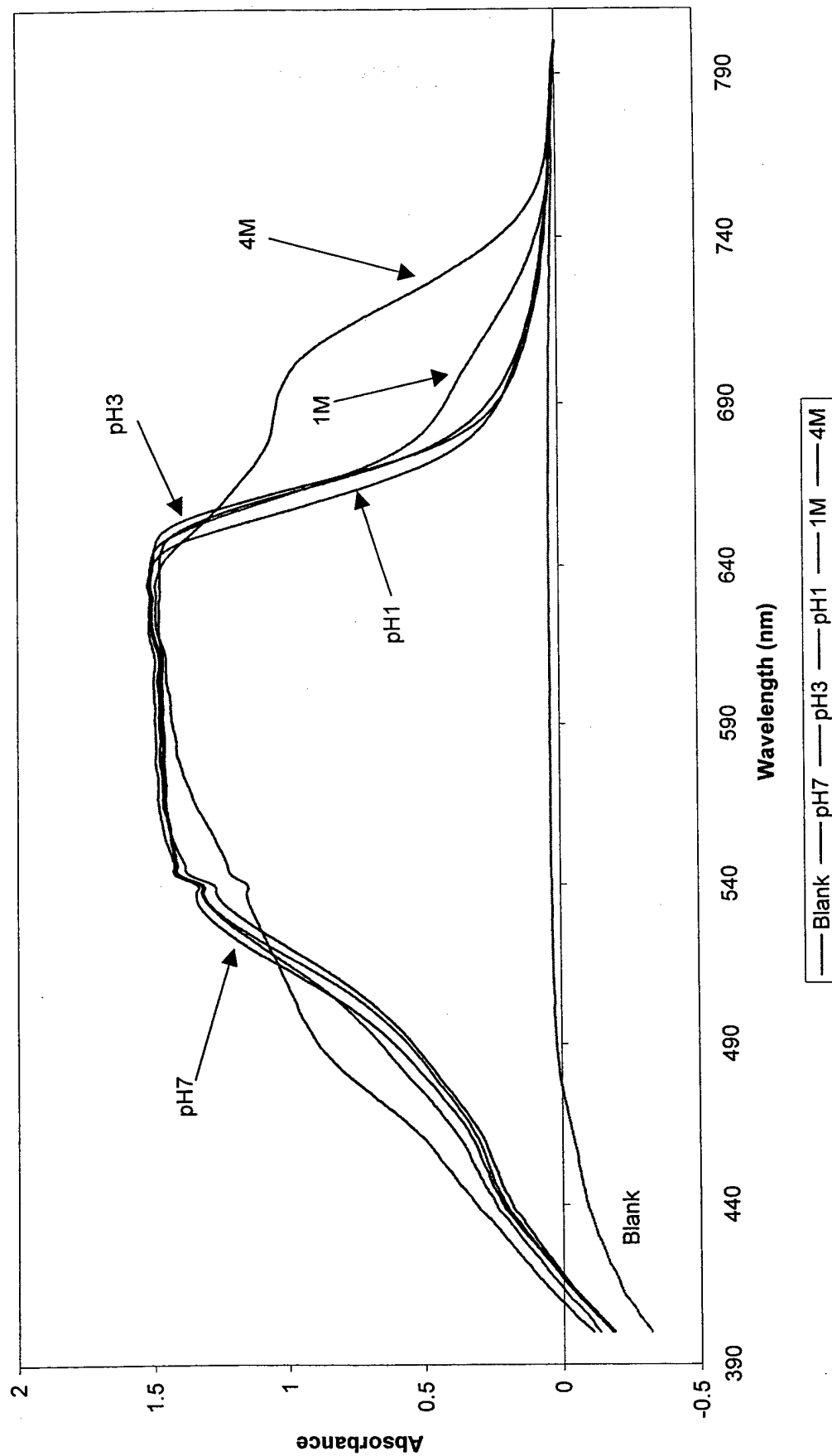
◆ 1st Run
■ 2nd Run
— Linear (1st Run)
— Linear (2nd Run)

Appendix 2, Annex H

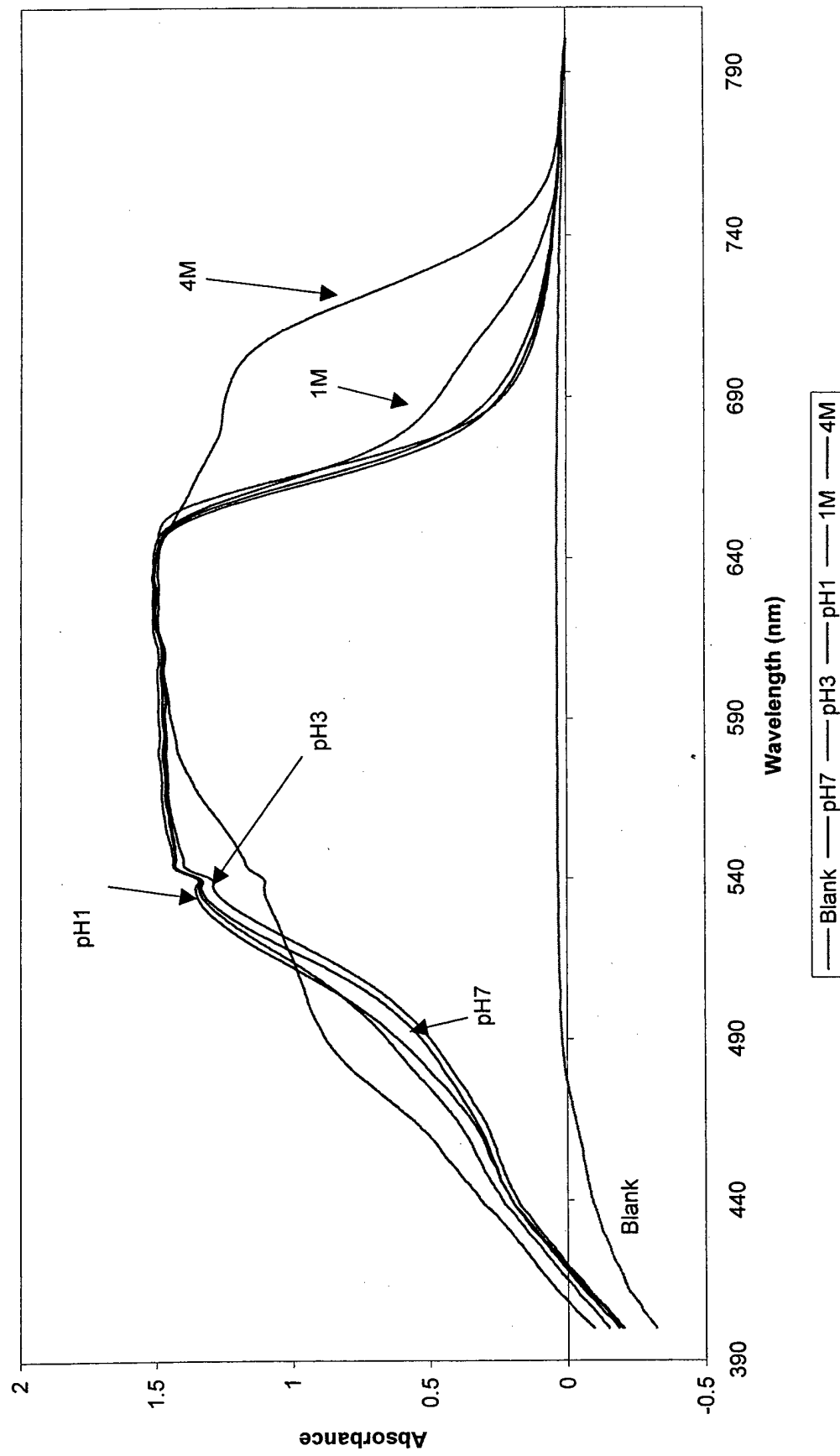
Brilliant Cresyl Blue Spectra Results with U(IV)

- H-1 BCB total with U(IV)
- H-2 BCB total without U(IV)
- H-3 BCB Complexation with U(IV) at pH7
- H-4 BCB Complexation with U(IV) at pH3
- H-5 BCB Complexation with U(IV) at pH1
- H-6 BCB Complexation with U(IV) at 1N HNO₃
- H-7 BCB Complexation with U(IV) at 4N HNO₃

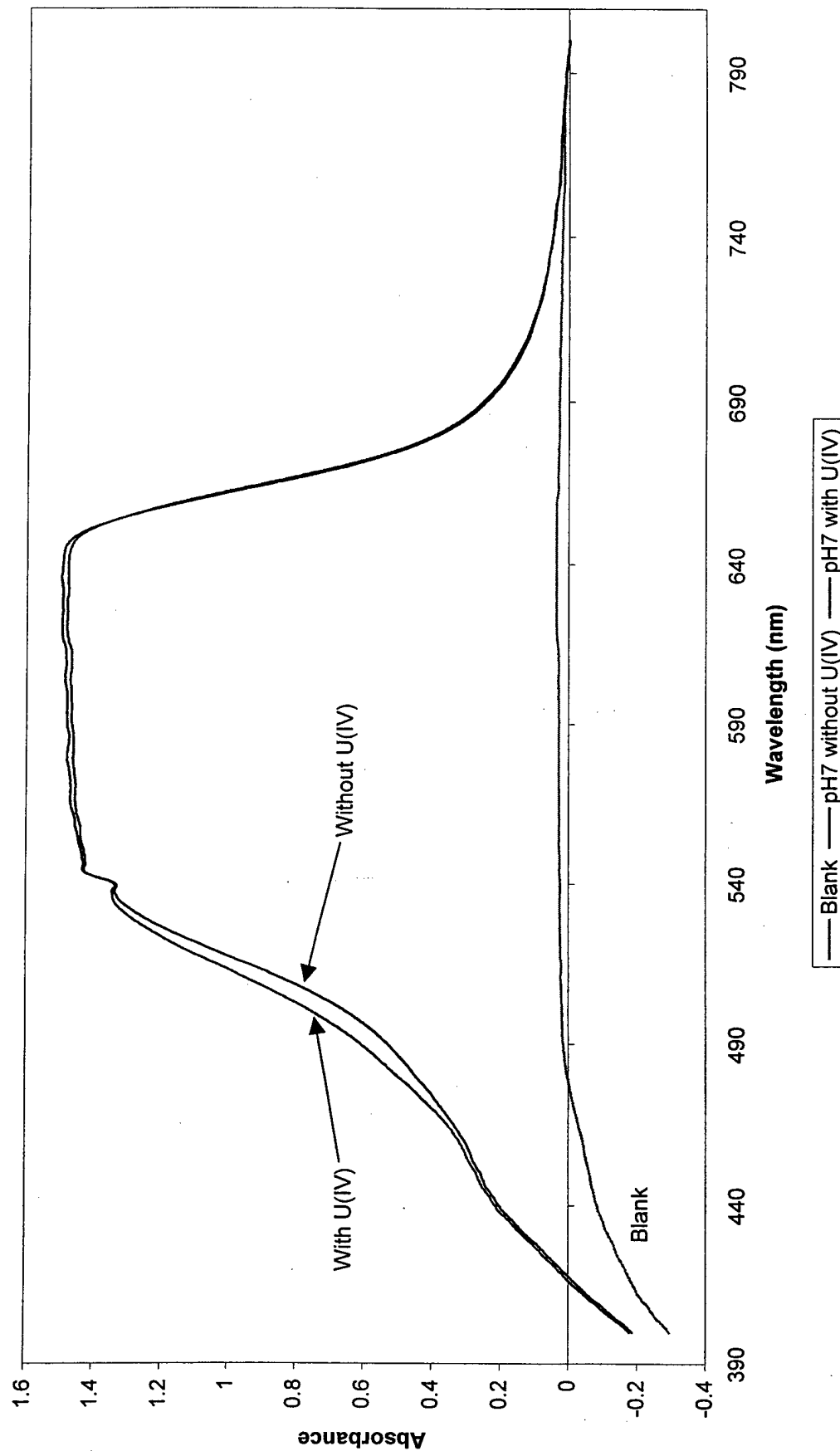
**BCB with U (IV) Metal Aqueous Species
(Normalized Values and Uncorrected for Background)**



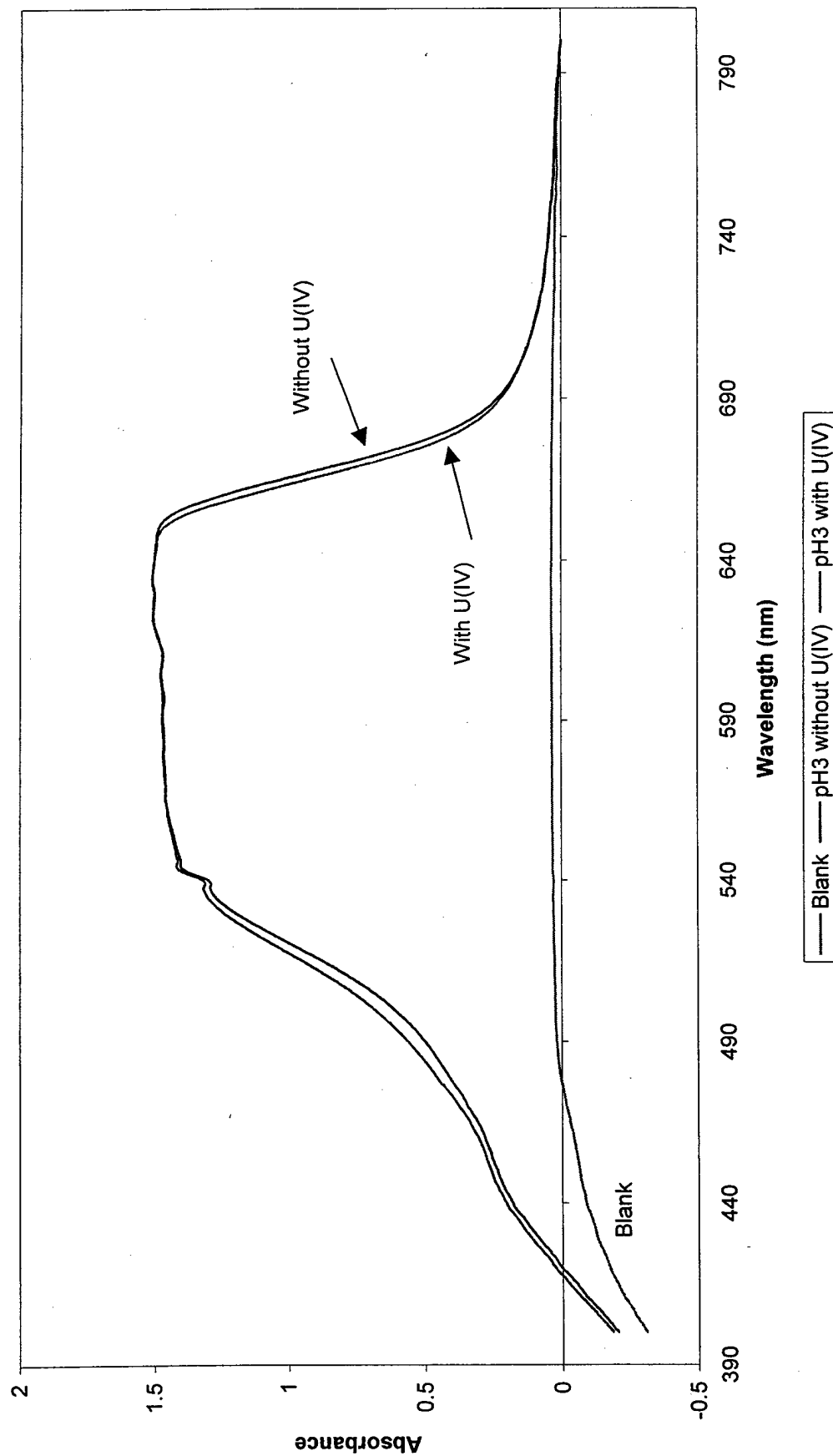
**BCB without U (IV) Metal Aqueous Species
(Normalized Values and Uncorrected for Background)**



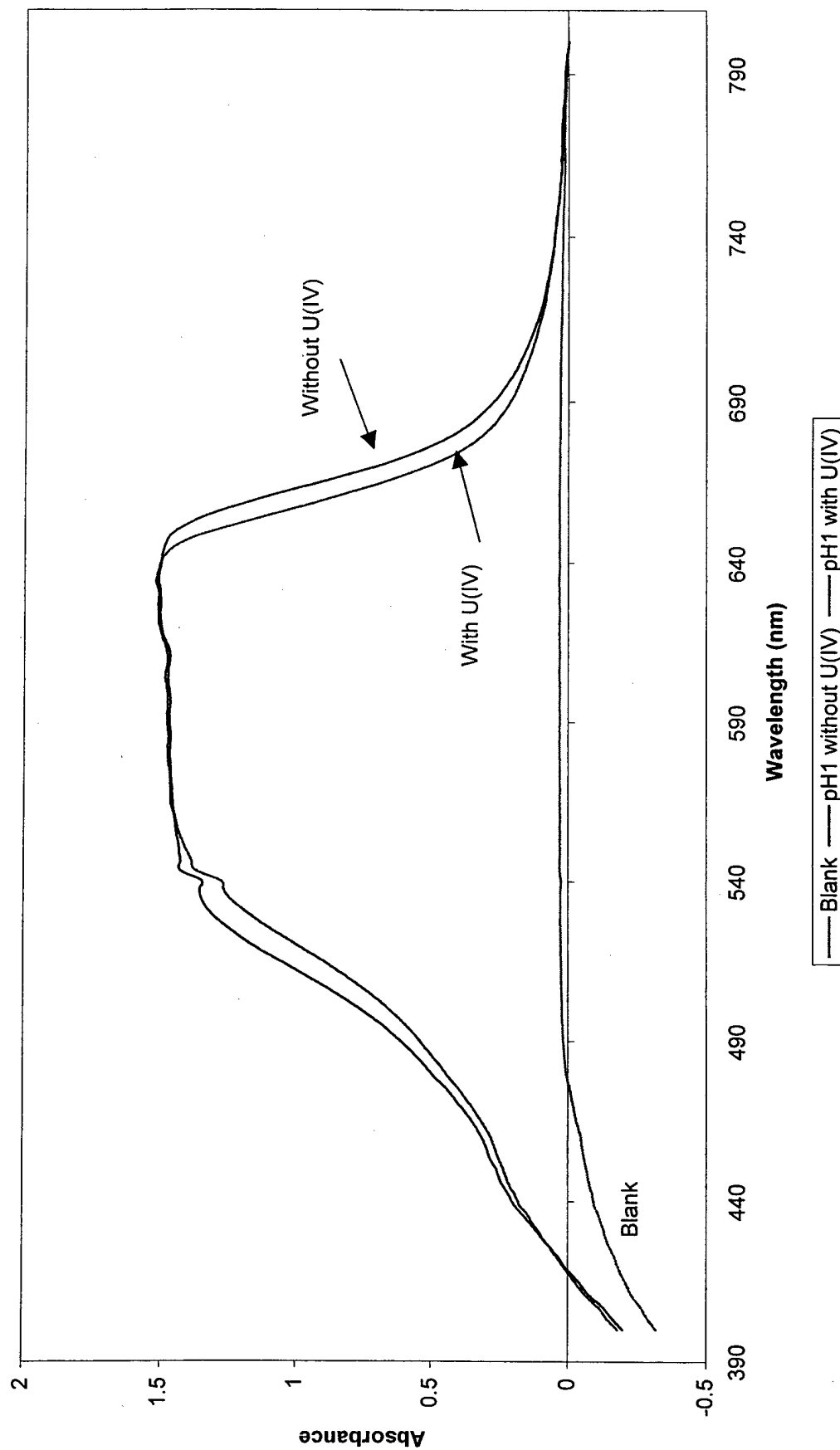
**BCB Complexation with U (IV) Metal Aqueous Species in pH7 Buffer
(Normalized Values and Uncorrected for Background)**



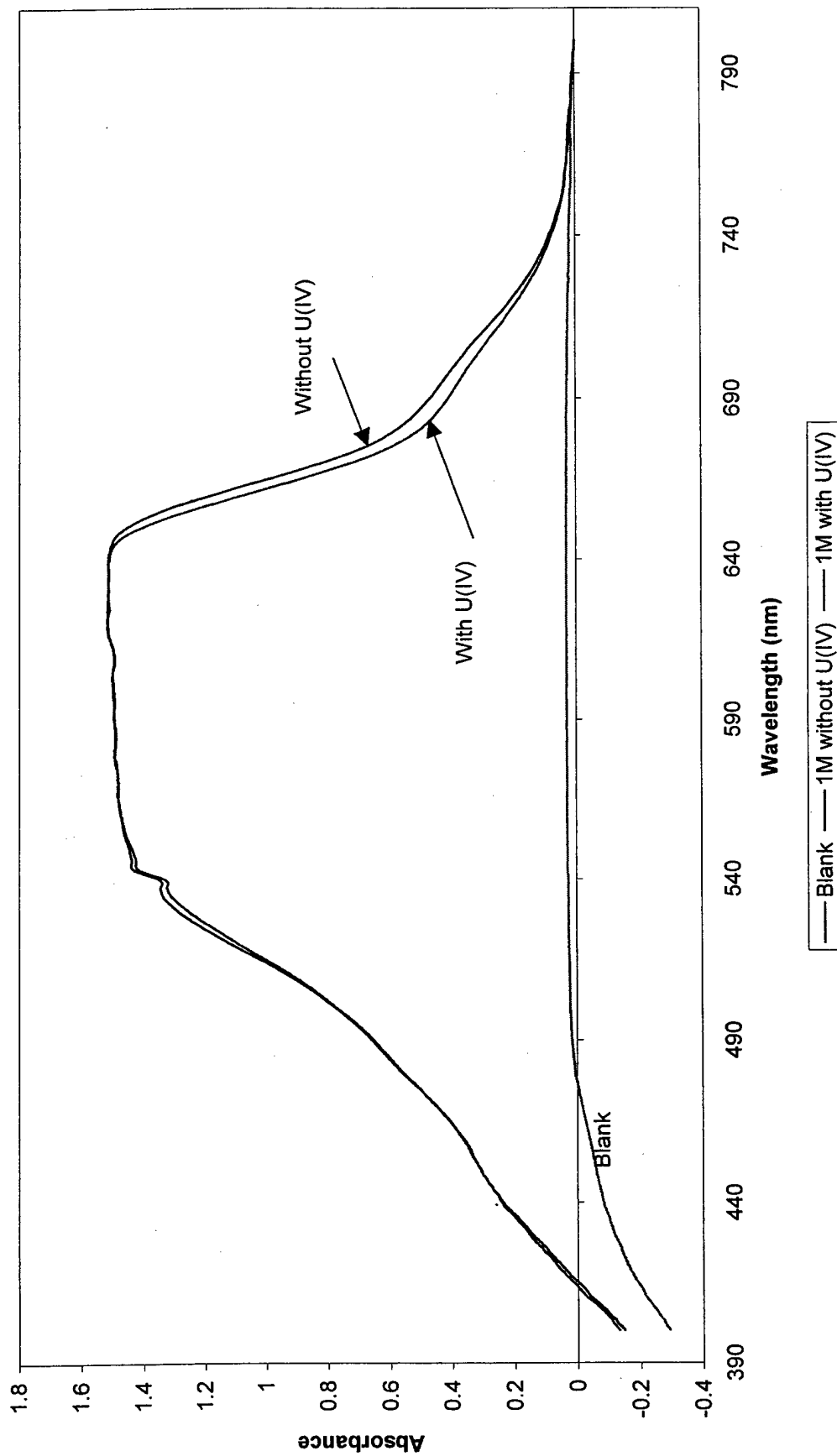
**BCB Complexation with U (IV) Metal Aqueous Species in pH3 Buffer
(Normalized Values and Uncorrected for Background)**



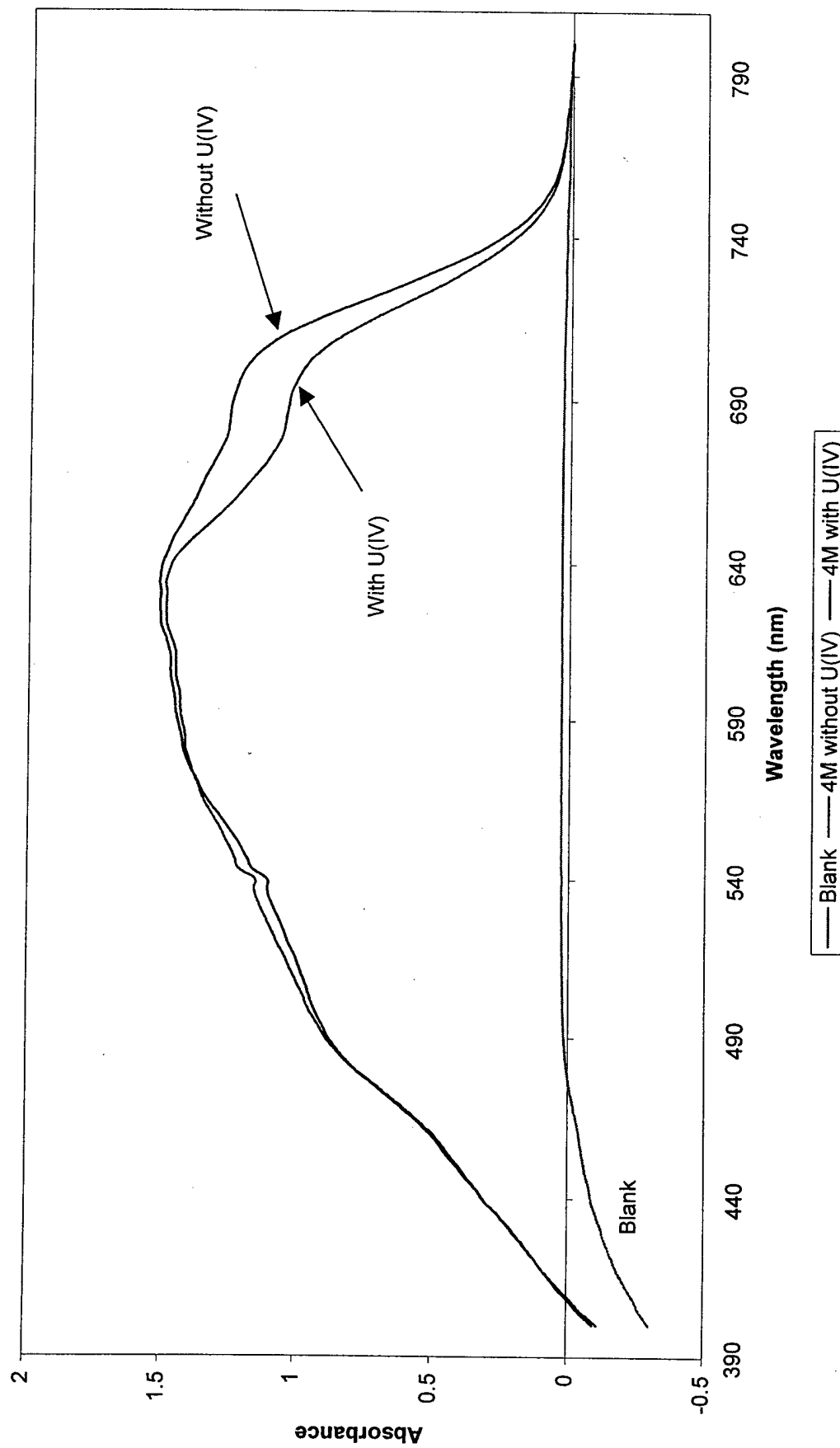
BCB Complexation with U (IV) Metal Aqueous Species in pH1 Buffer
(Normalized Values and Uncorrected for Background)



BCB Complexation with U (IV) Metal Aqueous Species in 1 M HNO₃
(Normalized Values and Uncorrected for Background)



BCB Complexation with U (IV) Metal Aqueous Species in 4 M HNO₃
(Normalized Values and Uncorrected for Background)

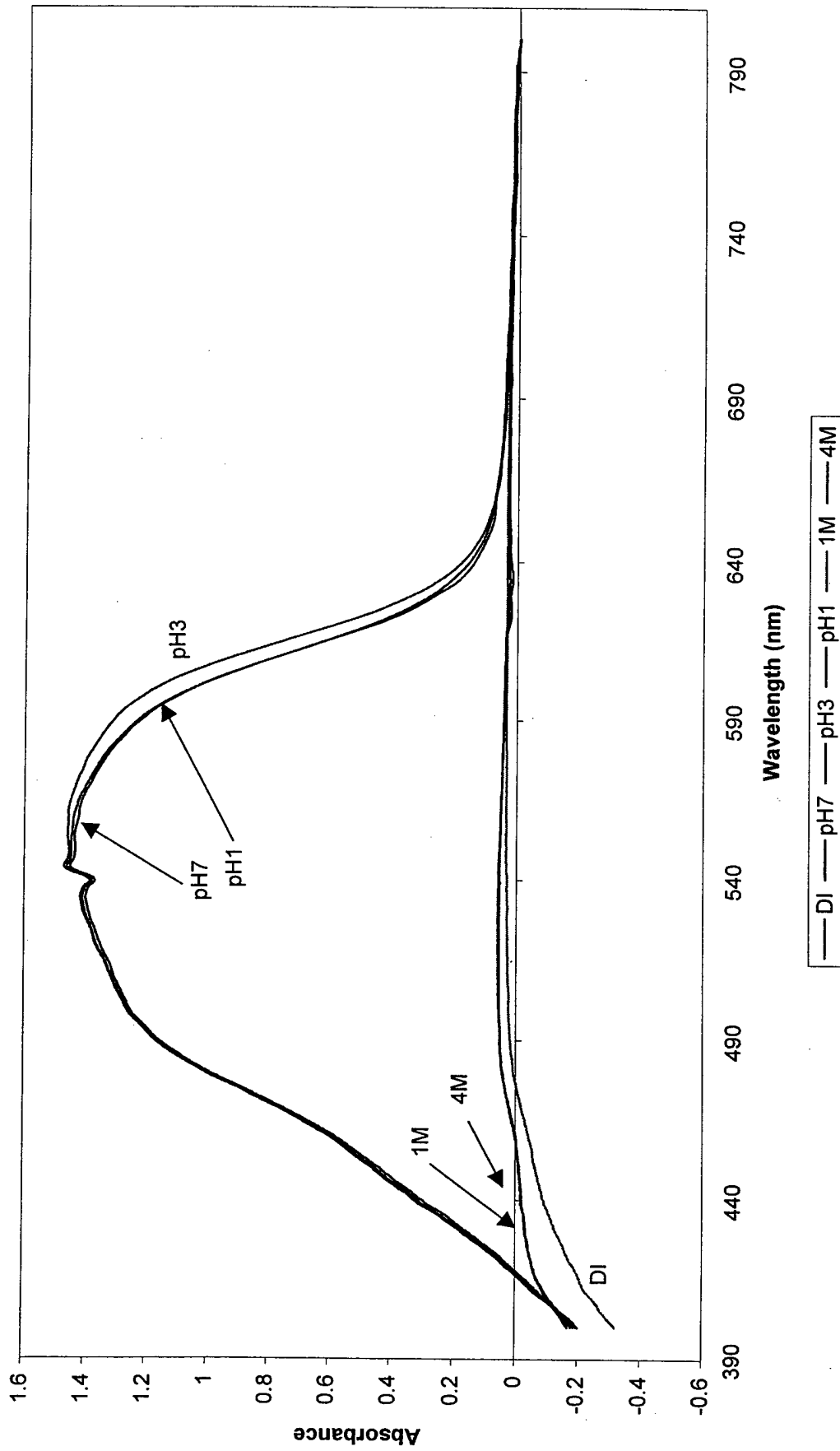


Appendix 2, Annex I

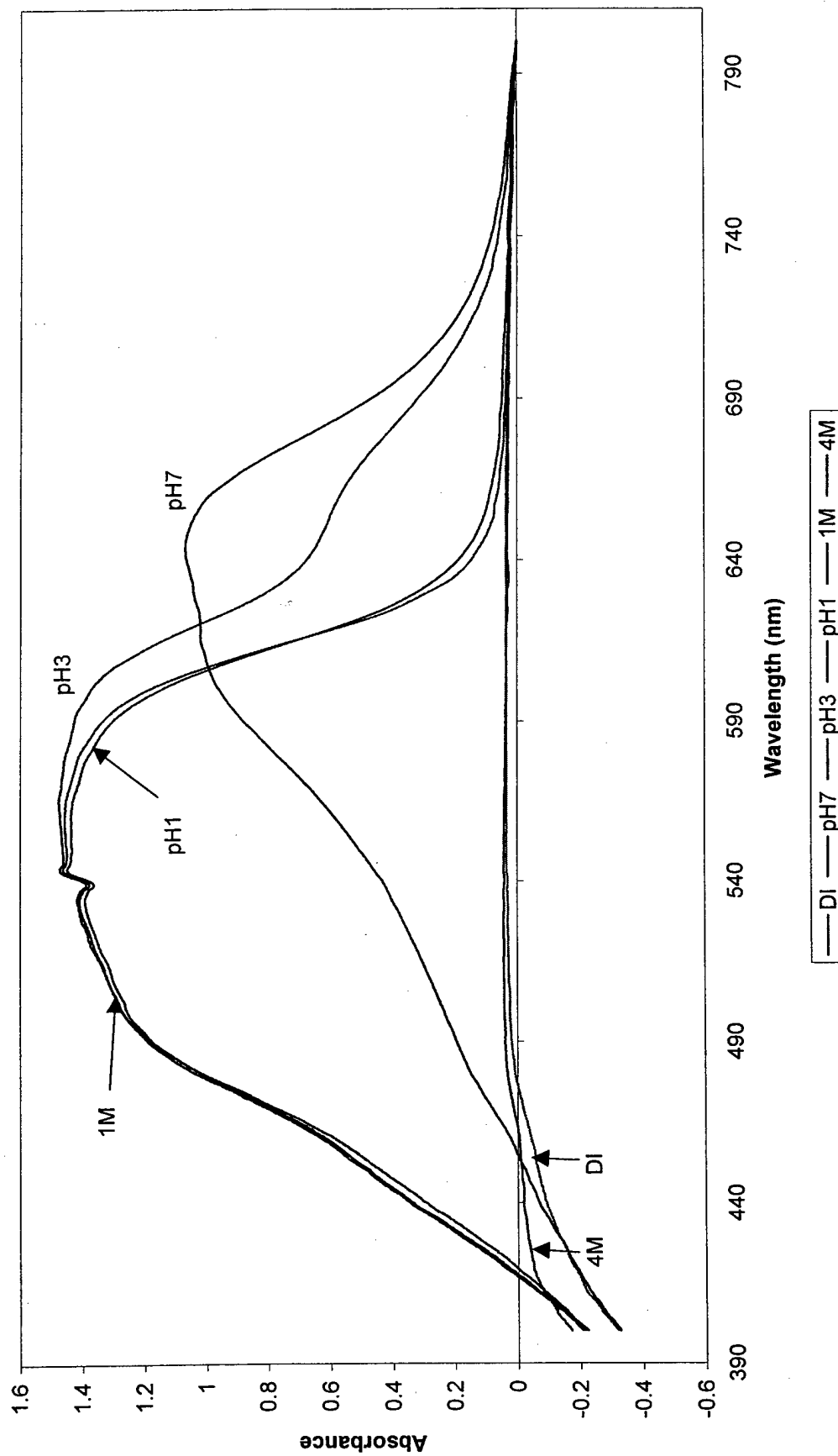
Celestine Blue Spectra Results with U(IV)

- I-1 CB total with U(IV)
- I-2 CB total without U(IV)
- I-3 CB Complexation with U(IV) at pH7
- I-4 CB Complexation with U(IV) at pH3
- I-5 CB Complexation with U(IV) at pH1
- I-6 CB Complexation with U(IV) at 1N HNO₃
- I-7 CB Complexation with U(IV) at 4N HNO₃

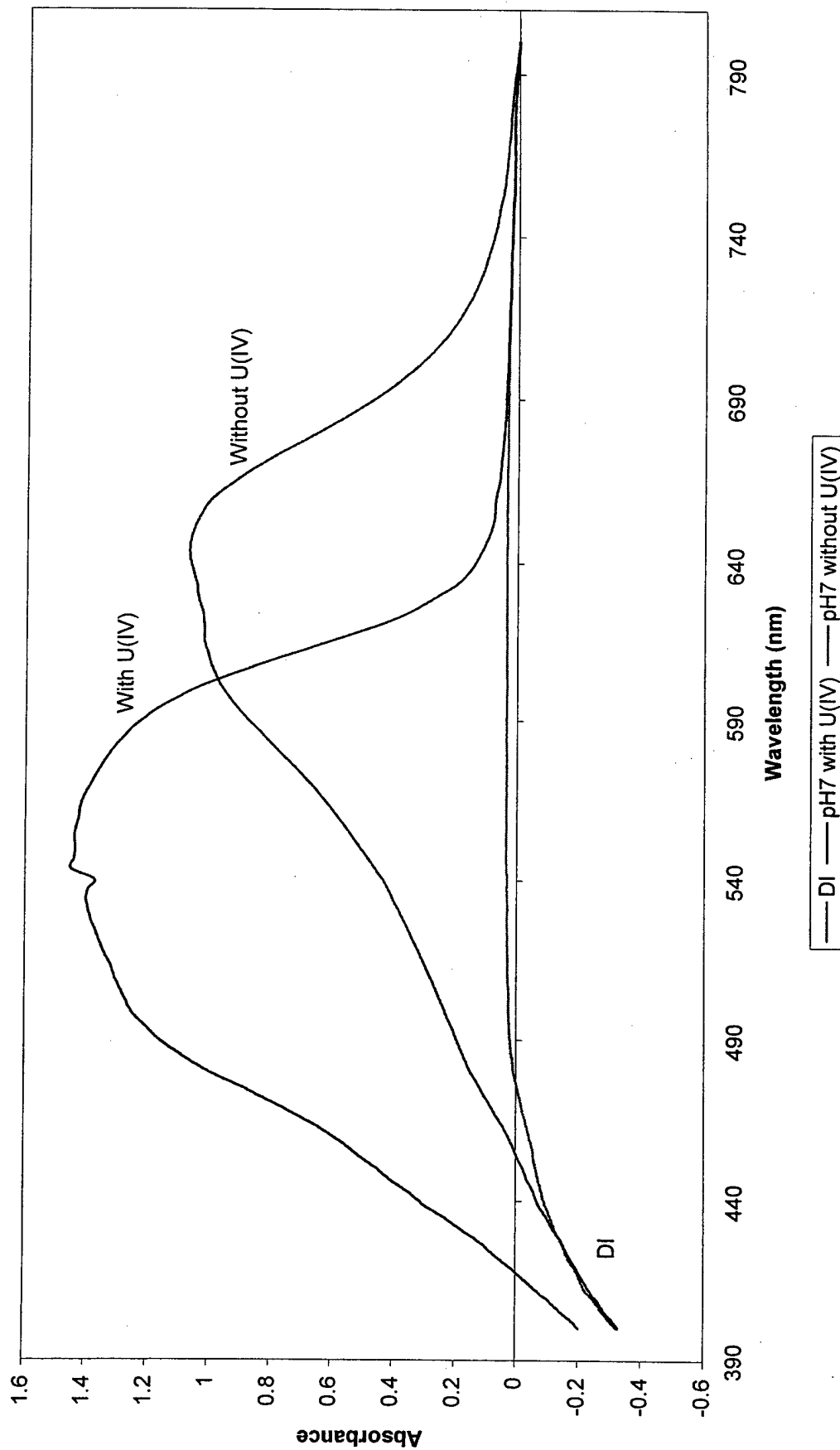
CB with U (IV) Metal Aqueous Species
(Normalized Values and Uncorrected for Background)



**CB without U (IV) Metal Aqueous Species
(Normalized Values and Uncorrected for Background)**



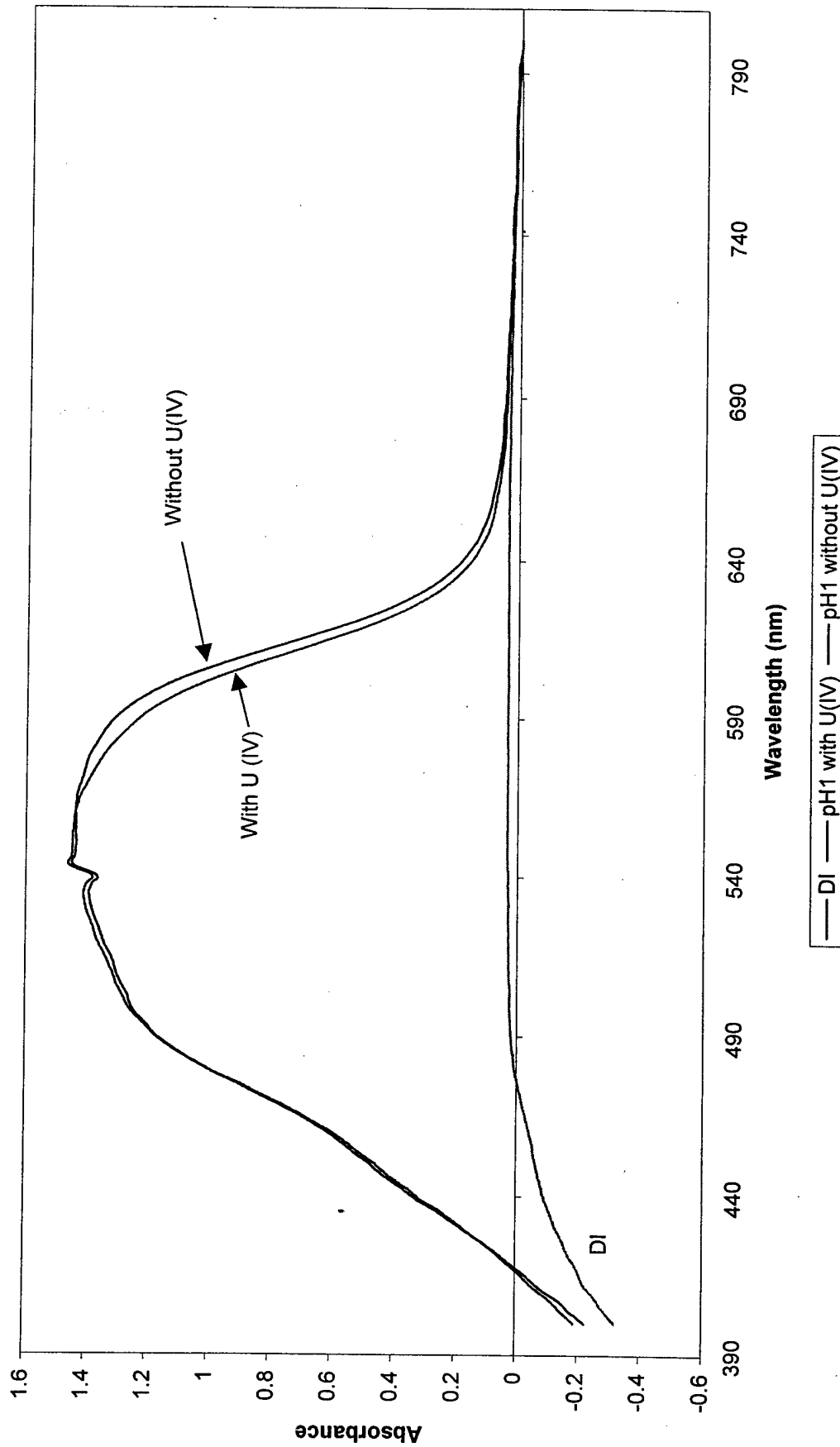
CB Complexation with U (IV) Metal Aqueous Species in pH7 Buffer (Normalized Values and Uncorrected for Background)



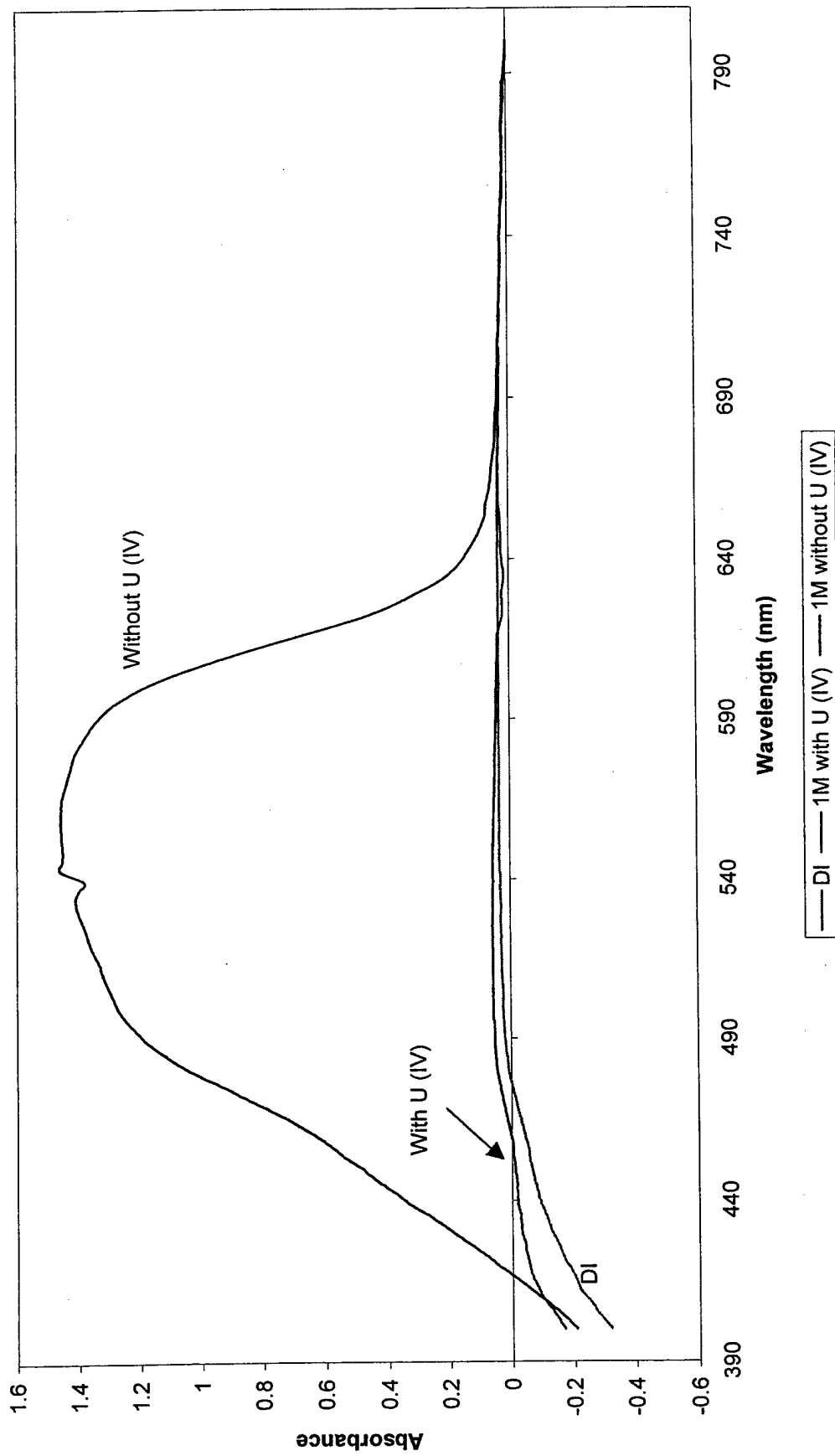
CB Complexation with U (IV) Metal Aqueous Species in pH3 Buffer (Normalized Values and Uncorrected for Background)



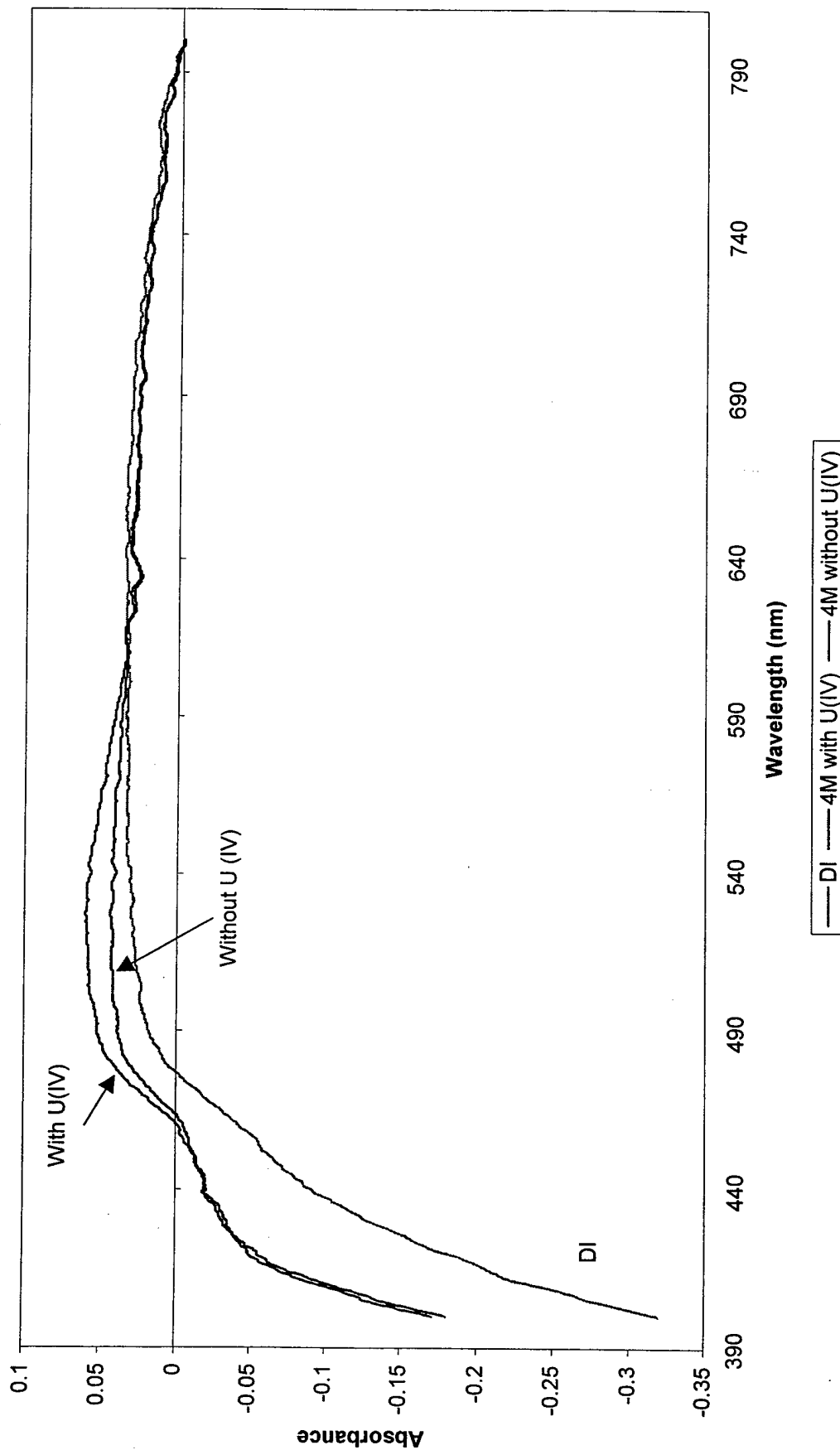
**CB Complexation with U (IV) Metal Aqueous Species in pH1 Buffer
(Normalized Values and Uncorrected for Background)**



CB Complexation with U (IV) Metal Aqueous Species in 1 M HNO₃ (Normalized Values and Uncorrected for Background)



CB Complexation with U (IV) Metal Aqueous Species in 4M HNO₃
(Normalized Values and Uncorrected for Background)

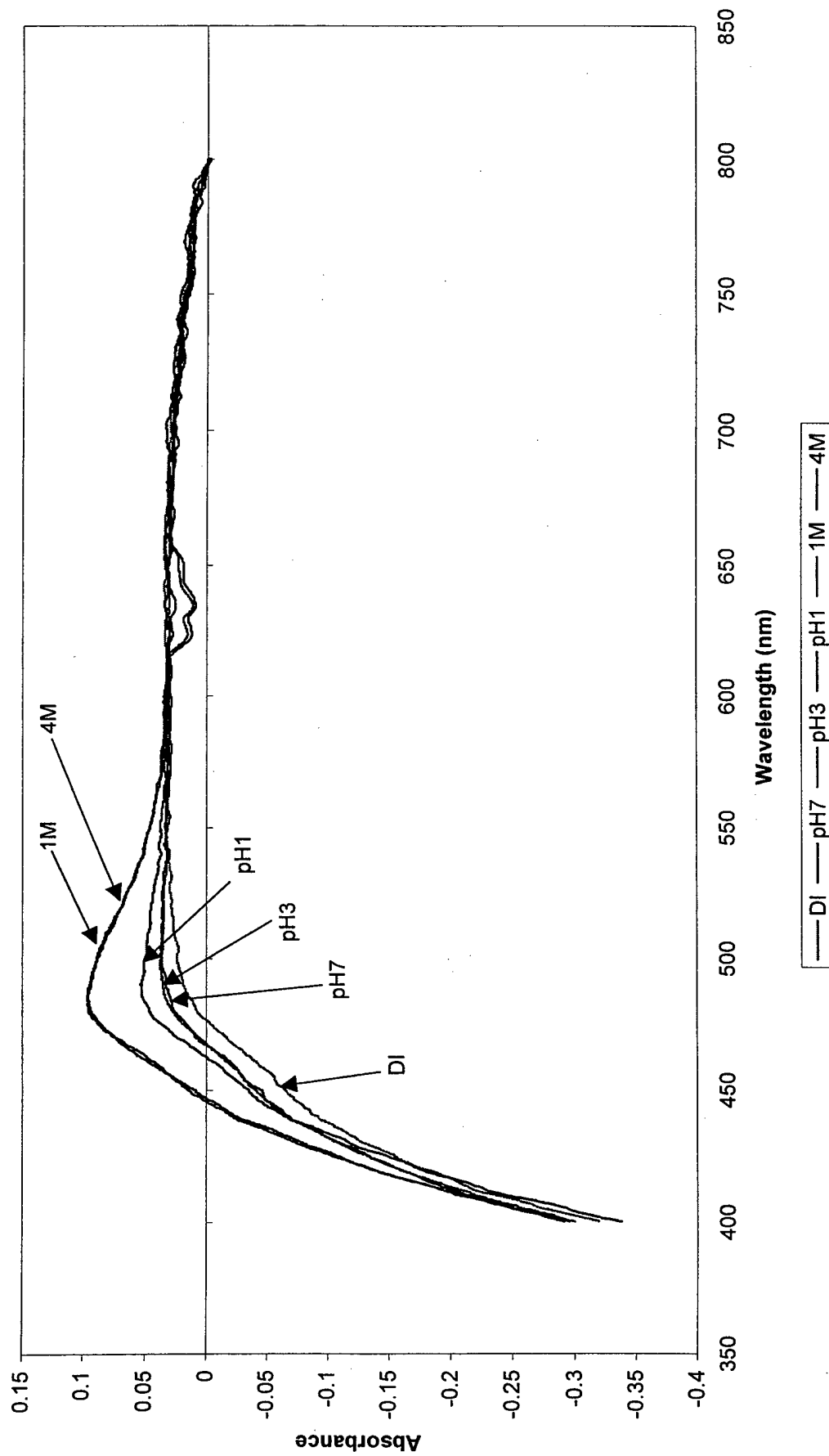


Appendix 2, Anne J

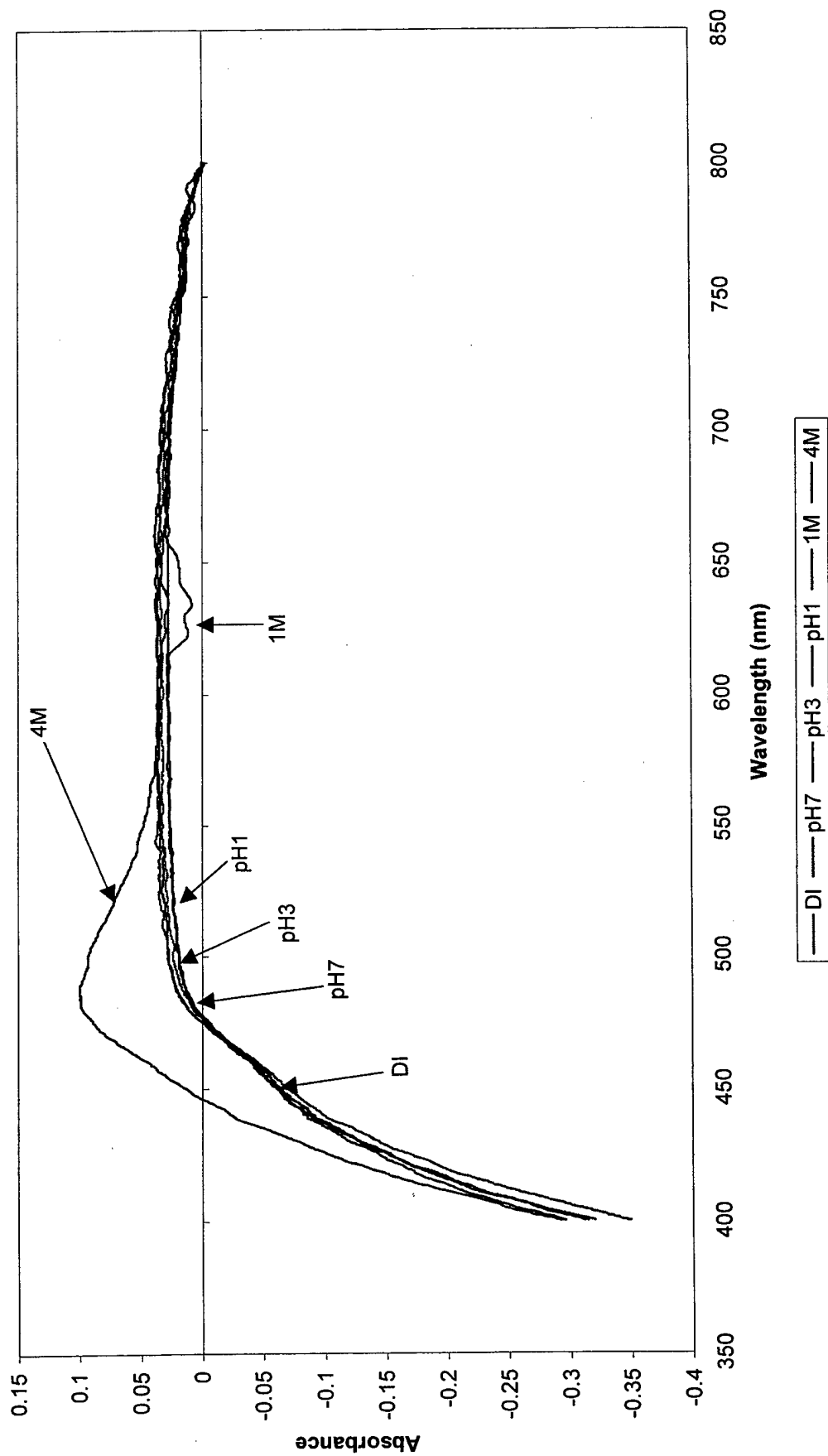
Gallomine Triethiodide Spectra Results with U(IV)

- J-1 GT total with U(IV)
- J-2 GT total without U(IV)
- J-3 GT Complexation with U(IV) at pH7
- J-4 GT Complexation with U(IV) at pH3
- J-5 GT Complexation with U(IV) at pH1
- J-6 GT Complexation with U(IV) at 1N HNO₃
- J-7 GT Complexation with U(IV) at 4N HNO₃

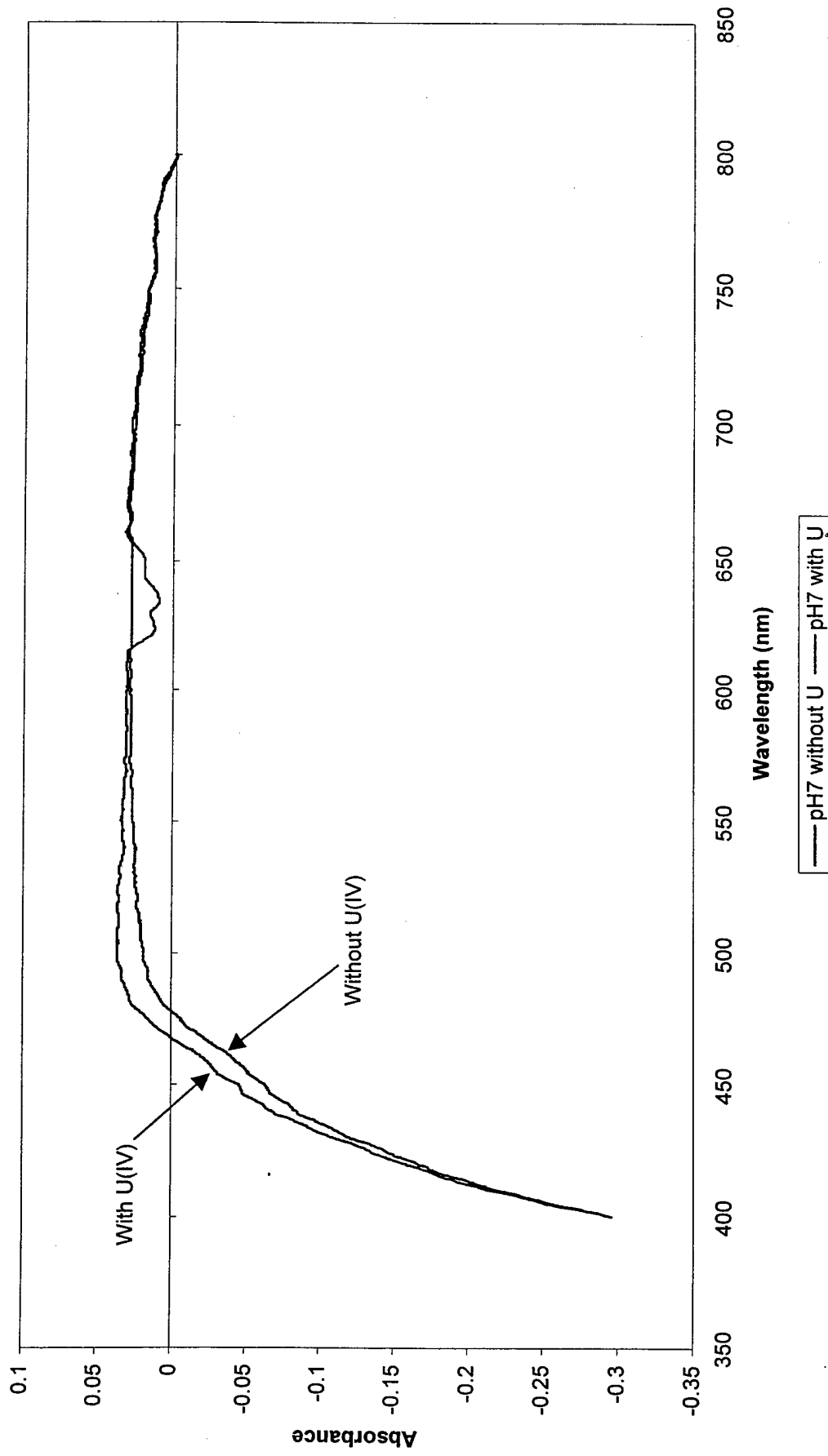
GT with U (IV) Metal Aqueous Species
(Normalized Values and Uncorrected for Background)



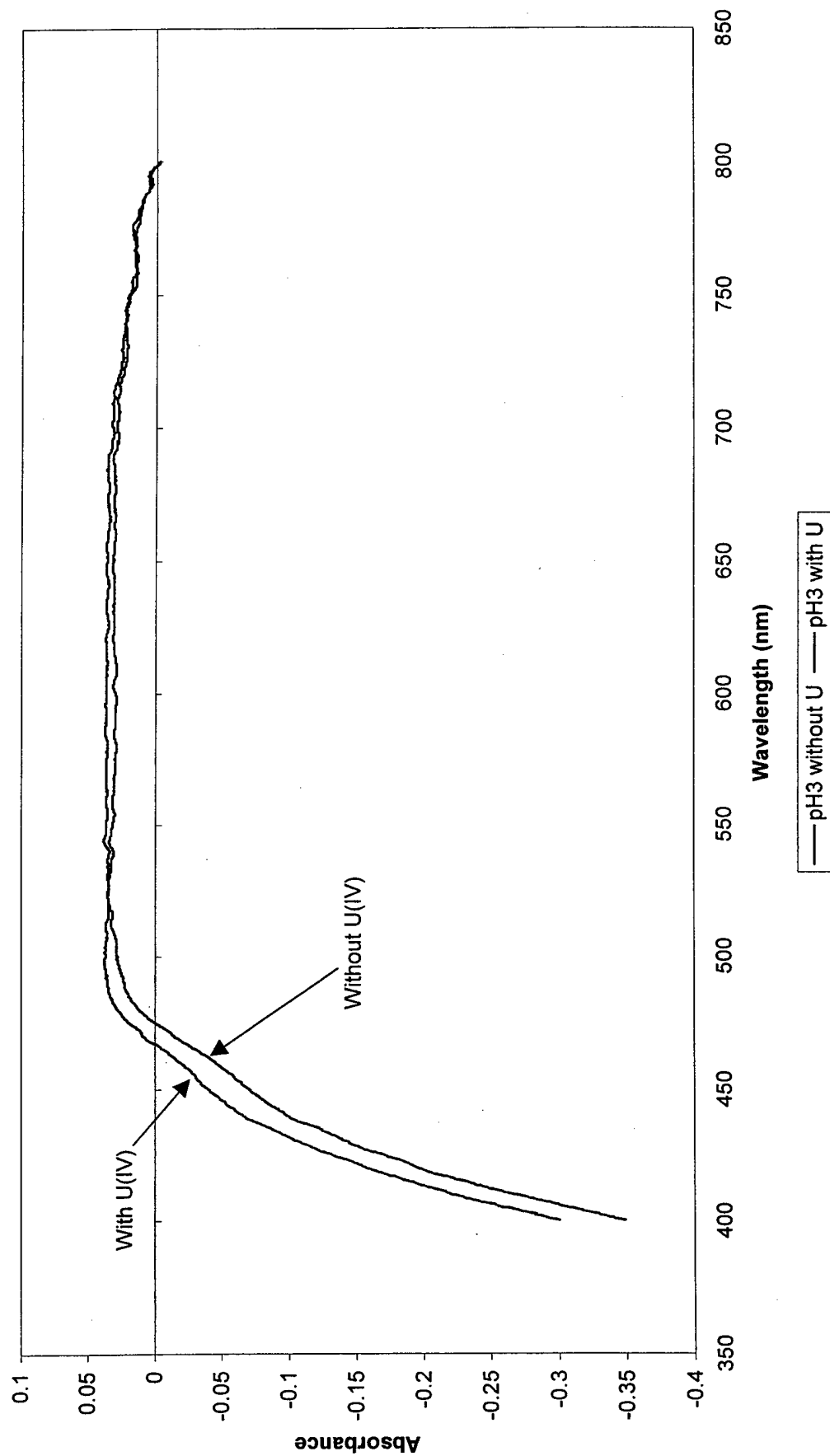
GT without U (IV) Metal Aqueous Species (Normalized Values and Uncorrected for Background)



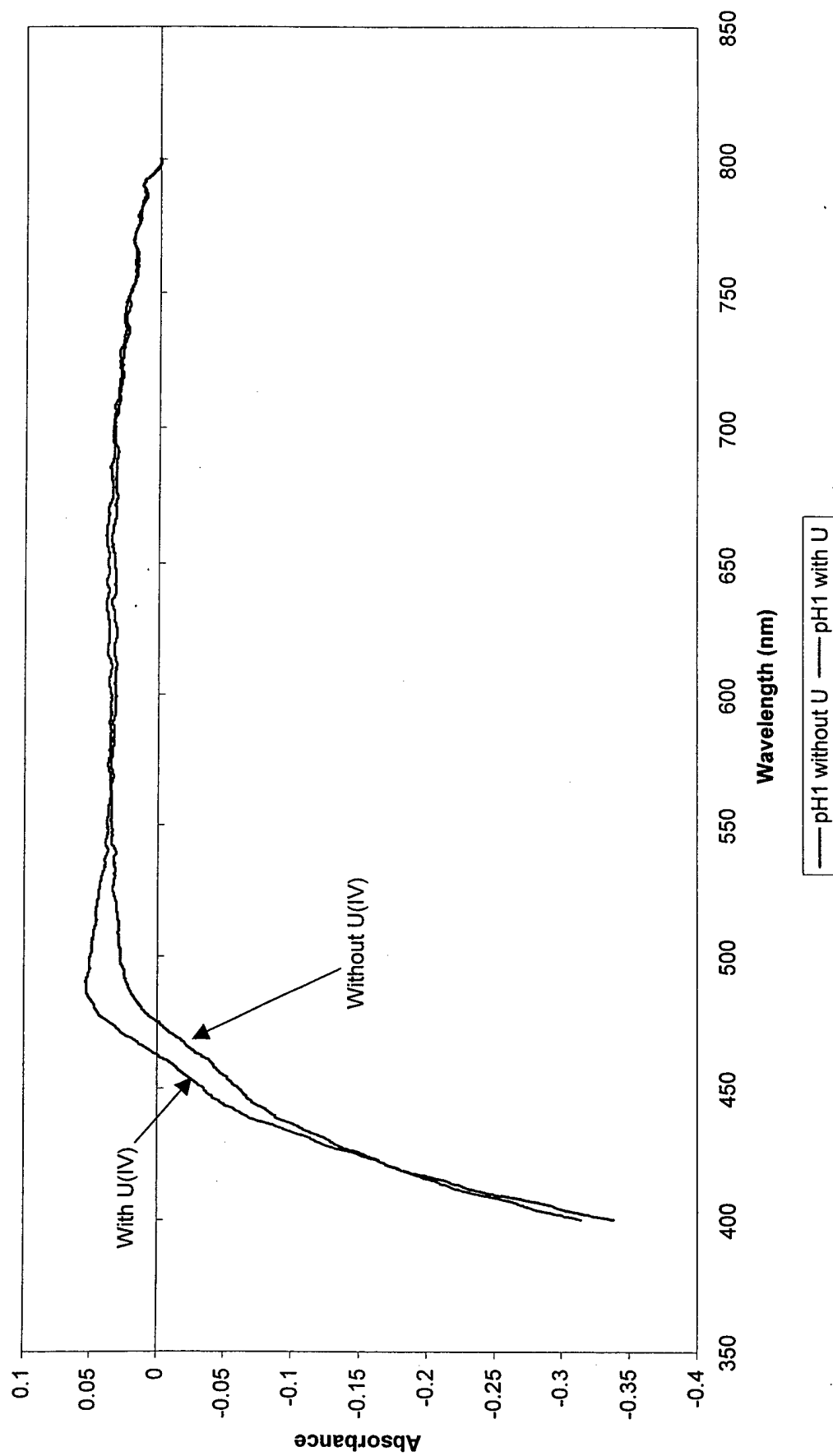
**GT Complexation with U (IV) Metal Aqueous Species in pH7 Buffer
(Normalized Values and Uncorrected for Background)**



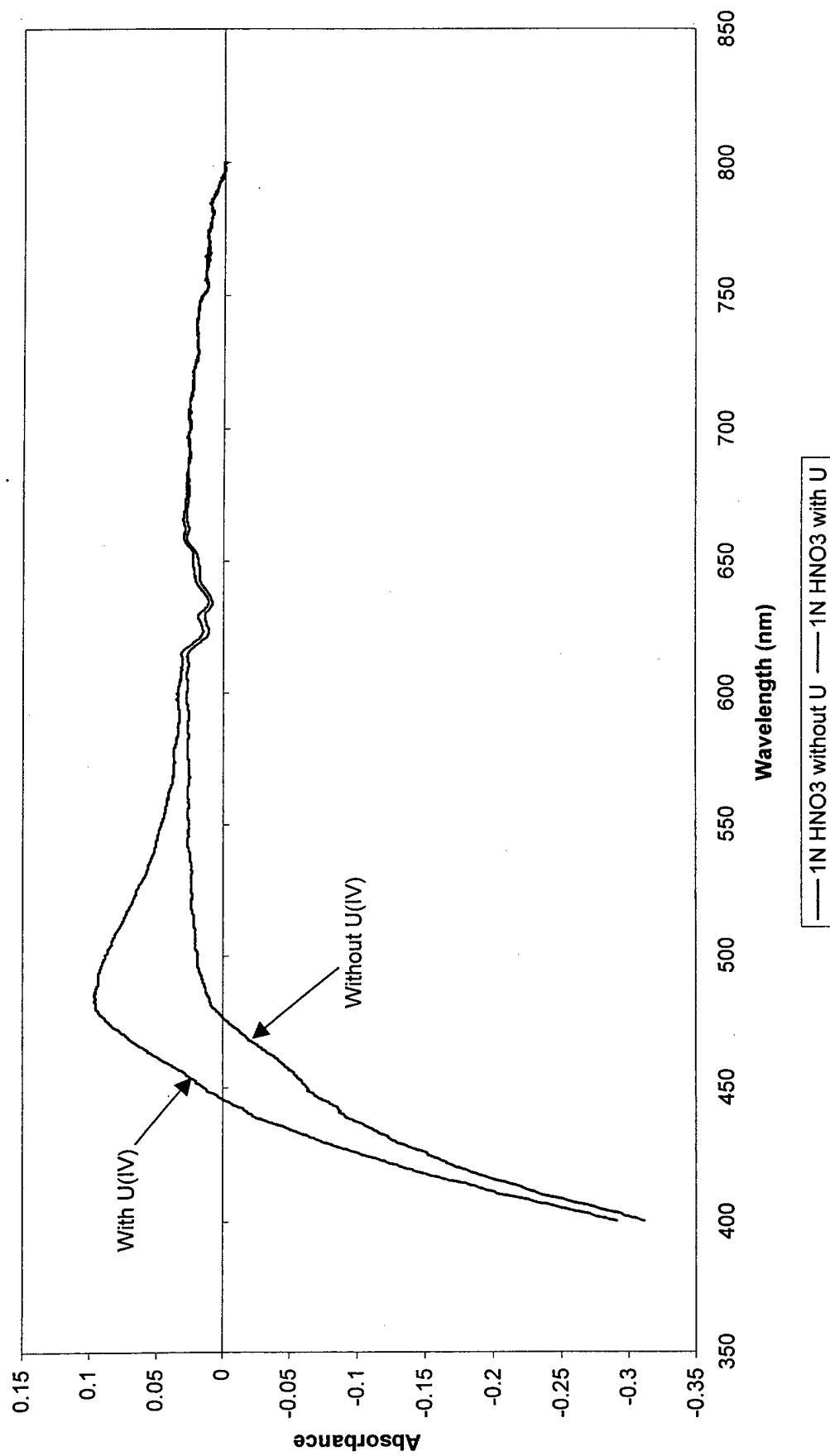
GT Complexation with U (IV) Metal Aqueous Species in pH3 Buffer (Normalized Values and Uncorrected for Background)



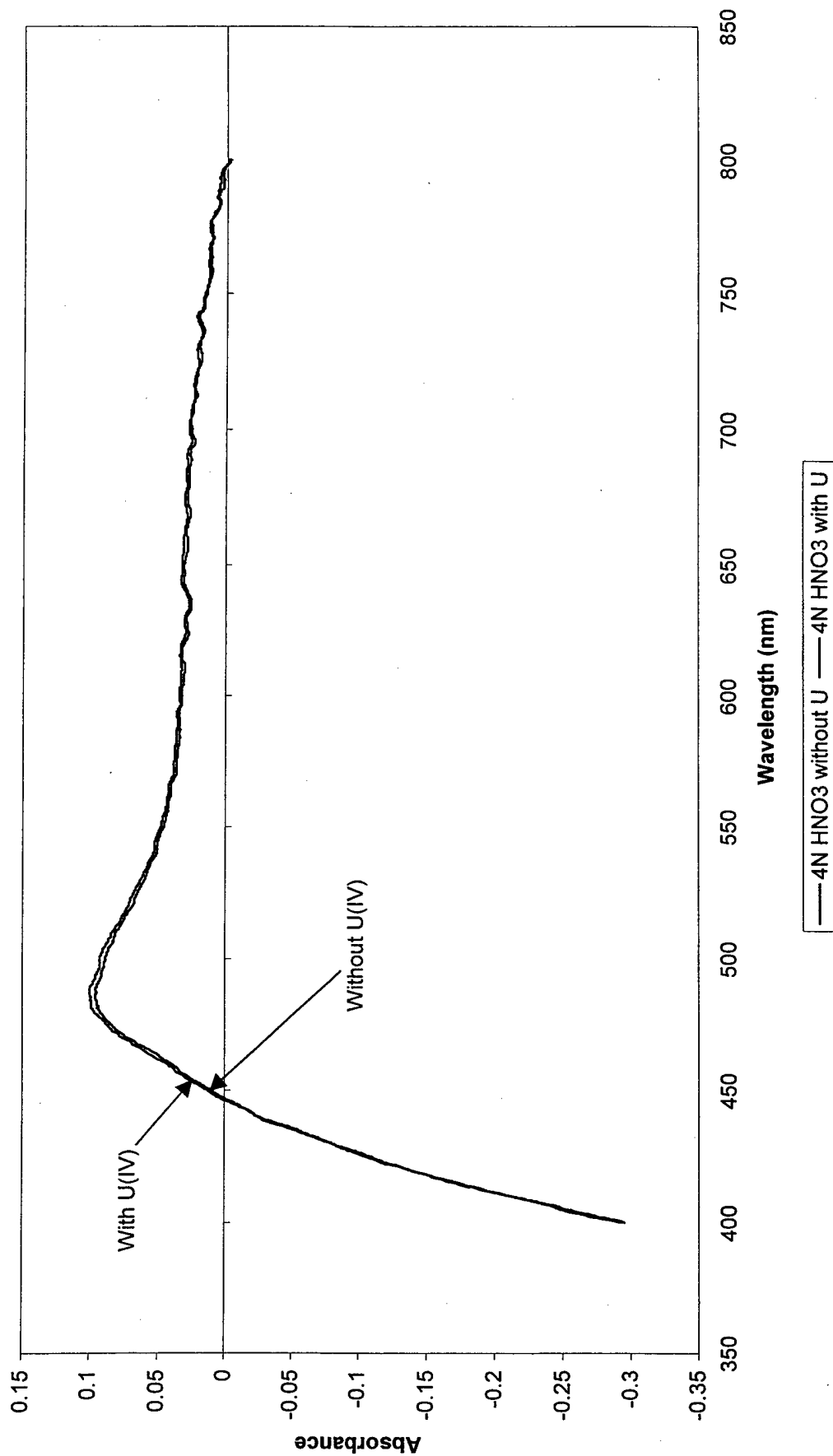
GT Complexation with U (IV) Metal Aqueous Species in pH1 Buffer (Normalized Values and Uncorrected for Background)



GT Complexation with U (IV) Metal Aqueous Species in 1 N HNO₃ (Normalized Values and Uncorrected for Background)



GT Complexation with U (IV) Metal Aqueous Species in 4 N HNO₃
(Normalized Values and Uncorrected for Background)

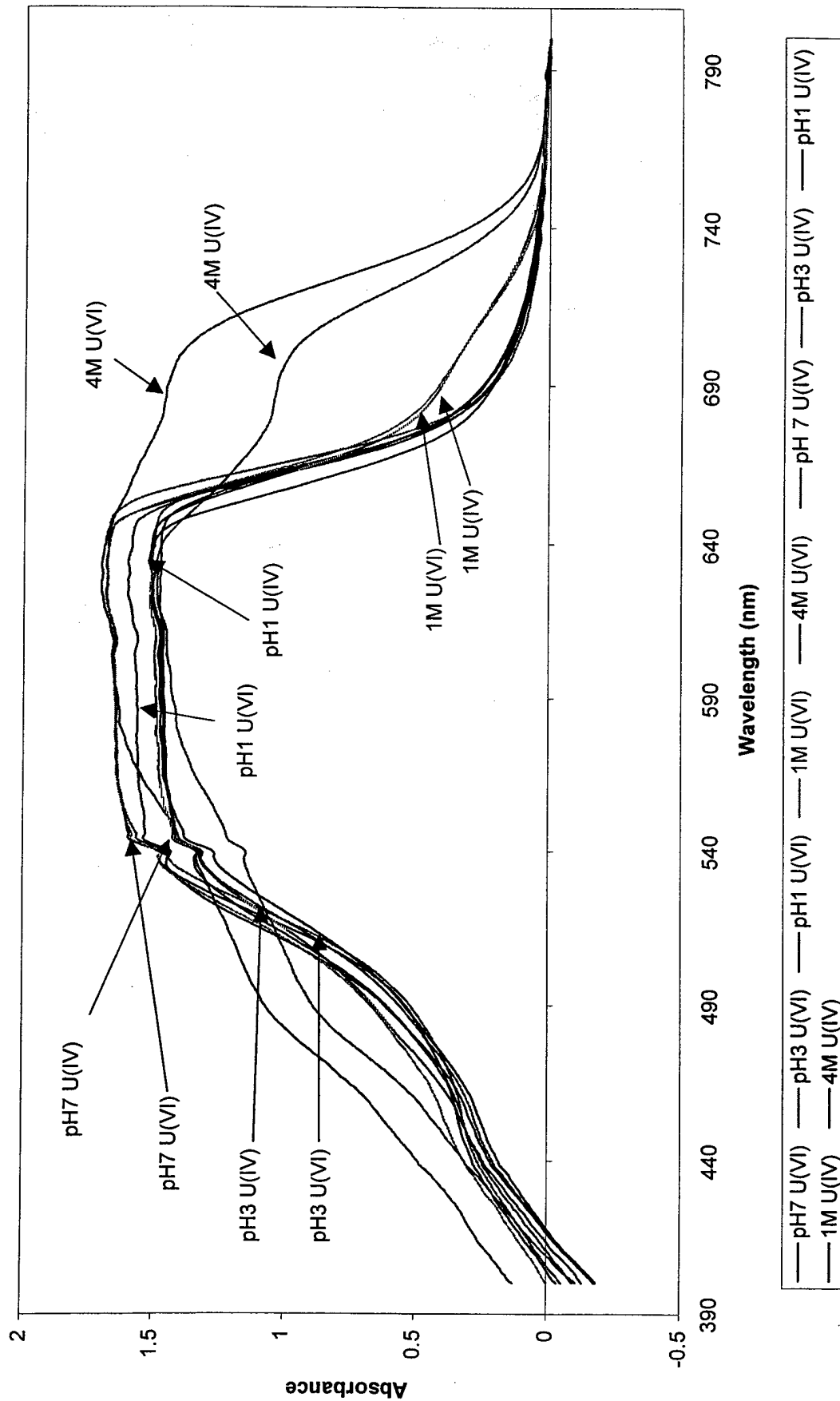


Appendix 2, Annex K

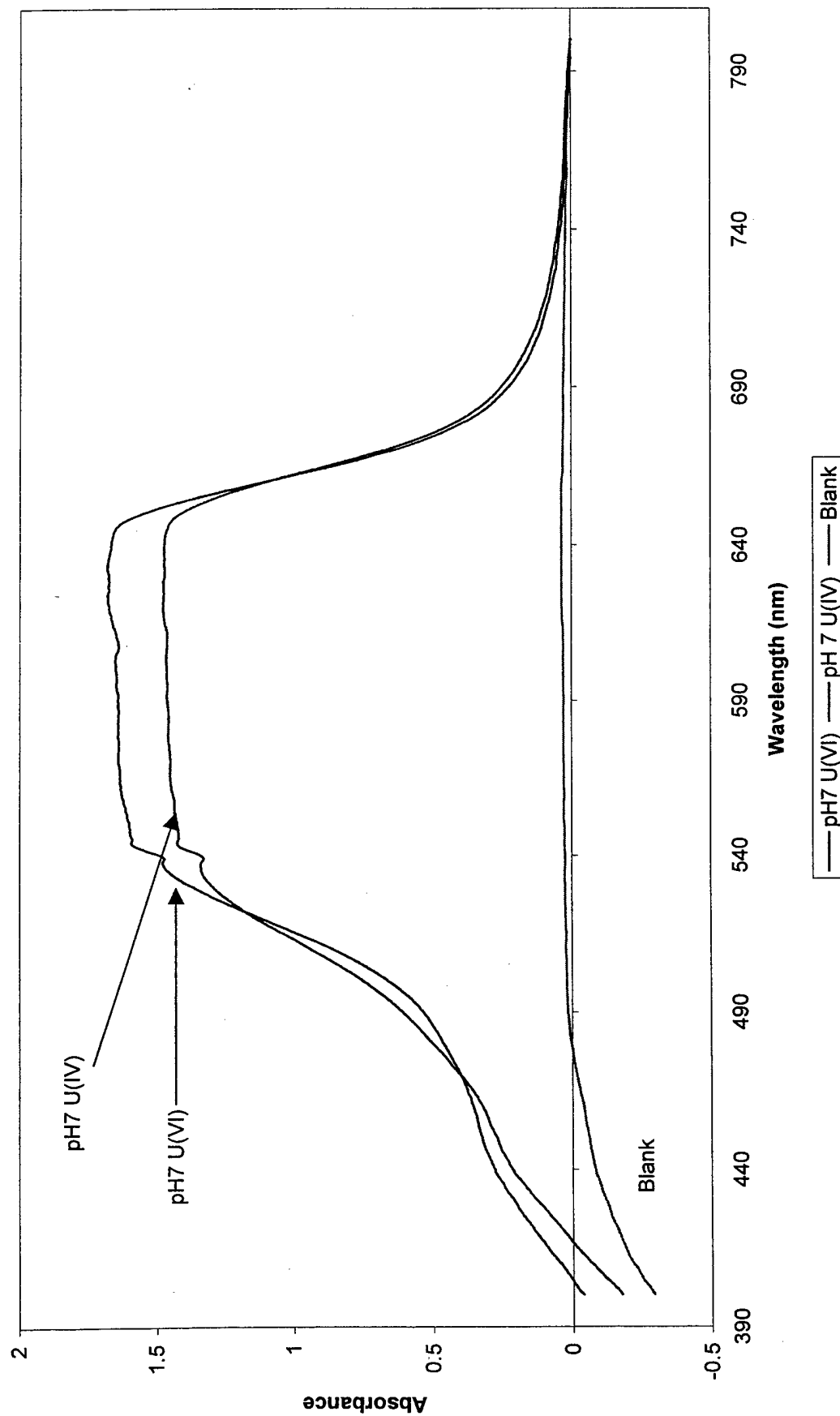
Brilliant Cresyl Blue Spectra Comparison of U(VI) and U(IV)

- K-1 BCB total with U(VI) and U(IV)
- K-2 BCB Complexation with U(VI) and U(IV) at pH7
- K-3 BCB Complexation with U(VI) and U(IV) at pH3
- K-4 BCB Complexation with U(VI) and U(IV) at pH1
- K-5 BCB Complexation with U(VI) and U(IV) at 1N HNO₃
- K-6 BCB Complexation with U(VI) and U(IV) at 4N HNO₃

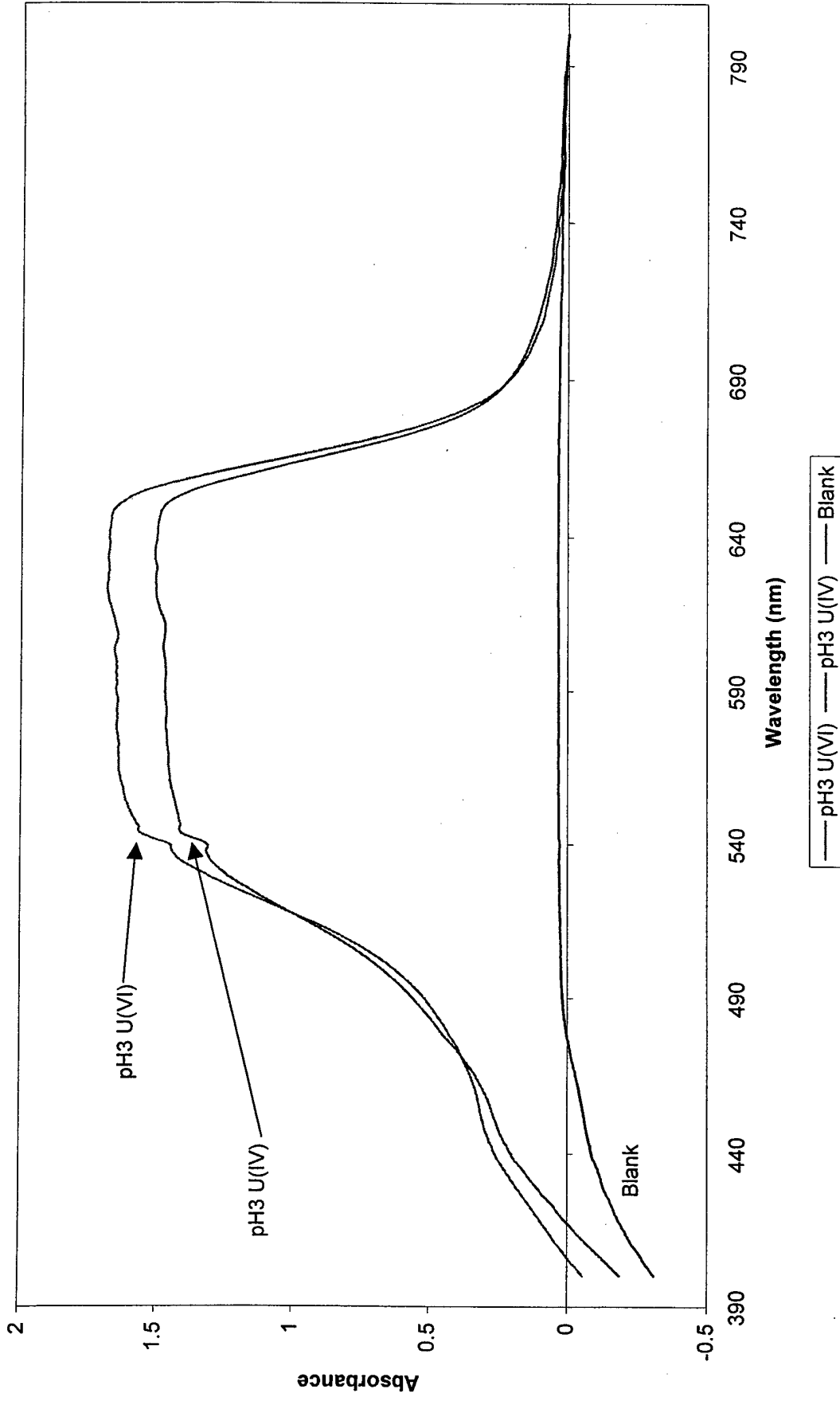
BCB with U(IV) and U(VI) Metal Aqueous Species (Normalized Values and Uncorrected for Background)



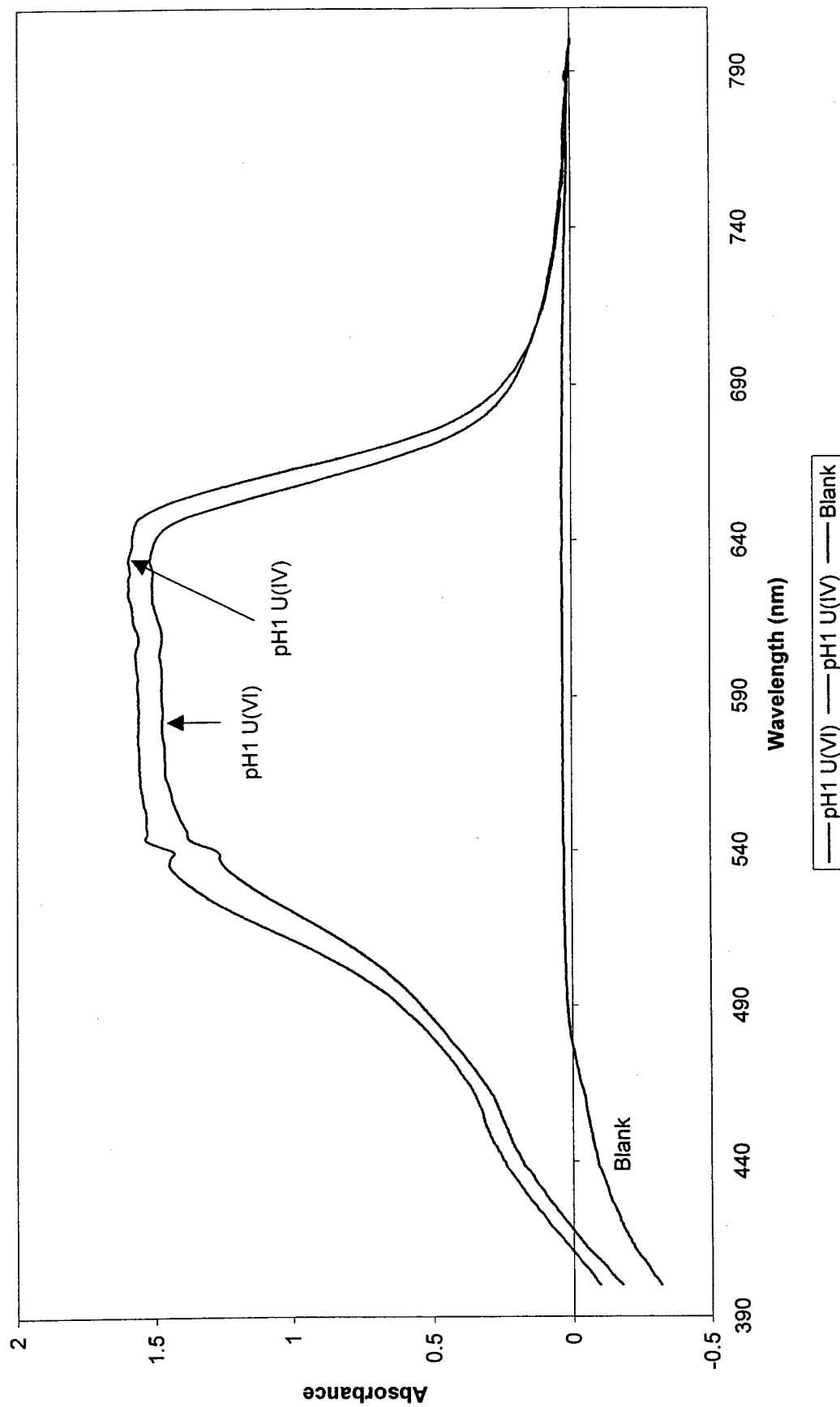
**BCB with U(IV) and U(VI) Metal Aqueous Species in pH7 Buffer
(Normalized Values and Uncorrected for Background)**



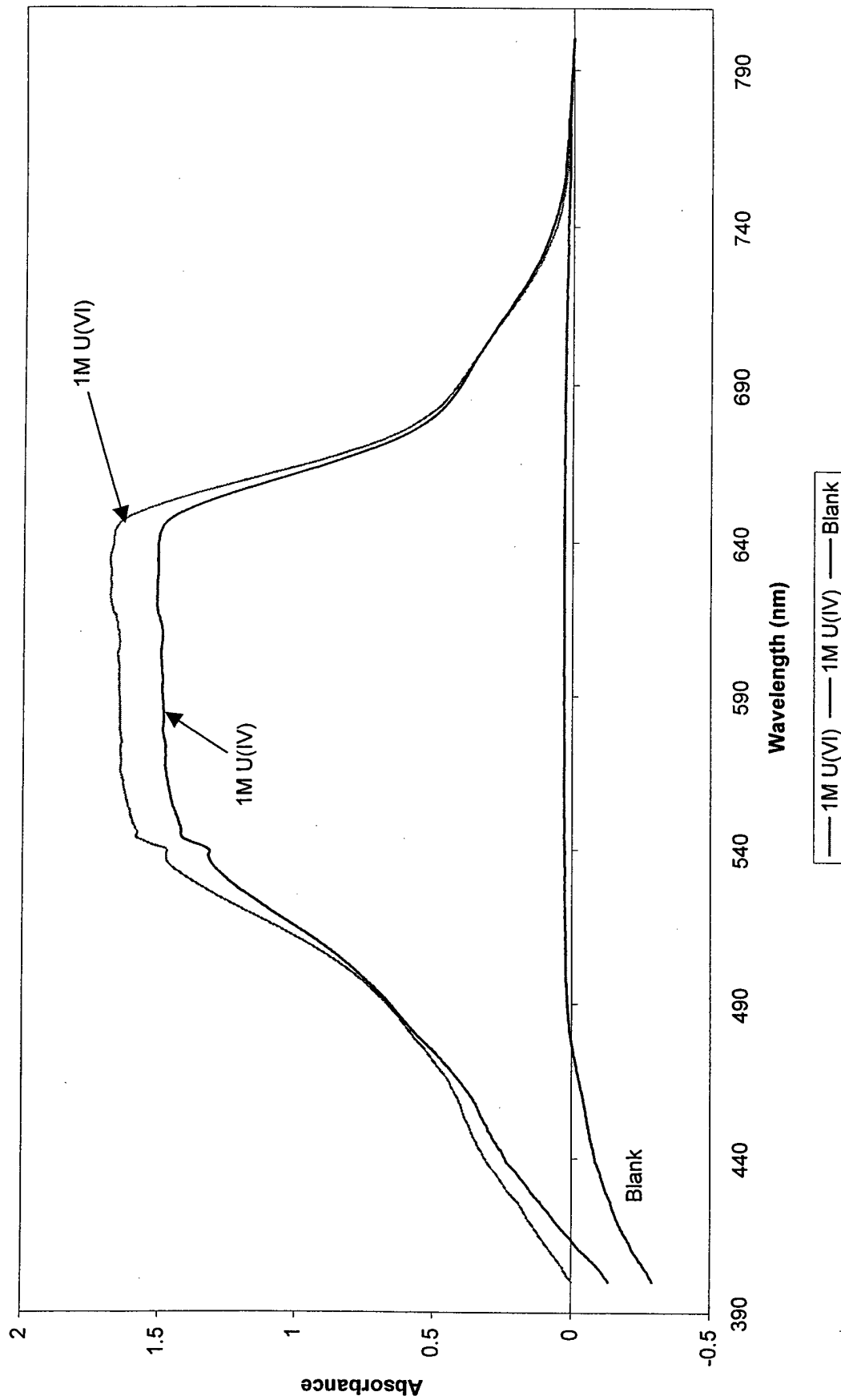
**BCB with U(IV) and U(VI) Metal Aqueous Species in pH3 Buffer
(Normalized Values and Uncorrected for Background)**



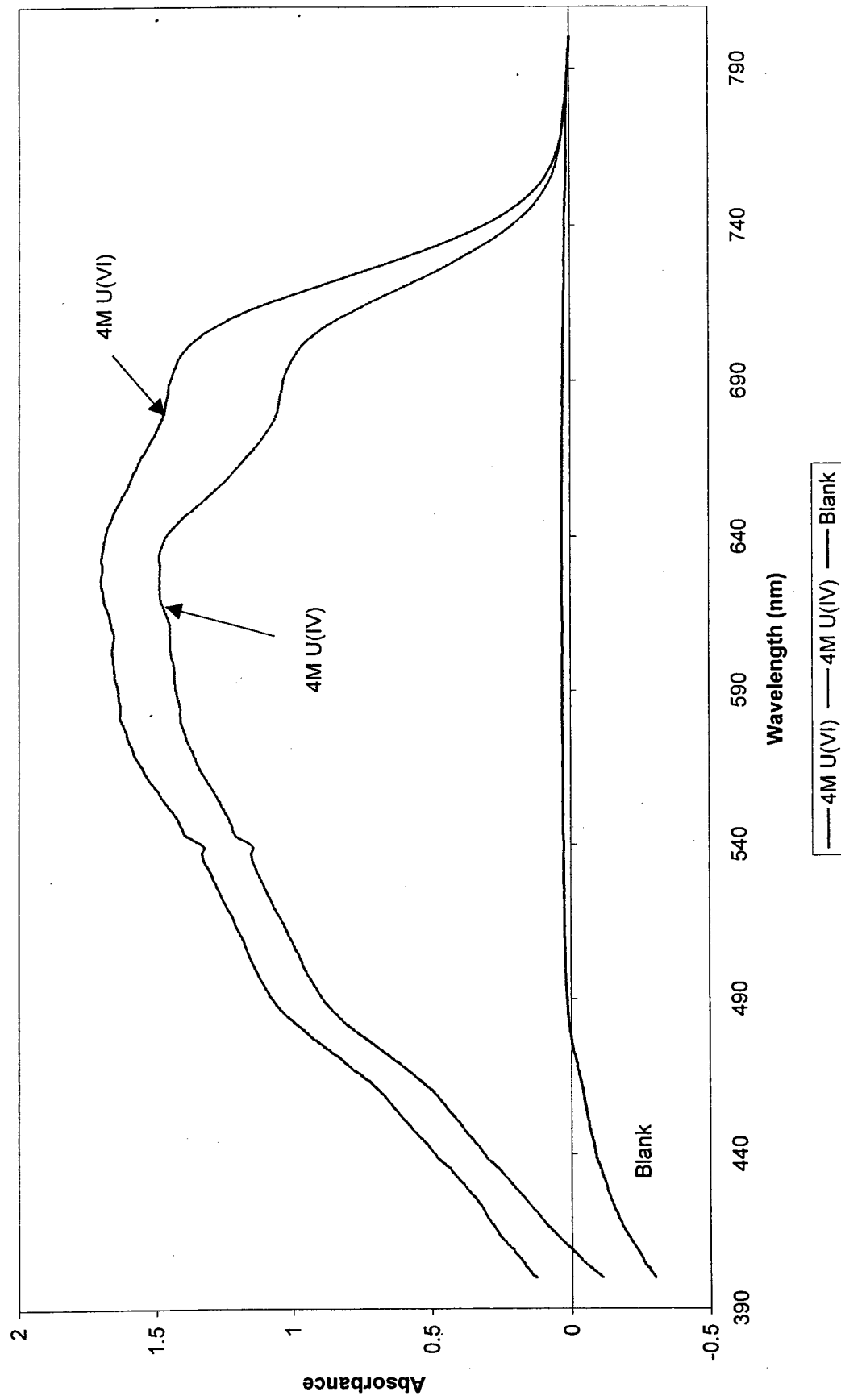
**BCB with U(IV) and U(VI) Metal Aqueous Species in pH1 Buffer
(Normalized Values and Uncorrected for Background)**



BCB with U(IV) and U(VI) Metal Aqueous Species in 1 M HNO₃
(Normalized Values and Uncorrected for Background)



BCB with U(IV) and U(VI) Metal Aqueous Species in 4M HNO₃
(Normalized Values and Uncorrected for Background)

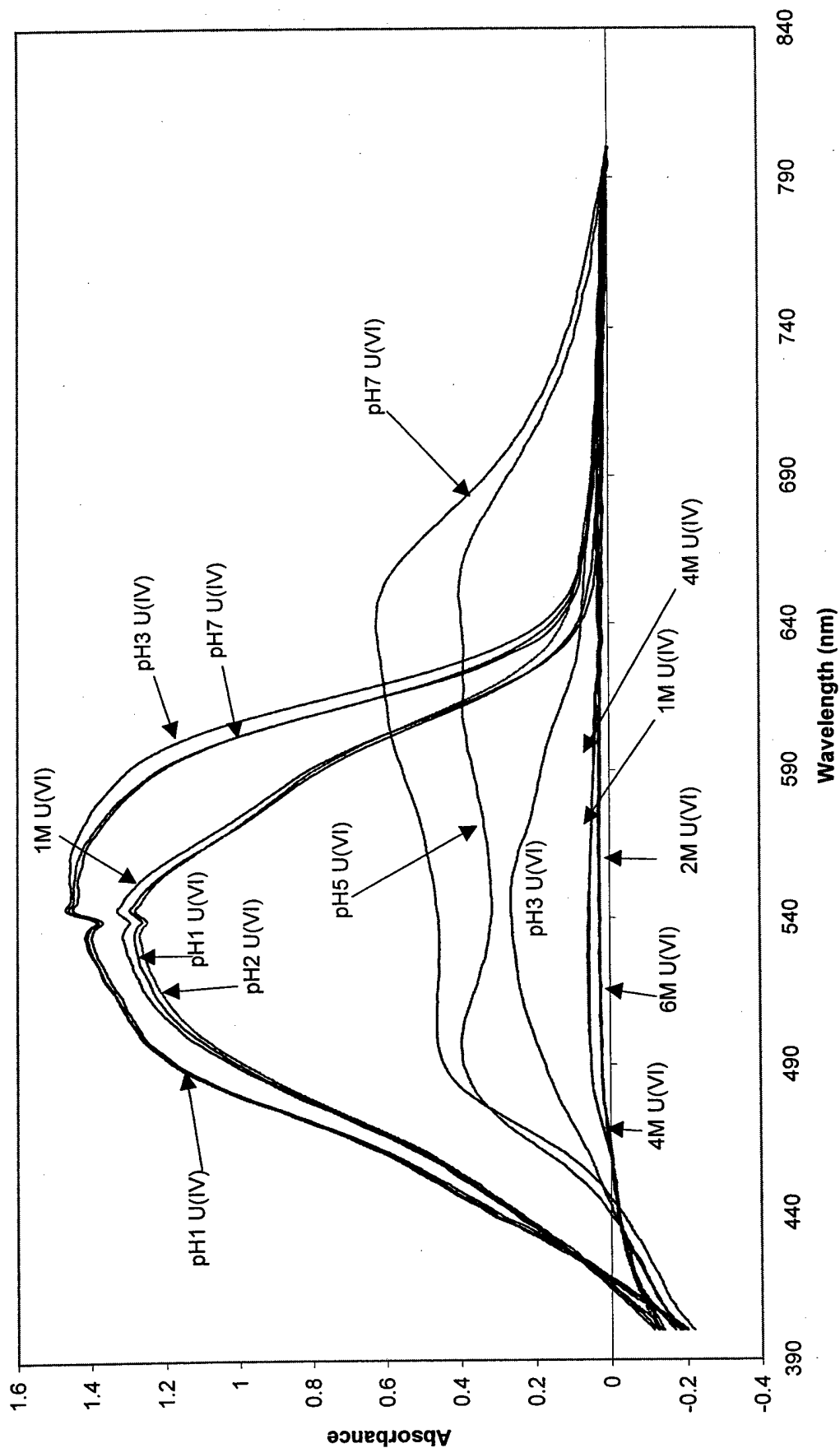


Appendix 2, Annex L

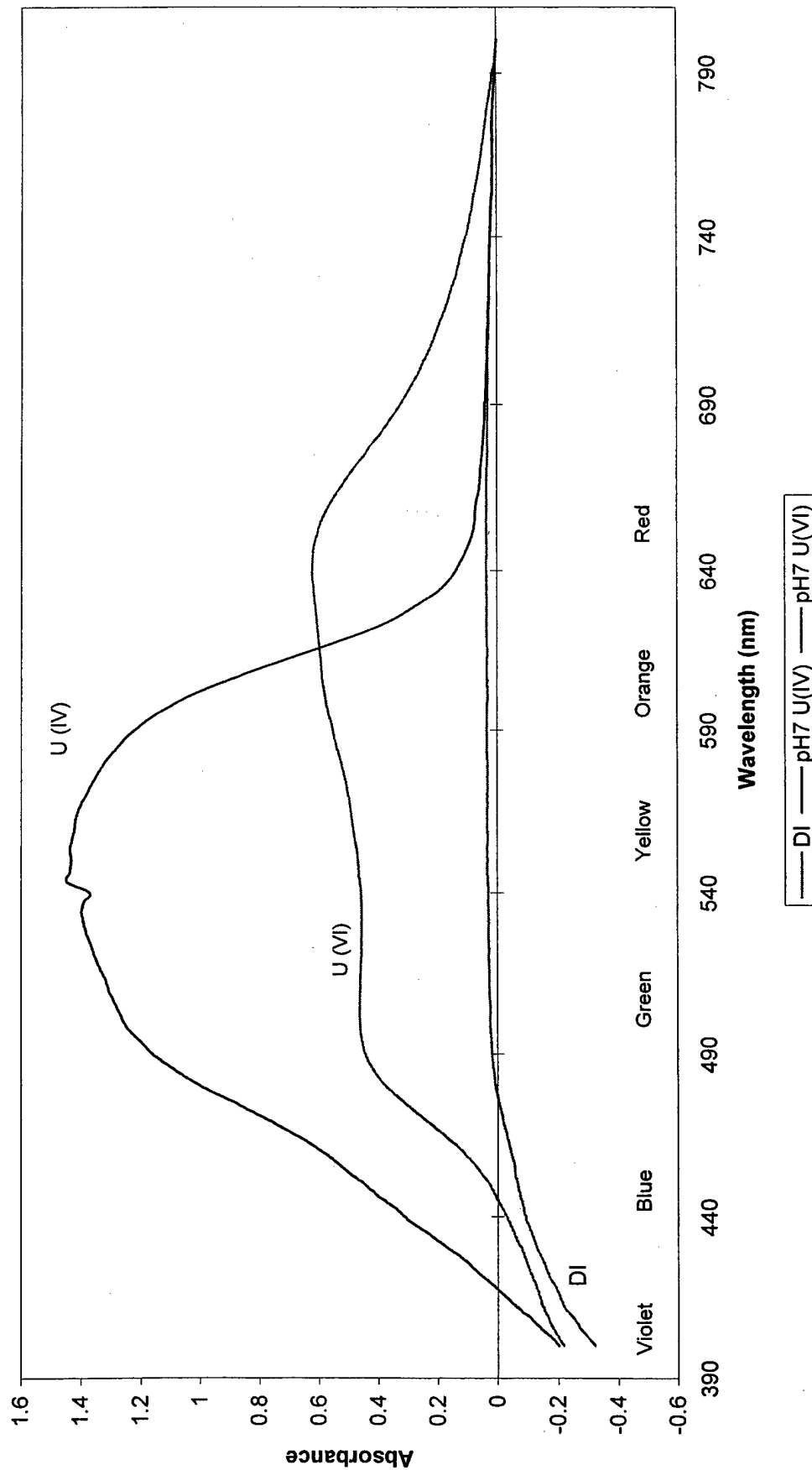
Celestine Blue Spectra Comparison of U(VI) and U(IV)

- L-1 CB total with U(VI) and U(IV)
- L-2 CB Complexation with U(VI) and U(IV) at pH7
- L-3 CB Complexation with U(VI) and U(IV) at pH3
- L-4 CB Complexation with U(VI) and U(IV) at pH1
- L-5 CB Complexation with U(VI) and U(IV) at 1N HNO₃
- L-6 CB Complexation with U(VI) and U(IV) at 4N HNO₃

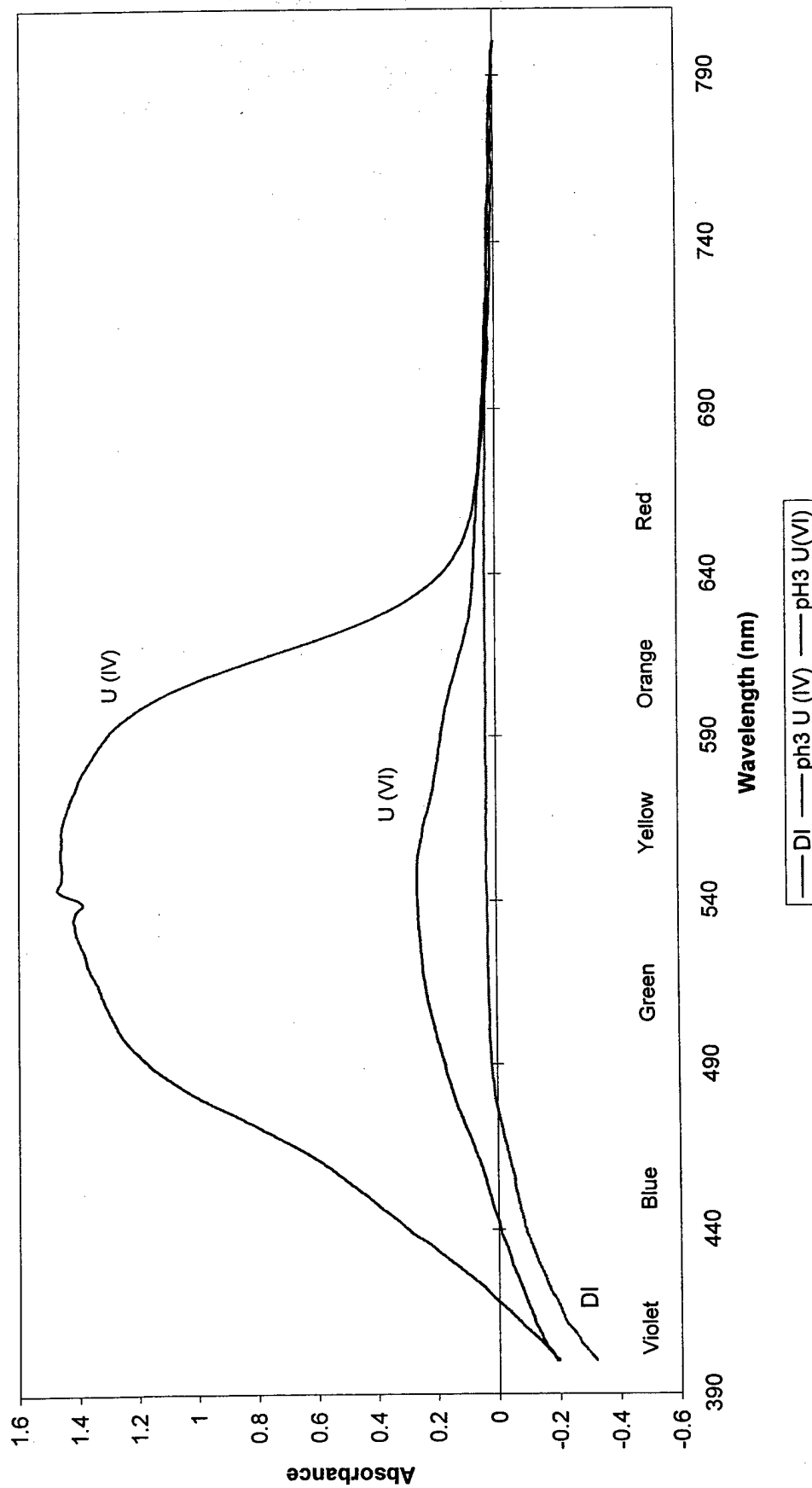
**CB with U(VI) and U(IV) Metal Aqueous Species
(Normalized Values and Uncorrected for Background)**



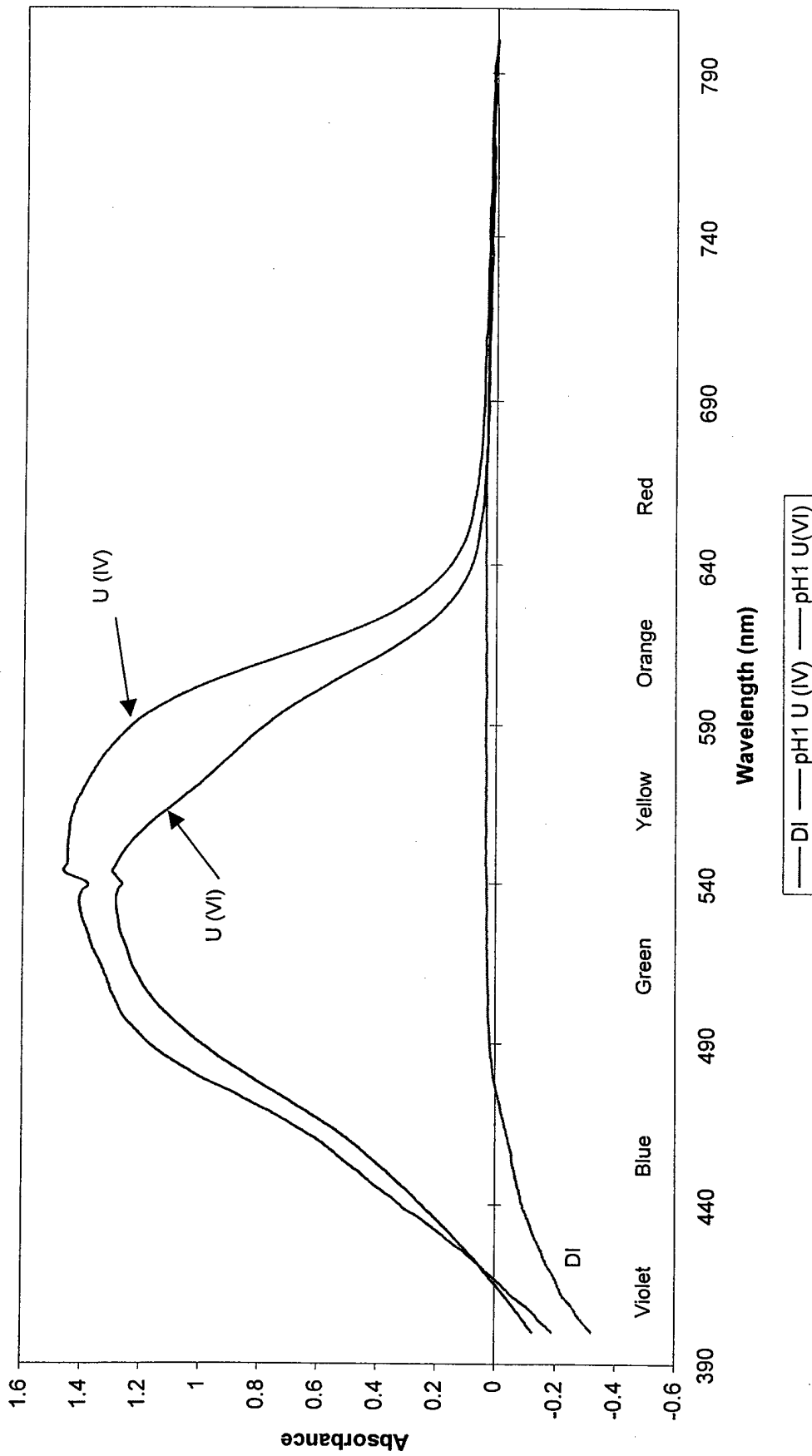
CB with U (IV) and U (VI)
Metal Aqueous Species in pH7 Buffer
(Normalized Values and Uncorrected for Background)



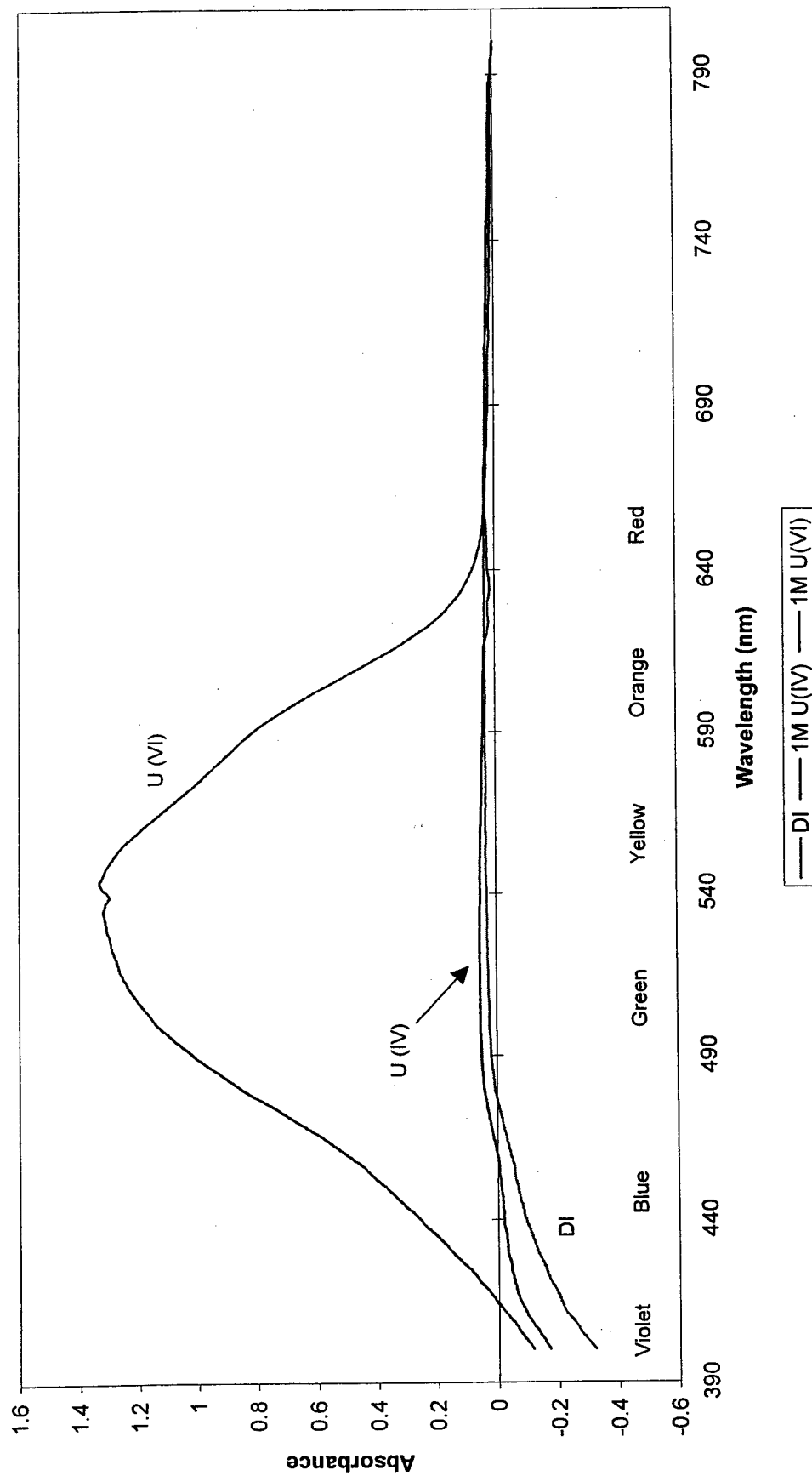
CB with U (IV) and U (VI)
Metal Aqueous Species in pH3 Buffer
(Normalized Values and Uncorrected for Background)



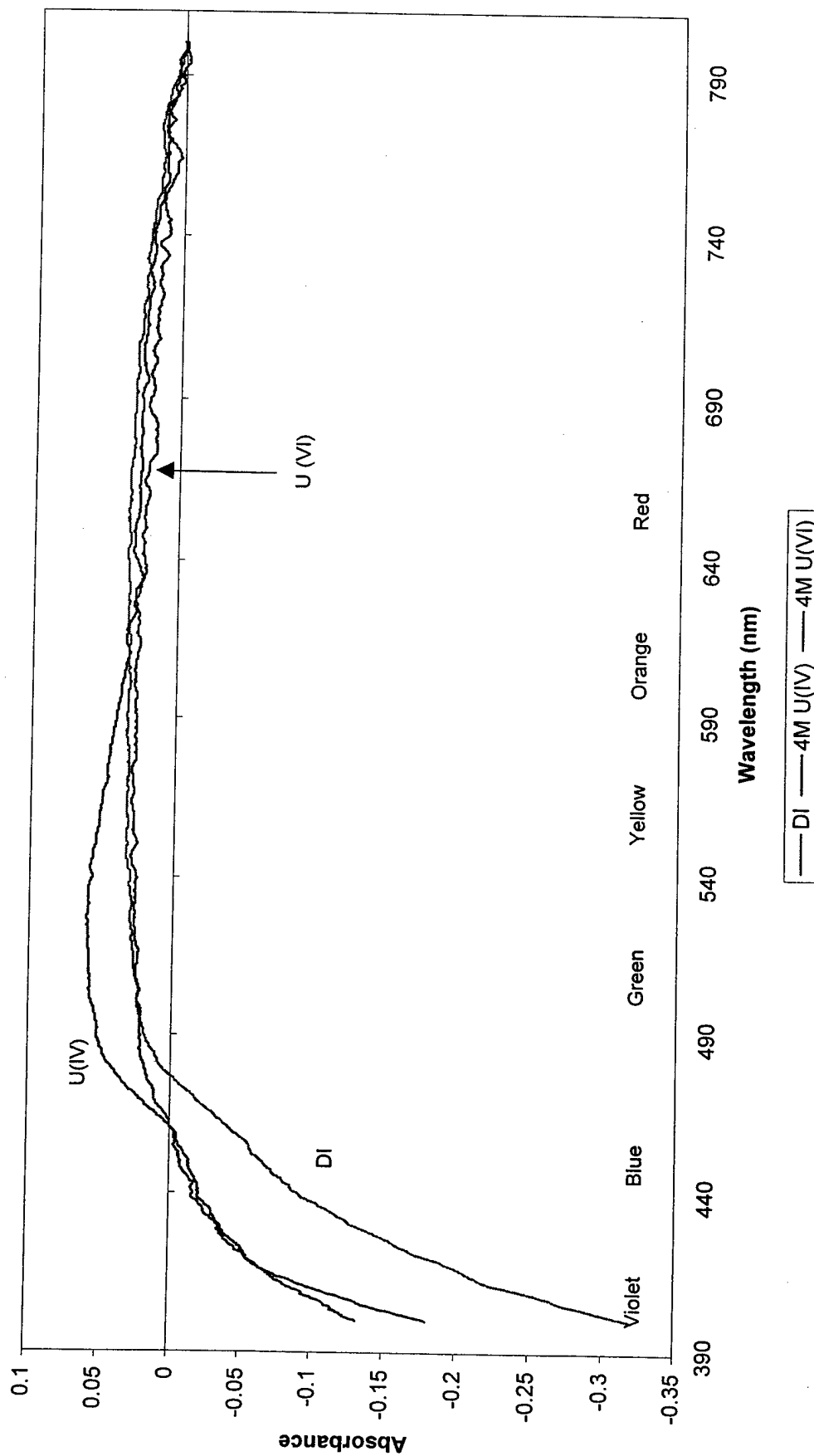
CB with U (IV) and U (VI)
Metal Aqueous Species in pH1 Buffer
(Normalized Values and Uncorrected for Background)



CB with U (IV) and U (VI)
Metal Aqueous Species in 1M HNO₃
(Normalized Values and Uncorrected for Background)



CB with U (IV) and U (VI)
Metal Aqueous Species in 4M HNO₃
(Normalized Values and Uncorrected for Background)

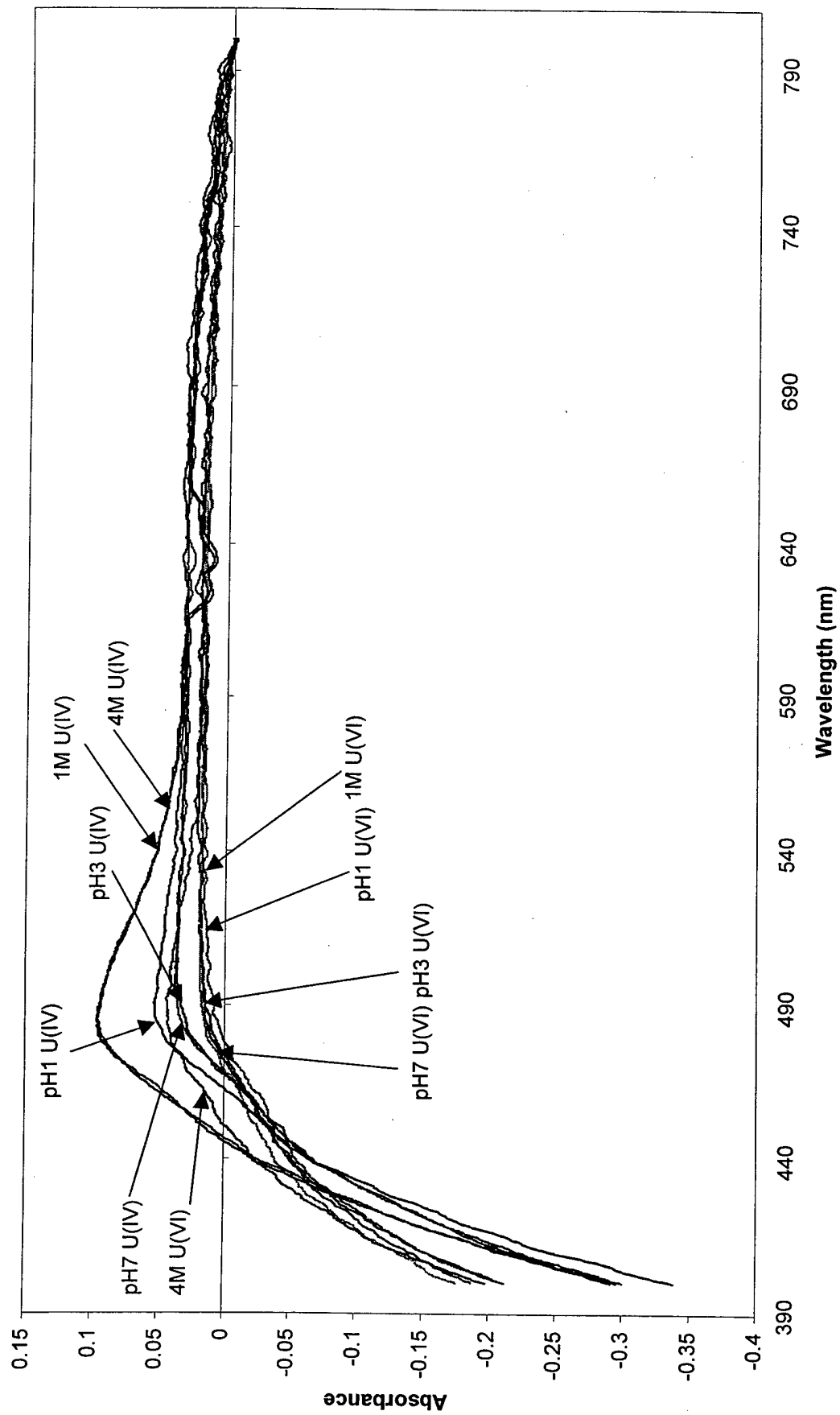


Appendix 2, Annex M

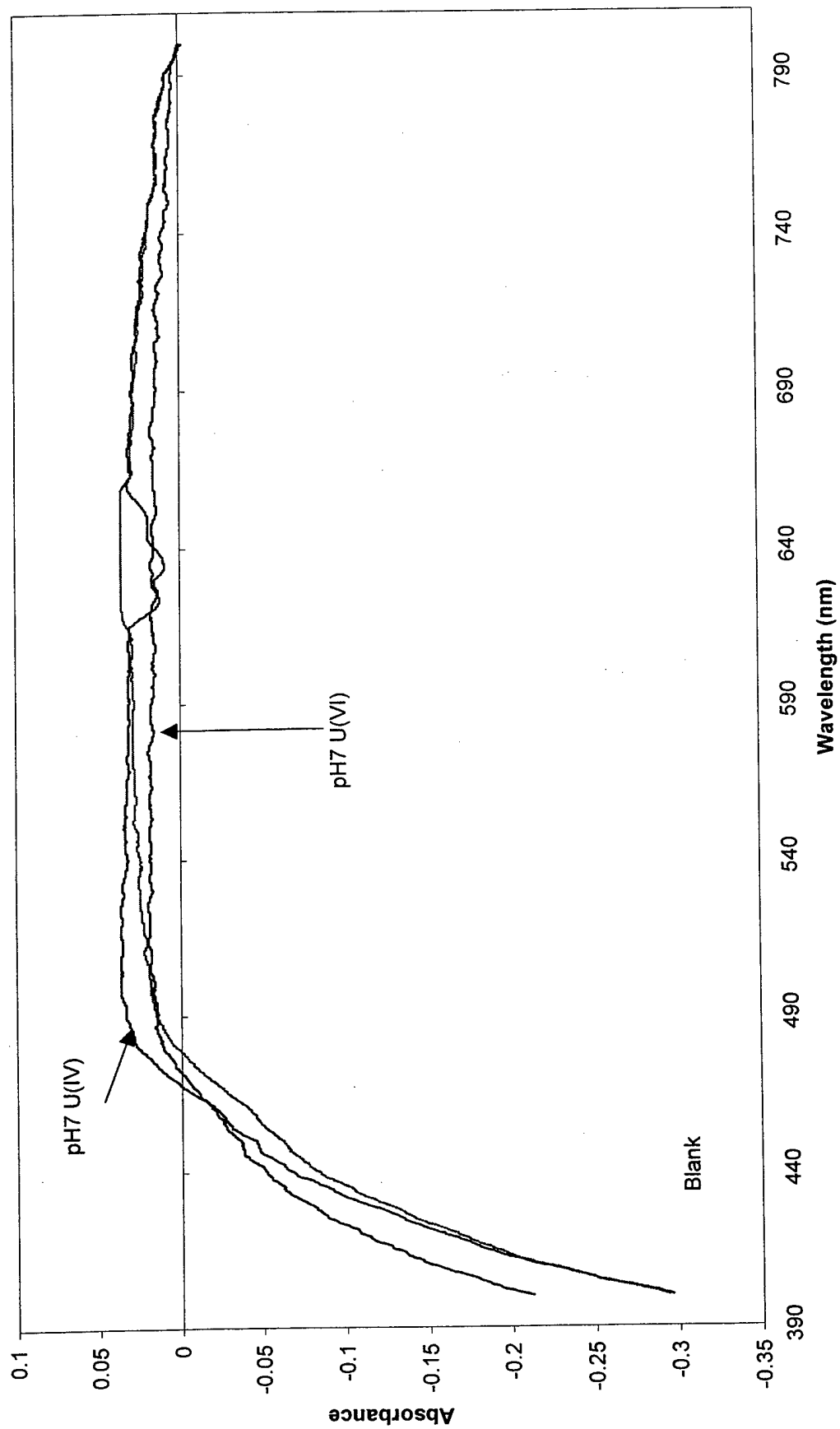
Gallomine Triethiodide Spectra Comparison of U(VI) and U(IV)

- M-1 GT total with U(VI) and U(IV)
- M-2 GT Complexation with U(VI) and U(IV) at pH7
- M-3 GT Complexation with U(VI) and U(IV) at pH3
- M-4 GT Complexation with U(VI) and U(IV) at pH1
- M-5 GT Complexation with U(VI) and U(IV) at 1N HNO₃
- M-6 GT Complexation with U(VI) and U(IV) at 4N HNO₃

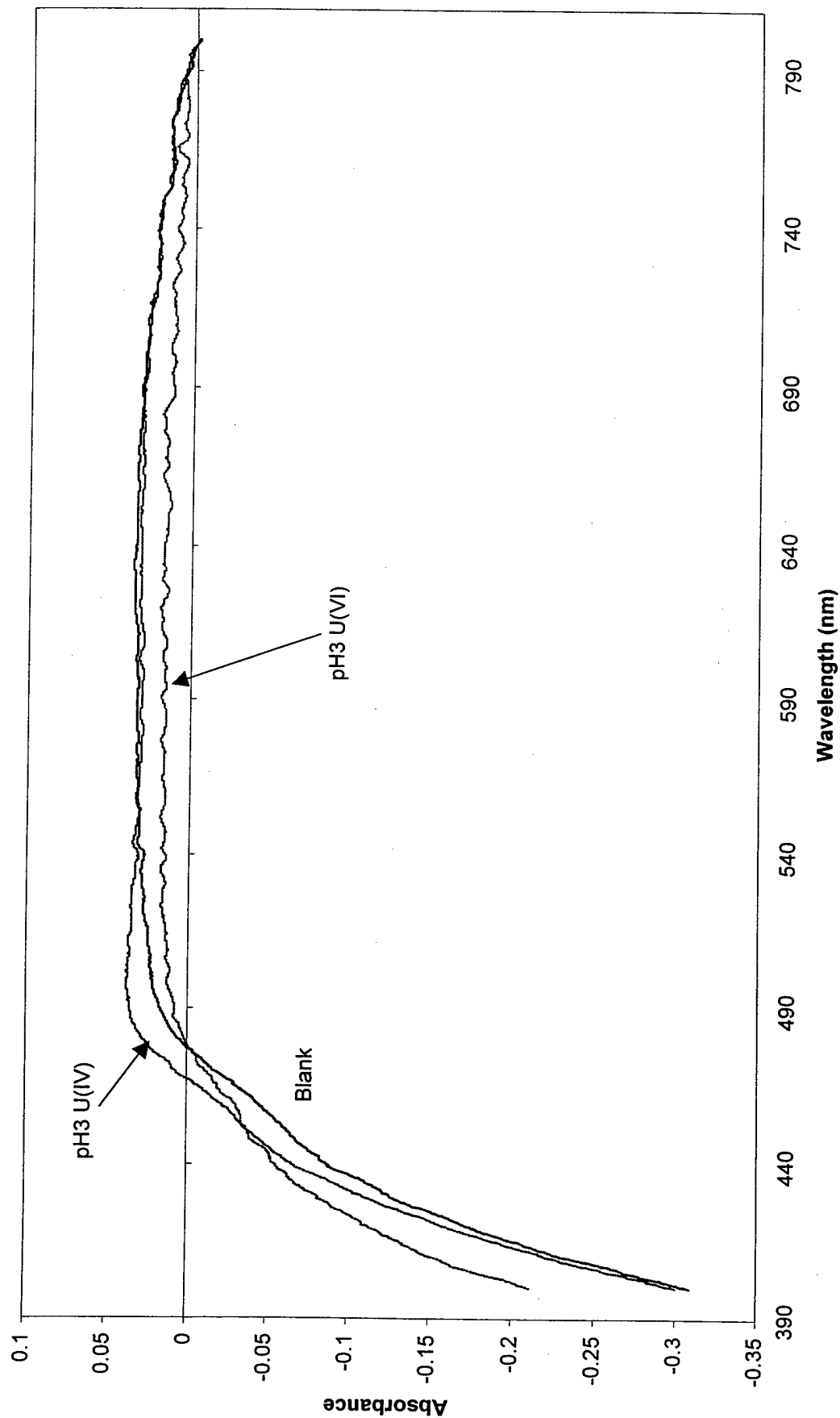
GT with U(IV) and U(VI) Metal Aqueous Species
(Normalized Values and Uncorrected for Background)



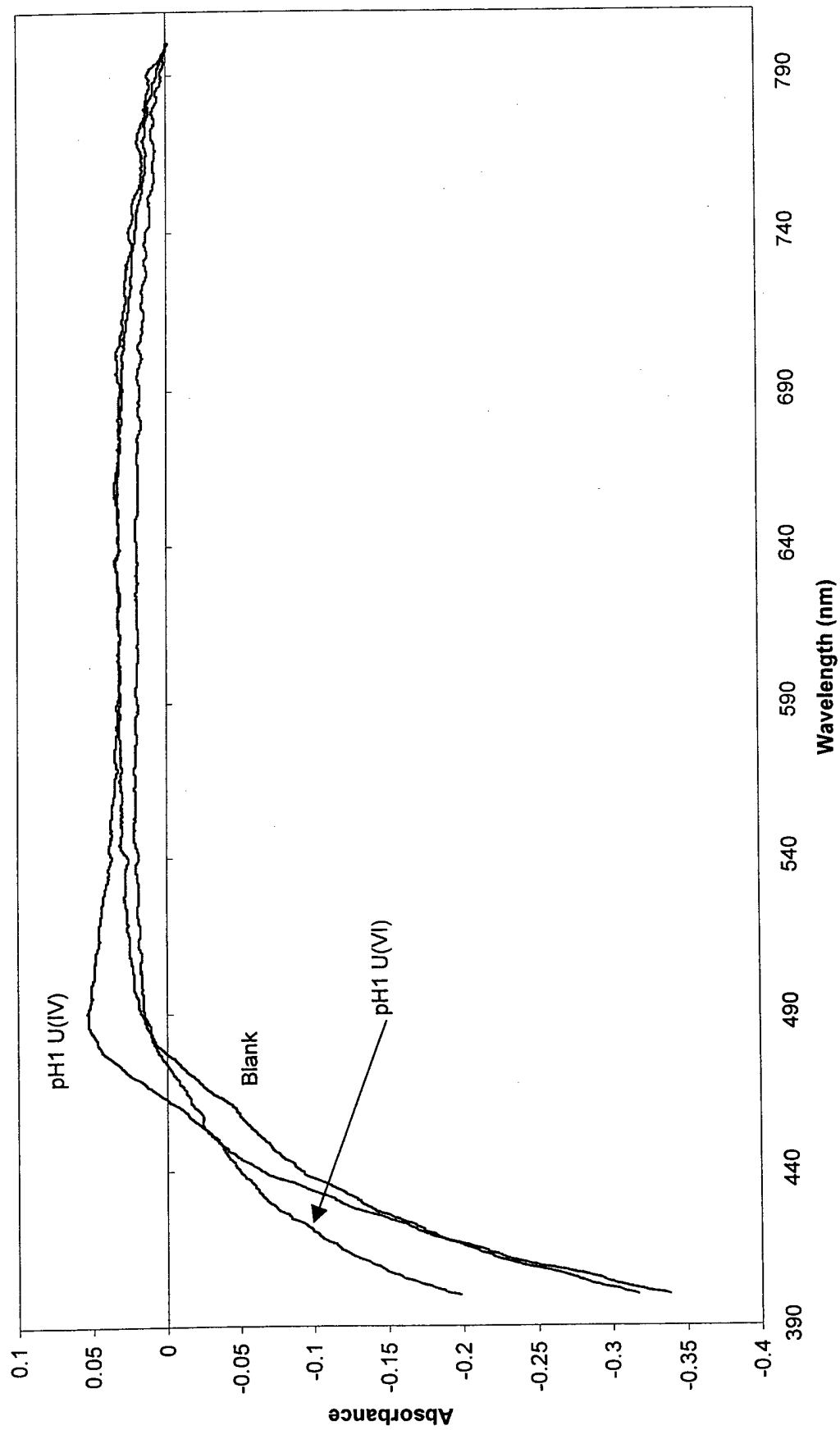
**GT with U(IV) and U(VI) Metal Aqueous Species in pH7 Buffer
(Normalized Values and Uncorrected for Background)**



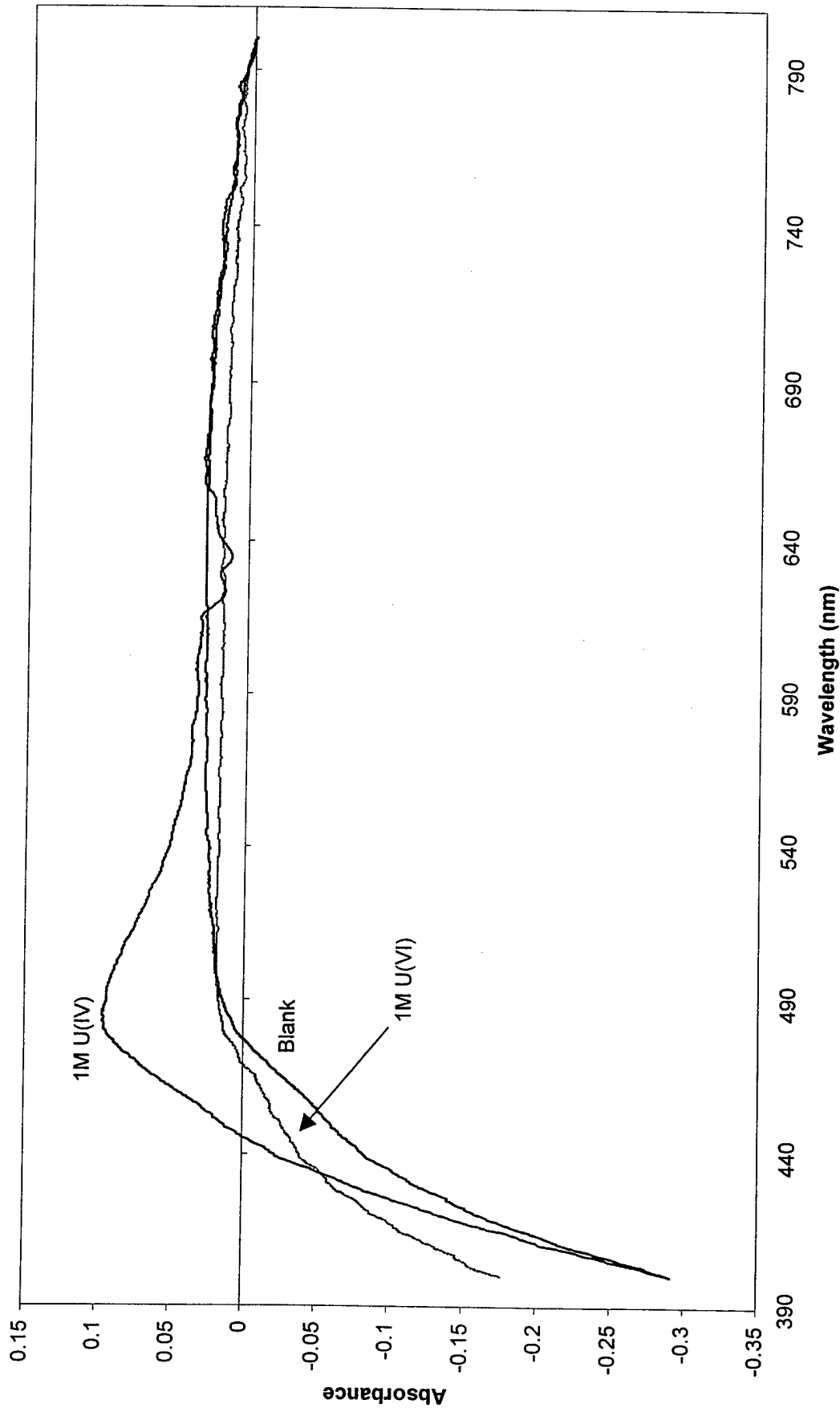
GT with U(IV) and U(VI) Metal Aqueous Species in pH3 Buffer
(Normalized Values and Uncorrected for Background)



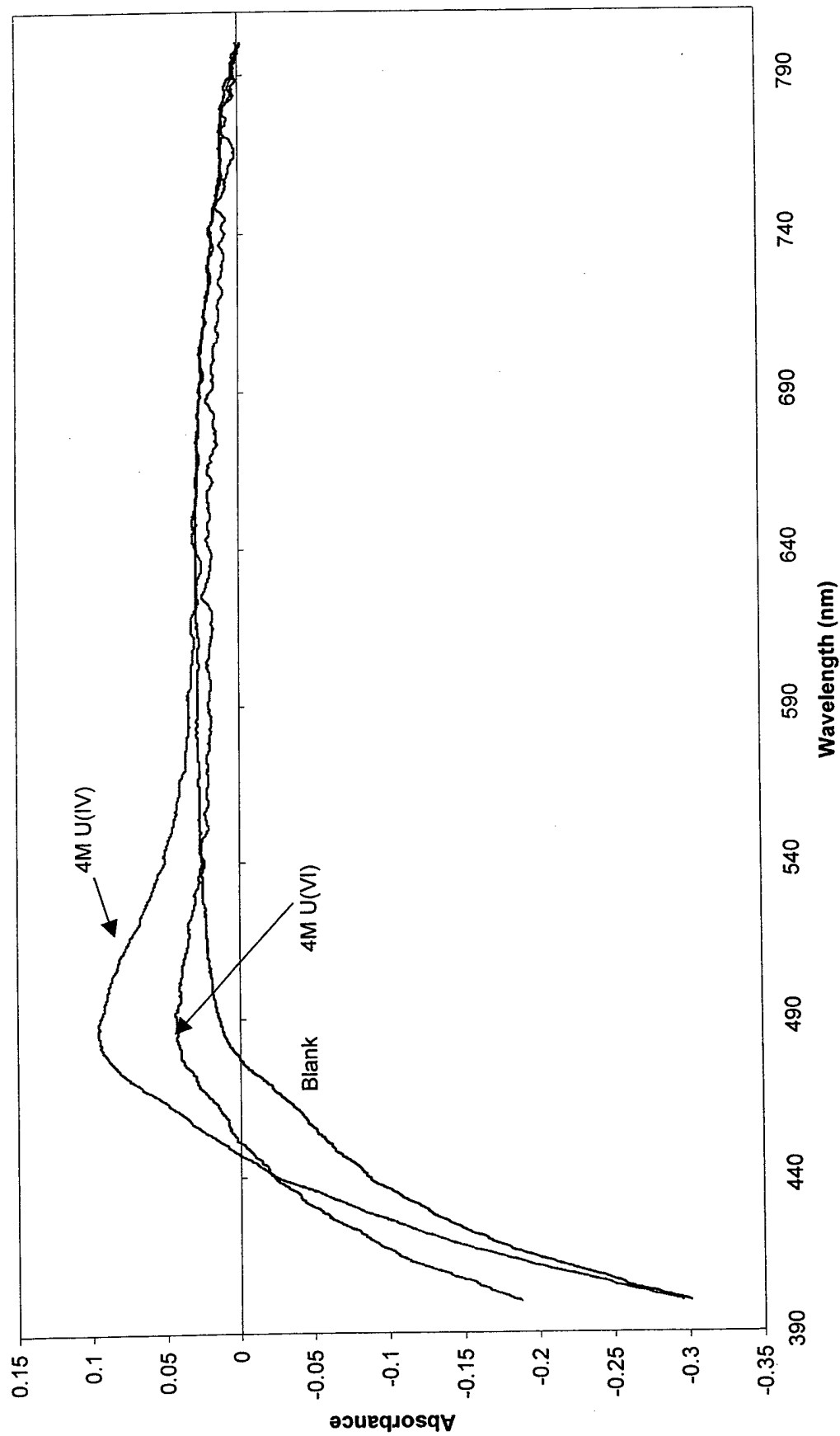
**GT with U(IV) and U(VI) Metal Aqueous Species in pH1 Buffer
(Normalized Values and Uncorrected for Background)**



GT with U(IV) and U(VI) Metal Aqueous Species in 1 M HNO₃
(Normalized Values and Uncorrected for Background)



GT with U(IV) and U(VI) Metal Aqueous Species in 4M HNO₃
(Normalized Values and Uncorrected for Background)



Appendix 3, Annex A

New Brunswick Laboratory

Certified Reference Material Certificate of Analysis

CRM U500

Uranium Isotopic Standard

	²³⁴ U	²³⁵ U	²³⁶ U	²³⁸ U
Atom Percent	0.5181	49.696	0.0755	49.711
	±0.0008	±0.050	±0.0003	±0.050
Weight Percent	0.5126	49.383	0.0754	50.029

The uncertainties for the isotopic composition are 95% confidence interval for a single determination.

July 5, 1994

Argonne, Illinois

(Revision of NBL Certificate Dated October 1, 1987)

Carleton D. Bingham

Director

Appendix 3, Annex B

ICP-AES Operating Instructions

1. Check to make sure that the exhaust system is on. The two circuit breaker power system switches are against the wall on collocated with the ICP-AES. They are usually never turned off.
2. Check coolant level. Remove reservoir cap and stick finger in reservoir to ensure that it is full.
3. Check the Argon tank. Open tank valve all the way and then back off a quarter turn. The gauge leading into the ICP-AES should read between 700-800 psi. The main argon tank pressure starts at 1400 psi. The ICP-AES burns approximately 500-600 psi an hour. When the tank reads less than 500 psi, the system should be shutdown and the tank replaced.
4. Turn the water cooling system ON. This is located in the right corner of the room (box on the floor). The temperature is set between 20°C and the re-circulation pump pressure is 78 psi.
5. Tighten the sampling tube. Stretches around the rotating circle. Work inside to outside and bottom to top. Once plastic fins on the tube are firmly in place, lock the tubing bracket down.
6. Check coolant flow rate. Open door to the torch and nebulizer assembly. (See photo in Chapter 3). The error light on the outside control switches flashes. Press the '+' button. Watch the upper right bubble meter labeled coolant. Then press Stop.

7. Check nebulizer press '-' and watch the bubble meter. The bubble shoots up and drops down and stabilizes.
8. Check the water level in the Argon Humidifier. Ensure that the water level is around one third full. If not, undo the cap and pour in water. The ICP runs a closed argon system. If undid cap, need to flush the system. Anytime there is a break in the line, the system needs to be flushed (Change gas cylinders, etc)
9. Check torch position and cleanliness of the quartz tube. Undo the protective plate with a phillips screwdriver. Look to make sure the bottom coil is above the inner part of the torch 1-2 mm and ensure the coil and torch are not touching. Put the protective plate and close the door.
10. Press Start on control panel. Now have to be very careful. Firing up the torch. When it starts, there are only a few seconds to look for a good burn. If other than a good burn, press stop There is a 60 second countdown: at 25-30 seconds and 10 second there is an audible click. At 0 seconds, there is an audible pop.
11. Press Pump on the control panel. Make sure orange sample line is in deionized water. Let the system run for 15 minutes with deionized water.
12. Log on to the software program.
13. Go to the operations menu. Instrument Generator Parameters. May change the pump step. Normally pump 2 for fast flush and 1 for samples.
14. Under method menu, select measure, quantitative, and the method Uranium (or other method for another analysis).

15. Output Format (Data file format) and Measurement Parameters (number of measurements, type of average, counting time factor, background correction) may be adjusted.
16. Switch the waste tanks just prior to placing in the samples.
17. Reprofile the optics. Looking for the characteristic wavelength of the element to analyze. Converts steps to energy values.
18. Type F3, type name of the measurement, switch tube, and then return
19. After the analysis (2-3 minutes), press F9 to print the results.

Appendix 3, Annex C

Detailed Media Contents for Cultivating *Shewanella Putrefaciens*

- 1) Vitamin Solution, 1000x (per liter medium added)
 - a) P-aminobenzonic acid
 - b) Biotin, 0.02 mg
 - c) Nicotinic acid, 0.05 mg
 - d) Ca-pantothenate, 0.05 mg
 - e) Thiamine HCl, 0.05mg
 - f) Pyridoein HCl (B), 0.1 mg
 - g) Cyano cobalamin (B12), 0.001 mg
- 2) Basal Solution, Stock Solution, 10x 1000ml (per liter medium added)
 - a) KH_2PO_4 , 0.2 g
 - b) NH_4Cl , 0.25 g
 - c) NaCl , 1.0 g
 - d) $\text{MgCl}_2 \cdot 6\text{H}_2\text{O}$, 0.4 g
 - e) KCl , 0.5 g
- 3) $\text{CaCl}_2 \cdot 2\text{H}_2\text{O}$ solution, 1000x 100ml per L medium 0.15 g
- 4) Trace Element Solution, 1000x 100ml (per liter of medium)
 - a) Conc HCl, 0.001 ml
 - b) $\text{MnCl}_2 \cdot 4\text{H}_2\text{O}$, 0.10 mg
 - c) $\text{CoCl}_2 \cdot 6\text{H}_2\text{O}$, 0.12 mg
 - d) ZnCl_2 , 0.07 mg

- e) H_3BO_3 , 0.06 mg
- f) $\text{NiCl}_2 \cdot 6\text{H}_2\text{O}$, 0.025 mg
- g) $\text{CuCl}_2 \cdot 2\text{H}_2\text{O}$, 0.015 mg
- h) $\text{Na}_2\text{MoO}_4 \cdot 2\text{H}_2\text{O}$, 0.025 mg
- i) $\text{FeCl}_2 \cdot 4\text{H}_2\text{O}$, 1.5 mg

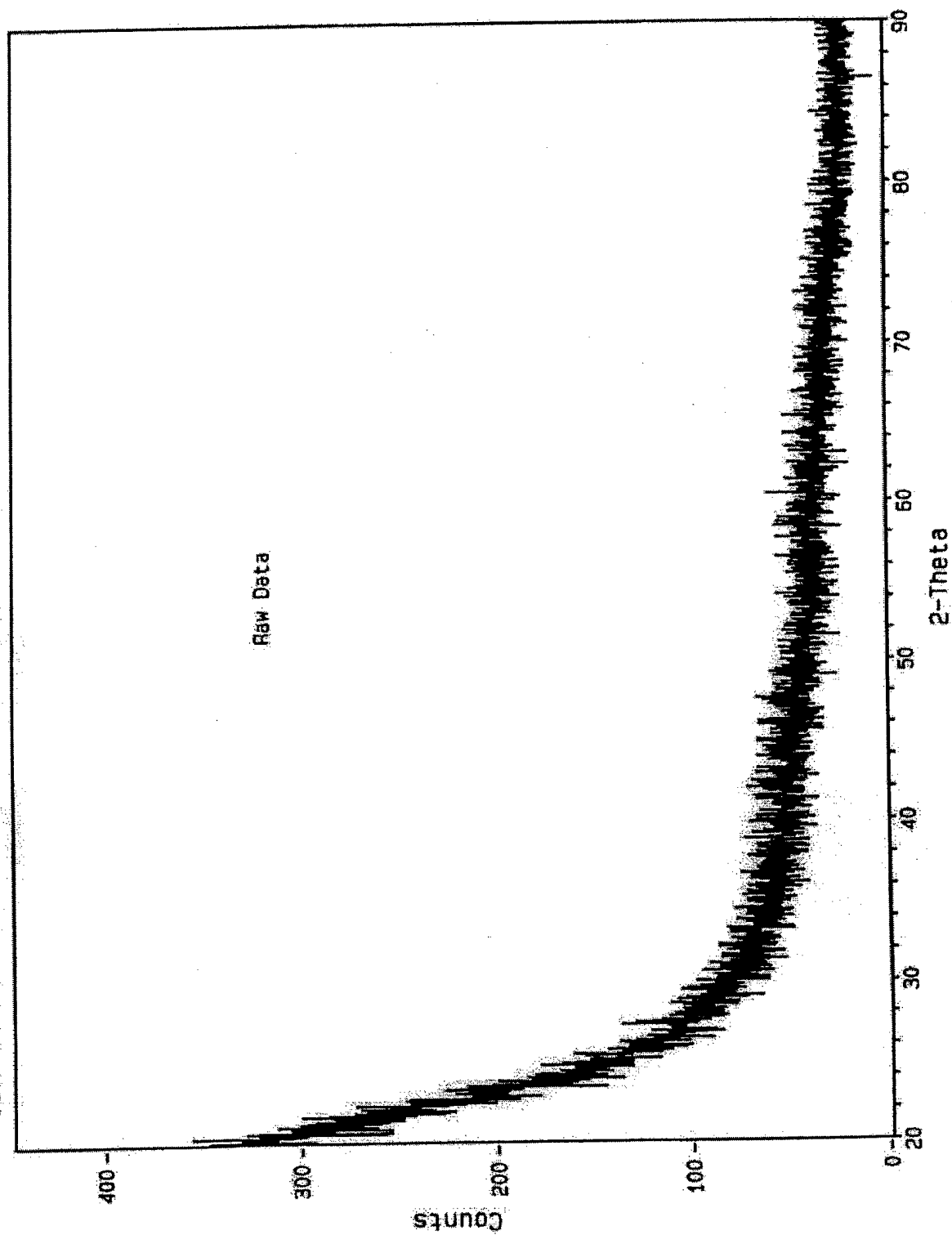
Appendix 3, Annex D

X-Ray Diffraction Graphs

- D-1 Raw Data Background Spectra.
- D-2 Raw Data of Bacterial Precipitate.
- D-3 Raw Data of both D-1 and D2 superimposed on each other.
- D-4 Raw Data with uraninite reference peak locations.
- D-5 Background and Ka2 subtracted spectra with:
 - 1 Uraninite peaks.
 - 2 2 θ Values.
- D-6 Peak Analysis for Bacterial Precipitate with Jade Software program.

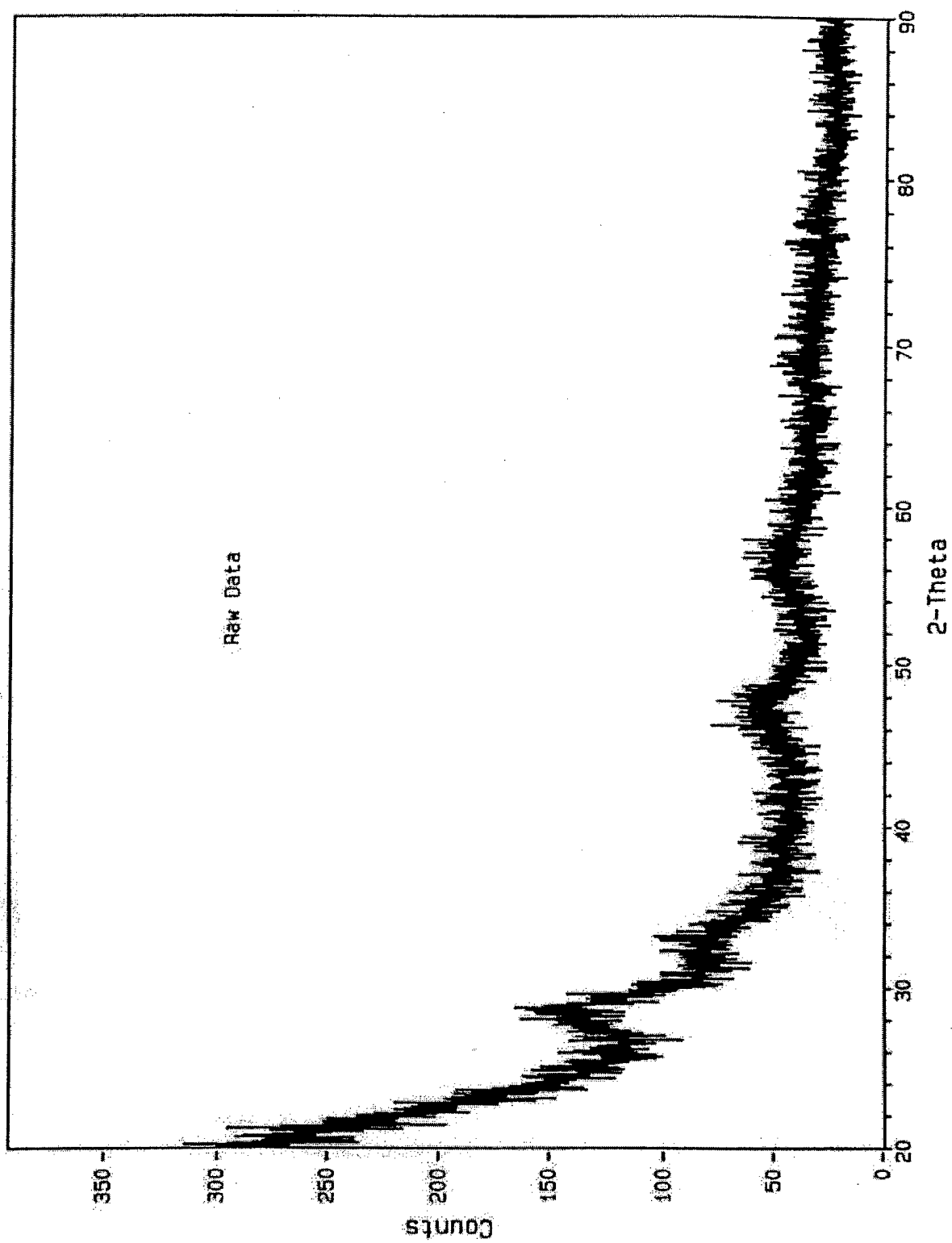
Appendix 3, Annex D-1

ID: SI ZERO BACKGROUND HOLDER W / COLLOIDION, 20-AUG-99014: 22
File: Z14544.RAW Scan: 20-90/02/ 1.5/#3501, Anode: CU



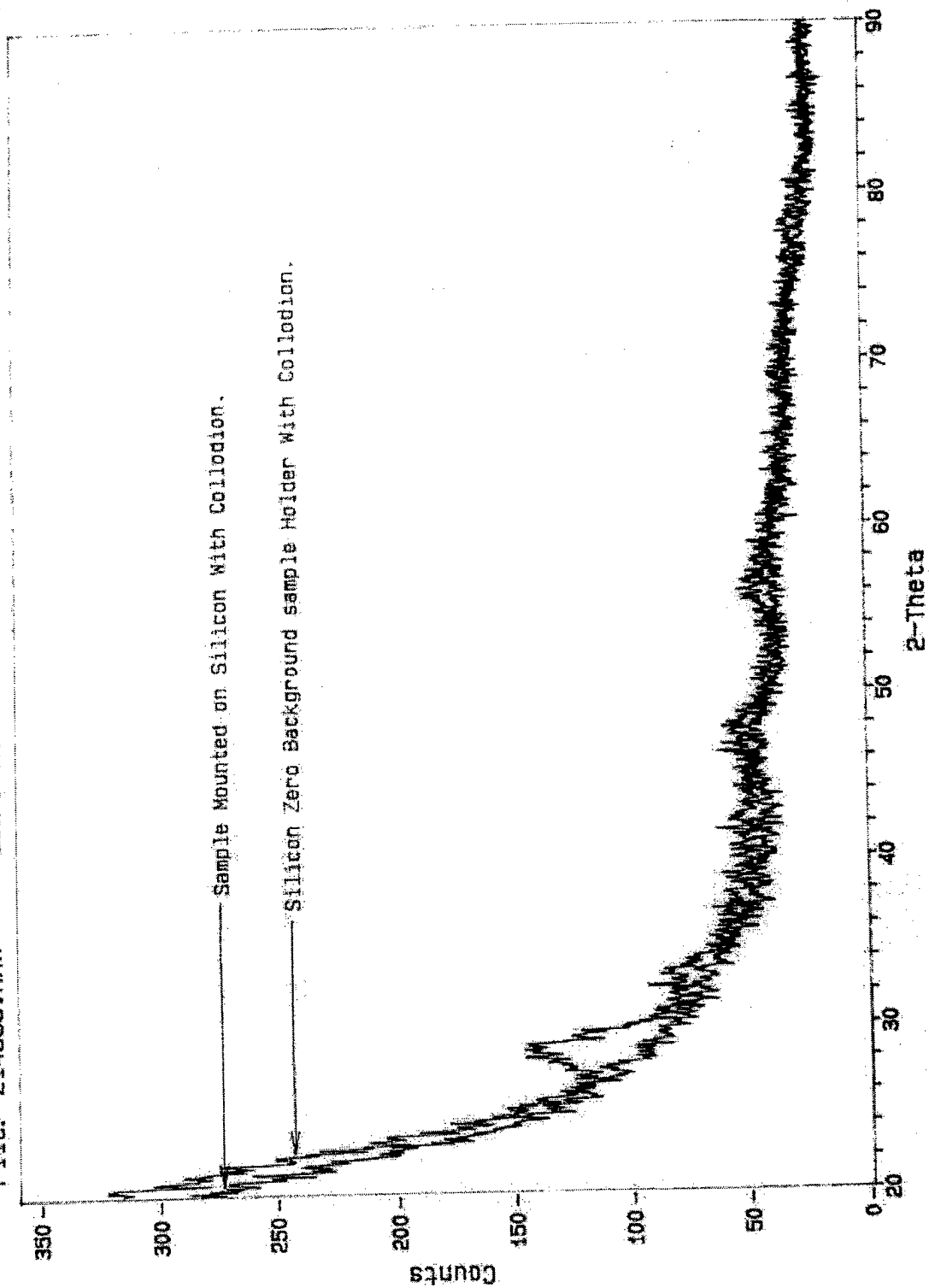
Appendix 3, Annex D-2

ID: LEWIS U027, 19-AUG-99@14:15
File: Z14535.RAW Scan: 20-90/.02/ 1.5/#3501, Anode: CU

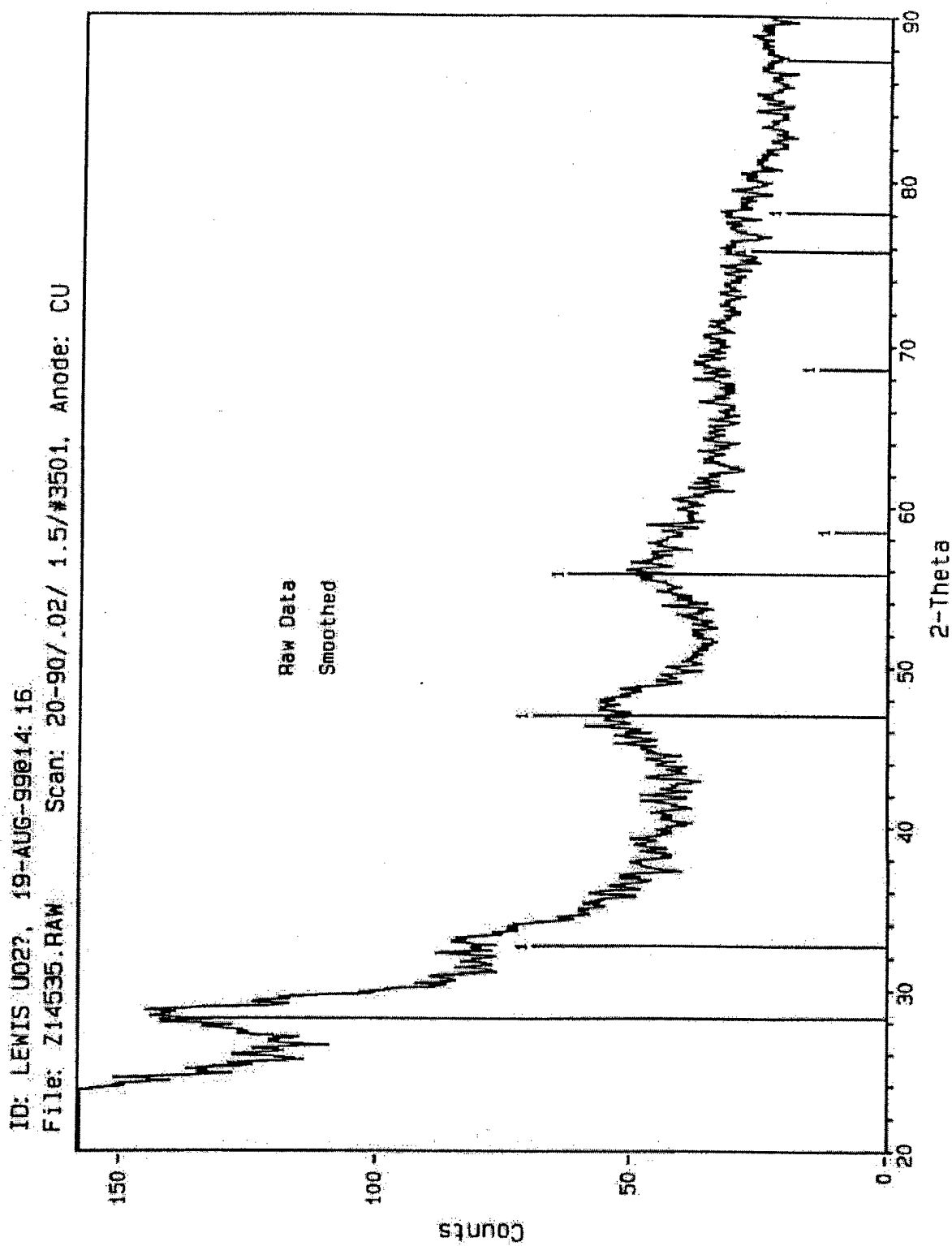


Appendix 3, Annex D-3

ID: LEWIS U022, 19-AUG-99 014:16
File: Z14535.RAW Scan: 20-90/.02/ 1.5/#3501, Anode: CU



Appendix 3, Annex D-4



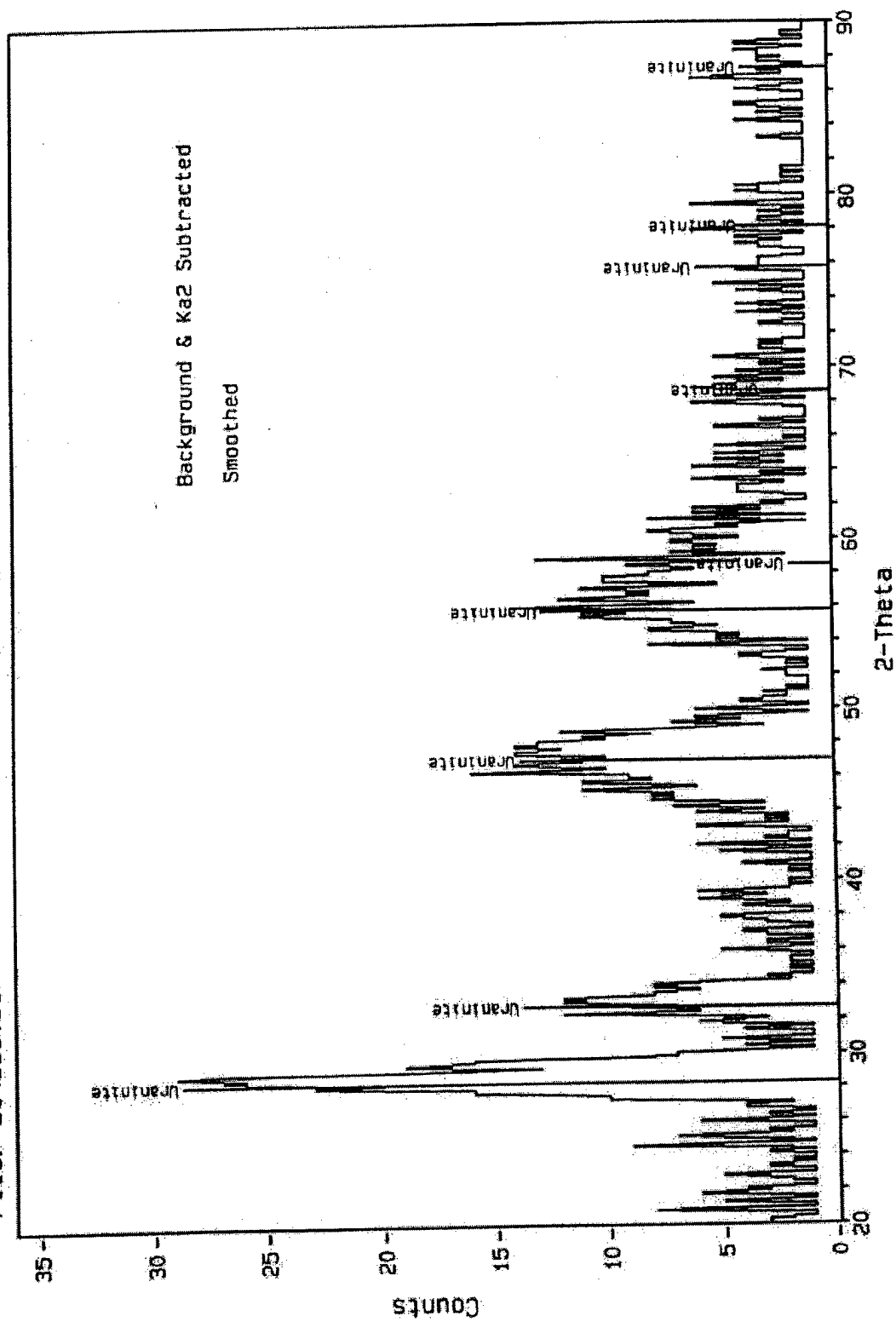
1> 41-1422: Uraninite-C - U02

Appendix 3, Annex D-5-1

ID: LEWIS 002? 19-AUG-99@14:16

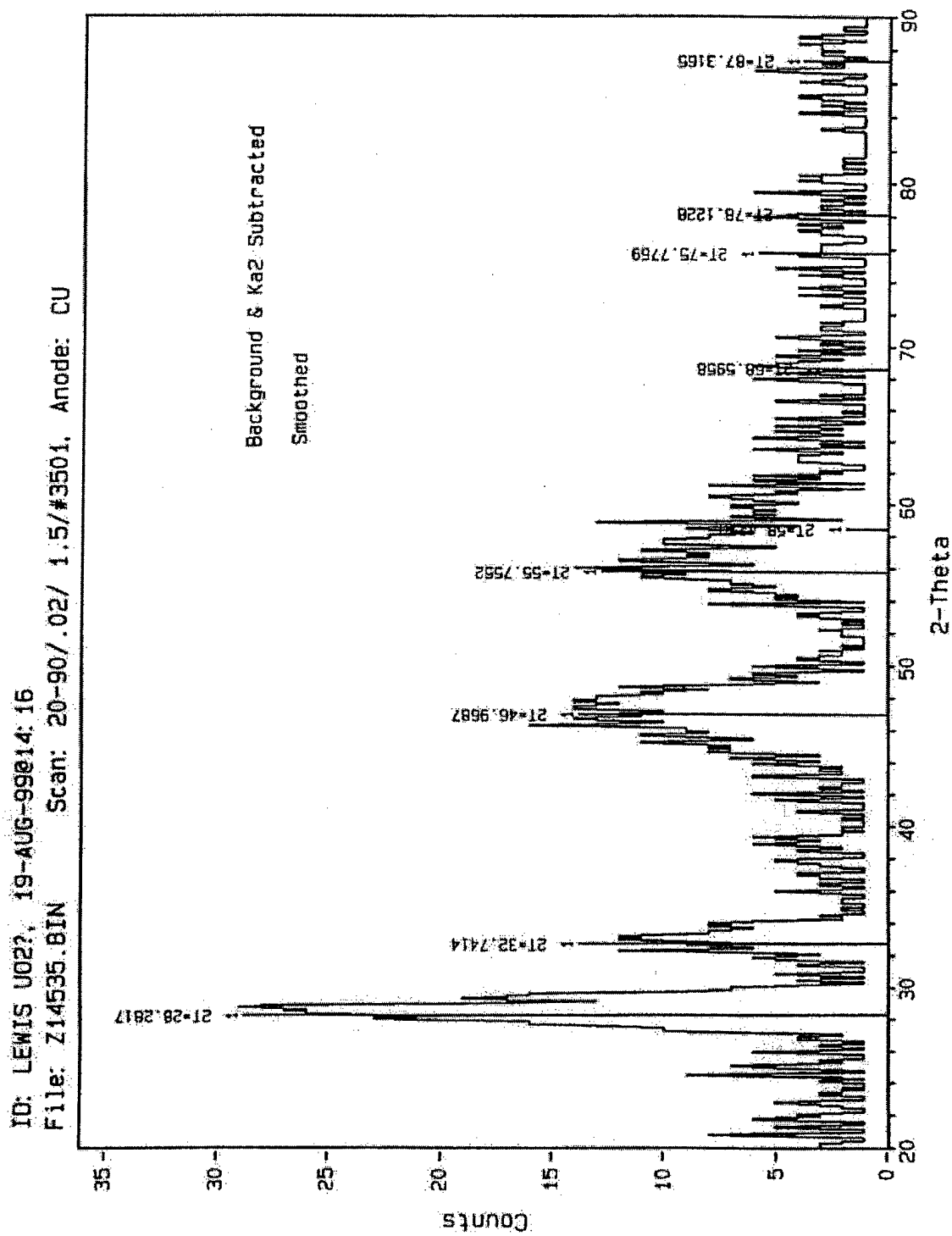
File: Z14535.BIN

Scan: 20-90/.02/ 1.5/#3501, Anode: CU



41-1422: Uraninite-C - U02

Appendix 3, Annex D-5-2



Appendix 3, Annex D-6

===== cmse @ MIT =====

Jade: Peak Listing

Thu Aug 19 1999 @3:07pm

File: Z14535.BIN> LEWIS UO2?, 19-AUG-99@14:16

----- Scan Parameters: -----				----- Search Parameters: -----			
Radiation	=	CU	1.54059	Filter length(pts)	=	9	
Scan Range	=	20	90	Noise level(sigmas)	=	4.0	
Step Size	=	.02		Intensity cutoff(%)	=	.1-100	
Count Time	=	1.5	sec.	2-Theta Zero (deg)	=	0	

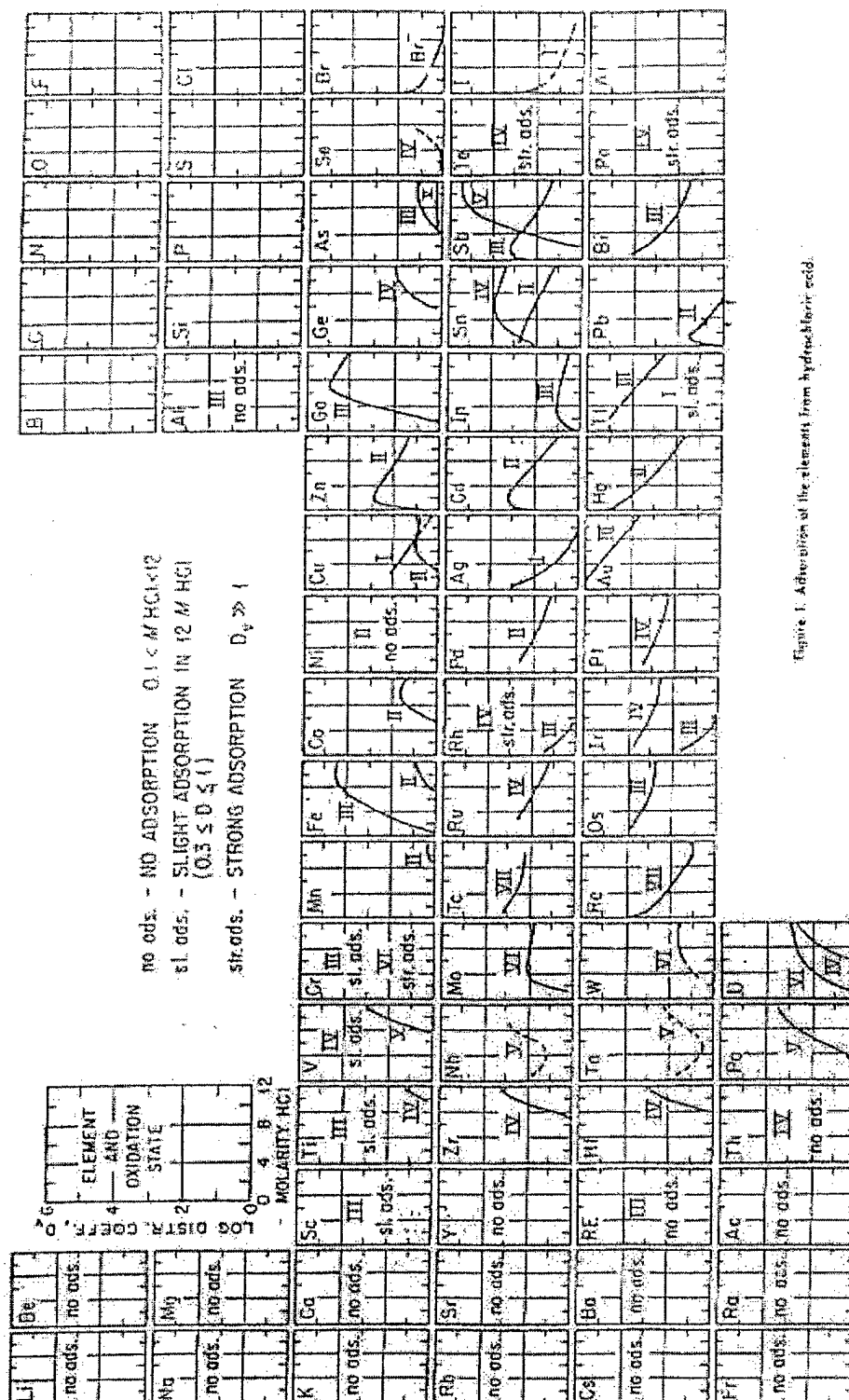
*** List of Integrated Peaks from Peak Edit ***

#	Centroid	2T & d	L&R-2Theta	L&R-Bkgrd	Peak	Area	FWHM	Size*	
1 -	28.574	3.1215	26.049	30.370	2	27	45	1.513	5.4
2 -	32.992	2.7129	30.947	35.700	2	10	14	1.301	6.4
3 -	46.832	1.9383	42.901	50.391	2	14	43	2.782	3.1

* Estimated crystallite size(nm).

Appendix 4, Annex A

Anion Exchange Resin Behavior for AG1-X8 Cl⁻ Form



Appendix 4, Annex B

Order in the Carousel

Supernatant Carousel

- 1 SOS
- 2 S4S
- 3 S8S
- 4 S24S
- 5 S95S
- 6 COS
- 7 C4S
- 8 C8S
- 9 C24S
- 10 C95S
- 11 BLANK 11
- 12 BLANK 12
- 13 BLANK 13
- 14 BLANK 14
- 15 BLANK 15

Precipitate Carousel

- 1 SOP
- 2 S4P
- 3 S8P
- 4 EMPTY
- 5 S24P
- 6 S95P
- 7 COP
- 8 C4P
- 9 C8P
- 10 C24P
- 11 C95P
- 12 EMPTY
- 13 EMPTY
- 14 EMPTY
- 15 EMPTY

Appendix 4, Annex C

Column Chemistry Log

Supernatant Columns

Pre-Clean reservoir	500 μ L	6 N HCl	1206	1 Feb 00
Clean	500 μ L	0.1 N HCl	1446	1 Feb 00
			1537	1 Feb 00
			1645	1 Feb 00
			0730	2 Feb 00
			0926	2 Feb 00
			1005	2 Feb 00
			1144	2 Feb 00
			1230	2 Feb 00
			1330	2 Feb 00
Equilibrate	200 μ L	3 N HCl	1417	2 Feb 00
Load Sample	150 μ L	3 N HCl	1517	2 Feb 00
Wash One Drop~30 μ L	30 μ L	3 N HCl	1546	2 Feb 00
			1603	2 Feb 00
			1614	2 Feb 00
Wash	200 μ L	3 N HCl	1629	2 Feb 00
Wash	200 μ L	6 N HCl	1647	2 Feb 00
Elute U	250 μ L	0.1 N HCl	1740	2 Feb 00
Precipitate Columns				
Pre-Clean reservoir	500 μ L	6 N HCl	1022	3 Feb 00
Clean	500 μ L	0.1 N HCl	1327	3 Feb 00
			1418	3 Feb 00
			1500	3 Feb 00
			1610	3 Feb 00
			1700	3 Feb 00
			0752	4 Feb 00
Equilibrate	200 μ L	3 N HCl	0853	4 Feb 00
Load Sample	150 μ L	3 N HCl	0947	4 Feb 00

Wash One Drop~30 μ L	30 μ L	3 N HCl	1006	4 Feb 00
			1016	4 Feb 00
			1032	4 Feb 00
Wash	200 μ L	3 N HCl	1041	4 Feb 00
Wash	200 μ L	6 N HCl	1130	4 Feb 00
Elute U	250 μ L	0.1 N HCl	1223	4 Feb 00

Appendix 4, Annex D

TIMS Turret Loading

Turret 1 15 Feb 00

Bead Name

- 1 1 μL U500, 1 μL 0.1 M H_3PO_4 , 1 μL Carbon
- 2 1 μL U500, 1 μL Carbon
- 3 1 μL U500, 1 μL Carbon
- 4 1 μL U500, 3 μL Carbon
- 5 1 μL U500, 3 μL Carbon
- 6 3 μL U500, 1 μL 0.1 M H_3PO_4 , 1 μL Carbon
- 7 3 μL U500, 1 μL Carbon
- 8 3 μL U500, 1 μL Carbon
- 9 3 μL U500, 3 μL Carbon
- 10 3 μL U500, 3 μL Carbon
- 11 U Blank 11
- 12 U Blank 12
- 13 U Blank 13
- 14 U Blank 14
- 15 U Blank 15
- 16 1 μL C0S, 3 μL Carbon
- 17 1 μL C4S, 3 μL Carbon
- 18 1 μL C8S, 3 μL Carbon
- 19 1 μL C24S, 3 μL Carbon
- 20 1 μL C95S, 3 μL Carbon

Turret 2 17 Feb 00

Bead Name

- 1 3 μL U500, 1 μL 1.0 M H_3PO_4 , Graphite Sandwich
- 2 3 μL U500, 1 μL 1.0 M H_3PO_4 , Graphite Sandwich
- 3 3 μL U500, 1 μL 1.0 M H_3PO_4 , Graphite Sandwich without top layer
- 4 3 μL U500, 1 μL 1.0 M H_3PO_4 , Graphite Sandwich without top layer
- 5 3 μL U500, 1 μL 0.1 M H_3PO_4 , Graphite Sandwich
- 6 3 μL U500, 1 μL 0.1 M H_3PO_4 , Graphite Sandwich
- 7 3 μL U500, 1 μL 0.1 M H_3PO_4 , Graphite Sandwich
- 8 Unrelated Experiment Sample
- 9 Unrelated Experiment Sample
- 10 Unrelated Experiment Sample

- 11 Unrelated Experiment Sample
- 12 Unrelated Experiment Sample
- 13 Unrelated Experiment Sample
- 14 Unrelated Experiment Sample
- 15 Unrelated Experiment Sample
- 16 Unrelated Experiment Sample
- 17 Unrelated Experiment Sample
- 18 Unrelated Experiment Sample
- 19 Unrelated Experiment Sample
- 20 Unrelated Experiment Sample

Turret 3 18 Feb 00

Bead Name

- 1 SOS-1
- 2 S4S-1
- 3 S8S-1
- 4 S24S-1
- 5 S95S-1
- 6 COS-2
- 7 C4S-2
- 8 S24P-1
- 9 S95P-1
- 10 S8P-1
- 11 Unrelated Experiment Sample
- 12 Unrelated Experiment Sample
- 13 Unrelated Experiment Sample
- 14 Unrelated Experiment Sample
- 15 Unrelated Experiment Sample
- 16 Unrelated Experiment Sample
- 17 Unrelated Experiment Sample
- 18 Unrelated Experiment Sample
- 19 Unrelated Experiment Sample
- 20 Unrelated Experiment Sample

Turret 4 19 Feb 00

Bead Name

- 1 Unrelated Experiment Sample
- 2 Unrelated Experiment Sample
- 3 Unrelated Experiment Sample
- 4 S24S-1
- 5 S95S-1
- 6 COS-1

- 7 S24P-1
- 8 S95P-1
- 9 S8P-1
- 10 Unrelated Experiment Sample
- 11 Unrelated Experiment Sample
- 12 Unrelated Experiment Sample
- 13 Unrelated Experiment Sample
- 14 Unrelated Experiment Sample
- 15 Unrelated Experiment Sample
- 16 Unrelated Experiment Sample
- 17 Unrelated Experiment Sample
- 18 Unrelated Experiment Sample
- 19 Unrelated Experiment Sample
- 20 Unrelated Experiment Sample

Turret 5 21 Feb 00

Bead Name

- 1 S4S-2
- 2 S8S-2
- 3 S24S-2
- 4 S95S-2
- 5 Unrelated Experiment Sample
- 6 Unrelated Experiment Sample
- 7 Unrelated Experiment Sample
- 8 Unrelated Experiment Sample
- 9 Unrelated Experiment Sample
- 10 Unrelated Experiment Sample
- 11 Unrelated Experiment Sample
- 12 Unrelated Experiment Sample
- 13 Unrelated Experiment Sample
- 14 Unrelated Experiment Sample
- 15 Unrelated Experiment Sample
- 16 Unrelated Experiment Sample
- 17 Unrelated Experiment Sample
- 18 Unrelated Experiment Sample
- 19 Unrelated Experiment Sample
- 20 Unrelated Experiment Sample

Turret 6 13 Mar 00

Bead Name

- 1 Unrelated Experiment Sample
- 2 Unrelated Experiment Sample
- 3 Unrelated Experiment Sample
- 4 Unrelated Experiment Sample

- 5 Unrelated Experiment Sample
- 6 Unrelated Experiment Sample
- 7 Unrelated Experiment Sample
- 8 Unrelated Experiment Sample
- 9 S4P-2
- 10 S8P-2
- 11 S24P-2
- 12 S95P-2
- 13 S4P-3
- 14 Unrelated Experiment Sample
- 15 Unrelated Experiment Sample
- 16 Unrelated Experiment Sample
- 17 Unrelated Experiment Sample
- 18 Unrelated Experiment Sample
- 19 Unrelated Experiment Sample
- 20 Unrelated Experiment Sample

Appendix 4, Annex E

TIMS Results of AO

E-1 Raw Database

E-2 Chart of Isotopic Ratios for AO as a function of time

E-3 Chart of Isotopic Ratios for AO as a function of temperature

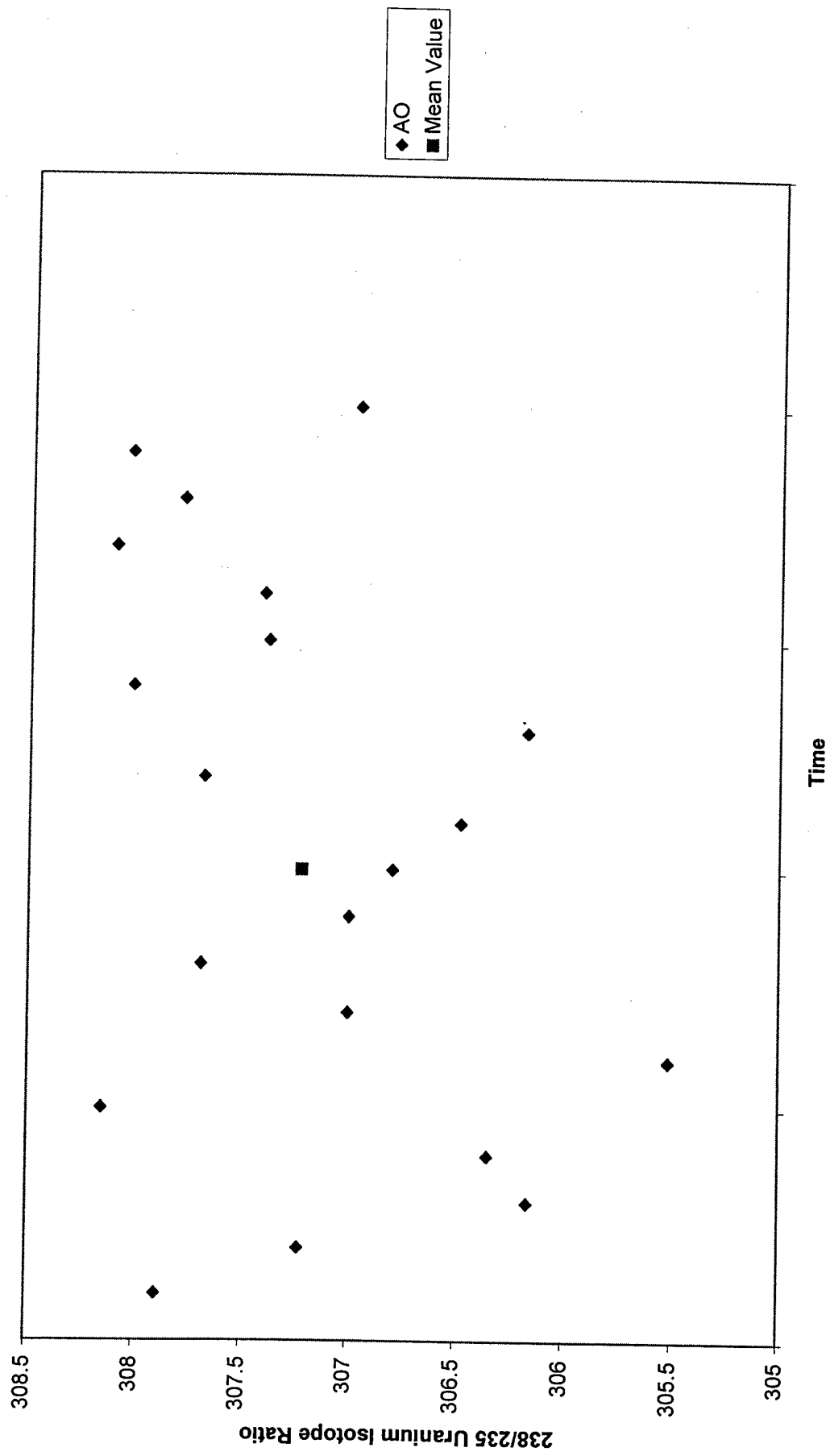
Appendix 4, Annex E-1

DTG 8/6/99 23:34

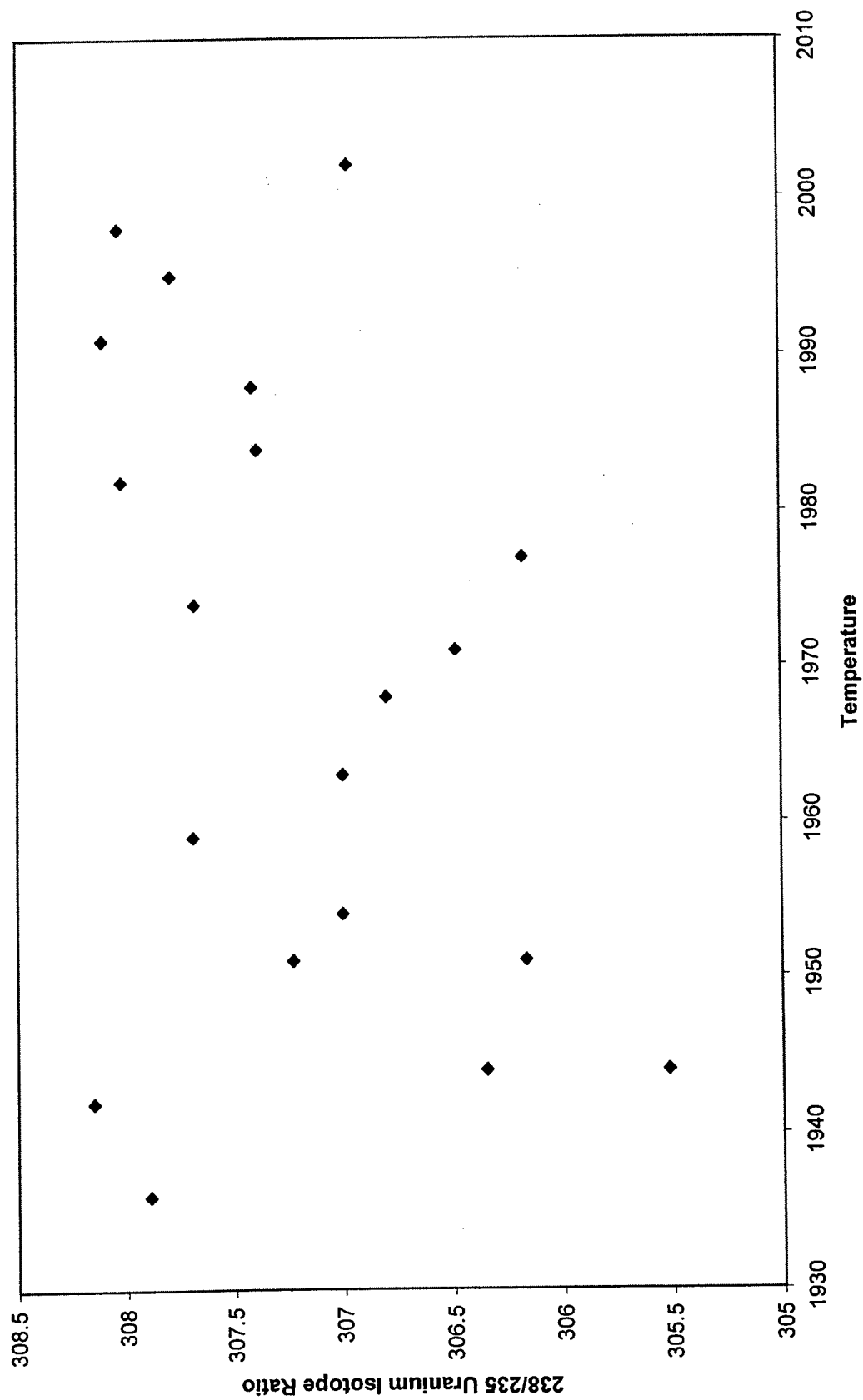
Bead: AO Liquid

Block	Amps	Temp	238 Intensity x10 ⁻¹² Amps	238/235	Std Error
1	4.365	1936	13	307.8946915	0.000848
2	4.425	1951	12	307.2289426	0.001215
3	4.425	1951	14	306.1648453	0.001201
4	4.425	1944	13	306.349651	0.000951
5	4.425	1942	12	308.1522157	0.001324
6	4.441	1944	11	305.515599	0.000768
7	4.487	1954	13	307.0044291	0.000550
8	4.508	1959	13	307.6943259	0.000806
9	4.521	1963	13	307.0027791	0.001515
10	4.537	1968	13	306.8023630	0.001034
11	4.547	1971	13	306.4843031	0.000937
12	4.561	1974	13	307.6876491	0.000801
13	4.572	1977	13	306.1741664	0.001213
14	4.585	1982	13	308.021916	0.001155
15	4.597	1984	13	307.393505	0.000931
16	4.613	1988	13	307.4171204	0.000749
17	4.625	1991	13	308.1089282	0.000949
18	4.638	1995	13	307.7959314	0.000924
19	4.646	1998	13	308.0395277	0.001187
20	4.658	2002	13	306.9769873	0.000066
Grand Mean				307.2272308	0.000267
			Mean	307.1954938	
			Std dev	0.760869347	

AO Turret
Isotopic Ratios as a Function of Consecutive Block Measurements



AO Turret
Isotopic Ratios as a Function of Filament Temperature



Appendix 4, Annex F

TIMS Results of Turret One

F-1 Raw Database

F-2 Charts

- 1 Chart of Isotopic Ratios for Supernatants of Control Samples
- 2 Chart of Isotopic Ratios Comparing Load Size
- 3 Chart of Isotopic Ratios for Bead One
- 4 Chart of Isotopic Ratios for Bead Two
- 5 Chart of Isotopic Ratios for Bead Three
- 6 Chart of Isotopic Ratios for Bead Four
- 7 Chart of Isotopic Ratios for Bead Five
- 8 Chart of Isotopic Ratios for Bead Six
- 9 Chart of Isotopic Ratios for Bead Nine A and B
- 10 Chart of Isotopic Ratios for Bead Nine Z
- 11 Chart of Isotopic Ratios for Bead Ten A and B
- 12 Chart of Isotopic Ratios for Bead Ten Z

Appendix 4, Annex F-1

U500 Standard Data		Mean	Standard Deviation	
Atom Percent	U238	49.711	0.05	
	U235	49.696	0.05	
	238/235	1.0003	0.0014	
		1.0003	0.0014	
DTG	2/15/00 15:44			
Bead: 1	U500 1ug 0.1 M H3PO4, 1ug Graphite. 1ug sample			
	238 Intensity			
	Temp	Amps	Std Error	Notes
Block	1	4.67	1.0014754	0.000024
	2	4.67	1.0018324	0.000026
	3	4.67	1.0024282	0.000021
	4	4.67	1.0028847	0.000038
	5	4.67	1.0029742	0.000016
	6	4.75	1.0036058	0.000036
	7	4.75	1.0042802	0.000050
	8	4.9	1.0056224	0.000056
	9	4.9	1.0076701	0.000064
	10	4.9	1.0083496	0.000024
Grand Mean			1.0041142	0.000225
	238 Intensity			
	Temp	Amps	Std Error	Notes
Block	1	4.67	0.9995538	0.000045
	2	4.67	0.9995982	0.000047
	3	4.75	1.0001144	0.000043
	4	4.75	1.0013944	0.000085
	5	4.9	1.0059420	0.000123
	6	4.9	1.0072561	0.000046
	7	4.9	1.0078927	0.000050
	8	4.9	1.0050436	0.000081
	9	5.1	1.0038564	0.000111
	10	5.1	1.0046866	0.000163
Grand Mean			1.0035417	0.000302

DTG 2/15/00 16:31 U500 1ug sample, 1ug Graphite
 Bead: 2 238 Intensity

Appendix 4, Annex F-1

DTG 2/15/00 17:14

Bead: 3A U500 1ug sample, 1ug Graphite

238 Intensity					238 Intensity				
Block	Amps	Temp	x10 ⁻¹² Amps	238/235	Std Error	Notes	Block	Amps	Temp
1	4.24	1952	4.9	0.9983398	0.000028		11	4.67	2030
2	4.24	1955	4.2	0.9989897	0.000039		12	4.74	2030
3	4.34	1982	3.6	0.9998665	0.000074		13	4.8	2030
4	4.34	1985	4.6	1.0002539	0.000040		14	4.8	2030
5	4.44	2011	3.4	1.0006404	0.000033		15	4.8	2030
6	4.5	2028	3.9	1.0003293	0.000053		16	4.8	2030
7	4.59	2030	3.8	1.0000273	0.000040		17	5.1	2030
8	4.59	2030	4.4	0.9999683	0.000041		Grand Mean		
9	4.67	2030	4.0	1.0004076	0.000019				
10	4.67	2030	4.6	1.0005891	0.000022				
Grand Mean					1.0001110	0.000051			

DTG 2/16/00 22:23

Bead: 3B U500 1ug sample, 1ug Graphite

238 Intensity					238 Intensity				
Block	Amps	Temp	x10 ⁻¹² Amps	238/235	Std Error	Notes	Block	Amps	Temp
11	4.67	2030	4.2	1.0039950	0.000046				
12	4.74	2030	3.7	1.0050950	0.000057				
13	4.8	2030	4.0	1.0069539	0.000024				
14	4.8	2030	4.4	1.0074936	0.000044				
15	4.8	2030	4.4	1.0075019	0.000040				
16	4.8	2030	4.5	1.0076786	0.000055				
17	5.1	2030	2.8	1.0046427	0.000085				
Grand Mean					1.0062172	0.000173			

DTG 2/15/00 18:20

Bead: 4A U500 1ug sample, 3ug Graphite

238 Intensity					238 Intensity				
Block	Amps	Temp	x10 ⁻¹² Amps	238/235	Std Error	Notes	Block	Amps	Temp
1	4.32	1933	4.7	0.9980246	0.000067		11	4.71	2030
2	4.37	1947	4.0	0.9986213	0.000033		12	4.71	2030
3	4.44	1966	3.9	0.9991732	0.000043		13	4.71	2030
4	4.44	1968	4.2	0.9993216	0.000034		14	4.77	2030
5	4.55	1994	3.6	0.9995308	0.000024		15	4.85	2030
6	4.55	1997	4.6	0.9998263	0.000039		16	4.96	2030
7	4.62	2015	3.8	0.9996885	0.000027		17	4.96	2030
8	4.62	2017	4.3	0.9995235	0.000031		18	5.09	2030
9	4.62	2020	4.0	0.9996211	0.000037		19	5.09	2030
10	4.69	2030	3.9	0.9996862	0.000048		20	5.09	2030
Grand Mean					0.9994307	0.000041	Grand Mean		

DTG 2/15/00 18:48

Bead: 4B U500 1ug sample, 3ug Graphite

238 Intensity					238 Intensity				
Block	Amps	Temp	x10 ⁻¹² Amps	238/235	Std Error	Notes	Block	Amps	Temp
11	4.71	2030	5.0	0.9998200	0.000027				
12	4.71	2030	4.7	0.9998044	0.000017				
13	4.71	2030	4.1	1.0001727	0.000024				
14	4.77	2030	3.7	1.0002493	0.000021				
15	4.85	2030	3.6	1.0006450	0.000034				
16	4.96	2030	3.6	1.0012306	0.000052				
17	4.96	2030	3.6	1.0031423	0.000070				
18	5.09	2030	2.9	1.0044903	0.000058				
19	5.09	2030	4.3	1.0057535	0.000030				
20	5.09	2030	4.3	1.0062167	0.000042				
Grand Mean					1.0021430	0.000241			

Appendix 4, Annex F-1

DTG		2/15/00 21:07		DTG		2/15/00 21:34	
Bead: 6A		U500 1ug 0.1 M H3PO4, 1ug Graphite. 3ug sample		Bead: 6B		U500 1ug 0.1 M H3PO4, 1ug Graphite. 3ug sample	
		238 Intensity				238 Intensity	
Block	Amps	Temp	x10 ⁻¹² Amps	Notes	Block	Amps	Temp
1	4.3	1986	5.1	Std Error 0.000031	11	4.49	2030
2	4.3	1988	4.9	0.9958543 0.000035	12	4.49	2030
3	4.3	1991	5.1	0.9960446 0.000022	13	4.49	2030
4	4.3	1992	5.0	0.9963261 0.000042	14	4.49	2030
5	4.3	1994	5.0	0.9964603 0.000019	15	4.49	2030
6	4.3	1995	5.0	0.9966538 0.000046	16	4.49	2030
7	4.3	1997	4.9	0.9969149 0.000037	17	4.49	2030
8	4.3	1998	4.9	0.9970054 0.000044	18	4.49	2030
9	4.3	1999	4.8	0.9972731 0.000037	19	4.49	2030
10	4.3	2000	4.8	0.9974742 0.000040	20	4.49	2030
Grand Mean				0.9976276 0.000058	Grand Mean		
				0.9967648 0.000058			
					238/235		
					0.9981593 0.000019		
					0.9983963 0.000017		
					0.9988328 0.000019		
					0.9990613 0.000034		
					0.9993246 0.000032		
					0.9994603 0.000040		
					0.9997326 0.000016		
					0.9999281 0.000018		
					1.0000759 0.000016		
					1.0002638 0.000019		
					0.9993223 0.000068		

DTG		2/15/00 22:02		DTG		2/15/00 22:45	
Bead: 6C		U500 1ug 0.1 M H3PO4, 1ug Graphite. 3ug sample		Bead: 10A		U500 3ug sample, 3ug Graphite	
		238 Intensity				238 Intensity	
Block	Amps	Temp	x10 ⁻¹² Amps	Notes	Block	Amps	Temp
21	4.62	2030	10.0	Std Error 0.000022	1	4.37	1955
22	4.62	2030	8.8	1.0002540 0.000070	2	4.37	1957
23	4.62	2030	4.0	1.0011367 0.000429	3	4.37	1959
24	4.62	2030	8.3	1.0026532 0.000176	4	4.44	1975
25	4.73	2030	2.9	1.0018449 0.000181	5	4.44	1976
26	4.73	2030	10.0	1.0020367 0.000099	6	4.44	1976
27	4.73	2030	10.0	1.0030255 0.000068	7	4.53	1996
28	4.73	2030	7.9	1.0033618 0.000073	8	4.53	1999
29	4.73	2030	5.1	1.0039291 0.000391	9	4.53	2000
30	4.91	2030	2.3	1.0157267 0.000393	10	4.53	2002
Grand Mean				1.0084611 0.000393	Grand Mean		
				1.0030988 0.000258			
					238/235		
					0.9980221 0.000031		
					0.9985254 0.000061		
					0.9989591 0.000037		
					0.9993859 0.000032		
					0.9996946 0.000046		
					0.9998834 0.000024		
					1.0002312 0.000054		
					1.0004716 0.000034		
					1.0007248 0.000032		
					1.0007774 0.000033		
					0.9996913 0.000088		

Appendix 4, Annex F-1

DTG 2/15/00 23:15

Bead: 10B U500 3ug sample, 3ug Graphite

238 Intensity					238 Intensity				
Block	Amps	Temp	x10 ⁻¹² Amps	238/235	Std Error	Notes	Block	Amps	Temp
11	4.74	2030	7.2	1.0010532	0.000025		1	4.3	1897
12	4.74	2030	6.5	1.0011561	0.000027		2	4.3	1898
13	4.74	2030	6.1	1.0020684	0.000069		3	4.3	1900
14	4.74	2030	5.8	1.0024856	0.000083		4	4.3	1901
15	4.74	2030	5.5	1.0017712	0.000036		5	4.3	1902
16	4.74	2030	5.3	1.0020099	0.000053		6	4.3	1903
17	4.74	2030	5.1	1.0022112	0.000041		7	4.3	1903
18	4.74	2030	5.0	1.0022866	0.000037		8	4.3	1904
19	4.74	2030	4.8	1.0026038	0.000049		9	4.3	1905
20	4.74	2030	4.7	1.0026752	0.000019		10	4.3	1906
Grand Mean				1.0020285	0.000055		Grand Mean		

DTG 2/15/00 23:54

Bead: 9A U500 3ug sample, 3ug Graphite

238 Intensity					238 Intensity				
Block	Amps	Temp	x10 ⁻¹² Amps	238/235	Std Error	Notes	Block	Amps	Temp
1	4.3	1897	6.1	0.9958752	0.000051		1	4.3	1897
2	4.3	1898	5.8	0.9963296	0.000026		2	4.3	1898
3	4.3	1900	5.8	0.9966995	0.000022		3	4.3	1900
4	4.3	1901	5.5	0.9970195	0.000025		4	4.3	1901
5	4.3	1902	5.3	0.9972799	0.000036		5	4.3	1902
6	4.3	1903	5.1	0.9975100	0.000026		6	4.3	1903
7	4.3	1903	4.9	0.9976830	0.000027		7	4.3	1903
8	4.3	1904	4.8	0.9979478	0.000036		8	4.3	1904
9	4.3	1905	4.7	0.9980727	0.000037		9	4.3	1905
10	4.3	1906	4.5	0.9981914	0.000055		10	4.3	1906
Grand Mean				0.9972928	0.000073		Grand Mean		

DTG 2/16/00 0:21

Bead: 9B U500 3ug sample, 3ug Graphite

238 Intensity					238 Intensity				
Block	Amps	Temp	x10 ⁻¹² Amps	238/235	Std Error	Notes	Block	Amps	Temp
11	4.34	1915	5.1	0.9984455	0.000015		1	4.225	2030
12	4.34	1916	4.9	0.9985223	0.000043		2	4.288	2030
13	4.34	1917	4.8	0.9986307	0.000018		3	4.394	2030
14	4.34	1918	4.6	0.9987310	0.000038		4	4.54	2030
15	4.34	1919	4.4	0.9988916	0.000041		5	4.52	2030
16	4.34	1919	4.2	0.9988751	0.000036		Grand Mean		
17	4.34	1920	4.1	0.9989818	0.000053				
18	4.34	1920	3.9	0.9989612	0.000037				
19	4.34	1921	3.8	0.9991232	0.000060				
20	4.34	1922	3.7	0.9990014	0.000047				
Grand Mean				0.9988169	0.000024				

DTG 2/16/00 1:10

Bead: 5 U500 1ug sample, 3ug Graphite

238 Intensity					238 Intensity				
Block	Amps	Temp	x10 ⁻¹² Amps	238/235	Std Error	Notes	Block	Amps	Temp
1	4.225	2030	3.9	1.0011902	0.000071		1	4.225	2030
2	4.288	2030	3.3	1.0030880	0.000071		2	4.288	2030
3	4.394	2030	3.2	1.0057448	0.000069		3	4.394	2030
4	4.54	2030	3.6	1.0074472	0.000090		4	4.54	2030
5	4.52	2030	3.6	1.0104298	0.000071		5	4.52	2030
Grand Mean				1.0055800	0.000462		Grand Mean		

Appendix 4, Annex F-1

DTG 2/16/00 1:45

Bead: 9X U500 3ug sample, 3ug Graphite
238 Intensity

Block	Amps	Temp	238/235	Std Error	Notes
1	4.402	1999	0.9996137	0.000017	
2	4.424	2005	0.9996999	0.000043	
3	4.433	2010	0.9997137	0.000037	
4	4.449	2015	0.9996612	0.000020	
5	4.468	2021	0.9997579	0.000035	
6	4.483	2027	0.9997906	0.000037	
7	4.501	2030	0.9998242	0.000030	
8	4.518	2030	0.9998369	0.000040	
9	4.456	1974	0.9990647	0.000038	
10	4.456	1973	0.9992576	0.000032	
Grand Mean			0.9996563	0.000023	

DTG 2/16/00 2:11

Bead: 9Y U500 3ug sample, 3ug Graphite
238 Intensity

Block	Amps	Temp	238/235	Std Error	Notes
11	4.456	1973	0.9993029	0.000034	
12	4.456	1973	0.9992870	0.000027	
13	4.456	1972	0.9994338	0.000029	
14	4.465	1975	0.9994078	0.000036	
15	4.474	1976	0.9994381	0.000049	
16	4.481	1977	0.9995891	0.000040	
17	4.49	1980	0.9995759	0.000028	
18	4.495	1982	0.9997250	0.000027	
19	4.504	1983	0.9996268	0.000036	
20	4.51	1985	0.9997616	0.000036	
Grand Mean			0.9995031	0.000018	

DTG 2/16/00 2:36

Bead: 9Z U500 3ug sample, 3ug Graphite
238 Intensity

Block	Amps	Temp	238/235	Std Error	Notes
21	4.516	1987	0.9998443	0.000041	
22	4.523	1988	0.9998600	0.000030	
23	4.529	1990	0.9999215	0.000034	
24	4.534	1992	0.9999397	0.000027	
25	4.540	1994	1.0000705	0.000044	
26	4.546	1996	1.0000618	0.000030	
27	4.554	1998	1.0001576	0.000041	
28	4.559	2000	1.0001444	0.000032	
29	4.567	2002	1.0001834	0.000029	
30	4.572	2004	1.0002165	0.000037	
Grand Mean			1.0000487	0.000016	

DTG 2/16/00 3:15

Bead: 10Z

Block	Amps	Temp	238/235	Std Error	Notes
1	4.249	2019	0.9998362	0.000040	
2	4.249	2030	1.0006140	0.000062	
3	4.300	2030	1.0024747	0.000294	
4	4.615	2030	1.0094765	0.000077	
Grand Mean			1.0031222	0.000618	

DTG 2/16/00 12:41
Bead: C0s A 1ul sample

238 Intensity					238 Intensity				
Block	Amps	Temp	x10 ⁻¹² Amps	Notes	Block	Amps	Temp	x10 ⁻¹² Amps	Notes
1	4.3	1950	4.6	0.9960357	0.000031	1	4.37	1976	0.9983544
2	4.3	1951	4.5	0.9963483	0.000040	2	4.37	1977	0.9985170
3	4.3	1953	4.6	0.9966350	0.000025	3	4.37	1979	0.9986261
4	4.3	1954	4.5	0.9968050	0.000034	4	4.37	1979	0.9987649
5	4.3	1954	4.5	0.9971045	0.000026	5	4.37	1982	0.9989107
6	4.3	1955	4.4	0.9972016	0.000027	6	4.37	1983	0.9989620
7	4.3	1956	4.3	0.9974797	0.000041	7	4.37	1984	0.9991223
8	4.3	1957	4.3	0.9975719	0.000018	8	4.37	1985	0.9991911
9	4.3	1958	4.3	0.9977715	0.000022	9	4.37	1985	0.9994335
10	4.3	1959	4.2	0.9979632	0.000051	10	4.37	1986	0.9994400
Grand Mean				0.9970946	0.000061	Grand Mean			0.9989365

DTG 2/16/00 13:37
Bead: C0s C 1ul sample

238 Intensity							238 Intensity						
Block	Amps	Temp	x10 ⁻¹² Amps	238/235	Std Error	Notes	Block	Amps	Temp	x10 ⁻¹² Amps	238/235	Std Error	Notes
1	4.4	1995	5.1	0.9997048	0.000026		1	4.3	1937	5.3	0.9957768	0.000029	
2	4.4	1996	5.0	0.9998680	0.000045		2	4.3	1938	5.1	0.9960958	0.000032	
3	4.4	1997	4.8	0.9998383	0.000027		3	4.3	1939	5.2	0.9964030	0.000037	
4	4.4	1999	4.7	1.0000415	0.000036		4	4.3	1940	5.1	0.9965662	0.000048	
5	4.4	2000	4.6	0.9999579	0.000031		5	4.3	1941	5.1	0.9967906	0.000027	
6	4.4	2001	4.5	1.0001183	0.000037		6	4.3	1941	5.1	0.9968852	0.000044	
7	4.4	2003	4.4	1.0002698	0.000023		7	4.3	1942	5.0	0.9970879	0.000034	
8	4.4	2004	4.3	1.0002996	0.000033		8	4.3	1943	5.0	0.9972258	0.000035	
9	4.4	2006	4.1	1.0003186	0.000037		9	4.3	1944	5.0	0.9973650	0.000041	
10	4.4	2007	4.0	1.0002449	0.000032		10	4.3	1945	4.9	0.9974924	0.000035	
Grand Mean				1.0000755	0.000023		Grand Mean				0.9967777	0.000054	

Appendix 4, Annex F-1

DTG 2/16/00 14:49
Bead: C4s B 1ul sample

Block	Amps	Temp	238 Intensity x10 ⁻¹² Amps	238/235	Std Error	Notes
1	4.37	1962	6.5	0.9977969	0.000025	
2	4.37	1961	6.4	0.9979093	0.000023	
3	4.37	1963	6.4	0.9980012	0.000021	
4	4.37	1964	6.4	0.9981869	0.000027	
5	4.37	1965	6.2	0.9982861	0.000029	
6	4.37	1966	6.1	0.9983721	0.000016	
7	4.37	1967	6.1	0.9984764	0.000026	
8	4.37	1967	6.1	0.9985143	0.000026	
9	4.37	1968	6.0	0.9986370	0.000024	
10	4.37	1969	6.0	0.9987914	0.000030	
Grand Mean				0.9982922	0.000031	

DTG 2/16/00 15:23
Bead: C4s C 1ul sample

Block	Amps	Temp	238 Intensity x10 ⁻¹² Amps	238/235	Std Error	Notes
1	4.44	1988	7.5	0.9993205	0.000012	
2	4.44	1989	7.4	0.9994170	0.000035	
3	4.44	1990	7.3	0.9995680	0.000018	
4	4.44	1992	7.1	0.9997146	0.000024	
5	4.44	1993	7.0	0.9999105	0.000020	
6	4.44	1994	6.9	0.9999620	0.000027	
7	4.44	1995	6.7	1.0001860	0.000035	
8	4.44	1996	6.6	1.0002845	0.000014	
9	4.44	1996	6.5	1.0004774	0.000030	
10	4.44	1998	6.2	1.0005908	0.000039	
Grand Mean				0.9999447	0.000043	

DTG 2/16/00 16:05
Bead: C8s A 1ul sample

Block	Amps	Temp	238 Intensity x10 ⁻¹² Amps	238/235	Std Error	Notes
1	4.3	1958	4.5	0.9961779	0.000031	
2	4.3	1960	4.4	0.9964683	0.000027	
3	4.3	1962	4.5	0.9966761	0.000019	
4	4.3	1963	4.5	0.9969991	0.000015	
5	4.3	1964	4.5	0.9972332	0.000035	
6	4.3	1965	4.4	0.9975124	0.000024	
7	4.3	1965	4.4	0.9976007	0.000017	
8	4.3	1966	4.3	0.9978111	0.000048	
9	4.3	1967	4.4	0.9980854	0.000029	
10	4.3	1968	4.3	0.9981249	0.000046	
Grand Mean				0.9972661	0.000065	

DTG 2/16/00 16:33
Bead: C8s B 1ul sample

Block	Amps	Temp	238 Intensity x10 ⁻¹² Amps	238/235	Std Error	Notes
1	4.37	1985	5.7	0.9985337	0.000024	
2	4.37	1985	5.6	0.9987143	0.000027	
3	4.37	1986	5.4	0.9988866	0.000048	
4	4.37	1987	5.3	0.9990035	0.000034	
5	4.37	1988	5.1	0.9992166	0.000032	
6	4.37	1989	5.0	0.9992787	0.000032	
7	4.37	1990	4.9	1.0003701	0.000024	
8	4.37	1991	4.8	0.9995752	0.000047	
9	4.37	1992	4.7	0.9997503	0.000037	
10	4.37	1993	4.6	0.9998850	0.000018	
Grand Mean				0.9993000	0.000054	

Appendix 4, Annex F-1

DTG 2/16/00 17:02
Bead: C8s C 1ul sample

Block	Amps	Temp	238 Intensity x10 ⁻¹² Amps
1	4.44	2011	5.9
2	4.44	2012	5.6
3	4.44	2014	5.3
4	4.44	2015	5.1
5	4.44	2016	4.9
6	4.44	2017	4.8
7	4.44	2019	4.6
8	4.44	2020	4.6
9	4.44	2022	4.4
10	4.44	2024	4.3
Grand Mean			

DTG 2/16/00 17:50
Bead: C95s A 1ul sample

Block	Amps	Temp	238 Intensity x10 ⁻¹² Amps	Std Error	Notes	238/235	Std Error	Notes
1	4.3	1957	3.8	0.000029		1.0001830	0.000029	
2	4.3	1961	3.8	0.000029		1.0002480	0.000029	
3	4.3	1963	3.8	0.000029		1.0002864	0.000029	
4	4.3	1965	3.7	0.000029		1.0003688	0.000029	
5	4.3	1967	3.6	0.000034		1.0004687	0.000034	
6	4.3	1968	3.5	0.000045		1.0006803	0.000045	
7	4.3	1970	3.4	0.000018		1.0007802	0.000018	
8	4.3	1971	3.3	0.000036		1.0008170	0.000036	
9	4.3	1972	3.2	0.000022		1.0011158	0.000022	
10	4.3	1973	3.2	0.000039		1.0011178	0.000039	
Grand Mean				0.000035		1.0006151	0.000035	

DTG 2/16/00 18:18
Bead: C95s B 1ul sample

Block	Amps	Temp	238 Intensity x10 ⁻¹² Amps
1	4.37	1990	4.1
2	4.37	1991	4.0
3	4.37	1993	3.7
4	4.37	1994	3.5
5	4.37	1995	3.4
6	4.37	1995	3.3
7	4.37	1998	3.2
8	4.37	1998	3.1
9	4.37	1999	3.0
10	4.37	2000	2.9
Grand Mean			

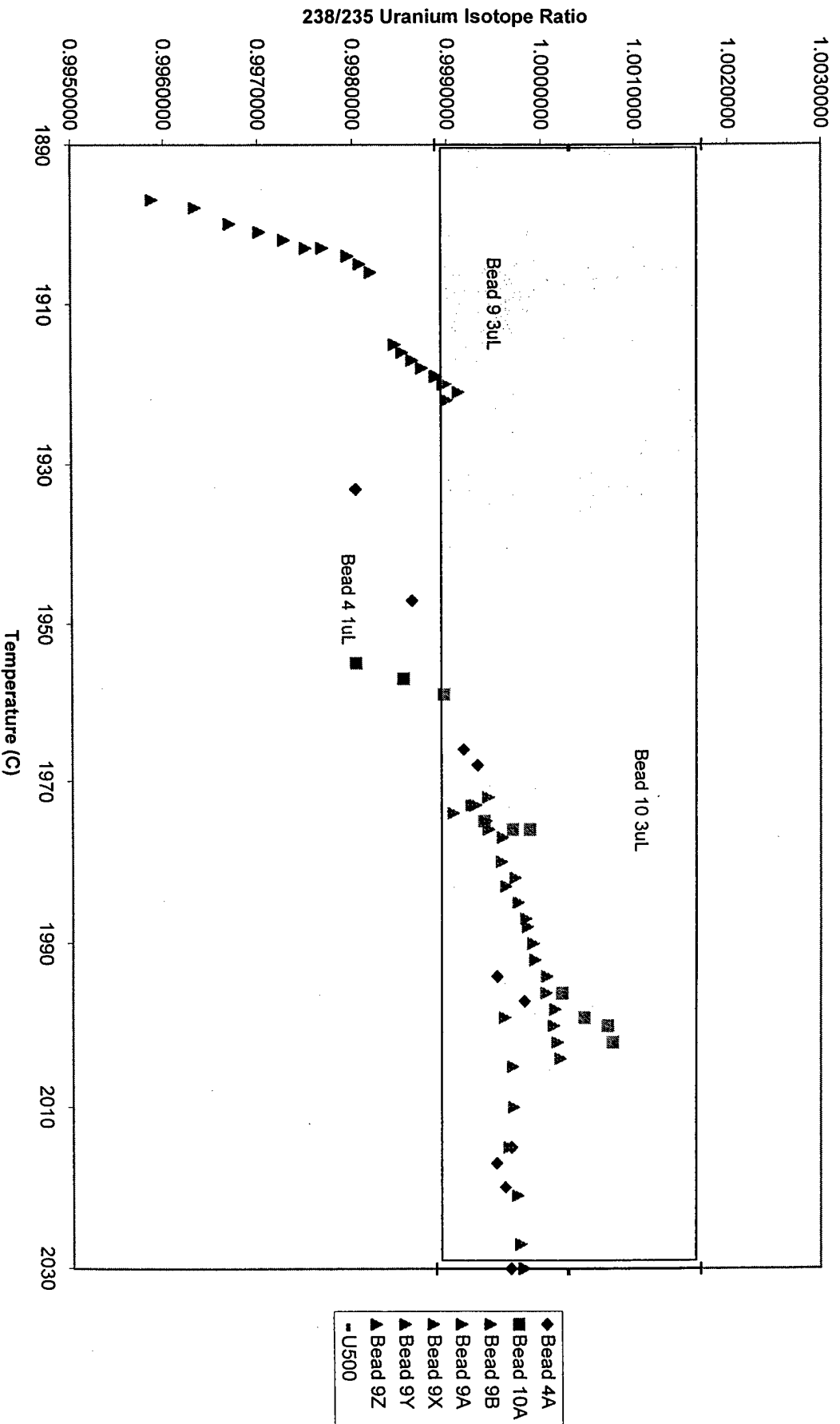
DTG 2/16/00 2:36
Bead: C95s C 1ul sample

Block	Amps	Temp	238 Intensity x10 ⁻¹² Amps	Std Error	Notes	238/235	Std Error	Notes
1	4.4	2010	3.2	0.000041		0.9988234	0.000041	
2	4.4	2011	3.1	0.000048		0.9989504	0.000048	
3	4.4	2012	3.1	0.000028		0.9988088	0.000028	
4	4.4	2013	3.0	0.000038		0.9988550	0.000038	
5	4.4	2015	2.9	0.000049		0.9990661	0.000049	
6	4.4	2016	2.8	0.000037		0.9990791	0.000037	
7	4.4	2018	2.8	0.000042		0.9992328	0.000042	
8	4.4	2018	2.7	0.000049		0.9991377	0.000049	
9	4.4	2019	2.6	0.000038		0.9993621	0.000038	
10	4.4	2020	2.5	0.000044		0.9993049	0.000044	
Grand Mean				0.000023		0.9990575	0.000023	

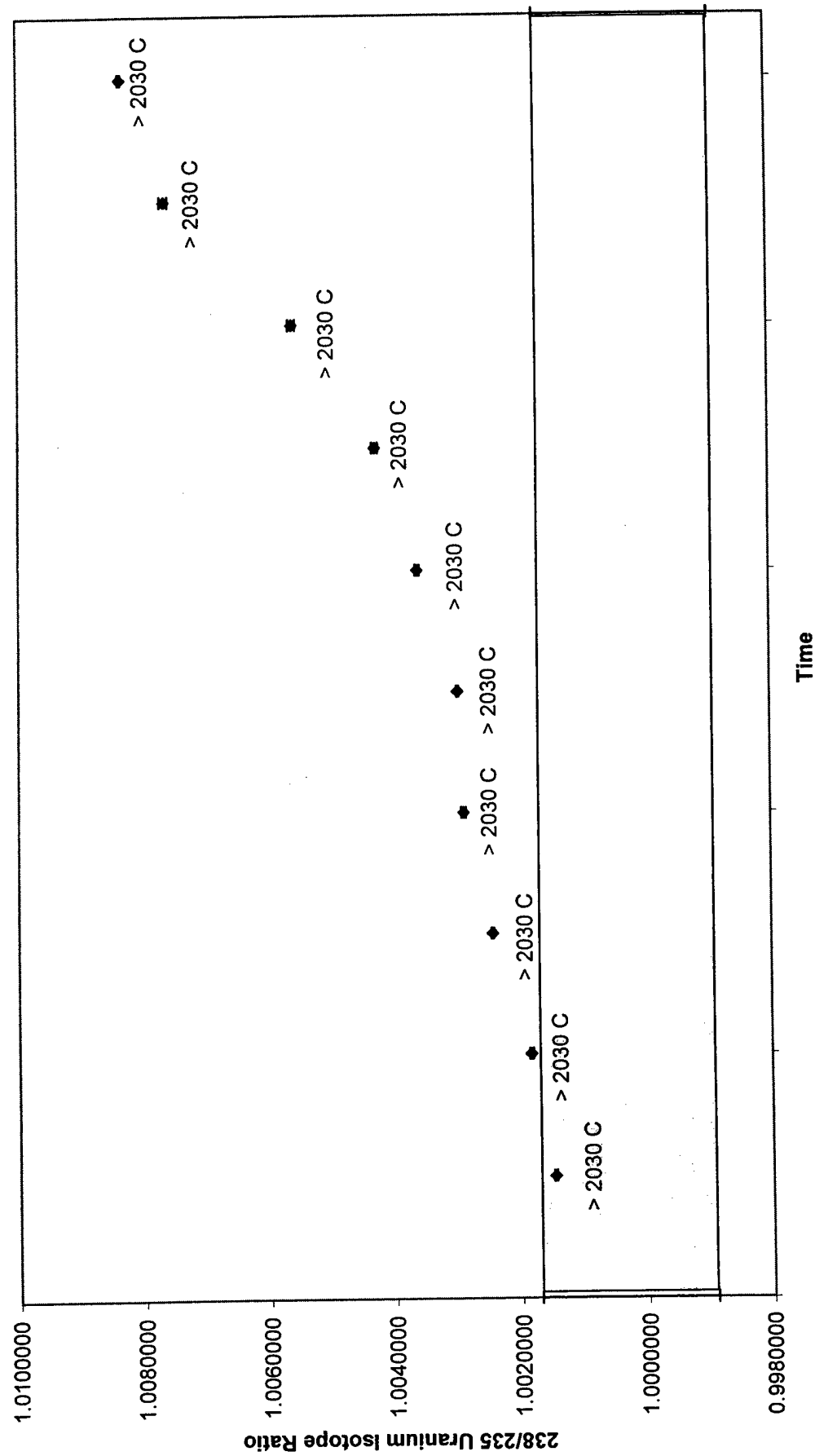
Turret One
Control Supernatant Samples



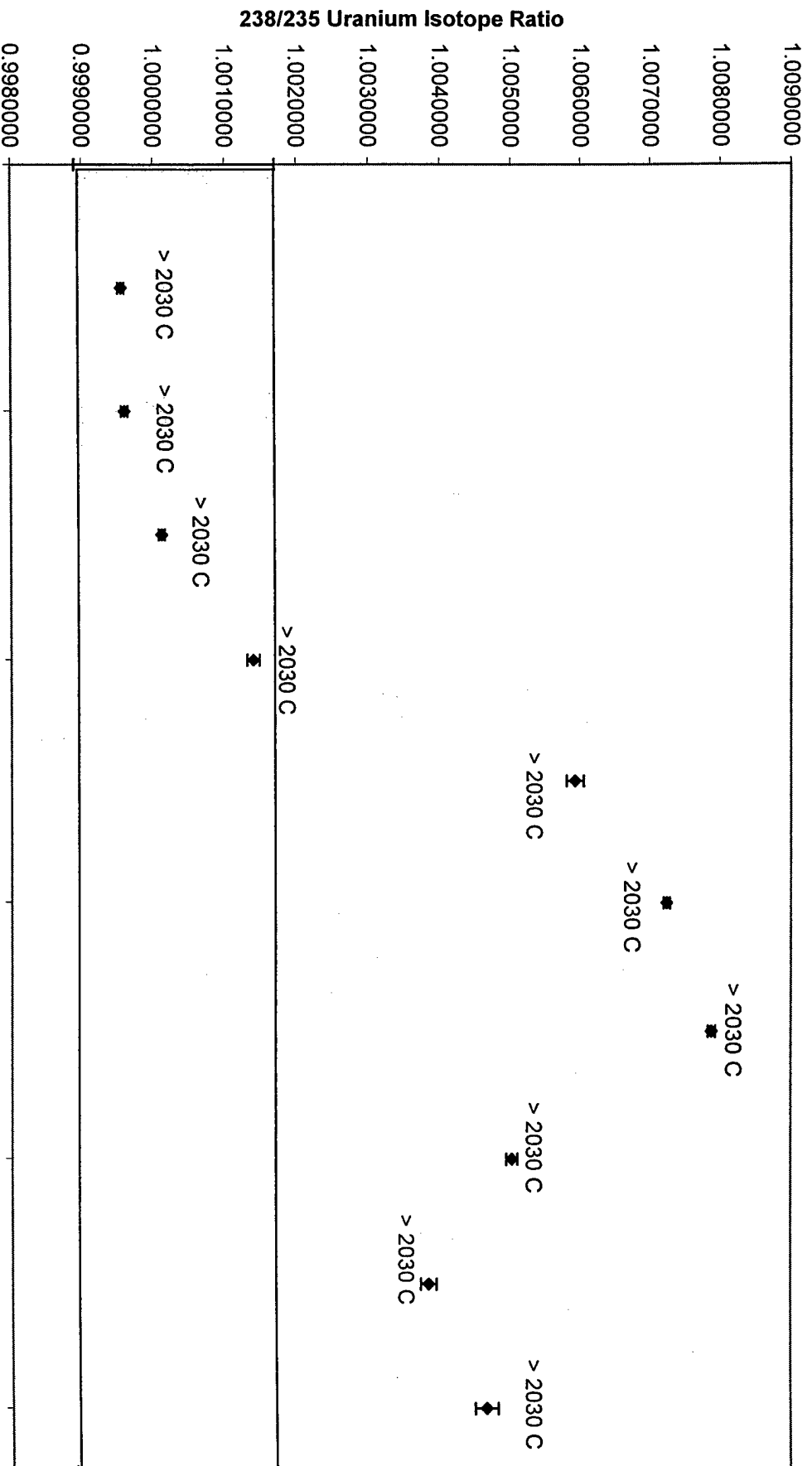
Comparison of Load Sample Size on Mass Fractionation 1uL versus 3uL with 3uL Graphite



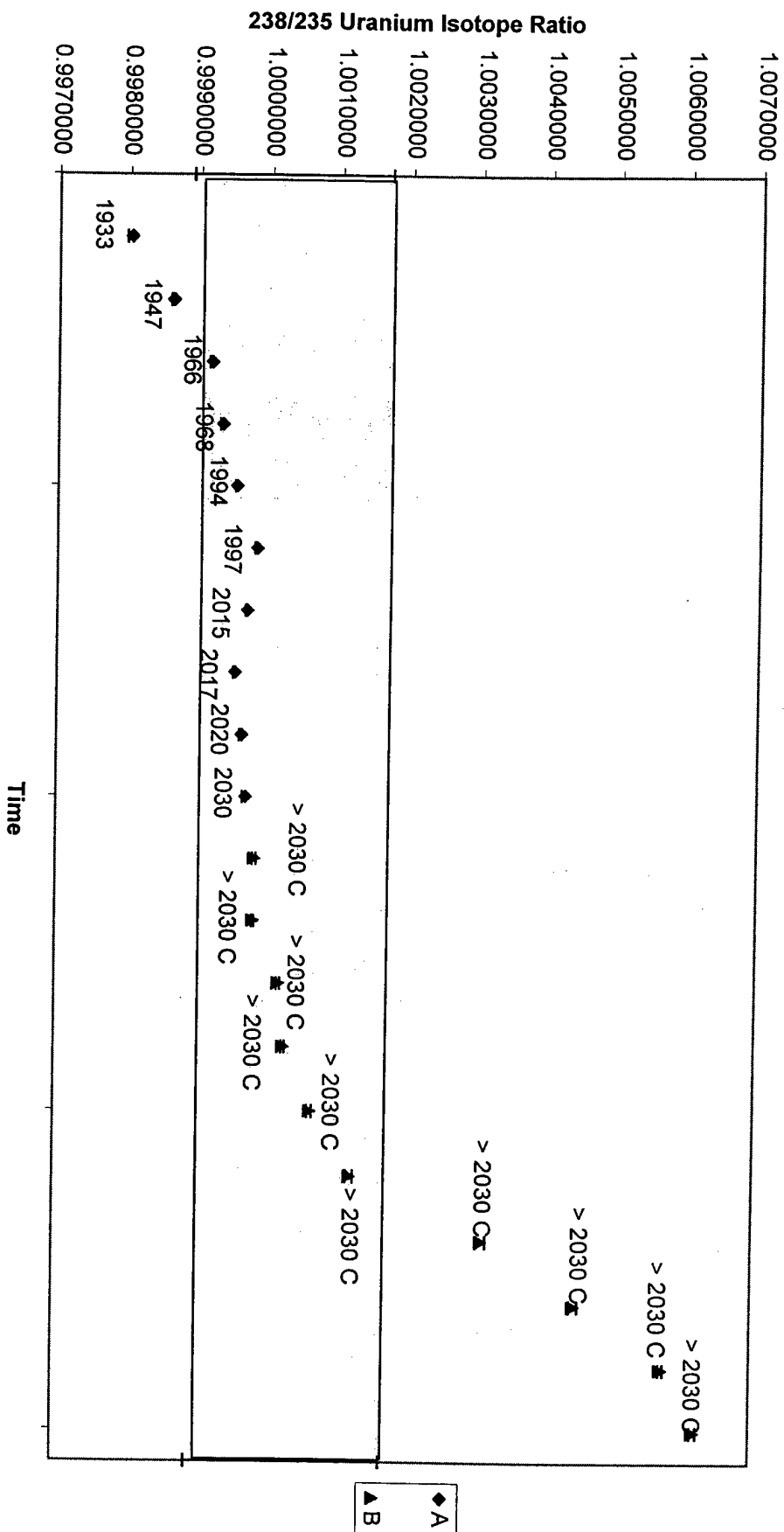
Turret One
Bead One
1 uL U500, 0.1 M H₃PO₄, 1 uL Graphite



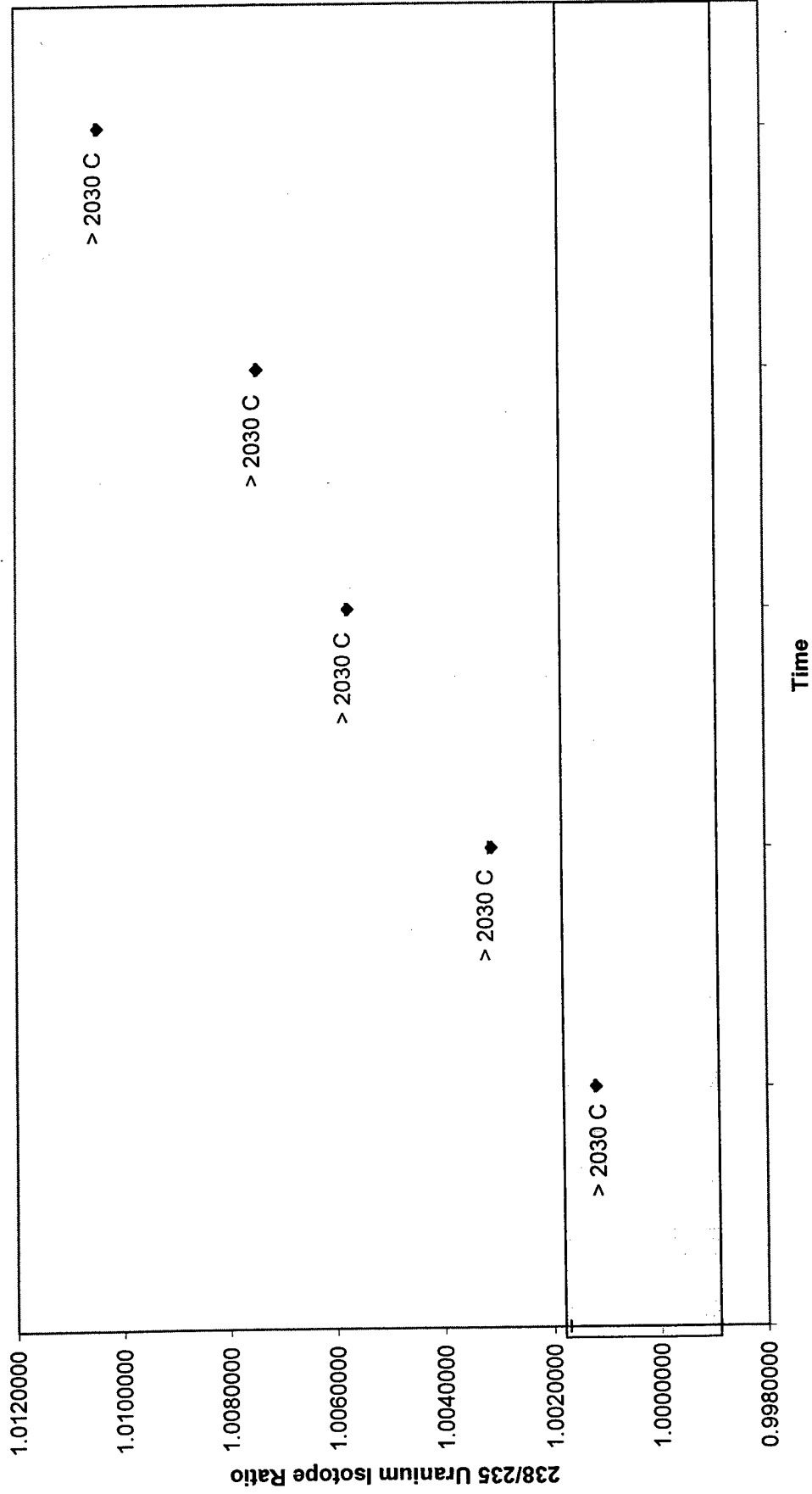
Turret One
Bead Two
1 uL U500, 1uL Graphite

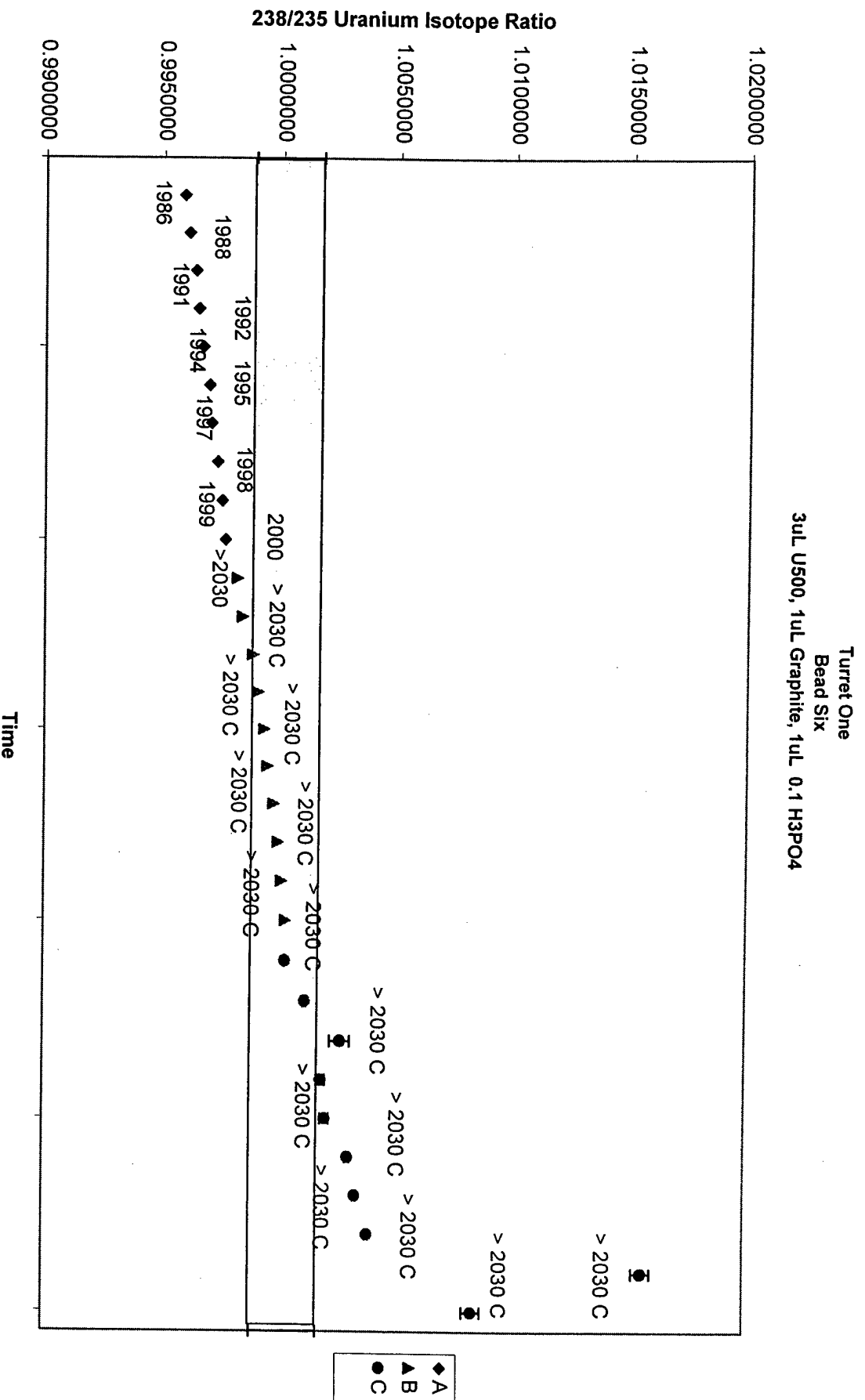


Turret One
Bead Four
1 uL U500, 3 uL Graphite

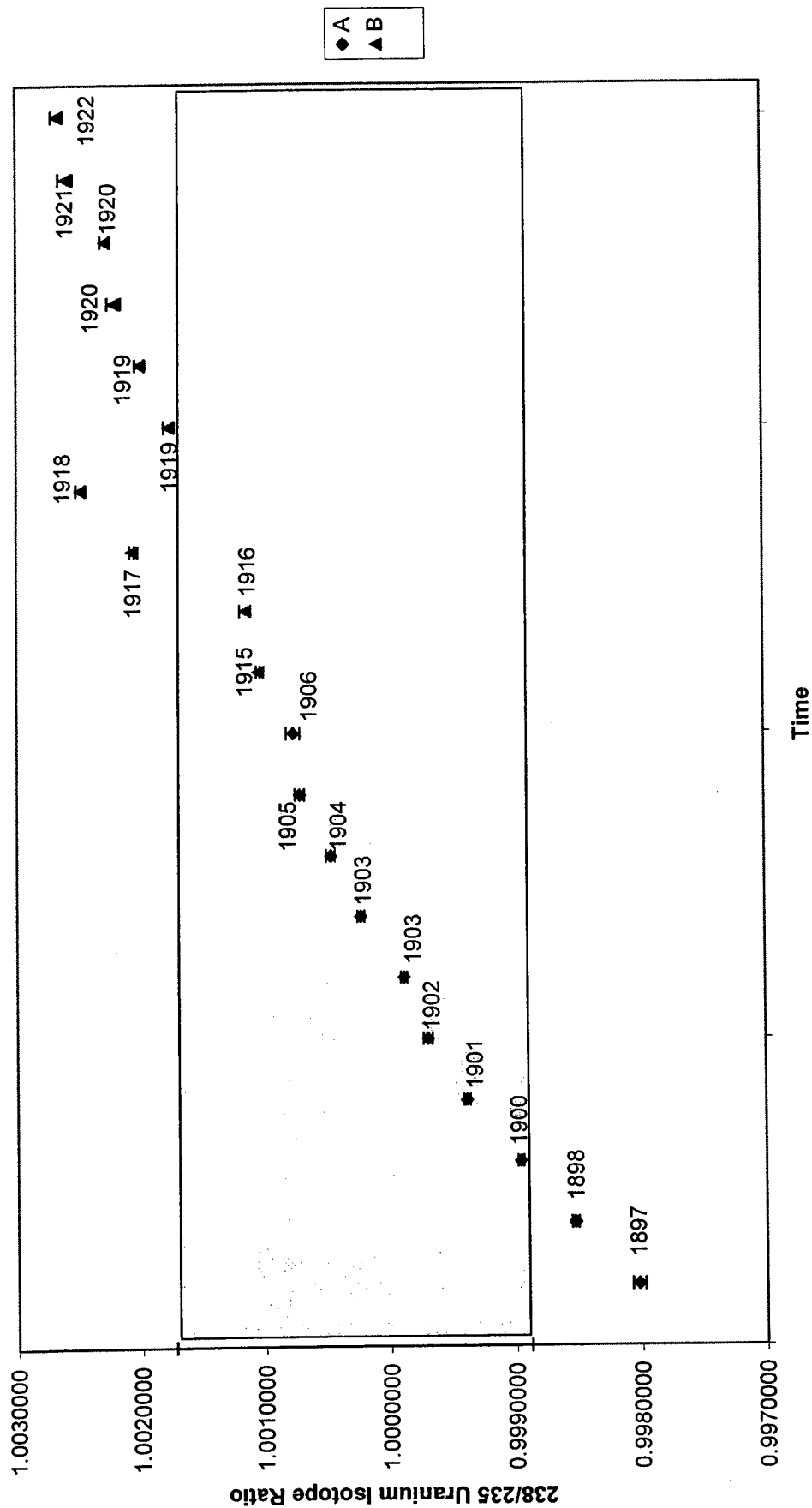


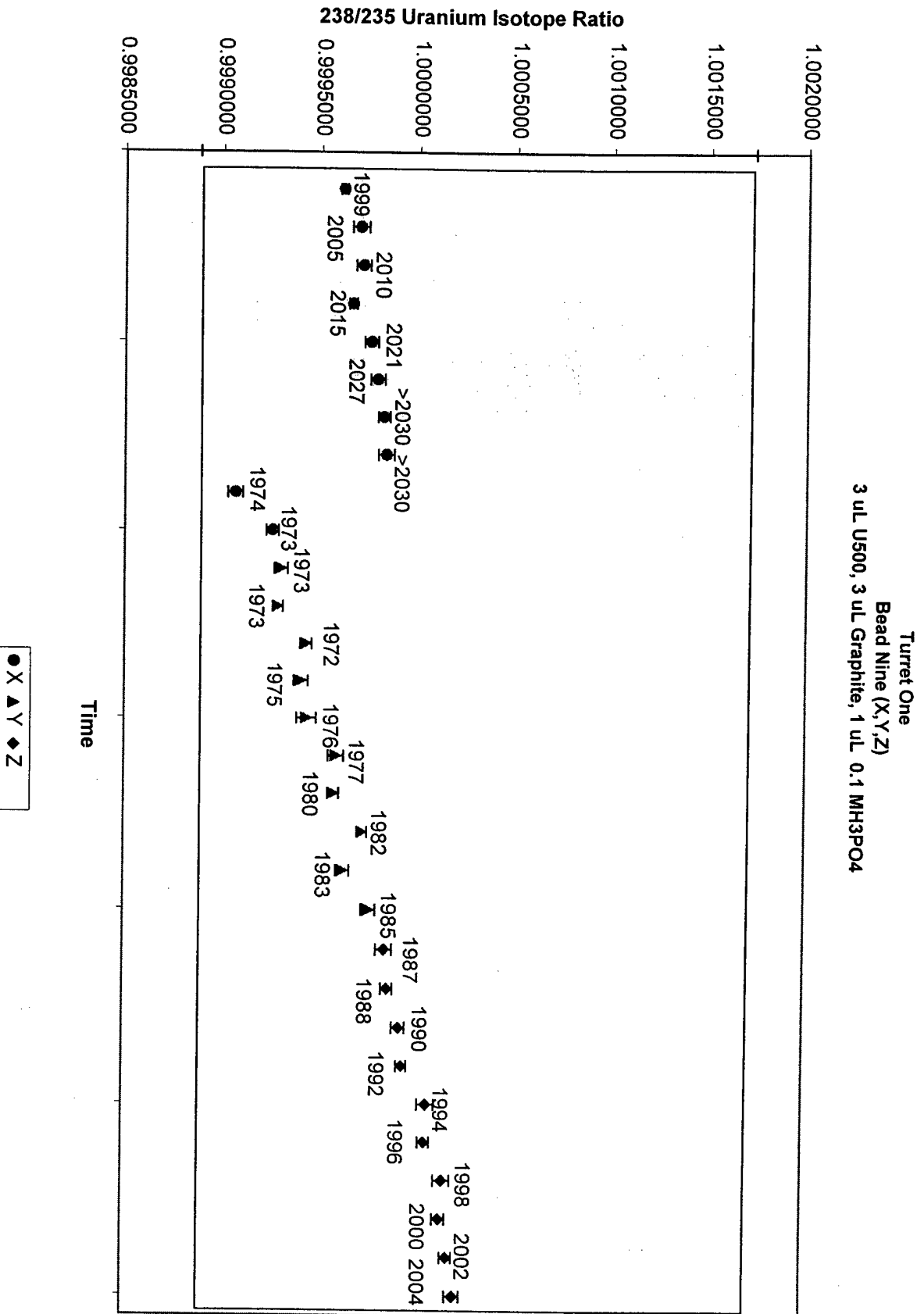
Turret One
Bead Five
1 uL U500,3 uL Graphite





Turret One
Bead Nine (A and B)
3 uL U500, 3 uL Graphite, 1 uL 0.1 M H₃PO₄

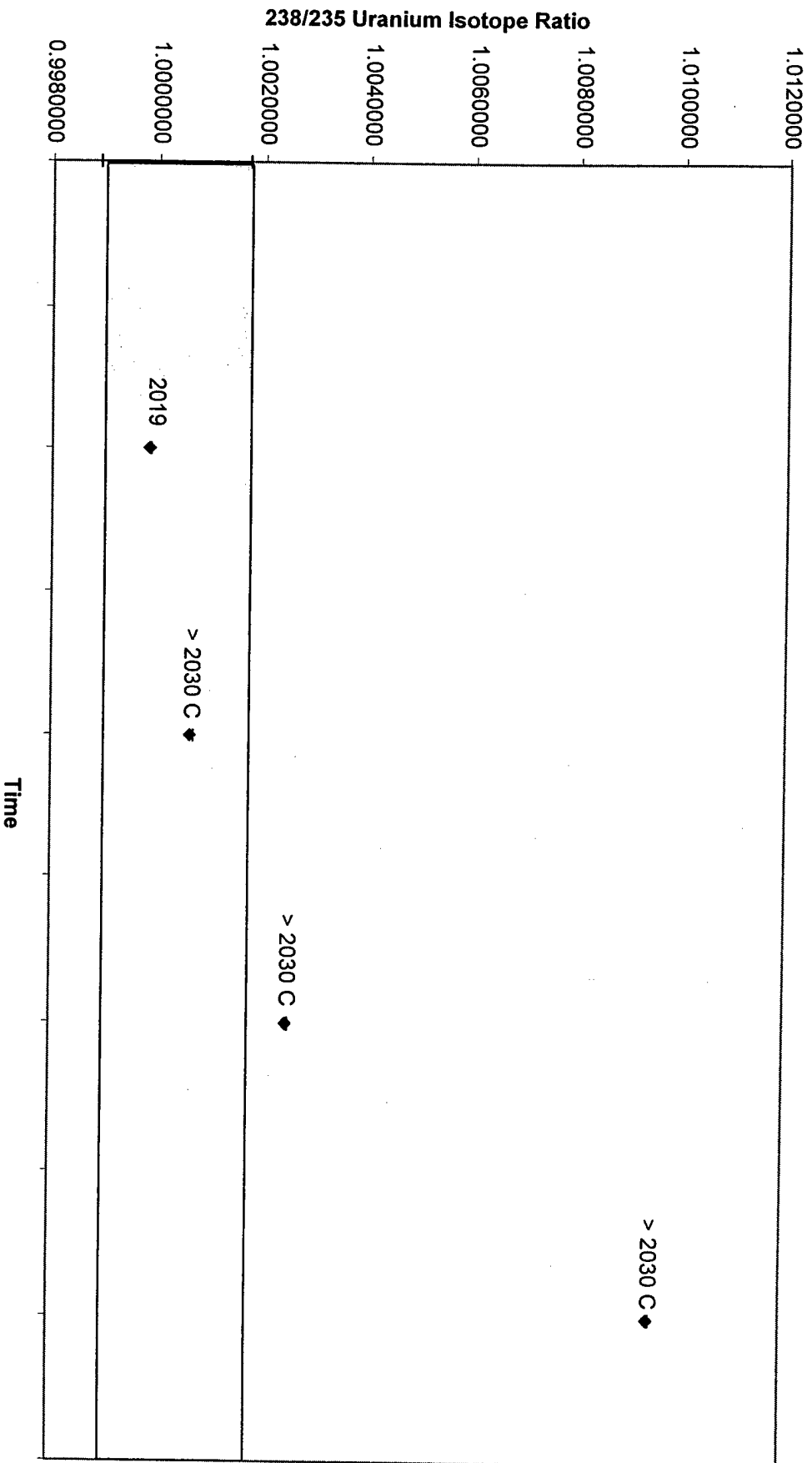




Turret One
Bead Ten (A and B)
3 uL U500, 3 uL Graphite



Turret One
Bead Ten(Z)
3 uL U500, 3 uL Graphite



Appendix 4, Annex G

TIMS Results of Turret Two

G-1 Raw Database

G-2 Charts

- 1 Chart of Isotopic Ratios for Bead One, Five through Seven
versus time
- 2 Chart of Isotopic Ratios for Bead One, Five through Seven
versus temperature
- 3 Chart of Isotopic Ratios for Bead One
- 4 Chart of Isotopic Ratios for Bead Five
- 5 Chart of Isotopic Ratios for Bead Six
- 6 Chart of Isotopic Ratios for Bead Seven

Appendix 4, Annex G-1

U500 Standard Data		Mean	Standard Deviation	
Atom Percent	U238	49.711	0.05	
	U235	49.696	0.05	
	238/235	1.0003	0.0014	
		1.0003	0.0014	
			10.5	0
			17.5	0
			20.5	0
			80.5	50
			50.5	0
			100.5	0
			100.5	80
			2030	1840

DTG 2/16/00 20:57

Bead: 5A U500 0.1M H₃PO₄ 3ug sample:sandwich

DTG 2/16/00 21:23

Bead: 5B U500 0.1M H₃PO₄ 3ug sample:sandwich

Block		Amps		Temp		238 Intensity		238/235		Std Error		Notes		Block		Amps		Temp		238 Intensity		238/235		Std Error		Notes	
1	4.3	1910	1.8	0.9953733	0.000052									11	4.33	1924	1.8	0.9977793	0.000045								
2	4.3	1911	1.7	0.9957583	0.000060									12	4.33	1924	1.8	0.9980103	0.000066								
3	4.3	1913	1.7	0.9959773	0.000040									13	4.33	1924	1.7	0.9979722	0.000053								
4	4.3	1913	1.7	0.9962591	0.000028									14	4.33	1924	1.7	0.9980080	0.000066								
5	4.3	1914	1.7	0.9965788	0.000054									15	4.33	1924	1.7	0.9983271	0.000067								
6	4.3	1914	1.7	0.9966127	0.000049									16	4.33	1924	1.6	0.9982470	0.000058								
7	4.3	1918	1.7	0.9972409	0.000039									17	4.33	1924	1.6	0.9984828	0.000048								
8	4.3	1918	1.7	0.9972267	0.000035									18	4.33	1924	1.5	0.9984433	0.000085								
9	4.3	1918	1.7	0.9973630	0.000028									19	4.33	1925	1.5	0.9987337	0.000051								
10	4.3	1918	1.6	0.9976256	0.000046									20	4.33	1925	1.4	0.9986319	0.000080								
Grand Mean				0.9966203	0.000073									Grand Mean								0.9982657	0.000034				

Appendix 4, Annex G-1

DTG	2/16/00 21:51		DTG	2/16/00 22:23			
Bead:	5C	U500 0.1M H ₃ PO ₄ 3ug sample:sandwich	Bead:	5D	U500 0.1M H ₃ PO ₄ 3ug sample:sandwich		
238 Intensity			238 Intensity				
Block	Amps	Temp	Notes	Block	Amps	Temp	Notes
21	4.4	1941	Std Error	31	4.47	1958	Std Error
22	4.4	1940	0.000059	32	4.47	1957	1.0000752 0.000057
23	4.4	1940	0.000035	33	4.47	1958	1.0001424 0.000071
24	4.4	1941	0.000032	34	4.47	1958	1.0001072 0.000079
25	4.4	1941	0.000056	35	4.47	1958	1.0002284 0.000059
26	4.4	1941	0.000084	36	4.47	1958	1.0001312 0.000043
27	4.4	1941	0.000060	37	4.47	1958	1.0003941 0.000041
28	4.4	1941	0.000075	38	4.47	1959	1.000362 0.000071
29	4.4	1941	0.000059	39	4.47	1959	1.0004193 0.000079
30	4.4	1941	0.000079	40	4.47	1959	1.0004332 0.000049
			0.000031				1.0004478 0.000047
Grand Mean			0.000034	Grand Mean			1.0002761 0.000021

DTG	2/16/00 22:51	DTG	2/17/00 16:49								
Bead:	5E U500 0.1M H ₃ PO ₄ 3ug sample:sandwich	Bead:	6A U500 0.1M H ₃ PO ₄ 3ug sample:sandwich								
238 Intensity		238 Intensity									
Block	Amps	Temp	x10 ⁻¹² Amps	Block	Amps	Temp	x10 ⁻¹² Amps	Std Error	Notes		
41	4.54	1974	1.7	1.0006661	0.000059	51	4.3	1990	2.3	0.9970045	0.000045
42	4.54	1974	1.7	1.0009765	0.000053	52	4.3	1994	2.1	0.9976379	0.000051
43	4.54	1975	1.6	1.0005374	0.000079	53	4.3	2000	2.2	0.9983110	0.000061
44	4.54	1975	1.6	1.0007978	0.000045	54	4.3	2004	2.1	0.9987955	0.000061
45	4.54	1975	1.5	1.0007245	0.000045	55	4.3	2009	2.0	0.9993478	0.000096
46	4.54	1975	1.4	1.0005755	0.000084	56	4.3	2013	1.8	0.9996195	0.000047
47	4.54	1976	1.4	1.0007234	0.000033	57	4.3	2018	1.6	1.0002852	0.000059
48	4.54	1976	1.3	1.0009233	0.000052	58	4.3	2021	1.5	1.0002752	0.000067
49	4.54	1976	1.3	1.0010377	0.000035	59	4.3	2024	1.3	1.0010087	0.000082
50	4.54	1976	1.3	1.0008536	0.000077	60	4.3	2026	1.1	1.0011694	0.000058
Grand Mean				1.0007896	0.000021	Grand Mean				0.9993428	0.000135

Appendix 4, Annex G-1

DTG 2/17/00 17:25

Bead: 6B U500 0.1M H₃PO₄ 3ug sample:sandwich

238 Intensity				
Block	Amps	Temp	x10 ⁻¹² Amps	238/235
61	4.4	2030	1.2	1.0039409
62	4.4	2030	1.0	1.0048671
63	4.4	2030	0.97	1.0083483
64	4.4	2030	0.91	1.0079813
65	4.4	2030	0.88	1.0097340
66	4.4	2030	0.82	1.0104557
67	4.4	2030	1.1	1.0077328
68	4.4	2030	1.1	1.0074377
69	4.4	2030	0.97	1.0090718
70	4.4	2030	0.86	1.0093458
Grand Mean				1.0081142

DTG 2/17/00 17:52

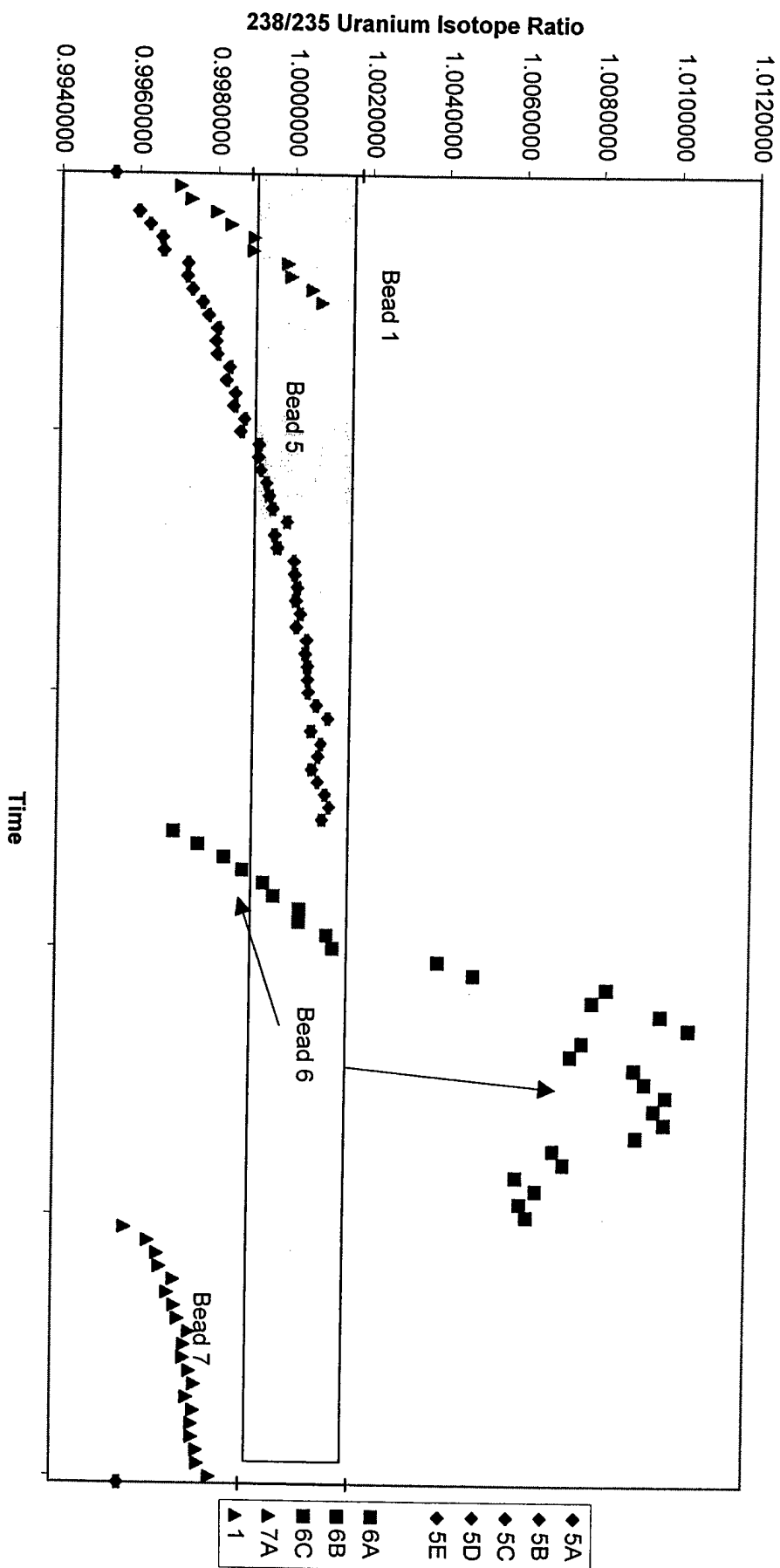
Bead: 6C U500 0.1M H₃PO₄ 3ug sample:sandwich

238 Intensity				
Block	Amps	Temp	x10 ⁻¹² Amps	238/235
71	4.47	2030	0.83	1.0098993
72	4.47	2030	0.68	1.0096028
73	4.47	2030	0.58	1.0098719
74	4.47	2030	0.40	1.0091496
75	4.47	2030	0.25	1.0070101
76	4.47	2030	0.20	1.0072899
77	4.47	2030	0.17	1.0060444
78	4.47	2030	0.14	1.0065636
79	4.47	2030	0.12	1.0061564
80	4.47	2030	0.11	1.0063312
Grand Mean				1.0078697

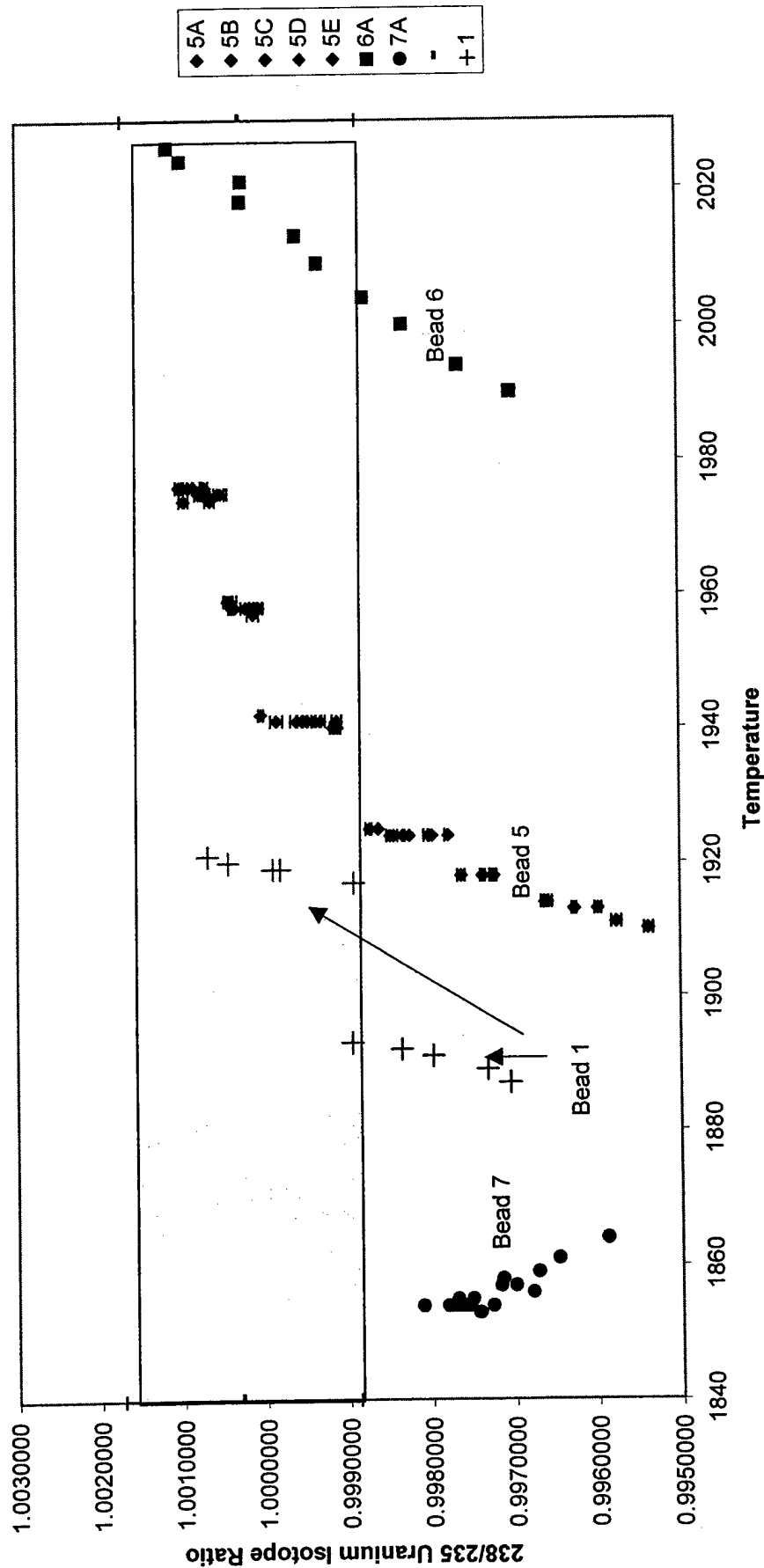
Appendix 4, Annex G-1

DTG		2/17/00 18:29		DTG		2/16/00 23:34							
Bead:		7A U500 0.1M H ₃ PO ₄ 3ug sample:sandwich		Bead:		1 U500 1M H ₃ PO ₄ 3ug sample:sandwich							
		238 Intensity				238 Intensity							
Block	Amps	Temp	x10 ⁻¹² Amps	Notes	Block	Amps	Temp	x10 ⁻¹² Amps	238/235	Std Error	Notes		
81	4.3	1864	1.8	0.9958887	0.000070	1	4.3	1887	1.20	0.9970432	0.000088		
82	4.3	1861	1.9	0.9964747	0.000072	2	4.3	1889	0.91	0.9973141	0.000104		
83	4.3	1859	1.8	0.9967247	0.000034	3	4.3	1891	0.74	0.9979705	0.000171		
84	4.3	1856	1.7	0.9967902	0.000080	4	4.3	1892	0.65	0.9983517	0.000101		
85	4.3	1858	1.7	0.9971501	0.000060	5	4.3	1893	0.59	0.9989528	0.000134		
86	4.3	1857	1.7	0.9969989	0.000048	6	4.4	1917	0.54	0.9989365	0.000108		
87	4.3	1857	1.6	0.9971758	0.000033	7	4.4	1919	0.82	0.9998297	0.000075		
88	4.3	1854	1.5	0.9972743	0.000048	8	4.4	1919	0.74	0.9999176	0.000118		
89	4.3	1854	1.5	0.9975577	0.000047	9	4.4	1920	0.69	1.0004604	0.000121		
90	4.3	1853	1.4	0.9974380	0.000029	10	4.4	1921	0.64	1.0007068	0.000075		
91	4.3	1853	1.4	0.9974243	0.000068	Grand Mean						0.9989632	0.000127
92	4.3	1854	1.4	0.9975827	0.000040								
93	4.3	1854	1.4	0.9977106	0.000027								
94	4.3	1855	1.4	0.9975177	0.000038								
95	4.3	1855	1.3	0.9976951	0.000059								
96	4.3	1854	1.4	0.9976512	0.000099								
97	4.3	1854	1.3	0.9976548	0.000076								
98	4.3	1854	1.3	0.9977879	0.000088								
99	4.3	1854	1.3	0.9978146	0.000051								
100	4.3	1854	1.3	0.9981142	0.000066								
Grand Mean				0.9973876	0.000033								

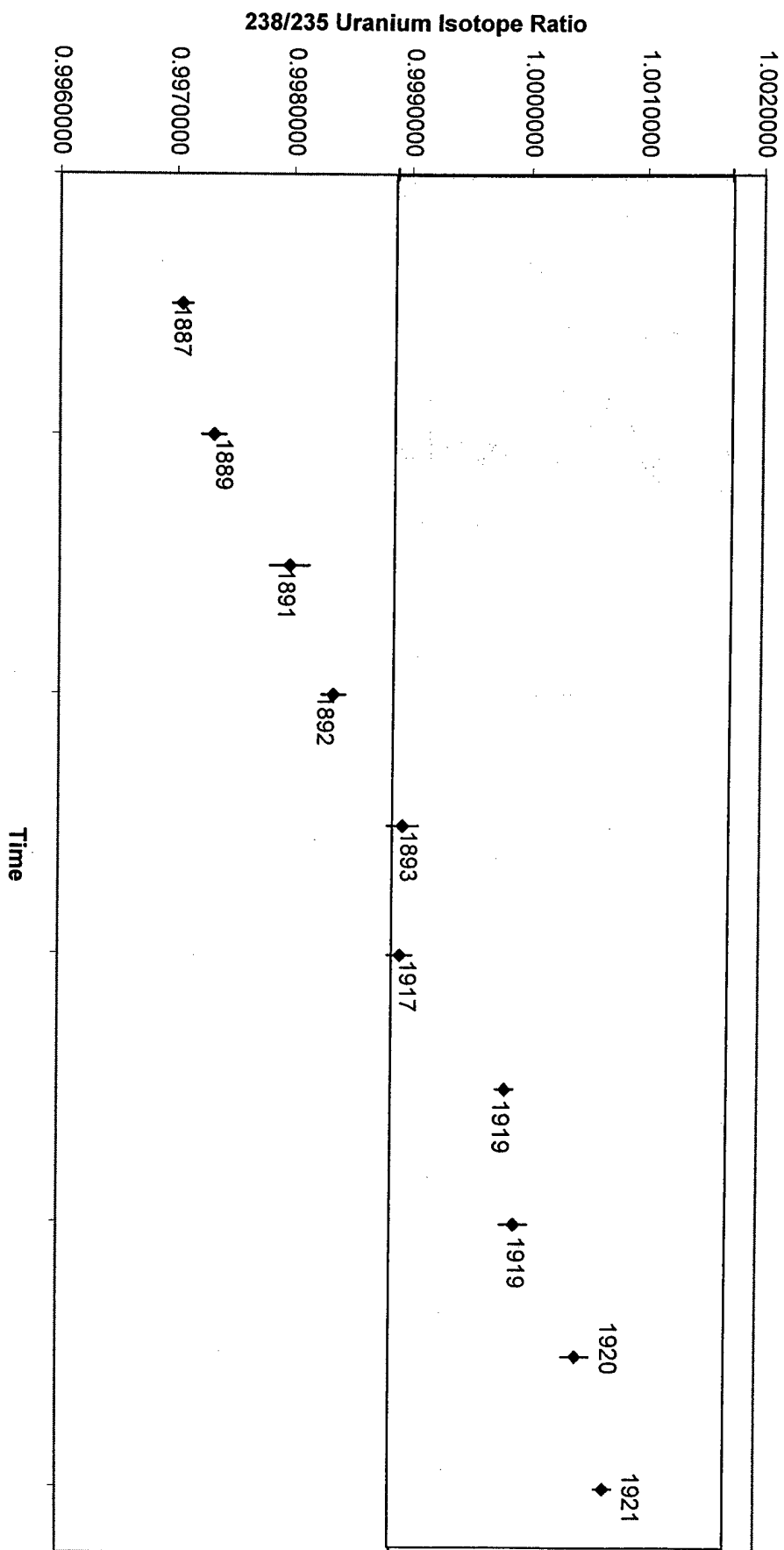
Turret Two
Bead 1, 5, 6, 7
U500 0.1 M H₃PO₄; 3uL Sample: Sandwich Load



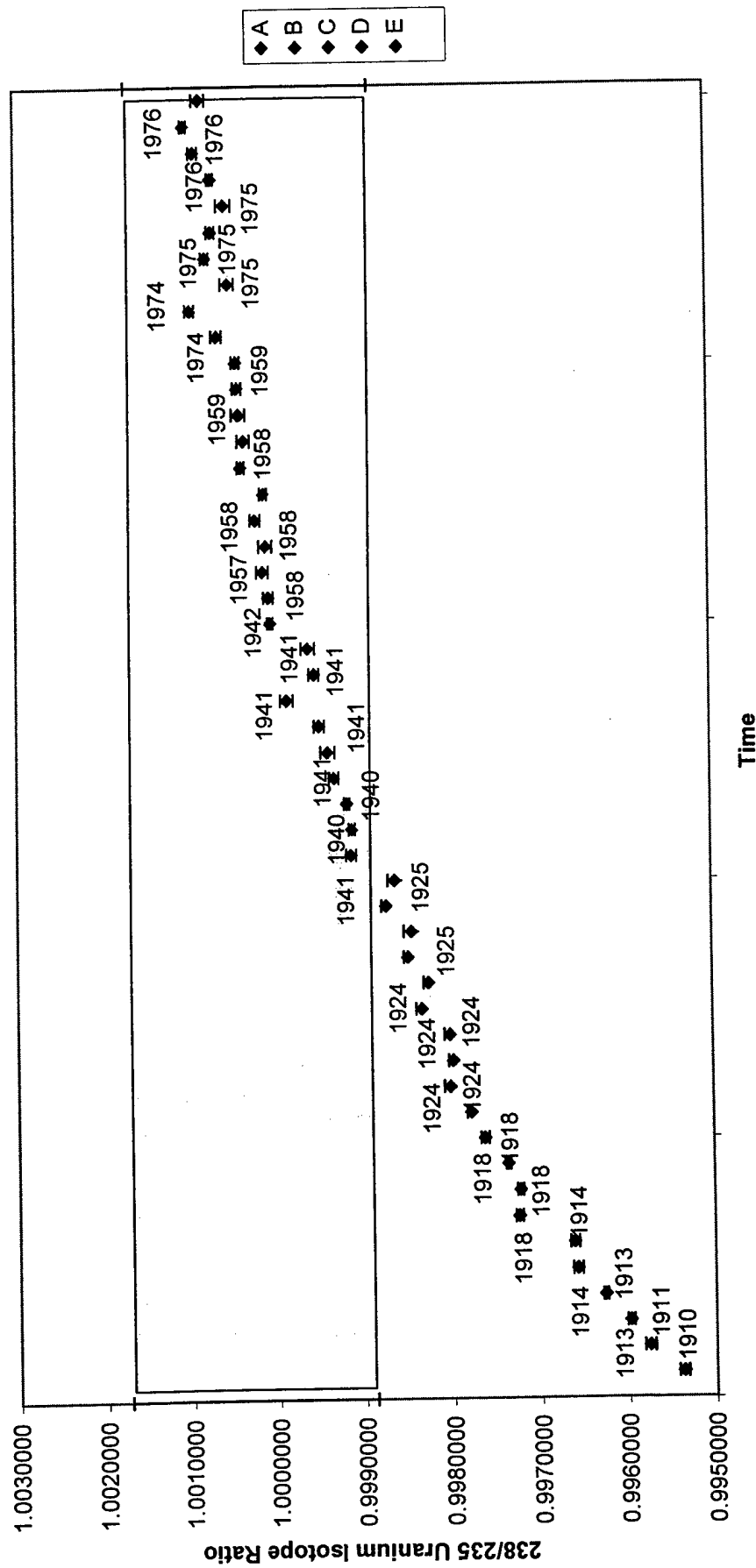
Turret Two
Bead 1, 5, 6, 7 versus Temperature
U500 0.1 M H₃PO₄; 3 uL Sample: Sandwich Load



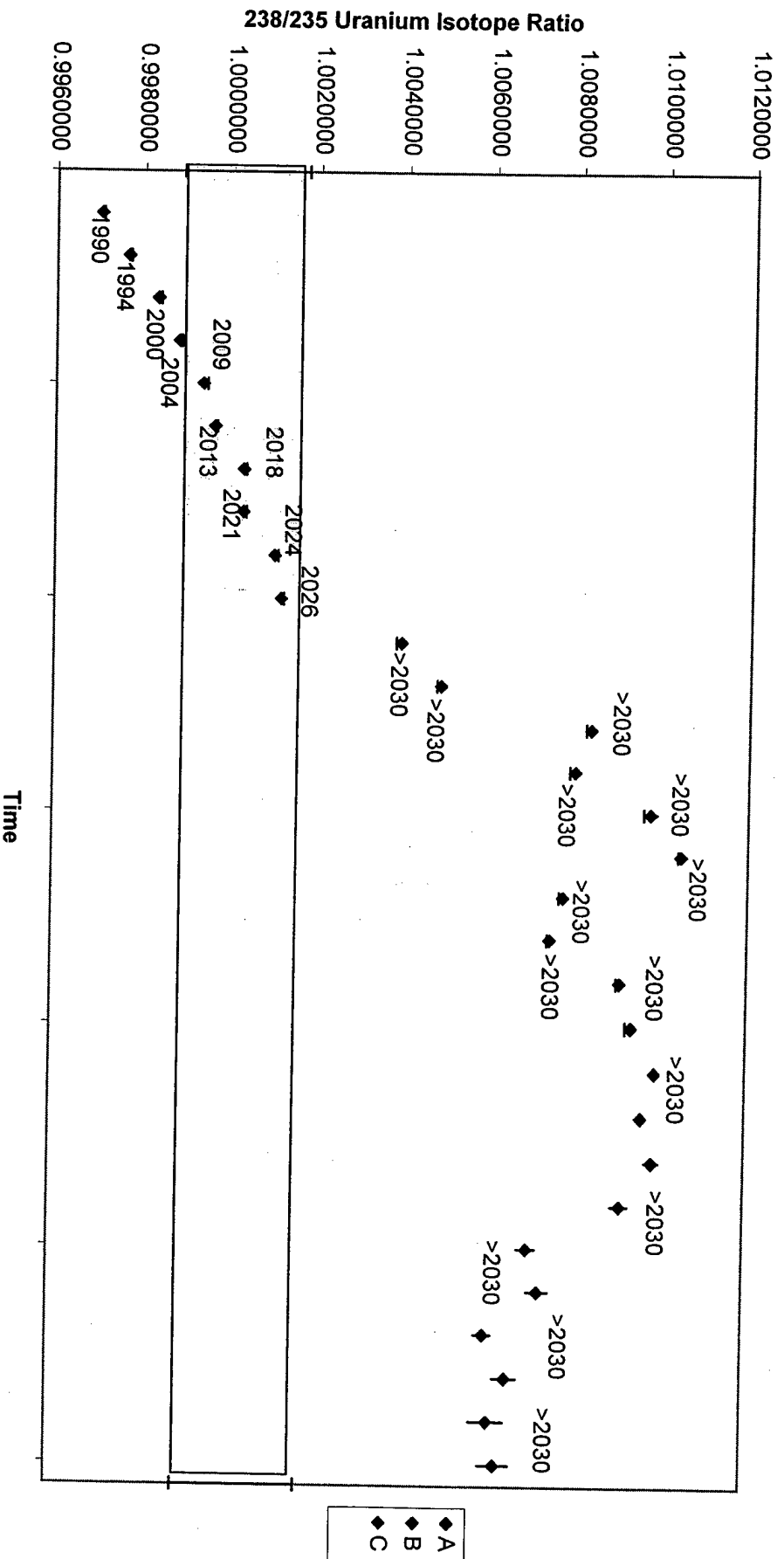
Turret Two
Bead One
U500 1 M H₃PO₄; 3uL Sample: Sandwich Load



Turret Two
Bead Five
U500 0.1 M H₃PO₄; 3 uL Sample: Sandwich Load



Turret Two
Bead Six
U500 0.1 M H₃PO₄; 3 uL Sample: Sandwich Load



Appendix 4, Annex H (cont)

- 18 Chart of Isotopic Ratios for sandwich and regular loaded S95 test sample supernatants and precipitates as a function of temperature
- 19 Chart of Isotopic Ratios for sandwich and regular loaded S95 test sample supernatants and precipitates as a function of consecutive block measurements

Appendix 4, Annex H-1

U500 Standard Data		Mean	Standard Deviation	
Atom Percent	U238	49.711	0.05	
	U235	49.696	0.05	
	238/235	1.0003	0.0014	
		1.0003	0.0014	
		85	160	400
		410	310	580
		1840	1840	1900
		2000	2040	2030
			250	2030
				0
				45
				100
				0
				215
				80
				240

DTG 2/18/00 18:43
Bead: SOS-1, A

DTG 2/18/00 19:10
Bead: SOS-1, B

Block		238 Intensity		Notes		Block		238 Intensity		Notes	
Amps	Temp	x10 ⁻¹² Amps	238/235	Std Error		Amps	Temp	x10 ⁻¹² Amps	238/235	Std Error	
131 4.3	1853	1.1	0.9964897	0.000088		141 4.37	1868	0.64	0.9995478	0.000080	
132 4.3	1852	0.92	0.9969788	0.000101		142 4.37	1868	0.60	0.9991681	0.000142	
133 4.3	1854	0.78	0.9973261	0.000100		143 4.37	1866	0.62	0.9992228	0.000074	
134 4.3	1854	0.71	0.9979687	0.000109		144 4.37	1866	0.58	0.9989373	0.000125	
135 4.3	1855	0.66	0.9978616	0.000112		145 4.37	1866	0.61	0.9990408	0.000041	
136 4.3	1855	0.62	0.9987152	0.000078		146 4.37	1865	0.57	0.9990912	0.000125	
137 4.3	1855	0.59	0.9983686	0.000092		147 4.37	1866	0.54	0.9991768	0.000122	
138 4.3	1855	0.55	0.9983588	0.000122		148 4.37	1866	0.50	0.9984868	0.000134	
139 4.3	1855	0.55	0.9987234	0.000115		149 4.37	1866	0.48	0.9993507	0.000104	
140 4.3	1854	0.52	0.9989482	0.000123		150 4.37	1866	0.46	0.9995949	0.000162	
Grand Mean			0.9980116	0.000080		Grand Mean			0.9991459	0.000042	

Appendix 4, Annex H

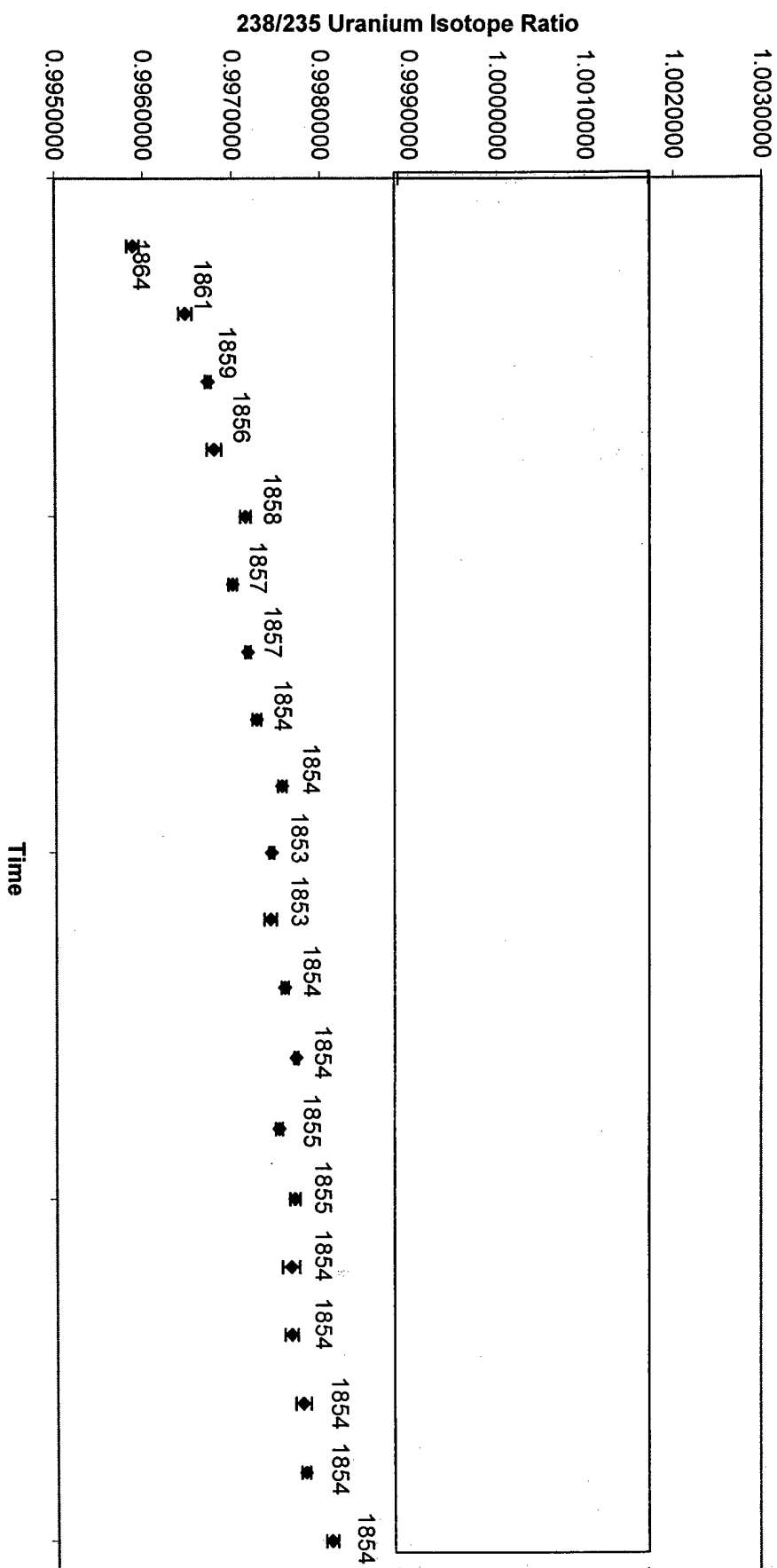
TIMS Results of Turrets Three through Five

H-1 Raw Database

H-2 Charts

- 1 Chart of Isotopic Ratios for regular loaded test sample supernatants as a function of temperature
- 2 Chart of Isotopic Ratios for regular loaded test sample supernatants as a function of consecutive block measurements
- 3 Chart of Isotopic Ratios for sandwich loaded test sample supernatants as a function of temperature
- 4 Chart of Isotopic Ratios for sandwich loaded test sample supernatants as a function of consecutive block measurements
- 5 Chart of Isotopic Ratios for sandwich loaded test sample precipitates as a function of consecutive block measurements
- 6 Chart of Isotopic Ratios for sandwich loaded test sample precipitates as a function of temperature
- 7 Chart of Isotopic Ratios for sandwich loaded 8 Hour test sample precipitates and supernatants as a function of consecutive block measurements
- 8 Chart of Isotopic Ratios for sandwich loaded 24 Hour test sample precipitates and supernatants as a function of consecutive block measurements
- 9 Chart of Isotopic Ratios for sandwich loaded 95 Hour test sample precipitates and supernatants as a function of consecutive block measurements
- 10 Chart of Isotopic Ratios for sandwich loaded S0 and C0 supernatants as a function of temperature
- 11 Chart of Isotopic Ratios for sandwich loaded S0 and C0 supernatants as a function of consecutive block measurements
- 12 Chart of Isotopic Ratios for sandwich and regular loaded S4 test sample supernatants as a function of temperature
- 13 Chart of Isotopic Ratios for sandwich and regular loaded S4 test sample supernatants as a function of consecutive block measurements
- 14 Chart of Isotopic Ratios for sandwich and regular loaded S8 test sample supernatants and precipitates as a function of temperature
- 15 Chart of Isotopic Ratios for sandwich and regular loaded S8 test sample supernatants and precipitates as a function of consecutive block measurements
- 16 Chart of Isotopic Ratios for sandwich and regular loaded S24 test sample supernatants and precipitates as a function of temperature
- 17 Chart of Isotopic Ratios for sandwich and regular loaded S24 test sample supernatants and precipitates as a function of consecutive block measurements

Turret Two
Bead Seven
U500 0.1 M H₃PO₄; 3 uL Sample: Sandwich Load



Appendix 4, Annex H-1

DTG 2/18/00 19:36
Bead: SOS-1, C

Block	Amps	Temp	238 Intensity $\times 10^{-12}$ Amps
151	4.47	1887	0.67
152	4.47	1885	0.65
153	4.47	1887	0.62
154	4.47	1887	0.61
155	4.47	1886	0.63
156	4.47	1887	0.67
157	4.47	1887	0.82
158	4.47	1887	0.98
159	4.47	1887	1.10
160	4.47	1887	1.00
Grand Mean			

DTG 2/18/00 20:02
Bead: SOS-1, D

Block	Amps	Temp	238 Intensity $\times 10^{-12}$ Amps	Notes	Std Error	238/235	Std Error	Notes
161	4.47	1888	0.91		0.00099	0.9999895	0.00099	
162	4.47	1889	0.82		0.000119	0.9997580	0.000119	
163	4.47	1889	0.77		0.000130	0.9996621	0.000130	
164	4.47	1890	0.73		0.000123	0.9992863	0.000123	
165	4.47	1891	0.72		0.000078	0.9993317	0.000078	
166	4.47	1891	0.65		0.000109	0.9987228	0.000109	
167	4.47	1889	0.62		0.000057	0.9986884	0.000057	
168	4.47	1891	0.65		0.000085	0.9990051	0.000085	
169	4.47	1890	0.60		0.000071	1.0003330	0.000071	
170	4.47	1890	0.58		0.000095	1.0004130	0.000095	
Grand Mean					0.000065	0.9994699	0.000065	

DTG 2/18/00 20:29
Bead: S4S-1, A

Block	Amps	Temp	238 Intensity $\times 10^{-12}$ Amps
41	4.7	1935	0.47
42	4.7	1935	0.30
43	4.7	1935	0.43
44	4.7	1934	0.43
45	4.7	1935	0.43
46	4.7	1934	0.43
47	4.7	1930	0.41
48	4.7	1926	0.35
49	4.7	1925	0.35
50	4.7	1917	0.37
Grand Mean			

DTG 2/18/00 21:15
Bead: S4S-1, B

Block	Amps	Temp	238 Intensity $\times 10^{-12}$ Amps	Notes	Std Error	238/235	Std Error	Notes
51	4.7	1918	0.36		0.000176	1.0012675	0.000176	
52	4.7	1918	0.39		0.000126	1.0029304	0.000126	
53	4.7	1919	0.43		0.000141	1.0131863	0.000141	
54	4.7	1918	0.46		0.000227	1.0123119	0.000227	
55	4.7	1918	0.83		0.000171	1.0120877	0.000171	
56	4.7	1918	0.82		0.000235	1.0125229	0.000235	
57	4.7	1918	0.76		0.000195	1.0103371	0.000195	
58	4.7	1918	0.73		0.000187	1.0077729	0.000187	
59	4.7	1918	0.69		0.000111	1.0068177	0.000111	
60	4.7	1919	0.67		0.000259	1.0060053	0.000259	
Grand Mean					0.000403	1.0085483	0.000403	

Appendix 4, Annex H-1

DTG 2/18/00 21:41
Bead: S4S-1, C

238 Intensity			
Block	Amps	Temp	$\times 10^{-12}$ Amps
61	4.7	1919	0.65
62	4.7	1919	0.63
63	4.7	1920	0.61
64	4.7	1920	0.60
65	4.7	1920	0.60
66	4.7	1921	0.60
67	4.7	1921	0.58
68	4.7	1921	0.58
69	4.7	1922	0.57
70	4.7	1922	0.56
Grand Mean			

DTG 2/18/00 22:46
Bead: S8S-1, B

238 Intensity			
Block	Amps	Temp	$\times 10^{-12}$ Amps
81	4.6	1905	0.40
82	4.6	1906	0.37
83	4.6	1906	0.37
84	4.6	1907	0.36
85	4.6	1907	0.36
86	4.6	1907	0.36
87	4.6	1907	0.37
88	4.6	1907	0.37
89	4.6	1907	0.36
90	4.6	1908	0.35
Grand Mean			

DTG 2/18/00 22:09
Bead: S8S-1, A

238 Intensity			
Block	Amps	Temp	$\times 10^{-12}$ Amps
71	4.4	1859	0.29
72	4.4	1858	0.23
73	4.4	1859	0.22
74	4.4	1859	0.19
75	4.4	1859	0.18
76	4.4	1881	0.17
77	4.4	1881	0.29
78	4.4	1882	0.27
79	4.4	1882	0.27
80	4.4	1882	0.24
Grand Mean			

DTG 2/19/00 12:05
Bead: S24S-1, A

238 Intensity			
Block	Amps	Temp	$\times 10^{-12}$ Amps
91	4.3	2030	1.4
92	4.3	2030	1.3
93	4.3	2030	1.5
94	4.3	2030	1.2
95	4.3	2030	1.1
96	4.3	2030	0.84
97	4.3	2030	0.61
98	4.3	2030	0.44
99	4.3	2030	0.65
100	4.3	2030	0.62
Grand Mean			

Appendix 4, Annex H-1

DTG 2/19/00 12:30
Bead: S24S-1, B

Block	Amps	Temp	238 Intensity x10 ⁻¹² Amps	238/235	Std Error	Notes	Block	Amps	Temp	238 Intensity x10 ⁻¹² Amps	238/235	Std Error	Notes
101	4.33	2030	0.67	1.0064214	0.000091		111	4.6	2030	0.43	1.0063431	0.000161	
102	4.33	2030	0.60	1.0060263	0.000149		112	4.6	2030	0.26	1.0052545	0.000146	
103	4.33	2030	0.47	1.0048496	0.000130		113	4.6	2030	0.18	1.0064788	0.000423	
104	4.33	2030	0.42	1.0042643	0.000088		114	4.6	2030	0.14	1.0059733	0.000415	
105	4.33	2030	0.38	1.0051074	0.000245		115	4.6	2030	0.099	1.0047003	0.000374	
106	4.33	2030	0.34	1.0051545	0.000139		116	4.6	2030	0.076	1.0060274	0.000680	
107	4.33	2030	0.30	1.0046494	0.000167		117	4.6	2030	0.055	1.0045281	0.000631	
108	4.33	2030	0.27	1.0054409	0.000131		118	4.6	2030	0.042	1.0052181	0.000978	
109	4.33	2030	0.24	1.0063950	0.000123		119	4.6	2030	0.028	1.0031259	0.001092	
110	4.33	2030	0.20	1.0060255	0.000357		120	4.6	2030	0.021	1.0062864	0.000921	
Grand Mean				1.0054108	0.000088		Grand Mean				1.0054417	0.000201	

DTG 2/19/00 12:56
Bead: S24S-1, C

Block	Amps	Temp	238 Intensity x10 ⁻¹² Amps	238/235	Std Error	Notes
111	4.6	2030	0.43	1.0063431	0.000161	
112	4.6	2030	0.26	1.0052545	0.000146	
113	4.6	2030	0.18	1.0064788	0.000423	
114	4.6	2030	0.14	1.0059733	0.000415	
115	4.6	2030	0.099	1.0047003	0.000374	
116	4.6	2030	0.076	1.0060274	0.000680	
117	4.6	2030	0.055	1.0045281	0.000631	
118	4.6	2030	0.042	1.0052181	0.000978	
119	4.6	2030	0.028	1.0031259	0.001092	
120	4.6	2030	0.021	1.0062864	0.000921	
Grand Mean				1.0054417	0.000201	

DTG 2/20/00 14:01
Bead: S95S-1, A

Block	Amps	Temp	238 Intensity x10 ⁻¹² Amps	238/235	Std Error	Notes
121	4.55	1924	0.20	0.9989060	0.000260	
122	4.55	1913	0.14	0.9992799	0.000468	
123	4.55	1892	0.14	1.0008614	0.000327	
124	4.55	1889	0.14	1.0005459	0.000499	
125	4.55	1884	0.13	1.0005919	0.000467	
126	4.55	1883	0.13	1.0011282	0.000250	
127	4.55	1883	0.13	1.0011900	0.000311	
128	4.55	1883	0.13	1.0019829	0.000506	
129	4.55	1882	0.13	1.0024223	0.000408	
130	4.55	1882	0.13	1.0014968	0.000470	
Grand Mean				1.0008373	0.000150	

DTG 2/20/00 14:38
Bead: S95S-1, B

Block	Amps	Temp	238 Intensity x10 ⁻¹² Amps	238/235	Std Error	Notes
131	4.75	1924	0.36	1.0029277	0.000209	
132	4.75	1924	0.30	1.0027973	0.000165	
133	4.75	1925	0.29	1.0027705	0.000142	
134	4.75	1925	0.28	1.0029668	0.000192	
135	4.75	1925	0.27	1.0038523	0.000147	
136	4.75	1925	0.27	1.0026515	0.000250	
137	4.75	1926	0.26	1.0030436	0.000207	
138	4.75	1926	0.26	1.0029396	0.000070	
139	4.75	1926	0.25	1.0032488	0.000107	
140	4.75	1926	0.25	1.0037610	0.000298	
Grand Mean				1.0030576	0.000065	

Appendix 4, Annex H-1

DTG 2/20/00 15:04
Bead: S95S-1, C

		238 Intensity	
Block	Amps	Temp	x10 ⁻¹² Amps
141	4.9	1955	0.47
142	4.9	1955	0.40
143	4.9	1955	0.37
144	4.9	1956	0.36
145	4.9	1958	0.37
146	4.9	1959	0.38
147	4.9	1961	0.37
148	4.9	1962	0.35
149	4.9	1963	0.34
150	4.9	1963	0.33
Grand Mean			1.0042468

DTG 2/20/00 15:30
Bead: S95S-1, D

		238 Intensity	
Block	Amps	Temp	x10 ⁻¹² Amps
151	4.9	1963	0.31
152	4.9	1964	0.30
153	4.9	1966	0.31
154	4.9	1966	0.30
155	4.9	1965	0.30
156	4.9	1965	0.29
157	4.9	1966	0.28
158	4.9	1967	0.28
159	4.9	1958	0.28
160	4.9	1958	0.25
Grand Mean			1.0026059

DTG 2/20/00 16:10
Bead: S95S-1, E

		238 Intensity	
Block	Amps	Temp	x10 ⁻¹² Amps
161	5.0	1976	0.35
162	5.0	1976	0.23
163	5.0	1976	0.26
164	5.0	1972	0.26
165	5.0	1973	0.25
166	5.0	1974	0.25
167	5.0	1974	0.23
168	5.0	1974	0.23
169	5.0	1974	0.23
170	5.0	1974	0.22
Grand Mean			1.0020956

DTG 2/20/00 16:44
Bead: S95S-1, F

		238 Intensity	
Block	Amps	Temp	x10 ⁻¹² Amps
171	5.13	2000	0.33
172	5.13	2001	0.30
173	5.13	2002	0.30
174	5.13	2002	0.30
175	5.13	2003	0.29
176	5.13	2004	0.28
177	5.13	1993	0.28
178	5.13	1993	0.30
179	5.13	1989	0.30
180	5.13	1989	0.30
Grand Mean			1.0022727

Appendix 4, Annex H-1

DTG 2/20/00 17:11
Bead: S95S-1, G

Block	Amps	Temp	238 Intensity $\times 10^{-12}$ Amps
181	5.25	2018	0.56
182	5.25	2019	0.47
183	5.25	2020	0.43
184	5.25	2020	0.39
185	5.25	2023	0.37
186	5.25	2026	0.35
187	5.25	2029	0.34
188	5.25	2030	0.33
189	5.25	2030	0.32
190	5.25	2030	0.31
191	5.25	2030	0.30
192	5.25	2030	0.31
193	5.25	2030	0.31
194	5.25	2030	0.31
195	5.25	2030	0.30
196	5.25	2030	0.29
197	5.25	2030	0.29
198	5.25	2030	0.28
199	5.25	2030	0.27
200	5.25	2030	0.26
201	5.25	2030	0.25
202	5.25	2030	0.25
203	5.25	2030	0.25
204	5.25	2030	0.24
205	5.25	2030	0.24
206	5.25	2030	0.24
207	5.25	2030	0.23
208	5.25	2030	0.22
209	5.25	2030	0.21
210	5.25	2030	0.21
Grand Mean			

DTG 2/20/00 19:02
Bead: S8P-1, A

Block	Amps	Temp	238 Intensity $\times 10^{-12}$ Amps	Notes	Std Error	238/235	Std Error	Notes
211	4.35	1929	0.24		0.000083	0.9962961	0.000288	
212	4.35	1930	0.24		0.000214	0.9962907	0.000166	
213	4.35	1931	0.27		0.000192	0.9963560	0.000106	
214	4.35	1931	0.27		0.000235	0.9970088	0.000229	
215	4.35	1932	0.29		0.000209	0.9977984	0.000203	
216	4.35	1932	0.29		0.000144	0.9977338	0.000174	
217	4.35	1932	0.29		0.000212	0.9984815	0.000181	
218	4.35	1932	0.29		0.000330	0.9980805	0.000112	
219	4.35	1932	0.30		0.000207	0.9985459	0.000183	
220	4.35	1933	0.31		0.000222	0.9982913	0.000096	
Grand Mean					0.000137	0.9975301	0.000101	

DTG 2/20/00 19:29
Bead: S8P-1, B

Block	Amps	Temp	238 Intensity $\times 10^{-12}$ Amps	Notes	Std Error	238/235	Std Error	Notes
221	4.35	1934	0.31		0.000243	0.9986069	0.000176	
222	4.35	1934	0.32		0.000224	0.9988070	0.000221	
223	4.35	1934	0.32		0.000221	0.9982823	0.000223	
224	4.35	1934	0.32		0.000204	0.9996125	0.000138	
225	4.35	1934	0.32		0.000219	0.9987596	0.000195	
226	4.35	1935	0.32		0.000255	0.9988637	0.000163	
227	4.35	1935	0.32		0.000250	0.9993615	0.000243	
228	4.35	1935	0.32		0.000252	0.9991077	0.000181	
229	4.35	1935	0.32		0.000151	0.9989222	0.000139	
230	4.35	1935	0.32		0.000241	0.9985413	0.000136	
Grand Mean					0.000285	0.9988864	0.000060	

Appendix 4, Annex H-1

DTG 2/20/00 20:00
Bead: S8P-1, C

Block	Amps	Temp	238 Intensity x10 ⁻¹² Amps	238/235	Std Error	Notes	Block	Amps	Temp	238 Intensity x10 ⁻¹² Amps	238/235	Std Error	Notes
231	4.35	1936	0.33	0.9993938	0.000157		241	4.47	1965	0.61	1.0001427	0.000113	
232	4.35	1936	0.33	0.9994952	0.000173		242	4.47	1965	0.60	1.0002282	0.000148	
233	4.35	1936	0.33	0.9991130	0.000101		243	4.47	1965	0.59	1.0001424	0.000130	
234	4.35	1937	0.33	0.9992337	0.000156		244	4.47	1965	0.59	1.0003473	0.000174	
235	4.35	1937	0.33	0.9996534	0.000224		245	4.47	1966	0.59	1.0005949	0.000056	
236	4.35	1937	0.33	0.9989901	0.000131		246	4.47	1966	0.59	1.0003773	0.000137	
237	4.35	1937	0.33	0.9997134	0.000150		247	4.47	1966	0.59	1.0004543	0.000075	
238	4.35	1937	0.33	0.9997493	0.000110		248	4.47	1967	0.59	1.0004827	0.000069	
239	4.35	1938	0.33	0.9997688	0.000188		249	4.47	1966	0.59	1.0006471	0.000150	
240	4.35	1938	0.33	0.9996211	0.000132		250	4.47	1966	0.59	1.000462	0.000090	
Grand Mean				0.9994315	0.000053		Grand Mean				1.0003956	0.000038	

DTG 2/20/00 21:05
Bead: S8P-1, E

Block	Amps	Temp	238 Intensity x10 ⁻¹² Amps	238/235	Std Error	Notes	Block	Amps	Temp	238 Intensity x10 ⁻¹² Amps	238/235	Std Error	Notes
251	4.54	1982	0.82	1.0011484	0.000096		261	4.64	2004	1.20	1.0019274	0.000117	
252	4.54	1982	0.80	1.0008708	0.000068		262	4.64	2004	1.20	1.0016630	0.000068	
253	4.54	1982	0.80	1.0014175	0.000087		263	4.64	2004	1.20	1.0016350	0.000056	
254	4.54	1982	0.80	1.0008789	0.000097		264	4.64	2005	1.20	1.0016069	0.000074	
255	4.54	1982	0.80	1.0010369	0.000146		265	4.64	2005	1.20	1.0017356	0.000092	
256	4.54	1983	0.80	1.0008808	0.000072		266	4.64	2005	1.20	1.0017811	0.000085	
257	4.54	1983	0.79	1.0011696	0.000107		267	4.64	2005	1.10	1.0021504	0.000062	
258	4.54	1983	0.79	1.0011143	0.000103		268	4.64	2006	1.10	1.0023810	0.000073	
259	4.54	1983	0.79	1.0017328	0.000135		269	4.64	2006	1.10	1.0023172	0.000090	
260	4.54	1983	0.79	1.0016863	0.000108		270	4.64	2006	1.10	1.0018535	0.000056	
Grand Mean				1.0011652	0.000039		Grand Mean				1.0018968	0.000035	

Appendix 4, Annex H-1

DTG 2/20/00 22:12

Bead: S95P-1, A

Block	Amps	Temp	238 Intensity		Notes
			x10 ⁻¹² Amps	Std Error	
271	4.15	1957	1.10	0.00056	
272	4.15	1960	1.10	0.00086	
273	4.15	1963	1.90	0.00034	
274	4.15	1965	1.80	0.00056	
275	4.15	1967	2.10	0.00039	
276	4.15	1968	2.00	0.00041	
277	4.15	1969	2.20	0.00045	
278	4.15	1970	2.10	0.00050	
279	4.15	1971	2.10	0.00028	
280	4.15	1971	2.10	0.00067	
Grand Mean				0.9958952	0.000029

DTG 2/20/00 23:04

Bead: S95P-1, C

Block	Amps	Temp	238 Intensity		Notes
			x10 ⁻¹² Amps	Std Error	
291	4.3	2010	4.80	0.00031	
292	4.3	2010	4.80	0.00023	
293	4.3	2011	5.20	0.00038	
294	4.3	2011	5.20	0.00021	
295	4.3	2012	5.50	0.00039	
296	4.3	2012	5.50	0.00022	
297	4.3	2012	5.50	0.00025	
298	4.3	2013	5.50	0.00024	
299	4.3	2013	5.50	0.00043	
300	4.3	2014	5.50	0.00024	
Grand Mean				0.9965747	0.000024

DTG 2/20/00 22:37

Bead: S95P-1, B

Block	Amps	Temp	238 Intensity		Notes
			x10 ⁻¹² Amps	Std Error	
281	4.2	1984	2.6	0.00024	
282	4.2	1985	2.6	0.00041	
283	4.2	1985	2.6	0.00030	
284	4.2	1985	2.6	0.00053	
285	4.2	1985	2.6	0.00060	
286	4.2	1986	2.6	0.00032	
287	4.2	1986	2.9	0.00025	
288	4.2	1986	2.9	0.00035	
289	4.2	1987	3.2	0.00062	
290	4.2	1987	3.2	0.00031	
Grand Mean				0.9959503	0.000015

DTG 2/20/00 23:29
Bead: S95P-1, D

Block	Amps	Temp	238 Intensity x10 ⁻¹² Amps
301	4.33	2021	6.3
302	4.33	2021	6.3
303	4.33	2022	6.3
304	4.33	2022	6.3
305	4.33	2023	6.3
306	4.33	2023	6.3
307	4.33	2024	6.2
308	4.33	2024	6.2
309	4.33	2025	6.2
310	4.33	2025	6.2
Grand Mean			

DTG 2/20/00 23:55
Bead: S95P-1, E

Block	Amps	Temp	238 Intensity x10 ⁻¹² Amps	238/235	Std Error	Notes
311	4.41	2030	9.10	0.9980018	0.000025	
312	4.41	2030	8.80	0.9980445	0.000016	
313	4.41	2030	8.80	0.9981575	0.000016	
314	4.41	2030	8.60	0.9982126	0.000027	
315	4.41	2030	Not Available	0.9984200	0.000026	Not available due to printer error.
316	4.41	2030	Not Available	0.9984066	0.000023	Data from electronic backup
317	4.41	2030	Not Available	0.9985786	0.000030	
318	4.41	2030	Not Available	0.9986043	0.000025	
319	4.41	2030	Not Available	0.998755	0.000018	
320	4.41	2030	Not Available	0.9988199	0.000028	
Grand Mean				0.9983959	0.000029	

Appendix 4, Annex H-1

DTG 2/20/00 0:21
Bead: S95P-1, F

Block	Amps	Temp	238 Intensity x10 ⁻¹² Amps
321	Not Available		Not Available
322	Not Available		Not Available
323	Not Available		Not Available
324	Not Available		Not Available
325	Not Available		Not Available
326	Not Available		Not Available
327	Not Available		Not Available
328	Not Available		Not Available
329	Not Available		Not Available
330	Not Available		Not Available
Grand Mean			

DTG 2/21/00 9:07
Bead: C0S-2, A

Block	Amps	Temp	238 Intensity x10 ⁻¹² Amps	238/235	Std Error	Notes
171	4.65	1962	2.00	0.9986004	0.000115	
172	4.65	1963	2.30	0.9988747	0.000028	
173	4.65	1963	1.80	0.9990008	0.000047	
174	4.65	1962	1.40	0.9990385	0.000028	
175	4.65	1962	1.20	0.9992231	0.000084	
176	4.65	1961	1.00	0.9990289	0.000091	
177	4.65	1961	0.92	0.9993442	0.000120	
178	4.65	1960	0.85	0.9995373	0.000064	
179	4.65	1957	0.86	0.9998374	0.000089	
180	4.65	1955	0.85	0.9974425	0.000071	
181	4.775	1980	1.30	0.9976120	0.000098	Refocus/A
182	4.775	1982	1.40	0.9974693	0.000074	mp
183	4.775	1983	1.40	0.9973356	0.000072	Change
184	4.775	1984	1.50	0.9975479	0.000044	
185	4.775	1985	1.50	0.9984735	0.000077	
186	4.775	1985	1.50	0.9976383	0.000043	
187	4.775	1985	1.50	0.9973955	0.000047	
188	4.775	1985	1.50	0.9975246	0.000064	
189	4.775	1985	1.50	0.9976934	0.000094	
190	4.775	1985	1.50	0.9978960	0.000056	
Grand Mean				0.9982418	0.000061	

Appendix 4, Annex H-1

DTG 2/21/00 10:21
Bead: S24P-1, A

Block	Amps	Temp	238 Intensity x10 ⁻¹² Amps
351	4.3	1904	0.22
352	4.3	1903	0.22
353	4.3	1904	0.27
354	4.3	1904	0.26
355	4.3	1904	0.28
356	4.3	1904	0.27
357	4.3	1904	0.29
358	4.3	1904	0.28
359	4.3	1904	0.29
360	4.3	1904	0.28
361	4.3	1904	0.32
362	4.3	1904	0.32
363	4.33	1911	0.31
364	4.33	1912	0.36
365	4.33	1912	0.36
366	4.33	1912	0.35
367	4.33	1911	0.35
368	4.33	1912	0.35
369	4.33	1911	0.34
370	4.33	1912	0.34

DTG 2/21/00 11:13
Bead: S24P-1, B

Block	Amps	Temp	238 Intensity x10 ⁻¹² Amps	238/235	Std Error	Notes
371	4.43	1935	0.52	0.9973268	0.000149	
372	4.43	1935	0.51	0.9969769	0.000097	
373	4.43	1935	0.50	0.9968167	0.000098	
374	4.43	1935	0.49	0.9971454	0.000155	
375	4.43	1935	0.49	0.996958	0.000124	
376	4.43	1935	0.48	0.9972348	0.000127	
377	4.43	1935	0.48	0.9965762	0.000115	
378	4.43	1934	0.48	0.9964472	0.000140	
379	4.43	1933	0.48	0.9964363	0.000157	
380	4.43	1932	0.47	0.9969386	0.000156	
Grand Mean				0.9969362	0.000047	

Appendix 4, Annex H-1

DTG 2/21/00 11:39
Bead: S24P-1, C

Block	Amps	Temp	238 Intensity $\times 10^{-12}$ Amps
381	4.57	1963	0.85
382	4.57	1963	0.84
383	4.57	1962	0.84
384	4.57	1962	0.84
385	4.57	1961	0.83
386	4.57	1961	0.82
387	4.57	1961	0.84
388	4.57	1960	0.83
389	4.57	1960	0.83
390	4.57	1960	0.83
Grand Mean			

DTG 2/21/00 12:05
Bead: S24P-1, D

Block	Amps	Temp	238 Intensity $\times 10^{-12}$ Amps	Std Error	Notes	238/235	Std Error	Notes
391	4.75	1998	1.70	0.000072		0.9969629	0.000072	
392	4.75	1998	1.50	0.000080		0.9971683	0.000080	
393	4.75	1999	1.70	0.000058		0.9968193	0.000058	
394	4.75	1998	1.70	0.000076		0.9969305	0.000076	
395	4.75	1997	1.60	0.000098		0.9972718	0.000098	
396	4.75	1997	1.40	0.000109		0.9969920	0.000109	
397	4.75	1997	1.50	0.000066		0.9967508	0.000066	
398	4.75	1997	1.40	0.000059		0.9971732	0.000059	
399	4.75	1996	1.80	0.000058		0.9970523	0.000058	
400	4.75	1996	1.80	0.000087		0.9972544	0.000087	
Grand Mean				0.000028		0.9970306	0.000028	

DTG 2/21/00 18:28
Bead: S4S-2,A

Block	Amps	Temp	238 Intensity $\times 10^{-12}$ Amps
401	4.3	1913	1.40
402	4.3	1915	1.40
403	4.3	1918	1.40
404	4.3	1919	1.40
405	4.3	1921	1.50
406	4.3	1922	1.50
407	4.3	1924	1.50
408	4.3	1925	1.50
409	4.3	1926	1.60
410	4.3	1927	1.60
Grand Mean			

DTG 2/21/00 18:55
Bead: S4S-2,B

Block	Amps	Temp	238 Intensity $\times 10^{-12}$ Amps	Std Error	Notes	238/235	Std Error	Notes
411	4.35	1939	2.00	0.000064		0.9945504	0.000064	
412	4.35	1940	2.00	0.000067		0.9946453	0.000067	
413	4.35	1942	0.76	0.002753	WEIRD	0.9976599	0.002753	
414	4.35	1943	0.76	0.000073		0.9951344	0.000073	
415	4.35	1945	1.90	0.000057		0.9954377	0.000057	
416	4.35	1946	1.90	0.000138		1.0064144	0.000138	
417	4.35	1947	1.90	0.000043		0.9957765	0.000043	
418	4.35	1949	1.90	0.000054		0.9960260	0.000054	
419	4.35	1950	1.90	0.000078		0.9961419	0.000078	
420	4.35	1951	1.90	0.000054		0.9963843	0.000054	
Grand Mean				0.000036		0.9970136	0.000036	

Appendix 4, Annex H-1

DTG 2/21/00 19:25
Bead: S4S-2,C

Block	Amps	Temp	238 Intensity x10 ⁻¹² Amps	Notes	Std Error	238/235	Std Error	Notes
421	4.4	1965	2.30		0.00040	0.9973175	0.00040	
422	4.4	1966	2.30		0.00083	0.9974354	0.00083	
423	4.4	1968	2.30		0.00055	0.9973961	0.00055	
424	4.4	1969	2.20		0.00059	0.9974864	0.00059	
425	4.4	1971	2.20		0.00081	0.9975731	0.00081	
426	4.4	1972	2.20		0.00066	0.9976095	0.00066	
427	4.4	1973	2.20		0.00043	0.9977047	0.00043	
428	4.4	1975	2.20		0.00057	0.9978937	0.00057	
429	4.45	1987	2.20		0.00027	0.9979554	0.00027	
430	4.45	1988	2.70		0.00046	0.9980512	0.00046	
431	4.45	1990	2.70		0.00032	0.9978555	0.00032	
432	4.45	1992	2.70		0.00033	0.9979479	0.00033	
433	4.45	1994	2.70		0.00048	0.9980857	0.00048	
434	4.45	1995	2.60		0.00033	0.9981589	0.00033	
435	4.45	1997	2.60		0.00033	0.9980722	0.00033	
436	4.45	1998	2.60		0.00035	0.9980897	0.00035	
437	4.45	2000	2.60		0.00044	0.9979538	0.00044	
438	4.45	2002	2.60		0.00039	0.9979829	0.00039	
Grand Mean						0.9978236	0.00022	

DTG 2/21/00 20:14
Bead: S4S-2,D

Block	Amps	Temp	238 Intensity x10 ⁻¹² Amps	Notes	Std Error	238/235	Std Error	Notes
439	4.5	2014	3.20		0.00030	0.9980441	0.00030	
440	4.5	2016	3.10		0.00027	0.9979502	0.00027	
441	4.5	2018	3.10		0.00044	0.9980986	0.00044	
442	4.5	2018	3.10		0.00054	0.9981129	0.00054	
443	4.5	2021	3.10		0.00032	0.9981607	0.00032	
Grand Mean						0.9980678	0.00019	

Appendix 4, Annex H-1

DTG 2/21/00 20:28
Bead: S4S-2,E

Block	Amps	Temp	238 Intensity x10 ⁻¹² Amps
444	4.55	2030	3.80
445	4.55	2030	3.70
446	4.55	2030	3.70
447	4.55	2030	3.70
448	4.55	2030	3.70
Grand Mean			

DTG 2/21/00 20:42
Bead: S4S-2,F

Block	Amps	Temp	238 Intensity x10 ⁻¹² Amps	Notes	Std Error	238/235	Std Error	Notes
2037	4.6	2030	4.60	2037	0.000070	0.9983534	0.000029	
450	4.6	2030	4.60		0.000147	0.9990356	0.000031	
451	4.6	2030	4.60		0.000043	0.9984243	0.000041	
452	4.6	2030	4.60		0.000054	0.9984235	0.000023	
453	4.65	2030	4.40		0.000038	0.9986064	0.000032	2072
454	4.65	2030	5.40		0.000032	0.9991326	0.000025	
455	4.65	2030	5.20		0.000038	0.9992207	0.000028	
456	4.65	2030	5.20		0.000035	0.9993392	0.000035	
457	4.7	2030	5.00		0.000027	0.9993619	0.000027	2090
458	4.7	2030	6.00		0.000020	0.9994580	0.000020	
459	4.7	2030	5.90		0.000095	0.9998213	0.000095	
460	4.7	2030	5.90		0.000020	0.9997081	0.000020	
Grand Mean						0.9991635	0.000031	

DTG 2/21/00 21:30
Bead: S8S-2,A

Block	Amps	Temp	238 Intensity x10 ⁻¹² Amps
461	4.3	1859	1.90
462	4.3	1861	1.70
463	4.3	1864	1.80
464	4.3	1866	1.70
465	4.3	1867	1.70
Grand Mean			

DTG 2/21/00 21:43
Bead: S8S-2,B

Block	Amps	Temp	238 Intensity x10 ⁻¹² Amps	Notes	Std Error	238/235	Std Error	Notes
466	4.35	1880	2.10		0.000023	0.9945352	0.000069	
467	4.35	1881	2.10		0.000045	0.9947195	0.000059	
468	4.35	1882	2.10		0.000040	0.9949782	0.000035	
469	4.35	1883	2.10		0.000045	0.9951146	0.000031	
470	4.35	1883	2.10		0.000059	0.9953480	0.000026	
Grand Mean						0.9949181	0.000042	

Appendix 4, Annex H-1

DTG 2/21/00 21:56
Bead: S8S-2,C

Block	Amps	Temp	238 Intensity x10 ⁻¹² Amps	238/235	Std Error	Notes	Block	Amps	Temp	238 Intensity x10 ⁻¹² Amps	238/235	Std Error	Notes
471	4.4	1897	2.60	0.9959585	0.000058		476	4.45	1919	3.50	0.9968299	0.000053	
472	4.4	1898	2.60	0.9960376	0.000045		477	4.45	1919	3.40	0.9969971	0.000021	
473	4.4	1904	2.60	0.9961079	0.000033		478	4.45	1920	3.40	0.9971939	0.000042	
474	4.4	1904	2.80	0.9964018	0.000058		479	4.45	1921	3.40	0.9971919	0.000046	
475	4.4	1906	2.80	0.9964716	0.000036		480	4.45	1922	3.30	0.9973742	0.000039	
Grand Mean				0.9961995	0.0034		Grand Mean				0.9971372	0.000030	

DTG 2/21/00 22:28
Bead: S8S-2,E

Block	Amps	Temp	238 Intensity x10 ⁻¹² Amps	238/235	Std Error	Notes	Block	Amps	Temp	238 Intensity x10 ⁻¹² Amps	238/235	Std Error	Notes
481	4.5	1933	4.10	0.9974052	0.000056		486	4.6	1960	5.40	0.9984081	0.000027	
482	4.5	1934	4.00	0.9976162	0.000024		487	4.6	1962	5.30	0.9984777	0.000031	
483	4.5	1935	4.00	0.9977030	0.000038		488	4.6	1963	5.20	0.9985736	0.000036	
484	4.5	1936	3.90	0.9978058	0.000050		489	4.6	1964	5.10	0.9986361	0.000030	
485	4.5	1937	3.80	0.9979314	0.000040		490	4.6	1965	5.00	0.9986886	0.000036	
Grand Mean				0.9977088	0.000029		Grand Mean				0.9985504	0.000019	

DTG 2/21/00 23:05
Bead: S8S-2,G

Block	Amps	Temp	238 Intensity x10 ⁻¹² Amps	238/235	Std Error	Notes	Block	Amps	Temp	238 Intensity x10 ⁻¹² Amps	238/235	Std Error	Notes
491	4.7	1987	7.20	0.9989206	0.000021		496	4.8	2024	8.50	0.9994949	0.000023	
492	4.7	1989	7.10	0.9990776	0.000025		497	4.8	2027	8.30	0.9995893	0.000030	
493	4.7	1991	6.90	0.9990861	0.000013		498	4.8	2029	8.10	0.9996571	0.000018	
494	4.7	1993	6.80	0.9991649	0.000025		499	4.8	2030	8.00	0.9997184	0.000017	
495	4.7	1995	6.70	0.9991915	0.000012		500	4.8	2030	7.90	0.9999582	0.000039	
Grand Mean				0.9990873	0.000016		Grand Mean				0.9996540	0.000021	

Appendix 4, Annex H-1

DTG 2/21/00 23:58
Bead: S24S-2,A

Block	Amps	Temp	238 Intensity x10 ⁻¹² Amps
501	4.3	1894	3.50
502	4.3	1896	3.10
503	4.3	1898	2.90
504	4.3	1899	2.80
505	4.3	1901	2.60
Grand Mean			

DTG 2/22/00 0:11
Bead: S24S-2,B

Block	Amps	Temp	238 Intensity x10 ⁻¹² Amps	Std Error	Notes	238/235	Std Error	Notes
506	4.35	1913	3.20	0.000031		0.9951043	0.000031	
507	4.35	1914	3.00	0.000044		0.9954883	0.000044	
508	4.35	1916	3.10	0.000028		0.9958505	0.000028	
509	4.35	1917	3.00	0.000067		0.9961001	0.000067	
510	4.35	1917	3.00	0.000044		0.9964804	0.000044	
Grand Mean				0.000073		0.9958040	0.000073	

DTG 2/22/00 0:25
Bead: S24S-2,C

Block	Amps	Temp	238 Intensity x10 ⁻¹² Amps	Std Error	Notes	238/235	Std Error	Notes
511	4.4	1930	3.70	0.000059		0.9976566	0.000059	
512	4.4	1932	3.60	0.000031		0.9979897	0.000031	
513	4.4	1934	3.50	0.000042		0.998269	0.000042	
514	4.4	1935	3.40	0.000016		0.9985306	0.000016	
515	4.4	1938	3.40	0.000032		0.9984439	0.000032	
Grand Mean				0.000045		0.9982133	0.000045	

DTG 2/22/00 0:38
Bead: S24S-2,D

Block	Amps	Temp	238 Intensity x10 ⁻¹² Amps	Std Error	Notes	238/235	Std Error	Notes
516	4.45	1951	4.20	0.000035		0.9987676	0.000035	
517	4.45	1952	4.10	0.000032		0.9989063	0.000032	
518	4.45	1954	4.00	0.000028		0.9989597	0.000028	
519	4.45	1956	3.90	0.000046		0.9990845	0.000046	
520	4.45	1958	3.80	0.000024		0.9990596	0.000024	
Grand Mean				0.000021		0.9989626	0.000021	

DTG 2/22/00 0:51
Bead: S24S-2,E

Block	Amps	Temp	238 Intensity x10 ⁻¹² Amps	Std Error	Notes	238/235	Std Error	Notes
521	4.5	1970	4.60	0.000045		0.9993447	0.000045	
522	4.5	1971	4.50	0.000047		0.9994258	0.000047	
523	4.5	1973	4.40	0.000046		0.9995365	0.000046	
524	4.5	1974	4.30	0.000025		0.9996093	0.000025	
525	4.5	1976	4.20	0.000043		0.9995661	0.000043	
Grand Mean				0.000021		0.9994974	0.000021	

DTG 2/22/00 1:04
Bead: S24S-2,F

Block	Amps	Temp	238 Intensity x10 ⁻¹² Amps	Std Error	Notes	238/235	Std Error	Notes
526	4.6	1996	6.10	0.000034		0.9996883	0.000034	
527	4.6	1998	5.80	0.000039		0.9997316	0.000039	
528	4.6	1998	5.50	0.000024		0.9998892	0.000024	
529	4.6	1999	5.30	0.000023		1.0000349	0.000023	
530	4.6	2000	5.10	0.000042		1.0000577	0.000042	
Grand Mean				0.000025		0.9998882	0.000025	

DTG 2/22/00 1:17
Bead: S24S-2,G

Dead. 3933-Z/A												
238 Intensity						238 Intensity						
Block	Amps	Temp	x10 ⁻¹² Amps	238/235	Std Error	Notes	Block	Amps	Temp	x10 ⁻¹² Amps	238/235	
531	4.7	2021	7.20	1.0001895	0.000029		536	4.35	1889	0.20	1.0004799	
532	4.7	2022	6.90	1.0003375	0.000026		537	4.35	1888	0.16	0.9980257	
533	4.7	2023	6.40	1.0005028	0.000028		538	4.35	1888	0.14	0.9980179	
534	4.7	2024	6.30	1.0005315	0.000021		539	4.35	1889	0.14	0.9987723	
535	4.7	2025	6.00	1.0006449	0.000034		540	4.35	1890	0.14	0.9989313	
Grand Mean							541	4.4	1903	0.16	0.9997544	
							542	4.4	1903	0.15	0.9992723	
							543	4.4	1903	0.15	0.9997550	
							544	4.4	1903	0.14	1.0004189	
							545	4.4	1903	0.14	1.0018125	
							546	4.4	1905	0.14	1.0021487	
							547	4.4	1906	0.13	1.0010510	
							548	4.4	1906	0.13	1.0021750	
							549	4.4	1907	0.13	1.0029728	
							550	4.4	1908	0.13	1.0015506	
							551	4.4	1908	0.13	1.0029935	
							Grand Mean					1.0002989
												0.000154

DTG 2/22/00 9:28
Bead: S95S-2,B

238 Intensity										238 Intensity										
Block	Amps	Temp	238 Intensity x10 ⁻¹² Amps	238/235	Std Error	Notes	Block	Amps	Temp	238 Intensity x10 ⁻¹² Amps	238/235	Std Error	Notes	Block	Amps	Temp	238 Intensity x10 ⁻¹² Amps	238/235	Std Error	Notes
552	4.445	1919	0.13	1.0018098	0.000278		557	4.5	1937	0.18	1.0040104	0.000245		552	4.445	1919	0.13	1.0018098	0.000278	
553	4.445	1919	0.13	1.0026725	0.000350		558	4.5	1940	0.17	1.0039540	0.000378		553	4.445	1919	0.13	1.0026725	0.000350	
554	4.445	1921	0.13	1.0023893	0.000451		559	4.5	1940	0.18	1.0040407	0.000291		554	4.445	1921	0.13	1.0023893	0.000451	
555	4.445	1921	0.13	1.0032057	0.000427		560	4.5	1941	0.18	1.0039469	0.000398		555	4.445	1921	0.13	1.0032057	0.000427	
556	4.445	1922	0.13	1.0036730	0.000366		561	4.5	1942	0.18	1.0051576	0.000198		556	4.445	1922	0.13	1.0036730	0.000366	
Grand Mean				1.0027569	0.000175		Grand Mean							Grand Mean				1.0042062	0.000151	

Appendix 4, Annex H-1

DTG 2/22/00 10:04
Bead: S95S-2,D

Block	Amps	Temp	238 Intensity x10 ⁻¹² Amps
562	4.6	1963	0.30
563	4.6	1964	0.27
564	4.6	1964	0.26
565	4.6	1965	0.26
566	4.6	1965	0.25
Grand Mean			

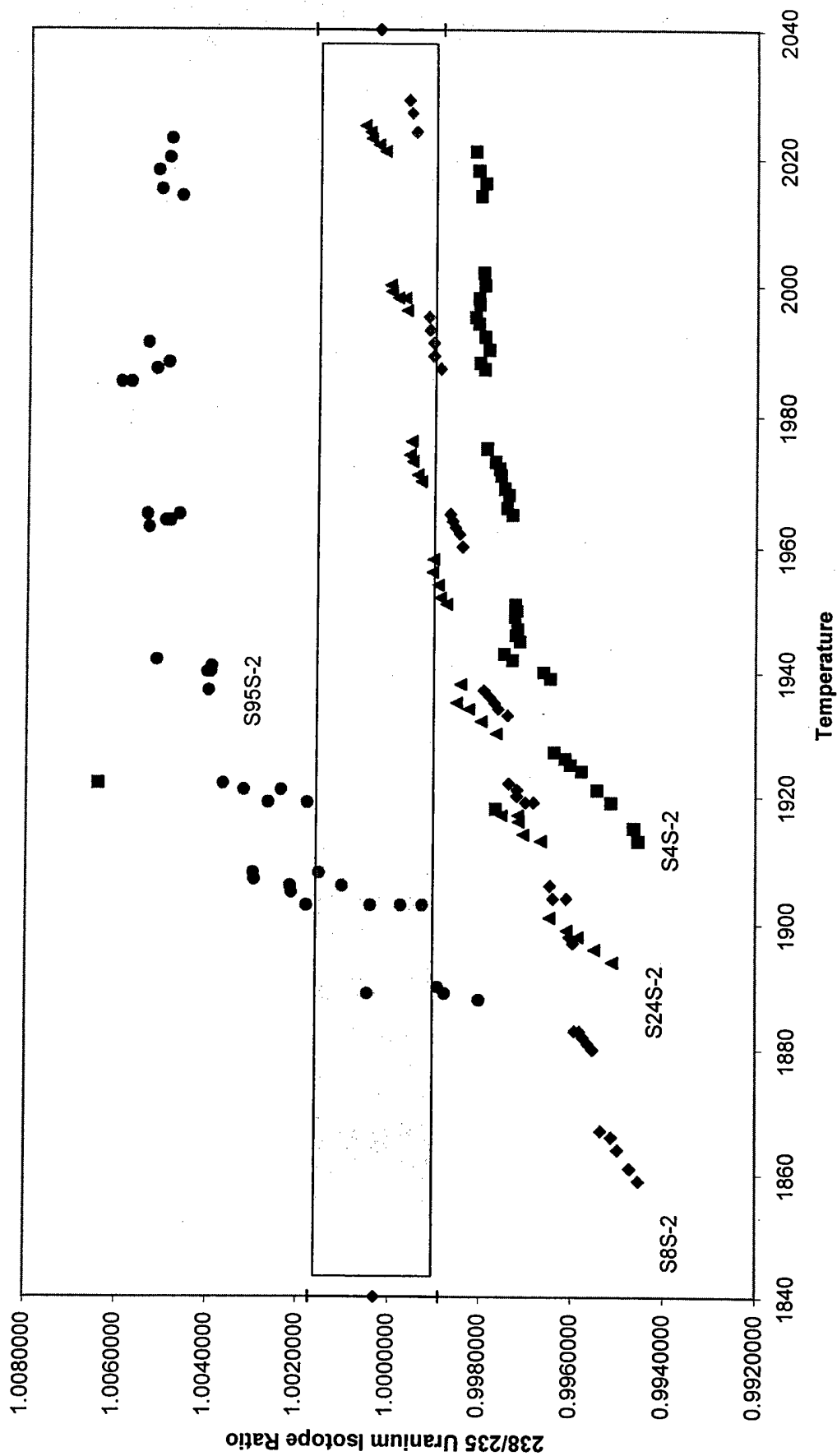
DTG 2/22/00 10:18
Bead: S95S-2,E

Block	Amps	Temp	238 Intensity x10 ⁻¹² Amps	Notes	Std Error	238/235	Std Error	Notes
567	4.7	1985	0.39		0.000181	1.0053408	0.000194	
568	4.7	1985	0.34		0.000115	1.0048769	0.000108	
569	4.7	1987	0.33		0.000311	1.0049737	0.000180	
570	4.7	1988	0.32		0.000173	1.0046829	0.000190	
571	4.7	1991	0.32		0.000159	1.0053769	0.000247	
Grand Mean					0.000095	1.0050478	0.000095	

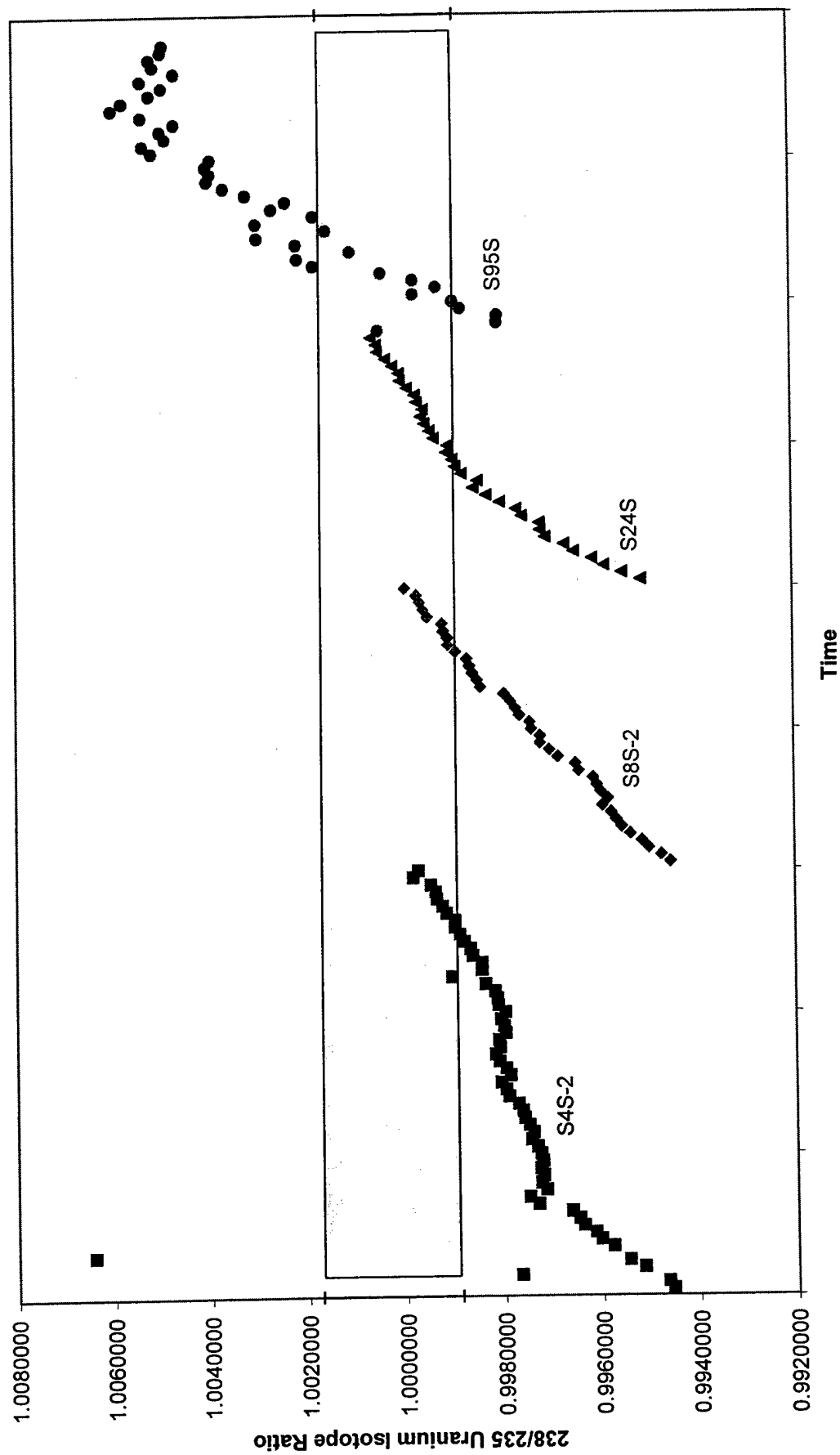
DTG 2/22/00 10:33
Bead: S95S-2,F

Block	Amps	Temp	238 Intensity x10 ⁻¹² Amps	Notes	Std Error	238/235	Std Error	Notes
572	4.8	2014	0.45		0.000219	1.0046760	0.000219	
573	4.8	2015	0.41		0.000117	1.0051176	0.000117	
574	4.8	2018	0.40		0.000107	1.0051962	0.000107	
575	4.8	2020	0.40		0.000150	1.0049549	0.000150	
576	4.8	2023	0.39		0.000094	1.0049118	0.000094	
Grand Mean					0.000059	1.0050259	0.000059	

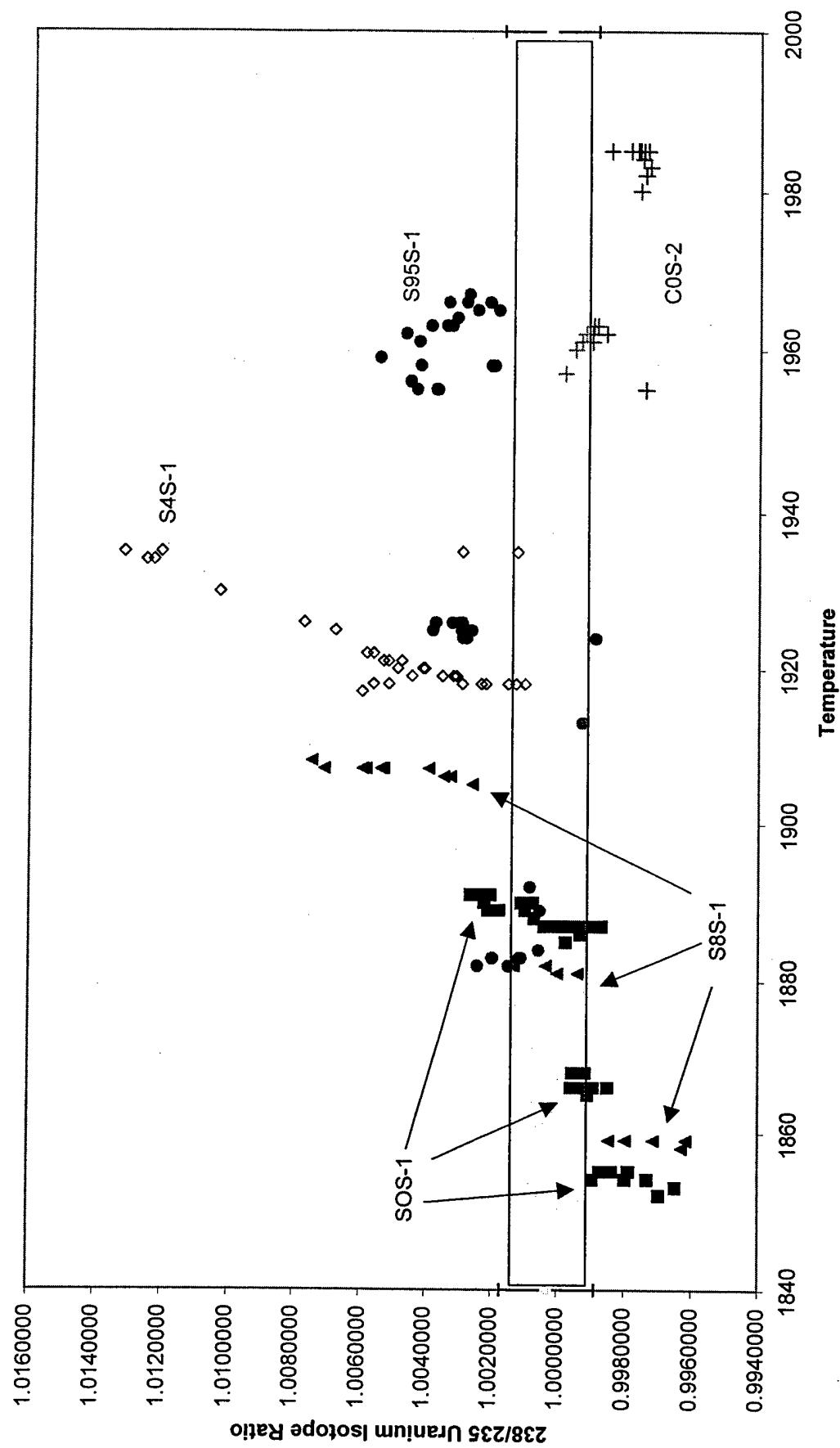
Turret Three through Five
Test Sample Supernatant Isotopic Ratios as a Function of Temperature
Regular Loading



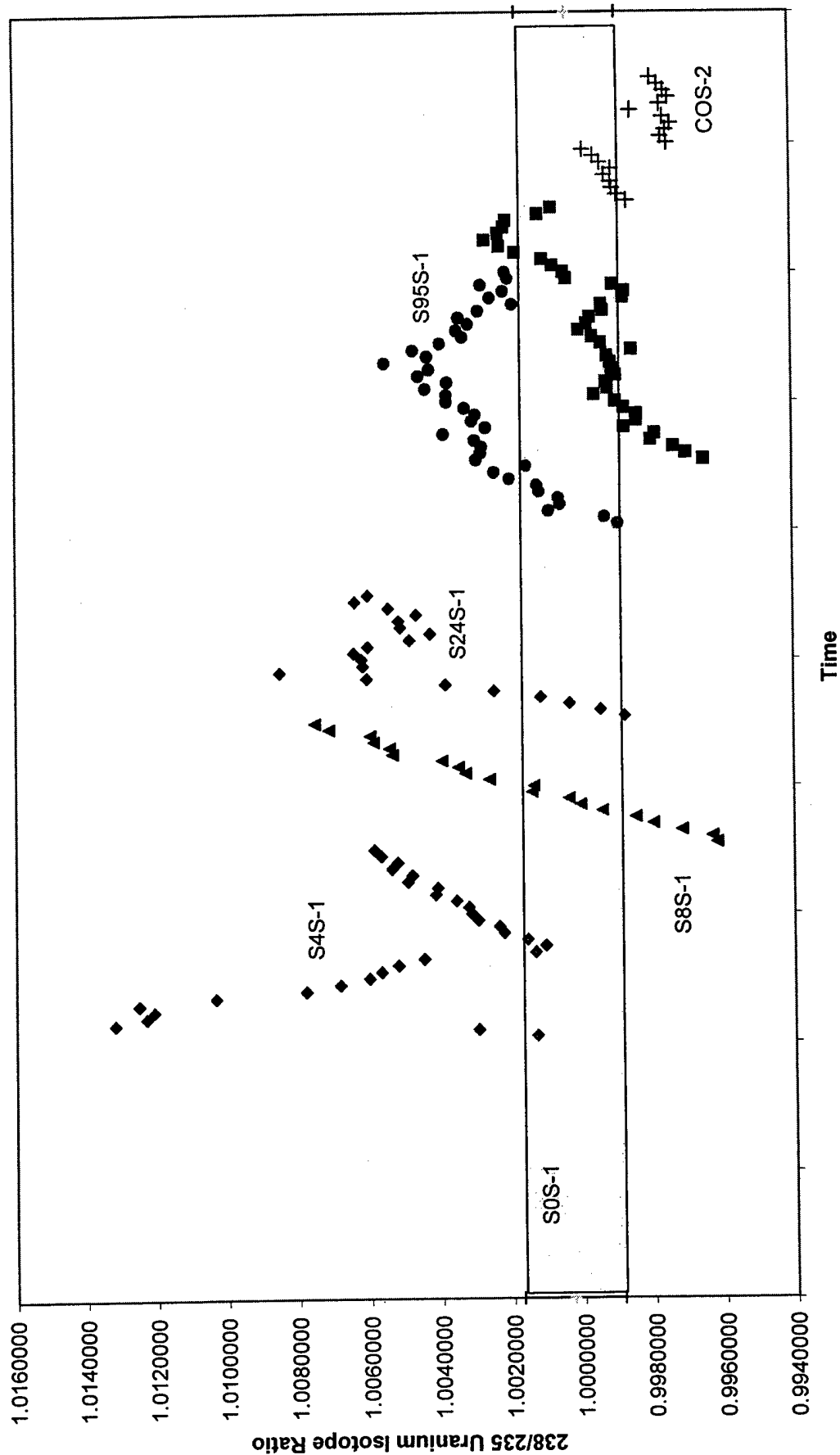
Turret Three through Five
Test Sample Supernatant Isotopic Ratios as a Function of Consecutive Block Measurements: Regular Loading



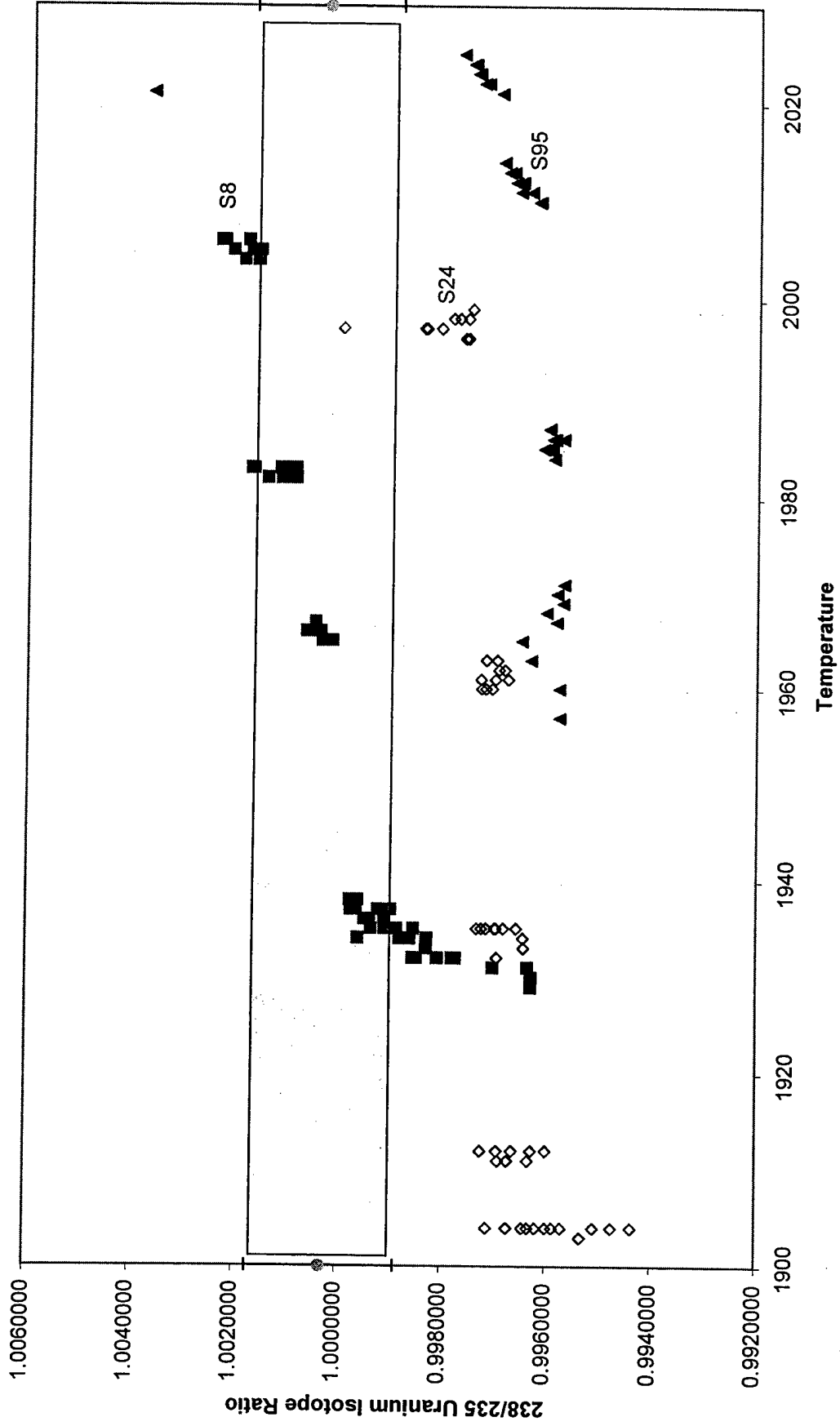
Turret Three through Five
Test Sample Supernatant Isotopic Ratios as a Function of Temperature
Sandwich Loading



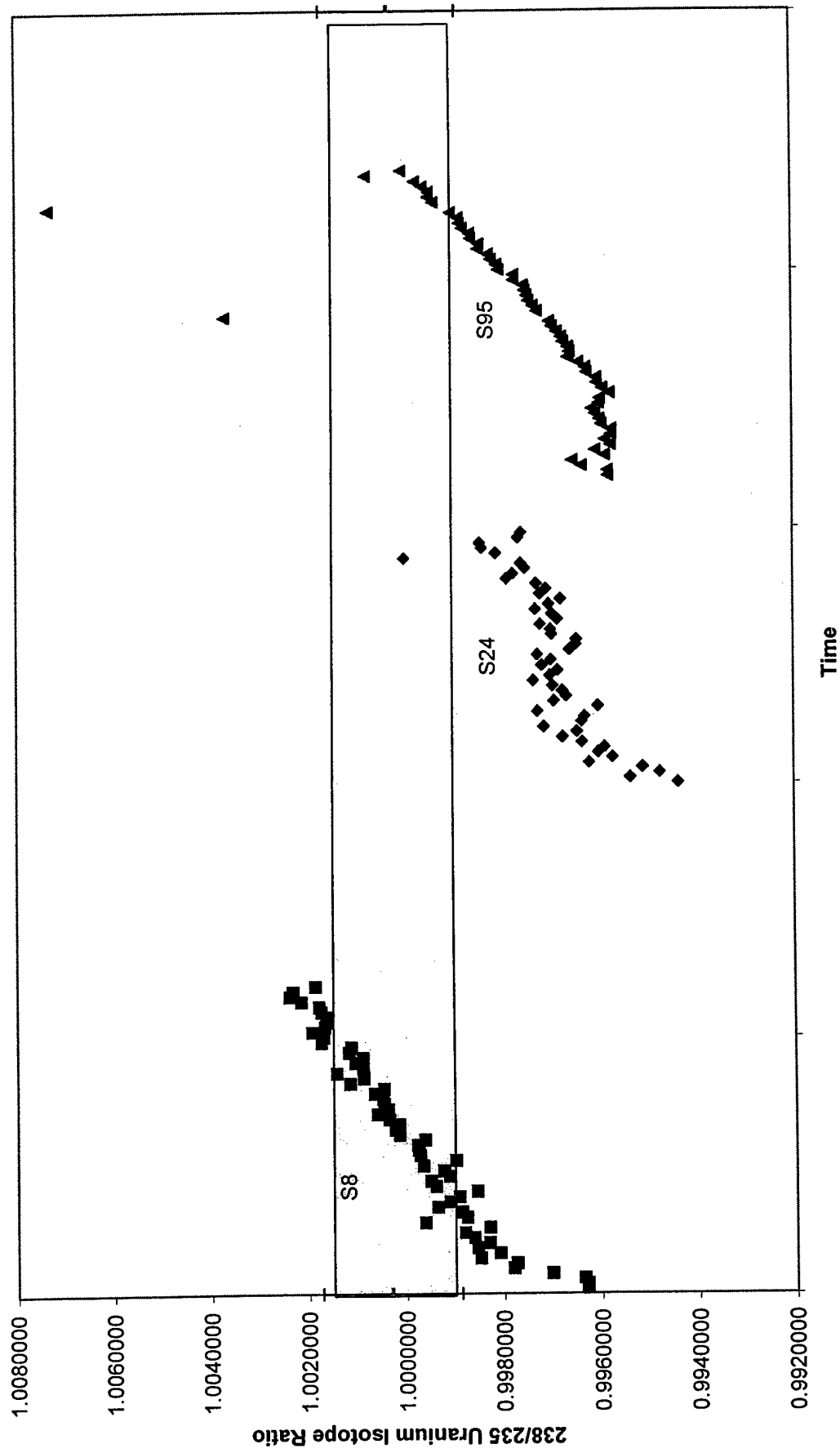
Turret Three through Five
Test Sample Supernatant Isotopic Ratios as a Function of Consecutive Block Measurements: Sandwich Loading



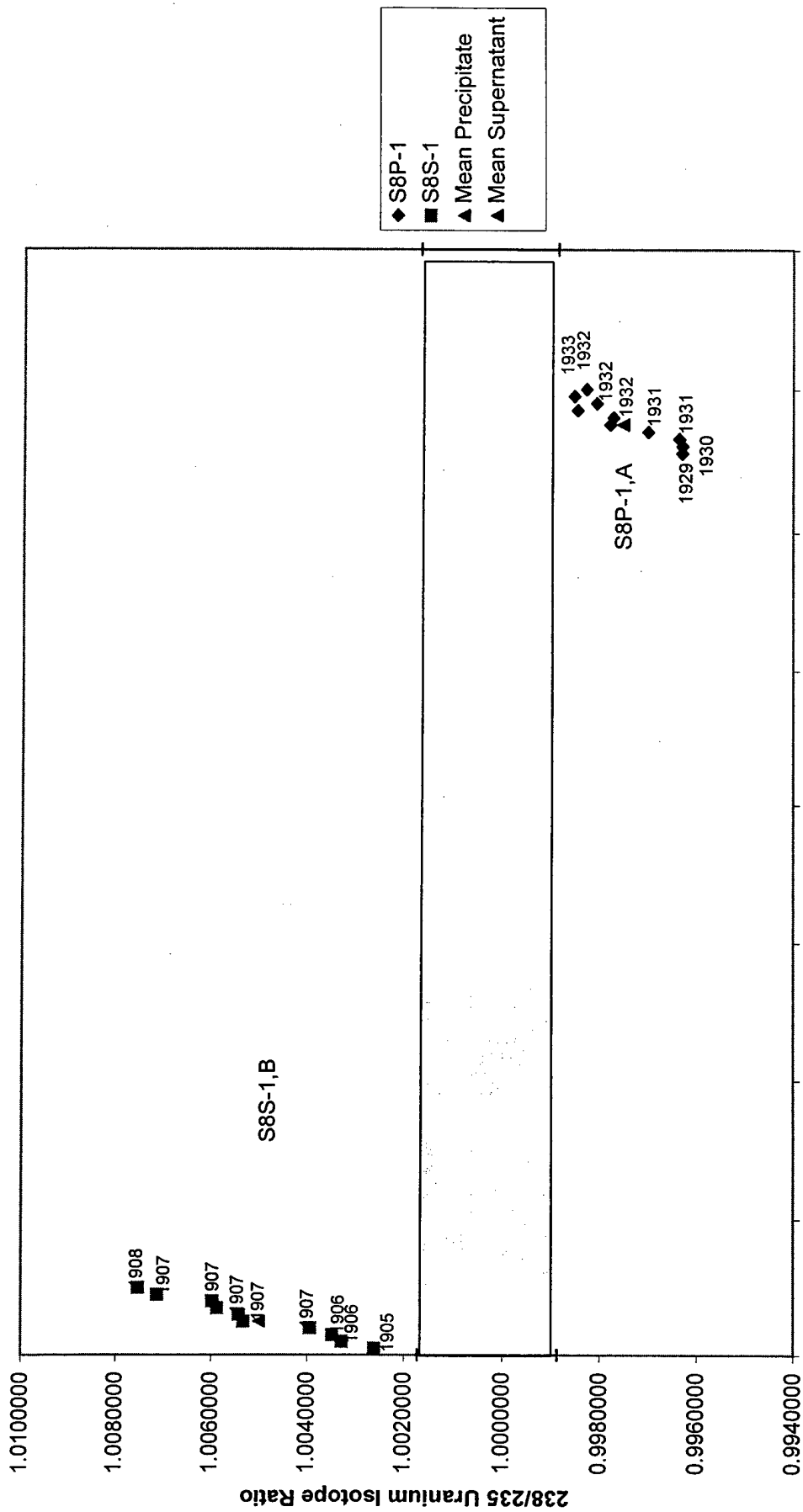
Turret Three through Five
Test Sample Precipitate Isotopic Ratios as a Function of Temperature
Sandwich Loading



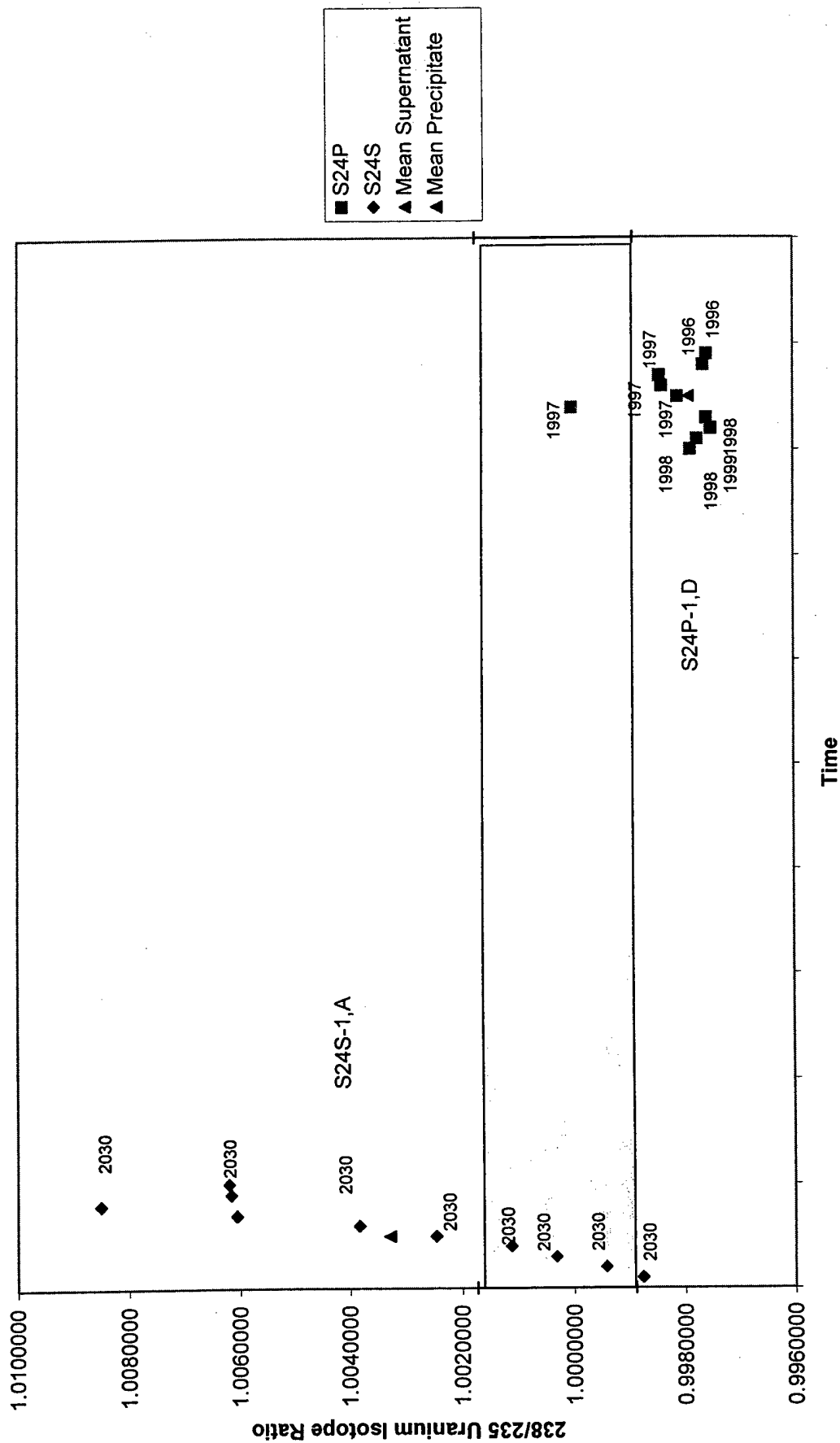
Turret Three through Five
Comparison of Precipitate Isotopic Ratios with Respect to Consecutive Block Measurements



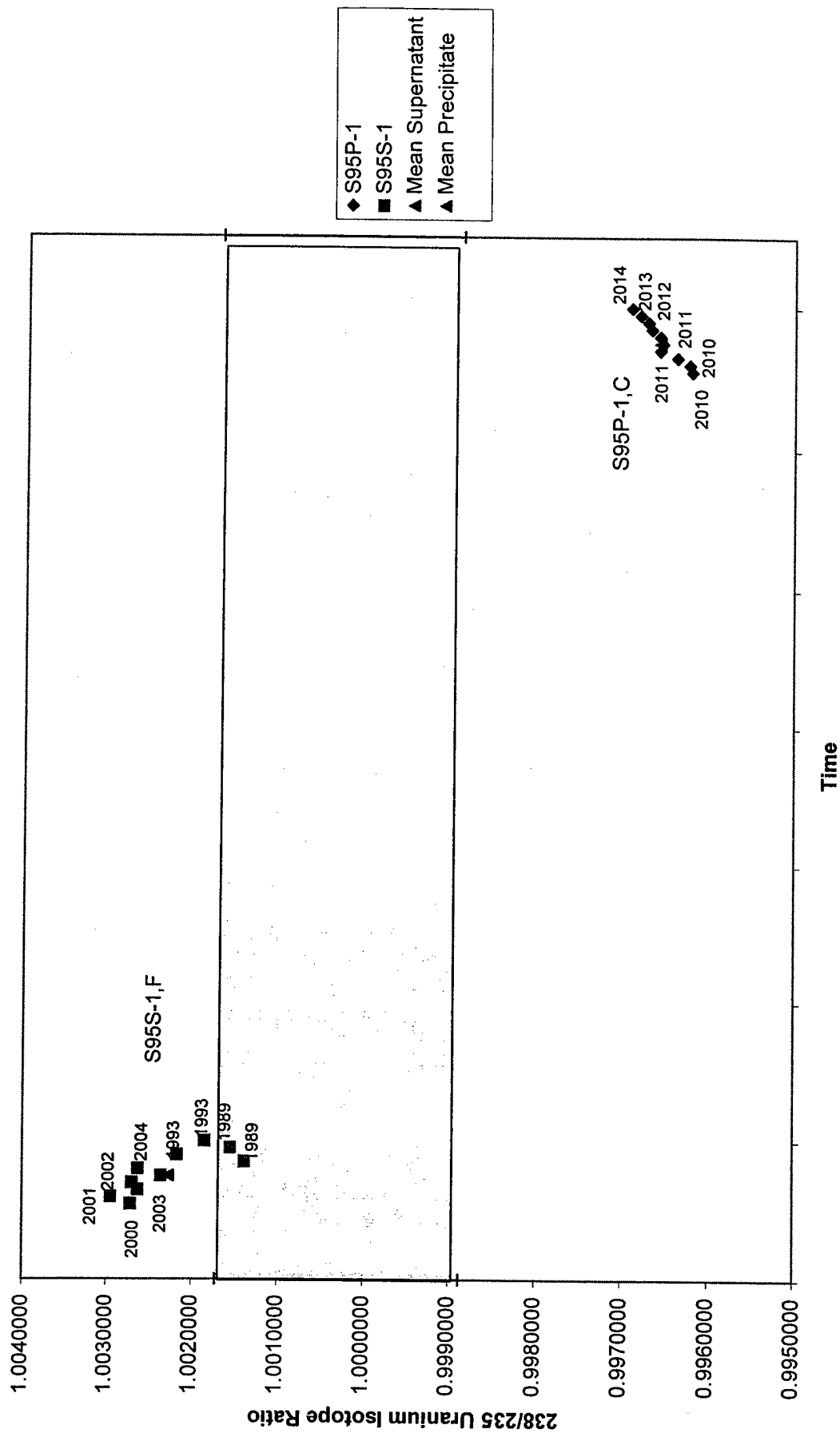
**Turret Three through Five
8 HOUR Supernatant and Precipitate Comparison Sandwich Style**



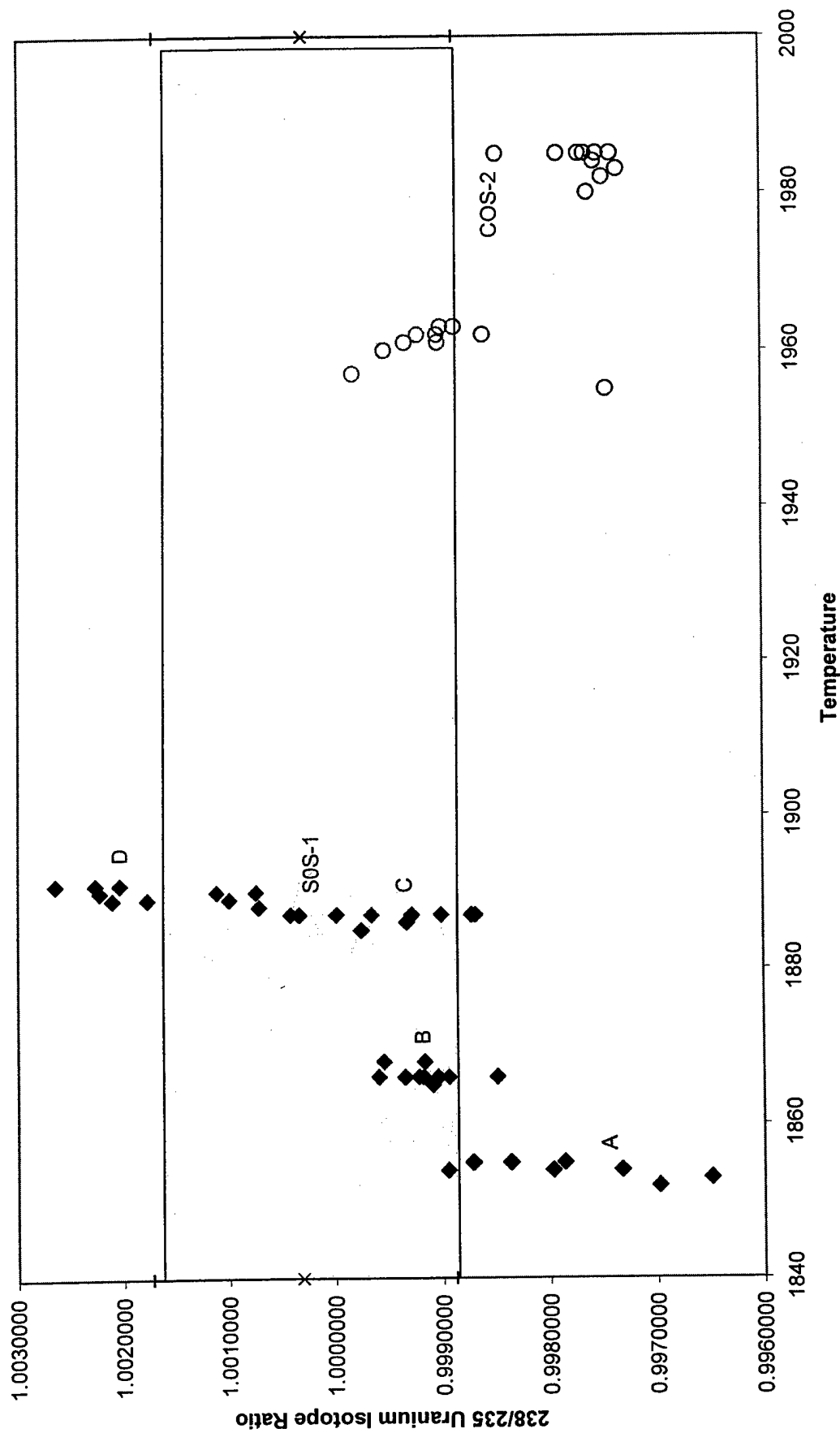
Turret Three through Five
24 HOUR Supernatant and Precipitate Comparison Sandwich Style



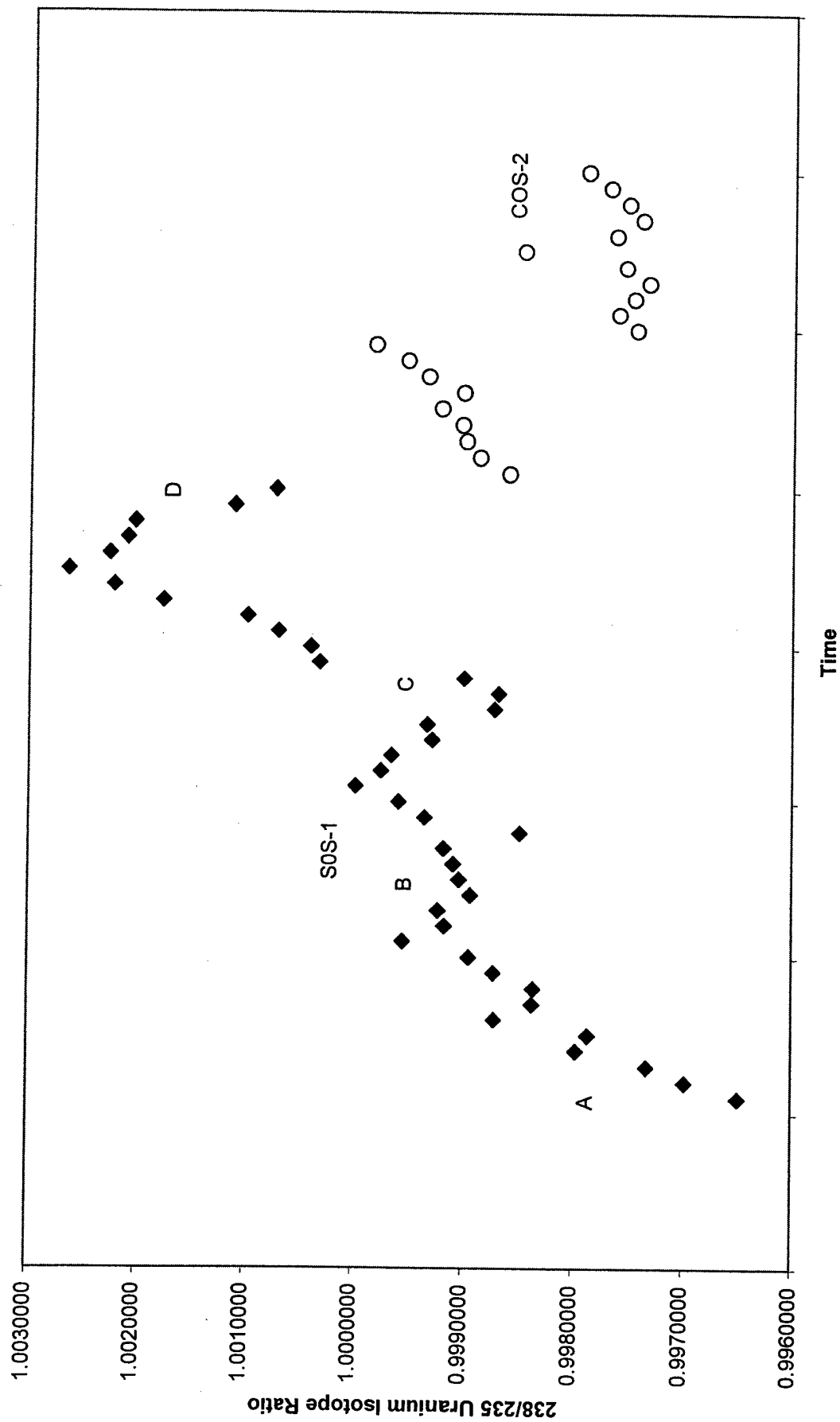
Turret Three through Five
95 HOUR Supernatant and Precipitate Comparison Sandwich Style



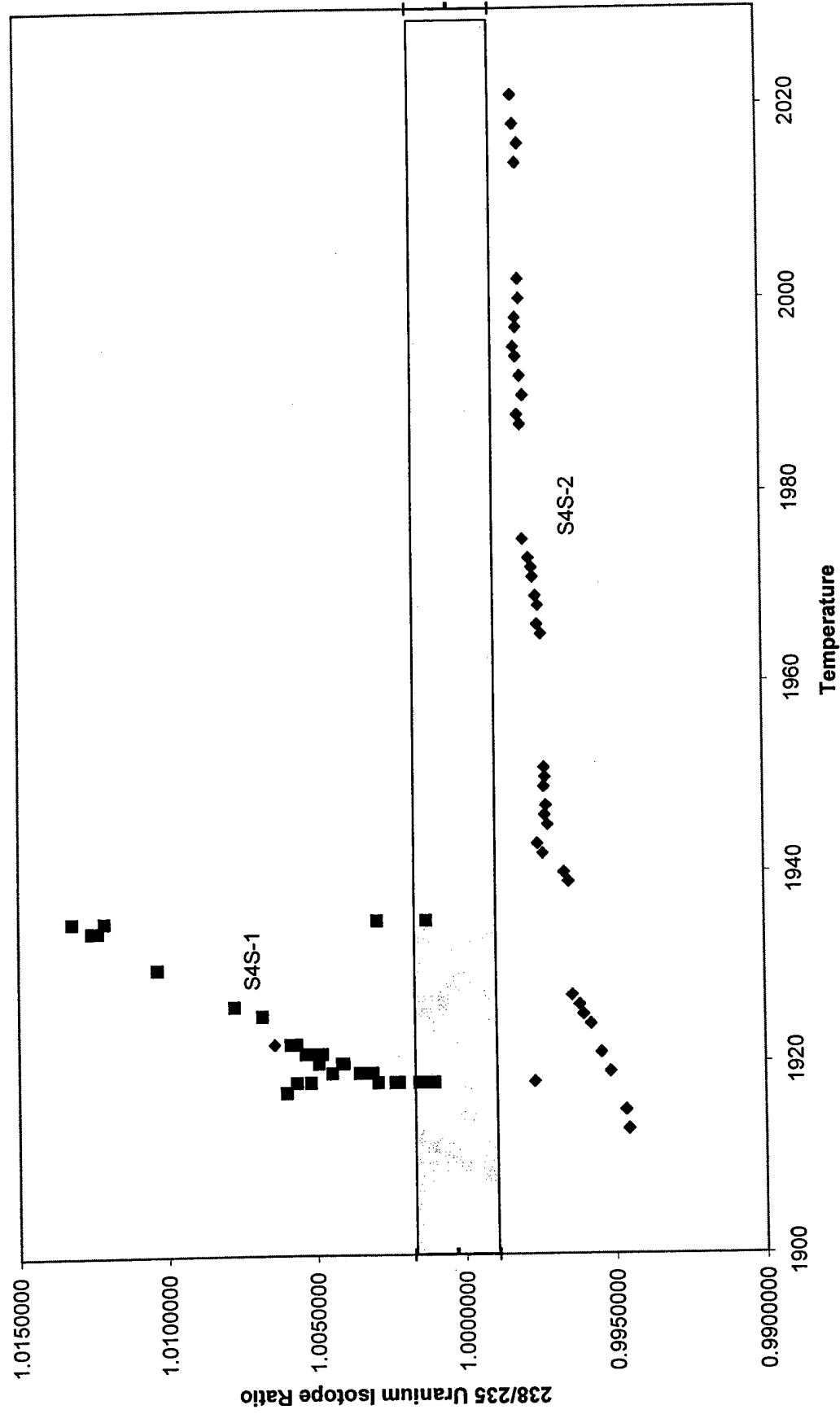
Turret Three through Five
SOS-1 (A-D) , COS-2 Sandwich versus Temperature



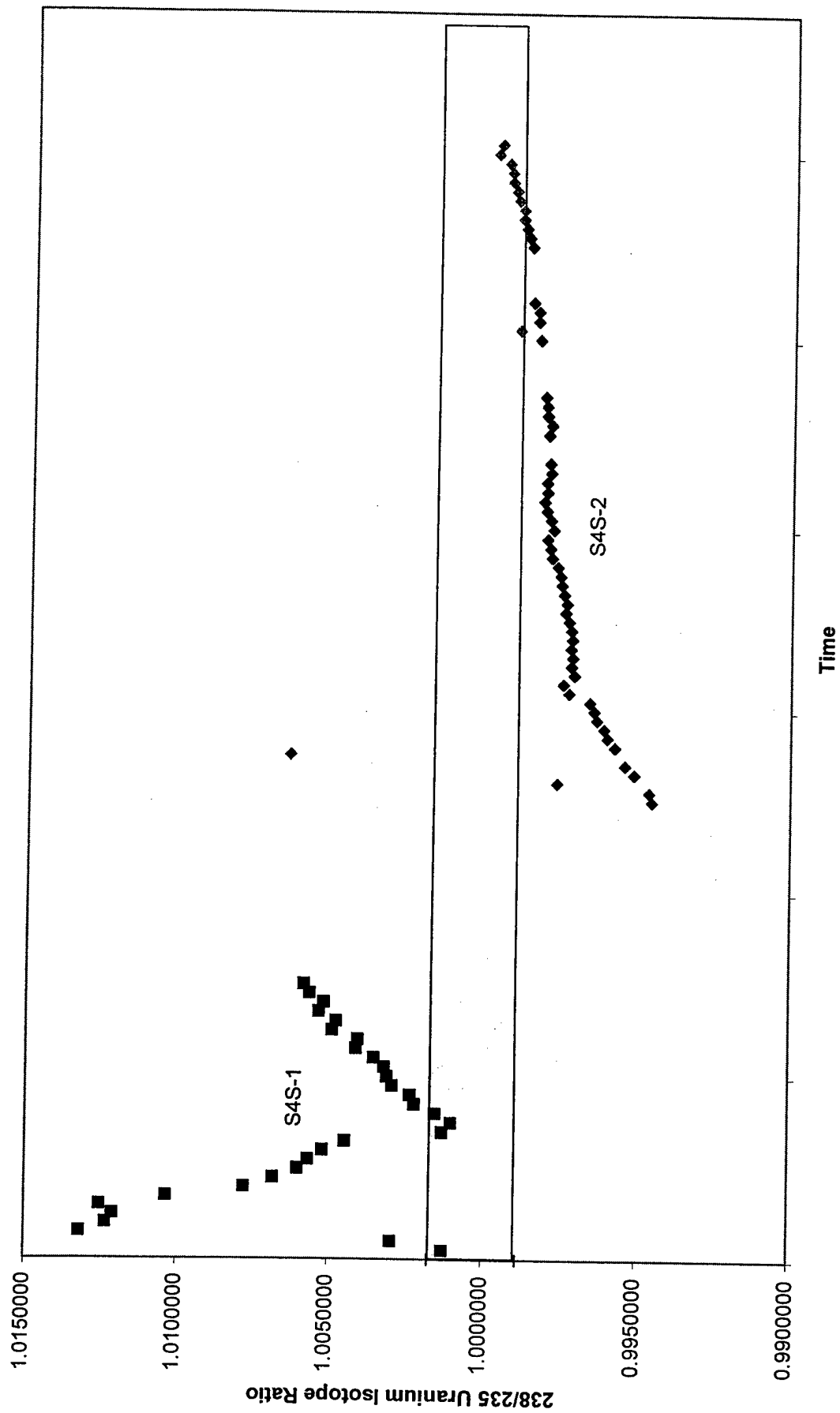
Turret Three through Five
S0S-1 (A-D) , C0S-2 Sandwich versus Consecutive Block Measurements



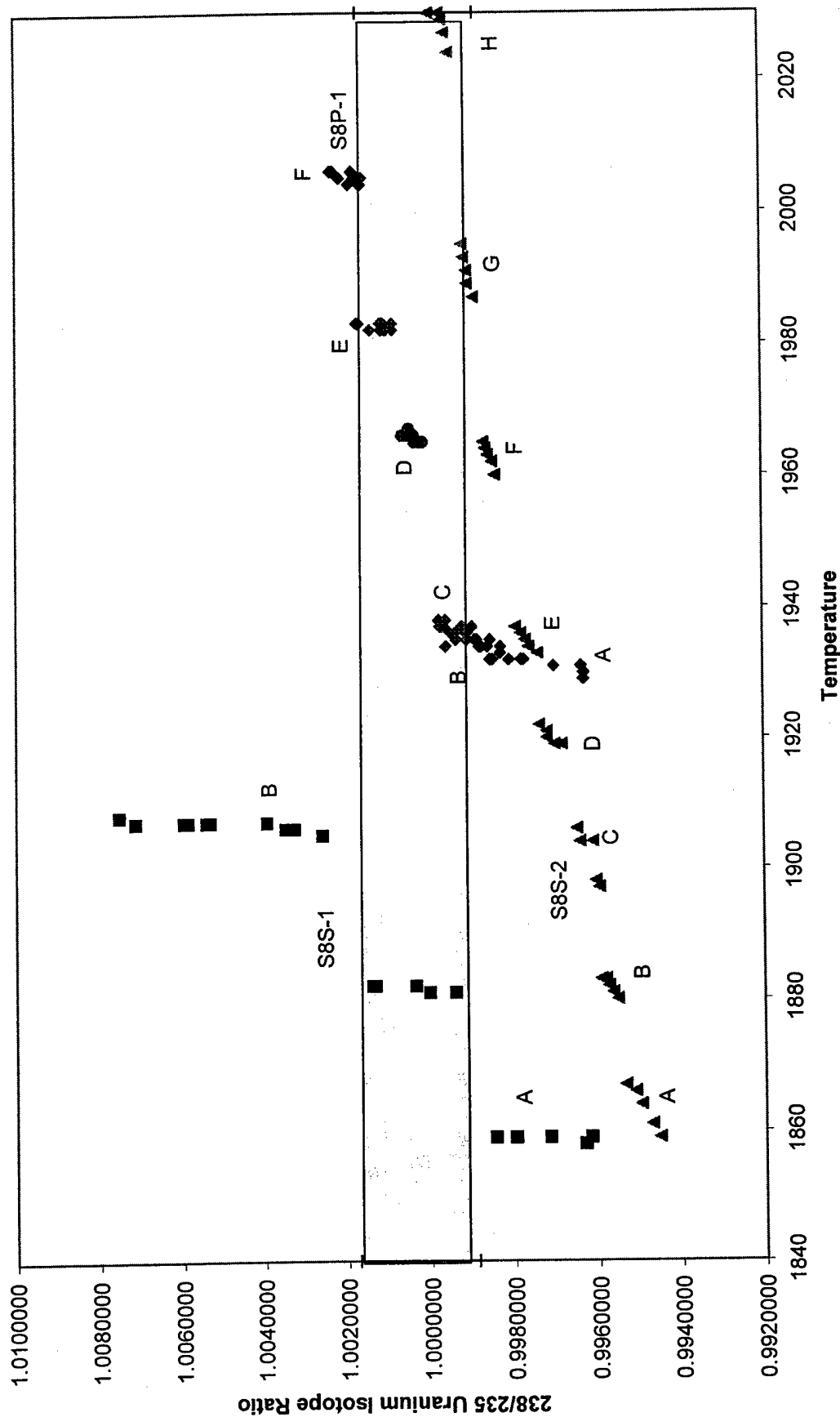
Turret Three through Five
S4S-1 (A-C) Sandwich and S4S-2 (A-F) Regular as a Function of Temperature



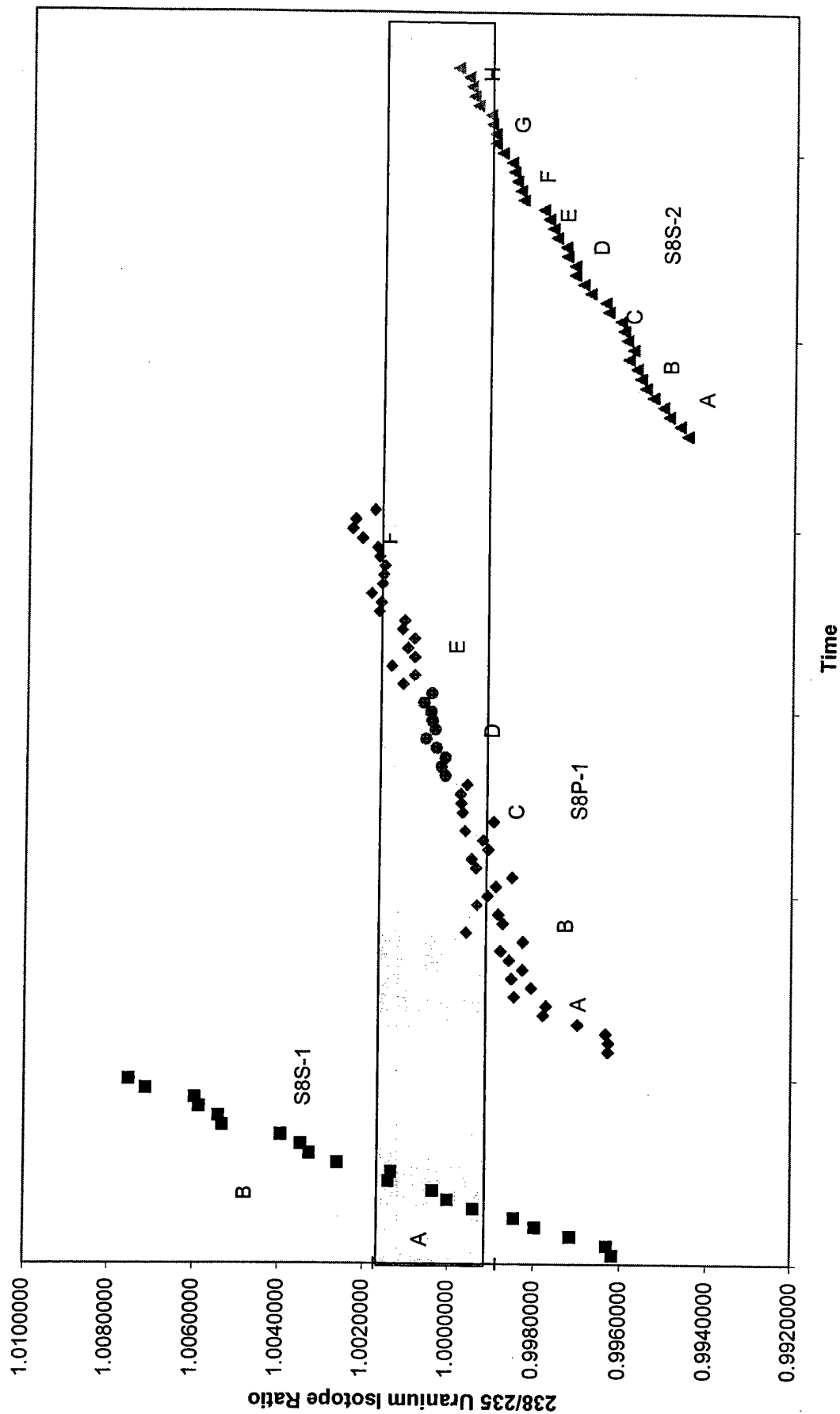
Turret Three through Five
S4S-1 (A-C) Sandwich and S4S-2 (A-F) Regular



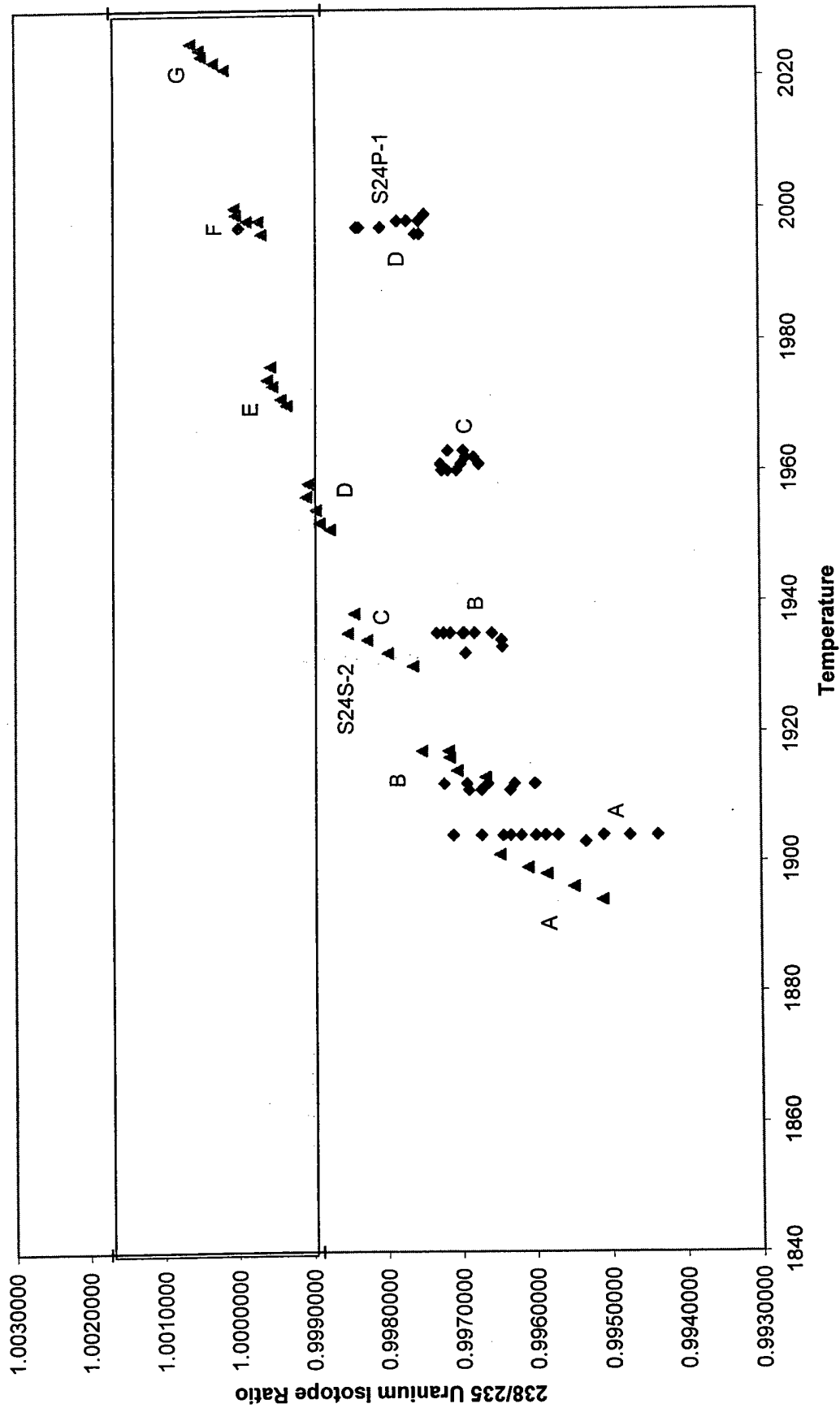
Turret Three through Five
S8S-1 (A-B), S8P-1 (A-F), Sandwich and S8S-2 (A-H) Regular as a Function of Temperature



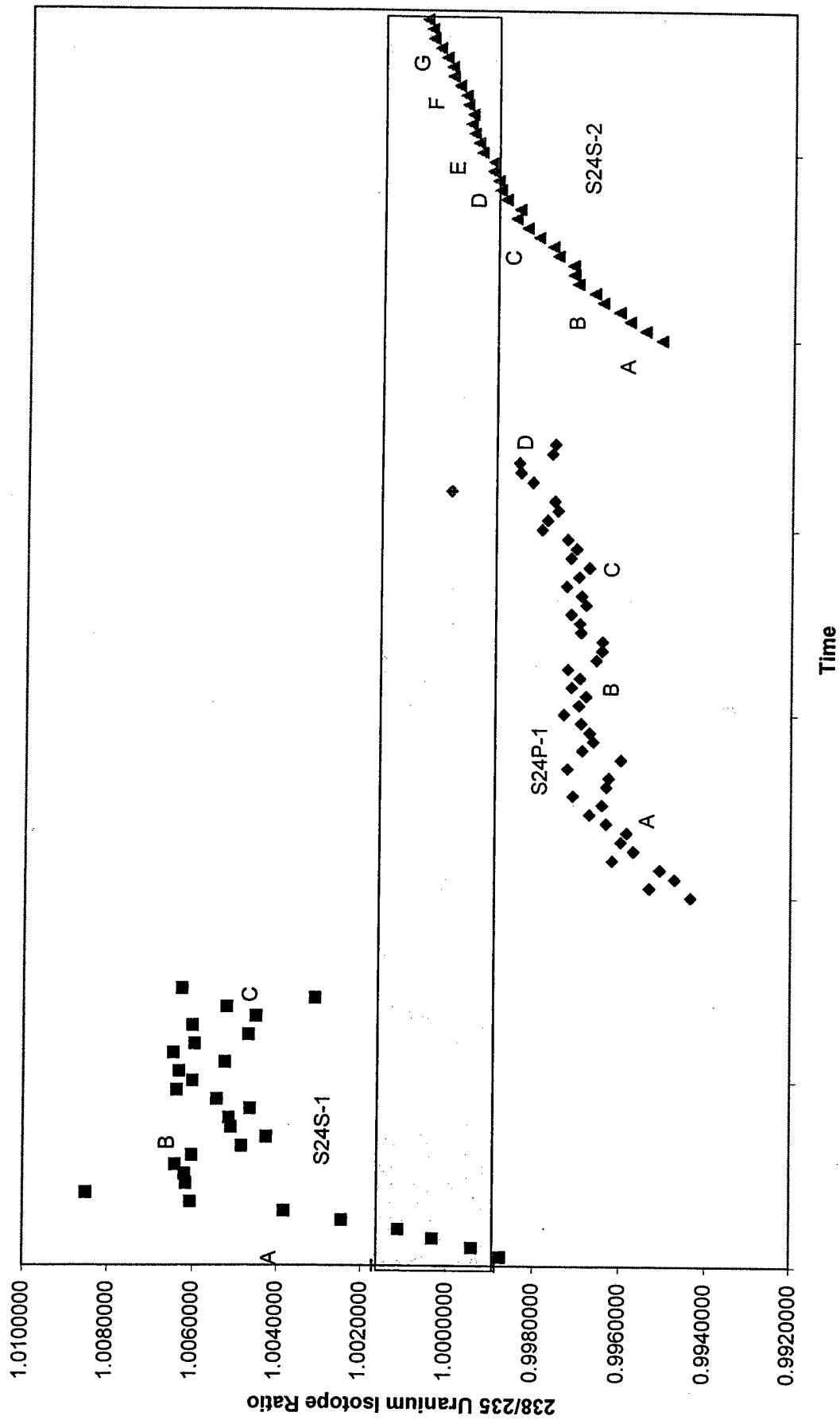
Turret Three through Five
S8S-1 (A-B), S8P-1 (A-F), Sandwich and S8S-2 (A-H) Regular



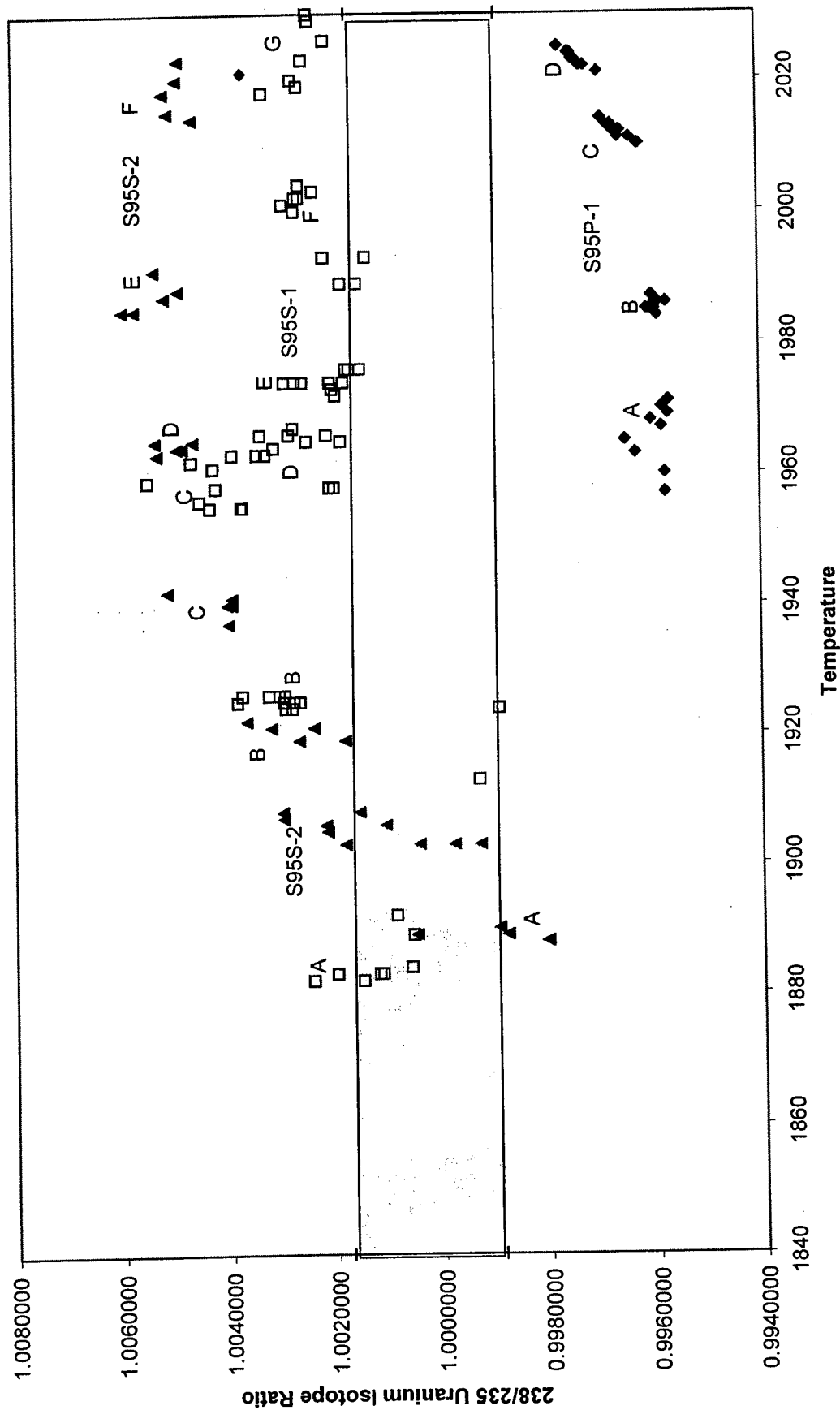
Turret Three through Five
S24S-1(A-C), S24P-1(A-D) Sandwich, and S24S-2 (A-G) Regular as a Function of Temperature



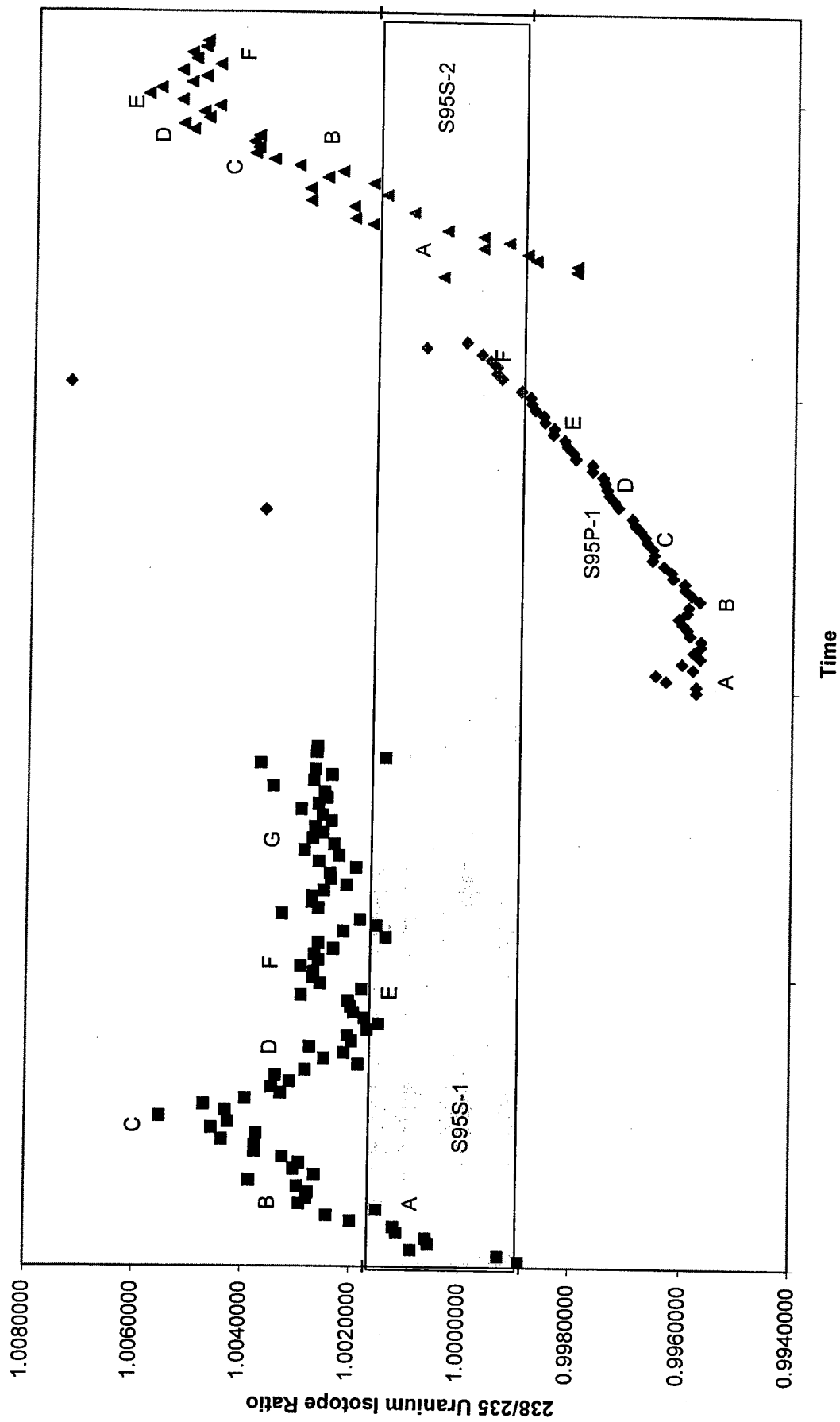
Turret Three through Five
S24S-1(A-C), S24P-1(A-D) Sandwich, and S24S-2 (A-G) Regular



Turret Three through Five
S95S-1(A-G), S95P-1(A-F) Sandwich, and S95S-2 (A-F) Regular as a Function of Temperature



Turret Three through Five
S95S-1(A-G), S95P-1(A-F) Sandwich, and S95S-2 (A-F) Regular



Appendix 4, Annex I

TIMS Results of Turret Six

I-1 Raw Database

I-2 Charts

- 1 Chart of Isotopic Ratios for regular loaded test sample precipitates as a function of temperature
- 2 Chart of Isotopic Ratios for regular loaded test sample precipitates as a function of consecutive block measurements
- 3 Chart of Isotopic Ratios for regular loaded 4 Hour test sample precipitates and supernatants, and C4 supernatant as a function of temperature
- 4 Chart of Isotopic Ratios for regular loaded 4 Hour test sample precipitates and supernatants, and C4 supernatant as a function of consecutive block measurements
- 5 Chart of Isotopic Ratios for regular loaded 8 Hour test sample precipitates and supernatants, and C8 supernatant as a function of temperature
- 6 Chart of Isotopic Ratios for regular loaded 8 Hour test sample precipitates and supernatants, and C8 supernatant as a function of consecutive block measurements
- 7 Chart of Isotopic Ratios for regular loaded 24 Hour test sample precipitates and supernatants as a function of temperature
- 8 Chart of Isotopic Ratios for regular loaded 24 Hour test sample precipitates and supernatants as a function of consecutive block measurements
- 9 Chart of Isotopic Ratios for regular loaded 95 Hour test sample precipitates and supernatants, and C95 supernatant as a function of temperature
- 10 Chart of Isotopic Ratios for regular loaded 95 Hour test sample precipitates and supernatants, and C95 supernatant as a function of consecutive block measurements

DTG										3/13/00 16:40										DTG										3/13/00 16:52									
Bead: 9										S4P-2,A										Bead: 9										S4P-2,B									
238										238										238										238									
Block										Amps										Temp										Intensity									
1										4.4										1910										1.8									
2										4.4										1909										1.7									
3										4.4										1908										1.7									
4										4.4										1908										1.6									
5										4.4										1906										1.6									
Grand Mean																														Grand Mean									
0.9964709																														0.9964709									
0.000046																														0.000046									
0.000059																														0.000059									
0.000072																														0.000072									
0.000044																														0.000044									
0.000033																														0.000033									
0.000045																														0.000045									
0.000046																														0.000046									
0.9961183																														0.9961183									
0.9962343																														0.9962343									
0.9964173																														0.9964173									
0.9968068																														0.9968068									
0.9968083																														0.9968083									
0.9964709																														0.9964709									
0.000046																														0.000046									
0.000059																														0.000059									
0.000072																														0.000072									
0.000044																														0.000044									
0.000033																														0.000033									
0.000045																														0.000045									
0.000046																														0.000046									
0.9961183																														0.9961183									
0.9962343																														0.9962343									
0.9964173																														0.9964173									
0.9968068																														0.9968068									
0.9968083																														0.9968083									
0.9964709																														0.9964709									
0.000046																														0.000046									
0.000059																														0.000059									
0.000072																														0.000072									
0.000044																														0.000044									
0.000033																														0.000033									
0.000045																														0.000045									
0.000046																														0.000046									
0.9961183																														0.9961183									
0.9962343																														0.9962343									
0.9964173																														0.9964173									
0.9968068																														0.9968068									
0.9968083																														0.9968083									
0.9964709																														0.9964709									
0.000046																														0.000046									
0.000059																														0.000059									
0.000072																														0.000072									
0.000044																														0.000044									
0.000033																														0.000033									
0.000045																														0.000045									
0.000046																														0.000046									
0.9961183																														0.9961183									
0.9962343																														0.9962343									
0.9964173																														0.9964173									
0.9968068																														0.9968068									
0.9968083																														0.9968083									
0.9964709																														0.9964709									
0.000046																														0.000046									
0.000059																														0.000059									
0.000072																														0.000072									
0.000044																														0.000044									
0.000033																														0.000033									
0.000045																														0.000045									
0.000046																														0.000046									
0.9961183																														0.9961183									
0.9962343																														0.9962343									
0.9964173																														0.9964173									
0.9968068																														0.9968068									
0.9968083																														0.9968083									

Appendix 4, Annex I-1

DTG		3/13/00 18:04		DTG		3/13/00 18:15	
Bead: 10		S8P-2,A		Bead: 10		S8P-2,B	
Block	Amps	Temp	Intensity	Block	Amps	Temp	Intensity
31	4.4	1937	4.4	36	4.5	1963	5.10
32	4.4	1938	4.1	37	4.5	1964	4.80
33	4.4	1939	3.9	38	4.5	1964	4.70
34	4.4	1939	3.7	39	4.5	1965	4.50
35	4.4	1939	3.5	40	4.5	1966	4.40
Grand Mean				Grand Mean			
							238/235
							0.9982921
							0.9986288
							0.9988439
							0.9990237
							0.9993061
							0.9988189
							Std Error
							0.00022
							0.00031
							0.00037
							0.00027
							0.00023
							0.00051
DTG		3/13/00 18:27		DTG		3/13/00 18:40	
Bead: 10		S8P-2,C		Bead: 10		S8P-2,D	
Block	Amps	Temp	Intensity	Block	Amps	Temp	Intensity
41	4.6	1989	6.4	46	4.65	2012	5.20
42	4.6	1992	6.1	47	4.65	2014	4.70
43	4.6	1994	5.7	48	4.65	2015	4.40
44	4.6	1997	5.6	49	4.65	2016	4.10
45	4.6	1998	5.2	50	4.65	2018	3.90
Grand Mean				Grand Mean			
							238/235
							1.0014881
							1.0016275
							1.0015458
							1.0015860
							1.0017168
							1.0015875
							Std Error
							0.00034
							0.00041
							0.00021
							0.00025
							0.00033
							0.00016
DTG		3/13/00 18:52		DTG		3/13/00 19:04	
Bead: 10		S8P-2,E		Bead: 10		S8P-2,F	
Block	Amps	Temp	Intensity	Block	Amps	Temp	Intensity
51	4.7	2030	4.4	56	4.75	2044	4.20
52	4.7	2030	4.2	57	4.75	2044	4.00
53	4.7	2030	4.1	58	4.75	2045	3.90
54	4.7	2030	3.8	59	4.75	2046	3.70
55	4.7	2032	3.6	60	4.75	2047	3.60
Grand Mean				Grand Mean			
							238/235
							1.0022389
							1.0022713
							1.0023628
							1.0025678
							1.0024979
							1.0023840
							Std Error
							0.00044
							0.00030
							0.00030
							0.00027
							0.00033
							0.00023

Appendix 4, Annex I-1

DTG 3/13/00 19:26
Bead: 11 S24P-2,A

Block	Amps	Temp	Intensity	238	238/235	Std Error	Notes	Block	Amps	Temp	238 Intensity	238/235	Std Error	Notes
61	4.4	1921	1.7	0.9952225	0.00083			66	4.5	1949	3.10	0.9965483	0.00048	
62	4.4	1923	1.8	0.9956565	0.00036			67	4.5	1949	3.10	0.9967218	0.00061	
63	4.4	1923	1.7	0.9959120	0.00055			68	4.5	1950	3.00	0.9969619	0.00034	
64	4.4	1925	1.9	0.9961736	0.00029			69	4.5	1950	2.90	0.9971553	0.00034	
65	4.4	1926	1.9	0.9963168	0.00077			70	4.5	1951	2.90	0.9974086	0.00059	
Grand Mean				0.9958869	0.00053			Grand Mean				0.9969440	0.00047	

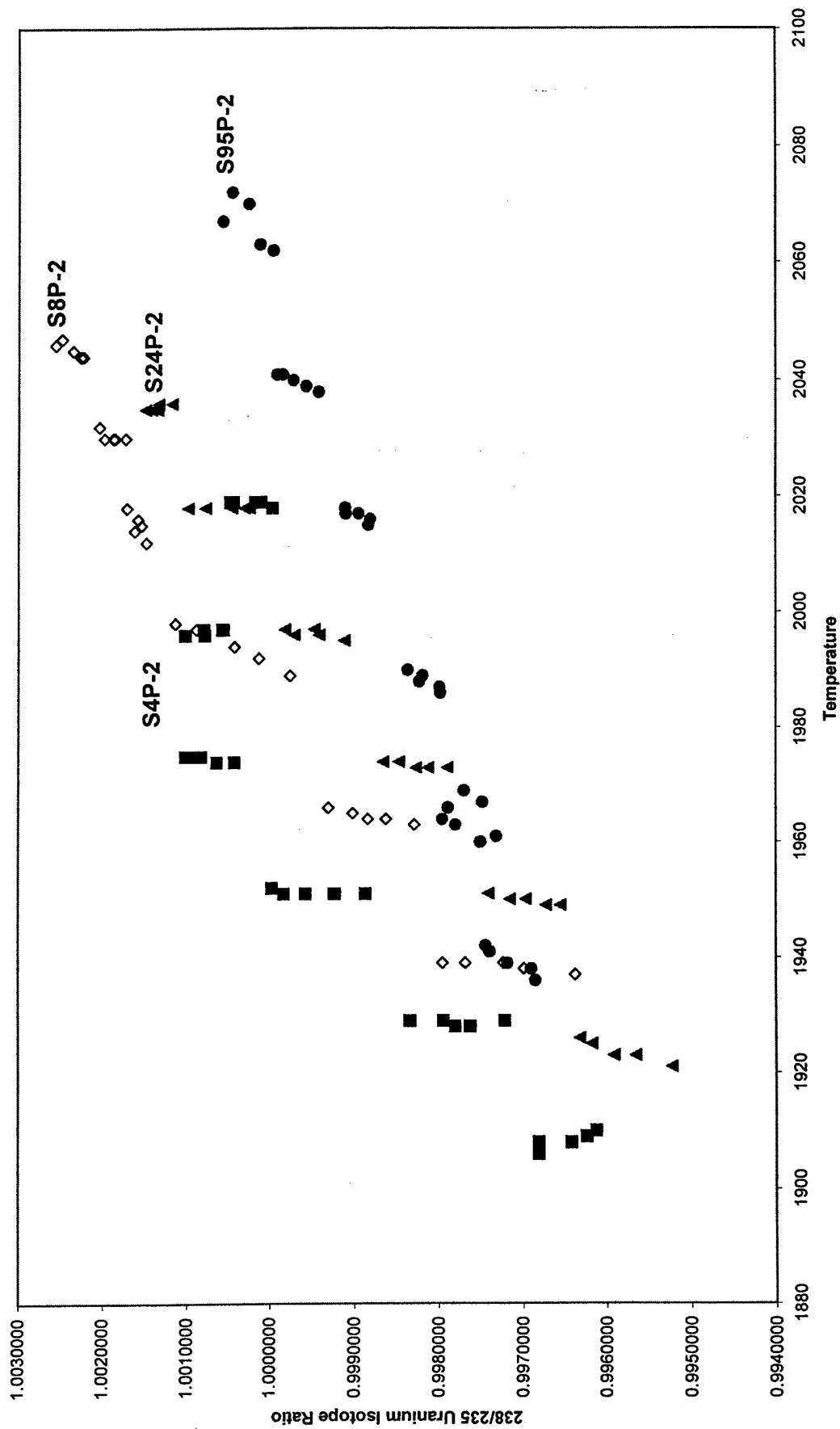
DTG 3/13/00 19:50
Bead: 11 S24P-2,C

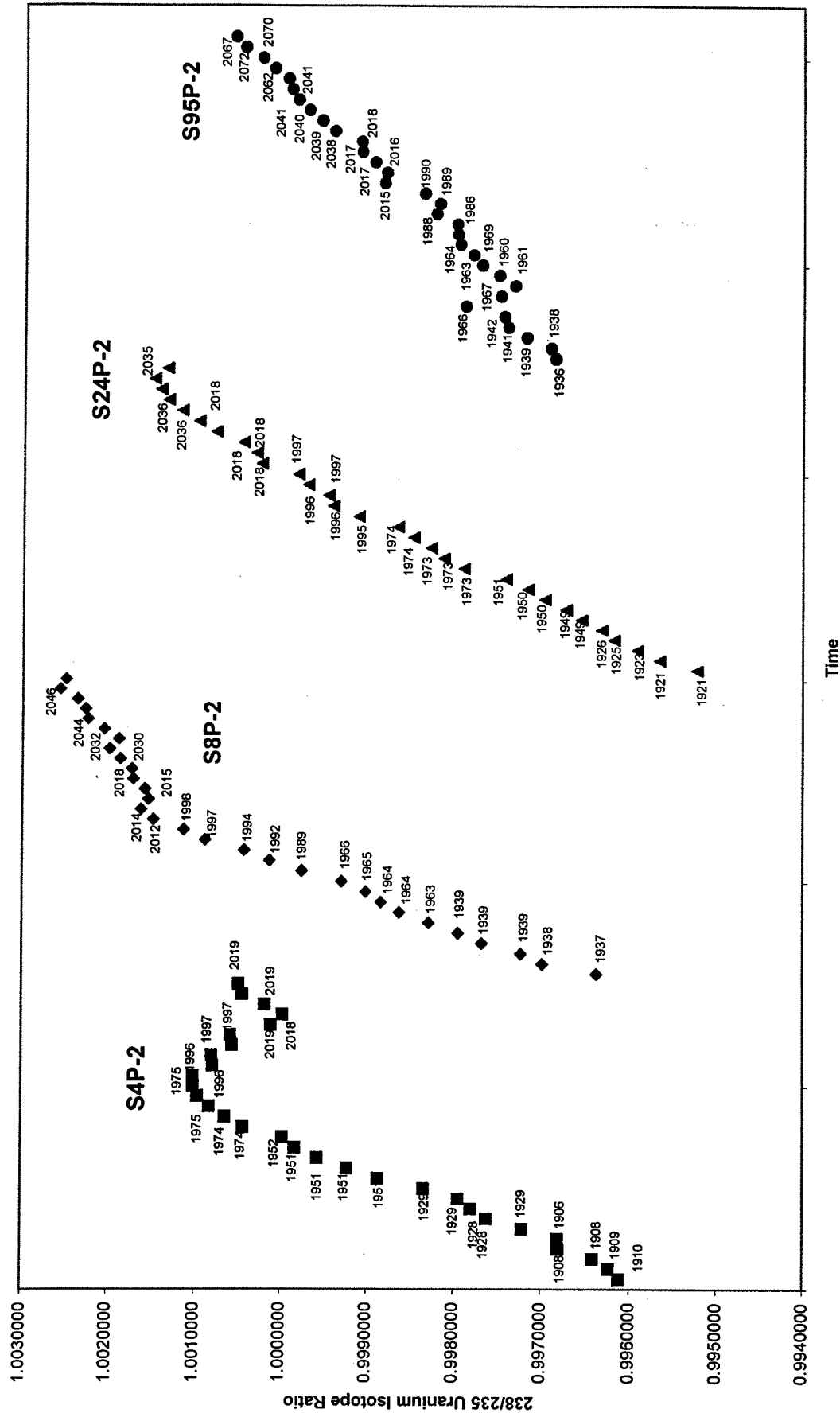
Block	Amps	Temp	Intensity	238	238/235	Std Error	Notes	Block	Amps	Temp	238 Intensity	238/235	Std Error	Notes
71	4.6	1973	4.3	0.9978962	0.00042			76	4.7	1995	5.20	0.9991258	0.00026	
72	4.6	1973	4.1	0.9981283	0.00036			77	4.7	1996	4.90	0.9994203	0.00037	
73	4.6	1973	4.0	0.9982746	0.00030			78	4.7	1997	4.70	0.9994775	0.00035	
74	4.6	1974	3.8	0.9984802	0.00044			79	4.7	1996	4.50	0.9997145	0.00018	
75	4.6	1974	3.7	0.9986610	0.00042			80	4.7	1997	4.30	0.9998291	0.00035	
Grand Mean				0.9982890	0.00039			Grand Mean				0.9995213	0.00037	

DTG 3/13/00 20:13
Bead: 11 S24P-2,E

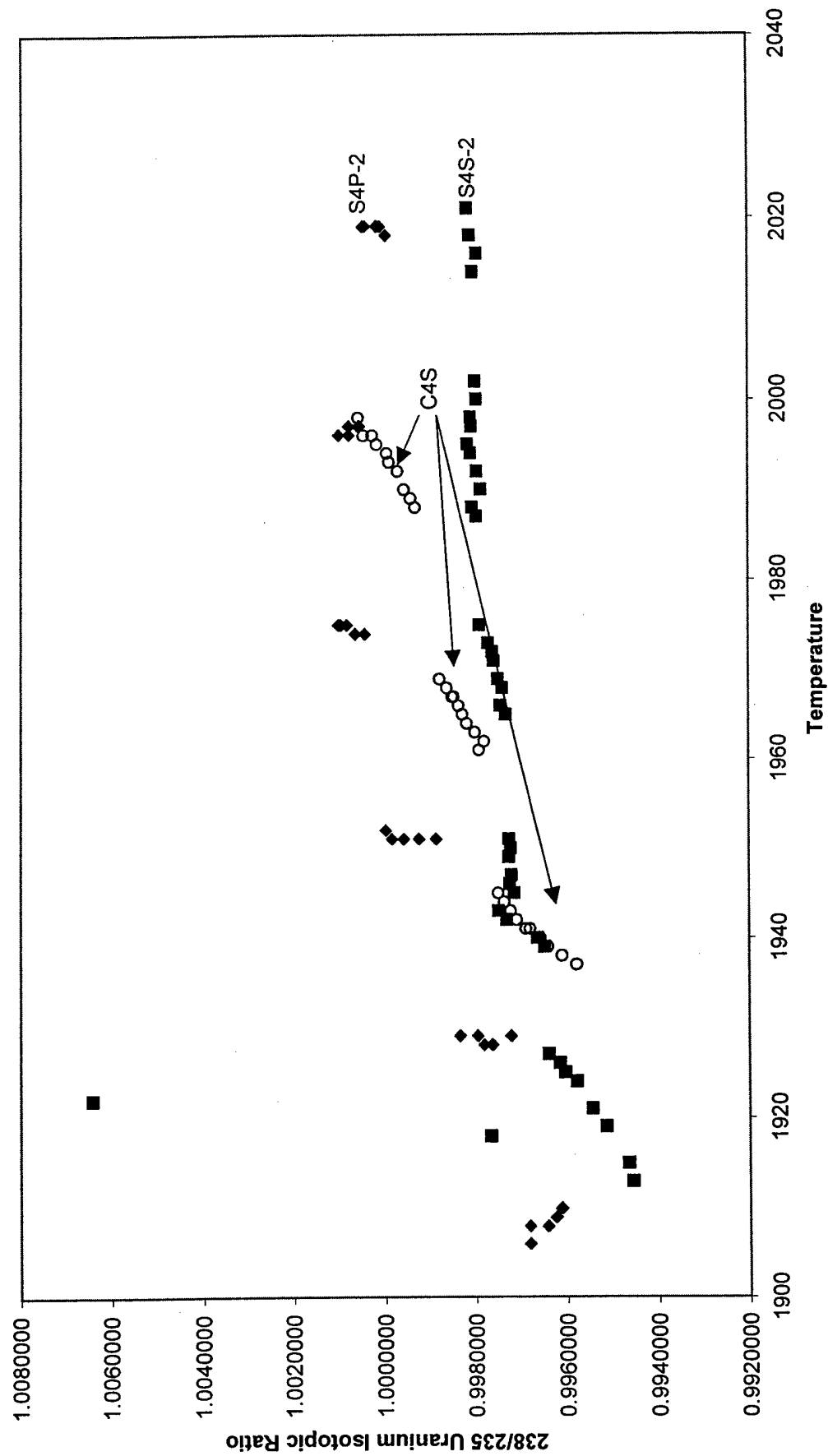
Block	Amps	Temp	Intensity	238	238/235	Std Error	Notes	Block	Amps	Temp	238 Intensity	238/235	Std Error	Notes
81	4.8	2018	5.5	1.0002568	0.00039			86	4.9	2036	5.80	1.0011861	0.00031	
82	4.8	2018	5.5	1.0003149	0.00026			87	4.9	2036	5.20	1.0013424	0.00023	
83	4.8	2018	5.1	1.0004673	0.00038			88	4.9	2035	4.80	1.0014288	0.00046	
84	4.8	2018	4.9	1.0007897	0.00012			89	4.9	2035	4.20	1.0015026	0.00028	
85	4.8	2018	4.7	1.0009906	0.00015			90	4.9	2035	3.80	1.0013561	0.00031	
Grand Mean				1.0005552	0.00042			Grand Mean				1.0013741	0.00020	

Turret Six
Precipitate Isotopic Ratios Regular Load

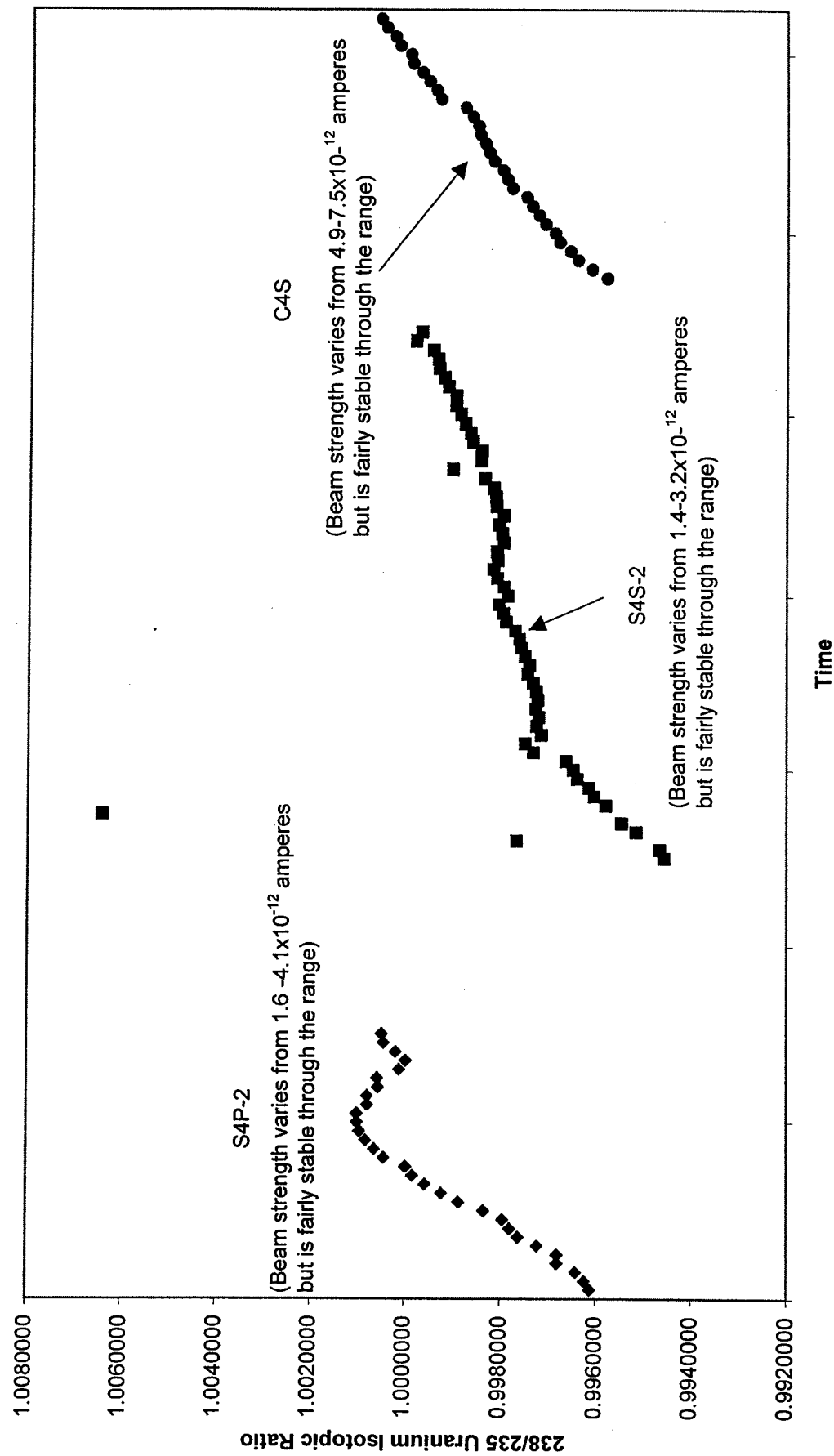




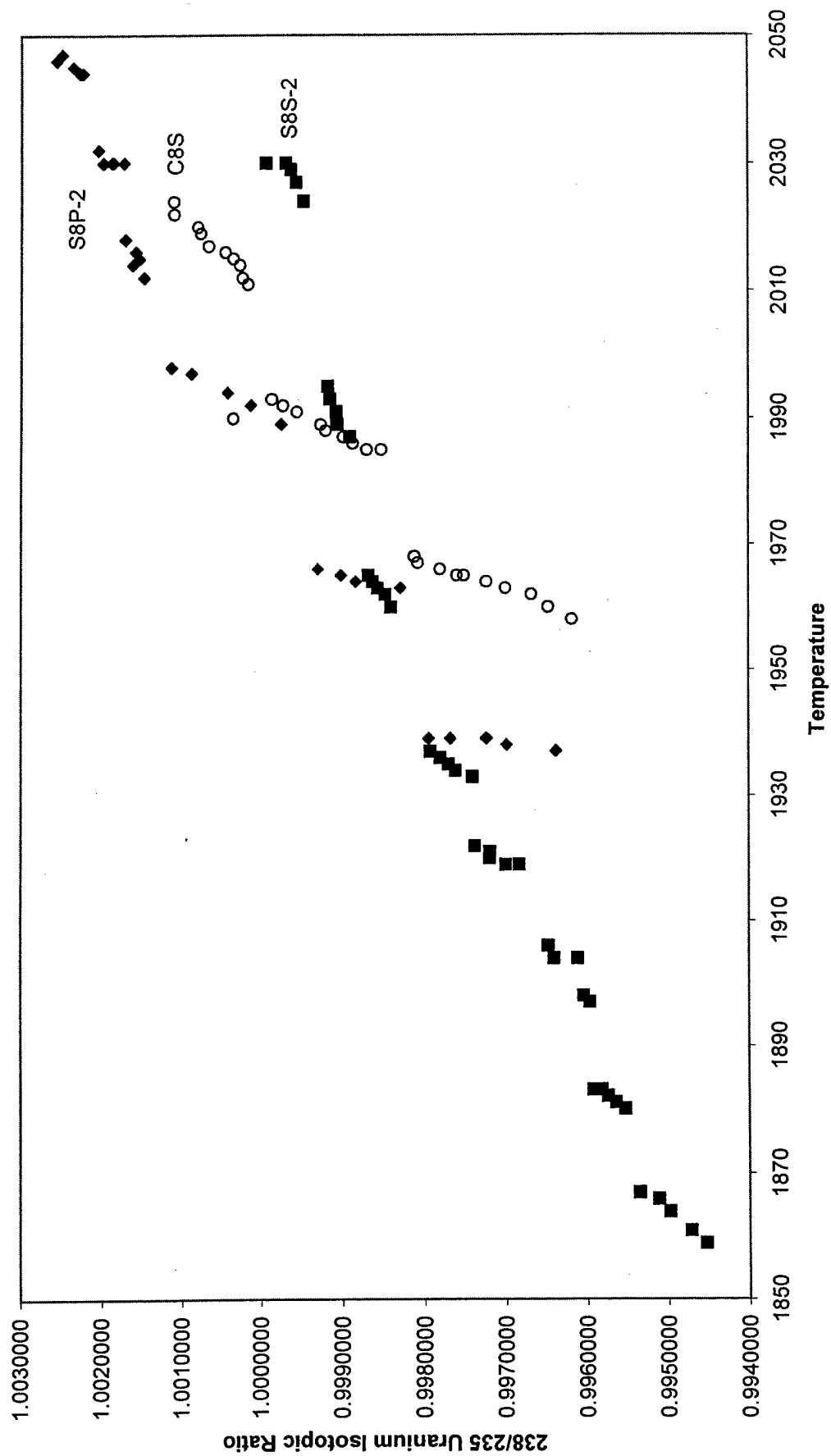
S4
Supernatant and Precipitate Ratio Comparison with respect to Temperature
Regular Loading Technique



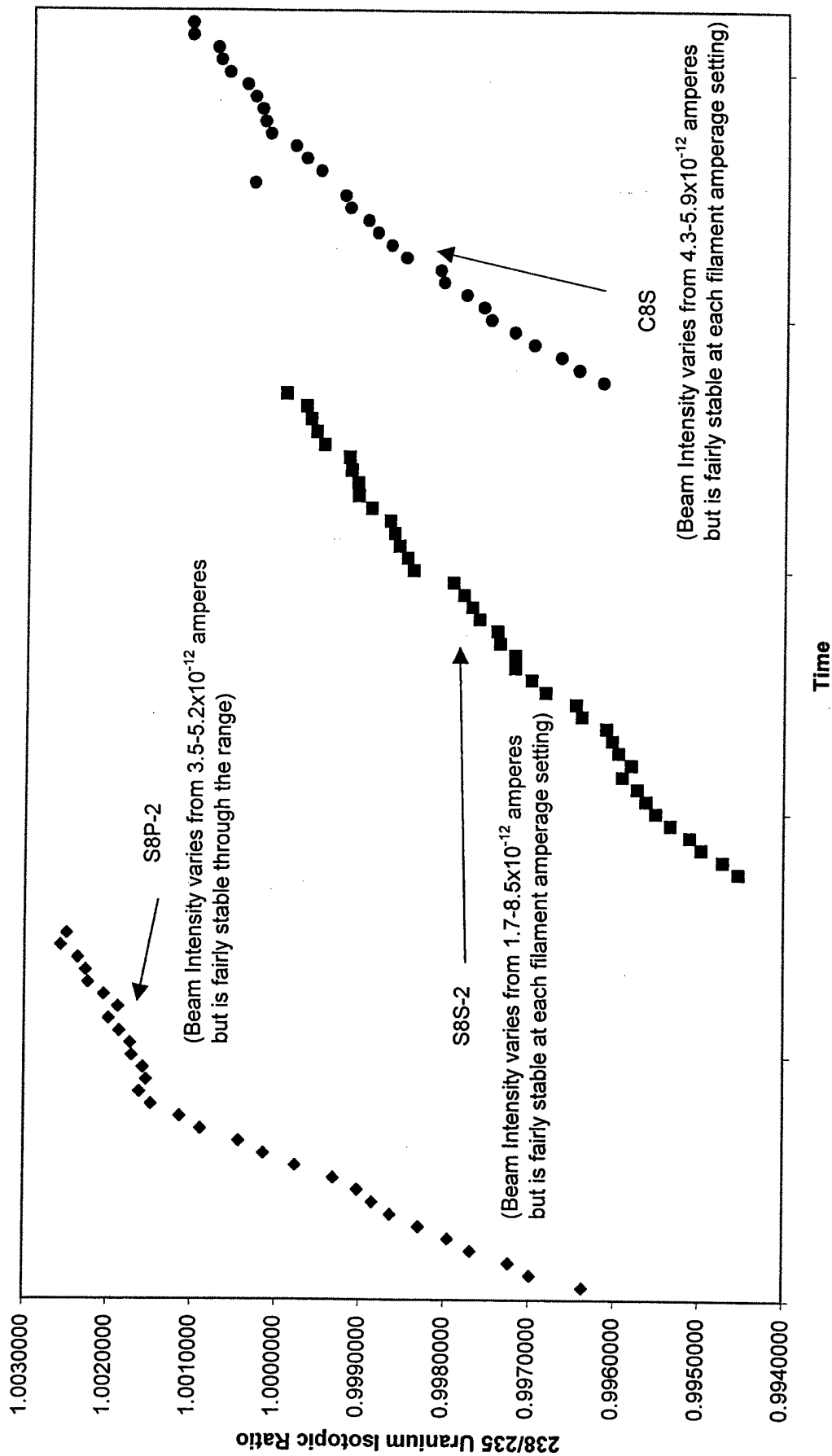
S4
Supernatant and Precipitate Ratio Comparison with respect to Time Steps
Regular Loading Technique



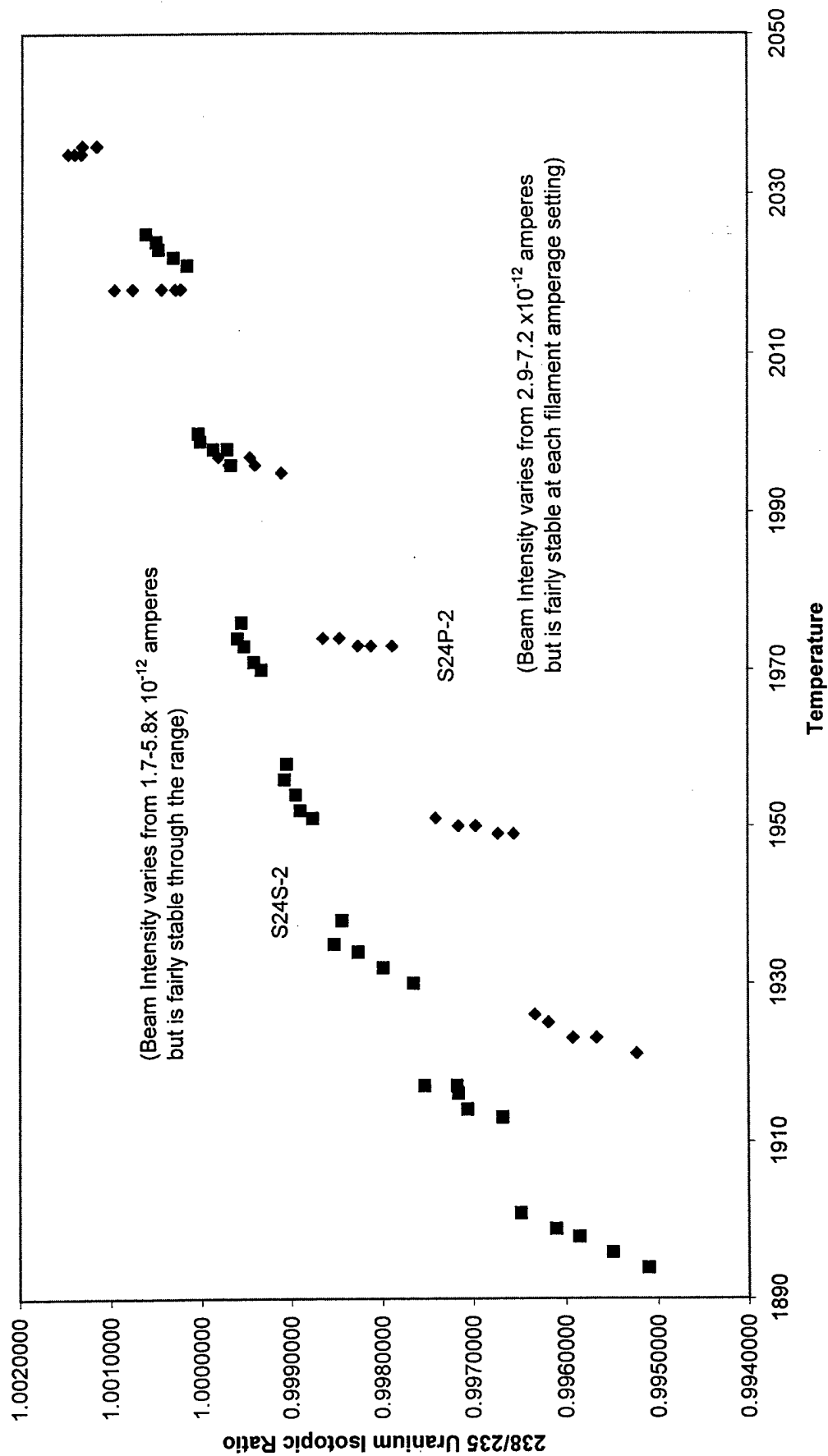
S8
Supernatant and Precipitate Ratio Comparison with respect to Temperature
Regular Loading Technique



S8
Supernatant and Precipitate Ratio Comparison with respect to Time Steps
Regular Loading Technique

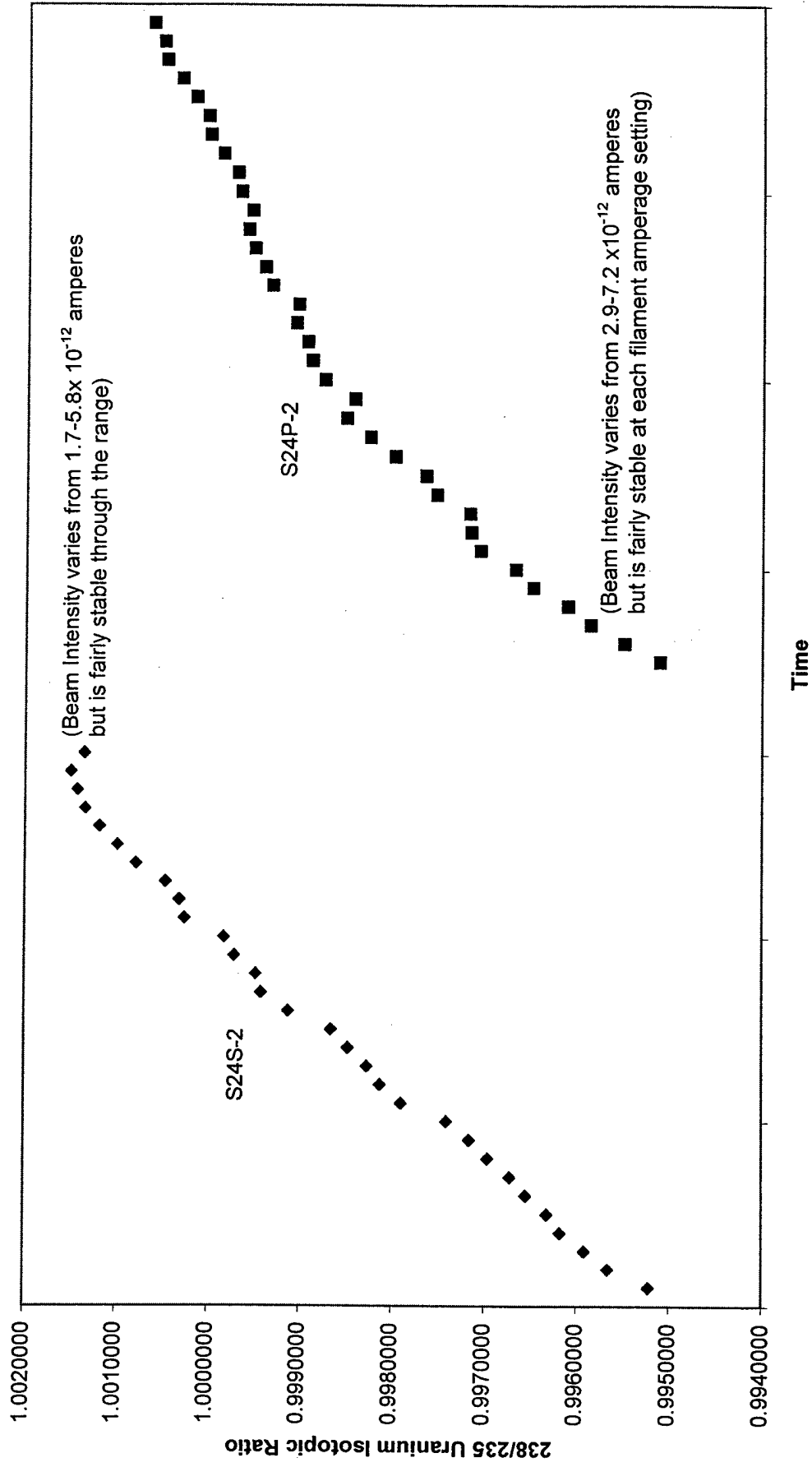


S24
Supernatant and Precipitate Ratio Comparison with respect to Temperature
Regular Loading Technique

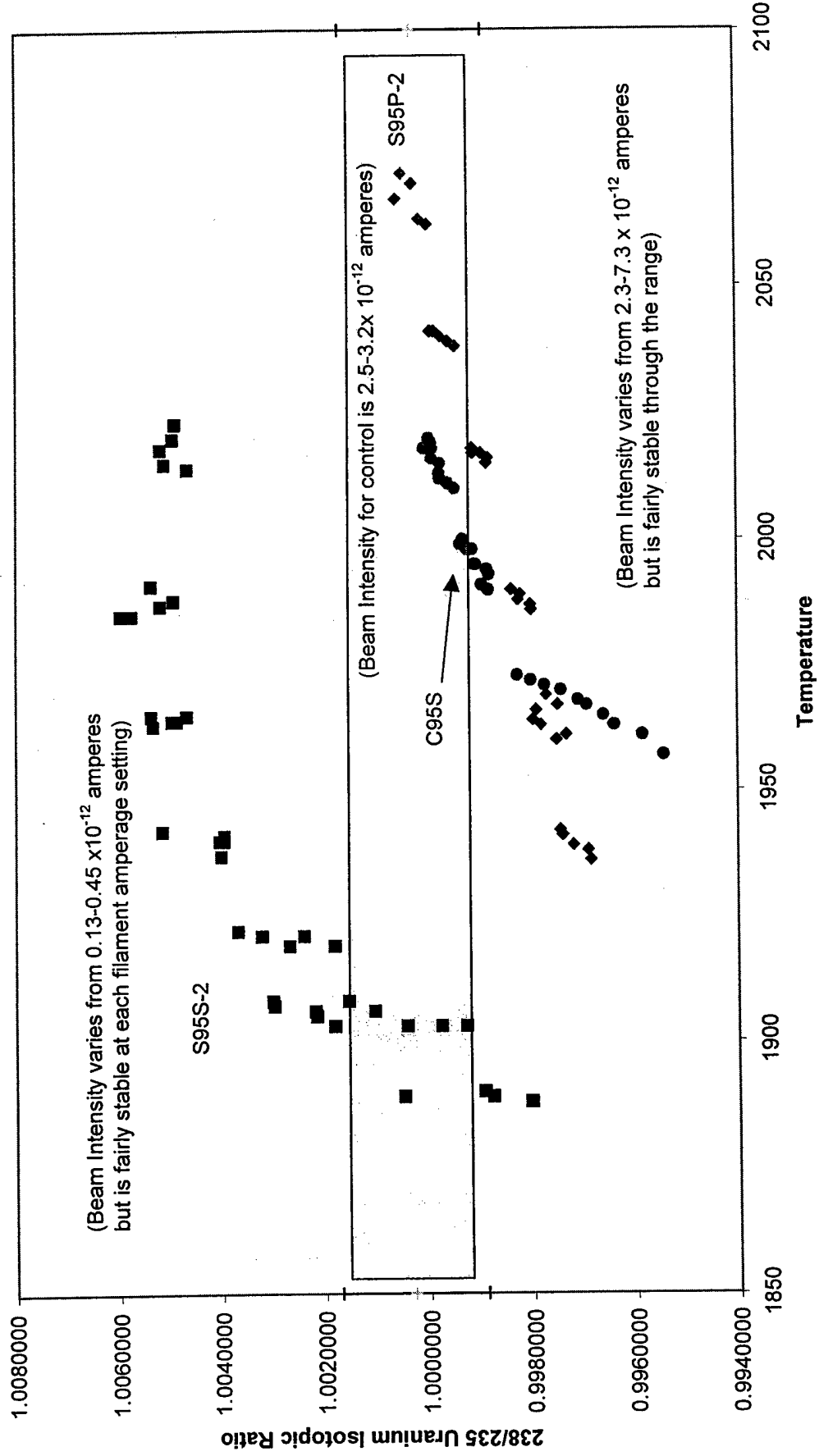


S24

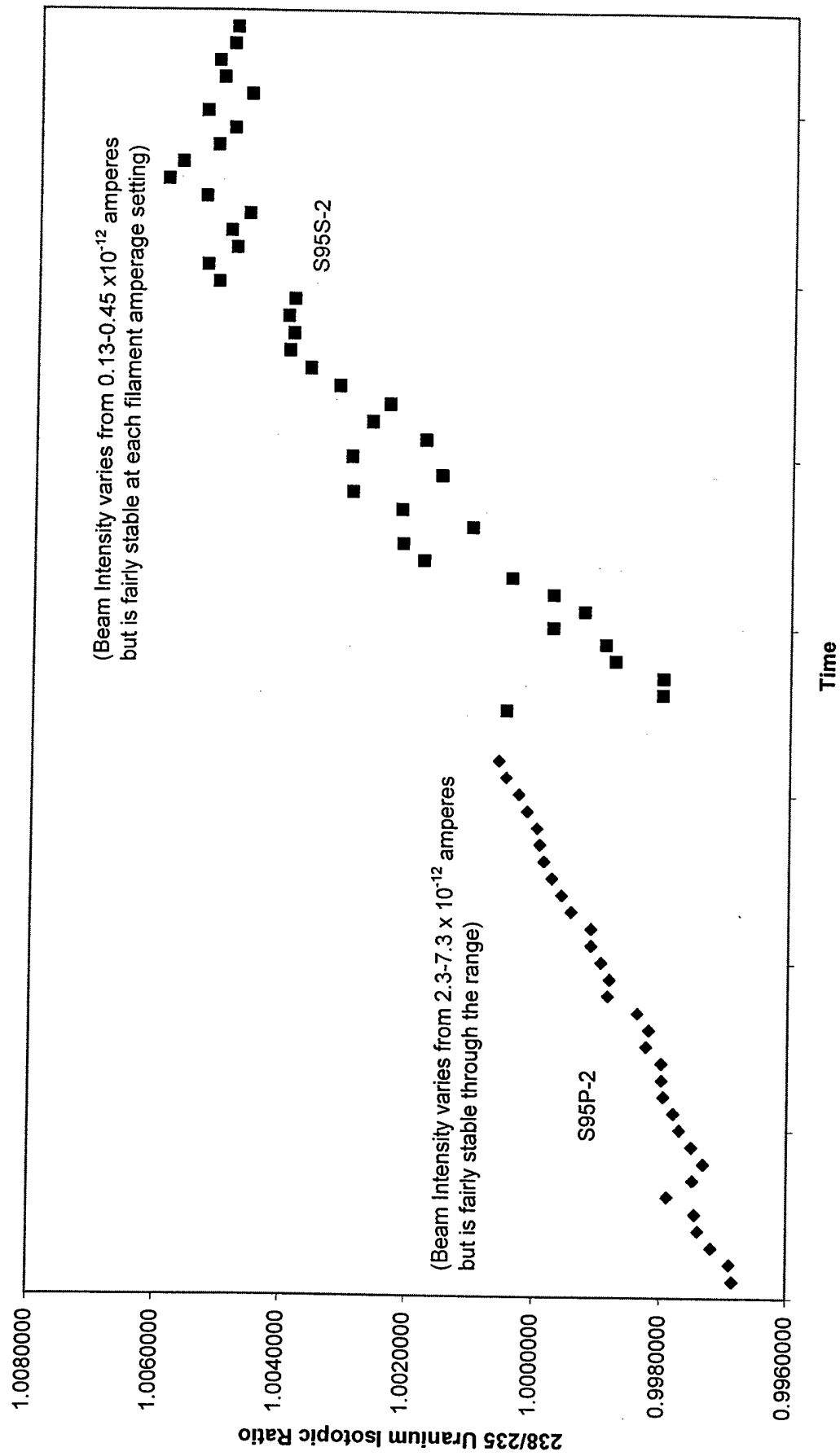
Supernatant and Precipitate Ratio Comparison with respect to Time Steps
Regular Loading Technique



S95
Supernatant and Precipitate Ratio Comparison with respect to Temperature
Regular Loading Technique



S95
Supernatant and Precipitate Ratio Comparison with respect to Time Steps
Regular Loading Technique



Appendix 4, Annex J

Estimated Concentration of the Precipitate Solutions

Test Sample *	ICP-AES		Uranium loss				Estimated		Estimated	
	Uranium Concentration in Supernatant (mM)	Uranium Concentration in Supernatant (Moles)	Uranium loss to in precipitate (mM)	Uranium loss to in precipitate and sorption (Moles)	Uranium in precipitate only (mM)	Uranium in precipitate only (Moles)	Concentration of the 1.5 mL centrifuge tube (M)	Concentration of the 15 mL centrifuge tube (M)	Estimated	Estimated
S0	1.842	1.050E-02	0	0	0	0	N/A	N/A	0	0
S4	1.535	8.750E-03	0.307	1.750E-03	0	0.000E+00	0	0	6.665E-01	1.162E+00
S8	1.231	7.017E-03	0.611	3.483E-03	0.304	1.733E-03	17.328	30.21	59.907	86.355
S24	1.005	5.729E-03	0.837	4.771E-03	0.53	3.021E-03	30.21	59.907	86.355	3.321E+00
S95	0.484	2.759E-03	1.358	7.741E-03	1.051	5.991E-03	59.907	86.355	3.321E+00	3.321E+00
	0.02	1.140E-04	1.822	1.039E-02	1.515	8.636E-03	86.355	3.321E+00	3.321E+00	3.321E+00

*Initial Concentration of Uranium Media
(discounting sorption, total volume 5.7 mL (5mL media+0.2 mL cellular inoculation+ 0.5 mL formaldehyde)

Bibliography

1. De Beer, H. & Coetzee. "Ion Chromatographic Separation and Spectrophotometric Determination of U(IV) and U(VI)." *Radiochimica Acta*, no. 57, (1992): 113-117.
2. Gorby, Yuri A. & Lovley, Derek. "Enzymatic Uranium Precipitation." *Environmental Science and Technology*, 26, (1992): 205-207.
3. Raju, K. Vijaya & Gautam, G. Madhu. "Iron (II) Titration of some Metal Ions with Oxazine Dye Indicators." *Talanta*, 35, no. 6, (1988): 490-492.
4. Grenthe, I., Fuger, J., Konings, R. J. M., Lemire, R. J., Muller, A. B., Nguyen-Trung, C., & Wanner, H. *Chemical Thermodynamics of Uranium, Volume 1*, Amsterdam: North Holland, 1992.
5. Cordfunke, E. H. *The Chemistry of Uranium*. New York, NY: Elsevier Publishing Company, 1969.
6. Polz, Martin. "Metal-metabolizing microbes reduce arsenic and uranium." *Civil and Environmental Engineering at MIT*, 13, no. 2, (Winter 1998-1999), 1-4.
7. Beard, Brian & Johnson, Clark M.. High precision iron isotope measurements of terrestrial and lunar materials. *Geochimica et Cosmochimica*, 63, no. 11/12, (1999): 1653-1660.
8. Oxtoby, David. *Principles of Modern Chemistry (Fourth Edition)*. New York, NY: Saunders College Publishing, (1999).
9. Gill, Robin *Modern Analytical Geochemistry*. Singapore, Indonesia: Longman Singapore Publishers Limited, (1997).
10. Wu, Jingfeng & Boyle, Edward A. "Determination of iron in seawater by high-resolution isotope dilution inductively coupled plasma mass spectrometry after $\text{Mg}(\text{OH})_2$ co-precipitation." *Analytica Chimica Acta*, 367, (1998): 183-191.
11. Trautmannsheimer, M., Schramel, P., Winkler, R., & Bunzel, K. "Chemical fractionation of some natural radionuclides in a soil contaminated by slags." *Environmental Science and Technology*, 32, no. 2, (1998): 238-243.

12. Iron Isotope Fractionation by the Bacteria *Shewanella* during Dissimilatory Reductive Dissolution of Ferrihydrite. ACS March 1999, 1 Abstracts, GEOC#068.
13. Golovnya, V.A. & Shubochkin, L.K. "The complex nature of uranyl acetate." Russian Journal of Inorganic Chemistry, 8, no. 5, (1963): 579-582.
14. Tanaka, Y., Fujii, Y., & Okamoto, M. "Raman spectroscopic and chromatographic study of uranium isotope effect in uranyl acetate complex formation." The Journal of Physical Chemistry, 86, no. 6, (1982): 1015-1018.
15. Inoue, Akihiko. "Mechanism of the oxidative dissolution of UO_2 in HNO_3 solution." Journal of Nuclear Materials, 138, (1986): 152-154.
16. Inoue, Akihiko & Tsujino, Takeshi Dissolution rates of U_3O_8 in nitric acid. Industrial Chemical Process Development, 23, (1984): 122-125.
17. Yasuike, Yoshiyuki, Ikeda, Yasuhisa, & Takashima, Yoichi "Kinetic study on dissolution of U_3O_8 powders in nitric acid." Journal of Nuclear Science and Technology, 32, no. 6, (1995): 596-598.
18. Fuger, J. & Oetting, F.L. The Chemical Thermodynamics of Actinide Elements and Compounds: Part 2 The Actinide Aqueous Ions. Vienna, Austria: International Atomic Energy Agency, 1976.
19. Palei, P.N. Analytical Chemistry of Uranium. Ann Arbor, Michigan: Ann Arbor-Humphrey Science Publishers, 1970.
20. Seaborg, Glenn T. and Katz, Joseph J. The Actinide Elements. New York, New York: McGraw-Hill Book Company, Inc., 1954.
21. Oxtoby, David W., Gillis, H.P., and Nachtrieb, Norman H. The Principles of Modern Chemistry. New York, New York: Saunders Golden Sunburst Publishing, 1999.
22. Benedict, Mason, Pigford, Thomas H., Levi, Hans Wolfgang. Nuclear Chemical Engineering. Boston, Massachusetts: McGraw-Hill Company, Inc., 1981.
23. Oxenberg, Tanya P. "The Use of Catchboxes to Minimize the Impact to the Environment from Testing Depleted Uranium Penetrators." Master's Thesis, Georgia Institute of Technology, 1997.
24. Owen, Paul E. "Waste Characteristics of Spent Fuel from a Pebble Bed Reactor." Masters Thesis, Massachusetts Institute of Technology, 1999.

25. Allen, Scott. "Concord Firm Halts Clean Up." The Boston Globe, 17 May 1999, p. B1, B5.
26. Oetting, F.L., Rand M.H., and Ackerman, R. J. The Chemical Thermodynamics of Actinide Elements and Compounds: Part 1 The Actinide Elements. Vienna, Austria: International Atomic Energy Agency, 1976.
27. Fuger, J. and Oetting F.L. The Chemical Thermodynamics of Actinide Elements and Compounds: Part 2 The Actinide Aqueous Ions. Vienna, Austria: International Atomic Energy Agency, 1976.
28. Cordfunke, E.H.P and O Hare, P.A.G. The Chemical Thermodynamics of Actinide Elements and Compounds: Part 3: Miscellaneous Actinide Compounds. Vienna, Austria: International Atomic Energy Agency, 1976.
29. Edelstein, Norman M. Actinides in Perspective. New York, New York: Pergamon Press, 1982.
30. Chernyaev, I.I. Complex Compounds of Uranium. Jerusalem, Israel: Academy of Sciences of the U.S.S.R., 1966.
31. Cordfunke, E.H.P. The Chemistry of Uranium. London, England: Elsevier Publishing Company, 1969.
32. Czerwinski, K.R., Buckau, G., Scherbaum, F., Kim, J.I. "Complexation of the Uranyl Ion with Aquatic Humic Acid." Radiochimica Acta, 65, (1994): 111-119.
33. Sherman, C. "Using Vegetation and Surface Water Samples to Trace Depleted Uranium Contamination from Starmet Corporation in Concord, MA." Bachelor of Science Thesis, Massachusetts Institute of Technology, 1998.
34. Walter J. Moore, Basic Physical Chemistry. London, England: Prentice Hall International, 1983.
35. Spectroflame Modula; Spectroflame EOP Operation Manual. Spectro Analytical Instruments GMBH. Kleve, Germany. (Not Dated)
36. SpectroFlame ICP Limits of Detection in Aqueous Solutions (2 s) in ppb. Spectro Analytical Instruments. Fitchburg, MA. (Not Dated)
37. Aldrich Catalog Handbook of Fine Chemicals (1998-1999), 127.

38. Parrington, Josef R., Knox, Harold D., Breneman, Susan L., Baum, Adward M., and Feiner, Frank. Nuclides and Isotopes, Fifteenth Edition. San Jose, Ca.: General Electric Company, 1996.
39. Guide to Ion Exchange (Bio Rad Catalog Number 140-9997).
40. Robert C. Weast and George L. Tuve. CRC Handbook of Chemistry and Physics. Cleveland, Ohio: Chemical Rubber Company, 1958.
41. David Lide and H.P.R. Frederikse. CRC Handbook of Chemistry and Physics 78th Edition. New York: Chemical Rubber Company, 1997.
42. Interview with Mark Schmitz, PhD student, Massachusetts Institute of Technology, 31 January 2000.